

COMPREHENSIVE METABOLOMICS REVEALS THE IMPACTS OF AFLATOXIN
B₁ AND GREEN TEA POLYPHENOLS ON GUT-MICROBIOTA DEPENDENT
METABOLISMS IN RODENT MODELS

by

JUN ZHOU

(Under the Direction of JIA-SHENG WANG)

ABSTRACT

Human commensal microorganisms play a critical role in regulating host physiology and health status. Xenobiotics can induce complex changes of gut-microbiota and cause significant impacts on host health, but the detailed mechanisms are not fully established. This dissertation project focused on the impacts of two representative natural products: aflatoxin B₁ (AFB₁) and green tea polyphenols (GTPs) on gut-microbiota dependent metabolisms and overall host physiological changes in model rats. The hypothesis is that the dynamics of gut-microbiome induced by xenobiotics may disrupt gut-microbiota dependent metabolisms and metabolic pathways, which contribute to the adverse health outcomes or promotion of host health status. Through 16S rRNA gene survey and metagenomic analysis, we found that AFB₁ and GTPs modified gut-microbiota community structure and gene orthologs with respect to energy metabolism, obesity, and inflammation. Adverse outcome pathways (AOPs) and nutritional beneficial effects were analyzed by integrating data collected from multiple analytical platforms, different

bioinformatics and biostatistics tools, as well as the reference data from validated pathological endpoints.

We found that AFB₁ significantly disrupted production of short chain fatty acids, secretion and metabolism of bile acids, absorption of long chain fatty acids, catabolism of phenylalanine, and the metabolisms of pyruvic acid, amino acids, and carbohydrates. These changes are associated with the alterations of community structure. The pathways all have key positions in the global metabolism of gut-microbiota and host health. Hence, gut-microbiota may partially be involved in the pathological mechanism of AFB₁-exposure induced adverse health outcomes in F344 rat model, and presumably also in humans.

On the other hand, GTPs caused reduction of calorific carbohydrates, elevation of vitamin production, decreases of bile constituents, and modified metabolic pattern of amino acids in the gut of GTPs-treated Sprague Dawley rats. A further examination on the key differential metabolites indicated a boost of gut-microbiota dependent mitochondrial TCA/Urea cycle following GTPs administration. Based on previous microbiome data and clinical chemical analysis, we believe that such changes may be a major contributor to the anti-obesity function of GTPs.

INDEX WORDS: aflatoxin B₁, green tea polyphenols, metabolomics, metabolic pathway analysis, bioinformatics, analytical chemistry, pathology, data integration

COMPREHENSIVE METABOLOMICS REVEALS THE IMPACTS OF AFLATOXIN
B1 AND GREEN TEA POLYPHENOLS ON GUT-MICROBIOTA DEPENDENT
METABOLISMS IN RODENT MODELS

by

JUN ZHOU

BA, Qingdao Agricultural University, China, 2008

MS, University of Chinese Academy of Sciences, China, 2012

A Dissertation Submitted to the Graduate Faculty of The University of Georgia in Partial
Fulfillment of the Requirements for the Degree

DOCTOR OF PHILOSOPHY

ATHENS, GEORGIA

2018

© 2018

Jun Zhou

All Rights Reserved

COMPREHENSIVE METABOLOMICS REVEALS THE IMPACTS OF AFLATOXIN
B1 AND GREEN TEA POLYPHENOLS ON GUT-MICROBIOTA DEPENDENT
METABOLISMS IN RODENT MODELS

by

JUN ZHOU

Major Professor: Jia-Sheng Wang
Committee: Brian S. Cummings
Tai L. Guo
Ye Shen

Electronic Version Approved:

Suzanne Barbour
Dean of the Graduate School
The University of Georgia
December, 2018

ACKNOWLEDGEMENTS

I would like to express my very great appreciation to my advisor Dr. Jia-Sheng Wang, my committee board members Drs. Brian S. Cummings, Tai Guo and Ye Shen. I would like to give my special thanks to Dr. Mathew Henderson in EPA's National Exposure Research Laboratory, Miss Joanne Mauro in Toxicology Program, Drs. Lili Tang, Erin K. Lipp and Kathy Xue in Toxicology Program and Environmental Health Science Department, University of Georgia. I also want to give my thanks to our collaborator Dr. Chwan-Li Shen in Department of Pathology, Texas Technology University, as well as the many hearty friends that helped and supported me so much in these years.

TABLE OF CONTENTS

ACKNOWLEDGEMENTS	iv
LIST OF TABLES	viii
LIST OF FIGURES	xii
CHAPTER 1. INTRODUCTION	1
1.1 Xenobiotics and gut-microbiota.....	1
1.2 Introduction to aflatoxin B ₁	2
1.3 Green Tea Polyphenols as chemoprevention and probiotic agent	13
1.4 Validation of animal models.....	20
1.5 Hypothesis of current dissertation	26
1.6 Methodology.....	27
1.7 Specific aims of research	29
CHAPTER 2. LITERATURE REVIEW	50
2.1 Gut-microbiota dependent metabolome.....	50
2.2 Statistical issues in metabolomics.....	81
2.3 Short chain fatty acids and chronic inflammatory diseases	87
2.4 Clinical references for omics data interpretation	132

CHAPTER 3. AFLATOXIN B ₁ DISRUPTS GUT-MICROBIAL METABOLISMS OF SHORT CHAIN FATTY ACIDS, LONG CHAIN FATTY ACIDS AND BILE ACIDS IN MALE F344 RATS.....	221
3.1 Introduction.....	221
3.2 Materials and methods	223
3.3 Results.....	229
3.4 Discussion.....	233
CHAPTER 4. ASSESSMENT OF THE ADVERSE IMPACTS OF AFLATOXIN B ₁ ON GUT-MICROBIOTA DEPENDENT METABOLISM IN F344 RATS	262
4.1 Introduction.....	262
4.2. Methods and material.....	265
4.3 Results.....	270
4.4 Discussion.....	273
CHAPTER 5. AFLATOXIN B ₁ DISRUPTS GUT-MICROBIOTA DEPENDENT METABOLIC PATHWAYS OF CALORIFIC CARBOHYDRATES, AMINO ACIDS, ORGANIC ACIDS AND LIPIDS MALE F344 RATS	301
5.1 Introduction.....	301
5.2 Method and materials.....	304
5.3 Results.....	311
5.4 Discussion.....	314
5.5 Conclusion	325

CHAPTER 6. GREEN TEA POLYPHENOLS MODIFY GUT-MICROBIOTA DEPENDENT METABOLISMS OF ENERGY, BILE CONSTITUENTS AND MICRONUTRIENTS IN FEMALE SPRAGUE-DAWLEY RATS.....	369
6.1 Introduction.....	369
6.2 Methods.....	373
6.3 Results.....	378
6.4 Discussion.....	382
CHAPTER 7. GREEN TEA POLYPHENOLS BOOST GUT-MICROBIOTA DEPENDENT MITOCHONDRIAL TCA/UREA CYCLE AND ENERGY CONVERSION OF IN SPRAGUE DAWLEY RATS.....	418
7.1 Introduction.....	418
7.2 Materials and methods	421
7.3 Results.....	424
7.4 Discussion.....	428
CHAPTER 8. SUMMARY.....	464

LIST OF TABLES

	Page
Table 1-1: Major metabolites of AFB ₁ and biochemical features.	8
Table 1-2: Reported aflatoxins and metabolites in human samples	9
Table 1-3: Important terms in metabolomics.....	27
Table 2-1: Summary of the in vitro studies to examine the immune regulatory effects of SCFAs.....	117
Table 2-2: Performance specifications and precisions for liver tests (%)	136
Table 2-3: American Medical Association (AMA) approved organ or disease-oriented panels for blood test	137
Table 2-4: Comparison of representative reference ranges of LFT	144
Table 2-5: Reference ranges of liver function related enzymatic activities.....	145
Table 2-6: Liver test results in the U.S. NHNES III, 1988-1994.....	146
Table 2-7: Suggested interpretation of LFT results from American Association for Clinical Chemistry (AACC)	146
Table 2-8: Estimate of liver function using the Child-Turcotte Class	148
Table 3-1: Analytical parameters of HPLC-profiling analysis used for the measurement of interested fecal metabolites.....	241
Table 3-2: Mixed-effects model analysis between AFB ₁ -treatment (dose, time and interaction) and fecal levels of SCFAs	243

Table 3-3: Results of precision and accuracy tests of 2-NPH derivatization combined HPLC-profiling analysis	244
Table 3-4: Fecal SCFA levels ($\mu\text{mole/g}$ feces) of rats treated with 0, 5, 25, and 75 μg AFB ₁ /kg B. W.....	246
Table 4-1: Detective channels and major analytes in UHPLC-profiling analysis	279
Table 4-2: Indicative peaks discovered in UHPLC-profiling analysis.	280
Table 4-3: Representative metabolites detected by UHPLC-MS based metabolomics....	281
Table 4-4: Gut-microbiota dependent metabolic pathways disrupted by AFB ₁	282
Table 4-5: Differential metabolites found by Random Forest and OPLS-DA models....	283
Table 5-1: Analytical parameters of GC-MS analysis used for the measurement of amino acids and carbohydrates	327
Table 5-2: Fecal concentrations of key carbohydrates and amino acids determined by standard calibration.....	329
Table 5-3: Key metabolites (GC-MS) extracted by Random Forests and OPLS-DA	331
Table 5-4: Key metabolites (nanoHPLC-MS/MS) extracted by Random Forests and OPLS-DA models.	332
SI Table 5-1: Comparison of the counts of peak detected by GC-MS by using different solvents for chemical derivatization	344
SI Table 5-2: Comparison of the counts of peaks detected by GC-MS analysis by using different solvents for sample extraction.....	345
SI Table 5-3: Fold-change and statistical parameters for the 60 differential metabolites detected by GC-MS.....	346

SI Table 5-4: Results of GC-MS pathway analysis (MSEA, only significant components included) performed using MetaboAnalyst	349
SI Table 5-5: Summary of nanoLC-MS/MS metabolomics data.....	351
Table 6-1: Analytical parameters of GC-MS analysis used for the measurement of key metabolites	390
Table 6-2: Analytical parameters of HPLC-profiling used for the measurements of key metabolites.....	392
Table 6-3: Two-way ANOVA examination on the statistical significance of the dose, time, and interaction effects of GTPs-treatment on the metabolites measured by GC-MS.....	394
Table 6-4: Significantly modified metabolic pathways revealed by MSEA	397
Table 7-1: Signature metabolites significantly affected by time/dose effects of GTPs treatment	436
Table 7-2: TCA/Urea cycle targeted metabolomic analysis performed with SRM.....	438
Table 7-3: Pathway impact analysis based on the metabolites showing remarkable change in targeted and untargeted metabolomic analysis	439
SI Table 7-1: Summary of untargeted metabolomic analysis.....	447
SI Table 7-2: Relative abundances of gut-microbiome family-level taxa in 1.5% GTPs-treated groups at 6-month	450
SI Table 7-3: Family-level OTU average gene diversities in the metabolic pathways stimulated by GTPs.....	452
SI Table 7-4: Relative contribution of family level OTUs to the gut-microbiota dependent metabolic pathways (1.5% GTPs-treated group, 6-month)	453

SI Table 7-5: Energy Conversion related gene orthologs (GO) significantly modified by GTPs.....	454
SI Table 7-6: Clinical chemistry data from reference serum analysis.....	455

LIST OF FIGURES

	Page
Figure 1-1: AFB ₁ bio-transformation and elimination in humans: a schematic diagram for the known pathways of AFB ₁ metabolism in human.....	6
Figure 1-2: Chemical structures of green tea polyphenols	15
Figure 1-3: Comparing adverse health outcomes induced by oral exposure to AFB ₁ with beneficial effects brought by administration of GTPs.	17
Figure 1-4: Previous studies of HCC prevention with GTPs administration.....	21
Figure 1-5: Major findings of previous studies in animal models	25
Figure 1-6: Composition of green tea polyphenol powder used in current study.....	26
Figure 1-7: Design of integrative metabolomics methodology.	29
Figure 2-1: Approximate composition of dehydrated human feces.....	52
Figure 2-2: General workflow of metabolomic analysis	60
Figure 2-3: General metabolic links of indole derivatives.....	62
Figure 2-4: General metabolic links of tryptophan.....	67
Figure 2-5: Metabolic pathway of glutamate.....	69
Figure 2-6: General metabolic links of phenylalanine and tyrosine	70
Figure 2-7: General metabolic links between L-tyrosine and p-Cresol.....	72
Figure 2-8: Metabolic pathway of L-carnitine to trimethylamine	80
Figure 2-9: Chemical entities of short chain fatty acids	90

Figure 3-1: HPLC-profiling chromatograms of fecal extracts from control (upper) and exposure group (lower) after 2-NPH derivatization.	247
Figure 3-2: Fecal SCFA levels of rats treated with 0, 5, 25, and 75 $\mu\text{g AFB}_1/\text{kg B. W.}$..	248
Figure 3-3: Hierarchical cluster tree and heat map to show cross correlations for short chain fatty acids and top 18 significantly altered gut microbial strains discovered by previous 16s rRNA data.....	249
Figure 3-4: Fecal concentrations of cholic acid, deoxycholic acid, linoleic acid, pentadecanoic acid, pyruvic acid and 3-phenyllactic acid measured from the experimental groups treated with 0, 5 and 25 $\mu\text{g AFB}_1/\text{kg B. W.}$ via HPLC-profiling analysis.....	250
Figure 3-5: Summary of the adverse health outcomes associated with dietary exposure to AFB_1 in F344 rat model.....	251
Figure 4-1: Representative chromatograms documented by UHPLC-profiling analysis of control sample.....	284
Figure 4-2: Heat map to show the correlations of 111 common metabolites upon AFB_1 -treatment	285
Figure 4-3: Volcano plots of all 335 differential metabolites detected by UHPLC-profiling analysis.....	286
Figure 4-4: Examination of multiple variable analysis (MVA) models to extract differential metabolites from data pool.....	287
Figure 4-5: Overview of the does-responses of metabolites with significant dose-respose to AFB_1 -exposure and the biochemical pathways that are associated with these metabolites	288

Figure 4-6: Evaluation of predictive power of indicative metabolites using receiver operating characteristic (ROC) curve based exploratory analysis (random forest model built-in)	289
Figure 4-7: Box plots to show the alterations of indicative metabolites induced by AFB ₁	290
SI Figure 4-1: Representative chromatograms documented by UHPLC-profiling analysis of control sample.....	291
Figure 5-1: Typical GC-MS total ion chromatogram (TIC) of fecal metabolites.....	333
Figure 5-2: Volcano plots of 1490 feature ions detected by GC-MS	334
Figure 5-3: Heatmap overview of the alterations of metabolites profiled by GC-MS between control and middle-dose groups	335
Figure 5-4: Differential metabolites measured by standard calibration.....	336
Figure 5-5: Score plot and model supervision of OPLS-DA model.....	337
Figure 5-6: Key metabolites (GC-MS) ranked by Random Forests model to evaluate the contribution of metabolites to the discrimination between control and AFB ₁ -treated groups.....	338
Figure 5-7: Metabolite set enrichment analysis (MSEA) and pathway enrichment analysis for the detected metabolites (KEGG rat database)	339
Figure 5-8: Cloud plot and data normalization of nanoHRLC-MS/MS data.....	340
Figure 5-9: Heat map based on the Pearson distance measure and the average cluster algorithm	341
Figure 5-10: Score plot and model supervision of OPLS-DA model for nanoLC-MS/MS metabolomics data	342

Figure 5-11: Comparison of intensities of signature lipid components between control group (upper) and exposure group (lower)	343
SI Figure 5-1: Global compound-gene network analysis of the metabolites detected in rat feces collected from the middle-dose group	356
SI Figure 5-2: Principal component analysis (PCA) for the 60 imputatively identified metabolites that were significantly altered by AFB ₁	357
Figure 6-1: GC-MS total ion chromatogram (TIC) of gut content metabolites.....	399
Figure 6-2: HPLC-profiling chromatograms of gut content metabolites from control (upper) and GTPs-treated group (lower)	400
Figure 6-3: Score plot of principal component analysis (PCA) of the 57 metabolites significantly modified by GTPs	401
Figure 6-4: Overview of the alterations of metabolites profiled by GC-MS during the course of GTPs-treatment	402
Figure 6-5: Box plots to show the alterations of eight signature metabolites that were affected by the dose, time and interaction effects of GTPs-treatment.....	403
Figure 6-6: Metabolite set enrichment analysis (MSEA) of detected metabolites and network view of GTPs-modified metabolic pathways.....	404
Figure 6-7: Global compound-gene network analysis of metabolites detected in feces of rats administered with 1.5% GTPs in drinking water	405
Figure 6-8: Key metabolites determined using HPLC-profiling and GC-MS analyses ..	406
Figure 7-1: Leverage/SPE scatter plots to screen the important metabolites that demonstrated significant responses to (A) time-, (B) dose-, and (C) interaction effects of GTPs administration	440

Figure 7-2: Correlation analysis of elevated and decreased operational taxonomic units (OTUs) of gut-microbiota	441
Figure 7-3: Relative contribution to gut-microbiota dependent metabolism by specific OTUs.....	442
Figure 7-4: Metabolic mapping of metabolomic and metagenomic data on KEGG map of gut-microbiota biosynthesis pathways	443
Figure 7-5: Relative abundances of TCA/Urea cycle related Gene Orthologs (GOs) revealed by metagenomic analysis that showed significant alteration in previous analysis.....	444
Figure 7-6: Serum chemistry analysis of the rats treated with GTPs	445
Figure 7-7: Summary of impact of GTPs on the mitochondrial TCA/urea cycle and associated metabolic pathways of gut-microbiota	446
Figure 8-1: Comparing the major impacts of AFB ₁ and GTPs on gut-microbiota.....	464

CHAPTER 1. INTRODUCTION

1.1 Xenobiotics and gut-microbiota

Commensal microorganisms in human and other animals play very important roles in regulating host physiology and health (Hooper and Gordon, 2001). However, this aspect has not been explored until recent years because of improvement of high-throughput technologies, especially next-generation sequencing (NGS) technologies. The known xenobiotic compounds and substances that may disrupt gut-microbiota include alcohol (Mutlu et al. 2009), metals (Liu et al. 2014), metalloids (Lu et al. 2014), nanoparticles (Han et al. 2014), anthropogenic chemicals (Zhang et al. 2015), natural toxins (Wang et al. 2016), food composition (Francino 2015), as well as many antibiotics and drugs (Jakobsson et al. 2010; Zaura et al. 2015). The interactions between gut microbiota and xenobiotics may affect the overall health of host in an interactive way. There are at least three aspects that need to be investigated. (1) the kinetics and dynamics of xenobiotics among different persons were affected by the different community structure of gut-microbiota that result in differences in metabolizing, activating, or deactivating a xenobiotic; (2) the community structure of gut microbiota could be modified by the xenobiotic in a significant way; (3) the “community structure”–“functional gene orthologs”–“metabolites”–“health outcomes” interactive links, which depends on the chemical features of the xenobiotics. Filling these gaps could largely update our knowledge on the effects of drugs/toxins/toxicants, as well as explain a number of issues in toxicology that have not been fully understood so far.

1.2 Introduction to aflatoxin B₁

1.2.1 *Dietary exposure to aflatoxin B₁*

The incidence rate of primary liver cancer has been on a rise since last 1970s (Deuffic *et al.*, 1998). This trend is estimated to continue in the world wide before 2030, which would lead to a 35% increase compared with 2005 (Valery *et al.*, 2018). According to a meta-analysis of the data collected from 2007 to 2016, the average annual percent change (AAPC) of incidence of liver cancer was 3.8% (95% C.I. 2.2% to 5.3%) in male Americans and 2.1 % (95% C.I. 1.5%–2.8%) in female Americans (Wong *et al.*, 2017). It was reported by American Cancer Society that in 2017 about 40,710 new cases will be diagnosed with primary liver cancer and intrahepatic bile duct cancer, and about 28,920 people will die of it (Goyal and Hu, 2017). The abnormal rise is considered to be associated with many risk factors such as hepatitis virus, cirrhosis, alcohol use, diabetes, smoking, unhealthy diets, metabolic syndrome and the oral exposure to food-borne aflatoxin B₁ (AFB₁) (Groopman *et al.*, 1996; Nderitu *et al.*, 2016; Wang and Groopman, 1999). AFB₁ is known as a potent carcinogenic mycotoxin produced by fungi *Aspergillus flavus* and *A. parasiticus*. The contamination of AFB₁ naturally occurs during post-harvest stage, frequently seen in hot, humid, and unsanitary environment (Wild and Hall, 2000). The fungi can easily colonize on the surface of cereals, groundnuts, and animal feedings at a moderate condition of temperature from 24 °C to 35 °C, which makes the contamination of AFB₁ a significant concern for agricultural and food industries in the worldwide. Dietary exposure to AFB₁ is associated with a wide array of adverse health effects in human and animals (Adedara *et al.*, 2014; Storvik *et al.*, 2011). Epidemiological studies have

demonstrated that the contamination of food with AFB₁ is the primary risk factor for human liver cancer (Madden *et al.*, 2002; Wang *et al.*, 2001).

Among the naturally occurred aflatoxins (B₁, B₂, G₁ and G₂), AFB₁ carries the highest hepatotoxicity and genotoxicity. It has a LD₅₀ of 1 to 50 mg/kg for most animal species and a LD₅₀ < 1 mg/kg for pigs, dogs, cats, rainbow trouts and ducklings (Diaz and Murcia, 2011). It is categorized as a Group I human carcinogen by the International Agency for Research on Cancer (IARC) (Eaton and Gallagher, 1994; Tang *et al.*, 2008). The mycotoxin can be found in corn, dried fruits, cereals and peanuts (Zeng *et al.*, 2017), as well as the meat, egg and milk products from the animals that have consumed contaminated feeds (Herzallah, 2009). A variety of acute and chronic toxicities have been reportedly observed or associated with dietary exposure to AFB₁ in human and other animals, e.g. hepatotoxicity and nephrotoxicity (Kensler *et al.*, 2011), as well as the Reye syndrome, immune deficiency, growth retardation and metabolic syndrome (Hogan, 1978; Wild and Hall, 2000; Zeng *et al.*, 2017).

The concern with the easy growth of aflatoxin-producing fungus, together with the many diseases mentioned above, have jointly led to the formulation of regulatory actions by many international organizations and regional agencies. Currently, there are several regulatory standards formulated by these agencies in monitoring aflatoxins in food, with special attention paid to AFB₁ and AFM₁ in food and milk products. The World Health Organization (WHO) has founded Codex Alimentarius Commission (Codex) as the body responsible for formulating the maximum level aflatoxins in foods (Organization, 2010). Codex prescribes a maximum level of 15 parts per billion (ppb) for total aflatoxins in peanuts, hazelnuts, pistachios, and almonds; 10 ppb for the processed nuts and rice. The

maximum level of AFM₁ is 0.5 parts per million (ppm) in milk. In North America, Canada and the United States have generally set aflatoxin standards of 15 to 20 ppb in any finished food products. In detail, the U.S. Food and Drug Administration (FDA) has set several action levels. For the feedstuff prepared for mature non-lactating animals: the action level is 100 to 300 ppb for total aflatoxins, specifically as: feed for breeding beef cattle, 100 ppb; feed for finishing swine, 200 ppb; feed for finishing beef cattle, 300 ppb. For commodities destined for human consumption and interstate commerce, the action level is 20 ppb for total aflatoxins. For dairy milk, the standard was at 0.5 ppb for AFM₁ (Food and Administration, 2000). The guidelines and monitoring limits show large variation for the region out of North America and E.U. (Anukul *et al.*, 2013), but such disparities are still comparable with the overall regulatory standards released by Codex.

1.2.2 *Metabolism and toxicity of AFB₁ in human*

The theory of cytochrome P450 enzyme-based hepatic metabolism of AFB₁ was established by Wogan Lab in Massachusetts Institute of Technology (MIT) last century (Groopman *et al.*, 1996). For oral exposure of AFB₁, a rapid absorption happens mostly via small intestinal passive diffusion. After that, AFB₁ is transported to the liver where it undergoes the classic two-phase hepatic metabolism and then exerts carcinogenicity and toxicity. The metabolic activation was driven by the collaboration of a group of liver cytochrome P450 enzymes such as 1A2, 2A6, 3A4, 2A13, and 3A5 (Kensler *et al.*, 2011; Kumagai, 1989; Tang *et al.*, 2009; Wild and Turner, 2002; Ziglari and Allameh, 2013). The reactions can also occur in intestinal enterocytes, lung, and kidney, with different enzymes enrolled, and this process largely depends on the species under exposure. **Figure**

1 illustrates the general biotransformation of AFB₁ in human liver. In the phase I reaction, the involved reactions include hydroxylation, reduction, demethylation and epoxidation, and the generated products are AFQ₁ (product of AFB₁ reduction), Aflatoxicol H₁ (derived from Q₁), AFM₁ (product of AFB₁ reduction), AFP₁ (product of AFB₁ demethylation), aflatoxicol (product of AFB₁ hydroxylation), AFB_{2a} (product of AFB₁ hydroxylation), AFB₁-8,9-epoxide (product of AFB₁ epoxidation) and AFB₁-mercapturic acid (produced by γ -glutamyl dipeptidase and N-acetyl transferase). Most AFB₁ Phase I reactions are oxidations catalyzed by cytochrome P450 (CYP450) enzymes, except for the reduction of AFB₁ to aflatoxicol (AFL) which is catalyzed by a cytosolic reductase. Phase II reactions are limited to conjugation of the AFB₁-exo-8,9-epoxide (AFBO) with glutathione, and conjugation of aflatoxins P₁ and M₁-P₁ with glucuronic acid. The conjugation of AFBO with GSH is catalyzed by specific glutathione transferase (GST) enzymes. The AFBO may also be hydrolyzed by an epoxide hydrolase (EPHX) to form AFB₁-exo-8,9-dihydrodiol. In rats and human, the dihydrodiol is in equilibrium with the dialdehyde phenolate form, which can be reduced by AFB₁ aldehyde reductase (AFAR), an enzyme that catalyzes the NADPH-dependent reduction of the dialdehyde to dialcohol phenolate (Guengerich *et al.*, 2001). AFB_{2a} (from AFB₁) and Aflatoxin B₁-2,3-dihydrodiol (from AFB₁-2,3-epoxide) can bind with amino acid-Schiff bases structures and cause toxic effects on protein (Neal *et al.*, 1981).

Binding of AFBO to the N7 position of guanine leads to the formation of the unstable trans-8,9-dihydro-(N7-guanyl)-9-hydroxy-AFB₁ adduct. Hydrolytic ring opening reaction further transfers the AFB₁-N7-adduct into the more stable formamidopyrimidine form (Giri *et al.*, 2002). Adverse consequences of the DNA binding include point mutations

and recombination in both prokaryotic and eukaryotic organisms. In bacteria, AFB₁ binding induces frameshift and missense mutations, mostly in form of G to T transversion. Hot spots for AFB₁ induced mutations include six contiguous G residues in the HPRT gene and the third position in codon 249 of the human p53 tumor suppressor gene (Shen and Ong, 1996). The surface binding and transmembrane passage of AFB₁ in gram-positive bacteria are more easily than gram-negative bacteria because of the structure of the cell wall (Oliveira *et al.*, 2013).

Though over 90% metabolized AFB₁ can be excreted through urea and feces, part of the absorbed mycotoxin is irreversibly retained in the liver, bound to tissue macromolecules, and cause further adverse effects (Gradelet *et al.*, 1998). Regarding the retention of AFB₁ in human, the most relevant data were collected from primate models with radioactive standards. Wong and Hsieh reported that 100 hours after [¹⁴C]AFB₁ dosing (1/10 of LD₅₀ i.v.), 13.6, 6.5 and 1.8% of the administrated dose was retained in monkey, rat and mouse liver (Wong and Hsieh, 1980). Dalezio and Wogan found that, 4 days after *i.p.* injection of 0.4 mg/kg [¹⁴C]AFB₁ into monkeys, 5.6% of the dose was retained by the liver, mostly conjugated with liver proteins (Dalezios and Wogan, 1972). The retained percentage is 5.8% when the dose was administrated orally (Dalezios *et al.*, 1973). Dalezio *et al.* also found in monkeys that about 80% of orally administrated AFB₁ (0.015 mg/kg) is excreted in 1 week but a tiny portion was retained in liver and peripheral circulation up to 5 weeks. After the oral dosing, rhesus monkeys excreted about 20% as aflatoxin M₁ during day 1 to 4. Unchanged AFB₁ accounted only for a small proportion and AFB₁ beta-glucuronide accounted for 5%, with 3.3% as glucuronide and 1.2% as sulfate conjugate. There was 5% dose excreted as B₁ and M₁ in the feces. Holeski *et al.*

found that 2 hours after administration of 0.25 mg/kg AFB₁ (via *i.p.*), 15% of the dose remained in the liver (Holeski *et al.*, 1987). Of the total measured radioactivity in the liver, 12% were from polar metabolites, 3% from nonpolar metabolites and 70% were from covalently bound adducts. In another study conducted in a rat model, over 80% of AFB₁ was found rapidly absorbed in the small intestine via passive diffusion (Kumagai, 1989). These findings are consistent with the lipophilic structure of aflatoxins, showing that AFB₁ can be immediately absorbed through passive diffusion and around 5% of the dosed AFB₁ or its metabolites can be retained in the liver.

Table 1-1. Major metabolites of AFB₁ and biochemical features.

AFB ₁ metabolites	Biochemical significance
AFB _{2a}	Microsomal metabolite of AFB ₁ , doubtful enzymatic formation, occurs non-enzymatically through hydration of furan double bond in absence of cofactors
AFP ₁	Mixed-function oxidase-catalyzed o-demethylase reaction in microsomes, major urinary metabolite in monkeys
AFM ₁	Hydroxylated metabolite, NADPH-dependent mixed function oxidase, major metabolite in milk and urine of animals fed AFB ₁ -contaminated diets
AFQ ₁	NADPH-dependent hepatic microsomal-mediated hydroxylation of AFB ₁ , major metabolite produced by primate microsomal metabolism
Aflatoxicol	Reversible reduction of AFB ₁ by reductase in the cytosol fraction, NADPH required as a cofactor, major metabolite of avian species
AFL-M ₁	Cytosol-catalyzed reduction of AFM ₁ or microsomal mixed-function oxidase-catalyzed hydroxylation of AFL
AFL-H ₁	Cytosol-catalyzed reduction of AFQ ₁ or by cytochrome P-450-catalyzed hydroxylation of AFL, major metabolite of AFB ₁ by humans or rhesus monkey
AFB ₁ -epoxide	Not isolatable from biological systems or synthesizable, formation deduced from production of AFB ₁ -dihydrodiol as acid hydrolysis product of metabolically or chemically generated AFB ₁ -nucleic acid adducts
AFB ₁ dihydrodiol	Formed by enzymatic or nonenzymatic hydrolysis of AFB ₁ -epoxide

*Table is excerpted from (Deshpande, 2002)

Several points in the metabolic pathway of AFB₁ are worthy of further discussion:

(1) among human aflatoxin-associated CYPs, CYP1A2 and CYP3A4 are the major AFB₁-

metabolizing enzymes found in human liver. AFB₁ is activated by CYP1A2 and 3A4 to AFB₁-8,9-exo-epoxide and AFB₁-8,9-endo-epoxide, but it is the exo-epoxide which binds to DNA to form the predominant 8,9-dihydro-8-(N7-guanyl)-9-hydroxy-AFB₁ (AFB₁-N7-Gua) adduct (Ramsdell *et al.*, 1991); (2) the major carcinogenic and mutagenic metabolites of AFB₁ are AFB₁-8,9-exo-epoxide, AFB₁-dihydroxide intermediate and AFM₁-8,9-epoxide, but the latter is relatively less active in the Ames mutagenesis test (Catterall *et al.*, 2003); (3) AFB_{2a} causes acute toxicity, liver necrosis and cellular metabolizing enzyme inhibition; (4) in the phase II conjugation, aflatoxin B₁-8,9-epoxide can bind with glutathione (GSH) by glutathione S transferase (GST), and the generated AFB₁-GSH is the major detoxicated metabolites excreted in bile. The detected aflatoxin metabolites are shown in **Table 1-2**. AFP₁, AFM₁ and AFM₁-P₁ (derived from P₁ or M₁) can be conjugated with glucuronic acid by UGT (Dohnal *et al.*, 2014). A biomarker is defined as the cellular, biochemical and molecular alteration that can be accurately measured in biological media, such as human tissues, cells or fluids. The measurement of these molecules can indicate the exposure of xenobiotics, induced effects or the susceptibility of subjects. Although many metabolites of AFB₁ have been detected from human samples (**Table 1-2**), not all of them are reliable for the use of biomarker. The biomarkers used for the control of AFB₁ include urine AFB₁-N7-guanine adduct, aflatoxin M₁, AFB₁-mercapturic acid and serum AFB₁-albumin adduct (Qian *et al.*, 2012; Tang *et al.*, 2009; Wang and Groopman, 1999; Wang *et al.*, 2008; Yu *et al.*, 2006).

Table 1-2. Reported aflatoxins and metabolites in human samples.

Human biofluid & tissue	Aflatoxins & Metabolites
Amnoiotic fluid	B ₁
Bile	B ₁

Blood	Aflatoxicol, B ₁ , B ₂ , G ₁ , G ₂ , M ₁ , M ₂
Brain	Aflatoxicol, B ₁ , B ₂ , G ₁ , G ₂ , M ₁ , M ₂
Breast milk	Aflatoxicol, B ₁ , B ₂ , G ₁ , G ₂ , M ₁ , M ₂
Feces	Aflatoxicol, B ₁ , B ₂ , G ₁ , G ₂ , M ₁ , M ₂ , Q ₁
Serum	Aflatoxicol, B ₁ , B ₂ , B _{2a} , G ₁ , G ₂ , G _{2a} , M ₁ , M ₂ , P, Q ₁
Urine	Aflatoxicol, B ₁ , B ₂ , B _{2a} , G ₁ , G ₂ , G _{2a} , M ₁ , M ₂ , P ₁ , Q ₁

*Table is excerpted and organized from (Weidenbörner, 2015).

1.2.3 Impairment of gut-microbiota dependent metabolites caused by AFB₁

In addition to above discussed liver cancer, dietary exposure to food-borne AFB₁ is also associated with a wide array of health problems in human and animals. The reported diseases include diarrhea, vomiting, tumors, deficient immunity, stunted growth, Reye's syndrome, metabolic syndrome, and liver diseases such as bile duct cirrhosis and non-alcoholic steatohepatitis (Kensler *et al.*, 2011; Weir *et al.*, 2013; Zeng *et al.*, 2017). The impact of such exposure on nutritional status and metabolism needs to be thoroughly investigated in order to better understand the pathological mechanisms of the associated disease outcomes. Gut-microbial metabolome, a collection of thousands of micronutrients and functional metabolites, has demonstrated a significant influence on host health nutritional status, as well as the susceptibility to diseases (Goffredo *et al.*, 2016; Randrianarisoa *et al.*, 2016). Assessment of the impact of AFB₁ on gut-microbial metabolome could, therefore, provide a mechanistic insight into the pathogenesis of AFB₁-induced health outcomes.

A wealth of recently advanced techniques, such as “next generation sequencing”, “single cell-based omics” and “high through-put metabolomics”, can be leveraged to analyze the genome and metabolome of the intestinal microbial flora. By now, researchers have already found over 1000 bacterial species and 100-fold more genes than host genome in the microbial community, in which more than 99% residents belong to *Firmicutes*,

Bacteroidetes, *Proteobacteria* and *Actinobacteria* classes (Qin *et al.*, 2010b). The scientific progress has brought new vision and strategy to the field of chemoprevention of liver diseases. The liver receives 70% of its blood supply from the intestine through the portal vein. Accordingly, it is the first and mostly exposed organ to gut-derived factors such as bacterial components, microbial derived nutrients, endotoxins, and peptidoglycans. Over 80% of hepatocellular carcinoma (HCC) are associated with the inflammation that accompanies with cirrhosis, fibrosis and compensatory hepatocyte proliferation (Baffy, 2013). It has been found that a number of hepatic cell types, e.g. Kupffer cells, sinusoidal cells, biliary epithelial cells, and hepatocytes carry pathogen-recognition-receptors that respond to the many microbial-derived products from the gut (Szabo *et al.*, 2010).

Actually, there have been many case reports which support that gut-microbiota and microbial metabolites are involved in the pathological process of liver diseases and other adverse health outcomes. Dumas *et al.* have previously found that the conversion of choline into methylamines by microbiota reduces the bioavailability of choline and lead to non-alcoholic fatty liver disease (NAFLD) in 129S6 rats with a high-fat diet (Dumas *et al.*, 2006a). Gaudet *et al.* designed an *in vitro* model using HEK 293T cells and several bacterial strains, which showed that *Neisseria spp.* may prevent liver carcinogenesis via microbial heptose-1,7-bisphosphate (HBP)-TRAF- forkhead associated domain (TIFA)-apoptosis pathway (Gaudet *et al.*, 2015). The disruption of gut-microbiota may lead to pro-inflammation in hepatic cells through the TLR4-TNF α -IL6 signaling that reduces oxidative and apoptotic stress (Darnaud *et al.*, 2013). The event was found being initiated by the lipopolysaccharide (LPS) or damage-associated molecular patterns (DAMP) secreted by gut-microbiota during dysbiosis and occurs mainly in Kupffer cells (Yu *et al.*, 2010). On

the other side, Zhang *et al* have shown in rat model of hepatocarcinoma which was created using diethylnitrosamine (DEN) via injected intraperitoneally (i.p.) administration, that the rats with liver cirrhosis and liver cancer frequently develop an intestinal dysbiosis, in which the *E. coli* growth rate was increased yet the benign bacteria which belong to *Lactobacillus*, *Bifidobacterium* and *Enterococcus* were significantly decreased (Zhang *et al.*, 2012). These evidences imply that the maintenance of gut-microbial homeostasis is tightly associated with liver health via gut-microbial metabolites and cellular components. In addition to liver diseases, the exposure to harmful xenobiotics is also known to be associated with metabolic syndrome, thrombophilia, atherosclerosis, hyperuricaemia and hyperglycaemia (Sears and Genus, 2012; Zhou, 2016). The modification of gut-microbiota may provide a new approach to AFB₁ associated liver diseases and other adverse health outcomes.

A wide range of xenobiotics, either naturally occurred or artificially synthesized, are known to be capable of disrupting the bio-chemical pathways or impairing the homeostasis of gut-microbiota (Maurice *et al.*, 2013). The xenobiotics include alcohol (Bala *et al.*, 2017; Mutlu *et al.*, 2009; Nolan, 1989; Yan *et al.*, 2011), heavy metals (Breton *et al.*, 2013; Fazeli *et al.*, 2011; Liu *et al.*, 2014), nanoparticles (Merrifield *et al.*, 2013; Sawosz *et al.*, 2007), anthropogenic chemicals (Xu *et al.*, 2014), antibiotics (Cho *et al.*, 2012; Dethlefsen and Relman, 2011; Francino, 2015), and natural toxins such as mycotoxins and microcystin-LR (Bennett and Klich, 2003; Lin *et al.*, 2015; Saint-Cyr *et al.*, 2013; Wache *et al.*, 2009). The impacts of xenobiotics on gut-microbiota and microbial derived nutrients are critical to host health. The exposure of gut commensal microbiota to certain natural products largely determines the delivering efficiency of nutrition from food

to host (Gibson and Roberfroid, 1995; Tuohy *et al.*, 2014). Many food ingredients and compositions are specially preferred by certain gut-microbial strains. L-carnitine is able to enrich the strains that belong to *Peptostreptococcaceae* and *Clostridiaceae* families, which in turn produce a high level of dimethylamine, trimethylamine (TMA) and trimethylamine-N-oxide (TMAO). These amines were previously found connected with primary sclerosing cholangitis (PSC) and inflammatory bowel disease in human (Kummen *et al.*, 2017). Genistein carries protective function from liver acute damage, liver inflammation (Tomas *et al.*, 2012), fibrosis (Burcelin *et al.*, 2011), hyperglycemia and glucose tolerance, and such function is associated with the modification of gut-microbiota (Qin *et al.*, 2010a). The triangle interaction between xenobiotic-microbiota-host, as discussed above, could thus play an un-ignorable etiological role in the incidence of xenobiotic-associated health problems or beneficial effects. Our preliminary 16s rRNA based analysis showed that oral exposure to AFB₁ resulted shift of gut-microbiota at phylogenetic level, featured by depletion of *Lactobacillus* and enrichment of *Firmicutes clostridiales* strains such as pro-inflammatory *Ruminococcus* (Jandhyala *et al.*, 2015). To further understand the complexities between gut-microbiota and AFB₁-induced health problems, it is necessary to elucidate the specific chemical composition of the flora. Fecal metabolomics analysis is an effective, non-sacrifice and non-invasive approach to achieve this goal.

1.3 Green Tea Polyphenols as chemoprevention and probiotic agent

1.3.1 *Introduction to green tea polyphenols*

The term “Probiotic” was first coined from the Greek language by Lilly *et al.*, meaning “for life” (Lilly and Stillwell, 1965). The concept was brought out by Gibson and

Roberfroid in 1995 and further refined by Roberfroid in 2007, presented as “a selectively fermented ingredient that allows specific changes, both in the composition and/or activity in the gastrointestinal microflora that confers benefits upon host well-being and health” (Roberfroid, 2007). The term also meantime defined by World Health Organization (WHO) and Food and Agriculture Organization of the United Nations (FAO) as ‘live microorganisms which when administered in adequate amounts confer a health benefit on the host’ (Morelli and Capurso, 2012). Probiotics are considered to have, yet not limited to, the following benefits: (1) reduction of *Helicobacter pylori* infection; (2) reduction of allergic symptoms; (3) relief from constipation; 4) relief from irritable bowel syndrome; (5) beneficial effects on mineral metabolism, particularly bone density and stability; (6) cancer prevention; and (7) reduction of cholesterol and triacylglycerol plasma concentrations (Schrezenmeir and de Vrese, 2001). The application of *Lactobacillus* has shown effects such as reduction of harmful strains in humanized mice (Martin *et al.*, 2008) and attenuation of chemical-induced colitis in mice (Kumar *et al.*, 2008). Li *et al.* administrated *Lactobacillus rhamnosus* GG to C57BL6/N mice one week before tumor induction and they found that probiotics shifted the gut-microbial community toward certain anti-inflammatory beneficial bacteria such as *Prevotella* and *Oscillibacter*, leading to reduced Th17 polarization and promoted anti-inflammatory T_{reg}/T_{r1} cells in the gut (Li *et al.*, 2016). Henrik *et al.* have reported the administration of *Lactobacillus acidophilus* NCFM in germ free Swiss Webster mice can modulate bile acid metabolism by deconjugation, as well as carbohydrate metabolism and Vitamin E acetate metabolism (Roager *et al.*, 2014). For these studies an effective dose around 1×10^8 to 1×10^{10} CFU/day is generally used.

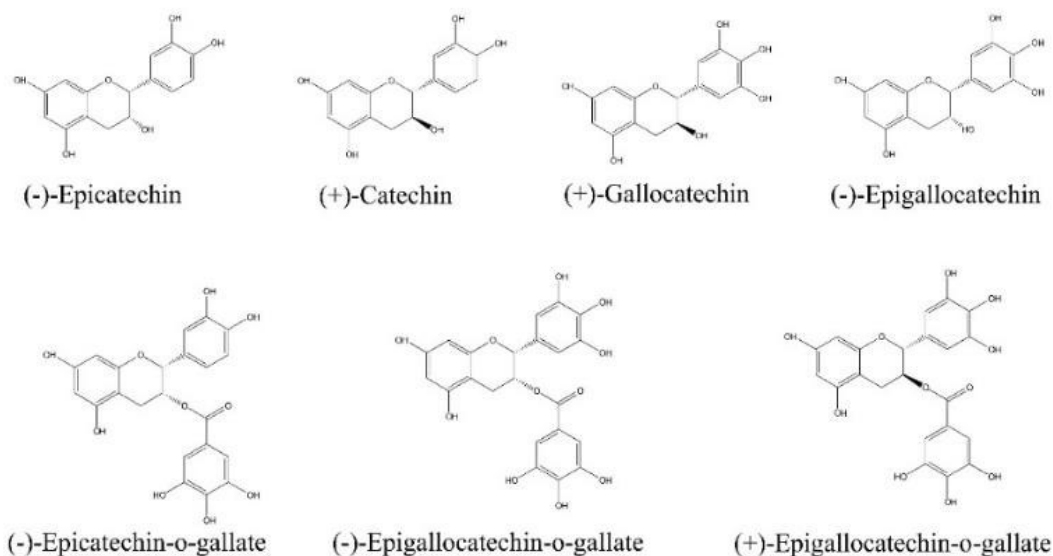


Figure 1-2. Green tea polyphenols.

Cancer chemoprevention is defined as the chronic administration of a synthetic, natural or biological agent to reduce or prevent the occurrence of malignancy (De Flora and Ferguson, 2005). Remarkable effort has been made to minimize the incidence of AFB₁-related HCC. In addition to the regulations discussed already, a significant effort of chemoprevention study has been made since last decade, such as oltipraz (Wang *et al.*, 1999), calcium montmorillonite clay (Mitchell *et al.*, 2014) and green tea polyphenols (Luo *et al.*, 2006a; Wang *et al.*, 2008). Polyphenol is defined as a compound containing more than one phenolic hydroxyl group. The primary polyphenols in green tea are flavanols, commonly known as catechins, including (–)-epicatechin, (–)-epicatechin-3-gallate, (–)-epigallocatechin, and (–)-epigallocatechin-3-gallate (EGCG). The major favorable functions of GTPs include: (1) protection against multiple carcinogenesis (Luo *et al.*, 2006a; Mukhtar and Ahmad, 2000; Qian *et al.*, 2012; Tang *et al.*, 2008; Wang *et al.*, 2008), (2)

amelioration of rheumatoid arthritis (Haqqi *et al.*, 1999; Riegsecker *et al.*, 2013; Singh *et al.*, 2010), (3) reduction of high blood pressure (Negishi *et al.*, 2004; Potenza *et al.*, 2007a; Potenza *et al.*, 2007b), (4) improvement of cardiovascular health (Babu and Liu, 2008; Wolfram, 2007), (5) enhancement of immune system (Katiyar *et al.*, 1999; Wong *et al.*, 2011) and the (6) prevention on tooth osteoporosis (Shen *et al.*, 2008).

However, there are many controversial observations on the effects of GTPs in human, such as its weight losing effect. During the last decade there are approximately over 30 studies conducted in human population, animal model and in vitro assays that were dedicated to collect evidences for this question (Hursel and Westerterp-Plantenga, 2013; Janssens *et al.*, 2015; Mielgo-Ayuso *et al.*, 2014; Phung *et al.*, 2010). Meanwhile, numerous potential mechanisms have been described, such as the involvement of chemokines, COX2, iNOS, NF-kB, AP-1 and such on (Frei and Higdon, 2003). These results are not well convincing because of the reasons such as the non-compatible composition of GTPs mixture between different studies, the involvement of caffeine when people drink tea, as well as the genetic polymorphism of the studied ethical populations. These functions cannot be completely explained by ligand-receptor theory. Emerging evidences have shown that polyphenols can be utilized by beneficial gut-microbial strains and modify the composition of the strains (Lee *et al.*, 2006; Rastmanesh, 2011; Tuohy *et al.*, 2012; Tuohy *et al.*, 2014). Tea polyphenol-contained galloyl moieties were found to act as inhibitors to glucosyltransferase from *Streptococcus sobrinus*, as well as collagenase from some eukaryotic and prokaryotic cells. The inhibitory effects on pathogens shown by

tea polyphenols are possibly contributed by the galloyl moiety (Sakanaka *et al.*, 1996). A metabolomics analysis of gut-microbial metabolome may help us better understand the beneficial functions of GTPs and clarify the many confusions.

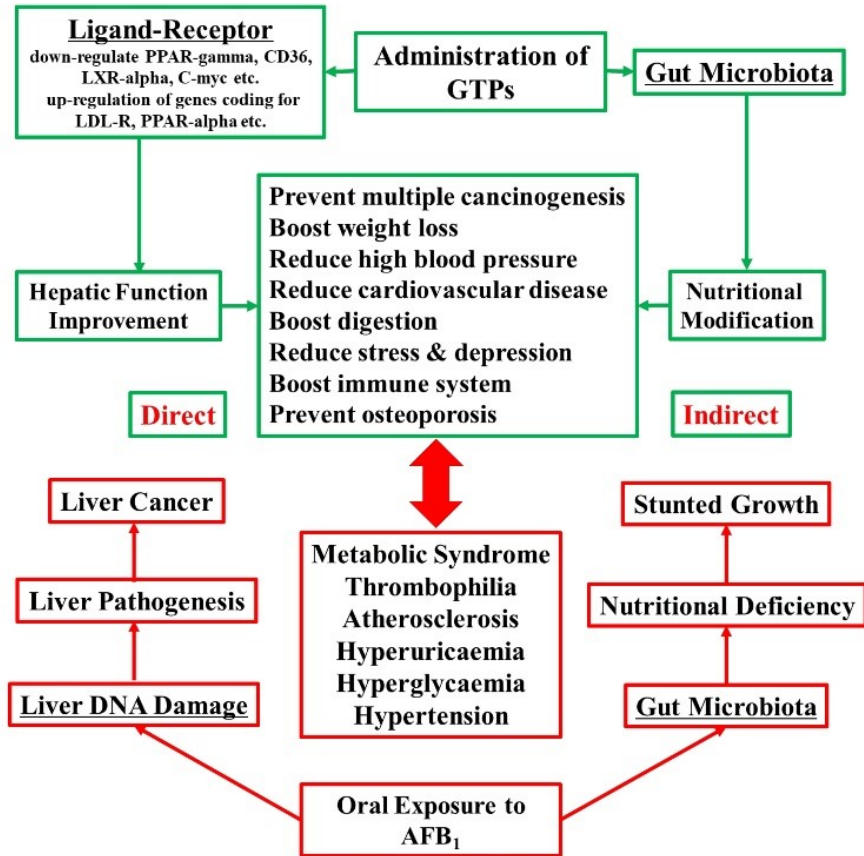


Figure 1-3. Comparing adverse health outcomes induced by oral exposure to AFB₁ with beneficial effects brought by administration of GTPs.

1.3.2 Previous studies on the beneficial functions of GTPs in human

The rationale of current dissertation is built based on a bunch of findings discovered in our lab. In last 90s, our lab did such phase IIa chemoprevention trial in Guangxi Zhuang Autonomous Region, People’s Republic of China, to examine the ameliorating effects of green tea polyphenols on carcinogen biomarkers and the possible adverse effect of GTPs

in the population with high risk of hepatocellular carcinoma (HCC) (Luo *et al.*, 2006a; Wang *et al.*, 2008). The study site is a rural farming community where major supply of food and cooking oil are produced from local corn and peanuts with severe contamination of aflatoxins. Serum and urine samples were collected from Sanhe and Zhuqing, two villages in Qujiu Township. The normalized HCC incidence and mortality is around 100 per 10 million for the last two decades.

The study measured hepatitis B virus (HBV) and aflatoxin biomarkers in 1200 blood samples and recruited 124 residents who were both HBsAg and AF-albumin adducts positive. These subjects were aged 20-55 with normal liver function test, serum alpha-fetoprotein negative, no personal history of cancer, and no use of prescribed medications. The selected 2 doses of GTPs were 500 mg and 1000 mg, equivalent to two and four cups of tea drink, respectively. Initial studies did not find significant differences on adverse effects and parameters representing liver and kidney function among 3 groups, indicating the relative safety of GTPs in human subjects. In the next step, follow-up studies were conducted to find and validate biomarker of exposure to GTPs from urine and plasma samples. The major findings are summarized in **Figure 1-4**.

(1) A total of 340 urine samples were collected at baseline, 1- and 3-month of the clinical trial. Trace amounts of GTPs components were detected for all 3 groups at baseline with no statistical significance ($p = 0.92$). Analysis of urine samples collected at 1- and 3-month revealed that levels of urinary EGC and EC were dose-dependently elevated in GTPs-treated groups. Mixed effects model showed significant differences between times and groups of treatment ($p < 0.05$) (Wang *et al.*, 2008).

(2) A total of 343 plasma samples collected at the same time points were analyzed. Similar pattern of dose-response was found in both urine and plasma samples, that the levels of EGCG and ECG in GTPs-treated groups were dose-dependently elevated. Significant differences between times and groups of treatment ($p < 0.05$) were also found. The results validated urinary excretion of EGC and EC and plasma levels of EGCG and ECG as biomarkers for green tea consumption (Luo *et al.*, 2006a). Luo *et al* also analyzed plasma sample via metabolomics approach and found that 56 of 106 detected metabolites were significantly modulated with administration of GTPs (Luo *et al.*, 2006b).

(3) Urinary 8-hydroxy deoxyguanosine (8-OHdG) was measured to reflect the modulative effect of GTPs on reactive oxygen species (ROS)-induced oxidative DNA damage. It was found that at the end of 3-month intervention, 8-OHdG levels decreased significantly in both GTPs-treated groups, suggesting a pronounced effect of GTPs in diminishing general oxidative DNA damage (Luo *et al.*, 2006a).

(4) A panel of biomarkers was introduced to estimate the exposure level of AFB₁ in the subjects and examine the mitigating effect of GTPs administration on the hepatic metabolism of AFB₁. It was found that: 1) By 1-month administration, the AF-albumin adduct levels in serum samples collected of the intervention was significantly decreased in the high-dose group ($p < 0.05$) than that in control; 2) by 3-month, the levels of AF-albumin-adducts in serum samples showed significant decrease in both the low- and the high-dose groups ($p < 0.05$); levels of AFM₁ in urine samples was significantly decreased in both low-dose and high-dose intervention groups. Treatment of GTPs elevated levels of AFB₁-NAC in GTPs-treated groups, which indicated an improved metabolism and

excretion of AFB₁. Thus, GTPs effectively inhibited phase I metabolic enzyme activities and boosted phase II metabolic enzyme activities.

(5) Based on the above findings, a long-term clinical trial with green tea polyphenols in Southern Guangxi, China. This study screened 10000 adult people and recruited 1826 HBsAg positive adults with normal liver function test, serum alpha-fetoprotein negative, no personal history of cancer, and no use of prescribed medications, in Guangxi, China. Two capsules (500 mg GTPs, or placebo), were instructed to be taken twice daily after meal. The HCC incidence rate for years 2 and 3 was significantly reduced in GTPs-treated group (443.46/100000 person each year) as compared to that of placebo group (1092.39/100000 person year) (p one-sided = 0.039) (Yu *et al.*, 2006).

1.4 Validation of animal models

In toxicological research, the use of animals to model human exposure strictly relies on the validation that basic mode of action (MOA) and mechanistic processes of experimental animals are similar with human. To validate an animal model, pharmacokinetic (PK)/pharmacodynamic (PD) or physiologically based pharmacokinetic (PBPK) models are widely used to gain information regarding “absorption, distribution, metabolism, and excretion (ADME)”, as well as the predictions of internal or target dose from environmental and pharmacologic chemical exposures. The oral LD₅₀ range of AFB₁ is estimated to be 1 to 50 mg/kg B. W. for most animal species. For rats, it shows gender differences with an oral LD₅₀ of 17.9 mg/kg B. W. in female rats and 7.2 mg/kg body weight in male rats (Agag, 2004). For the latter, AFB₁ is an incredibly potent carcinogen with a TD₅₀ of 0.0032 mg/kg/day (Butler, 1964).

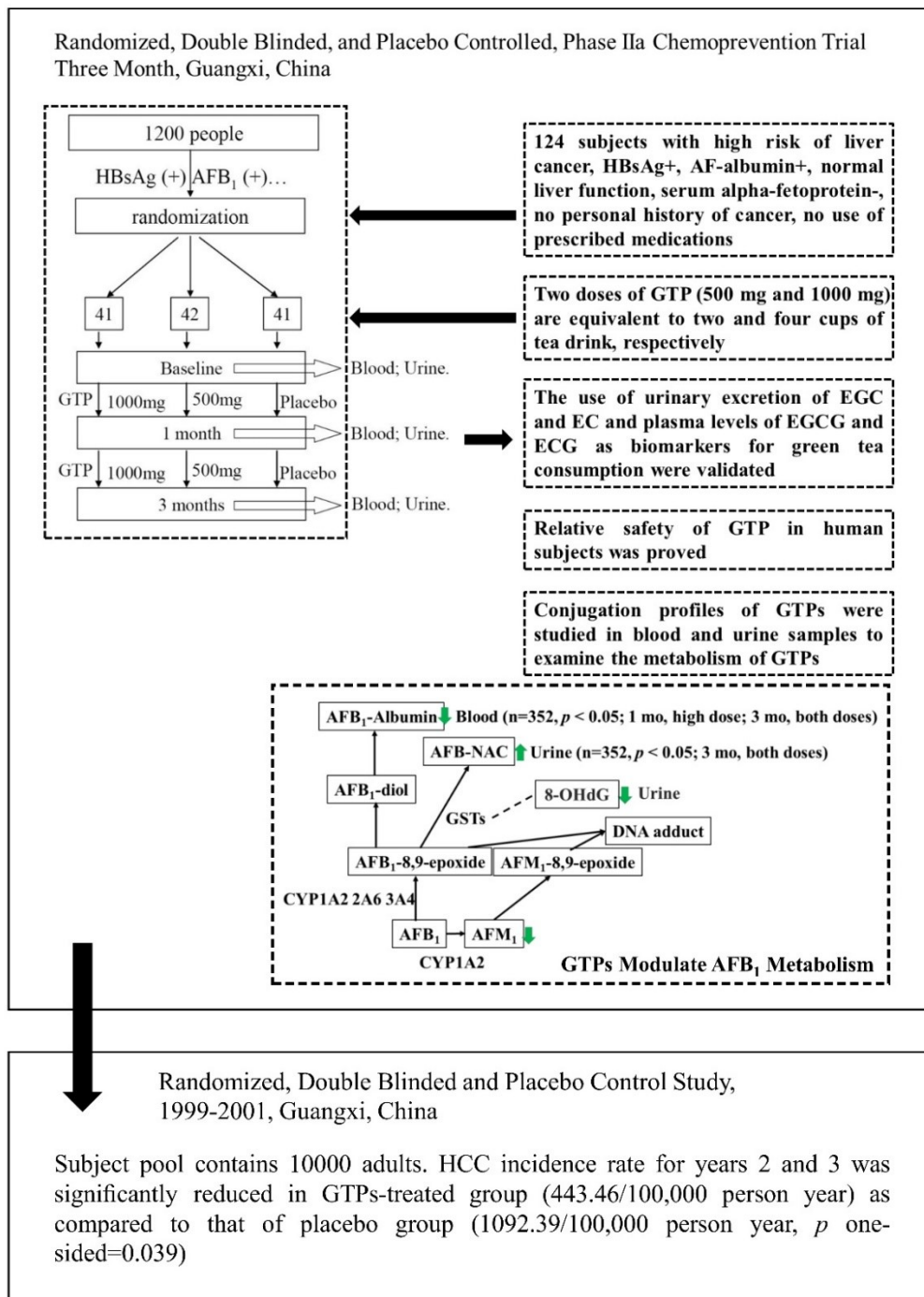


Figure 1-4. Previous studies of HCC prevention with GTPs administration.

Fischer 344 is the most widely used inbred rat strain for general purposes, being particularly favored for cancer research and toxicology. There is now substantial background information on its strain characteristics, including life-span, spontaneous diseases and response to chemicals. In the current study, Fischer 344 male rats were used as the animal model and validated by previous lab member Dr. Guoqing Qian. The detailed protocol was validated and reported in our previous publications, together with body indexes, histopathological assessment and AFB₁-lys pharmacokinetic data (Qian *et al.*, 2014; Qian *et al.*, 2013a; Qian *et al.*, 2013b). The dosage applied in AFB₁ study was transferred from several reports for Kenya, Ghana, and Guangxi, China, where the mean AFB₁ levels were found to be 100 to 1000 µg/kg in corn (Azziz-Baumgartner *et al.*, 2005; Groopman *et al.*, 1992; Tang *et al.*, 2009). The reference amount of corn consumption was 300 to 400 g/day for local residents (Li *et al.*, 2001), thus the minimal exposure level is estimated to be 0.45 µg/kg B. W. per day for adult with body weight of 65 kg. By applying a conversion factor of 6.2, the theoretical dose for rat of 150 g is 2.79 µg/kg B. W. per day (Nair and Jacob, 2016). Considering the working hours and actual B. W. (110 to 120 g) of rat, the minimal dose for gavage in this study is 5 µg/kg B. W. per day during working days. The original no-observed-effect-level (NOEL) for AFB₁ oral exposure in rat is 100 µg/kg for single dosing, and the maximum repeated dose in this study is 75 µg/kg B. W., a dose inducing significant liver cirrhosis in rats of the current study. Specifically, male Fischer 344 rats (100 to 120 g) were purchased from Harlan Laboratory (Indianapolis, IN). The animal housing environment is under controlled light/dark cycle (12 hr/12 hr) with a temperature of 22 ± 2 °C and relative humidity of 50 to 70%. Purified AIN 76A diet and tap water were maintained every day. We did not examine dietary aflatoxins in this study.

Upon arrival, animals were allowed for one week of environmental acclimation. One hundred male F344 rats were divided into 4 groups, with gavage of 0, 5, 25, 50 and 75 μg AFB₁/kg B. W. per day respectively. DMSO was used as vehicle solvent. Fecal samples collected from 0, 5, 25 and 75 μg AFB₁/kg B. W. were used for metabolomics analysis.

With the AFB₁ doses of 5, 10, 25, 50 and 75 μg /kg B. W. per day, the major pathological changes are listed on **Figure 1-5**, including the effects of exposure on the histological, immune-histological, clinical biochemical parameters, cell-specific cytokine secretion in splenic lymphocytes through both single-dose and repeated-dose treatment protocols (Qian *et al.*, 2014; Qian *et al.*, 2016; Qian *et al.*, 2013a; Qian *et al.*, 2013b; Qian *et al.*, 2012). In repeated-dose protocol, a linear increase of serum AFB-lys was observed for animals that received 5 to 25 μg AFB₁/kg B. W. daily, leading to a 1.0 to 1.5 times increase after five weeks compared to that after one week, suggesting its potential use as a long-term biomarker. For the application of highest dose, serum AFB-lys reached a maximum level after 2 weeks for animals that received a high daily dose of 75 μg /kg B. W. The dose-biomarker fitted curve matches Gaussian curve and may reflect a variation in the metabolic balance between AFB-epoxide formation and detoxification or enzymatic induction of glutathione S transferase (GST). This result is consistent with the alternative signs of toxicity found at this dose (see **Figure 1-5** for details). After 3 weeks exposure to 75 μg /kg B. W., bile duct proliferation, liver GST-P+ foci co-occurred, followed by proliferation foci formation after 4-week and dramatic ALT, AST and CK elevations after 5-week exposure. Thus, the maximum dose chosen in this study is 75 μg /kg B. W.

Sprague Dawley (SD) female rats were used as animal model for GTPs study. SD rat is an outbred multipurpose breed of albino rat used extensively in medical and

nutritional research. The rat model was evaluated by our collaborator Dr. Chwan-Li (Leslie) Shen, Texas Tech University Health Sciences Center. Shen Lab has by now assessed the chronic safety in middle-aged ovariectomized rats supplemented with different doses of GTPs in drinking water. The experiment used 6-month old sham (n = 39) and ovariectomized (OVX, n = 143) female rats. For comparison, all sham (n = 39) and equal number of the OVX animals received no GTPs treatment and were used as control. The samples were collected for outcome measures at baseline, 3 month and 6- month (n = 13 per group for each). The left OVX animals were randomized into 4 treatment groups and receive 0.15%, 0.5%, 1%, and 1.5% (n = 26 for each) of GTPs (wt/vol), in drinking water for 3 and 6 months.

During the veterinary examination, they found no mortality or abnormal treatment-related findings in clinical observations or ophthalmologic examinations (Shen *et al.*, 2017). Also, no treatment-related macroscopic or microscopic findings were noted for animals administered with the highest dose. Throughout the study, there was no difference in the body weight among all OVX groups. By the end of 6 month, GTPs intake did not affect most hematological indexes and parameters of clinical chemistry. However, the phosphorus and blood urea nitrogen were increased, and the total cholesterol, lactate dehydrogenase, and urine pH were decreased.

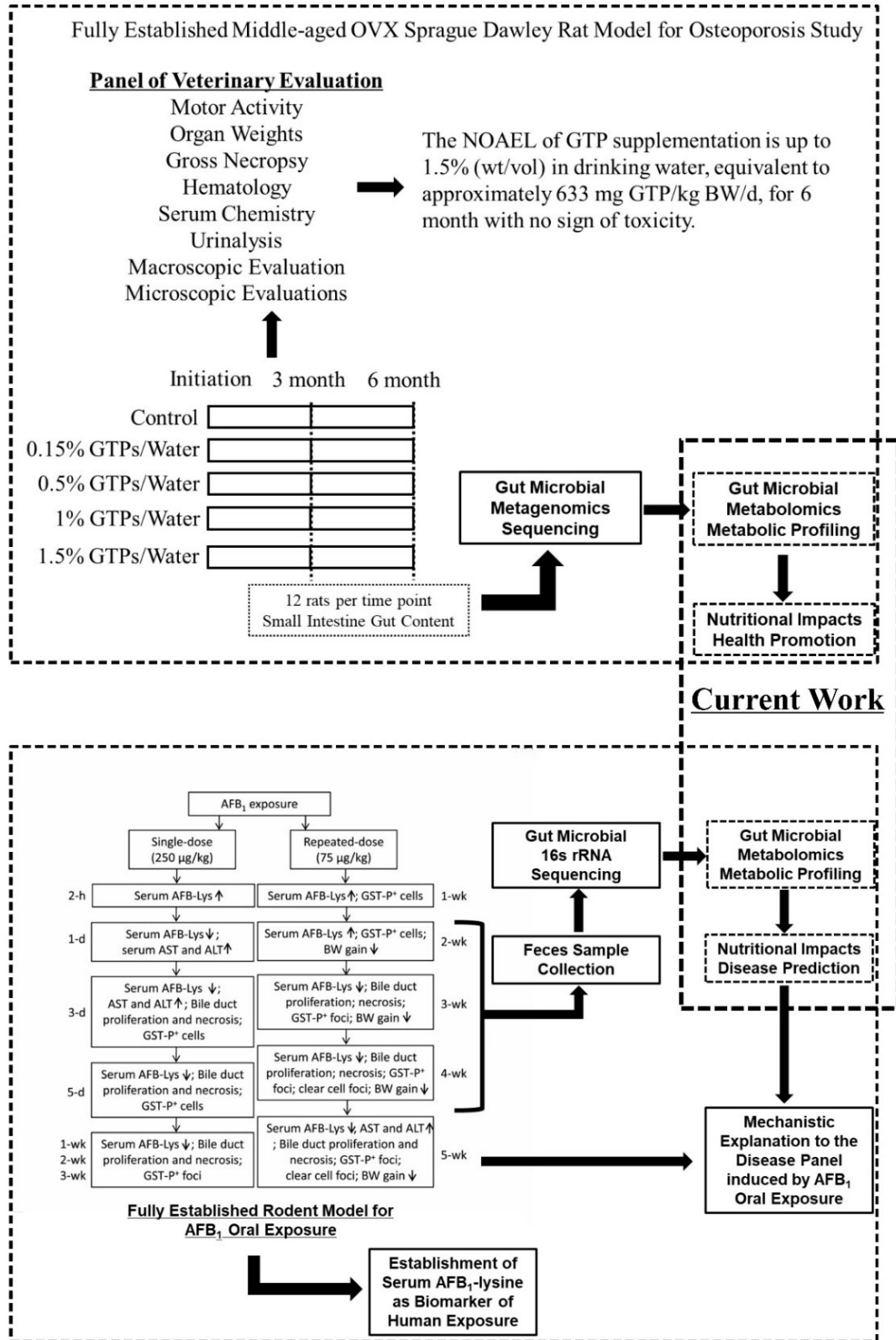
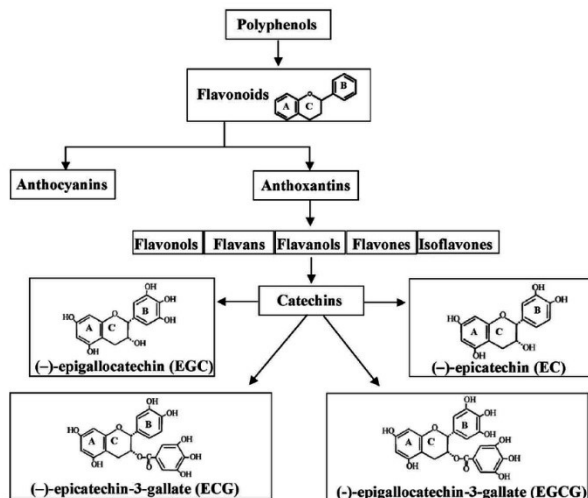


Figure 1-5. Major findings of previous studies in animal models.



Composition of GTP Powder

EGCG **464** mg
 ECG **112** mg
 EC **100** mg
 EGC **78** mg
 (-)-gallocatechin gallate (GCG) **96** mg
 Catechin **44** mg

 per **1000** mg powder in this study

*HPLC-ECD and HPLC-UV analysis

Figure 1-6. Composition of green tea polyphenol powder used in current study.

1.5 Hypothesis of current dissertation

As discussed above, oral exposure to AFB₁ are associated with liver cancer, metabolic syndrome and a number of hepato-intestinal diseases. The recently revealed intricate “three-way” connection among xenobiotics, gut-microbiota, and host health may involve in these situations by disrupting homeostasis of gut-microbiota and their functional metabolites. However, the administration of dietary prebiotics such as GTPs could improve host health by enriching beneficial bacteria such as *Lactobacillales* and the metabolites e.g. SCFAs. Our earlier 16s rDNA data has already discovered the dose-dependent change of gut-microbial strains and functional enzymes upon exposure to AFB₁ (Wang *et al.*, 2015). Such change may have an important role in the etiology of AFB₁-induced diseases, ailments and health problems. The hypothesis here is that the impacts of AFB₁ and GTPs on host health might be opposite and GTPs could potentially reverse the negative effects on AFB₁ on gut-microbiota dependent metabolites. More evidences are needed to justify this hypothesis.

1.6 Methodology

Metabolomics has been extensively employed to capture interested bio-chemical changes in cells, tissues and bio-fluids (Vernocchi *et al.*, 2016). The most frequently used instruments are the ‘hyphenated’ analytical platforms that are constructed with chromatography and mass-spectrometry (MS). With properly developed method this combination is able to profile hundreds to thousands of metabolites showing in sample simultaneously, according to their m/z , retention time and ionized fragments. So far, both liquid chromatography-mass spectrometry (LC-MS) with electrospray ionization (ESI) and gas chromatography-mass spectrometry (GC-MS) with Electron ionization (EI) serve as basic approach for metabolomics studies (Wang *et al.*, 2010). They have been used to perform a number of complex tasks, e.g. elucidation of mechanism, biomarker search and pharmaceutical intervention (Patti *et al.*, 2012; Ramautar *et al.*, 2013). However, both LC-MS and GC-MS are not perfect, in that the detective scope of GC-MS is generally limited to volatile molecules; whereas the data acquired by LC-MS are affected by factors, such as the ionization mode, design of analyzer, mobile phases, the voltages of capillary tube and cone (Beckonert *et al.*, 2007). A second round of complication is introduced during the process of raw data, which heavily depends on the selected processing suites (e.g. XCMS, OpenMS, MaxQuant and SMART), as well as the numerous algorithms to be tuned for feature detection, chromatogram building, deconvolution, isotope grouping and alignment (Lindahl *et al.*, 2017).

Table 1-3. Important terms in metabolomics

Term	Definition
------	------------

Metabolite	Small molecules that participate in general metabolic reactions and that are required for the maintenance, growth and normal function of a cell.
Metabolome	A complete set of metabolites in an organism, tissue, site, organ or cell of interest.
Metabolomics	Identification and quantification of all metabolites in a metabolome.
Metabolic Profiling	Quantitative analysis of set of metabolites in a selected biochemical pathway or a specific category or categories of compounds.
Metabolic Fingerprinting	Extraction of distinctive metabolites in response to disease, environmental or genetic perturbations that can be used to distinguish samples of different treatments.
Metabolomic Feature	A molecular entity with a unique m/z and retention time. It could be a precursor ion, product ion or polymer ion or different adducts generated during ionization, depending on the specific ionizer and analyzer.

The terms are organized from (Dumas *et al.*, 2006b) and (Dettmer *et al.*, 2007).

To conduct comprehensive assessment of the gut-microbial metabolome, in this study we established an integrative analytical methodology which includes a group of state-of-the-art analytical platforms. The whole system includes: (1) gas chromatography (GC)-electron ionization (EI)-quadrupole (Q) mass spectrometer (MS)-based metabolomics analysis; (2) high resolution (HR) liquid chromatography (LC)-linear ion trap quadrupole (LTQ)-orbitrap hybrid MS-based metabolomics analysis; (3) in-house profiling library that contains 34 saccharides, organic acids, vitamins and amino acids via HPLC and GC-EI-Q MS profiling analyses; (4) high-throughput chromatographic profiling analysis through eight channel ultra-high performance liquid chromatography (UHPLC)-diode array (DAD)-fluorescence (FLD) that couples with UHPLC-triple quadrupole (TsQ)-MS metabolomics analysis (presentation in SESOT 2017); (5) XCMS and MZmine-based processing of raw MS files; (6) multiple variate analysis (MVA)-based statistical models, and (7) KEGG and HMDB-leveraged bioinformatics analysis such as enrichment analysis

and network analysis of metabolic pathways. The pre-treatment of fecal samples, derivatization of extract, data collection, and parameters of module algorithms of MZmine were all optimized in our lab.

Integrative Metabolomics to Build a Database

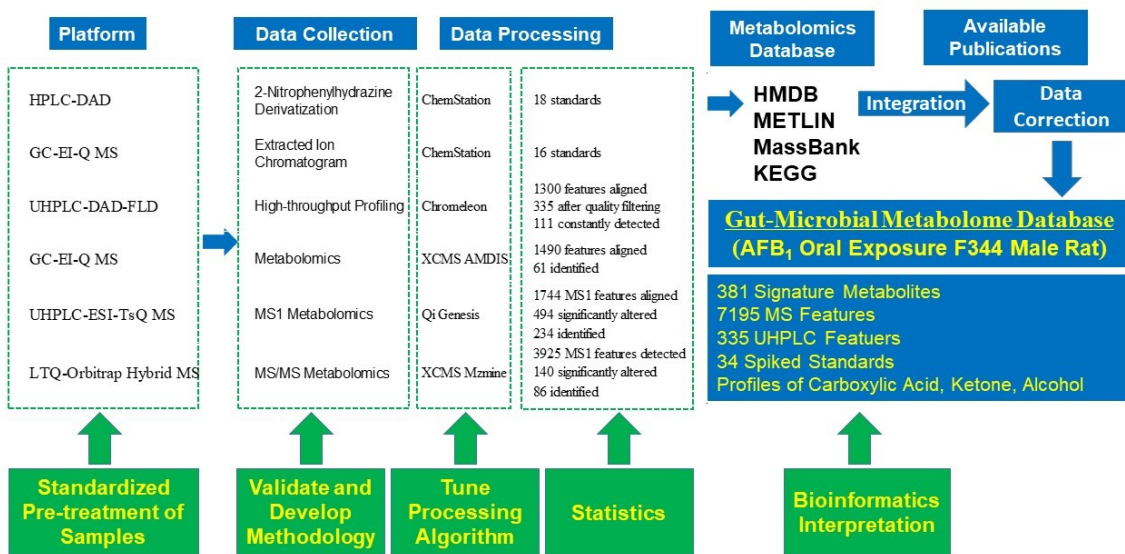


Figure 1-7. Design of integrative metabolomics methodology.

1.7 Specific aims of research

The principal goal of current dissertation study is to elucidate the impacts of AFB₁ and GTPs on gut-microbial metabolome in rat models using comprehensive metabolomics approach. This study has the following goals to achieve:

- (1) Establish multiple platforms-based methodology that integrates the standard metabolic profiling and metabolomics analysis.
- (2) Evaluate and apply statistical models to mine the metabolomics database, and also compare the efficacy of these models in order to refine dataset.
- (3) Validate the consistency between histopathological findings, metagenomics

data and metabolomics data of gut-microbiota under the same study design.

(4) Provide bioinformatics explanation on AFB₁-induced adverse health outcomes, as well as the health-improving effect of GTPs from a view of gut-microbial metabolome.

In the long term, the established methods and database can be used to assess the adverse or beneficial effects of all kinds of food additives, preservatives, contaminants, and food-borne toxins on nutritional status through in vitro, in vivo and ex vivo experiments. The whole system holds several advantages: (1) all analytical protocols are elongated therefore they can be applied to different kinds of samples; (2) the integrated database and bioinformatics analysis can be conveniently updated and extended once open-access databases such as KEGG, HMDB and METLIN are upgraded; (3) any interested hot-spot chemicals can be examined and quantified in this database with external standards; (4) novel methods in data science can be applied to this database and enable a vision of systems biology.

Reference

- Adedara, I. A., Nanjappa, M. K., Farombi, E. O., and Akingbemi, B. T. (2014). Aflatoxin B 1 disrupts the androgen biosynthetic pathway in rat Leydig cells. *Food Chem Toxicol* **65**, 252-259.
- Agag, B. (2004). Mycotoxins in foods and feeds: 1-aflatoxins. *Ass Univ Bull Environ Res* **7**(1), 173-205.
- Anukul, N., Vangnai, K., and Mahakarnchanakul, W. (2013). Significance of regulation limits in mycotoxin contamination in Asia and risk management programs at the national level. *J Food Drug Anal* **21**(3), 227-241.

- Azziz-Baumgartner, E., Lindblade, K., Gieseke, K., Rogers, H. S., Kieszak, S., Njapau, H., Schleicher, R., McCoy, L. F., Misore, A., and DeCock, K. (2005). Case-control study of an acute aflatoxicosis outbreak, Kenya, 2004. *Environ Health Perspect* **113**(12), 1779.
- Babu, P. V., and Liu, D. (2008). Green tea catechins and cardiovascular health: an update. *Curr Med Chem* **15**(18), 1840-50.
- Baffy, G. (2013). Hepatocellular Carcinoma in Non-alcoholic Fatty Liver Disease: Epidemiology, Pathogenesis, and Prevention. *J Clin Transl Hepatol* **1**(2), 131-7.
- Bala, S., Csak, T., Kodys, K., Catalano, D., Ambade, A., Furi, I., Lowe, P., Cho, Y., Iracheta-Vellve, A., and Szabo, G. (2017). Alcohol-induced miR-155 and HDAC11 inhibit negative regulators of the TLR4 pathway and lead to increased LPS responsiveness of Kupffer cells in alcoholic liver disease. *J Leukoc Biol* **102**(2), 487-498.
- Beckonert, O., Keun, H. C., Ebbels, T. M., Bundy, J., Holmes, E., Lindon, J. C., and Nicholson, J. K. (2007). Metabolic profiling, metabolomic and metabonomic procedures for NMR spectroscopy of urine, plasma, serum and tissue extracts. *Nat Protoc* **2**(11), 2692-2703.
- Bennett, J. W., and Klich, M. (2003). Mycotoxins. *Clin Microbiol Rev* **16**(3), 497-516.
- Breton, J., Daniel, C., Dewulf, J., Pothion, S., Froux, N., Sauty, M., Thomas, P., Pot, B., and Foligne, B. (2013). Gut microbiota limits heavy metals burden caused by chronic oral exposure. *Toxicol Lett* **222**(2), 132-8.

- Burcelin, R., Serino, M., Chabo, C., Blasco-Baque, V., and Amar, J. (2011). Gut microbiota and diabetes: from pathogenesis to therapeutic perspective. *Acta Diabetol* **48**(4), 257-273.
- Butler, W. H. (1964). Acute Toxicity of Aflatoxin B1 in Rats. *Br J Cancer* **18**(4), 756-&.
- Catterall, F., Copeland, E., Clifford, M. N., and Ioannides, C. (2003). Effects of black tea theaflavins on aflatoxin B(1) mutagenesis in the Ames test. *Mutagenesis* **18**(2), 145-50.
- Cho, I., Yamanishi, S., Cox, L., Methe, B. A., Zavadil, J., Li, K., Gao, Z., Mahana, D., Raju, K., Teitler, I., *et al.* (2012). Antibiotics in early life alter the murine colonic microbiome and adiposity. *Nature* **488**(7413), 621-6 (10.1038/nature11400).
- Dalezios, J. I., Hsieh, D. P., and Wogan, G. N. (1973). Excretion and metabolism of orally administered aflatoxin B1 by rhesus monkeys. *Food Cosmet Toxicol* **11**(4), 605-16.
- Dalezios, J. I., and Wogan, G. N. (1972). Metabolism of aflatoxin B 1 in rhesus monkeys. *Cancer Res* **32**(11), 2297-303.
- Darnaud, M., Faivre, J., and Moniaux, N. (2013). Targeting gut flora to prevent progression of hepatocellular carcinoma. *J Hepatol* **58**(2), 385-7.
- De Flora, S., and Ferguson, L. R. (2005). Overview of mechanisms of cancer chemopreventive agents. *Mutat Res* **591**(1-2), 8-15.
- Deshpande, S. (2002). *Handbook of Food Toxicology*. CRC Press.
- Dethlefsen, L., and Relman, D. A. (2011). Incomplete recovery and individualized responses of the human distal gut microbiota to repeated antibiotic perturbation. *Proc Natl Acad Sci U S A* **108** Suppl 1(Supplement 1), 4554-61.

- Dettmer, K., Aronov, P. A., and Hammock, B. D. (2007). Mass spectrometry-based metabolomics. *Mass Spectrom Rev* **26**(1), 51-78.
- Deuffic, S., Poynard, T., Buffat, L., and Valleron, A. J. (1998). Trends in primary liver cancer. *Lancet* **351**(9097), 214-5.
- Diaz, G. J., and Murcia, H. W. (2011). Biotransformation of aflatoxin B1 and its relationship with the differential toxicological response to aflatoxin in commercial poultry species. In *Aflatoxins-Biochemistry and Molecular Biology*. InTechOpen.
- Dohnal, V., Wu, Q., and Kuca, K. (2014). Metabolism of aflatoxins: key enzymes and interindividual as well as interspecies differences. *Arch Toxicol* **88**(9), 1635-44.
- Dumas, M.-E., Barton, R. H., Toye, A., Cloarec, O., Blancher, C., Rothwell, A., Fearnside, J., Tatoud, R., Blanc, V., Lindon, J. C., *et al.* (2006a). Metabolic profiling reveals a contribution of gut microbiota to fatty liver phenotype in insulin-resistant mice. *Proc Natl Acad Sci U S A* **103**(33), 12511-12516.
- Dumas, M. E., Barton, R. H., Toye, A., Cloarec, O., Blancher, C., Rothwell, A., Fearnside, J., Tatoud, R., Blanc, V., Lindon, J. C., *et al.* (2006b). Metabolic profiling reveals a contribution of gut microbiota to fatty liver phenotype in insulin-resistant mice. *Proc Natl Acad Sci U S A* **103**(33), 12511-6.
- Eaton, D. L., and Gallagher, E. P. (1994). Mechanisms of aflatoxin carcinogenesis. *Annu Rev Pharmacol Toxicol* **34**(1), 135-72.
- Fazeli, M., Hassanzadeh, P., and Alaei, S. (2011). Cadmium chloride exhibits a profound toxic effect on bacterial microflora of the mice gastrointestinal tract. *Hum Exp Toxicol* **30**(2), 152-9.

- Food, U., and Administration, D. (2000). Guidance for industry: action levels for poisonous or deleterious substances in human food and animal feed. *USFDA, Washington, DC*.
- Francino, M. P. (2015). Antibiotics and the human gut microbiome: dysbioses and accumulation of resistances. *Front Microbiol* **6**, 1543.
- Frei, B., and Higdon, J. V. (2003). Antioxidant activity of tea polyphenols in vivo: evidence from animal studies. *J Nutr* **133**(10), 3275S-84S.
- Gaudet, R. G., Sintsova, A., Buckwalter, C. M., Leung, N., Cochrane, A., Li, J., Cox, A. D., Moffat, J., and Gray-Owen, S. D. (2015). INNATE IMMUNITY. Cytosolic detection of the bacterial metabolite HBP activates TIFA-dependent innate immunity. *Science* **348**(6240), 1251-5.
- Gibson, G. R., and Roberfroid, M. B. (1995). Dietary modulation of the human colonic microbiota: introducing the concept of prebiotics. *J Nutr* **125**(6), 1401-12.
- Giri, I., Johnston, D. S., and Stone, M. P. (2002). Mispairing of the 8,9-dihydro-8-(N7-guanyl)-9-hydroxy-aflatoxin B1 adduct with deoxyadenosine results in extrusion of the mismatched dA toward the major groove. *Biochemistry* **41**(17), 5462-72.
- Goffredo, M., Mass, K., Parks, E. J., Wagner, D. A., McClure, E. A., Graf, J., Savoye, M., Pierpont, B., Cline, G., and Santoro, N. (2016). Role of gut microbiota and short chain fatty acids in modulating energy harvest and fat partitioning in youth. *J Clin Endocrinol Metab* **101**(11), 4367-4376.
- Goyal, H., and Hu, Z. D. (2017). Prognostic value of red blood cell distribution width in hepatocellular carcinoma. *Ann Transl Med* **5**(13), 271.
- Gradelet, S., Le Bon, A. M., Berges, R., Suschetet, M., and Astorg, P. (1998). Dietary carotenoids inhibit aflatoxin B1-induced liver preneoplastic foci and DNA damage

- in the rat: role of the modulation of aflatoxin B1 metabolism. *Carcinogenesis* **19**(3), 403-11.
- Groopman, J. D., Jiaqi, Z., Donahue, P. R., Pikul, A., Lisheng, Z., Jun-shi, C., and Wogan, G. N. (1992). Molecular dosimetry of urinary aflatoxin-DNA adducts in people living in Guangxi Autonomous Region, People's Republic of China. *Cancer Res* **52**(1), 45-52.
- Groopman, J. D., Wang, J. S., and Scholl, P. (1996). Molecular biomarkers for aflatoxins: from adducts to gene mutations to human liver cancer. *Can J Physiol Pharmacol* **74**(2), 203-9.
- Guengerich, F. P., Cai, H., McMahon, M., Hayes, J. D., Sutter, T. R., Groopman, J. D., Deng, Z., and Harris, T. M. (2001). Reduction of aflatoxin B1 dialdehyde by rat and human aldo-keto reductases. *Chem Res Toxicol* **14**(6), 727-37.
- Han, X., Geller, B., Moniz, K., Das, P., Chippindale, A.K., and Walker, V.K. (2014) Monitoring the developmental impact of copper and silver nanoparticle exposure in *Drosophila* and their microbiomes. *Sci Total Environ*, 487, 822–829.
- Haqqi, T. M., Anthony, D. D., Gupta, S., Ahmad, N., Lee, M. S., Kumar, G. K., and Mukhtar, H. (1999). Prevention of collagen-induced arthritis in mice by a polyphenolic fraction from green tea. *Proc Natl Acad Sci U S A* **96**(8), 4524-9.
- Herzallah, S. M. (2009). Determination of aflatoxins in eggs, milk, meat and meat products using HPLC fluorescent and UV detectors. *Food Chem* **114**(3), 1141-1146.
- Hogan, G. (1978). Aflatoxin B1 and reye's syndrome. *Lancet* **311**(8063), 561.

- Holeski, C. J., Eaton, D. L., Monroe, D. H., and Bellamy, G. M. (1987). Effects of phenobarbital on the biliary excretion of aflatoxin P1-glucuronide and aflatoxin B1-S-glutathione in the rat. *Xenobiotica* **17**(2), 139-53.
- Hooper, L.V. and Gordon, J.I. (2001) Commensal host-bacterial relationships in the gut. *Science*, **292**, 1115–1118.
- Hursel, R., and Westerterp-Plantenga, M. S. (2013). Catechin- and caffeine-rich teas for control of body weight in humans. *Am J Clin Nutr* **98**(6), 1682s-1693s.
- Jakobsson, H.E., Jernberg, C., Andersson, A.F., Sjölund-Karlsson, M., Jansson, J.K., and Engstrand, L. (2010) Short-term antibiotic treatment has differing long-term impacts on the human throat and gut microbiome. *PLoS ONE*, **5**, e9836.
- Jandhyala, S. M., Talukdar, R., Subramanyam, C., Vuyyuru, H., Sasikala, M., and Nageshwar Reddy, D. (2015). Role of the normal gut microbiota. *World J Gastroenterol* **21**(29), 8787-803.
- Janssens, P. L., Hursel, R., and Westerterp-Plantenga, M. S. (2015). Long-term green tea extract supplementation does not affect fat absorption, resting energy expenditure, and body composition in adults. *J Nutr* **145**(5), 864-870.
- Katiyar, S. K., Matsui, M. S., Elmets, C. A., and Mukhtar, H. (1999). Polyphenolic antioxidant (-)-epigallocatechin-3-gallate from green tea reduces uvb-Induced inflammatory responses and infiltration of leukocytes in human skin. *Photochem Photobiol* **69**(2), 148-153.
- Kensler, T. W., Roebuck, B. D., Wogan, G. N., and Groopman, J. D. (2011). Aflatoxin: a 50-year odyssey of mechanistic and translational toxicology. *Toxicol Sci* **120**(Suppl 1), S28-S48.

- Kumagai, S. (1989). Intestinal absorption and excretion of aflatoxin in rats. *Toxicol Appl Pharmacol* **97**(1), 88-97.
- Kumar, N. S. N., Balamurugan, R., Jayakanthan, K., Pulimood, A., Pugazhendhi, S., and Ramakrishna, B. S. (2008). Probiotic administration alters the gut flora and attenuates colitis in mice administered dextran sodium sulfate. *J Gastroenterol Hepatol* **23**(12), 1834-1839.
- Kummen, M., Vesterhus, M., Trøseid, M., Moum, B., Svardal, A., Boberg, K. M., Aukrust, P., Karlsen, T. H., Berge, R. K., and Hov, J. R. (2017). Elevated trimethylamine-N-oxide (TMAO) is associated with poor prognosis in primary sclerosing cholangitis patients with normal liver function. *United European Gastroenterol J* **5**(4), 532-541.
- Lee, H. C., Jenner, A. M., Low, C. S., and Lee, Y. K. (2006). Effect of tea phenolics and their aromatic fecal bacterial metabolites on intestinal microbiota. *Res Microbiol* **157**(9), 876-84.
- Li, F.-Q., Yoshizawa, T., Kawamura, O., Luo, X.-Y., and Li, Y.-W. (2001). Aflatoxins and fumonisins in corn from the high-incidence area for human hepatocellular carcinoma in Guangxi, China. *J Agric Food Chem* **49**(8), 4122-4126.
- Li, J., Sung, C. Y., Lee, N., Ni, Y., Pihlajamaki, J., Panagiotou, G., and El-Nezami, H. (2016). Probiotics modulated gut microbiota suppresses hepatocellular carcinoma growth in mice. *Proc Natl Acad Sci U S A* **113**(9), E1306-15.
- Lilly, D. M., and Stillwell, R. H. (1965). Probiotics: growth-promoting factors produced by microorganisms. *Science* **147**(3659), 747-8.

- Lin, J., Chen, J., He, J., Chen, J., Yan, Q., Zhou, J., and Xie, P. (2015). Effects of microcystin-LR on bacterial and fungal functional genes profile in rat gut. *Toxicon* **96**, 50-6.
- Lindahl, A., Sääf, S., Lehtiö, J., and Nordström, A. (2017). Tuning metabolome coverage in reversed phase LC-MS metabolomics of MeOH extracted samples using the reconstitution solvent composition. *Anal Chem* **89**(14), 7356-7364.
- Liu, Y., Li, Y., Liu, K., and Shen, J. (2014). Exposing to cadmium stress cause profound toxic effect on microbiota of the mice intestinal tract. *PLoS One* **9**(2), e85323.
- Luo, H., Tang, L., Tang, M., Billam, M., Huang, T., Yu, J., Wei, Z., Liang, Y., Wang, K., Zhang, Z. Q., *et al.* (2006a). Phase IIa chemoprevention trial of green tea polyphenols in high-risk individuals of liver cancer: modulation of urinary excretion of green tea polyphenols and 8-hydroxydeoxyguanosine. *Carcinogenesis* **27**(2), 262-8.
- Luo, H. T., Cox, S. B., Gao, W. M., Yu, J. H., Tang, L. L., and Wang, J. S. (2006b). Metabolic profiling in validation of plasma biomarkers for green tea polyphenols. *Metabolomics* **2**(4), 235-241.
- Madden, C. R., Finegold, M. J., and Slagle, B. L. (2002). Altered DNA mutation spectrum in aflatoxin B1-treated transgenic mice that express the hepatitis B virus X protein. *J Viro* **76**(22), 11770-11774.
- Martin, F. P. J., Wang, Y., Sprenger, N., Yap, I. K., Lundstedt, T., Lek, P., Rezzi, S., Ramadan, Z., Van Bladeren, P., and Fay, L. B. (2008). Probiotic modulation of symbiotic gut microbial–host metabolic interactions in a humanized microbiome mouse model. *Mol Syst Biol* **4**(1), 157.

- Maurice, C. F., Haiser, H. J., and Turnbaugh, P. J. (2013). Xenobiotics shape the physiology and gene expression of the active human gut microbiome. *Cell* **152**(1-2), 39-50.
- Merrifield, D. L., Shaw, B. J., Harper, G. M., Saoud, I. P., Davies, S. J., Handy, R. D., and Henry, T. B. (2013). Ingestion of metal-nanoparticle contaminated food disrupts endogenous microbiota in zebrafish (*Danio rerio*). *Environ Pollut* **174**, 157-63.
- Mielgo-Ayuso, J., Barrenechea, L., Alcorta, P., Larrarte, E., Margareto, J., and Labayen, I. (2014). Effects of dietary supplementation with epigallocatechin-3-gallate on weight loss, energy homeostasis, cardiometabolic risk factors and liver function in obese women: randomised, double-blind, placebo-controlled clinical trial. *Br J Nutr* **111**(7), 1263-71.
- Mitchell, N. J., Xue, K. S., Lin, S., Marroquin-Cardona, A., Brown, K. A., Elmore, S. E., Tang, L., Romoser, A., Gelderblom, W. C., and Wang, J. S. (2014). Calcium montmorillonite clay reduces AFB1 and FB1 biomarkers in rats exposed to single and co-exposures of aflatoxin and fumonisin. *J Appl Toxicol* **34**(7), 795-804.
- Morelli, L., and Capurso, L. (2012). FAO/WHO guidelines on probiotics: 10 years later. *J Clin Gastroenterol* **46 Suppl**, S1-2.
- Mukhtar, H., and Ahmad, N. (2000). Tea polyphenols: prevention of cancer and optimizing health. *Am J Clin Nutr* **71**(6 Suppl), 1698S-702S; discussion 1703S-4S.
- Mutlu, E., Keshavarzian, A., Engen, P., Forsyth, C. B., Sikaroodi, M., and Gillevet, P. (2009). Intestinal dysbiosis: a possible mechanism of alcohol - induced endotoxemia and alcoholic steatohepatitis in rats. *Alcohol Clin Exp Res* **33**(10), 1836-1846.

- Nair, A. B., and Jacob, S. (2016). A simple practice guide for dose conversion between animals and human. *J Basic Clin Pharm* **7**(2), 27-31.
- Nderitu, P., Garmo, H., Holmberg, L., Malmstrom, H., Hammar, N., Walldius, G., Jungner, I., Lambe, M., and Van Hemelrijck, M. (2016). Association between metabolic syndrome components and the risk of primary liver cancer and cirrhosis. *European J Surg Oncol* **42**(11), S231.
- Neal, G. E., Judah, D. J., Stirpe, F., and Patterson, D. S. P. (1981). The formation of 2,3-dihydroxy-2,3-dihydro-aflatoxin-b1 by the metabolism of aflatoxin-b1 by liver-microsomes isolated from certain avian and mammalian-species and the possible role of this metabolite in the acute toxicity of aflatoxin-B1. *Toxicol Appl Pharm* **58**(3), 431-437.
- Negishi, H., Xu, J. W., Ikeda, K., Njelekela, M., Nara, Y., and Yamori, Y. (2004). Black and green tea polyphenols attenuate blood pressure increases in stroke-prone spontaneously hypertensive rats. *J Nutr* **134**(1), 38-42.
- Nolan, J. P. (1989). Intestinal endotoxins as mediators of hepatic injury—an idea whose time has come again. *Hepatology* **10**(5), 887-891.
- Oliveira, C. A. F., Bovo, F., Corassin, C. H., Jager, A. V., and Reddy, K. R. (2013). Recent trends in microbiological decontamination of aflatoxins in foodstuffs. In *Aflatoxins-recent advances and future prospects*. InTech.
- Organization, W. H. (2010). International experts limit melamine levels in food. *World Health Organization, Geneva, Switzerland*.
- Patti, G. J., Yanes, O., and Siuzdak, G. (2012). Metabolomics: the apogee of the omic triology. *Nat Rev Mol Cell Biol* **13**(4), 263.

- Phung, O. J., Scholle, J. M., Talwar, M., and Coleman, C. I. (2010). Effect of noninsulin antidiabetic drugs added to metformin therapy on glycemic control, weight gain, and hypoglycemia in type 2 diabetes. *JAMA* **303**(14), 1410-8.
- Potenza, M. A., Marasciulo, F. L., Tarquinio, M., Tiravanti, E., Colantuono, G., Federici, A., Kim, J.-a., Quon, M. J., and Montagnani, M. (2007a). EGCG, a green tea polyphenol, improves endothelial function and insulin sensitivity, reduces blood pressure, and protects against myocardial I/R injury in SHR. *Am J Physiol Endocrinol Metab* **292**(5), E1378-E1387.
- Potenza, M. A., Marasciulo, F. L., Tarquinio, M., Tiravanti, E., Colantuono, G., Federici, A., Kim, J. A., Quon, M. J., and Montagnani, M. (2007b). EGCG, a green tea polyphenol, improves endothelial function and insulin sensitivity, reduces blood pressure, and protects against myocardial I/R injury in SHR. *Am J Physiol Endocrinol Metab* **292**(5), E1378-87.
- Qian, G., Tang, L., Guo, X., Wang, F., Massey, M. E., Su, J., Guo, T. L., Williams, J. H., Phillips, T. D., and Wang, J. S. (2014). Aflatoxin B1 modulates the expression of phenotypic markers and cytokines by splenic lymphocytes of male F344 rats. *J Appl Toxicol* **34**(3), 241-9.
- Qian, G., Tang, L., Lin, S., Xue, K. S., Mitchell, N. J., Su, J., Gelderblom, W. C., Riley, R. T., Phillips, T. D., and Wang, J. S. (2016). Sequential dietary exposure to aflatoxin B1 and fumonisin B1 in F344 rats increases liver preneoplastic changes indicative of a synergistic interaction. *Food Chem Toxicol* **95**, 188-95.

- Qian, G., Tang, L., Wang, F., Guo, X., Massey, M. E., Williams, J. H., Phillips, T. D., and Wang, J. S. (2013a). Physiologically based toxicokinetics of serum aflatoxin B1-lysine adduct in F344 rats. *Toxicology* **303**, 147-51.
- Qian, G., Wang, F., Tang, L., Massey, M. E., Mitchell, N. J., Su, J., Williams, J. H., Phillips, T. D., and Wang, J. S. (2013b). Integrative toxicopathological evaluation of aflatoxin B(1) exposure in F344 rats. *Toxicol Pathol* **41**(8), 1093-105.
- Qian, G., Xue, K., Tang, L., Wang, F., Song, X., Chyu, M. C., Pence, B. C., Shen, C. L., and Wang, J. S. (2012). Mitigation of oxidative damage by green tea polyphenols and Tai Chi exercise in postmenopausal women with osteopenia. *PLoS One* **7**(10), e48090.
- Qin, J., Li, R., Raes, J., Arumugam, M., Burgdorf, K. S., Manichanh, C., Nielsen, T., Pons, N., Levenez, F., Yamada, T., *et al.* (2010a). A human gut microbial gene catalog established by metagenomic sequencing. *Nature* **464**(7285), 59-65.
- Qin, J. J., Li, R. Q., Raes, J., Arumugam, M., Burgdorf, K. S., Manichanh, C., Nielsen, T., Pons, N., Levenez, F., Yamada, T., *et al.* (2010b). A human gut microbial gene catalogue established by metagenomic sequencing. *Nature* **464**(7285), 59-U70.
- Ramautar, R., Berger, R., van der Greef, J., and Hankemeier, T. (2013). Human metabolomics: strategies to understand biology. *Current opinion in chemical biology* **17**(5), 841-846.
- Ramsdell, H. S., Parkinson, A., Eddy, A. C., and Eaton, D. L. (1991). Bioactivation of aflatoxin B1 by human liver microsomes: role of cytochrome P450 IIIA enzymes. *Toxicol Appl Pharmacol* **108**(3), 436-47.

- Randrianarisoa, E., Lehn-Stefan, A., Wang, X., Hoene, M., Peter, A., Heinzmann, S. S., Zhao, X., Königsrainer, I., Königsrainer, A., and Balletshofer, B. (2016). Relationship of serum trimethylamine N-oxide (TMAO) levels with early atherosclerosis in humans. *Scientific reports* **6**.
- Rastmanesh, R. (2011). High polyphenol, low probiotic diet for weight loss because of intestinal microbiota interaction. *Chem Biol Interact* **189**(1-2), 1-8.
- Riegsecker, S., Wiczynski, D., Kaplan, M. J., and Ahmed, S. (2013). Potential benefits of green tea polyphenol EGCG in the prevention and treatment of vascular inflammation in rheumatoid arthritis. *Life Sci* **93**(8), 307-12.
- Roager, H. M., Sulek, K., Skov, K., Frandsen, H. L., Smedsgaard, J., Wilcks, A., Skov, T. H., Villas-Boas, S. G., and Licht, T. R. (2014). Lactobacillus acidophilus NCFM affects vitamin E acetate metabolism and intestinal bile acid signature in monocolonized mice. *Gut Microbes* **5**(3), 296-303.
- Roberfroid, M. (2007). Prebiotics: the concept revisited. *J Nutr* **137**(3 Suppl 2), 830S-7S.
- Saint-Cyr, M. J., Perrin-Guyomard, A., Houee, P., Rolland, J. G., and Laurentie, M. (2013). Evaluation of an oral subchronic exposure of deoxynivalenol on the composition of human gut microbiota in a model of human microbiota-associated rats. *PLoS One* **8**(11), e80578.
- Sakanaka, S., Aizawa, M., Kim, M., and Yamamoto, T. (1996). Inhibitory effects of green tea polyphenols on growth and cellular adherence of an oral bacterium, Porphyromonas gingivalis. *Biosci Biotechnol Biochem* **60**(5), 745-9.
- Sawosz, E., Binek, M., Grodzik, M., Zielinska, M., Sysa, P., Szmidt, M., Niemiec, T., and Chwalibog, A. (2007). Influence of hydrocolloidal silver nanoparticles on

- gastrointestinal microflora and morphology of enterocytes of quails. *Arch Anim Nutr* **61**(6), 444-51.
- Schrezenmeir, J., and de Vrese, M. (2001). Probiotics, prebiotics, and synbiotics—approaching a definition. *Am J Clin Nutr* **73**(2), 361s-364s.
- Sears, M. E., and Genuis, S. J. (2012). Environmental determinants of chronic disease and medical approaches: recognition, avoidance, supportive therapy, and detoxification. *J Environ Public Health* **2012**, 15.
- Shen, C. L., Brackee, G., Song, X., Tomison, M. D., Finckbone, V., Mitchell, K. T., Tang, L., Chyu, M. C., Dunn, D. M., and Wang, J. S. (2017). Safety evaluation of green tea polyphenols consumption in middle-aged ovariectomized rat model. *J Food Sci* **82**(9), 2192-2205.
- Shen, C. L., Wang, P., Guerrieri, J., Yeh, J. K., and Wang, J. S. (2008). Protective effect of green tea polyphenols on bone loss in middle-aged female rats. *Osteoporos Int* **19**(7), 979-90.
- Shen, H. M., and Ong, C. N. (1996). Mutations of the p53 tumor suppressor gene and ras oncogenes in aflatoxin hepatocarcinogenesis. *Mutat Res* **366**(1), 23-44.
- Singh, R., Akhtar, N., and Haqqi, T. M. (2010). Green tea polyphenol epigallocatechi-3-gallate: Inflammation and arthritis. *Life Sci* **86**(25-26), 907-918.
- Storvik, M., Huuskonen, P., Kyllönen, T., Lehtonen, S., El-Nezami, H., Auriola, S., and Pasanen, M. (2011). Aflatoxin B₁-a potential endocrine disruptor—up-regulates CYP19A1 in JEG-3 cells. *Toxicol lett* **202**(3), 161-167.
- Szabo, G., Bala, S., Petrasek, J., and Gattu, A. (2010). Gut-liver axis and sensing microbes. *Dig Dis* **28**(6), 737-44.

- Tang, L., Tang, M., Xu, L., Luo, H., Huang, T., Yu, J., Zhang, L., Gao, W., Cox, S. B., and Wang, J. S. (2008). Modulation of aflatoxin biomarkers in human blood and urine by green tea polyphenols intervention. *Carcinogenesis* **29**(2), 411-7.
- Tang, L., Xu, L., Afriyie-Gyawu, E., Liu, W., Wang, P., Tang, Y., Wang, Z., Huebner, H., Ankrah, N.-A., and Ofori-Adjei, D. (2009). Aflatoxin–albumin adducts and correlation with decreased serum levels of vitamins A and E in an adult Ghanaian population. *Food Addit Contam* **26**(1), 108-118.
- Tomas, J., Langella, P., and Cherbuy, C. (2012). The intestinal microbiota in the rat model: major breakthroughs from new technologies. *Anim Health Res Rev* **13**(1), 54-63.
- Tuohy, K. M., Conterno, L., Gasperotti, M., and Viola, R. (2012). Up-regulating the human intestinal microbiome using whole plant foods, polyphenols, and/or fiber. *J Agric Food Chem* **60**(36), 8776-8782.
- Tuohy, K. M., Fava, F., and Viola, R. (2014). ‘The way to a man's heart is through his gut microbiota’—dietary pro-and prebiotics for the management of cardiovascular risk. *Proc Nutr Soc* **73**(2), 172-185.
- Valery, P. C., Laversanne, M., Clark, P. J., Petrick, J. L., McGlynn, K. A., and Bray, F. (2018). Projections of primary liver cancer to 2030 in 30 countries worldwide. *Hepatology* **67**(2), 600-611.
- Vernocchi, P., Del Chierico, F., and Putignani, L. (2016). Gut microbiota profiling: metabolomics based approach to unravel compounds affecting human health. *Front Microbiol* **7**(1144).

- Wache, Y. J., Valat, C., Postollec, G., Bougeard, S., Burel, C., Oswald, I. P., and Fravallo, P. (2009). Impact of deoxynivalenol on the intestinal microflora of pigs. *Int J Mol Sci* **10**(1), 1-17.
- Wang, J.-S., Huang, T., Su, J., Liang, F., Wei, Z., Liang, Y., Luo, H., Kuang, S.-Y., Qian, G.-S., and Sun, G. (2001). Hepatocellular carcinoma and aflatoxin exposure in Zhuqing village, Fusui county, People's Republic of China. *Cancer Epidemiol Biomarkers Prev* **10**(2), 143-146.
- Wang, J., Tang, L., Glenn, T. C., and Wang, J.-S. (2015). Aflatoxin B1 induced compositional changes in gut microbial communities of male F344 rats. *Toxicol Sci* **150**(1), 54-63.
- Wang, J. H., Byun, J., and Pennathur, S. (2010). Analytical approaches to metabolomics and applications to systems biology. *Semin Nephrol* **30**(5), 500-511.
- Wang, J. S., and Groopman, J. D. (1999). DNA damage by mycotoxins. *Mutat Res* **424**(1-2), 167-81.
- Wang, J. S., Luo, H., Wang, P., Tang, L., Yu, J., Huang, T., Cox, S., and Gao, W. (2008). Validation of green tea polyphenol biomarkers in a phase II human intervention trial. *Food Chem Toxicol* **46**(1), 232-40.
- Wang, J. S., Shen, X., He, X., Zhu, Y. R., Zhang, B. C., Wang, J. B., Qian, G. S., Kuang, S. Y., Zarba, A., Egner, P. A., *et al.* (1999). Protective alterations in phase 1 and 2 metabolism of aflatoxin B1 by oltipraz in residents of Qidong, People's Republic of China. *J Natl Cancer Inst* **91**(4), 347-54.
- Weidenbörner, M. (2015). *Natural Mycotoxin Contamination in Humans and Animals*. Springer.

- Weir, T. L., Manter, D. K., Sheflin, A. M., Barnett, B. A., Heuberger, A. L., and Ryan, E. P. (2013). Stool Microbiome and Metabolome Differences between Colorectal Cancer Patients and Healthy Adults. *PLoS ONE* **8**(8), e70803.
- Wild, C. P., and Hall, A. J. (2000). Primary prevention of hepatocellular carcinoma in developing countries. *Mutat Res* **462**(2-3), 381-93.
- Wild, C. P., and Turner, P. C. (2002). The toxicology of aflatoxins as a basis for public health decisions. *Mutagenesis* **17**(6), 471-481.
- Wolfram, S. (2007). Effects of green tea and EGCG on cardiovascular and metabolic health. *J Am Coll Nutr* **26**(4), 373S-388S.
- Wong, C. P., Nguyen, L. P., Noh, S. K., Bray, T. M., Bruno, R. S., and Ho, E. (2011). Induction of regulatory T cells by green tea polyphenol EGCG. *Immunol Lett* **139**(1-2), 7-13.
- Wong, M. C., Jiang, J. Y., Goggins, W. B., Liang, M., Fang, Y., Fung, F. D., Leung, C., Wang, H. H., Wong, G. L., Wong, V. W., *et al.* (2017). International incidence and mortality trends of liver cancer: a global profile. *Sci Rep* **7**, 45846.
- Wong, Z. A., and Hsieh, D. P. (1980). The comparative metabolism and toxicokinetics of aflatoxin B1 in the monkey, rat, and mouse. *Toxicol Appl Pharmacol* **55**(1), 115-25.
- Xu, C., Liu, Q., Huan, F., Qu, J. H., Liu, W., Gu, A. H., Wang, Y. B., and Jiang, Z. Y. (2014). Changes in gut microbiota may be early signs of liver toxicity induced by epoxiconazole in rats. *Chemotherapy* **60**(2), 135-142.

- Yan, A. W., Fouts, D. E., Brandl, J., Starkel, P., Torralba, M., Schott, E., Tsukamoto, H., Nelson, K. E., Brenner, D. A., and Schnabl, B. (2011). Enteric dysbiosis associated with a mouse model of alcoholic liver disease. *Hepatology* **53**(1), 96-105.
- Yu, J., Huang, T., Zhang, L., Wei, Z., Liang, Y., Li, Y., Wang, K., Shi, J., Luo, H., and Tang, L. (2006). Chemoprevention trial of green tea polyphenols in high-risk population of liver cancer in southern Guangxi, China. In AACR.
- Yu, L. X., Yan, H. X., Liu, Q., Yang, W., Wu, H. P., Dong, W., Tang, L., Lin, Y., He, Y. Q., Zou, S. S., *et al.* (2010). Endotoxin accumulation prevents carcinogen-induced apoptosis and promotes liver tumorigenesis in rodents. *Hepatology* **52**(4), 1322-33.
- Zaura, E., Brandt, B.W., Teixeira de Mattos, M.J., Buijs, M.J., Caspers, M.P.M., Rashid, M.-U., Weintraub, A., Nord, C.E., Savell, A., Hu, Y., *et al.* (2015) Same exposure but two radically different responses to antibiotics: resilience of the salivary microbiome versus long-term microbial shifts in feces. *mBio*, 6, e01693-15-e01693-15.
- Zeng, H., Lin, H., Liu, W., Wang, J., Wang, L., Zheng, C., Tan, Y., Huang, Y., He, L., Luo, J., *et al.* (2017). Prevalence of metabolic syndrome among adults with liver function injury in rural area of Southwest China: A cross-sectional study. *Sci Rep* **7**(1), 5518.
- Zhang, H. L., Yu, L. X., Yang, W., Tang, L., Lin, Y., Wu, H., Zhai, B., Tan, Y. X., Shan, L., Liu, Q., *et al.* (2012). Profound impact of gut homeostasis on chemically-induced pro-tumorigenic inflammation and hepatocarcinogenesis in rats. *J Hepatol* **57**(4), 803-12.
- Zhou, C. (2016). Novel functions of PXR in cardiometabolic disease. *Biochim Biophys Acta* **1859**(9), 1112-20.

Ziglari, T., and Allameh, A. (2013). The Significance of Glutathione Conjugation in Aflatoxin Metabolism. In *Aflatoxins - Recent Advances and Future Prospects* (M. Razzaghi-Abyaneh, Ed.) doi: 10.5772/52096, pp. Ch. 13. InTech, Rijeka.

CHAPTER 2. LITERATURE REVIEW

2.1 Gut-microbiota dependent metabolome

2.1.1 *Review criteria*

“PubMed” and “Google Scholar” were used to search for the literatures with interested topics. The keywords input for literature searching include a primary term “gut microbiota”, or “intestinal content”, or “gut content”, and the following secondary terms: “indole”, “tryptophan”, “kynurenine”, “bile acid”, “secondary bile acid”, “phenyl acid”, “phenylalanine”, “tyrosine”, “vitamin”, “probiotic”, “quorum sensing”, “signaling molecule”, “organic acid”, “organic amine”, “lipid inflammatory factor”, “reactive oxygen”, and “aldehyde”.

2.1.2 *Concepts and terminology*

The concept of the human microbiota was first coined by Nobel laureate Joshua Lederberg on 2001, described as “*the ecological community of commensal, symbiotic, and also pathogenic microorganisms that share our body space and have been all but ignored as determinants of health and disease*” (Lederberg and McCray, 2001). Human gastrointestinal (GI) tract contains the largest surface of ~2,700 square feet in the human body, exceeding the total area of skin, lungs and body cavities (Leal-Lopes *et al.*, 2015). Human GI tract harbors a microbial community that contains over 1000 bacterial species and 100–fold more genes than host genome. Over 99% of the gut microbiota are *Firmicutes*,

Bacteroidetes, *Proteobacteria*, and *Actinobacteria* classes, with 64% of attached colonic species as *Firmicutes* and 23% of normal specie belonging to *Bacteroidetes* (Sartor, 2008). The microbial community demonstrate influences on various aspects of host physiology, including nutritional metabolism, resistance to infection, and the general performance of immune system as well.

Current evidences suggest that gut-microbiota is inherited from maternal placenta and vagina during vaginal birth, and is adjusted following the changes of host health condition, physiology and dietary pattern after then (Neu and Rushing, 2011). In addition, accumulating data have indicated that gut-microbiota has co-evolved with the host over thousands of years before the formulation of an intricate and mutually beneficial relationship (Neish, 2009). The connection between individual and gut-microbiota is similar with the term “endosymbiosis”—a term used to describe the integrated internal symbiosis, in which one organism takes up permanent residence inside another and eventually evolves into a single biological lineage (Embley and Martin, 2006; Margulis, 1981). This mutual connection is a good example to exhibit the complex links between eukaryotic system and prokaryotic cells. The two systems are believed to initially exist indifferently. According to the fundamental theory of evolutionary biology, eukaryotic cells were generated through the symbiotic union of separate prokaryotic cells, supported by the prokaryotic features of mitochondria and prokaryotic/eukaryotic features demonstrated by ribosome (Mereschkowsky, 1905; Wallin, 1927). Actually, with the accumulation of relevant data, researchers have identified a number of similarities existing between host/gut-microbiota and eukaryotic cells/mitochondria (Shapira, 2016).

So far, the most common practice to investigate gut-microbiota is fecal analysis, because feces contain representative portion of gut-microbiome and gut-microbiota dependent metabolites (**Figure 2-1**) and the collection of feces is a repeatable and non-invasive process (Barbosa, 2013). Through omics based fecal analysis, Wang *et al.* have identified both genomic and metabolic differences between formula-fed (FF) infants and breast-fed (BF) infants of 3-month (Wang *et al.*, 2013; Wang *et al.*, 2015a). Compared with FF infants, in the gut of BF infants there are higher relative abundances of *Bacteroides*, lower proportions of *Clostridium* XVIII, *Lachnospiracea incertae sedis*, *Streptococcus*, *Enterococcus* and *Veillonella*. Besides, galactitol, 15-methylhexadecanoic acid and maltose were found to be the abundant metabolites enriched in BF infants, whereas beta-alanine, dodecanoic acid, glycolic acid, decanoic acid and tyramine were the major metabolites associated with FF.

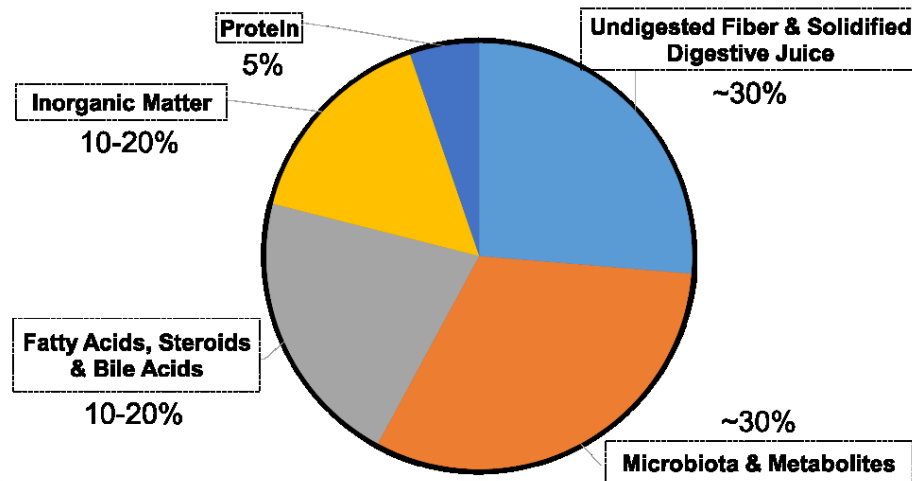


Figure 2-1. Approximate composition of dehydrated human feces. Pie chart is constructed based on the data published by Barbosa *et al* (Barbosa, 2013).

2.1.3 Analytical approaches to the study of gut-microbiota

The study of gut-microbiota is driven by the development and upgrade of polymerase chain reaction (PCR) based genetic and genomic analytical techniques. The most featured methods include qPCR, real-time PCR, denaturing gradient gel electrophoresis (DGGE), temperature gradient gel electrophoresis (TGGE), 5'-rapid amplification of cDNA ends (5'-RACE PCR), terminal restriction fragment length polymorphism (T-RFLP), DNA/RNA microarray, 16S rRNA sequencing, shotgun sequencing and the “next-generation sequencing” such as illumina sequencing, Roche 454 sequencing, Ion torrent/Proton/PGM sequencing (Fraher *et al.*, 2012). These techniques were designed to extract, enrich, separate, sequence and quantify both cytoplasm nucleotides or nuclear genome in a high throughput manner (Gong and Yang, 2012; Karlsson *et al.*, 2013). In addition to the sequencing-based studies, germ-free animal models are administrated with hypothesized functional microbes so that the connection between certain microbial inhabits and host health outcomes can be examined. In an early analysis of the ileal contents from germ free mice model the inoculation of *Bacteroides thetaiotaomicron* was found to modulate gut-associated lymph tissue (GALT)—an intestinal immune tissue with immune regulatory functions such as enhancing the integrity of ileal squamous epithelial barrier and promoting the enrollment of IgA-producing B cells (Hooper *et al.*, 2001). A number of aspects of host health and disease conditions have been associated with gut-microbiota, e. g. immune system, fat storage, energy metabolism, hepatic steatosis, atherosclerosis, cardiovascular diseases, tissue lipid composition, periodontitis, motor activity and enteroendocrine metabolism (Burcelin *et al.*, 2011). Recent findings have also suggested that perturbations of gut-microbiota community

structure may increase the predisposition to different disease phenotypes and cancer incidences, such as colorectal cancer, hepatic cancer, pancreatic cancer, chronic diarrhea, obesity, autism, allergy and inflammation (Carding *et al.*, 2015; Clemente *et al.*, 2012). The application of probiotics may mitigate these abnormal changes by performing beneficial functions like the amelioration of gut inflammation and enhancement of epithelial integrity (Hemarajata and Versalovic, 2012).

However, the phylogenetic analysis may sometimes fail to explain or correlate with the above adverse health outcomes, for reason that in clinical environment the microbial communities are extremely complicated and diverse among individuals and populations (Yatsunenکو *et al.*, 2012). In one study investigating the intestinal microbial composition of patients with severe obesity, decreased *Firmicutes/Bacteroidetes* ratio was identified (Schwiertz *et al.*, 2010). In another study with similar goal obesity was associated with a significant decrease at the level of alpha-diversity, fewer *Bacteroidetes*, more *Actinobacteria*, yet with no significant change of *Firmicutes* discovered (Turnbaugh *et al.*, 2009). Not consistently, in an investigation using both animal models and human feces samples, a decreased ratio of *Firmicutes/Bacteroidetes* was found to be associated with weight-losing diet (Jumpertz *et al.*, 2011). The disparities of these studies reflect a random competition amongst bacterial species, archaeal species, and various microbial eukaryotes living in mammal intestinal tracts (DiBaise *et al.*, 2012). Besides, birth-delivery modes, dietary history and administrative history of antibiotics could further complicate the gut-microbiota community structure (Jandhyala *et al.*, 2015; Nohr *et al.*, 2015). Accordingly, application of metagenomics analysis without auxiliary may not generate reliable results in assessing the influence of shift of gut-microbiota on host health.

Some transcriptomics and genomics-based studies have reported that gut-microbiome with different community structures may eventually result in comparable metabolic status (Gosalbes *et al.*, 2012). It seems that through the analysis of metabolites researchers could gain more reliable findings on the composition and function of gut-microbiota. The collection of these metabolites covers host-secreted regulatory molecules, gut-microbiota derived dietary metabolites, and the cell components of microbes such as lipoteichoic acid, lipopolysaccharide, peptidoglycan and nucleotide acids (Cunha *et al.*, 2012; Gareau *et al.*, 2010; Lebeer *et al.*, 2010). The major components of this metabolome are the metabolites derived from daily diets, such as indole derivatives, phenyl acids, fatty acids, secondary bile acids and neurotransmitters like melatonin, serotonin and gamma-amino butyric acid (Donia and Fischbach, 2015; Han *et al.*, 2014; Holmes *et al.*, 2012; Swann *et al.*, 2011). Through these functional components, a three-way reciprocal connection is established by gut-microbiota, host metabolism and environmental input. By analyzing the metabolic profiles of feces, researchers are able to reveal the association between gut-microbiota and adverse health outcomes (Calvani *et al.*, 2010; Qin *et al.*, 2010b). For example, one HT29/c1 and T84 colonic epithelial cell based study suggested that the domination of *Bacteroides* may lead to inflammation and cancer by increasing gut spermine oxidase (SMO) of enterotoxigenic *Bacteroides fragilis* (Goodwin *et al.*, 2011). SMO can be elevated by inflammatory stimuli or *Helicobacter pylori* (*H. pylori*) infection, and a high SMO level has been associated with the overproduction of reactive oxygen species (ROS) and DNA damage on gastric epithelium (Chaturvedi *et al.*, 2011; Handa *et al.*, 2010). *Bacteroides spp.* were found to be enriched by chlorpyrifos induced dysbiosis (Claus *et al.*, 2016). A recent mice study has demonstrated that the reduction of fecal bile

acid level in combination with elevated gut microbial microbial bile salt hydrolase (BSH), can modulate host lipid metabolism, cholesterol metabolism and eventually lead to weight loss, regardless of specific phylogenetic compositions (Joyce *et al.*, 2014). This finding is consistent with the observations on the subjects in human epidemic intervention studies, as well as the many observations on chickens and pigs (Guban *et al.*, 2006; Jones *et al.*, 2012; Smet *et al.*, 2007). High level of BSH has been found in many probiotic strains like *Lactobacillus*, *Bifidobacterium*, *Enterococcus*, *Clostridium* and *Bacteroides* spp., but is rarely seen in pathogen or opportunistic pathogens such as *Listeria monocytogenes*, *Enterococcus faecalis* and *Xanthomonas maltophilia* (Begley *et al.*, 2006). These findings have jointly indicated that a metabolite-based analysis of intestinal microbiota is reliable and trustable. Accordingly, some researchers have turned to the end products and metabolites of the gut-microbiota to investigate its influence on host health. Actually, there has been a long history for the compositional analysis of feces with the aim to examine host health. In an early work published in *Journal of Chromatography* (1975) done by George *et al.*, 6 indole and tryptophan derivatives were successfully extracted from 3 g rat feces for quantitatively analysis (Anderson, 1975). The concentrations of the metabolites measured in the samples included indole 4.5–7.8 µg/g, skatole 0–0.78 µg/g, indole-3-acetic acid 0.53–3.5 µg/g, indole-3-propionic acid 0.34–4.5 µg/g, tryptamine 0.17–1.7 µg/g, tryptophan 0.92–1.8 µg/g. In addition, indole-3-acetamide, tryptophol, indole-3-lactic acid, indole-3-acrylic acid, kynurenine and anthranilic acid fell out of the detection limit for quantitative analysis, though still detectable. Later in 1994, with the advancement of chromatography, Mogens *et al.* reported the measurement of indoles and skatole from 10 g pig feces using gas-chromatography (GC) (Jensen *et al.*, 1995). The lower limit of

detection (LLOD) for indole and 3-methylindole was both 20 µg/kg, largely below the values typically found in intestinal contents by biochemical measurement (100 mg/kg). On the other hand, the fecal levels of skatole and indole were 2.3 µg/g and 10 µg/g via high-performance liquid chromatography (HPLC) based method, but the recoveries were lower than GC method (Claus *et al.*, 1993).

2.1.4 Birth of metabolomics

In 1999, Jeremy K. Nicholson, John C. Lindon and Elaine Holmes, three biochemists from Imperial College of Science, Technology and Medicine, University of London, together published the first metabolomics study on the journal *Xenobiotica*, in which “Metabolomics” is defined as “*the quantitative measurement of the dynamic multi-parametric metabolic response of living systems to pathophysiological stimuli or genetic modification*” (Nicholson, 2006). Ten years later, the complete concepts of the metabolomics, as well as metabolome wide association study (MWAS), was formally forged by the same group of researchers (Holmes *et al.*, 2008). As an approach of analysis, metabolomics usually acquires data via gas or liquid chromatography combined with detectors like diode array detector (DAD), fluorescence detectors (FLD), electron capture detector (ECD), mass-spectrometer (MS) and nuclear magnetic resonance spectroscopy (NMR) etc., and the generated data are processed with thoughtful biostatistics and database-leveraging bioinformatics methods to extract useful information regarding biological effects and changes (Byrne *et al.*, 2015; Wishart *et al.*, 2007b). A broader detective scope could be achieved by combining data collected through different platforms, since the “next-generation” MS are constructed using a variety of ionization sources,

selectors, detectors and analyzers, such as electrospray ionization (ESI), atmospheric pressure chemical ionization (APCI), electron ionization (EI), chemical ionization (CI), triple quadrupole, time-of-flight detector, orbitrap, fourier-transform ion cyclotron resonance and so on (Dettmer *et al.*, 2007). In the last decade, metabolomics has been boosted by the introduction of ultra-high performance liquid chromatography (UHPLC), which is able to achieve efficient separation of mixed compounds with outstanding peak shape and accuracy, and enhance the signal-to-noise ratio (S/N) (Nordstrom *et al.*, 2006). Different with genomics, transcriptomics and proteomics, the principal task of metabolic profiling and metabolomics is to look at the final phenotype side of a biological process or event. The advantage of metabolomics includes its non-invasive sampling method, convenient sample preparation, and preclinical diagnosis of drug toxicity and disease/pre-disease conditions (Kildegaard *et al.*, 2013; Schmidt, 2004). The five most important key steps for metabolomics study include: comprehensive understanding on the study design and purpose, complete master of the instrumental platform of metabolomics study, case-to-case optimization of sample pre-treatment, raw data processing, and the strategies used for data analysis.

Currently, both bottom-up untargeted metabolomics and top-down targeted metabolomics approaches are widely used. In mass spectrometry (MS)-based bottom-up untargeted metabolomics, no standard would be spiked in the beginning except for internal standards. Since the MS analysis is untargeted, there would be a large amount of ion peaks detected. These peaks would be filtered, deconvoluted and aligned using processing modules such as online XCMS or offline MZmine (Huan *et al.*, 2017; Pluskal *et al.*, 2010). The attribution of detected feature ions is based on fragmentation spectrum (GC/MS),

accurate mass (LC/MS), retention time and reference tandem mass spectrometry (MS/MS) data, all of which can be found by open-access data bases such as Human Metabolome Database (HMDB), massBank and METLIN, or trustable literatures (Smith *et al.*, 2005; Wishart *et al.*, 2007a). Through statistical modeling and analysis, usually 10–15 key metabolites would be retained from a data pool of several thousands of feature ions. This untargeted metabolomics workflow could help gain insights into the global metabolic changes in the biological system and discover the “black matters” that have never been characterized (Peisl *et al.*, 2017).

Regarding top-down metabolomic analysis, triple quadrupole (QqQ, or TsQ) LC-MS based targeted metabolomic workflow is the mostly employed instrument (Lu *et al.*, 2008; Yuan *et al.*, 2012). In such practice, standard compounds for the metabolites of interest are first used to set up selected reaction monitoring (SRM) library based on retention time and ion pair transition. Instrument voltages used for ionization and parent-product fragmentation are determined and response curves are optimized for absolute quantification. Global metabolites are usually extracted from tissues, biofluids or cell cultures using either general methods or the strategies that can enhance the detection of certain metabolites. Top-down approach is aimed to concisely assess certain metabolic pathways (Bajad *et al.*, 2006; Lu *et al.*, 2008; Lu *et al.*, 2010).

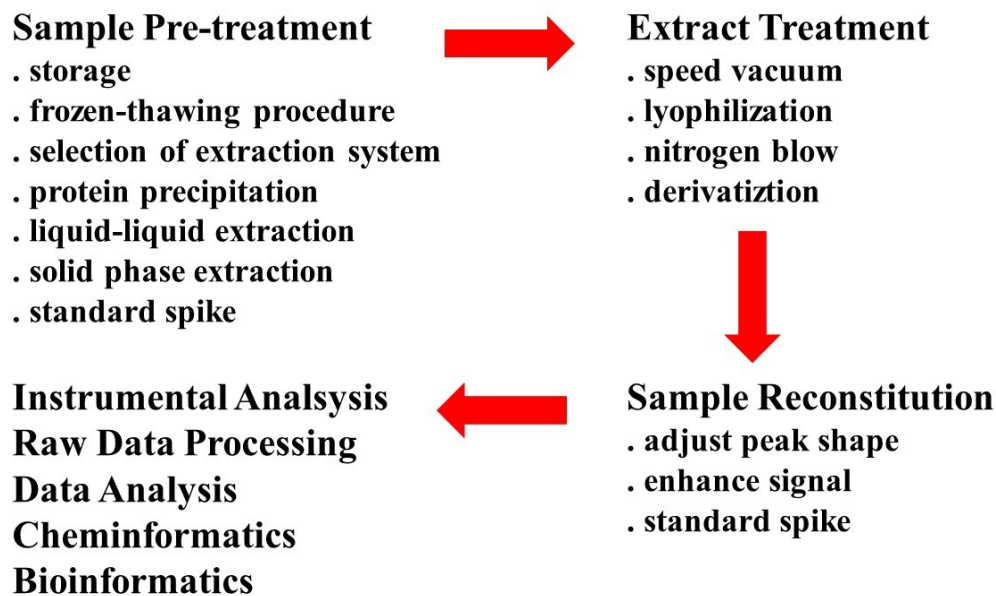


Figure 2-2. General workflow of metabolomic analysis.

2.1.5 Application of metabolomics to the analysis of gut-microbiota

Fecal metabolomics is considered to be a non-invasive way and proxy to qualify or quantify gut-microbiota dependent metabolites, therefore to assess the metabolic condition of gut-microbiota and predict its impacts on host health (Wikoff *et al.*, 2009). For example, significant shift of gut-microbiota dependent metabolome has been found in the patients with Crohn's Disease (CD) by using metabolomics techniques (Jansson *et al.*, 2009; Willing *et al.*, 2010). The potential impacts of this metabolic shift on host include disruptions of tyrosine catabolism, bile acid metabolism, fatty acid biosynthesis, prostaglandin metabolism, as well as the metabolisms of tyrosine, tryptophan and phenylalanine. In addition to these house-keeping metabolisms, many findings have shown that gut-microbiota dependent metabolome may significantly influence host neurophysiology and behaviors (Anderson and Maes, 2015; Daulatzai, 2015; de Magistris

et al., 2016; Hemarajata and Versalovic, 2012; Hsiao *et al.*, 2013). This is not surprising, since in human ~90% percent of serotonin is synthesized in gut from diet (Yano *et al.*, 2015). In germ-free mice, or the mice depleted of gut-microbiota, researchers have observed substantial alterations in the behaviors and the neuropathology that are associated with neurodevelopmental, psychiatric and neurodegenerative disorders (Sampson and Mazmanian, 2015). It seems the components of gut-microbiota dependent metabolome have significant influence on other organs and systems, yet this metabolite pool has not been thoroughly investigated so far. The purpose of current review is thus to review the primary metabolites shown in the intestine metabolome in order to better interpret the data collected from metabolomics.

2.1.6 Gut-microbiota dependent metabolites

2.1.6.1 Indole and indole derivatives in tryptophan pathway

Indole is a widely studied aromatic heterocyclic organic compound that is normally present in human feces at a concentration ranging from 0.25 to 1.2 mM (Karlin *et al.*, 1985). In human gut, a notable quantity of indole and derivatives are produced by gut-microbiota. They serve as intercellular, interspecies and interkingdom signaling molecules (Akiyama *et al.*). Indole acetic acid is one of such indole derivatives. It can be produced from aromatic and branched-chain amino acids by *Enterobacter cloacae* (Leyn *et al.*, 2016). Indole acetic acid is a major precursor of skatole (3-methyl indole)—a mildly toxic white crystalline organic compound belonging to the indole family. Skatole occurs naturally in feces, produced from tryptophan in the mammalian digestive tract, and has a strong fecal odor (Schmid-Schonbein and Delano, 2009). Tryptophan, a well-known precursor of the

neurotransmitter serotonin, can be generated from indole by gut-microbiota (Pandey *et al.*, 2013). The biosynthesis of tryptamine generally proceeds from tryptophan pathway. Tryptamine is the pivot precursor molecule of many hormones and neurotransmitters which are tryptamine derivatives. The most well-known tryptamine derivatives are serotonin, an important neurotransmitter, and melatonin, a hormone involved in regulating the sleep-wake cycle (Mozaffari *et al.*, 2010).

Indole is also known to be able to modulate intestinal epithelial metabolism by regulating incretin peptide glucagon-like peptide-1 (GLP-1) (Drucker and Nauck, 2006). It can widen the action potential of enteroendocrine L cells and result in the influx of extracellular calcium and the exocytosis of GLP-1 loaded vesicles. GLP-1 is known to inhibit glucagon release and stimulate insulin release, thus lower blood glucose. Prolonged exposure to indole may inhibit ATP production and GLP-1 secretion (Chimerel *et al.*, 2014).

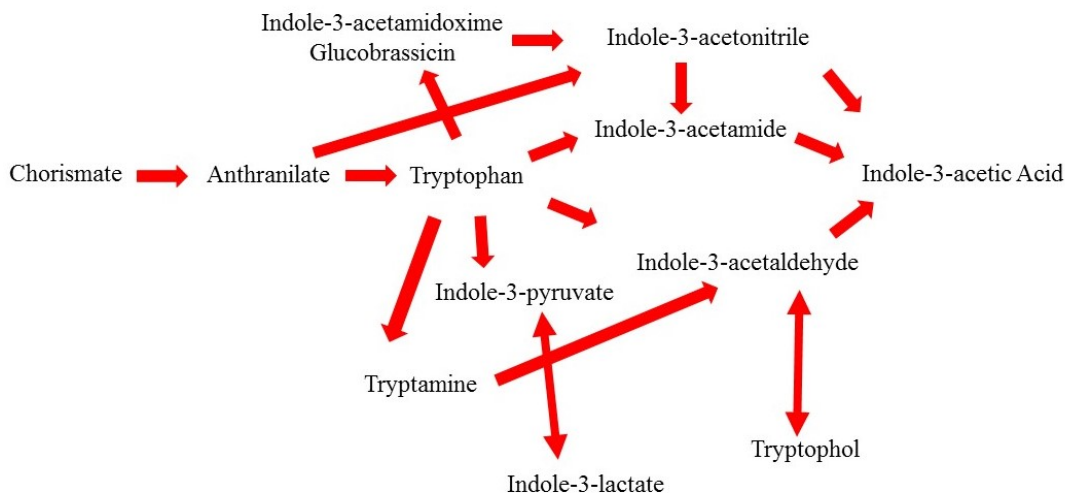


Figure 2-3. General metabolic links of indole derivatives. The structures are not intended to convey any stereochemical information.

Lee *et al.* found that the bacterial biofilm formation of *E. coli* O157 : H7 can be reduced by 83% by indole and 90% by 7-hydroxy indole (Lee *et al.*, 2007). Indole-3-acetaldehyde can be largely generated by intestinal *Rhodococcus sp.* BFI 332, and was reported to inhibit *Escherichia coli* O157: H7 biofilm formation (Lee *et al.*, 2012). Some indole derivatives like indole-3-acetic acid (IAA), carry with anti-pathogen activity (Spaepen *et al.*, 2007). Kazuhiko *et al.* have proposed that the molecular size of indole derivative is a primary factor determining the their inhibitory effect on pathogens—higher activity was observed when the substitute moeity is of smaller molecule size (Matsuda *et al.*, 1998).

In clinical medicine, indole and derivatives are frequently co-administered with non-steroidal anti-inflammatory drugs (NSAIDs). Indole and derivatives are able to reduce the generation of reactive oxidative species (ROS), and therefore enhance the efficiency of NSAIDs (Wallace, 2012). Indole-3-propionic acid (IPA) has shown significant mitigating and preventive effects on neuro damage by reducing ROS. The cell death and damage of primary neurons caused by ROS is one of the most prominent neuro-pathologic features of Alzheimer's disease (Guzior *et al.*, 2015). IPA is also an inhibitor of beta-amyloid fibril formation and a potent neuro-protectant against oxidotoxins (Chyan *et al.*, 1999). Amyloids are abnormal fibrous, extracellular, proteinaceous deposits found in organs and tissues. They are insoluble and are structurally dominated by β -sheets with no common primary structure. The accumulation of amyloids in neuron system is associated with amyloidosis (Glennner, 1980; Haass and Selkoe, 2007). These diseases include Alzheimer's, the spongiform encephalopathies and type II diabetes (Rambaran and Serpell, 2008). Indole-3-acetamide (I3A) is the intermediate metabolite in the conversion from tryptophan

to indole-3-acetic acid. I3A is an antioxidant reagent and also inhibitor of phospholipases A2. The latter enzymes function to release fatty acids from the second carbon group of glycerol, and mice deficient in sPLA2 isoenzymes have shown less atherosclerosis formation (Gao *et al.*, 2013).

Indole-3-carbinol (I3C) is a hydrolysis product of glucobrassicin, a compound that is of large amount in a number of vegetables of the Brassica genus such as cabbage (0.1–1.9 mmol/kg), cauliflower (0.1–1.6 mmol/kg), and brussels sprouts (0.5–3.2 mmol/kg) (Bjeldanes *et al.*, 1991). I3C is known to be a dietary modulator of carcinogenesis, showing the potential to be used as chemoprevention agent. Data have also shown that, with sufficient administration before carcinogen exposure, both the incidence of neoplasia and the formation of covalent adduct of carcinogen with DNA were reduced (Fujioka *et al.*, 2016). The functionality might be achieved through the binding activity of I3C with aryl hydrocarbon receptor (Chen *et al.*, 1996). In fact, as early as last 80s, Wattenberg *et al.* have already shown that I3C can suppress 7,12-dimethylbenz(a)anthracene-induced mammary tumor formation in female Sprague-Dawley rats and on benzo(a)pyrene-induced neoplasia of the forestomach in female ICR/Ha mice (Wattenberg and Loub, 1978). In addition, I3C has also shown regulatory effects on estradiol metabolism and can inhibit spontaneous mammary tumors in mice (Bradlow *et al.*, 1991). The National Institutes of Health (NIH) has reviewed indole-3-carbinol as a possible cancer preventive agent in last 90s and had supported its using for breast and colon cancer prevention (Greenwald, 2004; Murillo and Mehta, 2001). The mechanism of the above anti-tumor function was further uncovered in the last decade by Chen *et al.* (Chen *et al.*, 1996). Their follow-up study reported that indole-3-carbinol and its metabolite 3,3'-diindolymethane (DIM) target

multiple aspects of cancer cell cycle regulation and survival including Akt-NF κ B signaling, caspase activation, cyclin-dependent kinase activities, estrogen metabolism, estrogen receptor signaling, endoplasmic reticulum stress and BRCA gene expression (Weng *et al.*, 2008). They have also found that indole-3-carbinol may inhibit tumorigenicity of hepatocellular carcinoma cells via suppression of microRNA-21, including miR-21 and miR-221 and miR-222, and the upregulation of phosphatase and tensin homolog (PTEN/AKT pathway) *in vivo* and *in vitro* (Deng *et al.*, 2015). In another study in mice with high-fat-diet-induced obesity, I3C administration was found to decrease the body weight, fat accumulation and infiltrated macrophages in epididymal adipose tissue. The reductions were associated with improved glucose tolerance and with modulated expression of adipokines, lipogenic-associated gene products such as acetyl coenzyme A carboxylase and peroxisome proliferator-activated receptor- γ (Chang *et al.*, 2011). Indole-3-acetonitrile was also abundant in cruciferous vegetables such as cabbage, cauliflower, broccoli, and brussels sprouts, in addition to the metabolic generation in the indole pathway. Studies have found that indole-3-acetonitrile can prevent tumor development in various animal models primarily by upregulating cytochrome P450 enzymes (Wattenberg and Loub, 1978).

Some biological effects of indole derivatives discovered in animal models or cell cultures may not apply to human. It was found in dogs with acute diarrhea that the serum concentrations of kynurenic acid, together with urine concentrations of 2-methyl indole and 3-formyl-5-methoxy indole, were all significantly decreased (Probert *et al.*, 2004; Tuomola *et al.*, 1996). However, no human evidence has been collected. In an early study, indole-3-acrylic acid was found to be able to inhibit the growth of mycelia of neurospora

crassa and cause accumulation of indoleglycerol phosphate in cultured cells (Matchett, 1972). But no obvious physiological function of indole-3-acrylic acid has been observed in human by now.

2.1.6.2 Tryptophan metabolism

Kynurenine and derivatives are major metabolites produced in tryptophan metabolic pathway and are considered to be beneficial to human health. Kynurenine can be generated by gut-microbial tryptophan dioxygenase and indole amine 2,3-dioxygenase (Kennedy *et al.*, 2017). In human body, the former is synthesized primarily, but not exclusively in the liver, and the latter is synthesized in many tissues in response to various immune activation (Jaspersen *et al.*, 2009). Kynurenine and its metabolic products have diverse biological functions, including dilating blood vessels during inflammation, and regulating the immune response (Qin *et al.*, 2010b). Epidemiological data have indicated that in lung cancer patients, serum kynurenine level is significantly higher than the healthy population (Suzuki *et al.*, 2010). Besides, evidence has suggested that the increase of kynurenine may alleviate the depressive symptoms that are caused by interferon therapy for hepatitis C (Gambhir *et al.*, 2012).

Kynurenine plays important roles in a variety of psychological processes (Lovelace *et al.*, 2016). Abnormal neuroactive metabolites of kynurenine have been closely linked to neurodegenerative diseases. For example, cognitive deficits in schizophrenia are associated with the dysfunctions of the enzymes that break down kynurenine (Muller *et al.*, 2011). Kynurenine production was found to be increased in Alzheimer's disease and is positively associated with the cognitive deficits and depressive symptoms with the disease

progression (Baran *et al.*, 1999). Dysfunctional state of kynurenine pathway, which may induce abnormal alteration of kynurenine, kynurenic acid, quinolinic acid, anthranilic acid, 3-hydroxykynurenine levels in gut, has been described for a number of disorders related with the above discussion (O Watzlawik *et al.*, 2016).

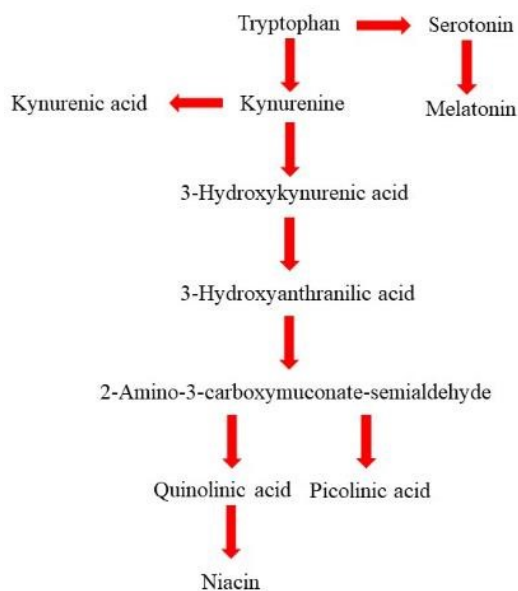


Figure 2-4. General metabolic links of tryptophan. The structures are not intended to convey any stereochemical information.

Quinolinic acid (QUIN or 2,3-Pyridinedicarboxylic acid) is a neuroactive metabolite generated in tryptophan pathway. QUIN is an agonist of N-methyl-D-aspartate (NMDA) receptors NR2A/B and is also considered to be an excitotoxin. As an endogenous neurotoxin with multiple target receptors, QUIN is implicated in the pathogenesis of a variety of human neurological diseases. In fact, QUIN is normally presented in nano molar concentrations in human brain and cerebrospinal fluid (CSF) (Davies *et al.*, 2010). Although QUIN can be specifically degraded by quinolinate phosphoribosyltransferase (QPRT), the enzyme is usually of low efficiency and is saturated rapidly (~300 nM). Accordingly, extra QUIN can continue stimulating NMDA receptor. This is different with

the uptake systems of glutamate and aspartate, the latter two metabolites are of same active level with QUIN yet they have fast uptake system available to remove them from neuro synapse (Choi, 1988). In general, QUIN neurotoxicity is considered to lead to presynaptic receptors, energetic dysfunction, oxidative stress, transcription factors, cytoskeletal disruption, behavior alterations and cell death (Lugo-Huitron *et al.*, 2013).

Serotonin (5-hydroxytryptamine, 5-HT) and melatonin are two important neurotransmitters produced in the kynurenine pathway, and show multiple hormonal bioactivity like sleep circle regulation, anti-oxidant and immune-modulation (Chowdhury and Maitra, 2012). Akihiko *et al.* have proven that melatonin is capable of reducing the susceptibility of the fetal rat brain to oxidative damage of lipids and DNA in rat model of fetal ischemia/reperfusion (Wakatsuki *et al.*, 1999). It has also been found that microbial strains containing tryptophan catabolism enzymes can be enriched in the disease-associated microbial community (DMC), including *Pseudomonas*, *Xanthomonas*, *Burkholderia*, *Stenotrophomonas*, *Shewanella*, *Bacillus*, *Rhodobacteraceae*, *Micrococcaceae* and *Halomonadaceae* (Vujkovic-Cvijin *et al.*, 2013). Abnormal 5-HT release after meal is associated with some postprandial symptoms that are accompanied with the irritable bowel syndrome (IBS) (Bearcroft *et al.*, 1998). Following the deterioration of intestinal ecology, the disruption of serotonin and melatonin synthesis may lead to sleepy disorder and immune deficiency.

2.1.6.3 Glutamate metabolism

Glutamate is the biological precursor of gamma-amino butyric acid (GABA). Glutamate is synthesized from the non-essential amino acid glutamine, and glutamate is converted into GABA by the enzyme glutamate decarboxylase. Glutamate decarboxylase uses Vitamin B6 as a cofactor (Peng *et al.*, 1994). David R Wise and Craig B Thompson have recently brought out a viewpoint that a restriction of dietary glutamine can be an effective cancer therapy. The perspective is based on the observations of the addiction that cancer cell lines that display to glutamine. Actually, in many cancer cell lines, glutamine was found to be the primary mitochondrial substrate maintaining mitochondrial membrane potential, integrity and the NADPH production (Wise and Thompson, 2010).

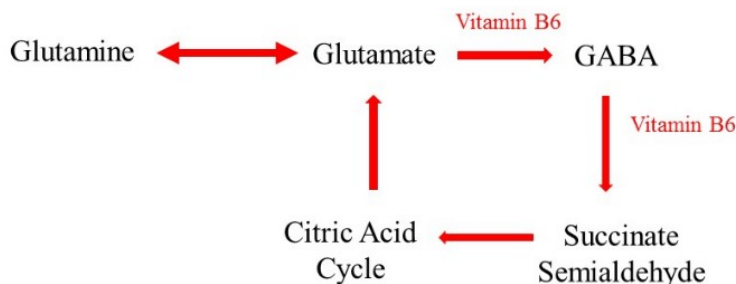


Figure 2-5. Metabolic pathway of glutamate. The structural representations provided are not intended to convey any stereochemical information.

GABA can be generated from glutamate pathway. As an inhibitory neurotransmitter, GABA functions to calm nervous activity, a reason why the anti-anxiety drugs like Valium and Xanax achieve functionality by targeting GABA receptors (Streeter *et al.*, 2012). Interestingly, John *et al.* have found that *Lactobacillus rhamnosus*, a common bacterium in human GI tract, can be passed to the intestine of rodent pups from dams

through the birth canal but not cesarean section. This strain is known to secrete a high intensity of GABA (Bravo *et al.*, 2011).

2.1.6.4 Phenyl acid and derivatives

Most phenyl acids and derivatives are harmful metabolites generated from phenylalanine. They were found to disrupt renal clearance and brain function (Smith *et al.*, 1945). Phenylalanine is a large, neutral amino acid which is capable of passing the blood-brain barrier (BBB) via the large neutral amino acid transporter (LNAAT) (Pietz *et al.*, 1999). Excessive phenylalanine in the blood may saturate the transporter and decrease the levels of other LNAAs, and further disrupts brain development in infants.

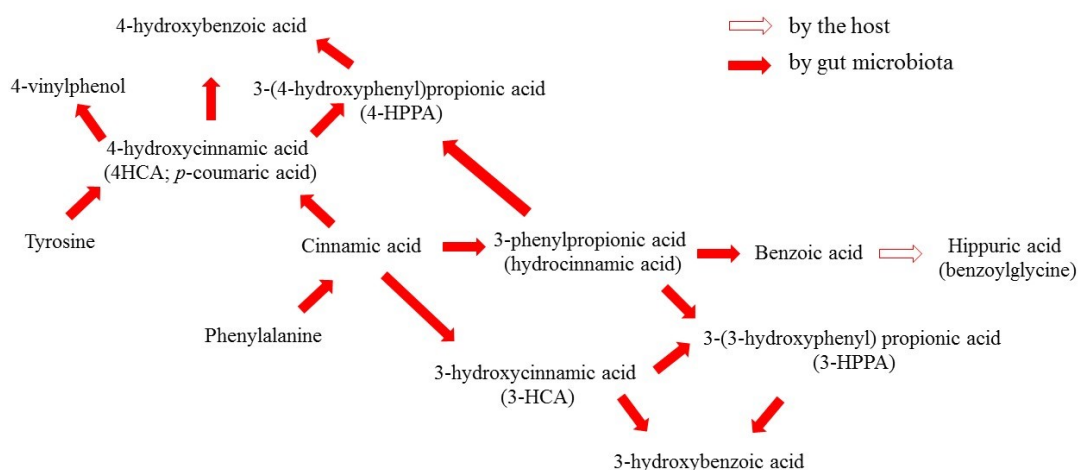


Figure 2-6. General metabolic links of phenylalanine and tyrosine. The structural representations provided are not intended to convey any stereochemical information.

Phenyl acetic acid and phenyl propionic acid are formed from the metabolism of phenylalanine by anaerobic bacteria (Clayton, 2012). The most well-known microbial mediated conversion of phenylalanine to phenylacetic acid is from phenylalanine to phenylpyruvic acid, and then to phenylacetic acid. On the other side, the conversion of tyrosine to *p*-cresol is first through tyrosine to 4-hydroxy phenyl pyruvic acid, and then to

4-hydroxyphenylacetic acid and *p*-cresol. In human, phenylacetic acid and *p*-cresol are further degraded into phenylacetylglutamine and *p*-cresol sulfate, respectively.

Phenylpyruvic acid is a pivot intermediate in several metabolic pathways. Besides, pyruvic acid can be produced from glucose through glycolysis, and can also be converted back to carbohydrates via gluconeogenesis (Dashty, 2013). Alternatively, pyruvic acid can be converted back to fatty acids through a reaction with acetyl-CoA (Williamson, 1967). Therefore, the endogenous concentration of phenylpyruvic acid might vary largely, depending on the global metabolic balance. Due to the accumulation of phenylacetic acid and phenylpyruvic acid, a “musty” odor of skin, hair, sweat, and urine might be generated, together with a tendency to hypopigmentation and eczema (Jiang *et al.*, 2008). It was also noticed that the neural-developmental disruption of phenylketonuria is primarily caused by the block of neurotransmitter synthesis. In detail, the path from phenylalanine to tyrosine is blocked because of the deficiency of phenylalanine hydroxylase, thus that the generation from tyrosine to melanin and dopamine is obstructed. Early this century, the National Institutes of Health Consensus Development Conference announced the need for more research on PKU to replace the therapy based on a simple dietary restriction (Panel, 2001). Among other suggestions were the practice of standard screening procedures: infants with blood phenylalanine levels greater than 10 mg/dL should be started on treatment within 7 to 10 days after birth. Appropriate treatment should be multidisciplinary with a lifelong duration.

2.1.6.5 L-Tyrosine to p-Cresol

p-Cresol is one of the major metabolites generated from tyrosine and to a certain extent it can also be produced during the catabolism of phenylalanine. In the latter pathway, phenylalanine is converted to 4-hydroxyphenyl acetic acid by intestinal bacteria and then decarboxylated to *p*-cresol (Vanholder *et al.*, 1999). The major contributing bacteria in this process are aerobes, mainly *Enterobacteria*, but anaerobes such as *Clostridium perfringens* may also take a producing role.

Specifically, *p*-cresol is a uremic toxin that is at least partially removed by peritoneal dialysis in haemodialysis patients and has been involved in the progression of renal failure. It was reported that 1 µg/g phenol and 50 µg/g *p*-cresol were detected from 0.45 to 0.55 g feces by using HPLC method (King *et al.*, 2009). *p*-Cresol has been reported to carry with several physiological functions: (1) diminishing the oxygen uptake of rat cerebral cortex; (2) increasing concentration of warfarin and diazepam of the free active form; (3) inducing growth retardation in the weanling pig; (4) altering cell membrane permeability of bacteria; (5) inducing lactate dehydrogenase (LDH or LD) leakage from rat liver; (6) causing susceptibility to auditive epileptic crisis; (7) blocking cell K⁺ channels.

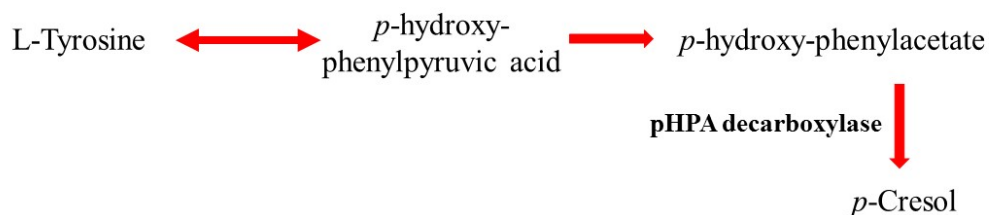


Figure 2-7. General metabolic links between L-tyrosine and *p*-Cresol. Structural representations provided are not intended to convey any stereochemical information.

The accumulation of 4-hydroxyphenylpyruvic acid is known to induce tyrosinemia type III like syndrome, an autosomal recessive disorder featured by elevated levels of blood tyrosine and massive excretion of tyrosine derivatives into urine (Tomoeda *et al.*, 2000). The 4-hydroxyphenylpyruvic acid dioxygenase (HPD) catalyzes 4-hydroxyphenylpyruvic acid into homogentisic acid in the tyrosine catabolism pathway. It has been shown that hawkinsinuria, an autosomal dominant disorder characterized by the excretion of “hawkinsin” may also be resulted by HPD deficiency (Endo *et al.*, 1995).

2.1.6.6 *Bile acids and secondary bile acids*

The major members of bile acids and secondary bile acids include cholic acid, chenodeoxycholic acid, α -muricholic acid, β -muricholic acid, hyocholic acid, deoxycholic acid (DCA), ω -muricholic acid, lithocholic acid, ursodeoxycholic acid and hyodeoxycholic acid. They are the steroid acids secreted by liver which are then stored in the bile of most vertebrates. Bile acid synthesis is operated by a class of liver cells, in which primary bile acids were synthesized via a multi-step process mediated by cytochrome P450 (Bjorkhem *et al.*, 1999). Different molecular forms of bile acids can be synthesized in the liver by different species. For human, cholic acid and chenodeoxycholic acid are the primary bile acids secreted in such cells (Parks *et al.*, 1999). It was estimated that on average, approximate 600 mg of bile salts are synthesized daily to replace bile acids lost in the feces (Wilson and Dietschy, 1972). Bile acids and neutral sterols are of interest due to the fact that they are of steric similarity to carcinogenic polycyclic aromatic hydrocarbons (Conney, 1982). Patrice *et al.* have reported an observation on the shift of gut-microbiota community structure caused by high fat diet in mice, consequently leading to the expansion of

deoxycholic acid-producing bacteria *Clostridium XI*. Once over generated, deoxycholic acid could induce a phenotypic change in hepatic stellate cells to secrete pro-inflammatory cytokines and eventually facilitates hepatocellular carcinoma (Cani *et al.*, 2007).

2.1.6.7 Vitamins and probiotics

The most featured benefit of gut probiotics—microorganisms that are believed to provide health benefits when consumed—is the production and provision of vitamins. Vitamins are essential micronutrients functioning as cofactors of the various enzymes. A routine exogenous supply of vitamins is necessary, because humans are incapable of synthesizing most vitamins. Since vitamins are involved in all the biochemical reactions in cells, they are necessary for the generation of many metabolites. For example, vitamin B6 (pyridoxine, pyridoxal and pyridoxamine) are necessary cofactors in the conversion of glutamate to GABA and further from GABA to succinic acid. In human it has been well documented that gut-microbiota are able to synthesize most of the water-soluble B vitamins, such as biotin (VB 6), cobalamin (VB 12), folates (VB 9), niacin (VB 3), panthotenic acid (VB 5), pyridoxine (VB 6), riboflavin (VB 2) and thiamine (VB 1). In contrast to the uptake of dietary vitamins that occurs in small intestine, the predominant absorption of microbial produced vitamins was in the colon (LeBlanc *et al.*, 2013). This portion of microbial produced vitamins is very necessary in maintaining routine need of vitamins, in that sometimes the deficiency of dietary vitamins can be resulted by insufficient food intake. Oral administration of fermented milk product that contains lactic acid bacteria is an effective way to supply B-group vitamins (LeBlanc *et al.*, 2011).

Generally speaking, there are two major genera of vitamin-producing intestinal microbiota: *Bifidobacterium* and *Lactobacilli* (Arena *et al.*, 2014). The genus *Bifidobacterium*, normally called *Lactobacillus bifidus*, encompasses 39 species. *Bifidobacterial* species can convert a number of dietary compounds to health-promoting bioactive molecules, such as conjugated linoleic acid and B vitamins. *Lactobacilli* species are known as vitamin and folate producers. This genus contains over 100 identified species of a remarkable phylogenetic, phenotypic and ecological diversity. The genetic characterization of *Lactobacilli* is much clearer than that of *Bifidobacteria*, but the molecular mechanisms driving their interaction with the human gut also remain largely unknown. Folate biosynthetic properties of *Bifidobacteria* have been well characterized. It was found that the folate biosynthesis appears to be restricted to certain species/strains. *Bifidobacterium bifidum* and *Bifidobacterium longum subsp. infantis* are known to be high level folate producing strains, whereas *Bifidobacterium breve*, *Bifidobacterium longum subsp. longum* and *Bifidobacterium adolescentis* are known to be low level folate-producing species.

Eight B group vitamins are reportedly generated by gut microbiota and the specific strains that can produce these vitamins have been well examined (Magnusdottir *et al.*, 2015). Riboflavin (VB 2), folate (VB 9) and cobalamin (VB 12), increased levels of other B-group vitamins like niacin (VB 3) and pyridoxine (VB 6), have been reported for certain LABs that appear in yoghurt, cheese and other types of fermentations. Elevated levels of thiamine (VB 1) and pyridoxine were found as a result of soy fermentation with *Streptococcus thermophilus* ST5, *Lactobacillus helveticus* R0052 or *B. longum* R0175. *Lactobacillus reuteri* CRL1098 was shown to be the first *Lactobacillales* (lactic acid

bacteria, LAB) strain that is able to produce a cobalamin-like compound. However, the biological activity of this pseudo vitamin B12 is still not clearly examined.

Vitamin K is featured by its antioxidant characteristic that scavenges free radicals with high efficiency (LeBlanc *et al.*, 2013). In fact, one study has shown that the antioxidant activity of vitamin K can protect against fetal brain injury. Bacteria in the gut flora can also convert K1 into vitamin K2. Certain gut microbiota can modify the isoprenoid side chain of vitamin K2 and produce a range of vitamin K2 forms. In fact, all forms of K2, other than MK-4, can only be produced by bacteria (Marques *et al.*, 2010).

2.1.6.8 Bacterial signaling molecules

Microbial signaling molecules are certain small diffusible molecules secreted by microbes, and function as sensor to the local environmental conditions and also regulator to synchronize multicellular behaviors (Lee and Lee, 2010). It has been well characterized that gram-positive bacteria can regulate gene expression at the population level via a molecule signaling system known as quorum sensing. The system is mediated by two-component systems (BceRS, LiaRS, PsdRS and YxdJK) and extracytoplasmic function σ factors (σ_M , σ_W and σ_X). This system has been widely investigated in both the *Firmicutes* (low genome GC percentage) and *Actinobacteria* (high genome GC percentage) branches of gram-positive bacteria.

Compared with other microbial strains, the signaling molecules identified in *Bacillus subtilis* have been studied more deeply. The identified molecules include: (1) a modified 5- to 10-amino-acid peptide called ComX; (2) lantibiotic peptides such as subtilin; (3) unmodified pentapeptide Phr peptides, including PhrA, PhrC, PhrE, PhrF, PhrG, PhrH,

PhrI, and PhrK. Phr family of extracellular signaling peptides of are extracellular signaling peptides that are identified in Gram-positive bacteria; (4) Tprs is a kind of signaling molecule which works with internalized Phr-like peptides (Pottathil and Lazazzera, 2003). The regulatory mechanisms of the related genes are poorly documented and thus calls for more explorations. Environmental input molecules are known to regulate gut microbiota through manipulation on such molecules. For example, glucose can inhibit expression of the Phr-like peptide gene via catabolic repression, further leading to elevated production of bacteriocin.

Autoinducer-2 (AI-2) is a furanosyl borate diester that functions as important signaling molecule in both gram-negative and gram-positive bacteria. The elevation of AI-2 can be induced by 1-deoxy-3-dehydro-D-ribulose with boric acid and is recognized by the two-component sensor kinase LuxPQ in Vibrionaceae.

2.1.6.9 LAB bacterial metabolites

Phenyl lactic and hydroxyphenyl lactic acids have also been found to be the major metabolites involved in the formation of cheese flavour and produced by LAB strains through phenylalanine (Phe) and tyrosine (Tyr) degradation, respectively. 3-hydroxylated fatty acids are mainly generated from *Firmicutes* LAB, covering any fatty acid with a hydroxy functional group in the β - or 3-position. β -Hydroxy fatty acids accumulate during cardiac hypoxia and can also be used as chemical markers of bacterial endotoxins.

Phenethyl amine can be generated by *Firmicutes* LAB. Phenylethylamine functions as a monoaminergic neuromodulator and a neurotransmitter in the human central nervous system (Zhang *et al.*, 2017). It is derived from the amino acid L-phenylalanine through an

enzymatic decarboxylation via the enzyme aromatic L-amino acid decarboxylase. Phenethylamine is mainly metabolized in the small intestine by monoamine oxidase B (MAO-B) and aldehyde dehydrogenase (ALDH), finally converting it to phenylacetic acid. Phenethylamine is also found in many other organisms and foods, especially the foods processed with various microbial fermentation. In clinics, phenethylamine is sold as a dietary supplement for increasing mood, focus, energy and losing weight.

2.1.6.10 *Inflammatory factors and lipid oxidation secondary products*

Reactive oxygen species (ROS) are chemically reactive chemicals containing oxygen, such as peroxides, superoxide, hydroxyl radical, singlet oxygen and so on. It has been recognized that the major sources of ROS include mitochondria, NADPH oxidase and 5-lipoxygenase. Plus, ROS can also be generated in many subcellular compartments by oxidases, peroxidases, mono-/di-oxygenases, P450 superfamily, lysyl oxidase and peroxisomal oxidases, which generally include glycolate oxidases, D-amino oxidases, ureate oxidases, fatty acid-CoA oxidases and L- α -hydroxyacid oxidases.

The production and accumulation of ROS in human body can occur in response to ultraviolet radiation, cigarette smoking, alcohol, nonsteroidal anti-inflammatory drugs, ischemia-reperfusion injury, chronic infections and inflammatory disorders. The appearance of ROS within the gastrointestinal (GI) tract is associated with the occurrence of various GI diseases, e.g. peptic ulcers, gastrointestinal cancers and inflammatory bowel disease, but the roles taken by ROS in the pathogenesis have not been well established (Bhattacharyya *et al.*, 2014).

Fecal ROS contents can be measured by using HPLC, yet a strict quenching process during the sample pretreatment step is needed (Owen *et al.*, 2000). Some studies have successfully correlated fecal ROS level with biased dietary habit, disorder of colorectal function and intestinal bowel disease (Orozco *et al.*, 2011). In fact, despite the protective barrier provided by the mucosa, certain food contained toxins, such as mycotoxins or microbial pathogens, can induce oxidative burst and cause inflammation in the epithelium. The pathogenesis of various GI diseases, including peptic ulcers, gastrointestinal cancers and inflammatory bowel disease, are partly due to this reason (Bhattacharyya *et al.*, 2014).

A variety of toxic lipid aldehydes are known to be generated in the peroxidation process of lipid layer. They mainly belong to the α , β -unsaturated reactive aldehyde class, such as malondialdehyde (MDA), 4-hydroxy-2-nonenal (4-HNE), 2-propenal (acrolein) and isoprostanes. Compared with the above discussed free radicals, these aldehydes are much more stable and can diffuse far away from the site of the origin. Some of these aldehydes have been shown oxidative reactivity with various biomolecules, including proteins, DNA, amino acids and phospholipids. Modification of amino acids by reactive aldehydes primarily occurs on the nucleophilic residues Cys, His and Lys. 4-HNE (4-hydroxy-2-nonenal) is a widely studied reactive aldehyde which has been proven as a cytotoxic and genotoxic lipid oxidation secondary product. It can be formed through either microbiota or endogenously upon peroxidation of cellular n-6 fatty acids. 4-HNE showed tight connection with microbial derived nitrosamine. It was found this metabolite can form mitochondrial protein, DNA or lipid adducts in cancer development, thus can serve as early biomarker of CRC (Deng *et al.*, 2015; Keller *et al.*, 2015; Surya *et al.*, 2016). The initialization and progress of colon cancer is almost usually associated with chronic

intestinal inflammation. Besides the inflammatory ROS and lipid aldehydes discussed above, the intestinal pathogen–host interaction can promote gut inflammation and stimulate host gut epithelium to secrete higher levels of sphingosine-1-phosphate, Chemokine (C-C motif) ligand 20 (CCL20), prostaglandin E2 (PGE2) etc. (Deng *et al.*, 2015).

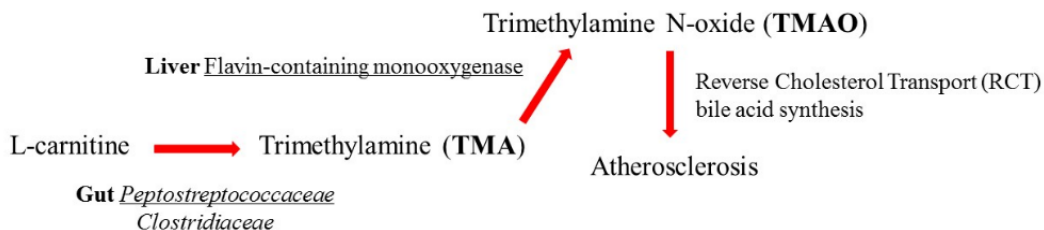


Figure 2-8. Metabolic pathway of L-carnitine to trimethylamine. Structural representations provided are not intended to convey any stereochemical information.

L-carnitine is an abundant in red meat and contains a trimethylamine structure similar to choline. L-carnitine is also widely used as functional component in commercial weight-loss pills. In human intestine, L-carnitine is metabolized into trimethylamine (TMA) by gut-microbiota, probably by *Peptostreptococcaceae* and *Clostridiaceae* families. Rat studies have indicated that, after uptake of intestinal tract via simple diffusion and carrier-mediated transport, TMA was rapidly distributed to all parts of the body, with the highest concentrations measured in the kidney and liver. In liver, TMA is further metabolized into Trimethylamine N-oxide (TMAO) by flavin monooxygenases (FMOs), and then distributed in peripheral circulating system. TMAO may increase atherosclerosis by suppressing reverse cholesterol transport (RCT) and bile acid synthesis. In addition, TMAO contributes to the incidence of cardiovascular disease by acting as ‘on’ switch for inflammatory cascade and cause damages to arteries. Consequently, the generated

cholesterol accumulates on the artery wall and form plaque. Besides, high levels of serum TMAO reduce the body's ability to get rid of low-density lipoprotein (LDL)—the so called “bad” cholesterol that tends to form blockage in vessels.

2.2 Statistical issues in metabolomics

2.2.1 *Review criteria*

“PubMed” and “Google Scholar” were used to search for the literatures with interested topics. The keywords input for literatures searching include a primary term “metabolomics”, or “metabolic profiling”, combined with the following secondary terms “false discovery rate”, “ α ”, “ β ”, “statistical power”, “q value”, “re-sampling technique”, “statistical models”.

2.2.2 *Data pre-processing*

The basis task of data analysis for most metabolomics studies is to examine whether a detected ion or compound has statistically significant change among the designed groups. In toxicology, the groups are usually differed by their exposure to the interested chemicals with different functions and levels, or other interested conditions like genotype, age, life style and ethnicity. These factors can essentially be taken as independent variables in the statistical analysis. Given the complexity of the content of bio-samples, it is not uncommon to see that in each bio-sample being analyzed, hundreds to thousands of features are recorded by the instrument. Therefore, multivariate analysis is widely used to handle the dataset of metabolomics, which can provide predictive biomarkers and a refined data pool for pathway analysis.

However, in practice, it is not surprising to see that during instrumental analysis, for each running of single measurement, there is minor shift of the recorded values. This unavoidable bias is caused by the continually accumulated contamination of the analytical parts, the loss of efficiency of chromatographic column, and the background noise of the bio-samples. For instance, it is easy to find the retention time or m/z of a detected feature show minor shift in different samples or batches of samples. Such instrumental bias is statistically fixable by a statistical process termed as ‘alignment’, which can be processed with either the online resources like XCMS and MetaboAnalyst, or the software such as IPA, genesis QI and a number of R packages. The next step of data-processing are the normalization and standardization of raw data, which are necessary for most statistical methods to be applied.

Centering converts all the concentrations to fluctuations around zero instead of around the mean of the metabolite concentrations. Hereby, it adjusts for differences in the offset between high and low abundant metabolites. It is therefore used to focus on the fluctuating part of the data and leaves only the relevant variation (being the variation between the samples) for analysis. Centering is applied in combination with all the methods described below. LOESS is very convenient for filling the missing data when the data size is large, with enough repeats performed. Analysis of the positive and negative correlations between metabolites can be performed by preparing a large number (typically 30–50) of apparently identical samples of, for instance, cultured cells. Although the measured concentrations of cellular metabolites in the individual samples will be identical within biological variation, that uniformity is achieved by numerous homeostatic mechanisms that will give rise to positive and negative correlations between metabolite concentrations. This

type of analysis is often referred to as metabolite–metabolite correlation analysis (MMCA) (Fiehn and Weckwerth, 2003; Kose *et al.*, 2001).

2.2.3 Familywise error rate in metabolomics

The possibility of making one or more false discoveries or type I error when performing multiple hypothesis test is termed as familywise error rate (FWER). The existence of false discovery in metabolomics is rooted in the test of multiple hypothesis which is also seen in genomics, proteomics and proteomics (Tyanova *et al.*, 2016). The causes of FWER include, but are not limited to, the improper sample size, excessive false discovery rate due to multiple hypothesis testing, inappropriate choice of particular numerical methods, and overfitting of the applied models (Broadhurst and Kell, 2006). The numerical modeling methods share some common processes: the features are treated equally; certain statistics or p -values are computed; and the false discovery rates or other controlling statistic are computed. To minimize statistical errors, adequate validation and cross-validations could be very helpful. However, for the excessive false discovery rate caused by the large abundance of dependent variables, the traditional p value simply does not work. If significant features need to be extracted from thousands of dependent variables, a p -value with threshold of 0.5 will lead to remarkable false positive results (Storey, 2003). The natural cubic spline algorithm-based calculation of q value is usually used in this situation to replace p -value, according to the strategy provided by Storey *et al.* (Storey and Tibshirani, 2003).

Regarding the metabolomic methods used in the current dissertation, the overall goal is to compare the differential impacts of oral exposure of xenobiotics, either harmful

or beneficial, on gut-microbiota dependent metabolites. The measured values of the metabolites are processed with biostatistical and bioinformatics analyses, so as to extract stimulated metabolic pathways, indicator metabolites, networks of gene-compounds, and comprehensive pictures under a systematic view. The highlights of results cover the xenobiotic-induced nutritional provision to host, the fecal indicator metabolites that are able to reflect such exposure, and the potentially associated disease situations.

The major statistical models used in the metabolomics are multivariate analyses, such as principal component analysis (PCA) and partial least squares discriminant analysis (PLS-DA) etc. There are several statistical parameters that frequently need to be carefully considered. (1) Alpha (α) value is the probability of committing a type I error, which is similar with the level of significance and is commonly set as 0.05 or 0.01. It represents the chance of rejecting a true null hypothesis. p -value is in general the smallest ' α ' for which the test would reject the null hypothesis. (2) Beta (β) is the probability of committing a type II error, which represents the probability to fail in rejecting a false null hypothesis.

The statistical power of any test is $(1 - \beta)$, indicating the probability to reject the false null hypothesis. The statistical factors that affect statistical power are: (1) the directional nature of the alternative hypothesis, i.e. one or two tails; (2) the level of significance (α); (3) n (sample size). Statistical power can be elevated by: (1) application of one-tailed tests; (2) increasing alpha; (3) increasing sample size; (4) improvement of technical precision and accuracy. These values are tightly associated with p -value and FWER and normally come with the final results for a metabolomics dataset (Trutschel *et al.*, 2015).

2.2.4 Enriched pathway analysis

Since the detected and identified metabolites always take certain roles in a number of bio-chemical pathways which relate to global functions and responses. A generally applied strategy to quantify the level of involvement of a specific pathway, i.e. a set of metabolites sharing same physiological signaling event, is the so called “enrichment pathway analysis”. It requires a dataset with X metabolites, N samples and Y factors being analyzed, such as different exposures, phenotypes and genotypes. The calculation of the involvement of a pathway is called enrichment score $ES(P_i)$, which are based on the association score of each gene/metabolite with the phenotype of interest, obtained from Pearson correlation or p -values of two-sample test (e.g. t-test).

$$T_{hit}(P_i, J) = \sum_{g_j \in P_i, j \leq J} \frac{|r_j|}{N(P_i)}, \text{ where } N(P_i) = \sum_{g_j \in P_i} |r_j|$$
$$T_{miss}(P_i, J) = \sum_{g_j \in P_i, j \leq J} \frac{1}{G - p_i}$$

With the above formula (Liu *et al.*, 2012; Subramanian *et al.*, 2005), the ES score is defined as $ES(P_i) = \max_J B(P_i, J) = \max_J T_{hit}(P_i, J) - T_{miss}(P_i, J)$. Again, if p -value is used, obviously there will be a huge FWER generated. The grouping of the metabolites is based on the online databases such as KEGG, Metline, HMDB etc., which are conveniently provided by the various online or offline tools as mentioned above. Thus, high FWER caused by the test of multiple hypothesis influences statistical analysis of a metabolomics dataset from so many aspects and q value is very useful in handling metabolomics data. To calculate q value, the R package ‘Qvalue’ can be leveraged, which is written by Storey (Storey and Tibshirani, 2003) and is available in Github or Bioconductor websites. Based on the p values input into the program, a list of q -value will be provided through algorithm

based on the combination of false discovery rate and interpolation of natural cubic spline (Hedenfalk *et al.*, 2001).

2.2.5 Two-sample t-test in metabolomics

Two sample t-tests are frequently used in metabolomics to preliminarily screen the metabolites that may differentiate the sample with different treatments. By doing this, researchers can preliminarily refine the metabolite pool before applying multivariate models. The original Student's t-test assumes normally distributed data with equal group variances. Welch's t-test allows for unequal variances. The Wilcoxon-Mann-Whitney test uses a ranked set of values, by which it can handle non-normally distributed data sets (Adedara *et al.*, 2014). It is very important to know that even a very small p value does not guarantee that the metabolite has sufficient power to separate the two groups in classification. Hence the metabolites with small p values must be further evaluated with classification models such as PLS-DA, logistic regression, support vector machine (SVM), and random forest. Here, when all p values are calculated, q values can be obtained for double checking purpose. The selected features can be input into classification models.

2.2.6 Resampling techniques in metabolomics

In omics studies, resampling is a popularly used technique to evaluate the performance of a statistical model. In general, a resampling procedure can be done by: (1) estimating the precision of sample statistics, including medians, variances and percentiles by using subsets of available data, which is the so called jackknifing, or drawing randomly with replacement from a set of data points, the so called bootstrapping; (2) exchanging

labels on data points when performing significance tests which is termed as permutation tests, also called exact tests, randomization tests, or re-randomization tests; (3) using random subsets, i.e. cross-validation (Efron and Gong, 1983).

Cross-validation is a statistical method for validating a predictive model. It especially fits metabolomics study in that one major goal of metabolomics is to obtain biomarkers for the prediction of exposure of toxin/toxicants, or other independent variables of samples. Usually, subsets of the data are held out for use as validating sets; a model is applied to the remained training dataset, which result model parameters that can predict for the validation set. Cross-validation can be done by either leaving out a single observation at a time, similar with the jackknife, or, splitting the data into K subsets, with each one held out in turn as the validation set (Triba *et al.*, 2015).

2.3 Short chain fatty acids and chronic inflammatory diseases

2.3.1 SCFAs and certain chronic inflammatory diseases

Chronic inflammatory diseases (CIDs) are featured by local or systematic over-recruitment of active immune cells and inflammatory factors over a long term. Emerging evidences indicate that a number of CIDs may be treated or modulated through nutritional approach. As major beneficial nutrients produced by gut-microbiota, short chain fatty acids (SCFAs) have shown immune regulatory effects on multiple organs, systems, and disease statuses. Growing evidences suggest that the mitigation of some CIDs by modifying intestinal and peripheral SCFAs is applicable. Here we systematically reviewed the relevant publications in this aspect and organized the major findings reported by these studies. Our review suggested that SCFAs have promising modulatory effects on obesity-

associated inflammation, liver inflammatory diseases, colorectal inflammation, as well as the nervous system disease-associated inflammation. The specific mechanisms differ largely. We call for more widely and innovative clinical use of SCFAs as the entry point to modulate and mitigate these CIDs.

The complex links between chronic inflammatory diseases (CIDs) and gut-microbiota have been noticed for more than a decade (Tlaskalova-Hogenova *et al.*, 2004; Tlaskalová-Hogenová *et al.*, 2011). In the past years, the advent of meta-genomics has enabled a systematic understanding on human gut-microbiota—an organ-like community which harbors more than 100 trillion cells from 400 microbial species and contains 150 times more genes than the human genome (Bourlioux *et al.*, 2003; Qin *et al.*, 2010a). The gut-microbiota has shown complex interactions with host, and has been proven to be a necessary and complimentary part to multiple metabolic pathways of host organs and systems, such as gut, liver, neuro and immune systems (Deng *et al.*, 2015; I Naseer *et al.*, 2014; Sun *et al.*, 2012; Tlaskalova-Hogenova *et al.*, 2011). Studies have demonstrated that the diversity, intensity and metabolites of the gut-microbiota are tightly correlated with host healthy conditions, especially the homogeneity and maintenance of immune system (Koren *et al.*, 2012; Neu and Rushing, 2011; Solis *et al.*, 2010; Yatsunenko *et al.*, 2012). Some basic understandings on this microbiota-driven regulation have been gained by analyzing gut-microbial derived metabolites such as trimethyl amine (TMA), trimethylamine *N*-oxide (TMAO), short chain fatty acids (SCFAs), tryptophan, secondary bile acids, 4-cresol, melatonin, serotonin and so on (Han *et al.*, 2014; Holmes *et al.*, 2012; Reddy *et al.*, 1977; Ridlon *et al.*, 2006). SCFAs have addressed special attention and

interests of medical professionals in the worldwide in light of the role of SCFAs in regulating host immune system, neuro function, and energy metabolism.

SCFAs are defined as aliphatic acids constructed by 1–6 carbon atom(s) (**Figure 2-11**), typically including formic acid, acetic acid, propionic acid, butyric acid, valeric acid and hexanoic acid. Regarding butyric acid, valeric acid and hexanoic acid, their methyl-branched fatty acids (FBMAs, i.e. iso-butyric acid, iso-valeric acid and iso-caproic acid) are sometimes also categorized into SCFAs (Torii *et al.*, 2010). In human gut, SCFAs are mainly generated from polysaccharide and oligosaccharide by the fermentation of resistant starches and insoluble fibers of intestinal anaerobic microbiota (Brockman, 2005). Besides, SCFAs can also be generated from protein, peptide, and glycoprotein precursors (Corte Osorio *et al.*, 2011). This process incorporates a variety of alternative and compromising pathways, e.g., fructans, starch, cellulose and galactomannans are metabolized into SCFAs through gut microbial glycolytic pathway; xylans and pectins can be transferred into SCFAs through pentose phosphate pathway; arabinogalactan can be degraded into SCFAs through both routes (Macfarlane and Macfarlane, 2003). The correlation between diet and gut-microbiota dependent production of SCFAs has been investigated in many studies (Corte Osorio *et al.*, 2011). However, the mechanism is complicated by the many receptors and signaling pathways involved in the production and function of SCFAs, as well as some contradictory findings and observations on the effects of SCFAs on CIDs. In this regard, we aimed to systematically review the major findings in these aspects so as to form a comprehensive picture that integrates the production, distribution, metabolism, physiological significances, and CIDs-modulating effects of SCFAs.

Lipid number	Common	Name		Formula		Mass
		Systematic	Molecular	Structural		
C1:0	Formic acid	Methanoic acid	CH ₂ O ₂	HCOOH	46.03	
C2:0	Acetic acid	Ethanoic acid	C ₂ H ₄ O ₂	CH ₃ COOH	60.05	
C3:0	Propionic acid	Propanoic acid	C ₃ H ₆ O ₂	CH ₃ CH ₂ COOH	74.08	
C4:0	Butyric acid	Butanoic acid	C ₄ H ₈ O ₂	CH ₃ (CH ₂) ₂ COOH	88.11	
C4:0	Isobutyric acid	2-Methylpropanoic acid	C ₄ H ₈ O ₂	(CH ₃) ₂ CHCOOH	88.11	
C5:0	Valeric acid	Pentanoic acid	C ₅ H ₁₀ O ₂	CH ₃ (CH ₂) ₃ COOH	102.13	
C5:0	Isovaleric acid	3-Methylbutanoic acid	C ₅ H ₁₀ O ₂	(CH ₃) ₂ CHCH ₂ COOH	102.13	

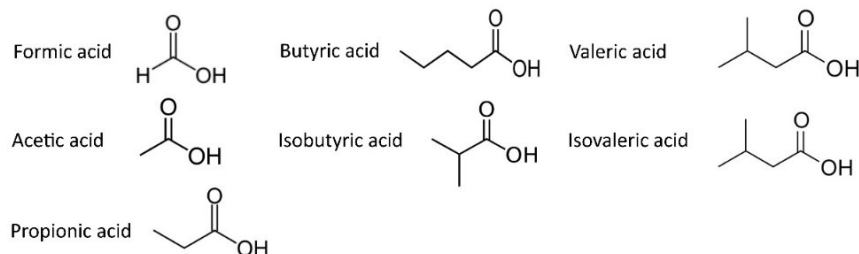


Figure 2-9. Chemical entities of short chain fatty acids.

2.3.2 Review criteria

“PubMed” and “Google Scholar” were used as engines to acquire the literatures of interests, either pre-clinical or clinical studies. The keywords used for the topic searching include: (1) a primary term “short chain fatty acids”, combined with secondary terms: acetic acid, acetic acid, butyric acid, butyric acid, propionic acid, propionic acid, valeric acid, valerate, pentanoic acid, caproic acid, hexanoic acid, synthesizing pathway, gut microbiota, intestinal microbiota, fermentation, administration, distribution, metabolism, excretion, fecal measurement G-protein receptors, GPR43, FFAR2, GPR41, FFAR3, OLF78, OR51E2, GPR109A, HM74a, HCA2, PUMA-G, ABC transporters, SMCT1, SLC5A8, BRCP, ABCG2, OAT7, SLC22, epigenetic regulations, HDACs; (2) a combination of “short chain fatty acids” and “metabolic diseases”, input with the following secondary terms: obesity, insulin resistance, satiety, PPAR γ , PPAR δ , PPAR α , LDL, LDLR,

type 2 diabetes mellitus, intestinal bowl diseases, cell cycle, apoptosis, TGF- β 1, NF- κ B, Treg cell, regulatory T cell, non-alcoholic fatty liver disease, steatohepatitis, neurodegenerative diseases, Parkinson's disease, Alzheimer's disease, colorectal cancer, gut auto-immune lymphatic tissue, GALT, auto-immune system, clinic applications, epidemiological study.

2.3.3 SCFAs: production and absorption

The production of SCFAs is affected by a number of factors, e.g. the community structure of gut-microbiota, host lifestyle, dietary habit, as well as host health status. The difference of community structure is believed to be the primary cause. It was found in a stool sample analysis that African Americans have lower SCFAs levels compared with other racial/ethnic groups (Topping and Clifton, 2001). One recent study explained this by analyzing the variation of microbiota and SCFAs levels among different racial/ethnic groups, and found that the members of the *Lachnospiraceae* and *Ruminococcaceae* families play the most deciding role in causing this variation (Marchesi *et al.*, 2011)—the mean averaged quantity of *Ruminococcaceae* families was higher in African Americans than European Americans, but the *Lachnospiraceae* family was lower than European Americans.

The most abundant three phyla of gut microbes in human intestine, i.e. *Bacteroidetes* (gram-negative), *Firmicutes* (gram-positive), and *Actinobacteria* (gram-positive), have shown significantly different patterns in producing SCFAs. *Bacteroidetes* phylum mainly produces acetic acid and propionic acid (Macfarlane and Macfarlane, 2003); members of *Actinobacteria* are known as propionic acid-producing bacteria; *Firmicutes*

phylum produces the majority of butyric acid as end product (Akasaka *et al.*, 2003). However, at genus level the gut microbes have a diversity of synthetic pathways to produce SCFAs. For instance, *Ruminococcus flavefaciens* and *Ruminococcus albus* mainly degrade cellulose (Flint *et al.*, 2008), whereas *Ruminococcus bromii* and *Ruminococcus callidus* prefer to degrade complex polysaccharides like starch or xylan (Leitch *et al.*, 2007). Cooperative production of SCFAs also exists. For example, *Archaea* can make use of CO₂ and H₂ to produce CH₄, then in the next step acetogenic bacteria could convert CO₂ into acetic acid (den Besten *et al.*, 2013). The synthesizing pathways of SCFAs are further complicated by a highly inter-strain co-metabolism (Louis *et al.*, 2014). A general synthetic pathway for SCFAs can be described as the following stages: (1) monosaccharides are first generated from the aerobic microbial degradation on the resistant starch and insoluble fiber, then go through acrylate pathway, succinate pathway and propanediol pathway to generate propionic acid; (2) pyruvate, an intermediate produced from hexoses and pentoses in acrylate pathway, is utilized as common substrate in generating acetic acid and butyric acid—from pyruvate, acetic acid can be generated through either Wood-Ljungdahl pathway or directly through acetyl-CoA reduction, and butyric acid is generated through butyryl-CoA reduction (Louis *et al.*, 2014); (3) valeric acid is generated by the additive reaction of acetic-CoA and butyric-CoA, whereas hexanoic acid is generated by acetic-CoA and propionyl-CoA, and the two reactions are catalyzed by CoA transferase (Khan, 2006). These metabolic events are integrated from microbes with different phylogenetic identities.

Up to 90–95% of the SCFAs present in the human colon are acetic acid (C₂), propionic acid (C₃), and butyric acid (C₄) (Mortensen and Clausen, 1996). The production

rate, ratio and the level of SCFAs depend on the factors like fermentable carbohydrate type, microbiome diversity and activity, as well as the gut transit time of food (Brinkworth *et al.*, 2009; Gao *et al.*, 2013; Murphy *et al.*, 2010; Schwiertz *et al.*, 2010; Wisker *et al.*, 1988). Evidences from both *in vivo* and *in vitro* studies have demonstrated that a longer transit process can increase SCFAs production by altering gut microbiota community (Macfarlane *et al.*, 1998; Macfarlane *et al.*, 1992). The total amount of SCFAs is estimated to range from 70 to 140 mM in the proximal colon, and around 20 to 70 mM in the distal colon (Cook and Sellin, 1998; Roberfroid, 2007; Topping and Clifton, 2001). Despite the individual factors, in healthy human gut the proportion of acetic acid : propionic acid : butyric acid concentrations in different regions of the large intestine were found to be stable as ~60 : 20 : 20 (Cummings *et al.*, 1987).

In terms of absorption, the three major SCFAs are generally absorbed at comparable rates in different regions of the colon (Engelhardt, 1995; Ruppin *et al.*, 1980). SCFAs serve as important energy source for mammals, and count approximately 1.2–10% energy intake from the typical western diet in human (McNeil, 1984). The absorption of SCFAs in the cecum and the colon is highly efficient, and only 5–10% is excreted in the feces (McNeil *et al.*, 1978; Roberfroid, 2004; Roediger and Moore, 1981). Although data from open-access sources have shown that the averaged total SCFAs concentration is around 9 mg/mL in human stool (Hester *et al.*, 2015), in human peripheral circulation SCFAs are at low level (Bowling *et al.*, 1993). Wolever *et al.* have shown that in human peripheral blood the concentration of SCFAs is around 100–150 μ M for acetic acid, 4.5–6.6 μ M for propionic acid, and 2.2–3.9 μ M for butyric acid (Wolever *et al.*, 1997). Cummings *et al.* have measured SCFAs from adults, and results showed highest level of acetic acid as 69.1

mmol/kg in caecum content, propionic acid as 26.7 mmol/kg in ascending part of large intestine content, butyric acid as 26.1 mmol/kg in caecum content; total SCFA in blood was: portal 375 ± 70 mM, hepatic 148 ± 42 mM and peripheral 79 ± 22 mM (Cummings *et al.*, 1987).

The intestinal absorption of SCFAs can be achieved by either diffusion of protonated SCFAs or anion exchange (Cook and Sellin, 1998). A human rectal infusion study has shown that, SCFAs with shorter chain length and higher concentration can be absorbed faster, which suggests passive diffusion as the predominant mechanism of absorption (Ruppin *et al.*, 1980). Indeed, at normal physiological conditions, around 60% SCFAs uptake is achieved via simple diffusion of protonated SCFAs, whereas the left intake is through anion exchange, with enhanced Na^+ and K^+ absorption and bicarbonate excretion (Fleming *et al.*, 1991). Cook *et al.* proposed that the anion exchange route was assumed to become dominant at higher concentrations over 80 mmol/L (Cook and Sellin, 1998; Harig *et al.*, 1996; Rajendran and Binder, 1994). Such transportation is correlated with water and is greater in distal part than in the proximal colon. Finally, the absorption of SCFAs demonstrates a synergistic pattern. Human study indicated that butyric acid absorption is higher ($n = 10$, $p = 0.12$) when it is co-administrated with acetic acid and/or propionic acid at physiological ratio (Vogt and Wolever, 2003).

The colonic uptake of butyric acid in human is achieved through two transporters: monocarboxylate transport proteins (MCT1) and sodium-linked monocarboxylate transporter (SMCT1, also called SLC5A8) (Blottiere *et al.*, 2003; Halestrap and Meredith, 2004). MCT1 and SMCT1 locate in the lumen side, whereas MCT4 and MCT5 locate on the basolateral membrane of portal vein. SMCT1 transports butyric acid faster than its

transportation of propionic acid and acetic acid (den Besten *et al.*, 2013). MCTs and SMCT1 are negatively associated with tumorigenesis. For example, tumor-specific methylation on promoter SMCT1 was observed in 33 of 40 serrated adenomas (Dong *et al.*, 2005). Also, in colonic epithelial tumor cells, a reduction in MCT1 and SMCT1 protein expression, and a consequent inhibited butyric acid absorption were observed (Goncalves and Martel, 2013). On the other side, the transporters of SCFAs are also indispensable in realizing physiological functions, and depletion of these transporters may lead to severe diseases or cancer. Gurav *et al.* have exhibited in an *ex vivo* study that SMCT1 takes an obligatory role in mucosal immune system (Gurav *et al.*, 2015). In a case-control study, the methylation of SMCT1 was observed in 38 of 64 primary colon cancers, meanwhile 35 of these 38 cases showing no methylation in matched healthy tissues (Blottiere *et al.*, 2003). In patients of intestinal bowl diseases, i.e. ulcerative colitis and Crohn's disease, colonic MCT1 was found significantly downregulated, yet glucose transporter GLUT1 was upregulated, indicating an energy-utilizing mechanism switch from butyric acid to glucose. Interestingly, in one study on colorectal cancer, MCT1 (also for isoforms 2 and 3) expression was shown a significant upregulation (n = 126) (Thibault *et al.*, 2010). The mechanism is discussed as that the unlimited cell division in cancer tissue requires an upregulation of glycolysis, so an upregulated MCT expression is compensated to release lactate (Hadjiagapiou *et al.*, 2000; Pinheiro *et al.*, 2008). Thus, the expression level of the transporter is associated with SCFAs level, cell status and many other factors.

Another transporter of butyric acid is breast cancer resistance protein 1 (BRCP, also referred to as ABCG2)—an ABC (ATP-binding cassette) transporter in the multi-drug resistance family. In colonocytes of normal status, butyric acid can be discharged to the

apical lumen side by BCRP, and this process can be facilitated with ATP consumption (Goncalves and Martel, 2013). Such activity is involved in the function of butyric acid to fasten cell proliferation (Goncalves *et al.*, 2011). By contrast, BCRP is downregulated in intestinal bowl diseases and in colorectal cancer cell lines, which may be resulted by a compensation of the higher level of butyric acid in cancerous colonocytes (Englund *et al.*, 2007). Finally, a very special transporter called OAT7 was found to locate in the sinusoidal membrane of hepatocyte, and this transporter genetically belongs to SLC22 family. This transporter can export liver generated sulfate-conjugated estrone into blood plasma, and intake butyric acid as exchange (Shin *et al.*, 2007). These evidences have indicated the essential role of SCFA transporters in realizing the physiological functions of SCFAs, rather than a singular transporting function.

2.3.4 SCFAs: distribution and metabolism

After absorption, SCFAs are mainly metabolized at three physiological sites, depending on the carbon number: (1) ceco-colonic epithelium uses butyric acid as major substrate for energy maintenance; (2) liver cells metabolize residual butyric acid, with large proportion of propionic acid for gluconeogenesis, and 50% to 70% of acetic acid for TCA cycle; (3) muscle and brain generate energy from oxidation of residual acetic acid (Roberfroid, 2007). For isolated healthy colonocytes, the oxidation of SCFAs account for 60–70% of the energy need, and this supply reduces the oxidation of glucose, pyruvate and glutamine (Butler *et al.*, 1990; LeBlanc *et al.*, 2017). Indeed, studies have shown that compared with glucose, pyruvate and glutamine, butyric acid is the preferred intestinal fuel (Roediger, 1980)

The distributions and metabolisms of SCFAs differ largely. In liver, acetic acid is involved in cholesterol synthesis (Siperstein and Guest, 1960). Around half of total acetic acid absorbed in intestine will be rapidly taken up by the liver and then promptly delivered to peripheral tissues where acetic acid can be utilized as substrate of ATP synthesis (Hijova and Chmelarova, 2007), e.g. muscle skeletal cells can generate energy from the oxidation of acetic acid via acetyl-CoA (Al-Lahham *et al.*, 2012). On the other hand, propionic acid, butyric acid and valeric acid are metabolized in both intestinal epithelium and liver, and are both glucogenic and ketogenic in liver (Hijova and Chmelarova, 2007). Propionic acid and butyric acid share many modulatory activities in the epithelia such as cell-cycle regulation (Hijova and Chmelarova, 2007; Topping and Clifton, 2001). However, butyric acid is still the preferred energy resource for colonic epithelia (Blottiere *et al.*, 2003). This fact has been well exhibited in many studies. Leschelle *et al.* have therefore concluded that the metabolism downstream of acetyl-CoA, i.e. oxidation step in tricarboxylic acid (TCA) cycle and lipid synthesis, may act as the regulator of butyric acid intracellular concentration, and β -oxidative pathway is believed as major pathway for colon utilization of butyric acid (Brockman, 2005; Clausen and Mortensen, 1995). An earlier rat study showed that in rat colon, butyric acid oxidation is faster than acetic acid and much faster than propionic acid (Fleming *et al.*, 1991), and in isolated human colonic cells, it was shown that butyric acid is metabolized more efficiently than acetic acid and propionic acid (Wong *et al.*, 2006). These findings, together support a unique role of butyric acid as energy source for colonic mucosa, whereas acetic acid is mainly functioning in peripheral tissue.

2.3.4.1 *Acetic acid in peripheral tissues*

As discussed above, a significant amount of acetic acid enters systemic circulation and reaches peripheral tissue, whereas propionic acid, after passing the portal circle, is primarily utilized in gluconeogenesis in the liver, and butyric acid majorly functions in gut epithelium (Anderson and Maes, 2015; Cummings *et al.*, 1987; Puddu *et al.*, 2014). Compared with butyric acid and propionic acid, acetic acid has the lowest affinity with G-protein receptors and also demonstrates weakest HDACi activity. However, it shows some special functions that are different with other SCFAs. Gary *et al.* performed *in vivo* ¹¹C-acetic acid administration and PET-CT (positron emission tomography–computed tomography) scanning in mouse model and showed that the ¹¹C-acetic acid administrated by intravenous injection or colonic infusion can come cross the blood–brain barrier (Frost *et al.*, 2014). It was demonstrated by ¹³C high-resolution magic-angle-spinning that ¹³C acetic acid from fermentation of ¹³C-labelled carbohydrate in the colon can increase hypothalamic ¹³C acetic acid. They further observed the increase of melanocortin precursor pro-opiomelanocortin (POMC), the suppressions of Neuropeptide Y (NPY) and agouti-related peptide (AgRP), and eventually a subsequent reduction in food intake. Similar with the above mechanism, it was found that acetic acid and propionic acid can significantly stimulate muscle and liver FA oxidation via increased activation of AMPK to pAMPK in cytoplasm and a PPAR δ -dependent mechanism in nuclear (den Besten *et al.*, 2015; Gao *et al.*, 2009). It was also shown in rats with obese phenotype that after 6 months of acetic acid injections (5.2 mg/kg of body weight) in skeletal muscle, glucose uptake was indirectly increased through an AMPK-dependent manner via GLUT4 receptor, and muscular insulin

sensitivity is also increased through systemic levels of gut-originated PYY and GLP-1 (Chambers *et al.*, 2015a).

Acetic acid has demonstrated apoptosis-inducing capacity on colorectal carcinoma cells HCT-15 and RKO at physiological relevant level (as low as 70 mM), which is involved with cathepsin D (CatD) releasing through lysosomal membrane permeabilization (LMP) (Marques *et al.*, 2013). The result is consistent with another study which analyzed the synergistic anti-tumor effect of SCFAs, revealing that lysosomal protease CatD, which is released from damaged mitochondria and independent of autophagy, suppressed butyric acid-mediated apoptosis. Thus, a co-administrated CatD inhibitor may largely elevate the anti-tumor activity of SCFAs (Oliveira *et al.*, 2015). Clinically, patients suffering from traumatic brain injury (TBI) show decreased N-acetylaspartate (NAA) and ATP in brain, which obstruct recovery of the injured area. Providing acetic acid would help compensate the lack of NAA and ATP levels, and also the nuclear histone acetylation reactions would help suppress inflammatory genes during cellular repair and recovery (Arun *et al.*, 2010).

2.3.4.2 *Butyric acid in colon and breast gland*

Compared with other SCFAs, butyric acid has shown the strongest anti-colon cancer effect, besides its energetic and epigenetic functions in maintaining healthy colonocytes (Cunha *et al.*, 2012; Donohoe *et al.*, 2014; Fung *et al.*, 2011). In a wide variety of neoplastic cells, butyric acid has been found to induce growth arrest, apoptosis and differentiation of cultured cells at mM concentrations, by altering the expression of a variety of genes through histone hyperacetylation, DNA hypomethylation and hypermethylation (Bordonaro and Lazarova, 2015; Lazarova and Bordonaro, 2016; Ortega

et al., 2016). Normally, cancer cell growth can be ceased through cell cycle arrest or histone deacetylase inhibition, and mitochondria mediated apoptosis is initiated by cell surface apoptotic receptor (Le Leu *et al.*, 2007; Soscia *et al.*, 2010). The proliferation of MCF-7 human breast cancer cells plated at 5×10^4 cells/mL was reduced 46 % by butyric acid (1 mM) combined with vitamin A (10 μ M) after 120 h treatment, significantly higher than 34 % and 10 % by butyric acid and vitamin A when used independently. This inhibition was achieved through the H3K9 targeted HDAC inhibitory effect of butyric acid that reactivates the promoter of *RAR β* , a cancer suppressive gene although the mutated CRBP-1 remained down-regulated in this cancer cell line so the ability of retinol storing is still aberrant (Andrade *et al.*, 2012). VEGF receptor neuropilin-1 (NRP-1) is expressed in a singly dispersed subpopulation of cells in the normal colonic epithelium, but that expression becomes dysregulated during colorectal carcinogenesis, highly indicating a poor prognosis of cancer development. The spatial distribution and morphology of NRP-1 expressing cells are altered in response to disease state including cancer and irritable bowel syndrome. The increase of NRP-1 is reversed by butyric acid in colon cancer cell lines *in vitro* and *in vivo* (Chang *et al.*, 2011). It was shown that butyric acid can suppress RKO colon cancer cell proliferation, migration by upregulating endocan through ERK2/MAPK signaling way (Zuo *et al.*, 2013). Similarly, an *in vitro* study using human colon cancer cell line Caco-2 has shown that the butyric acid-induced cell differentiation was via p38-MAPK pathway, which leads to the upregulation of the vitamin D receptor (VDR) (Bermudez *et al.*, 2011).

Butyric acid has a contradictory role in regulating colon metabolism is termed as “Butyric acid Paradox”. It has been shown that butyric acid stimulates the physiological

pattern of proliferation in the basal crypt in the colon, whereas it reduces the number and the size of aberrant crypt focus, the earliest detectable neoplastic lesions in the colon. This ‘Butyric acid Paradox’ was recently associated with “Warburg Effect”, basically describing a shift from mitochondrial oxidative respiration to aerobic glycolysis in cancer cell development. A study conducted in HCT116 cancer cells has demonstrated that the “Warburg effect” may combine with histone acetylation to induce the “Butyric acid Paradox” (Donohoe *et al.*, 2012). The hypothesis was shown in cancer cells, that the Ca²⁺ hemostasis in cytoplasm is deviated by “Warburg Effect”. Zhang *et al.* showed that sodium butyric acid increases endoplasmic reticulum stress by altering intracellular calcium levels, a well-known autophagy trigger, and then lead to apoptotic response in human colorectal cancer cells lines HCT-116 and HT-29 with sodium butyric acid at concentrations ranging from 0.5 to 5 mM (Zhang *et al.*, 2016). Moreover, because of “Warburg Effect”, in tumor cells the metabolism of butyric acid is slow, thus the accumulated butyric acid exerts a higher activity on apoptosis and cell proliferation (Donohoe *et al.*, 2014). The contradictory effects of butyric acid on colorectal inflammation and cancer progress can be seen in many studies of irritable bowel syndrome (Finnie *et al.*, 1993; Jørgensen and Mortensen, 2001). Such inconsistent bioactivities indicate that the function of butyric acid largely depend on the severity and specific progression of intestinal inflammation and cancer.

2.3.4.3 Propionic acid in liver

The distribution, metabolism and functioning of propionic acid are mainly in liver. Bindels *et al.* reported that in mice model of aggressive malignancy that is induced by Bcr-Abl-transfected Ba/F3 cells transplantation, administration of inulin-type fructans (ITF)

via drinking water could modulate compositions of gut-microbiota, enrich *Bifidobacteria* and *Lactobacilli* species and elevate portal propionic acid level, which further reduced hepatic BaF3 cell infiltration and inflammation via a cAMP level-dependent pathway (Bindels *et al.*, 2012). They have also demonstrated that oral administration of inulin-type fructans can generate more propionic acid by elevating gut-microbiota dependent fermentation of starch, which further counteract the malignant cell proliferation in liver (Bindels *et al.*, 2012). Another unique benefit of propionic acid is its capacity of stimulating insulin secretion. Evidences have shown that it can modulate Akt2 knockout-induced cardiomyocyte contractile dysfunction (Al-Lahham *et al.*, 2012).

2.3.4.4 Other SCFAs

Currently there is little knowledge about iso-butyric acid, valeric acid, iso-valeric acid, caproic acid and iso-caproic acid. Solid evidences have suggested that the synthesizing pathway of valeric acid, caproic acid and branched SCFAs are largely distinct with major SCFAs. In general, straight SCFAs are considered as products of microbial fermentation on hydrocarbons, whereas branched SCFAs like iso-butyric and iso-valeric acids are fermented from protein sources. It was demonstrated in canine that a high protein diet, compared with baseline diet, can lead to 24-fold increase of valeric acid production, 79.5% increase of iso-butyric acid and 42.4% increase of iso-valeric acid. Of note, production of propionic acid was reduced by 43.3%; the production of acetic acid was reduced by 25.0%; and the production of butyric acid was reduced by 10.2% (Huurinainen, 2009). The increase of branched chain fatty acids was not as significant as valeric acids and may not be affected by dietary adaptation to a high protein composition. The positive

correlation between the productions of iso-butyric and iso-valeric acids, plus the evidence that their production is almost independent of species, age, diet and living conditions, has suggested that the source of their production is intestinal sloughed cells (Cardona *et al.*, 2005). Valeric and hexanoic acid (caproic acid) have shown similar yet weaker HDACi activity compared with butyric acid, and can decrease pro-inflammatory cytokine expression within dendritic cells meanwhile promote Treg induction (Arpaia *et al.*, 2013). Han *et al.* have shown that propionic acid and valeric acid are able to elevate insulin-stimulated glucose uptake in 3T3-L1 adipocyte via GPCR41 (Chimerel *et al.*, 2014). Hexanoic acid is also positively associated with *Salmonella* infection in gut (Van Immerseel *et al.*, 2004).

2.3.5 Mechanism of function: G-protein receptors and downstream events

Epidemiological studies have confirmed the association between higher fiber intake, increased intestinal SCFAs and reduced risk of a range of CIDs, such as irritable bowel syndrome, inflammatory bowel disease, cardiovascular inflammation, diabetes, and colon cancer (Galisteo *et al.*, 2008). There are sufficient evidences showing that the administration of SCFAs has a positive effect on the treatment of ulcerative colitis, Crohn's disease, antibiotic-associated diarrhea, blood glucose homeostasis, insulin sensitivity, adipogenesis, lipid levels, the immune functions of colonic environment, intestinal mucosal growth and integrity, blood flow and obesity (Binder, 2010; Chambers *et al.*, 2015b; Di Sabatino *et al.*, 2005; Neut *et al.*, 1995; Roy *et al.*, 2006; Vinolo *et al.*, 2011; Wong *et al.*, 2006).

SCFAs enable their functional regulation on target cells in two ways, either by the histone deacetylase (HDAC) activity after entering cell nuclear, or by directly coupling with membrane G-protein receptors to modulate downstream pathways (Canfora *et al.*, 2015).. In the latter aspect, they act as signal transduction molecules via G-protein coupled receptors like GPR43 (free fatty acid receptor 2, FFAR2), GPR41 (free fatty acid receptor 3, FFAR3), OLF78 (human ortholog as OR51E2), GPR109A (also named HM74a, HCA2 or PUMA-G). GPR41 has 52% similarity and 43% identity with GPR43, and the SCFAs response profiles between human and rat GPR41 receptor are similar, indicating that the receptor is evolutionarily conserved (Brown *et al.*, 2003a).

The affinities of SCFAs to GPR41 and GPR43 differ with the carbon length of the ligands. In CHO-GPR41 or CHO-GPR43 cells, GTP γ [35S] binding assay showed that propionic acid EC₅₀ to GPR41 and GPR43 are ~274 μ M and ~259 μ M, respectively; acetic acid EC₅₀ to GPR41 was ~1300 μ M and to GPR43 was ~537 μ M. Pluznick *et al.* measured in HEK293T using luciferase assay, that OLF78 responds solely to acetic acid and propionic acid and the EC₅₀ for OLF78 was 920 μ M for propionic acid, 2.35 mM for acetic acid (Pluznick, 2014; Pluznick, 2013). GPR109A responds only to butyric acid with an EC₅₀ as 1.6 mM (Ahmed *et al.*, 2009).

In addition to affinity, the three major SCFAs also demonstrated different potents in activating GPRs. Propionic acid has highest potent in activating GPRs, and acetic acid has lowest potent. Propionic acid is the most potent substrate to GPR41 and GPR43, whereas butyric acid is preferred by GPR41, and acetic acid has higher affinity with GPR43. Brown *et al.* conducted membrane GTP γ [35S] binding assay in HEK293T cell and showed that formic acid EC₅₀ to GPR43 and GPR41, were ~5640 \pm 1480 μ M and ~7760

$\pm 3870 \mu\text{M}$; acetic acid EC₅₀ to GPR43 and GPR41 were $431 \pm 85 \mu\text{M}$ and $1020 \pm 200 \mu\text{M}$; propionic acid EC₅₀ to GPR43 and GPR41 were $\sim 290 \pm 42 \mu\text{M}$ and $\sim 127 \pm 14 \mu\text{M}$; butyric acid EC₅₀ to GPR43 and GPR41 were $\sim 371 \pm 81 \mu\text{M}$ and $\sim 158 \pm 35 \mu\text{M}$; valerate EC₅₀ to GPR43 and GPR41 were $\sim 876 \pm 206 \mu\text{M}$ and $\sim 142 \pm 87 \mu\text{M}$; hexanoate EC₅₀ to GPR43 was $\sim 1300 \mu\text{M}$ but no result for GPR41. The EC₅₀ of propionic acid, butyric acid and valerate to rGPR41 are close, between ~ 31 and $\sim 41 \mu\text{M}$ (Brown *et al.*, 2003a).

GPR41 and GPR43 were G protein-coupled receptors of same homologous family (Brown *et al.*, 2003a; Le Poul *et al.*, 2003; Nilsson *et al.*, 2003). They are tandemly encoded at a single chromosomal locus in both humans and mice. GPR41 couples to Gi, and GPR43 was found to couple to both Gi and Gq. Downstream of Gi and Gq proteins include several important cellular pathways containing adenylate cyclase, small G proteins, mitogen-activated protein kinases (MAPK), phospholipase C(PLC) and A2(PLA2), inositol 1,4,5-trisphosphate formation after phospholipase stimulation, inhibition of cAMP accumulation, ion channels and many transcription factors (Hirata *et al.*, 1980; Hong *et al.*, 2005; Redfern *et al.*, 2000; Robishaw *et al.*, 1986; Taylor *et al.*, 1991). The protein-based physiological detection of these receptors is limited by the lack of reliable monoclonal antibody, therefore most findings are approached by nucleotide-based methods. GPR41 is mainly distributed in colon, with a cellular population density of 0.01 ± 0.01 cells/crypt. Although the population density of GPR41 is smaller than that of GPR43 (0.33 ± 0.01 cells/crypt) in the human colon, the response of GPR41 to SCFAs, of which propionic acid > butyric acid > acetic acid, is matching with the potency order of SCFA-induced phasic contraction of colonic smooth muscle, while GPR43 responsive potency order is propionic acid, butyric acid, acetic acid. Therefore, GPR41 may function as primary sensor for luminal SCFAs in

human gut, while GPR43 plays unique roles in other organs (Tazoe *et al.*, 2009). Indeed, *GPR43* mRNA has been found in cardiovascular epithelium, intestinal epithelium, and immune cells like lymphocytes, neutrophils, monocytes, the peripheral blood mononuclear cells (PBMCs), brain, liver, muscle, bone marrow, immune system, lung, pancreas, gut epithelium, mature white adipose tissue, but not in the brown adipose tissue or pre-adipocytes (Karaki *et al.*, 2006; Kimura *et al.*, 2011; Tazoe *et al.*, 2009; Xiong *et al.*, 2004). GPR41, GPR43 and OLF78 proteins were found being expressed in the kidney and the vasculature, yet not like OLF78, both GPR41 and GPR43 show other physiological expressions and corresponding functions (Pluznick, 2014): (1) GPR41 protein is found in human blood vessel, colon mucosa enterocytes and enteroendocrine cells, as well as in mouse autonomic and somatic sensory ganglia (Brown *et al.*, 2003a; Pluznick, 2013); (2) GPR41 protein has also been detected in mice kidney blood vessels, and in several types of mice neuron and ganglia as well, such as autonomic and somatic sensory ganglia (Nohr *et al.*, 2015; Pluznick, 2014); (3) GPR43 protein has been detected in human and mouse colon epithelial cells (Karaki *et al.*, 2006; Tang *et al.*, 2011), whereas *Gpr43* mRNA was detected in human blood vessel endothelium, colon enterocytes, rat peptide YY (PYY) expressing enteroendocrine cells, and rat 5-HT expressing mast cells in the *lamina propria* (but not in muscle or submucosa) (Karaki *et al.*, 2006; Karaki *et al.*, 2008).

A variety of physiological functions are associated with the above receptors. Evidences collected from *in vitro*, *in vivo* and epidemiological studies have clearly demonstrated that vasculature localized GPR41 has an inhibitory effect on blood pressure (Pluznick, 2013). For gut-localized GPR41, transgenic mice revealed that GPR41 is associated with reduced expression of peptide YY (PYY), an enteroendocrine cell-derived

hormone that regulates gut motility and reduced harvest of energy from the diet (Samuel *et al.*, 2008). Cell line studies have illustrated that GPR41 may inhibit cell proliferation and induces apoptosis via the activation of p53 and MAPK (Yonezawa *et al.*, 2009). On the other hand, the primary beneficial function of GPR43 is highly related with cancer occurrence and immunity modulation (Pluznick, 2013). Cytokine-stimulation can induce GPR43 expression in bone marrow cells (Senga *et al.*, 2003). It has been shown in both cultured intestinal epithelial cells and in mice, that SCFAs activate cytokines and chemokines in a GPR43 dependent way. The immune response was absent in Gpr43 $-/-$ mice, which exhibited extensive dysregulation of inflammatory responses in models of colitis, arthritis and asthma (Kim *et al.*, 2013).

The maintenance or promotion of gut epithelium by SCFAs can be enabled by their binding with GPR43 and GPR109A to stimulate K^+ efflux and hyperpolarization (Macia *et al.*, 2015). GPR43 was also shown an important role in adipose insulin regulation, and the signaling is achieved by increasing phospholipase C (PLC), protein kinase C, phosphatase and tensin homolog (PTEN), thus inhibiting phosphatidylinositol (3,4,5)-trisphosphate (PIP3) synthesis and reducing bioactivity of insulin (Kimura *et al.*, 2013). A phenylacetamide derivative, CMTB, as specific GPR43 agonist has showed equal activity on Gi and Gq pathway, and cell-proliferation inhibiting activity on two human cancer cell lines, U937 cells and K562 cells (Qin *et al.*, 2010b). These data have indicated a very complex and broad downstream of SCFA G-receptors. The corresponding pathways are in reality overlapped with epigenetic regulation and also energy homeostasis that centers in TCA circle.

The other two receptors for SCFAs, i.e. GPR109A and Olfr78, are less known. GPR109A has multiple ligand affinities and also demonstrate multiple functions, depending on the specific organ where it is expressed. It was measured by [³⁵S]GTP γ S binding assay using GPR109A expressing CHO-K1 cells that GPR109A responded to butyric acid and β -hydroxybutyric acid, an endogenous ketone derivative of butyric acid generated in starvation, with EC₅₀ 1.6 mmol/L for butyric acid and 0.7 mmol/L for β -hydroxybutyric acid (Elangovan *et al.*, 2014; Taggart *et al.*, 2005). Besides butyric acid and β -hydroxybutyric acid, GPR109A can also be stimulated by niacin and phenolic acids and then inhibit the oncogenes in multiple organs including gut, breast gland and lung. However, the normal physiologic level of butyric acid in circulation, approximately 10 μ mol/L, is insufficient to activate GPR109A in most tissues, except for colon and mammalian gland, because colon microbial derived butyric acid can reach a concentration of \sim 10 mM and in mammalian gland butyric acid is also of high concentration (Ochoa-Zarzosa *et al.*, 2009). It has been recognized for a long time, that butyric acid can decrease the development of carcinogen-induced mammary tumor, suppressing the expression of estrogen receptor ER α and progesterone receptor, thereby inducing growth arrest in breast cancer cell lines (Defazio *et al.*, 1992; Graham and Buick, 1988; Horwitz *et al.*, 1982). The deletion of the GPR109A receptor in GPR109A^{-/-} mice will lead to higher incidence of lung metastasis, and the similar immune dysfunctional symptoms was shown in GPR43^{-/-} mice (Elangovan *et al.*, 2014). GPR109A also demonstrated immune modulatory function. In retinal pigment epithelial cells, the activation of GPR109A leads to inhibition of TNF- α induced IL-6 and Ccl2 production (Gambhir *et al.*, 2012). Reduction of adipose lipolysis is another well-known function of GPR109A, triggered by binding of nicotinic

acid (Ahmed *et al.*, 2009). GPR109A activation in adipose tissue decreases adenylyl cyclase efficiency and thus lead to lower cellular levels of cyclic AMP (cAMP) (Brown *et al.*, 2003b; Soga *et al.*, 2003; Tunaru *et al.*, 2003). Finally, it has been shown that nicotinic acid can inhibit progression of atherosclerosis in mouse model through its receptor GPR109A in immune cells (Lukasova *et al.*, 2011). Also, it has been observed that GPR109A expression demonstrated positive correlation with squamous cell carcinoma both *in vivo* and *in vitro*, though the increased GPR109A expressions are nonfunctional for unknown reason (Bermudez *et al.*, 2011). The high similarity of response to SCFAs indicates that GPR109A is evolutionarily conservative like GPR41 (Pluznick, 2013).

Mice *Olf78* (human ortholog as OR51E2) is one of the sensory receptors that play important yet undefined roles in a variety of tissues and physiological processes. *OLFR78* can be activated by acetic acid and propionic acid, and the EC50 values are 2.35 mM and 920 μ M, respectively (Kasubuchi *et al.*, 2015). For human OR51E2, the EC50 is 2.93 mM for acetic acid and 2.16 mM for propionic acid (Pluznick, 2013). The binding of acetic acid and propionic acid to *OLFR78* induces the release of renin, an enzyme that is involved in the regulation of blood pressure (Pluznick, 2014; Pluznick, 2013). *Gpr43* and *Olf78* are both expressed in the kidney and cardiovascular system (Pluznick, 2014). Renal *Olf78* is expressed in renal juxtaglomerular apparatus vessel and is involved in renin secretion (Pluznick, 2013).

Finally, the modulatory function of SCFAs on disease and ailments can be achieved by multiple receptors discussed above. For example, SCFAs can reduce blood pressure through at least two separated ways (Pluznick, 2014). SCFAs can bind with renal *Olf78* in the afferent arteriole and modulate renin release, which can lead to change of blood

pressure after several hours or days. The regulation could also be achieved by stimulate peripheral OLF78 and GPR41 receptors, and such change could happen in several seconds, through an acute adaptation in vascular tone. On the other side, independent regulations initiated by different receptors can be integrated in one physiological process. For example, specific in white adipose tissue, SCFAs were shown to upregulate leptin secretion through GPR41 (Xiong *et al.*, 2004). Meanwhile, in adipose tissue the activation of GPR43 and GPR109A can suppress lipolysis, and the latter also decreases adenylyl cyclase efficiency and lower cellular levels of cyclic AMP (cAMP) (Zaibi *et al.*, 2010).

2.3.6 Mechanism of function: epigenetic regulations

Besides coupling with G-protein receptors, SCFAs can also achieve complex regulations by their inhibitory activities on histone deacetylase (HDACs) in cytoplasm. Histones are a group of proteins in eukaryotic nuclei that construct chromatin, which allows for additional gene regulatory controls and modification of DNA packing. The basic unit of chromatin consists of a tetra-histone formed octamer. The eight core histones (duplicated H2A, H2B, H3, and H4) are wrapped around 145–146 bp of DNA. The core histones are rich in lysine or arginine residues, which are subject to posttranslational modifications such as methylation and acetylation (Berger, 2002; Strahl and Allis, 2000). For example, H3 hyperacetylation (H3ac) or trimethylation at lysine 4 (H3K4me3) is often associated with genes of high activity (Santos-Rosa *et al.*, 2002), whereas trimethylation of the same protein at lysine 9 or 27 (H3K9me3 or H3K27me3) is generally found in chromatin containing silent genes (Litt *et al.*, 2001). Chromatin realizes a dynamic equilibrium between the two states (Baldwin *et al.*, 2013). The above epigenetic regulation of

chromatin structure is realized by the interplay between histone acetyltransferases (HATs) and histone deacetylases (HDACs), which targets on histone proteins at Lys (K) residues. Typically, acetylation results in a more relaxed chromatin conformation which promotes most transcription factors (TFs) interaction with specific gene promoters, thus upregulating certain gene expression (Chuang *et al.*, 2009). Deficiencies in histone acetylation and transcriptional dysfunctions have been well noted in cancer pathology and neurodegenerative diseases (Hinnebusch *et al.*, 2002; Mariadason *et al.*, 2000; Waldecker *et al.*, 2008), such as Huntington's, Parkinson's and Alzheimer's diseases, amyotrophic lateral sclerosis, spinal muscular atrophy and stroke (Bates *et al.*, 2006; Pallos *et al.*, 2008; Steffan *et al.*, 2001).

SCFAs are able to inhibit the activities of Class I/II HDACs, and downregulate the expression of sirtuin-1 (SIRT1, a Class III HDAC) (Nakahata *et al.*, 2008). In addition, SCFAs can promote H3K27Me3 and H3K9Me3, the repressive histone trimethylation on histone 3, by affecting the enhancer of zeste homolog2 (EZH2) and the suppressor of variegation 3-9 homolog1 (SUV39H1) (Schotta *et al.*, 2003; Sun *et al.*, 1998). A large abundance of studies have demonstrated that the immune ameliorating and cancer prevention capacity of SCFAs are mainly enabled by their inhibitory effect on HDAC (Candido *et al.*, 1978; Sealy and Chalkley, 1978). One test performed in calf thymus showed that butyric acid has the highest inhibitory potent on the enzyme activity of HDAC 1/2 (80% of maximum level), whereas acetic acid showed the lowest inhibitory activity (10% of maximum level). The inhibitory efficiencies of other three SCFAs, propionic acid, valeroic acid and hexanoic acid are 60%, 65% and 30%, respectively (Cousens *et al.*, 1979).

However, there is still argument on whether acetic acid is an actual histone deacetylase inhibitor (HDACi). Some studies reported negative observation on the HDACi activity of acetic acid (Hinnebusch *et al.*, 2002; Kiefer *et al.*, 2006; Waldecker *et al.*, 2008), yet in many other studies, either in peripheral circulation or brain, the results are positive (Bhattacharyya *et al.*, 2014; Soliman and Rosenberger, 2011). Markus *et al.* have conducted a luciferase-assay in HeLa Mad 38 cells, showing that acetic acid has merely no HDACi activity from 0 to 20 mM, and butyric acid showed the highest such potent at extremely low concentration that is close to physiological environment (1-2 mM). (Waldecker *et al.*, 2008). In one study aimed to explore novel HDACi activity of acetic acid, researchers showed that acetic acid is a necessary co-operator in determining the specificity between HDAC8 and some amino-acid derived ligands (Whitehead *et al.*, 2011). By contrast, butyric acid and propionic acid are widely recognized HDACi, as is discussed above, that can inhibit cell growth and promote cell differentiation (Bultman, 2014)—actually, as early as last mid-1970s, sodium butyric acid was already found can halt DNA synthesis, cell proliferation and regulate gene expression and cell morphology (Prasad and Sinha, 1976). Later, some studies have reported that some other phenolic acids, which are formed during the intestinal microbial degradation of polyphenolic constituents of fruits and vegetables, also carry inhibitory activity on global HDAC (Bearcroft *et al.*, 1998; James *et al.*, 2004; Jenner *et al.*, 2005). However, among all these organic acids, butyric acid and propionic acid have demonstrated highest potent HDACi activity in HT-29 human colon carcinoma cells and a whole-cell HeLa Mad 38-based reporter gene assay (Waldecker *et al.*, 2008). Thus, compared with butyric acid and propionic acid, acetic acid is more like a a co-factor or mediator of HDACi activity.

Mechanistically, SCFAs function as non-competitive inhibitors of HDACs. It has been shown that butyric acid and propionic acid have preference on inhibiting HDAC1, HDAC2 and HDAC3. Typically, it is believed butyric acid prefers HDAC1 and propionic acid prefers HDAC3 (Thangaraju *et al.*, 2009; Zimmerman *et al.*, 2012). Recently, anti-inflammatory effects of HDAC inhibitors have been confirmed in several murine disease models like chronic inflammatory bowel disease, systemic lupus erythematosus, rheumatoid arthritis, and endotoxemia (Biddle *et al.*, 2013). For example, the long existing assumption of the epigenetic link between microbiota and obese and T2DM has also been confirmed by comparing patients with lean control subjects (Remely *et al.*, 2014). It was reported that the diversity of the gut microbiota and the degree of methylation of the GPR41 promoter region were significantly lower in the obese and type 2 diabetic patients compared to lean individuals, demonstrating a correlation between a higher body mass index and lower methylation of GPR41 (Remely *et al.*, 2014). This result indicated that in long term, the epigenetic aspect of SCFAs modulation may come across the “border” to affect the functions that initialized by G-protein receptors of SCFAs.

2.3.7 Effects of SCFAs on carcinogenesis and immune system

The regulatory effects of SCFAs on carcinogenesis and immune system are tightly linked with the above two aspects of mechanisms. The cancer prevention effects of SCFAs are mainly achieved by inducing apoptosis and the arrest of uncontrolled cell proliferation.

In colon cancer cells, the apoptosis can be initiated through the inhibition of Bcl-2, Bcl-xL, cyclin D1, and activation of the death receptor signaling pathway. In neutrophils the apoptosis would be achieved via a caspase-dependent way (Thangaraju *et al.*, 2009).

One study in 2003 has uncovered how SCFAs can interfere cancer cells via an epigenetic regulation (Davie, 2003). It was demonstrated in p21^{Waf1/Cip1} gene of MCF-7 (T5) human breast cancer cells, Sp1 and Sp3 are hyperactive in recruiting HDAC1 and HDAC2, leading to deacetylation in the promotor area and thus cause silence of p21 expression. Butyric acid inhibits HDACs and induce expression of p21^{Waf1/Cip1}. The upregulated p21 thereby inhibited cyclin E–Cdk2 activity and halted the cells from entering into S phase. The cell cycle–arrested cancer cells may then differentiate or undergo cell death by apoptosis.

How could SCFAs epigenetically modulate the cell cycle of cancer cells? Kilner *et al.* applied iTRAQ tandem mass-spectrometry workflow and high-throughput analysis microscopy (HCA) to acquire information on the cell cycle and the cytoskeletal structure upon SCFAs administration. They reported that butyric acid has the most biological potent of SCFAs to inhibit human colon carcinoma and induce G2 phase arrest and consequent apoptosis in HCT116 cell line. They summarized that butyric acid, valerate and propionic acid carry specific effect of the modulatory activity: butyric acid and butyric acid sodium show more pronounced increasing effects on the keratin 19 and actin; valerate increases the keratin 19 and β -tubulin 2C; propionic acid displayed an intermediate effect, involving in both functions (Kilner *et al.*, 2012). Other experimental evidences showed that SCFAs may possess anti-mitotic capabilities in colon cancer cells by disrupting microtubule (MT) structural integrity via dysregulation of β -tubulin isotypes. In one study, the simulations of propionic acid and valerate displayed increased catastrophe frequencies and longer periods of MT-fibre shrinkage (Kilner *et al.*, 2016). In Wistar rats with Hartmann’s end colostomy, tumorous signs like hyperemia, increased number of vessels, bleeding and mucus discharge can be significantly restored by 8 wks administration of enemas containing butyric acid.

And the density of collagen fibers, the number of goblet cells and the apoptosis rate returned to normal value after treatment (Pacheco *et al.*, 2012). A number of evidences support that such regulations on cell cycle progression and apoptosis are achieved through HADC and HAT homeostasis on related cytoskeleton unit genes (Aebersold and Mann, 2003; Drake *et al.*, 2008; Khan *et al.*, 2011; Kilner *et al.*, 2011; Ku *et al.*, 1999; Leech *et al.*, 2008).

Several *in vitro* and *in vivo* studies have demonstrated the innate-immune modulation of SCFAs on peripheral blood mononuclear cells (PBMCs) such as lymphocyte, monocyte, or macrophage. The immune modulatory function of butyric acid is most remarkable among all SCFAs. Ohira *et al.* tested butyric acid effect on a co-culture of 3T3-L1 adipocyte and RAW264.7 macrophage and found that butyric acid can significantly reduce the cell secreted TNF- α , MCP-1, IL-6, free glycerol and FFAs in the co-culture medium (Ohira *et al.*, 2013). Butyric acid can inhibit the phosphorylation of MAPKs and the activity of NF- κ B in co-cultured macrophages and suppress the activities of several lipases, including adipose triglyceride lipase, hormone sensitive lipase and the fatty acid-binding protein in adipocytes. Consistent with this finding, a shared NF- κ B suppressive activity of three major SCFAs was observed in the LPS induced RAW264.7 cells that showed increased nitric oxide and pro-inflammatory cytokines. The production of pro-inflammatory factors, including TNF- α , IL-1 β , IL-6 and NO was largely reduced by three SCFAs, and meantime the anti-inflammatory cytokine IL-10 was increased by SCFAs (Bhattacharyya *et al.*, 2014). An *in vitro* study has tested SCFAs immune-modulatory ability and approved that in lipopolysaccharide (LPS)-stimulated PBMCs, SCFAs can down-regulate tumor necrosis factor alpha (TNF- α), interleukin (IL)-12, interferon gamma

(IFN- γ) and transforming growth factor beta-1 (TGF- β 1), and up-regulated IL-4, IL-10. Meantime there is no significant effect on PBMCs in the control group, indicating that SCFAs regulated cytokine milieu in LPS-stimulated PBMCs to anti-inflammatory cytokines (Asarat *et al.*, 2015). A transcript level evidence supported the selective immune modulatory effects of SCFAs, showing that in HT-29 colon epithelial cells, SCFAs enhanced TLR5-induced transcription of TNF α but abolished the TLR5-mediated induction of IL-8 and monocyte chemoattractant protein 1 (Anderson and Maes, 2015). The dendritic cells (DCs) separated from wild type mice were exposed to butyric acid, and the expression of immunosuppressive enzymes indoleamine 2, 3-dioxygenase 1 (IDO1) and aldehyde dehydrogenase 1A2 (Aldh1A2) were then upregulated. Consequently, the conversion of naive T-cells into immunosuppressive forkhead box P3+ (i.e. FoxP3+) regulatory T-cells (Tregs) was promoted, and the conversion of naive T cells into pro-inflammatory interferon (IFN)- γ -producing cells was suppressed.

NF- κ B is the pivot in the release of the inflammatory cytokines mentioned above (Hayden *et al.*, 2006). Butyric acid and propionic acid were shown to reduce TNF- α level and NF- κ B activity in PBMCs in a similar manner with HDAC inhibitor Trichostatin A (TSA) (Usami *et al.*, 2008). Although global inhibition of HDAC activity was also observed in *ex vivo* rodent neutrophils after addition of acetic acid, propionic acid, or butyric acid (Vinolo *et al.*, 2011), acetic acid may mediate its anti-inflammatory effects through GPCR activation, rather than HDAC inhibition (Maslowski *et al.*, 2009). Vinolo *et al.* reported that in monocytes acetic acid failed to same effect as butyric acid and propionic acid, which can reduce LPS-induced TNF α expression and NOS expression in rodent neutrophils (Vinolo *et al.*, 2011). Importantly, the weak HDAC-inhibitory activity

of acetic acid was also noted in other cases. For example, acetic acid failed to down-regulate NF- κ B activation, yet butyric acid and propionic acid can successfully activate NF- κ B (Davie, 2003). HDACi activity of butyric acid and propionic acid can also stimulate lipolysis in 3T3-L1 adipocytes in a glucose-dependent way, while aminobutyric acid and acetic acid failed to show this effect (Rumberger *et al.*, 2014).

Similar with the myeloid cells discussed above, the HDACi-driven immune modulation by SCFAs can also be seen in lymphocytes. The inhibition of HDAC9 can increase expression of the forkhead box P3 (Foxp3) transcription factor in mice, which boosts proliferation and bioactivity of Tregs (Lucas *et al.*, 2009; Tao *et al.*, 2007). In-depth mechanistic explanations were provided by two groups on 2013. Arpaia *et al.* reported that in mice model propionic acid and butyric acid are able to upregulate peripheral regulatory T-cells in different ways. Butyric acid increases Treg-cell numbers by potentiating extrathymic differentiation of Treg-cells, and this process depends on acetylation of *Foxp3* intronic enhancer CNS1 (conserved non-coding sequence 1), which is necessary for extrathymic but dispensable for thymic Treg-cell differentiation. On the other hand, *de novo* Treg-cell generation in the periphery was potentiated by propionic acid but not butyric acid or acetic acid, which has weak HDAC-inhibitory activity. Arpaia *et al.* also briefly mentioned that this periphery immune stimulation is different with that in the colon—they found that Treg-cells in the gut was stimulated by acetic acid and propionic acid in a CNS1-independent manner, but was not significantly promoted by butyric acid (Arpaia *et al.*, 2013). The above immune regulatory effects of SCFAs are summarized in **Table 2-1**.

Table 2-1. Summary of the *in vitro* studies to examine the immune regulatory effects of SCFAs.

Cell line	Effect observed	SCFAs	Reference
-----------	-----------------	-------	-----------

Raw 264.7 cells	↓TNF- α , IL-6, IL-1 β , NO, ↑IL-10	Ac, Pr, Bt	(Bhattacharyya <i>et al.</i> , 2014; Chakravortty <i>et al.</i> , 2000; Park <i>et al.</i> , 2007)
Mononuclear cells	↓TNF- α , ↑PGE2	Bt	(Usami <i>et al.</i> , 2008)
Monocytes and Macrophages	↓TNF- α	Bt	(Fukae <i>et al.</i> , 2005)
Macrophages	↓TNF- α , IL-6, IL-8	Ac	(Kendrick <i>et al.</i> , 2010)
Monocytes	↓TNF- α , IL-12, IFN- γ , ↑IL-10	Bt	(Saemann <i>et al.</i> , 2000)
	↓MCP-1, IL-10, ↑PGE2	Ac, Pr, Bt	(Cox <i>et al.</i> , 2009)
Microglial cells N9 cells	↑IL-6, NO	Pr, Bt	(Huuskonen <i>et al.</i> , 2004)
Rat Primary Microglia	↓TNF- α , IL-6, NO	Bt	(Huuskonen <i>et al.</i> , 2004)
Murine BV2 cell	↓NO	Bt	(Dong <i>et al.</i> , 2005)
Mesencephalic Neuron-glia	↓TNF- α , NO	Bt	(Chen <i>et al.</i> , 2007)
Co-culture of 3T3-L1 Adipocyte & RAW 264.7 Macrophage	↓TNF- α , MCP-1, IL-6, NF- κ B	Bt	(Ohira <i>et al.</i> , 2013)
Kupffer cells	↓TNF- α , ↑PGE2	Bt	(Perez <i>et al.</i> , 1998)
Human Monocyte-Derived DC	↓ CCL3, CCL4, CCL5, CXCL9, CXCL10; ↓ IL-6, IL-12p40	Pr, Bt	(Nastasi <i>et al.</i> , 2015)
Rat Neutrophils	↓TNF- α , CINC-2 $\alpha\beta$, NO	Pr, Bt	(Vinolo <i>et al.</i> , 2011)
Human HUVECs	↑ICAM-1, E-selectin	Bt	(Miller <i>et al.</i> , 2005)

Abbreviations: acetic acid (Ac), propionic acid (Pr), butyric acid (Bt), interferon- γ (IFN- γ), interleukin-6 (IL-6), interleukin-10 (IL-10), interleukin-12 (IL-12), macrophage chemoattractant protein (MCP), nitric oxide (NO), prostaglandin E2 (PGE2), tumor necrosis factor- α (TNF- α), dendritic cells (DC), human umbilical vein endothelial cells (HUVECs), intercellular adhesion molecule-1 (ICAM-1). (↑) increase and (↓) reduction. **The table is modified and updated from reference (Vinolo *et al.*, 2011).

2.3.8 SCFAs and obesity, insulin resistance and Type II diabetes mellitus

Obesity, insulin resistance, and Type II diabetes mellitus (T2DM) are risk factors for a number of systematic CIDs, such as allergy, asthma, autoimmune diseases, and lupus

(Bastard *et al.*, 2006; Festa *et al.*, 2000). The modulatory effects of SCFAs on obesity can be achieved via a number of different aspects, such as appetite satiety, insulin sensitivity, lipolysis, adipogenesis, liver/muscular energy metabolism, gluconeogenesis and glucose uptake (Arora *et al.*, 2011; den Besten *et al.*, 2013; Diamant *et al.*, 2011; Greiner and Backhed, 2011; Hong *et al.*, 2005). Such positive function may further modulate innate immune system, leptin secretion, modulate immune disorder, and T2DM (Al-Lahham *et al.*, 2012; Al-Lahham *et al.*, 2010; den Besten *et al.*, 2015). Studies have shown that oral and intravenous administration of acetic acid (den Besten *et al.*, 2015; Kondo *et al.*, 2009; Sakakibara *et al.*, 2006; Yamashita *et al.*, 2007), butyric acid (den Besten *et al.*, 2015) and propionic acid (den Besten *et al.*, 2015) in obesity and T2DM models can reduce liver lipid storage and improve glucose tolerance. A human epidemiological study has proved that acetic acid can fasten glucose metabolism, promote endothelial function and reduce circulating lipid level in subjects with impaired glucose tolerance (Mitrou *et al.*, 2015). In detail, the researchers observed enhancement of muscle blood flow, improvement of muscular glucose uptake, and amelioration of postprandial hyperinsulinaemia/triglyceridaemia after administration of acetic acid. These findings indicate a modulatory function of SCFAs for metabolic disorder and insulin resistance—the primary factor responsible for T2DM.

A large bunch of evidences gathered from *in vivo*, *ex vivo* and *in vitro* studies, have well depicted the mechanistic map that how SCFAs could mitigate and prevent obesity and related secondary diseases. There are three major routes in such beneficial regulation.

(1) The first route to achieve this function is through a comprehensive regulatory effect on energy homeostasis, which contains insulin sensitivity, lipolysis, adipogenesis

and fatty acid synthesis/oxidation in liver, muscle and adipose tissue. The process involves the stimulation of mitochondrial driven fatty acid oxidation in muscle, liver and brown adipose tissue, and also the suppression of fatty acid synthesis in liver (den Besten *et al.*, 2015; Gao *et al.*, 2009). The achievement of this modulation in liver and adipocyte is through increased activation of AMPK to pAMPK in a PPAR γ -dependent way, while in skeletal muscle the FA oxidation was approached via a PPAR δ -dependent way. SCFAs reduce expression of PPAR γ —and its target genes *CD36*, *LPL*, *FABP4*, and *PLTP* in liver and adipose tissue, but not in muscle (den Besten *et al.*, 2015). The initiation of AMPK upregulation is caused by changed AMP/ATP ratio in liver (den Besten *et al.*, 2013; Kondo *et al.*, 2009). Importantly, mice study showed that in brown fat tissue and skeletal muscle, a further upregulation of PGC-1 α , the peroxisome proliferator-activated receptor PPAR-coactivator (PGC)-1 α is involved, but such change was not observed in liver and white adipose (den Besten *et al.*, 2015; Gao *et al.*, 2009). The modulatory activity of SCFAs in white adipose tissue is different with the regulations of SCFAs in liver, muscle and brown adipose tissue, which is considered via either GPR41 or GPR43. By using siRNA targeting on GPR43 in 3T3-L1 cell lines, and also through *ex vivo* studies, Hong *et al.* have showed that acetic acid and propionic acid achieve influence on adipose via GPR43 but not GPR41 (Hong *et al.*, 2005). To add up, the regulation of obesity of SCFAs shows highly tissue-specificity but are meantime well connected among different systems.

Besides the content discussed above, the downstream of PPARs regulation on nuclear transcription factors (TFs) is also an important part of the modulatory function of SCFAs. LDL receptor and CD36 (a lipoprotein receptor/fatty acid transporter) were assumed to be a mediators of PPAR γ -regulated lipid clearance. The association between

PPAR γ and LDL receptor was found in liver (Yu *et al.*, 2003). The co-upregulation of PPAR γ and CD36 was found in many other tissues including adipose, muscle, liver, and macrophages (Akiyama *et al.*, 2002; Gerhold *et al.*, 2002; Memon *et al.*, 2000). Although the inactivation of CD36 gene reduced fatty acid uptake in adipose tissue, skeletal muscle and heart, the effect was not observed in liver (Coburn *et al.*, 2000).

Taken together, the downstream events of SCFAs lipid regulation may finally through nuclear regulation on gene expressions of LDLR and CD36, following activation of PPAR γ driven TFs. Specifically, upregulated LDLR leads to an increased receptor-mediated endocytosis of LDL; whereas CD36 exhibits three functions in this process: (1) accumulation of cholesterol ester in cytoplasm; (2) generating more HDL and ApoA1; (3) LDL scavenge function (Marleau *et al.*, 2005). These events will combine with PPARs mediated mitochondrial fatty acid oxidation reduce cellular lipid content (McGarry and Foster, 1980; Reddy and Rao, 2006).

(2) The second route SCFAs mitigate obesity is through intestinal gluconeogenesis (IGN). Propionic acid and butyric acid are able to elevate IGN (De Vadder *et al.*, 2014). And the elevation of blood glucan from IGN can be detected by hepatoportal glucose sensor, thus able to generate a satiety feeling that decreases food intake. The upregulation of IGN is resulted by butyric acid and propionic acid through different mechanisms: butyric acid acts through a cAMP-dependent mechanism and can induce IGN genes *in vivo* and *in vitro*; propionic acid, as a substrate of IGN, can directly initiate a GPR41 dependent gut-brain neural circuit, but the observation is not observed *in vitro*. Following the preliminary stimulation, the glucose released by IGN can be detected by portal vein glucose sensor that connects with liver, and further transmit sensed signal to the brain through either vagus

nerve or spinal cord. Finally, SCFAs can falsify a c-fos-brought satiety to brain through colon IG1N, as c-fos in is a well-known pivot in generating satiety upon food intake (Batterham *et al.*, 2002).

(3) Colon-originated hormone regulation is the third route by which SCFAs can influence obesity and related secondary symptoms. The relationship between neuro hormone/transmitter and SCFAs have been noticed for a long time. Fukumoto *et al.* showed in rats, that the released 5-HT from EC cells in response to SCFAs, can upregulate 5-HT₃ receptors in the colonic mucosa, which may cure diarrhea and colonic transit problem (Fukumoto *et al.*, 2003). Byrne *et al.* showed that, fermentable hydrocarbons (FCs), or SCFAs themselves, can stimulate the production of anorectic gut hormones, such as glucagon-like peptide-1 (GLP-1) and peptide YY (PYY), which can reduce the energy intake (Byrne *et al.*, 2015). Samuel *et al.* and Psichas *et al.* have confirmed that SCFAs modulate obesity by regulating colon-generated glucagon-like peptide-1 (GLP-1) and peptide YY (PYY). They have conducted a serial of studies approached by KO rodent models *in vivo* and *ex vivo* cell lines. Their work, from functional genomic, biochemical, and physiologic aspects, showed that butyric acid and propionic acid can increase level of a variety of anorectic gut hormones, such as GLP-1 and PYY. The regulation mainly depends on GPR41 (Chambers *et al.*, 2015a; Samuel *et al.*, 2008). GLP-1 and PYY are well known hormones that can increase insulin secretion and reduce lipid storage, and these hormones are tightly associated many other physiological events related to obesity and TDM2. Nøhr *et al.* showed in monomeric red fluorescent protein (mRFP)-labeled GPR41 mice, that there is a “CCK-secretin-GIP-neurotensin-GLP-1-PYY lineage” that can be upregulated, after stimulation of GPR41-expression in enteroendocrine cells along the

intestine, from duodenum, jejunum, ileum to colon and rectum. In contrast, such co-stimulation pattern was not observed in GPR43. However, GPR43-mRFP reporter was found strongly expressed in a large population of leukocytes in the *lamina propria*, particularly in small intestine, but very weakly in a proportion of enteroendocrine cells, in which co-upregulation of GPR43, GLP-1 and mobilized intracellular Ca^{2+} were observed (Nøhr *et al.*, 2013). Collectively, evidences support that SCFAs carry with modulatory activities on a variety of gut hormone peptides, and can achieve a neuron and hormone ruling on obesity related aspects like glucose homeostasis, insulin sensitivity, appetite, gut motivation performance.

2.3.9 SCFAs and non-alcoholic fatty liver disease (NAFLD)

Adult nonalcoholic fatty liver disease (NAFLD) is featured by portal chronic inflammation (Brunt *et al.*, 2009). NAFLD has a prevalence of 20% in worldwide, a condition associated with an increased risk of developing T2DM, obesity, insulin resistance etc. The prevalence of NAFLD in the United States is reported to be between 10% and 30%, with similar rates reported from Europe and Asia. As the most prevalent liver disease in the US, NAFLD is defined by the presence of $\geq 5\%$ hepatic macrovesicular steatosis, in the condition that the patient consumes less than 20 g of alcohol per day (Farrell *et al.*, 2013; Vernon *et al.*, 2011). As a matter of fact, NAFLD connects many other metabolic diseases and symptoms. First, NAFLD can induce a range of secondary diseases like Nonalcoholic steatohepatitis (NASH), fibrosis, cirrhosis and portal hypertension (Browning *et al.*, 2004; Clark *et al.*, 2002). Once NAFLD came to the stage of cirrhosis, around 30%–40% patients will die of liver failure in 10 years (McCullough, 2006). Second,

a remarked association with obesity, metabolic/insulin resistance syndrome and dyslipidemia was unveiled (Adams and Angulo, 2006). NAFLD shows a significant association with obesity, T2DM and many other metabolic symptoms. For instance, NAFLD has been reported in over 76% of T2DM (Portillo-Sanchez *et al.*, 2015). Furthermore, over 90% of severely obese patients undergoing bariatric surgery have NAFLD (Kasturiratne *et al.*, 2013; Portillo-Sanchez *et al.*, 2015; Yamazaki *et al.*, 2015). A meta-analysis by Younossi *et al.* have shown that global prevalence of NAFLD is 25.24%, and in all patients with NAFLD: 51.34% have obesity, 22.51% have T2DM, 69.16% have hyperlipidemia and 42.54% have metabolic syndrome (Younossi *et al.*, 2015). Among these obese subjects, around 70%–80% have NAFLD and 15%–20% have NASH (Bugianesi *et al.*, 2002). Insulin resistance syndrome A was observed in 88% of patients with NASH (Marchesini *et al.*, 2003), and T2DM was found co-occurred with 30%–80% NAFLD patients (Marchesini *et al.*, 1999; Silverman *et al.*, 1989). A strong co-occurrence of NASH and obese has been observed under a background of obesity epidemic in the US and elsewhere (Calle *et al.*, 1999; Flegal *et al.*, 1998; James *et al.*, 2004; Livingstone, 2000). It has been reported that All patients with NAFLD show symptom of insulin resistance to some extent (Tolman and Dalpiaz, 2007).

Endogenous alcohol and microbial LPS, which can be generated by either infection or invaded bacteria from gut, are believed to be among the major factors that induce NAFLD (Deng *et al.*, 2015). And the gut microbial generated alcohol serves an important role in NAFLD etiology, which is suggested by the increased abundance of alcohol-producing bacteria, elevated blood-ethanol concentration, and biomarkers of alcohol induced oxidative stress in NASH patients (Tang *et al.*, 2013). On the other hand, LPS and

other microbial components can enter liver and bind to the specific receptor-activating TLRs signaling in different liver cell populations, triggering the activation of cytokines like pro-IL-1 β and pro-IL-18, and promote inflammation and fibrogenic pathway (De Minicis *et al.*, 2014).

Propionic acid has a high liver concentration and carries with a comprehensive modulatory effect on NAFLD. It was found in rats that an addition of 0.5% sodium propionic acid in cholesterol diet can significantly reduce liver and serum cholesterol level, compared with the control group, though serum triglyceride concentrations were not changed (Chen *et al.*, 1984). Additionally, it was reported that propionic acid can downregulate hepatic lipogenic enzymes, specifically fatty acid synthase (FAS) (Parnell and Reimer, 2010). Chambers *et al.* developed a novel inulin-propionic acid ester (IPE), in which propionic acid is bounded with dietary fiber inulin, and is released upon microbial fermentation (Byrne *et al.*, 2015). In their study, 16 participants (40–65 years) with NAFLD were recruited and were provided with either 10 g/day IPE (n = 11) or 10 g/day inulin control (n = 5) and a significant reduction in intrahepatocellular lipid (IHCL) content post-intervention was observed. However, some researchers reported that at the concentrations that are significantly higher than normal level, propionic acid may accumulate in liver mitochondria in the form of propionyl-CoA, and inhibit liver mitochondrial function (Matsuishi *et al.*, 1991).

2.3.10 Modulatory effects of SCFAs on inflammatory bowel disease

It is known that the hereditary forms of colon cancer only count around 15–30 % of the total incidence of colorectal cancer (CRC) (Taylor *et al.*, 2010). Most CRC cases

(50–75 %) could be prevented by adapting dietary patterns to a healthy diet (Englund *et al.*, 2007). Epidemiological data have shown that a routine diet covering fish, dairy foods, poultry meat, high fiber diets, and daily coffee or tea drinking can significantly reduce the incidence of colon cancer; while red meat, pickled vegetables, processed meat products are proven risk factors for colon cancer incidence (Chao *et al.*, 2005; Chavarro *et al.*, 2008; Clausen *et al.*, 1991; Larsson *et al.*, 2005; Lee and Lee, 2010; Mirvish *et al.*, 2008; Willett *et al.*, 1990). Cohort studies in Europe and China have consistently revealed that patients with T2DM had a lower proportion of butyric acid-producing and a larger proportion of non-butyric acid-producing *Clostridiales* (Karlsson *et al.*, 2013; Qian *et al.*, 2013). A case-control study has demonstrated that the significant association of reduced level and uncommon ratio of SCFAs with inflammatory bowel disease (IBD) (Huda-Faujan *et al.*, 2010). In this study, fecal samples were obtained from 50 healthy subjects (male = 18, female = 32) and 8 IBD (male = 6, female = 2) subjects from March 2007 to December 2008 in Selangor, Malaysia. The age of the studied patients ranged from 34 to 68 years and the age for the healthy subjects ranged from 22 to 55 years. SCFAs ratio and level indicate gut microbiota condition and proportions, and also the general healthy situation. Besides, *Firmicutes* phylum could significantly decrease in inflammatory bowel disease (Frank *et al.*, 2007). It has been found that the increased gene expression of inflammatory mediators like TNF- α , interleukin 6 (IL-6) and inducible nitric oxide synthase (iNOS) in both human samples and animal models of obesity (Hemmrich *et al.*, 2007; Weisberg *et al.*, 2003). Butyric acid can exert its anti-proliferative properties by altering colon cancer cells that are initially highly glycolytic to butyric acid utilizing phenotype. A cross-sectional study for which 93 CRC patients, 27 healthy individuals and 22 healthy individuals with adenoma

were enrolled, has shown that, the concentrations of SCFAs were significantly decreased in the CRC group and the pH was increased, while adenoma group were intermediate to CRC group and non-adenoma group (Ohigashi *et al.*, 2013). In human, a case control study showed that one mechanistic aspect of SCFAs chemoprevention was achieved through SOD2, with increased level of mRNA as 1.96-fold; protein as 1.41-fold and enzymatic activity as 1.8-fold (n = 21 in case group, mean age 66 ± 13 yrs, $p < 0.05$) (Jahns *et al.*, 2015).

To increase butyric acid concentration in colon, there have been several methods tested so far, including vehicle/booster molecule of SCFAs, and various SCFA-generating probiotics. For the former one, oligosaccharide acarbose can act as α -glucosidase inhibitor and indirectly increase colonic butyric acid concentration by enabling more starch to arrive colon. Tributyrin, which contain three butyric acid molecules, can augment butyric acid concentrations through hydrolysis of pancreatic and gastric lipases (Weaver *et al.*, 1997; Wolever and Chiasson, 2000). Consumption of butyric acid-producing probiotic bacterial strains like *Butyrivibrio fibrisolvens* and *Clostridium butyricum* has been modeled in rats and mice (Araki *et al.*, 2004; Araki *et al.*, 2000; Ohkawara *et al.*, 2005). It has been shown in MCF-7 human breast and HT-29 human colon cancer cells that novel SCFA-acylated daunorubicin–GnRH-III bioconjugates can serve as drug delivery systems for targeted cancer chemotherapy (Hegedus *et al.*, 2012). Thirabunyanon *et al.* have screened *Pediococcus pentosaceus* FP3, *Lactobacillus salivarius* FP25, *Lactobacillus salivarius* FP35 and *Enterococcus faecium* FP51 from infant feces and showed that they are probiotic bacteria that have anti-proliferative effect on colon cancer cells by generating butyric and propionic acids (Thirabunyanon and Hongwittayakorn, 2013).

2.3.11 SCFAs, gut-microbiota and nervous system associated inflammation

Meta-genomics studies have uncovered a permeable boundary between gut-microbiota, gut-autoimmune-lymphatic-tissue (GALT), intestinal endocrine system and the gut-brain neuro axis (Carabotti *et al.*, 2015). The microbiota-brain link is also mutually regulated (Cryan and Dinan, 2012; El Aidy *et al.*, 2016; Mayer *et al.*, 2015). The influence of the gut microbiota on brain has been demonstrated in host's intelligent/emotional performances and autonomic nerve functions like sleep, hunger and satiety. Epidemiological studies have demonstrated a significant association between dysbiosis and CNS disorders including autism, anxiety, depression, schizophrenia, atherosclerosis, neuromyelitis optica, Guillain-Barre syndrome, meningitis, chronic fatigue syndrome, Parkinson's disease (PD) and Alzheimer's disease (AD) (Cryan and Dinan, 2012; Daulatzai, 2015; El Aidy *et al.*, 2015; I Naseer *et al.*, 2014; Kist and Bereswill, 2001; Ochoa-Reparaz and Kasper, 2014; Tsang, 2002). The misfolded plaques or oligomers of disease-induced immune proteins like β -amyloid, tau, α -synuclein, huntingtin and TDP-43 have been considered to be the major inducer of the above neuro diseases (Goate *et al.*, 1991; Murrell *et al.*, 1991; Poorkaj *et al.*, 1998; Weiss *et al.*, 2012).

As the second most common neurodegenerative disease, PD is estimated to affect 1%–2% of the population over 65 years old, and more than 4% of the population by the age of 85 years in the world wide (De Rijk, 2000). The primary neuropathology of PD is the loss of midbrain dopaminergic neurons and the following characteristic motor deficits (Alexander, 2004). The initiation of PD is believed to be a multifactorial process, and the major causes include immune abnormality, alpha-synuclein abnormality, LRRK2 gene mutations (up to 80 types of pathogenic variants), PARKIN gene mutations (parkin, pivot

regulator of mitochondria shape and ubiquitin-proteasome system), autosomal recessive etc. (Corti *et al.*, 2011). The motor deficiency is the clinical diagnostic standard, but the patients also have a number of non-motor symptoms (NMS), such as gastrointestinal disturbances, pain, psychiatric disorders, depression and anxiety (Chaudhuri *et al.*, 2006). These syndromes generally happen before the motor symptoms and are highly associated with a dysfunction in the communication between gut and brain (Baig *et al.*, 2015; Pfeiffer, 2003). These non-motor PD symptoms are highly associated with gut-microbial imbalance, with affects that often precede motor symptoms, whereas the administration of gut-probiotics can ameliorate such symptoms (Barichella *et al.*, 2009). These findings lead to the hypothesis that gut microbial disorder happens before the appearance of neurodegenerative cases and some studies were conducted to explain this phenomenon. Several pathological studies have shown the spatial-temporal association between neuro diseases and the changes of certain immune proteins, with widely observations from *in vivo*, *in vitro* and *ex vivo* studies in diseases such as Alzheimer's, Parkinson's, Huntington's, amyotrophic lateral sclerosis (ALS) (Bhattacharyya *et al.*, 2014; Deng *et al.*, 2015; Goedert and Spillantini, 2006; Kumar *et al.*, 2016; Mulak and Bonaz, 2015; Pfeiffer, 2003; Stefanis, 2012; Tada *et al.*, 2011). As a major route for pathogens to enter human body and induce disturbance in immune system, intestinal epithelium has attracted attention from scientists in many different fields. To correlate gut microbial metabolites with the healthy condition, or to manipulate the metabolic composition of intestinal microbiota, are therefore of highly clinical significance.

Gut-microbiota is considered to be a major link of PD, immune disorder, and a number of CIDs. Persistent and excessive stimulation of the GALT would result in

symptoms like gut dysbiosis, bacterial overgrowth and increased intestinal permeability. The activation of enteric neurons and enteric glial cells may contribute to the initiation of alpha-synuclein misfolding. And chronic stimulation would result in accumulation of alpha-synuclein. The alpha-synuclein have cytotoxic misfolding and/or excessive secretion that affect all levels of the brain-gut axis, including the central, autonomic, and enteric nervous systems (Stefanis, 2012). In addition, the adaptive immune system may be misled by bacterial proteins and cross-react with human antigens, thereby resulting a variety of auto-immune diseases (Tlaskalova-Hogenova *et al.*, 2011).

In addition, small intestinal bacterial overgrowth (SIBO) and *H. Pylori* infection may also contribute to the incidence of PD. SIBO and *H. Pylori* infection usually lead to abdominal pain caused by the damage of small intestinal and gastric mucosa, via bacterial adherence and enterotoxin production (Sachdev and Pimentel, 2013). The microbial toxins can either act locally on enteric nerves, or translocate via humoral or vagal afferent pathways to affect neuro duct to induce pain (Kountouras *et al.*, 2012). Such observation is consistent with the detected migration of immune cells stimulated in the intestine and appearing in distal sites, and is also backed up by the systemic diffusion of microbial metabolites, or the invaded bacteria from integrity-impaired intestinal barrier (Wang *et al.*, 2015b). In an epidemiology study conducted by Fasano *et al.*, the presence of SIBO was reported in 54% of PD patients and is associated not only with the GI symptoms but also with the motor symptoms. The motor fluctuations were significantly promoted by treatment with Rifaximin (Fasano *et al.*, 2013). In another study, SIBO was detected in 25% of PD patients, and showed early occurrence in the disease progress (Bhattacharyya *et al.*, 2014). Accordingly, it is assumed that SIBO induces the impairment of small intestinal

integrity and thus leads to the PD symptoms discussed above. Another example to show the association between gut-microbiota and neurodegenerative diseases is the link between gut pathogens and AD—the most common neurodegenerative disease. It was uncovered by Tanzi *et al.* that amyloid-beta, an anti-microbial peptide, can bind with microbial cell wall, and the formed A β oligomers are able to develop protofibrils on-site, to inhibit pathogen adhesion to host cells. Their *in vivo* models of both mouse and nematode have indicated that, persistently disturbed immune responses to invaded pathogens can stimulate the over-production of amyloid-beta, which gathers tough fibril-like structures called amyloid plaques within the brains of patients (Kumar *et al.*, 2016; Soscia *et al.*, 2010).

Could administration of SCFAs modulate neuro diseases and related inflammation? Very likely. It is believed that to modify gut microbiota composition in PD patients would influence the cascade of neurodegeneration in PD (Mulak and Bonaz, 2015). A recent finding has uncovered that, the formation of alpha-synuclein aggregates in gut enteric nervous system (ENS), both the submucosal plexus (i.e. Meissner's plexus) and myenteric plexus (i.e. Auerbach's plexus), is prior to their appearance in CNS (Felice *et al.*, 2016). This report has well backed up the hypothesis that PD can be initiated from gut microbial disturbance on GALT. Mechanistically, there is a close mutual relationship between gut dysbiosis, intestinal permeability and gut inflammation. The changes of intestinal permeability may stimulate the translocation of bacteria and endotoxins across the epithelial barrier, thereby inducing the immunological responses that secret pro-inflammatory cytokines. In such process, the intensively disturbed enteric neurons and glial cells in the gut *lamina propria* may result in neurological dysfunction along the whole brain-gut axis (de Magistris *et al.*, 2016; Felice *et al.*, 2016; Mulak and Bonaz, 2015).

Therefore, the application of SCFAs may protect and maintain the epithelium so as to prevent the incidence of such dysfunction.

2.3.12 *Conclusion and future perspectives*

In this work, we have collected the relevant studies in terms of the various associations between gut-microbiota dependent SCFAs and CIDs. The major findings reported by these studies suggested that SCFAs carry with the modulatory effects on a number of CIDs, e.g. obesity-associated inflammation, liver inflammatory diseases, colorectal inflammation, and the nervous system disease-associated inflammatory status. The available mechanism and evidences demonstrated that the use of SCFAs in preventing and mitigating CIDs is applicable. The clinical use of SCFAs seems to be a promising approach to adjust the endogenous level of intestinal SCFAs, as well as their absorption, distribution, and metabolisms. And we are looking forward to see more innovative application of SCFAs in the field of clinical nutrition which may incorporate novel vehicles, prebiotics or probiotics as facilitating tools.

2.4 Clinical references for omics data interpretation

2.4.1 *In Vitro test for liver abnormality and metabolic disorder*

Traditionally, in the fields of toxicology, pharmacology, nutrition and so on, biofluid-based biochemical analysis serves as a basic way of *in vitro* examination to preliminarily probe individual health status. The tested samples are mainly the blood, urine and feces collected from patients and the acquired information can well reflect the physiological status of organs and systems, the adverse affects of xenobiotics and the

effectiveness of medical treatment (Miri-Dashe *et al.*, 2014). Among the various tests, probably the most widely used one is the lab based blood test (Baron, 1996; MacLennan *et al.*, 2007). In America, the blood test technique has been gradually established since last 1940s, marked by the milestones such as the official introduction of Coombs test in 1945 (Coombs *et al.*, 1945), and the marriage license-required blood test for syphilis in 1947 (Brandt, 1988). With all the improvements made by the researchers in the worldwide, by now blood test has become a standard, convenient and reliable tool for clinical diagnosis. In America, standardized panels and processes are designed and certified by professional agencies such as Clinical Laboratory Improvement Amendments (CLIA), American Medical Association (AMA) (Ehrmeyer and Laessig, 2004).

The nature of human blood is a complex and dynamic liquid mixture that compositionally include erythrocytes, leucocytes, thrombocytes and plasma. There are all kinds of nutrients, immune factors and metabolites transported in the plasma. The metabolites can either be exogenous or endogenous, containing drug metabolites, lipids, glucoses, nucleoside triphosphate, functional nucleotides, cytokines, virus, enzymes, short peptides and amino acids like glutamine, homocysteine, creatinine, lipoprotein, albumin and C-reactive protein (CRP) (MacLennan *et al.*, 2007). Many hydrophobic components like bilirubin, or enzymes such as alkaline transferase are conjugated with carrier protein like albumin and lipoprotein (Miri-Dashe *et al.*, 2014). Unless otherwise specified, blood sample is mainly the arterial blood collected by arm venipuncture with vacuum tube (MacLennan *et al.*, 2007). Rarely, for some specialized tests like arterial blood gas test, the artery blood is needed. The collected artery blood is analyzed to monitor carbon dioxide and oxygen levels related to pulmonary function, and also offers information on the blood

pH and bicarbonate levels. Blood test is also a proven way to examine virus infection. One such contribution of blood test is the screening of hepatitis virus such as HAV, HBV and HCV, which is considered to be a significant contribution in some countries with epidemic of viral hepatitis such as China (Gao *et al.*, 2009).

The routine method to prepare serum or plasma sample from blood sample, is via the centrifugation of blood sample, using inert gel barrier inserted evacuated tubes. The inert gel polymers have a specific gravity between the serum/plasma and the cellular portion of blood (Smith, 1989). In the case that plasma sample is needed, several strategies have been applied for the anticoagulation, i.e. EDTA-treated, normally with lavender cap; citrate-treated anticoagulant tubes, normally with light-blue cap; heparinized tubes which normally have green tops (Penetar *et al.*, 2008). It is worthy noting that heparin can often be accompanied with endotoxin, which can stimulate white blood cells to release cytokines, thus related immuno assays need to be cautious in sample preparation (Theoharides *et al.*, 2012). The second step for plasma preparation is the centrifugation, through which the liquid portion of blood sample can be separated from the cellular components that disrupt the consequent analysis. However, in the process of centrifugation the pellet spun down sometimes migrates up again and contaminates the supernatant part needed (Yagi, 1984). By contrast, serum is much easier to be separated with the solid portion of blood, in that it is free of cells and platelets which are precipitated away with the fibrin meshwork of the clot, though there is still contamination generated in the platelet clotting (Bruce *et al.*, 2009; Yagi, 1984). Regarding which type of blood sample, plasma or serum should be used for lab tests, a debate exists. Yet in most cases serum is considered the gold standard and the

majority of lab reference ranges are based on serum, though a 30 min clotting time is required (Penetar *et al.*, 2008).

Blood tests are often performed in health care to investigate liver function, metabolic homeostasis and disease progression (Table 2-2). In practice, multiple tests for targetted blood components are often grouped together into one blood test panel, e.g. blood glucose test and cholesterol test (Burtis *et al.*, 2012). A typical metabolic panel includes measurement of sodium, potassium, chloride, bicarbonate, blood urea nitrogen (BUN), magnesium, creatinine, glucose, and sometimes calcium (Burtis *et al.*, 2012; Higgins, 2007; Saathoff *et al.*, 2008). Another frequently performed test is cholesterol level panel, which typically includes LDL and HDL cholesterol levels, as well as triglyceride levels (Castelli and Anderson, 1986). The cholesterol test panel is especially important for the aged population. Some tests require specially designed process at different time points, such as the regular glucose test which is taken at a certain point in time; and the glucose tolerance test, for which repeated testing is needed to determine the rate at which glucose is physiologically processed (Nichols *et al.*, 2008). The metabolic panel is another case in which complex blood analysis can be useful. The phenotypes of this syndrome include elevations of remnant lipoproteins, fasting glucose, blood pressure, circulating inflammatory cytokines, prothrombotic factors and suppressed levels of high density lipoproteins (HDL). A group of biomarkers have been associated with metabolic syndrome, e.g. non-esterified fatty acids, leptin, adiponectin, resistin, angiotensinogen, insulin, insulin-like growth factor binding protein-2 (Heald *et al.*, 2006; Reaven, 2005; Trayhurn, 2005). These components can be examined together from blood sample and serve as a test panel.

The most performed test for general examination is the liver function test (LFT) (Hoekstra *et al.*, 2013). The principle of it lies in that the physiological status of liver can be reflected by the blood enzymes and proteins secreted by liver and released from liver upon damage. So far, LFT has been proven as an efficient and effective approach to evaluate liver status. It normally consists of several metrics that can be performed at the same time. Typically, in order to conduct a reliable examination, subjects are asked to avoid eating or drinking for a consecutive 8 hours. Even though, the normal ranges for liver function tests still variate largely by the age, gender, race and region (Dufour *et al.*, 2000). Therefore, different labs may have different reference ranges applied which have numeric difference.

Table 2-2. Performance specifications and precisions for liver tests (%).

Reference source	Type of standard	Specifications of measurements					
		ALT	AST	ALP	GGT	Albumin	Bilirubin
Standard imprecision, %							
CLIA	Mandate standard	TE = 20	TE = 20	TE = 30	NS	TE = 10	TE = 20
European	Biological variation	I = 13.6	I = 7.2	I = 3.4	NS	I = 1.4	I = 11.3
		B = 13.6	B = 6.2	B = 6.4	NS	B = 1.1	B = 9.8
		TE = 36	TE = 18	TE = 12	NS	TE = 3.4	TE = 28
Ricos et al.	Biological variation	I = 12.2	I = 6.0	I = 3.2	I = 6.9	I = 1.6	I = 12.8
		B = 12.2	B = 5.4	B = 6.4	B = 10.8	B = 1.3	B = 10
		TE = 32	TE = 15	TE = 12	TE = 22	TE = 3.9	TE = 31
Skendzel et al.	Clinician opinion	NS	TE = 26	NS	NS	NS	TE = 23
Within-laboratory imprecision, %							
Lott et al.	Proficiency tests	8	9	5	6	NS	NS
Ross et al.	Proficiency tests	NS	NS	NS	NS	4.4	8.9

Abbreviations: ALT, alanine transaminase; AST, aspartate transaminase; ALP, alkaline phosphatase; GGT, gamma-glutamyltransferase. TE, total error; I, imprecision or degree of reproducibility; B, bias or difference from correct result; NS, not specified. The table is modified from (Dufour *et al.*, 2000). Related references are from Westgard *et al.* (Westgard

et al., 1994), Ricos *et al.* (Ricos *et al.*, 1999), Skendzel *et al.* (Skendzel *et al.*, 1985), Lott *et al.* (Lott *et al.*, 1988), Ross *et al.* (Ross and Lawson, 1995).

Table 2-3. American Medical Association (AMA) approved organ or disease oriented panels for blood test.

Panel Component	Basic Metabolic Panel 80048	Comprehensive Metabolic Panel 80053	Electrolyte Panel 80051	Hepatic Function Panel 80076	Acute Hepatitis Panel 80074	Lipid Panel 80061	Obstetric Panel 80055	Renal Function Panel 80069
ABO, 86900							■	
RH(D), 86901							■	
Antibody Screen, 86850							■	
Rubella Antibody IgG, 86762							■	
Hepatitis B Surface Antigen, 87340							■	
VDRL, 86592							■	
CBC w/Differential & Plt., 85025							■	
Phosphorus, Inorganic, 84100								■
Carbon Dioxide, 82374	■	■	■					■
Chloride, 82435	■	■	■					■
Potassium, 84132	■	■	■					■
Sodium, 84295	■	■	■					■
Creatinine, 82565	■	■						■

Glucose, 82947	■	■						■
BUN, 84520	■	■						■
Calcium, 82310	■	■						■
Albumin, 82040		■		■				■
AST (SGOT), 84450		■		■				
Alkaline Phosphatas e, 84075		■		■				
Bilirubin, Total, 82247		■		■				
Protein, Total, 84155		■		■				
ALT (SGPT), 84460		■		■				
Bilirubin, Direct, 82248				■				
Hepatitis A Antibody, IgM, 86709					■			
Hepatitis B Surface Antigen, 87340					■			
Hepatitis B Core Antibody, IgM, 86705					■			
Hepatitis C Antibody, 86803					■			
Cholesterol , 82465						■		
HDL Cholesterol , 83718						■		

LDL Cholesterol (Calculation), 83718						■		
Triglycerides, 84478						■		

2.4.2 Alanine aminotransferase (ALT or SGPT)

ALT has two isoforms, named as ALT1 and ALT2. The major expression of ALT1 was found in liver, skeletal muscle and kidney, with relatively lower level in heart muscle. On the other hand, high level of ALT2 can be detected in skeletal and heart muscle (Lindblom *et al.*, 2007). The measurement of blood ALT activity is very useful in checking hepatitis, and is taken as a specific biomarker of hepatocellular injury (Kim *et al.*, 2008). Abnormal high level of ALT frequently cooccurred with infection of acute hepatitis, while moderate increase can be seen accompanied with chronic hepatitis. Importantly, the uptake of certain drugs or during exercise also lead to elevation of ALT.

2.4.3 Aspartate aminotransferase (AST or SGOP)

AST is an enzyme mainly distributing in the liver, heart and the muscular tissues around the whole body. AST has two isoenzymes: mitochondrial type and cytosolic type (Baudhuin *et al.*, 1964). The mitochondrial form is located in hepatocytes, functionally reacting to membrane oxidative stresses, taking a role similar with ALT. The cytosolic form is usually present in skeletal muscle, heart muscle and kidney tissue. Similar to ALT, a very high level of AST is frequently seen with acute hepatitis, and usually the rise of blood AST occurs in conjunction with ALT. The ratio of AST/ALT is conventionally used to estimate different types of hepatocellular injury. An AST/ALT ratio equal to 1:1, yet

with both levels elevated, would suggest acute viral hepatitis or drug-related liver injury. An AST/ALT ratio higher than 2:1, as mentioned above, would indicate alcoholic liver disease. Importantly, an AST/ALT ratio higher than 1:1 could also indicate cirrhosis if there is no alcoholic hepatitis found in patients (Pratt and Kaplan, 2000). When liver damage is induced by alcohol, AST often increases much more than ALT, a pattern rarely observed with few other liver diseases (Giannini *et al.*, 2005). An elevated AST level can also be found after heart attacks and muscle injury (Giboney, 2005). Besides, during chronic hepatitis, blocked bile ducts, cirrhosis and liver cancer, AST level may be moderately increased as well (Green and Flamm, 2002).

2.4.4 Alkaline phosphatase (ALP)

ALP is an enzyme primarily generated in the bile ducts but also produced by the bones and intestines. The enzyme is produced by the epithelial cells lining bile ducts and canaliculi, and is released in response to the accumulation of bile salts or cholestasis (Hatoff and Hardison, 1982). ALP may be significantly increased with obstructed bile ducts, cirrhosis, liver cancer, and also with bone disease (Kaplan and Righetti, 1969). Since ALP is also generated in the kidney, intestine, leukocytes, placenta and bone, functional elevation of ALP can be seen during female pregnancy or in the growing period for children, whereas abnormal rise of level could occur in Paget's disease, renal disease and bone metastases (Lehmann, 1975). To detect ALP with special origin, monoclonal based ELISA can be very useful (Gomez *et al.*, 1995). For example, Du *et al.* reported that in nineteen trials with 3268 subjects included, the mean level of serum bone ALP was 41.50 ± 26.61 $\mu\text{g/L}$ (216.90 ± 139.00 U/L) in patients with osseous metastases and 14.49 ± 5.52 $\mu\text{g/L}$

(103.30 ± 39.44 U/L) in patients without osseous metastases. The serum level of B-ALP was significant higher in the osseous metastases group than that in the control group ($p < 0.05$) (Bhattacharyya *et al.*, 2014).

2.4.5 Gamma-glutamyl transferase (GGT)

GGT is primarily present in liver, kidney, pancreas and intestine, but the majority of GGT in serum is released from liver. The enzyme is a cell-surface protein featured for its function to the extracellular catabolism of glutathione (GSH). In liver, it can be found in the microsomes of hepatocytes and biliary epithelial cells. A physiological elevation is found to be induced by chronic alcohol use or intake of rifampicin and phenytoin (Hall and Cash, 2012). An elevation of GGT, in association with a rise of ALP, highly suggests of a biliary tract obstruction, known as a cholestatic picture. A GGT test may be used to help determine the cause of an elevated ALP. It is worth noting that both ALP and GGT are elevated in bile duct and liver disease, but only ALP will be elevated in bone disease (Siris *et al.*, 1998).

Importantly, high level of GGT has been associated with increased risk of atherosclerotic cardiovascular disease (CVD). Lee *et al.* reported that in 3451 Framingham Study participants (mean age of 44 years old, 52% women), an increased serum GGT predicted the onset of metabolic syndrome and the occurrence of CVD and death; moreover, the highest GGT quartile experienced a 67% increase in CVD incidence. In this study the association of GGT concentrations with CVD and mortality remained significant after adjustment for traditional cardiac risk factors and C-reactive protein level, a metric reflecting general levels of inflammation (Lee *et al.*, 2007).

2.4.6 Bilirubin

Bilirubin is a yellow pyrrole compound generated in the catabolic pathway of heme break down, a routine physiological process in the vertebrate reticuloendothelial cells in liver, spleen and bone marrow (Wolkoff *et al.*, 1983). Free bilirubin is transported to liver after binding with circulating albumin, in which case the conjugated bilirubin is also called “direct” bilirubin. In liver bilirubin is conjugated with glucuronic acid by the enzyme glucuronyl transferase and then excreted into the small intestine via bile ducts (Erlinger *et al.*, 2014). The level of bilirubin is especially important if a person has jaundice. High bilirubin level is very common in newborns from 1 to 3 days old. In many healthy persons, the serum unconjugated bilirubin is mildly elevated to a concentration of 2 to 3 mg/dL (equal to 34–51 $\mu\text{mol/L}$) after a 24-hour fasting. However, if unconjugated bilirubin is high yet it is the only abnormality, while the conjugated bilirubin level and complete blood count being normal, the diagnosis is usually assumed to be Gilbert syndrome (Vitek *et al.*, 2002). The syndrome was recently shown to correlate with to a variety of partial defects in uridine diphosphate-glucuronosyl transferase, which conjugates bilirubin with albumin for transportation (Johnston, 1999). Interestingly, bilirubin can behave as an antioxidant or pro-oxidant, depending on specific situations. In neonatal jaundice, bilirubin at low concentration is an antioxidant, yet in the case of haemolysis it is of high chance that albumin may be over-generated and lead to systematic oxidative stressing (Mizejewski *et al.*, 2013).

2.4.7 Albumin

Hydrophobic substances can only be transported in the blood when they are attached to carrier proteins. Albumin is one such carrier protein and, as already discussed,

is the primary carrier protein for the transportation of bilirubin. Albumin is synthesized from amino acids in the liver, and typically is at normal level upon liver disease. As the main protein generated by the liver, the level of albumin can be affected by the functional changes of liver and kidney, since a deficiency of renal filtering function would release albumin in urine (Foley *et al.*, 1996). More frequently, decreased blood albumin is induced by nutritional deficiency, a phenomenon frequently seen in Crohn disease, Low-protein diets, Celiac disease and Whipple disease (Russell, 1986; Zeuzem, 2000). In practice, patients with low serum albumin concentrations yet no other LFT abnormalities are most likely to have a non-hepatic cause for low albumin. Such causes include proteinuria, acute or chronic inflammation in burns, trauma and sepsis, and active rheumatic disorders or severe end-stage malnutrition (Johnston, 1999). Severe liver function decrease can be indicated by a measured results of total serum bilirubin concentration > 2.0 mg/dL and serum albumin concentration < 3.5 g/dL (Kamath *et al.*, 2001). Plasma bilirubin/albumin ratio (B/A) in newborn may be used to identify newborns at risk for bilirubin encephalopathy and neurotoxicity (Iskander *et al.*, 2014).

Depending on specific situation, there may be many other metrics added into a regular LFT, e.g. lactate dehydrogenase (LD), prothrombin time (PT), alpha-feto protein (AFP) and autoimmune antibodies. These tests are very useful to understand certain disease incidence and staging. Lactate dehydrogenase (LD) is a non-specific marker of tissue damage and may be elevated with acute liver disease or liver tumors, yet it is also elevated with a number of other conditions that do not affect the liver. A prolonged or increased Prothrombin time (PT) can be seen with liver disease or coagulation factor deficiency. Different estimates or reference values exist, based on specific population statistics (**Table**

2-4). Because the standard normal ranges of blood test variate with a number of factors such as age, gender, region, life styles and genetics (Table 2-5).

Table 2-4. Comparison of representative reference ranges of LFT.

Parameter	Nigeria	Kenya	Tanzania	Tanzania (Mbeya)	U.S.	FDA
Urea Nitrogen mmol/L M	3.0 (2.2-4.8)	2.8 (1.5-4.6)	1.5-5.0	2.77 (1.57-5.01)	3.6-7.1	3.32-6.68
Urea Nitrogen mmol/L F	3.3 (2.5-5.8)	2.5 (1.4-4.6)		2.55 (1.47-4.61)		
Creatine μ mol/L M	85.8 (76.3-111.1)	77 (62.0-106.0)	0-90	56 (40-81)	0-133	88.4-176.8
Creatine μ mol/L F	79.3 (63-117.8)	66 (51-91)		69 (48-96)		
Glucose mmol/L M	4.9 (3.7-7.9)	4.1 (3.0-5.6)	2.9-5.2	4.16 (2.88-5.3)	4.2-6.4	4.4-6.7
Glucose mmol/L F	5.9 (4.4-9.6)	4 (3.2-5.7)		3.95 (3.3-5.06)		
AST (U/L) M	33.1 (26.0-49.4)	23.9 (14.9-45.3)	0-48	28.2 (15.2-53.4)	0-35	0-40
AST (U/L) F	33 (22-58.4)	19.1 (13.1-38.1)		20.1 (13.5-35.2)		
ALT (U/L) M	24.4 (17.3-48.4)	22.3 (10.8-53.9)	0-48	24.7 (9.1-55.3)	0-35	0-30
ALT (U/L) F	24.1 (19-38)	16.8 (8.6-47)		16.6 (6.7-44.9)		
Total bilirubin μ mol/L M	6.8 (3.4-17.1)	12.2 (5.6-42.9)	5.2-41	13.9 (6-42)	5.1-17	Total < 17.1
Total bilirubin μ mol/L F	2.3 (0.3-10.6)	9.6 (4.4-26.8)		10 (4.5-31.3)		Direct < 6.84
Total cholesterol (mmol/L) M	4.8 (3.2-5.3)	3.8 (2.5-5.5)	0-5.5	3.77 (2.32-5.67)	0-6.2	<5.82
Total cholesterol (mmol/L) F	4 (3.1-5.6)	3.9 (2.6-5.9)		3.92 (2.82-5.50)		
Triglyceride (mmol/L) M	1.1 (0.7-2.2)	0.9 (0.4-2.7)	0-2.9	0.91 (0.39-3.01)	0-1.8	0.45-2.26
Triglyceride (mmol/L) F	1.0 (0.6-2.1)	0.8 (0.4-2.5)		0.79 (0.38-2.18)		

In this modified table, references from other African region and U.S. are added for comparison (Adedara *et al.*, 2014; Kratz *et al.*, 2004; Saathoff *et al.*, 2008). The calculated ranges are very useful, in that currently there is a strong demand of improving personal health in the large amount of underdeveloped countries and developing countries in Africa (Bultman, 2014).

Table 2-5. Reference ranges of liver function related enzymatic activities.

Sources	Total bilirubin	ALT	AST	GGT	ALP	Albumin
Reference 1, 25 °C	0.2–1 mg/dL	8–30 U/L	10–40 U/L	Female U/L Male U/L	4–18 6–28 U/L	14–80 U/L NA
Reference 2, 37 °C	< 17 µmol/L	10–37 U/L	NA	Female Male	23 33 U/L	39– 128 U/L 35–50 g/L
Reference 3, 37 °C	0.2-1.2 mg/dL/(0–0.4 mg/dL)	Female U/L Male U/L	10–28 13–40	10–59 U/L	Female U/L Male U/L	1–24 2–30 U/L 14–80 U/L NA

Reference 1 is excerpted from (Koff, 1980); Reference 2 excerpted from (Blann, 2013; Higgins, 2007); Reference 3 is excerpted from (Burtis *et al.*, 2012).

Specifically for America, a representative and useful reference range was generated from the third National Health and Nutrition Examination Survey (NHANES III, **Table 2-6**), which is essentially a large cross-sectional study of the civilian noninstitutionalized U.S. population, conducted from 1988 to 1994 (Lazo *et al.*, 2008). The participants are 1864 adults with equal sex distribution, aged over 18 years old, also with equally split between age 20 to 39 years and age 40 years or older. In the study, alanine aminotransferase (ALT), aspartate aminotransferase (AST), γ -glutamyltransferase, alkaline phosphatase, and total bilirubin were selected as major tested biomarkers. It was calculated from the study, the upper limit of cutoff values for the normal levels of the liver test results are suggested as: AST levels higher than 37 U/L for men and 31 U/L for women, ALT levels higher than 40 U/L for men and 31 U/L for women, γ -glutamyltransferase levels

higher than 51 U/L for men and 33 U/L for women, alkaline phosphatase levels higher than 177 U/L, and total bilirubin levels higher than 17.1 $\mu\text{mol/L}$ ($> 1 \text{ mg/dL}$).

Table 2-6. Liver test results in the U.S. NHNES III, 1988-1994.

Serum composition	Median level & range
Alanine transferase	13 U/L (3–40 U/L)
Aspartate transaminase	19 U/L (8–37 U/L)
Gamma-glutamyltransferase	19 U/L (3–51 U/L)
Alkaline phosphatase	82 U/L (17–174 U/L)
Total Bilirubin	9 $\mu\text{mol/L}$ (1.7–17.1 $\mu\text{mol/L}$)

Abnormal results of LFT test may entail a repeat analysis of one or more components, or the whole panel. In the case that a person with liver disease is being medically treated, results of the liver panel can help to determine if liver function or damage is worsening or improving. The LFT results from American Association for Clinical Chemistry (AACC, **Table 2-7**) Child-Turcotte class (**Table 2-8**), known as the “Child” class, can be very helpful in monitoring the prognosis of liver functionality. By using this table, a “Child” score is calculated by adding the points as determined by the patient's laboratory results: class A = 0 to 1; class B = 2 to 4; class C = 5 and higher. The results can approximately estimate the severity of liver dysfunction: class A is associated with a good prognosis, and class C is associated with limited life expectancy. Ascites and encephalopathy are graded as “none”, “controlled with routine medical therapy” or “refractory to medical therapy” (Pugh *et al.*, 1973).

Table 2-7. Suggested interpretation of LFT results from American Association for Clinical Chemistry (AACC).

Type of liver abnormality	Bilirubin	ALT AST	and	ALP	Albumin	Blood prothrombin time
---------------------------	-----------	------------	-----	-----	---------	------------------------

Acute liver infarction damage due to infection, toxins or drugs, etc.	normal or increased usually after alt and ast are already increased	Usually greatly increased (> 10 times); ALT is usually higher than AST	normal or moderately increased	normal	usually normal
Chronic forms of various liver disorders	normal or increased	Mildly or moderately increased; ALT is persistently increased	normal to slightly increased	normal	normal
Alcoholic Hepatitis	normal or increased	AST is moderately increased, usually at least twice the level of ALT	normal or moderately increased	normal	normal
Cirrhosis	may be increased but this usually occurs later in the disease	AST is usually higher than ALT but levels are usually lower than in alcoholic disease	normal or increased	normal or decreased	usually prolonged
Bile duct obstruction, cholestasis	normal or increased; increased in complete obstruction	Normal to moderately increased	increased; often greater than 4 times what is normal	normal or decrease if chronic	usually normal
Metastasized cancer in liver	usually normal	Normal or slightly increased	usually greatly increased	normal	normal
Cancer originating in the liver (hepatocellular carcinoma, HCC)	may be increased, especially if the disease has progressed	AST higher than ALT but levels lower than that seen in alcoholic disease	normal or increased	normal or decreased	usually prolonged

Autoimmune Deficiency normal or increased Moderately increased; ALT usually higher than AST normal or slightly increased or usually decreased normal

Retrieved from liver function test interpretation, Lab Tests Online, American Association for Clinical Chemistry, last modified on March 10, 2016.

Table 2-8. Estimate of liver function using the Child-Turcotte Class.

Metrics	Points		
	0	1	2
Albumin	More than 3.5 g/dL (35 g/L)	2.8 to 3.5 g/dL (28 to 35 g/L)	Less than 2.8 g/dL (28 g/L)
Bilirubin	Less than 2 mg/dL (34 µmol/L)	2 to 3 mg/dL (34 to 51 µmol/L)	More than 3 mg/dL
Prolongation of prothrombin time	Less than 4 seconds	4 to 6 seconds	More than 6 seconds
Ascites	None	Controlled	Refractory
Encephalopathy	None	Controlled	Refractory

2.4.8 Liver and sex endocrine disorder

Besides assessing liver function and metabolic homeostasis, LFT is also important in the diagnostics of endocrine disorder. Liver serves as a pivotal and central axis connecting the environment input, endogenous homeostasis, blood cleaning, detoxification of xenobiotics, the metabolism and delivery of nutrients (Hoekstra *et al.*, 2013; Kamath *et al.*, 2001; Pratt and Kaplan, 2000). It is the most critical organ in maintaining metabolic and endocrine homeostasis. There are numerous and constant relationships and feedback mechanisms between liver and other endocrine organs including pituitary gland, thyroid gland, adrenal gland, pancreas, ovary, testis etc. For this reason, abnormality of liver may become the cause of other endocrine disorders (Johnston, 1999). Regarding such correlation, there are many clinical examples, e.g. hypothyroidism can be induced by

primary biliary cirrhosis (Huang and Liaw, 1995); hyperthyroidism can be induced by chronic liver inflammation (Babb, 1984); Cushing's syndrome has been reported to be caused by chronic liver inflammation (Burra, 2013); polycystic ovary syndrome which can be caused by nonalcoholic steatohepatitis and nonalcoholic fatty liver disease (Setji *et al.*, 2006).

Clinical documents have shown statistically significant connection between hypogonadism and liver abnormalities (Bannister *et al.*, 1986). The mechanism of the association between liver dysfunction and hypogonadism is complex. Male cirrhotic patients often show feminization, gynecomastia and redistribution of body fat, loss of libido and impotence during sex. In patients and rodent models with liver cirrhosis, a higher ratio of estrogen/androgen is noticed, with lower levels of testosterone and androstenedione (Coburn *et al.*, 2000; Kew, 1987). The isolated Leydig cells, testes and testicular homogenates have all demonstrated reduced level of testosterone (Maheshwari and Thuluvath, 2011). The current opinion on the etiology is that these phenotypes are resulted from impaired estrogen metabolism in liver and consequent estrogenemia. Specifically, the damage of liver leads to deficient metabolism and secretion of estrogen, which in turn lifts the estrogen level in serum and gonads. Though similarly, androstenedione is not efficiently metabolized by liver, yet once coming into the circulation it is aromatised to estrone and estradiol in skin and adipose tissues. Also, estradiol can stimulate the production of sex hormone binding protein (SHBG) in testis, which preferably binds to testosterone and further decrease free testosterone/estrogen ratio (Gluud, 1988). SHBG or sex steroid-binding globulin (SSBG) is a glycoprotein that binds to androgen and estrogen and mask biological activities. Other steroid hormones such as progesterone, cortisol, and

other corticosteroids are bound by transcortin. The relative binding affinity of various sex steroids for SHBG is dihydrotestosterone (DHT) > testosterone > androstenediol > estradiol > estrone (Becker, 2001). In line with the theory being discussed here, it has been noted that orally administered estrogen, progesterone, or commercial drugs of analogs, are inductive factors of hepatic adenomas, focal nodular hyperplasia and haemangiomas which are partly induced by the disruption of the metabolic pathway of steroid hormones in liver (Maheshwari and Thuluvath, 2011). In addition to the above theory, other induction of liver-related induction of hypogonadism include: (1) impaired supply of LDL-cholesterol from liver; (2) impaired secretion of insulin-like growth factor 1 (IGF-1 or somatomedin C) by liver, which eventually affects hypothalamus-pituitary-gonad axis.

The measurement of circulating androgens can be exploited as a biomarker of hypogonadism. In human body, the main subset of androgens, known as adrenal androgens, is composed of 19-carbon steroids synthesized in the zona reticularis, the innermost layer of the adrenal cortex. The primary and most well-known androgen is testosterone. Dihydrotestosterone (DHT) and androstenedione (A4) are generally less known but are of equal importance in male development. DHT in the embryo life causes differentiation of penis, scrotum and prostate. Later in life DHT contributes to balding, prostate growth and sebaceous gland activity. Adrenal androgens function as weak steroids (though some are precursors), and the subset includes dehydroepiandrosterone (DHEA), dehydroepiandrosterone sulfate (DHEA-S), and androstenediol (A5). Although androgens are described as male sex hormones, both males and females have them to varying degrees, as is also true of estrogens. They are one of three types of sex hormones—the other types are estrogens such as estradiol and progestogens such as progesterone.

To summarize, liver function test is an important clinical reference which is needed for precise analysis of disease progress and evaluation of individual nutritional status. Gut-microbiota dependent metabolism is a kind of frontier “center” which links environmental chemical input, endogenous functional metabolites and host physiology. Accordingly, a version that integrates gut-microbiota, intestinal epithelium, gut associated lymph tissue (GALT), endocrine system and liver function is very necessary and helpful. The combination of traditional clinical reference data, such as biopsy and liver function test, with novel omics-based analysis, bioinformatics and biostatistics may largely enhance the overall strength and precision of clinical medical treatment as well as the various researches conducted in laboratory environment.

Reference

- Adams, L. A., and Angulo, P. (2006). Treatment of non-alcoholic fatty liver disease. *Postgrad Med J* **82**(967), 315-22.
- Adedara, I. A., Nanjappa, M. K., Farombi, E. O., and Akingbemi, B. T. (2014). Aflatoxin B1 disrupts the androgen biosynthetic pathway in rat Leydig cells. *Food Chem Toxicol* **65**, 252-9.
- Aebersold, R., and Mann, M. (2003). Mass spectrometry-based proteomics. *Nature* **422**(6928), 198-207.
- Ahmed, K., Tunaru, S., and Offermanns, S. (2009). GPR109A, GPR109B and GPR81, a family of hydroxy-carboxylic acid receptors. *Trends Pharmacol Sci* **30**(11), 557-62.

- Akasaka, H., Ueki, A., Hanada, S., Kamagata, Y., and Ueki, K. (2003). *Propionicimonas paludicola* gen. nov., sp. nov., a novel facultatively anaerobic, Gram-positive, propionate-producing bacterium isolated from plant residue in irrigated rice-field soil. *Int J Syst Evol Microbiol* **53**(Pt 6), 1991-8.
- Akiyama, T. E., Sakai, S., Lambert, G., Nicol, C. J., Matsusue, K., Pimprale, S., Lee, Y.-H., Ricote, M., Glass, C. K., and Brewer, H. B. (2002). Conditional disruption of the peroxisome proliferator-activated receptor γ gene in mice results in lowered expression of ABCA1, ABCG1, and apoE in macrophages and reduced cholesterol efflux. *Mol Cell Biol* **22**(8), 2607-2619.
- Al-Lahham, S., Roelofsen, H., Rezaee, F., Weening, D., Hoek, A., Vonk, R., and Venema, K. (2012). Propionic acid affects immune status and metabolism in adipose tissue from overweight subjects. *Eur J Clin Invest* **42**(4), 357-364.
- Al-Lahham, S. H., Roelofsen, H., Priebe, M., Weening, D., Dijkstra, M., Hoek, A., Rezaee, F., Venema, K., and Vonk, R. J. (2010). Regulation of adipokine production in human adipose tissue by propionic acid. *Eur J Clin Invest* **40**(5), 401-407.
- Alexander, G. E. (2004). Biology of Parkinson's disease: pathogenesis and pathophysiology of a multisystem neurodegenerative disorder. *Dialogues Clin Neurosci* **6**(3), 259-80.
- Anderson, G., and Maes, M. (2015). The gut-brain axis: The role of melatonin in linking psychiatric, inflammatory and neurodegenerative conditions. *Adv Integr Med* **2**(1), 31-37.
- Anderson, G. M. (1975). Quantitation of tryptophan metabolites in rat feces by thin-layer chromatography. *J Chromatogr* **105**(2), 323-8.

- Andrade, F. O., Nagamine, M. K., Conti, A. D., Chaible, L. M., Fontelles, C. C., Jordao Junior, A. A., Vannucchi, H., Dagli, M. L., Bassoli, B. K., Moreno, F. S., *et al.* (2012). Efficacy of the dietary histone deacetylase inhibitor butyrate alone or in combination with vitamin A against proliferation of MCF-7 human breast cancer cells. *Braz J Med Biol Res* **45**(9), 841-50.
- Araki, Y., Andoh, A., Takizawa, J., Takizawa, W., and Fujiyama, Y. (2004). Clostridium butyricum, a probiotic derivative, suppresses dextran sulfate sodium-induced experimental colitis in rats. *Int J Mol Med* **13**(4), 577-80.
- Araki, Y., Fujiyama, Y., Andoh, A., Koyama, S., Kanauchi, O., and Bamba, T. (2000). The dietary combination of germinated barley foodstuff plus Clostridium butyricum suppresses the dextran sulfate sodium-induced experimental colitis in rats. *Scand J Gastroenterol* **35**(10), 1060-7.
- Arena, M. P., Russo, P., Capozzi, V., Lopez, P., Fiocco, D., and Spano, G. (2014). Probiotic abilities of riboflavin-overproducing Lactobacillus strains: a novel promising application of probiotics. *Appl Microbiol Biotechnol* **98**(17), 7569-81.
- Arora, T., Sharma, R., and Frost, G. (2011). Propionate. Anti-obesity and satiety enhancing factor? *Appetite* **56**(2), 511-5.
- Arpaia, N., Campbell, C., Fan, X., Dikiy, S., van der Veeken, J., deRoos, P., Liu, H., Cross, J. R., Pfeffer, K., Coffey, P. J., *et al.* (2013). Metabolites produced by commensal bacteria promote peripheral regulatory T-cell generation. *Nature* **504**(7480), 451-5 (Letter).

- Arun, P., Ariyannur, P. S., Moffett, J. R., Xing, G., Hamilton, K., Grunberg, N. E., Ives, J. A., and Namboodiri, A. M. (2010). Metabolic acetate therapy for the treatment of traumatic brain injury. *J Neurotrauma* **27**(1), 293-8.
- Asarat, M., Apostolopoulos, V., Vasiljevic, T., and Donkor, O. (2015). Short-chain fatty acids produced by synbiotic mixtures in skim milk differentially regulate proliferation and cytokine production in peripheral blood mononuclear cells. *Int J Food Sci Nutr* **66**(7), 755-65.
- Babb, R. R. (1984). Associations between Diseases of the Thyroid and the Liver. *American J Gastroenterol* **79**(5), 421-423.
- Baig, F., Lawton, M., Rolinski, M., Ruffmann, C., Nithi, K., Evetts, S. G., Fernandes, H. R., Ben-Shlomo, Y., and Hu, M. (2015). Delineating nonmotor symptoms in early Parkinson's disease and first-degree relatives. *Movement Disorders* **30**(13), 1759-1766.
- Bajad, S. U., Lu, W., Kimball, E. H., Yuan, J., Peterson, C., and Rabinowitz, J. D. (2006). Separation and quantitation of water soluble cellular metabolites by hydrophilic interaction chromatography-tandem mass spectrometry. *J Chromatogr A* **1125**(1), 76-88.
- Baldwin, K. M., Haddad, F., Pandorf, C. E., Roy, R. R., and Edgerton, V. R. (2013). Alterations in muscle mass and contractile phenotype in response to unloading models: role of transcriptional/pretranslational mechanisms. *Front Physiol* **4**, 284.
- Bannister, P., Handley, T., Chapman, C., and Losowsky, M. S. (1986). Hypogonadism in chronic liver disease: impaired release of luteinising hormone. *Br Med J (Clin Res Ed)* **293**(6556), 1191-3.

- Baran, H., Jellinger, K., and Deecke, L. (1999). Kynurenine metabolism in Alzheimer's disease. *J Neural Transm (Vienna)* **106**(2), 165-81.
- Barbosa, M. R. (2013) Chemical composition and formation of human feces-Problems and solutions of large mergers demographics in developing countries. In 10th International Symposium on Recent Advances in Environmental Health Research.
- Barichella, M., Cereda, E., and Pezzoli, G. (2009). Major nutritional issues in the management of Parkinson's disease. *Mov Disord* **24**(13), 1881-92.
- Baron, S. (1996). *Epidemiology--Medical Microbiology*. University of Texas Medical Branch at Galveston.
- Bastard, J. P., Maachi, M., Lagathu, C., Kim, M. J., Caron, M., Vidal, H., Capeau, J., and Feve, B. (2006). Recent advances in the relationship between obesity, inflammation, and insulin resistance. *Eur Cytokine Netw* **17**(1), 4-12.
- Bates, E. A., Victor, M., Jones, A. K., Shi, Y., and Hart, A. C. (2006). Differential contributions of *Caenorhabditis elegans* histone deacetylases to huntingtin polyglutamine toxicity. *J Neurosci* **26**(10), 2830-8.
- Batterham, R. L., Cowley, M. A., Small, C. J., Herzog, H., Cohen, M. A., Dakin, C. L., Wren, A. M., Brynes, A. E., Low, M. J., Ghatei, M. A., *et al.* (2002). Gut hormone PYY3-36 physiologically inhibits food intake. *Nature* **418**(6898), 650-654.
- Baudhuin, P., Beaufay, H., Rahman-Li, Y., Sellinger, O. Z., Wattiaux, R., Jacques, P., and De Duve, C. (1964). Tissue fractionation studies. 17. Intracellular distribution of monoamine oxidase, aspartate aminotransferase, alanine aminotransferase, D-amino acid oxidase and catalase in rat-liver tissue. *Biochem J* **92**(1), 179-84.

- Bearcroft, C. P., Perrett, D., and Farthing, M. J. (1998). Postprandial plasma 5-hydroxytryptamine in diarrhoea predominant irritable bowel syndrome: a pilot study. *Gut* **42**(1), 42-6.
- Becker, K. L. (2001). *Principles and practice of endocrinology and metabolism*. Lippincott Williams & Wilkins.
- Begley, M., Hill, C., and Gahan, C. G. (2006). Bile salt hydrolase activity in probiotics. *Appl Environ Microbiol* **72**(3), 1729-38.
- Berger, S. L. (2002). Histone modifications in transcriptional regulation. *Curr Opin Genet Dev* **12**(2), 142-8.
- Bermudez, Y., Benavente, C. A., Meyer, R. G., Coyle, W. R., Jacobson, M. K., and Jacobson, E. L. (2011). Nicotinic acid receptor abnormalities in human skin cancer: implications for a role in epidermal differentiation. *PLoS One* **6**(5), e20487.
- Bhattacharyya, A., Chattopadhyay, R., Mitra, S., and Crowe, S. E. (2014). Oxidative stress: an essential factor in the pathogenesis of gastrointestinal mucosal diseases. *Physiol Rev* **94**(2), 329-54.
- Biddle, A., Stewart, L., Blanchard, J., and Leschine, S. (2013). Untangling the genetic basis of fibrolytic specialization by Lachnospiraceae and Ruminococcaceae in diverse gut communities. *Diversity* **5**(3), 627-640.
- Bindels, L. B., Porporato, P., Dewulf, E. M., Verrax, J., Neyrinck, A. M., Martin, J. C., Scott, K. P., Buc Calderon, P., Feron, O., Muccioli, G. G., *et al.* (2012). Gut microbiota-derived propionate reduces cancer cell proliferation in the liver. *Br J Cancer* **107**(8), 1337-44.

- Binder, H. J. (2010). Role of colonic short-chain fatty acid transport in diarrhea. *Annu Rev Physiol* **72**, 297-313.
- Bjeldanes, L. F., Kim, J. Y., Grose, K. R., Bartholomew, J. C., and Bradfield, C. A. (1991). Aromatic hydrocarbon responsiveness-receptor agonists generated from indole-3-carbinol in vitro and in vivo: comparisons with 2,3,7,8-tetrachlorodibenzo-p-dioxin. *Proc Natl Acad Sci U S A* **88**(21), 9543-7.
- Bjorkhem, I., Diczfalusy, U., and Lutjohann, D. (1999). Removal of cholesterol from extrahepatic sources by oxidative mechanisms. *Curr Opin Lipidol* **10**(2), 161-165.
- Blann, A. (2013). *Routine Blood Results Explained 3/e: A guide for Nurses & Allied Health Professionals*. M&K Update Ltd.
- Blottiere, H. M., Buecher, B., Galmiche, J. P., and Cherbut, C. (2003). Molecular analysis of the effect of short-chain fatty acids on intestinal cell proliferation. *Proc Nutr Soc* **62**(1), 101-6.
- Bordonaro, M., and Lazarova, D. L. (2015). CREB-binding protein, p300, butyrate, and Wnt signaling in colorectal cancer. *World J Gastroenterol* **21**(27), 8238-48.
- Bourlioux, P., Koletzko, B., Guarner, F., and Braesco, V. (2003). The intestine and its microflora are partners for the protection of the host: report on the Danone Symposium "The Intelligent Intestine," held in Paris, June 14, 2002. *Am J Clin Nutr* **78**(4), 675-683.
- Bowling, T. E., Raimundo, A. H., Grimble, G. K., and Silk, D. B. (1993). Reversal by short-chain fatty acids of colonic fluid secretion induced by enteral feeding. *Lancet* **342**(8882), 1266-8.

- Bradlow, H. L., Michnovicz, J., Telang, N. T., and Osborne, M. P. (1991). Effects of dietary indole-3-carbinol on estradiol metabolism and spontaneous mammary tumors in mice. *Carcinogenesis* **12**(9), 1571-4.
- Brandt, A. M. (1988). The syphilis epidemic and its relation to AIDS. *Science* **239**(4838), 375-80.
- Bravo, J. A., Forsythe, P., Chew, M. V., Escaravage, E., Savignac, H. M., Dinan, T. G., Bienenstock, J., and Cryan, J. F. (2011). Ingestion of Lactobacillus strain regulates emotional behavior and central GABA receptor expression in a mouse via the vagus nerve. *Proc Natl Acad Sci U S A* **108**(38), 16050-5.
- Brinkworth, G. D., Noakes, M., Clifton, P. M., and Bird, A. R. (2009). Comparative effects of very low-carbohydrate, high-fat and high-carbohydrate, low-fat weight-loss diets on bowel habit and faecal short-chain fatty acids and bacterial populations. *Br J Nutr* **101**(10), 1493-1502.
- Broadhurst, D. I., and Kell, D. B. (2006). Statistical strategies for avoiding false discoveries in metabolomics and related experiments. *Metabolomics* **2**(4), 171-196.
- Brockman, R. (2005). Glucose and short-chain fatty acid metabolism. *Quantitative Aspects of Ruminant Digestion and Metabolism*. J. Dijkstra, JM Forbes, and J. France, ed. CAB International, Wallingford, UK, 291-310.
- Brown, A. J., Goldsworthy, S. M., Barnes, A. A., Eilert, M. M., Tcheang, L., Daniels, D., Muir, A. I., Wigglesworth, M. J., Kinghorn, I., and Fraser, N. J. (2003a). The Orphan G protein-coupled receptors GPR41 and GPR43 are activated by propionate and other short chain carboxylic acids. *J Biol Chem* **278**(13), 11312-11319.

- Brown, A. J., Goldsworthy, S. M., Barnes, A. A., Eilert, M. M., Tcheang, L., Daniels, D., Muir, A. I., Wigglesworth, M. J., Kinghorn, I., Fraser, N. J., *et al.* (2003b). The Orphan G protein-coupled receptors GPR41 and GPR43 are activated by propionate and other short chain carboxylic acids. *J Biol Chem* **278**(13), 11312-9.
- Browning, J. D., Szczepaniak, L. S., Dobbins, R., Nuremberg, P., Horton, J. D., Cohen, J. C., Grundy, S. M., and Hobbs, H. H. (2004). Prevalence of hepatic steatosis in an urban population in the United States: impact of ethnicity. *Hepatology* **40**(6), 1387-95.
- Bruce, S. J., Tavazzi, I., Parisod, V., Rezzi, S., Kochhar, S., and Guy, P. A. (2009). Investigation of Human Blood Plasma Sample Preparation for Performing Metabolomics Using Ultrahigh Performance Liquid Chromatography/Mass Spectrometry. *Anal Chem* **81**(9), 3285-3296.
- Brunt, E. M., Kleiner, D. E., Wilson, L. A., Unalp, A., Behling, C. E., Lavine, J. E., Neuschwander-Tetri, B. A., and Appendix, N. C. R. N. I. o. m. o. t. N. S. C. R. N. c. b. f. i. t. (2009). Portal chronic inflammation in nonalcoholic fatty liver disease (NAFLD): a histologic marker of advanced NAFLD-Clinicopathologic correlations from the nonalcoholic steatohepatitis clinical research network. *Hepatology* **49**(3), 809-20.
- Bugianesi, E., Leone, N., Vanni, E., Marchesini, G., Brunello, F., Carucci, P., Musso, A., De Paolis, P., Capussotti, L., Salizzoni, M., *et al.* (2002). Expanding the natural history of nonalcoholic steatohepatitis: from cryptogenic cirrhosis to hepatocellular carcinoma. *Gastroenterology* **123**(1), 134-40.

- Bultman, S. J. (2014). Molecular pathways: gene-environment interactions regulating dietary fiber induction of proliferation and apoptosis via butyrate for cancer prevention. *Clin Cancer Res* **20**(4), 799-803.
- Burcelin, R., Serino, M., Chabo, C., Blasco-Baque, V., and Amar, J. (2011). Gut microbiota and diabetes: from pathogenesis to therapeutic perspective. *Acta Diabetol* **48**(4), 257-273.
- Burra, P. (2013). Liver abnormalities and endocrine diseases. *Best Pract Res Clin Gastroenterol* **27**(4), 553-63.
- Burtis, C. A., Ashwood, E. R., and Bruns, D. E. (2012). *Tietz textbook of clinical chemistry and molecular diagnostics*. Elsevier Health Sciences.
- Butler, R. N., Stafford, I., Triantafillos, E., O'Dee, C. D., Jarrett, I. G., Fettman, M. J., and Roberts-Thomson, I. C. (1990). Pyruvate sparing by butyrate and propionate in proliferating colonic epithelium. *Comp Biochem Physiol B* **97**(2), 333-7.
- Byrne, C. S., Chambers, E. S., Morrison, D. J., and Frost, G. (2015). The role of short chain fatty acids in appetite regulation and energy homeostasis. *Int J Obes* **39**(9), 1331-8.
- Calle, E. E., Thun, M. J., Petrelli, J. M., Rodriguez, C., and Heath, C. W. (1999). Body-mass index and mortality in a prospective cohort of US adults. *N Engl J Med* **341**(15), 1097-1105.
- Calvani, R., Miccheli, A., Capuani, G., Tomassini Miccheli, A., Puccetti, C., Delfini, M., Iaconelli, A., Nanni, G., and Mingrone, G. (2010). Gut microbiome-derived metabolites characterize a peculiar obese urinary metabotype. *Int J Obes* **34**(6), 1095-8.

- Candido, E. P., Reeves, R., and Davie, J. R. (1978). Sodium butyrate inhibits histone deacetylation in cultured cells. *Cell* **14**(1), 105-13.
- Canfora, E. E., Jocken, J. W., and Blaak, E. E. (2015). Short-chain fatty acids in control of body weight and insulin sensitivity. *Nat Rev Endocrinol* **11**(10), 577-91 (Review).
- Cani, P. D., Neyrinck, A. M., Fava, F., Knauf, C., Burcelin, R. G., Tuohy, K. M., Gibson, G. R., and Delzenne, N. M. (2007). Selective increases of bifidobacteria in gut microflora improve high-fat-diet-induced diabetes in mice through a mechanism associated with endotoxaemia. *Diabetologia* **50**(11), 2374-2383.
- Carabotti, M., Scirocco, A., Maselli, M. A., and Severi, C. (2015). The gut-brain axis: interactions between enteric microbiota, central and enteric nervous systems. *Ann Gastroenterol* **28**(2), 203-209.
- Carding, S., Verbeke, K., Vipond, D. T., Corfe, B. M., and Owen, L. J. (2015). Dysbiosis of the gut microbiota in disease. *Microb Ecol Health Dis* **26**, 26191.
- Cardona, M. E., Collinder, E., Stern, S., Tjellström, B., Norin, E., and Midtvedt, T. (2005). Correlation between faecal iso-butyric and iso-valeric acids in different species. *Microb Ecol Health Dis* **17**(3), 177-182.
- Castelli, W. P., and Anderson, K. (1986). A Population at Risk - Prevalence of High Cholesterol Levels in Hypertensive Patients in the Framingham-Study. *Am J Med* **80**(2a), 23-32.
- Chakravorty, D., Koide, N., Kato, Y., Sugiyama, T., Mu, M. M., Yoshida, T., and Yokochi, T. (2000). The inhibitory action of butyrate on lipopolysaccharide-induced nitric oxide production in RAW 264.7 murine macrophage cells. *J Endotoxin Res* **6**(3), 243-7.

- Chambers, E., Viardot, A., Psichas, A., Morrison, D., Murphy, K., Zac-Varghese, S., Preston, T., Tedford, C., Bell, J., Thomas, L., *et al.* (2015a). Effects of Elevating Colonic Propionate on Liver Fat Content in Adults with Non-Alcoholic Fatty Liver Disease. *The FASEB Journal* **29**(1 Supplement).
- Chambers, E. S., Viardot, A., Psichas, A., Morrison, D. J., Murphy, K. G., Zac-Varghese, S. E., MacDougall, K., Preston, T., Tedford, C., Finlayson, G. S., *et al.* (2015b). Effects of targeted delivery of propionate to the human colon on appetite regulation, body weight maintenance and adiposity in overweight adults. *Gut* **64**(11), 1744-54.
- Chang, H.-P., Wang, M.-L., Chan, M.-H., Chiu, Y.-S., and Chen, Y.-H. (2011). Antiobesity activities of indole-3-carbinol in high-fat-diet–induced obese mice. *Nutrition* **27**(4), 463-470.
- Chao, A., Thun, M. J., Connell, C. J., McCullough, M. L., Jacobs, E. J., Flanders, W. D., Rodriguez, C., Sinha, R., and Calle, E. E. (2005). Meat consumption and risk of colorectal cancer. *JAMA* **293**(2), 172-82.
- Chaturvedi, R., Asim, M., Romero-Gallo, J., Barry, D. P., Hoge, S., de Sablet, T., Delgado, A. G., Wroblewski, L. E., Piazuelo, M. B., Yan, F., *et al.* (2011). Spermine oxidase mediates the gastric cancer risk associated with *Helicobacter pylori CagA*. *Gastroenterology* **141**(5), 1696-708 e1-2.
- Chaudhuri, K. R., Healy, D. G., Schapira, A. H., and National Institute for Clinical, E. (2006). Non-motor symptoms of Parkinson's disease: diagnosis and management. *Lancet Neurol* **5**(3), 235-45.

- Chavarro, J. E., Stampfer, M. J., Hall, M. N., Sesso, H. D., and Ma, J. (2008). A 22-y prospective study of fish intake in relation to prostate cancer incidence and mortality. *Am J Clin Nutr* **88**(5), 1297-303.
- Chen, H. W., Fang, B. S., and Hu, Z. D. (2007). Simultaneous HPLC determination of four key metabolites in the metabolic pathway for production of 1,3-propanediol from glycerol. *Chroma* **65**(9-10), 629-632.
- Chen, I., Safe, S., and Bjeldanes, L. (1996). Indole-3-carbinol and diindolylmethane as aryl hydrocarbon (Ah) receptor agonists and antagonists in T47D human breast cancer cells. *Biochem Pharmacol* **51**(8), 1069-1076.
- Chen, W. J. L., Anderson, J. W., and Jennings, D. (1984). Propionate May Mediate the Hypocholesterolemic Effects of Certain Soluble Plant Fibers in Cholesterol-Fed Rats. *P Soc Exp Biol Med* **175**(2), 215-218.
- Chimerel, C., Emery, E., Summers, D. K., Keyser, U., Gribble, F. M., and Reimann, F. (2014). Bacterial metabolite indole modulates incretin secretion from intestinal enteroendocrine L cells. *Cell Rep* **9**(4), 1202-8.
- Choi, D. W. (1988). Glutamate neurotoxicity and diseases of the nervous system. *Neuron* **1**(8), 623-34.
- Chowdhury, I., and Maitra, S. K. (2012). Melatonin time line: from discovery to therapy. In *Melatonin in the promotion of health*, pp. 1-60. Taylor & Francis, Boca Raton, FL.
- Chuang, D. M., Leng, Y., Marinova, Z., Kim, H. J., and Chiu, C. T. (2009). Multiple roles of HDAC inhibition in neurodegenerative conditions. *Trends Neurosci* **32**(11), 591-601.

- Chyan, Y.-J., Poeggeler, B., Omar, R. A., Chain, D. G., Frangione, B., Ghiso, J., and Pappolla, M. A. (1999). Potent neuroprotective properties against the Alzheimer β -amyloid by an endogenous melatonin-related indole structure, indole-3-propionic acid. *J Biol Chem* **274**(31), 21937-21942.
- Clark, J. M., Brancati, F. L., and Diehl, A. M. (2002). Nonalcoholic fatty liver disease. *Gastroenterology* **122**(6), 1649-57.
- Claus, R., Dehnhard, M., Herzog, A., Bernalbarragan, H., and Gimenez, T. (1993). Parallel Measurements of Indole and Skatole (3-Methylindole) in Feces and Blood-Plasma of Pigs by Hplc. *Livest Prod Sci* **34**(1-2), 115-126.
- Claus, S. P., Guillou, H., and Ellero-Simatos, S. (2016). The gut microbiota: a major player in the toxicity of environmental pollutants? *NPJ Biofilms Microbiomes* **2**, 16003.
- Clausen, M. R., Bonnen, H., and Mortensen, P. B. (1991). Colonic fermentation of dietary fibre to short chain fatty acids in patients with adenomatous polyps and colonic cancer. *Gut* **32**(8), 923-8.
- Clausen, M. R., and Mortensen, P. B. (1995). Kinetic studies on colonocyte metabolism of short chain fatty acids and glucose in ulcerative colitis. *Gut* **37**(5), 684-9.
- Clayton, T. A. (2012). Metabolic differences underlying two distinct rat urinary phenotypes, a suggested role for gut microbial metabolism of phenylalanine and a possible connection to autism. *FEBS Lett* **586**(7), 956-61.
- Clemente, J. C., Ursell, L. K., Parfrey, L. W., and Knight, R. (2012). The impact of the gut microbiota on human health: an integrative view. *Cell* **148**(6), 1258-70.

- Coburn, C. T., Knapp, F. F., Jr., Febbraio, M., Beets, A. L., Silverstein, R. L., and Abumrad, N. A. (2000). Defective uptake and utilization of long chain fatty acids in muscle and adipose tissues of CD36 knockout mice. *J Biol Chem* **275**(42), 32523-9.
- Conney, A. H. (1982). Induction of microsomal enzymes by foreign chemicals and carcinogenesis by polycyclic aromatic hydrocarbons: GHA Clowes Memorial Lecture. *Cancer Res* **42**(12), 4875-4917.
- Cook, S. I., and Sellin, J. H. (1998). Review article: short chain fatty acids in health and disease. *Aliment Pharmacol Ther* **12**(6), 499-507.
- Coombs, R. R., Mourant, A. E., and Race, R. (1945). A new test for the detection of weak and "incomplete" Rh agglutinins. *Br J Exp Pathol* **26**(4), 255.
- Corte Osorio, L. Y., Martinez Flores, H. E., and Ortiz Alvarado, R. (2011). [Effect of dietary fiber in the quantitative expression of butyrate receptor GPR43 in rats colon]. *Nutr Hosp* **26**(5), 1052-8.
- Corti, O., Lesage, S., and Brice, A. (2011). What genetics tells us about the causes and mechanisms of Parkinson's disease. *Physiol Rev* **91**(4), 1161-218.
- Cousens, L. S., Gallwitz, D., and Alberts, B. M. (1979). Different accessibilities in chromatin to histone acetylase. *J Biol Chem* **254**(5), 1716-23.
- Cox, M. A., Jackson, J., Stanton, M., Rojas-Triana, A., Bober, L., Laverty, M., Yang, X. X., Zhu, F., Liu, J. J., Wang, S. K., *et al.* (2009). Short-chain fatty acids act as antiinflammatory mediators by regulating prostaglandin E-2 and cytokines. *World J Gastroenterol* **15**(44), 5549-5557.
- Cryan, J. F., and Dinan, T. G. (2012). Mind-altering microorganisms: the impact of the gut microbiota on brain and behaviour. *Nat Rev Neurosci* **13**(10), 701-12.

- Cummings, J. H., Pomare, E. W., Branch, W. J., Naylor, C. P., and Macfarlane, G. T. (1987). Short chain fatty acids in human large intestine, portal, hepatic and venous blood. *Gut* **28**(10), 1221-7.
- Cunha, C., Carvalho, A., Esposito, A., Bistoni, F., and Romani, L. (2012). DAMP signaling in fungal infections and diseases. *Front Immunol* **3**, 286.
- Dashty, M. (2013). A quick look at biochemistry: Carbohydrate metabolism. *Clin Biochem* **46**(15), 1339-1352.
- Daulatzai, M. A. (2015). Non-celiac gluten sensitivity triggers gut dysbiosis, neuroinflammation, gut-brain axis dysfunction, and vulnerability for dementia. *CNS Neurol Disord Drug Targets* **14**(1), 110-31.
- Davie, J. R. (2003). Inhibition of histone deacetylase activity by butyrate. *J Nutr* **133**(7 Suppl), 2485S-2493S.
- Davies, N. W., Guillemin, G., and Brew, B. J. (2010). Tryptophan, Neurodegeneration and HIV-Associated Neurocognitive Disorder. *Int J Tryptophan Res* **3**, 121-40.
- de Magistris, L., Siniscalco, D., Bravaccio, C., and Loguercio, C. (2016). Gut–Brain Axis: A New Revolution to Understand the Pathogenesis of Autism and Other Severe Neurological Diseases. In *Human Nutrition from the Gastroenterologist's Perspective*, pp. 49-65. Springer.
- De Minicis, S., Rychlicki, C., Agostinelli, L., Saccomanno, S., Candelaresi, C., Trozzi, L., Mingarelli, E., Facinelli, B., Magi, G., Palmieri, C., *et al.* (2014). Dysbiosis contributes to fibrogenesis in the course of chronic liver injury in mice. *Hepatology* **59**(5), 1738-49.

- De Rijk, M. (2000). Prevalence of Parkinson's disease in Europe: A collaborative study of. *Neurology* **54**(5), s214323.
- De Vadder, F., Kovatcheva-Datchary, P., Goncalves, D., Vinera, J., Zitoun, C., Duchamp, A., Backhed, F., and Mithieux, G. (2014). Microbiota-generated metabolites promote metabolic benefits via gut-brain neural circuits. *Cell* **156**(1-2), 84-96.
- Defazio, A., Chiew, Y. E., Donoghue, C., Lee, C. S. L., and Sutherland, R. L. (1992). Effect of Sodium-Butyrate on Estrogen-Receptor and Epidermal Growth-Factor Receptor Gene-Expression in Human Breast-Cancer Cell-Lines. *J Biol Chem* **267**(25), 18008-18012.
- den Besten, G., Bleeker, A., Gerding, A., van Eunen, K., Havinga, R., van Dijk, T. H., Oosterveer, M. H., Jonker, J. W., Groen, A. K., and Reijngoud, D.-J. (2015). Short-chain fatty acids protect against high-fat diet-induced obesity via a ppar γ -dependent switch from lipogenesis to fat oxidation. *Diabetes* **64**(7), 2398-2408.
- den Besten, G., van Eunen, K., Groen, A. K., Venema, K., Reijngoud, D.-J., and Bakker, B. M. (2013). The role of short-chain fatty acids in the interplay between diet, gut microbiota, and host energy metabolism. *J Lipid Res* **54**(9), 2325-2340.
- Deng, Z., Mu, J., Tseng, M., Wattenberg, B., Zhuang, X., Egilmez, N. K., Wang, Q., Zhang, L., Norris, J., Guo, H., *et al.* (2015). Enterobacteria-secreted particles induce production of exosome-like S1P-containing particles by intestinal epithelium to drive Th17-mediated tumorigenesis. *Nat Commun* **6**, 6956 (Article).
- Dettmer, K., Aronov, P. A., and Hammock, B. D. (2007). Mass spectrometry-based metabolomics. *Mass Spectrom Rev* **26**(1), 51-78.

- Di Sabatino, A., Morera, R., Ciccocioppo, R., Cazzola, P., Gotti, S., Tinozzi, F. P., Tinozzi, S., and Corazza, G. R. (2005). Oral butyrate for mildly to moderately active Crohn's disease. *Aliment Pharmacol Ther* **22**(9), 789-94.
- Diamant, M., Blaak, E., and De Vos, W. (2011). Do nutrient–gut–microbiota interactions play a role in human obesity, insulin resistance and type 2 diabetes? *Obesity Rev* **12**(4), 272-281.
- DiBaise, J. K., Frank, D. N., and Mathur, R. (2012). Impact of the Gut Microbiota on the Development of Obesity: Current Concepts. *Am J Gastroenterol Suppl* **1**(1), 22-27.
- Dong, S. M., Lee, E. J., Jeon, E. S., Park, C. K., and Kim, K. M. (2005). Progressive methylation during the serrated neoplasia pathway of the colorectum. *Mod Pathol* **18**(2), 170-8.
- Donia, M. S., and Fischbach, M. A. (2015). HUMAN MICROBIOTA. Small molecules from the human microbiota. *Science* **349**(6246), 1254766.
- Donohoe, D. R., Collins, L. B., Wali, A., Bigler, R., Sun, W., and Bultman, S. J. (2012). The Warburg effect dictates the mechanism of butyrate-mediated histone acetylation and cell proliferation. *Mol Cell* **48**(4), 612-26.
- Donohoe, D. R., Holley, D., Collins, L. B., Montgomery, S. A., Whitmore, A. C., Hillhouse, A., Curry, K. P., Renner, S. W., Greenwalt, A., Ryan, E. P., *et al.* (2014). A gnotobiotic mouse model demonstrates that dietary fiber protects against colorectal tumorigenesis in a microbiota- and butyrate-dependent manner. *Cancer Discov* **4**(12), 1387-97.

- Drake, P. J., Griffiths, G. J., Shaw, L., Benson, R. P., and Corfe, B. M. (2008). Application of high-content analysis to the study of post-translational modifications of the cytoskeleton. *J Proteome Res* **8**(1), 28-34.
- Drucker, D. J., and Nauck, M. A. (2006). The incretin system: glucagon-like peptide-1 receptor agonists and dipeptidyl peptidase-4 inhibitors in type 2 diabetes. *Lancet* **368**(9548), 1696-705.
- Dufour, D. R., Lott, J. A., Nolte, F. S., Gretch, D. R., Koff, R. S., and Seeff, L. B. (2000). Diagnosis and monitoring of hepatic injury. I. Performance characteristics of laboratory tests. *Clin Chem* **46**(12), 2027-49.
- Efron, B., and Gong, G. (1983). A Leisurely Look at the Bootstrap, the Jackknife, and Cross-Validation. *Am Stat* **37**(1), 36-48.
- Ehrmeyer, S. S., and Laessig, R. H. (2004). Has compliance with CLIA requirements really improved quality in US clinical laboratories? *Clin Chim Acta* **346**(1), 37-43.
- El Aidy, S., Dinan, T. G., and Cryan, J. F. (2015). Gut Microbiota: The Conductor in the Orchestra of Immune–Neuroendocrine Communication. *Clin Ther* **37**(5), 954-967.
- El Aidy, S., Stilling, R., Dinan, T. G., and Cryan, J. F. (2016). Microbiome to Brain: Unravelling the Multidirectional Axes of Communication. In *Microbial Endocrinology: Interkingdom Signaling in Infectious Disease and Health*, pp. 301-336. Springer.
- Elangovan, S., Pathania, R., Ramachandran, S., Ananth, S., Padia, R. N., Lan, L., Singh, N., Martin, P. M., Hawthorn, L., Prasad, P. D., *et al.* (2014). The niacin/butyrate receptor GPR109A suppresses mammary tumorigenesis by inhibiting cell survival. *Cancer Res* **74**(4), 1166-78.

- Embley, T. M., and Martin, W. (2006). Eukaryotic evolution, changes and challenges. *Nature* **440**(7084), 623-30.
- Endo, F., Awata, H., Katoh, H., and Matsuda, I. (1995). A nonsense mutation in the 4-hydroxyphenylpyruvic acid dioxygenase gene (Hpd) causes skipping of the constitutive exon and hypertyrosinemia in mouse strain III. *Genomics* **25**(1), 164-9.
- Engelhardt, W. (1995). Absorption of short-chain fatty acids from the large intestine. *Physiological and clinical aspects of short-chain fatty acids*, 149.
- Englund, G., Jacobson, A., Rorsman, F., Artursson, P., Kindmark, A., and Ronnblom, A. (2007). Efflux transporters in ulcerative colitis: decreased expression of BCRP (ABCG2) and Pgp (ABCB1). *Inflamm Bowel Dis* **13**(3), 291-7.
- Erlinger, S., Arias, I. M., and Dhumeaux, D. (2014). Inherited Disorders of Bilirubin Transport and Conjugation: New Insights Into Molecular Mechanisms and Consequences. *Gastroenterology* **146**(7), 1625-1638.
- Farrell, G. C., Wong, V. W.-S., and Chitturi, S. (2013). NAFLD in Asia—as common and important as in the West. *Nat Rev Gastroenterol* **10**(5), 307-318.
- Fasano, A., Bove, F., Gabrielli, M., Petracca, M., Zocco, M. A., Ragazzoni, E., Barbaro, F., Piano, C., Fortuna, S., Tortora, A., *et al.* (2013). The role of small intestinal bacterial overgrowth in Parkinson's disease. *Mov Disord* **28**(9), 1241-9.
- Felice, V. D., Quigley, E. M., Sullivan, A. M., O'Keeffe, G. W., and O'Mahony, S. M. (2016). Microbiota-gut-brain signalling in Parkinson's disease: Implications for non-motor symptoms. *Parkinsonism Relat Disord* **27**, 1-8.

- Festa, A., D'Agostino, R., Howard, G., Mykkanen, L., Tracy, R. P., and Haffner, S. M. (2000). Chronic subclinical inflammation as part of the insulin resistance syndrome - The Insulin Resistance Atherosclerosis Study (IRAS). *Circulation* **102**(1), 42-47.
- Fiehn, O., and Weckwerth, W. (2003). Deciphering metabolic networks. *Eur J Biochem* **270**(4), 579-88.
- Finnie, I. A., Taylor, B. A., and Rhodes, J. M. (1993). Ileal and Colonic Epithelial Metabolism in Quiescent Ulcerative-Colitis - Increased Glutamine-Metabolism in Distal Colon but No Defect in Butyrate Metabolism. *Gut* **34**(11), 1552-1558.
- Flegal, K. M., Carroll, M. D., Kuczmarski, R. J., and Johnson, C. L. (1998). Overweight and obesity in the United States: prevalence and trends, 1960–1994. *Int J Obes Relat Metab Disord* **22**(1).
- Fleming, S. E., Choi, S. Y., and Fitch, M. D. (1991). Absorption of short-chain fatty acids from the rat cecum in vivo. *J Nutr* **121**(11), 1787-97.
- Flint, H. J., Bayer, E. A., Rincon, M. T., Lamed, R., and White, B. A. (2008). Polysaccharide utilization by gut bacteria: potential for new insights from genomic analysis. *Nat Rev Microbiol* **6**(2), 121-31.
- Foley, R. N., Parfrey, P. S., Harnett, J. D., Kent, G. M., Murray, D. C., and Barre, P. E. (1996). Hypoalbuminemia, cardiac morbidity, and mortality in end-stage renal disease. *J Am Soc Nephrol* **7**(5), 728-36.
- Fraher, M. H., O'Toole, P. W., and Quigley, E. M. M. (2012). Techniques used to characterize the gut microbiota: a guide for the clinician. *Nat Rev Gastroenterol Hepatol* **9**(6), 312-322 (10.1038/nrgastro.2012.44).

- Frank, D. N., St Amand, A. L., Feldman, R. A., Boedeker, E. C., Harpaz, N., and Pace, N. R. (2007). Molecular-phylogenetic characterization of microbial community imbalances in human inflammatory bowel diseases. *Proc Natl Acad Sci U S A* **104**(34), 13780-5.
- Frost, G., Sleeth, M. L., Sahuri-Arisoylu, M., Lizarbe, B., Cerdan, S., Brody, L., Anastasovska, J., Ghourab, S., Hankir, M., Zhang, S., *et al.* (2014). The short-chain fatty acid acetate reduces appetite via a central homeostatic mechanism. *Nat Commun* **5**, 3611.
- Fujioka, N., Fritz, V., Upadhyaya, P., Kassie, F., and Hecht, S. S. (2016). Research on cruciferous vegetables, indole-3-carbinol, and cancer prevention: A tribute to Lee W. Wattenberg. *Mol Nutr Food Res* **60**(6), 1228-1238.
- Fukae, J., Amasaki, Y., Yamashita, Y., Bohgaki, T., Yasuda, S., Jodo, S., Atsumi, T., and Koike, T. (2005). Butyrate suppresses tumor necrosis factor α production by regulating specific messenger RNA degradation mediated through a cis-acting AU-rich element. *Arthritis Rheum* **52**(9), 2697-2707.
- Fukumoto, S., Tatewaki, M., Yamada, T., Fujimiya, M., Mantyh, C., Voss, M., Eubanks, S., Harris, M., Pappas, T. N., and Takahashi, T. (2003). Short-chain fatty acids stimulate colonic transit via intraluminal 5-HT release in rats. *Am J Physiol Regul Integr Comp Physiol* **284**(5), R1269-76.
- Fung, K. Y., Brierley, G. V., Henderson, S., Hoffmann, P., McColl, S. R., Lockett, T., Head, R., and Cosgrove, L. (2011). Butyrate-induced apoptosis in HCT116 colorectal cancer cells includes induction of a cell stress response. *J Proteome Res* **10**(4), 1860-9.

- Galisteo, M., Duarte, J., and Zarzuelo, A. (2008). Effects of dietary fibers on disturbances clustered in the metabolic syndrome. *J Nutr Biochem* **19**(2), 71-84.
- Gambhir, D., Ananth, S., Veeranan-Karmegam, R., Elangovan, S., Hester, S., Jennings, E., Offermanns, S., Nussbaum, J. J., Smith, S. B., Thangaraju, M., *et al.* (2012). GPR109A as an anti-inflammatory receptor in retinal pigment epithelial cells and its relevance to diabetic retinopathy. *Invest Ophthalmol Vis Sci* **53**(4), 2208-17.
- Gao, X., Gong, H., Men, P., Zhou, L., and Ye, D. (2013). Design, synthesis, and biological evaluation of novel dual inhibitors of secretory phospholipase A2 and sphingomyelin synthase. *Chin J Chem* **31**(9), 1164-1170.
- Gao, Z., Yin, J., Zhang, J., Ward, R. E., Martin, R. J., Lefevre, M., Cefalu, W. T., and Ye, J. (2009). Butyrate improves insulin sensitivity and increases energy expenditure in mice. *Diabetes* **58**(7), 1509-1517.
- Gareau, M. G., Sherman, P. M., and Walker, W. A. (2010). Probiotics and the gut microbiota in intestinal health and disease. *Nat Rev Gastroenterol* **7**(9), 503-514.
- Gerhold, D. L., Liu, F., Jiang, G., Li, Z., Xu, J., Lu, M., Sachs, J. R., Bagchi, A., Fridman, A., and Holder, D. J. (2002). Gene expression profile of adipocyte differentiation and its regulation by peroxisome proliferator-activated receptor- γ agonists. *Endocrinology* **143**(6), 2106-2118.
- Giannini, E. G., Testa, R., and Savarino, V. (2005). Liver enzyme alteration: a guide for clinicians. *CMAJ* **172**(3), 367-79.
- Giboney, P. T. (2005). Mildly elevated liver transaminase levels in the asymptomatic patient. *Am Fam Physician* **71**(6), 1105-10.

- Glennner, G. G. (1980). Amyloid deposits and amyloidosis. The beta-fibrilloses (first of two parts). *N Engl J Med* **302**(23), 1283-92.
- Gluud, C. (1988). Testosterone and alcoholic cirrhosis. Epidemiologic, pathophysiologic and therapeutic studies in men. *Dan Med Bull* **35**(6), 564-75.
- Goate, A., Chartier-Harlin, M. C., Mullan, M., Brown, J., Crawford, F., Fidani, L., Giuffra, L., Haynes, A., Irving, N., James, L., *et al.* (1991). Segregation of a missense mutation in the amyloid precursor protein gene with familial Alzheimer's disease. *Nature* **349**(6311), 704-6.
- Goedert, M., and Spillantini, M. G. (2006). A century of Alzheimer's disease. *Science* **314**(5800), 777-81.
- Gomez, B., Jr., Ardakani, S., Ju, J., Jenkins, D., Cerelli, M. J., Daniloff, G. Y., and Kung, V. T. (1995). Monoclonal antibody assay for measuring bone-specific alkaline phosphatase activity in serum. *Clin Chem* **41**(11), 1560-6.
- Goncalves, P., Gregorio, I., and Martel, F. (2011). The short-chain fatty acid butyrate is a substrate of breast cancer resistance protein. *Am J Physiol Cell Physiol* **301**(5), C984-94.
- Goncalves, P., and Martel, F. (2013). Butyrate and colorectal cancer: the role of butyrate transport. *Curr Drug Metab* **14**(9), 994-1008.
- Gong, J., and Yang, C. B. (2012). Advances in the methods for studying gut microbiota and their relevance to the research of dietary fiber functions. *Food Res Int* **48**(2), 916-929.
- Goodwin, A. C., Destefano Shields, C. E., Wu, S., Huso, D. L., Wu, X., Murray-Stewart, T. R., Hacker-Prietz, A., Rabizadeh, S., Woster, P. M., Sears, C. L., *et al.* (2011).

- Polyamine catabolism contributes to enterotoxigenic *Bacteroides fragilis*-induced colon tumorigenesis. *Proc Natl Acad Sci U S A* **108**(37), 15354-9.
- Gosalbes, M. J., Abellan, J. J., Durban, A., Perez-Cobas, A. E., Latorre, A., and Moya, A. (2012). Metagenomics of human microbiome: beyond 16s rDNA. *Clin Microbiol Infect* **18 Suppl 4**, 47-9.
- Graham, K. A., and Buick, R. N. (1988). Sodium butyrate induces differentiation in breast cancer cell lines expressing the estrogen receptor. *J Cell Physiol* **136**(1), 63-71.
- Green, R. M., and Flamm, S. (2002). AGA technical review on the evaluation of liver chemistry tests. *Gastroenterology* **123**(4), 1367-84.
- Greenwald, P. (2004). Clinical trials in cancer prevention: current results and perspectives for the future. *J Nutr* **134**(12 Suppl), 3507S-3512S.
- Greiner, T., and Backhed, F. (2011). Effects of the gut microbiota on obesity and glucose homeostasis. *Trends Endocrinol Metab* **22**(4), 117-23.
- Guban, J., Korver, D. R., Allison, G. E., and Tannock, G. W. (2006). Relationship of dietary antimicrobial drug administration with broiler performance, decreased population levels of *Lactobacillus salivarius*, and reduced bile salt deconjugation in the ileum of broiler chickens. *Poult Sci* **85**(12), 2186-94.
- Gurav, A., Sivaprakasam, S., Bhutia, Y. D., Boettger, T., Singh, N., and Ganapathy, V. (2015). Slc5a8, a Na⁺-coupled high-affinity transporter for short-chain fatty acids, is a conditional tumour suppressor in colon that protects against colitis and colon cancer under low-fibre dietary conditions. *Biochem J* **469**(2), 267-278.

- Guzior, N., Wieckowska, A., Panek, D., and Malawska, B. (2015). Recent development of multifunctional agents as potential drug candidates for the treatment of Alzheimer's disease. *Curr Med Chem* **22**(3), 373-404.
- Haass, C., and Selkoe, D. J. (2007). Soluble protein oligomers in neurodegeneration: lessons from the Alzheimer's amyloid β -peptide. *Nat Rev Mol Cell Biol* **8**(2), 101.
- Hadjiagapiou, C., Schmidt, L., Dudeja, P. K., Layden, T. J., and Ramaswamy, K. (2000). Mechanism(s) of butyrate transport in Caco-2 cells: role of monocarboxylate transporter 1. *Am J Physiol Gastrointest Liver Physiol* **279**(4), G775-80.
- Halestrap, A. P., and Meredith, D. (2004). The SLC16 gene family—from monocarboxylate transporters (MCTs) to aromatic amino acid transporters and beyond. *Pflügers Archiv* **447**(5), 619-628.
- Hall, P., and Cash, J. (2012). What is the real function of the liver 'function' tests. *Ulster Med J* **81**(1), 30-36.
- Han, J. H., Kim, I. S., Jung, S. H., Lee, S. G., Son, H. Y., and Myung, C. S. (2014). The effects of propionate and valerate on insulin responsiveness for glucose uptake in 3T3-L1 adipocytes and C2C12 myotubes via G protein-coupled receptor 41. *PLoS One* **9**(4), e95268.
- Handa, O., Naito, Y., and Yoshikawa, T. (2010). Helicobacter pylori: a ROS-inducing bacterial species in the stomach. *Inflamm Res* **59**(12), 997-1003.
- Harig, J. M., Ng, E. K., Dudeja, P. K., Brasitus, T. A., and Ramaswamy, K. (1996). Transport of n-butyrate into human colonic luminal membrane vesicles. *Am J Physiol Gastrointest Liver Physiol* **271**(3), G415-G422.

- Hatoff, D. E., and Hardison, W. G. (1982). Bile Acid-Dependent Secretion of Alkaline Phosphatase in Rat Bile. *Hepatology* **2**(4).
- Hayden, M. S., West, A. P., and Ghosh, S. (2006). NF-kappaB and the immune response. *Oncogene* **25**(51), 6758-80.
- Heald, A. H., Kaushal, K., Siddals, K. W., Rudenski, A. S., Anderson, S. G., and Gibson, J. M. (2006). Insulin-like growth factor binding protein-2 (IGFBP-2) is a marker for the metabolic syndrome. *Exp Clin Endocrinol Diabetes* **114**(7), 371-6.
- Hedenfalk, I., Duggan, D., Chen, Y., Radmacher, M., Bittner, M., Simon, R., Meltzer, P., Gusterson, B., Esteller, M., Kallioniemi, O. P., *et al.* (2001). Gene-expression profiles in hereditary breast cancer. *N Engl J Med* **344**(8), 539-48.
- Hegedus, R., Manea, M., Orban, E., Szabo, I., Kiss, E., Sipos, E., Halmos, G., and Mezo, G. (2012). Enhanced cellular uptake and in vitro antitumor activity of short-chain fatty acid acylated daunorubicin-GnRH-III bioconjugates. *Eur J Med Chem* **56**, 155-65.
- Hemarajata, P., and Versalovic, J. (2012). Effects of probiotics on gut microbiota: mechanisms of intestinal immunomodulation and neuromodulation. *Therap Adv Gastroenterol* **6**(1), 39-51.
- Hemmrich, K., Thomas, G. P., Abberton, K. M., Thompson, E. W., Rophael, J. A., Penington, A. J., and Morrison, W. A. (2007). Monocyte Chemoattractant Protein-1 and Nitric Oxide Promote Adipogenesis in a Model That Mimics Obesity. *Obesity* **15**(12), 2951-2957.

- Hester, C. M., Jala, V. R., Langille, M. G., Umar, S., Greiner, K. A., and Haribabu, B. (2015). Fecal microbes, short chain fatty acids, and colorectal cancer across racial/ethnic groups. *World J Gastroenterol* **21**(9), 2759-69.
- Higgins, C. (2007). *Understanding laboratory investigations for nurses and health professionals*. Wiley-Blackwell.
- Hijova, E., and Chmelarova, A. (2007). Short chain fatty acids and colonic health. *Bratisl Lek Listy* **108**(8), 354-8.
- Hinnebusch, B. F., Meng, S., Wu, J. T., Archer, S. Y., and Hodin, R. A. (2002). The effects of short-chain fatty acids on human colon cancer cell phenotype are associated with histone hyperacetylation. *J Nutr* **132**(5), 1012-7.
- Hirata, F., Schiffmann, E., Venkatasubramanian, K., Salomon, D., and Axelrod, J. (1980). A phospholipase A2 inhibitory protein in rabbit neutrophils induced by glucocorticoids. *Proc Natl Acad Sci U S A* **77**(5), 2533-6.
- Hoekstra, L. T., de Graaf, W., Nibourg, G. A., Heger, M., Bennink, R. J., Stieger, B., and van Gulik, T. M. (2013). Physiological and biochemical basis of clinical liver function tests: a review. *Ann Surg* **257**(1), 27-36.
- Holmes, E., Li, J. V., Marchesi, J. R., and Nicholson, J. K. (2012). Gut microbiota composition and activity in relation to host metabolic phenotype and disease risk. *Cell Metab* **16**(5), 559-64.
- Holmes, E., Loo, R. L., Stamler, J., Bictash, M., Yap, I. K., Chan, Q., Ebbels, T., De Iorio, M., Brown, I. J., Veselkov, K. A., *et al.* (2008). Human metabolic phenotype diversity and its association with diet and blood pressure. *Nature* **453**(7193), 396-400.

- Hong, Y. H., Nishimura, Y., Hishikawa, D., Tsuzuki, H., Miyahara, H., Gotoh, C., Choi, K. C., Feng, D. D., Chen, C., Lee, H. G., *et al.* (2005). Acetate and propionate short chain fatty acids stimulate adipogenesis via GPCR43. *Endocrinology* **146**(12), 5092-9.
- Hooper, L. V., Wong, M. H., Thelin, A., Hansson, L., Falk, P. G., and Gordon, J. I. (2001). Molecular analysis of commensal host-microbial relationships in the intestine. *Science* **291**(5505), 881-4.
- Horwitz, K. B., Mockus, M. B., and Lessey, B. A. (1982). Variant T47D human breast cancer cells with high progesterone-receptor levels despite estrogen and antiestrogen resistance. *Cell* **28**(3), 633-42.
- Hsiao, E. Y., McBride, S. W., Hsien, S., Sharon, G., Hyde, E. R., McCue, T., Codelli, J. A., Chow, J., Reisman, S. E., Petrosino, J. F., *et al.* (2013). Microbiota modulate behavioral and physiological abnormalities associated with neurodevelopmental disorders. *Cell* **155**(7), 1451-63.
- Huan, T., Forsberg, E. M., Rinehart, D., Johnson, C. H., Ivanisevic, J., Benton, H. P., Fang, M., Aisporna, A., Hilmers, B., Poole, F. L., *et al.* (2017). Systems biology guided by XCMS Online metabolomics. *Nat Methods* **14**(5), 461-462.
- Huang, M. J., and Liaw, Y. F. (1995). Clinical Associations between Thyroid and Liver-Diseases. *J Gastroenterol Hepatol* **10**(3), 344-350.
- Huda-Faujan, N., Abdulmir, A. S., Fatimah, A. B., Anas, O. M., Shuhaimi, M., Yazid, A. M., and Loong, Y. Y. (2010). The impact of the level of the intestinal short chain Fatty acids in inflammatory bowel disease patients versus healthy subjects. *Open Biochem J* **4**, 53-8.

- Huurinainen, O. (2009). Dietary protein and carbohydrate modify volatile fatty acid (VFA) profile in canine faeces. University of Helsinki, Faculty of Veterinary Medicine, Department of Equine and Small Animal Medicine. *Thesis*
- Huuskonen, J., Suuronen, T., Nuutinen, T., Kyrylenko, S., and Salminen, A. (2004). Regulation of microglial inflammatory response by sodium butyrate and short-chain fatty acids. *Br J Pharm* **141**(5), 874-880.
- I Naseer, M., Bibi, F., H Alqahtani, M., G Chaudhary, A., I Azhar, E., A Kamal, M., and Yasir, M. (2014). Role of gut microbiota in obesity, type 2 diabetes and Alzheimer's disease. *CNS Neurol Disord Drug Targets* **13**(2), 305-311.
- Iskander, I., Rasha G., Salma E. H., Amira E. S., Iman S., Nesrin E. G., Hazem A.-Y., Aleksandr A., and Richard P. W. (2014) Serum bilirubin and bilirubin/albumin ratio as predictors of bilirubin encephalopathy. *Pediatrics* 134(5): 1330-1339.
- Jahns, F., Wilhelm, A., Jablonowski, N., Mothes, H., Greulich, K. O., and Gleib, M. (2015). Butyrate modulates antioxidant enzyme expression in malignant and non-malignant human colon tissues. *Mol Carcinog* **54**(4), 249-60.
- James, P. T., Rigby, N., Leach, R., and International Obesity Task, F. (2004). The obesity epidemic, metabolic syndrome and future prevention strategies. *Eur J Cardiovasc Prev Rehabil* **11**(1), 3-8.
- Jandhyala, S. M., Talukdar, R., Subramanyam, C., Vuyyuru, H., Sasikala, M., and Nageshwar Reddy, D. (2015). Role of the normal gut microbiota. *World J Gastroenterol* **21**(29), 8787-803.
- Jasperson, L. K., Bucher, C., Panoskaltis-Mortari, A., Mellor, A. L., Munn, D. H., and Blazar, B. R. (2009). Inducing the tryptophan catabolic pathway, indoleamine 2,3-

- dioxygenase (IDO), for suppression of graft-versus-host disease (GVHD) lethality. *Blood* **114**(24), 5062-70.
- Jenner, A. M., Rafter, J., and Halliwell, B. (2005). Human fecal water content of phenolics: the extent of colonic exposure to aromatic compounds. *Free Radic Biol Med* **38**(6), 763-72.
- Jensen, M. T., Cox, R. P., and Jensen, B. B. (1995). 3-Methylindole (skatole) and indole production by mixed populations of pig fecal bacteria. *Appl Environ Microbiol* **61**(8), 3180-4.
- Jiang, Y., Jolly, P. E., Preko, P., Wang, J. S., Ellis, W. O., Phillips, T. D., and Williams, J. H. (2008). Aflatoxin-related immune dysfunction in health and in human immunodeficiency virus disease. *Clin Dev Immunol* **2008**, 790309.
- Johnston, D. E. (1999). Special considerations in interpreting liver function tests. *Am Fam Physician* **59**(8), 2223-30.
- Jones, M. L., Martoni, C. J., Parent, M., and Prakash, S. (2012). Cholesterol-lowering efficacy of a microencapsulated bile salt hydrolase-active *Lactobacillus reuteri* NCIMB 30242 yoghurt formulation in hypercholesterolaemic adults. *Br J Nutr* **107**(10), 1505-13.
- Jørgensen, J., and Mortensen, P. B. (2001). Substrate utilization by intestinal mucosal tissue strips from patients with inflammatory bowel disease. *Am J Physiol Gastrointest Liver Physiol* **281**(2), G405-G411.
- Joyce, S. A., MacSharry, J., Casey, P. G., Kinsella, M., Murphy, E. F., Shanahan, F., Hill, C., and Gahan, C. G. (2014). Regulation of host weight gain and lipid metabolism

- by bacterial bile acid modification in the gut. *Proc Natl Acad Sci U S A* **111**(20), 7421-6.
- Jumpertz, R., Le, D. S., Turnbaugh, P. J., Trinidad, C., Bogardus, C., Gordon, J. I., and Krakoff, J. (2011). Energy-balance studies reveal associations between gut microbes, caloric load, and nutrient absorption in humans. *Am J Clin Nutr* **94**(1), 58-65.
- Kamath, P. S., Wiesner, R. H., Malinchoc, M., Kremers, W., Therneau, T. M., Kosberg, C. L., D'Amico, G., Dickson, E. R., and Kim, W. R. (2001). A model to predict survival in patients with end-stage liver disease. *Hepatology* **33**(2), 464-70.
- Kaplan, M. M., and Righetti, A. (1969). Induction of liver alkaline phosphatase by bile duct ligation. *Biochim Biophys Acta* **184**(3), 667-9.
- Karaki, S., Mitsui, R., Hayashi, H., Kato, I., Sugiya, H., Iwanaga, T., Furness, J. B., and Kuwahara, A. (2006). Short-chain fatty acid receptor, GPR43, is expressed by enteroendocrine cells and mucosal mast cells in rat intestine. *Cell Tissue Res* **324**(3), 353-360.
- Karaki, S., Tazoe, H., Hayashi, H., Kashiwabara, H., Tooyama, K., Suzuki, Y., and Kuwahara, A. (2008). Expression of the short-chain fatty acid receptor, GPR43, in the human colon. *J Mol Histol* **39**(2), 135-42.
- Karlin, D. A., Mastromarino, A. J., Jones, R. D., Stroehlein, J. R., and Lorentz, O. (1985). Fecal skatole and indole and breath methane and hydrogen in patients with large bowel polyps or cancer. *J Cancer Res Clin Oncol* **109**(2), 135-41.
- Karlsson, F., Tremaroli, V., Nielsen, J., and Backhed, F. (2013). Assessing the human gut microbiota in metabolic diseases. *Diabetes* **62**(10), 3341-9.

- Kasturiratne, A., Weerasinghe, S., Dassanayake, A. S., Rajindrajith, S., Silva, A. P., Kato, N., Wickremasinghe, A. R., and Silva, H. J. (2013). Influence of non-alcoholic fatty liver disease on the development of diabetes mellitus. *J Gastroenterol Hepatol* **28**(1), 142-147.
- Kasubuchi, M., Hasegawa, S., Hiramatsu, T., Ichimura, A., and Kimura, I. (2015). Dietary gut microbial metabolites, short-chain fatty acids, and host metabolic regulation. *Nutrients* **7**(4), 2839-49.
- Keller, J., Baradat, M., Jouanin, I., Debrauwer, L., and Guéraud, F. (2015). “Twin peaks”: Searching for 4-hydroxynonenal urinary metabolites after oral administration in rats. *Redox Biol* **4**, 136-148.
- Kendrick, S. F., O'Boyle, G., Mann, J., Zeybel, M., Palmer, J., Jones, D. E., and Day, C. P. (2010). Acetate, the key modulator of inflammatory responses in acute alcoholic hepatitis. *Hepatology* **51**(6), 1988-97.
- Kennedy, P. J., Cryan, J. F., Dinan, T. G., and Clarke, G. (2017). Kynurenine pathway metabolism and the microbiota-gut-brain axis. *Neuropharmacology* **112**(Pt B), 399-412.
- Kew, M. (1987). Sexual dysfunction in men with chronic liver disease. *Hepatology (Baltimore, Md.)* **8**(2), 429-431.
- Khan, A., Shaw, L., Drake, P., Griffiths, G., Brown, S., and Corfe, B. (2011). Application of high content biology demonstrates differential responses of keratin acetylation sites to short chain fatty acids and to mitosis. *J Integr OMICS* **1**(2), 253-259.
- Khan, M. A. (2006). Regulation of volatile fatty acid synthesis in *Megasphaera elsdenii* and hexanoic acid utilisation by *Pseudomonas putida*. Victoria University.

- Kiefer, J., Beyer-Sehlmeyer, G., and Pool-Zobel, B. L. (2006). Mixtures of SCFA, composed according to physiologically available concentrations in the gut lumen, modulate histone acetylation in human HT29 colon cancer cells. *Br J Nutr* **96**(5), 803-10.
- Kildegaard, H. F., Baycin-Hizal, D., Lewis, N. E., and Betenbaugh, M. J. (2013). The emerging CHO systems biology era: harnessing the 'omics revolution for biotechnology. *Curr Opin Biotechnol* **24**(6), 1102-7.
- Kilner, J., Corfe, B., and Wilkinson, S. (2011). Modelling modifications affecting the tubulin code as a route to study the chemopreventive and chemotherapeutic actions of SCFAs as HDAC inhibitors. *Mol. Biosyst* **7**, 975-983.
- Kilner, J., Corfe, B. M., McAuley, M. T., and Wilkinson, S. J. (2016). A deterministic oscillatory model of microtubule growth and shrinkage for differential actions of short chain fatty acids. *Mol Biosyst* **12**(1), 93-101.
- Kilner, J., Waby, J. S., Chowdry, J., Khan, A. Q., Noirel, J., Wright, P. C., Corfe, B. M., and Evans, C. A. (2012). A proteomic analysis of differential cellular responses to the short-chain fatty acids butyrate, valerate and propionate in colon epithelial cancer cells. *Mol Biosyst* **8**(4), 1146-56.
- Kim, M. H., Kang, S. G., Park, J. H., Yanagisawa, M., and Kim, C. H. (2013). Short-chain fatty acids activate GPR41 and GPR43 on intestinal epithelial cells to promote inflammatory responses in mice. *Gastroenterology* **145**(2), 396-406 e1-10.
- Kim, W. R., Flamm, S. L., Di Bisceglie, A. M., Bodenheimer, H. C., and A, P. P. C. A. (2008). Serum activity of alanine aminotransferase (ALT) as an indicator of health and disease. *Hepatology* **47**(4), 1363-1370.

- Kimura, I., Inoue, D., Maeda, T., Hara, T., Ichimura, A., Miyauchi, S., Kobayashi, M., Hirasawa, A., and Tsujimoto, G. (2011). Short-chain fatty acids and ketones directly regulate sympathetic nervous system via G protein-coupled receptor 41 (GPR41). *Proc Natl Acad Sci U S A* **108**(19), 8030-5.
- Kimura, I., Ozawa, K., Inoue, D., Imamura, T., Kimura, K., Maeda, T., Terasawa, K., Kashihara, D., Hirano, K., Tani, T., *et al.* (2013). The gut microbiota suppresses insulin-mediated fat accumulation via the short-chain fatty acid receptor GPR43. *Nat Commun* **4**, 1829 (Article).
- King, R. A., May, B. L., Davies, D. A., and Bird, A. R. (2009). Measurement of phenol and p-cresol in urine and feces using vacuum microdistillation and high-performance liquid chromatography. *Anal Biochem* **384**(1), 27-33.
- Kist, M., and Bereswill, S. (2001). *Campylobacter jejuni*. *Contrib Microbiol* **8**, 150-65.
- Koff, R. S. (1980). Toxic injury of the liver, part B. The liver: Normal function and disease series, volume 2. *Gastroenterology* **79**(2), 403.
- Kondo, T., Kishi, M., Fushimi, T., and Kaga, T. (2009). Acetic acid upregulates the expression of genes for fatty acid oxidation enzymes in liver to suppress body fat accumulation. *J Agric Food Chem* **57**(13), 5982-6.
- Koren, O., Goodrich, J. K., Cullender, T. C., Spor, A., Laitinen, K., Backhed, H. K., Gonzalez, A., Werner, J. J., Angenent, L. T., Knight, R., *et al.* (2012). Host remodeling of the gut microbiome and metabolic changes during pregnancy. *Cell* **150**(3), 470-80.

- Kose, F., Weckwerth, W., Linke, T., and Fiehn, O. (2001). Visualizing plant metabolomic correlation networks using clique–metabolite matrices. *Bioinformatics* **17**(12), 1198-1208.
- Kountouras, J., Zavos, C., Polyzos, S., Deretzi, G., Vardaka, E., Giartza-Taxidou, E., Katsinelos, P., Rapti, E., Chatzopoulos, D., and Tzilves, D. (2012). Helicobacter pylori infection and Parkinson's disease: apoptosis as an underlying common contributor. *Eur J Neurol* **19**(6), e56-e56.
- Kratz, A., Ferraro, M., Sluss, P. M., and Lewandrowski, K. B. (2004). Normal reference laboratory values. *N Engl J Med* **351**(15), 1548-1563.
- Ku, N. O., Zhou, X., Toivola, D. M., and Omary, M. B. (1999). The cytoskeleton of digestive epithelia in health and disease. *Am J Physiol* **277**(6 Pt 1), G1108-37.
- Kumar, D. K., Choi, S. H., Washicosky, K. J., Eimer, W. A., Tucker, S., Ghofrani, J., Lefkowitz, A., McColl, G., Goldstein, L. E., Tanzi, R. E., *et al.* (2016). Amyloid-beta peptide protects against microbial infection in mouse and worm models of Alzheimer's disease. *Sci Transl Med* **8**(340), 340ra72.
- Larsson, S. C., Bergkvist, L., and Wolk, A. (2005). High-fat dairy food and conjugated linoleic acid intakes in relation to colorectal cancer incidence in the Swedish Mammography Cohort. *Am J Clin Nutr* **82**(4), 894-900.
- Lazarova, D. L., and Bordonaro, M. (2016). Vimentin, colon cancer progression and resistance to butyrate and other HDACis. *J Cell Mol Med* **20**(6), 989-93.
- Lazo, M., Selvin, E., and Clark, J. M. (2008). Brief communication: clinical implications of short-term variability in liver function test results. *Ann Intern Med* **148**(5), 348-52.

- Le Leu, R. K., Brown, I. L., Hu, Y., Esterman, A., and Young, G. P. (2007). Suppression of azoxymethane-induced colon cancer development in rats by dietary resistant starch. *Cancer Biol Ther* **6**(10), 1621-6.
- Le Poul, E., Loison, C., Struyf, S., Springael, J.-Y., Lannoy, V., Decobecq, M.-E., Brezillon, S., Dupriez, V., Vassart, G., and Van Damme, J. (2003). Functional characterization of human receptors for short chain fatty acids and their role in polymorphonuclear cell activation. *J Biol Chem* **278**(28), 25481-25489.
- Leal-Lopes, C., Velloso, F. J., Campopiano, J. C., Sogayar, M. C., and Correa, R. G. (2015). Roles of Commensal Microbiota in Pancreas Homeostasis and Pancreatic Pathologies. *J Diabetes Res* **2015**, 284680.
- Lebeer, S., Vanderleyden, J., and De Keersmaecker, S. C. (2010). Host interactions of probiotic bacterial surface molecules: comparison with commensals and pathogens. *Nat Rev Microbiol* **8**(3), 171-84.
- LeBlanc, J., Laiño, J., del Valle, M. J., Vannini, V., Van Sinderen, D., Taranto, M., de Valdez, G. F., de Giori, G. S., and Sesma, F. (2011). B-Group vitamin production by lactic acid bacteria—current knowledge and potential applications. *J Appl Microbiol* **111**(6), 1297-1309.
- LeBlanc, J. G., Chain, F., Martin, R., Bermudez-Humaran, L. G., Courau, S., and Langella, P. (2017). Beneficial effects on host energy metabolism of short-chain fatty acids and vitamins produced by commensal and probiotic bacteria. *Microb Cell Fact* **16**(1), 79.

- LeBlanc, J. G., Milani, C., de Giori, G. S., Sesma, F., van Sinderen, D., and Ventura, M. (2013). Bacteria as vitamin suppliers to their host: a gut microbiota perspective. *Curr Opin Biotechnol* **24**(2), 160-168.
- Lederberg, J., and McCray, A. T. (2001). Ome SweetOmics--A Genealogical Treasury of Words. *The Scientist* **15**(7), 8-8.
- Lee, D. S., Evans, J. C., Robins, S. J., Wilson, P. W., Albano, I., Fox, C. S., Wang, T. J., Benjamin, E. J., D'Agostino, R. B., and Vasan, R. S. (2007). Gamma glutamyl transferase and metabolic syndrome, cardiovascular disease, and mortality risk: the Framingham Heart Study. *Arterioscler Thromb Vasc Biol* **27**(1), 127-33.
- Lee, J. H., Kim, Y. G., Kim, C. J., Lee, J. C., Cho, M. H., and Lee, J. (2012). Indole-3-acetaldehyde from *Rhodococcus* sp. BFI 332 inhibits *Escherichia coli* O157:H7 biofilm formation. *Appl Microbiol Biotechnol* **96**(4), 1071-8.
- Lee, J. H., and Lee, J. (2010). Indole as an intercellular signal in microbial communities. *FEMS Microbiol Rev* **34**(4), 426-44.
- Leech, S. H., Evans, C. A., Shaw, L., Wong, C. H., Connolly, J., Griffiths, J. R., Whetton, A. D., and Corfe, B. M. (2008). Proteomic analyses of intermediate filaments reveals cytokeratin8 is highly acetylated--implications for colorectal epithelial homeostasis. *Proteomics* **8**(2), 279-288.
- Lehmann, F.-G. (1975). Immunological relationship between human placenta and intestinal alkaline phosphatase. *Clin Chim Acta* **65**(3), 257-269.
- Leitch, E. C., Walker, A. W., Duncan, S. H., Holtrop, G., and Flint, H. J. (2007). Selective colonization of insoluble substrates by human faecal bacteria. *Environ Microbiol* **9**(3), 667-79.

- Leyn, S. A., Suvorova, I. A., Kazakov, A. E., Ravcheev, D. A., Stepanova, V. V., Novichkov, P. S., and Rodionov, D. A. (2016). Comparative genomics and evolution of transcriptional regulons in Proteobacteria. *Microb Genom* **2**(7), e000061.
- Lindblom, P., Rafter, I., Copley, C., Andersson, U., Hedberg, J. J., Berg, A. L., Samuelsson, A., Hellmold, H., Cotgreave, I., and Glinghammar, B. (2007). Isoforms of alanine aminotransferases in human tissues and serum--differential tissue expression using novel antibodies. *Arch Biochem Biophys* **466**(1), 66-77.
- Litt, M. D., Simpson, M., Gaszner, M., Allis, C. D., and Felsenfeld, G. (2001). Correlation between histone lysine methylation and developmental changes at the chicken β -globin locus. *Science* **293**(5539), 2453-2455.
- Liu, T., Li, J., Liu, Y., Xiao, N., Suo, H., Xie, K., Yang, C., and Wu, C. (2012). Short-chain fatty acids suppress lipopolysaccharide-induced production of nitric oxide and proinflammatory cytokines through inhibition of NF-kappaB pathway in RAW264.7 cells. *Inflammation* **35**(5), 1676-84.
- Livingstone, B. (2000). Epidemiology of childhood obesity in Europe. *Eur J Pediatr* **159 Suppl 1**(1), S14-34.
- Lott, J. A., Tholen, D. W., and Massion, C. G. (1988). Proficiency testing of enzymes. Charting the way toward standardization. *Arch Pathol Lab Med* **112**(4), 392-8.
- Louis, P., Hold, G. L., and Flint, H. J. (2014). The gut microbiota, bacterial metabolites and colorectal cancer. *Nat Rev Microbiol* **12**(10), 661-72 (Review).
- Lovelace, M. D., Varney, B., Sundaram, G., Franco, N. F., Ng, M. L., Pai, S., Lim, C. K., Guillemin, G. J., and Brew, B. J. (2016). Current Evidence for a Role of the

- Kynurenine Pathway of Tryptophan Metabolism in Multiple Sclerosis. *Front Immunol* **7**, 246.
- Lu, W., Bennett, B. D., and Rabinowitz, J. D. (2008). Analytical strategies for LC–MS-based targeted metabolomics. *J Chromatogr B* **871**(2), 236-242.
- Lu, W., Clasquin, M. F., Melamud, E., Amador-Noguez, D., Caudy, A. A., and Rabinowitz, J. D. (2010). Metabolomic analysis via reversed-phase ion-pairing liquid chromatography coupled to a stand alone orbitrap mass spectrometer. *Anal Chem* **82**(8), 3212-21.
- Lucas, J. L., Mirshahpanah, P., Haas-Stapleton, E., Asadullah, K., Zollner, T. M., and Numerof, R. P. (2009). Induction of Foxp3⁺ regulatory T cells with histone deacetylase inhibitors. *Cell Immunol* **257**(1-2), 97-104.
- Lugo-Huitron, R., Ugalde Muniz, P., Pineda, B., Pedraza-Chaverri, J., Rios, C., and Perez-de la Cruz, V. (2013). Quinolinic acid: an endogenous neurotoxin with multiple targets. *Oxid Med Cell Longev* **2013**, 104024.
- Lukasova, M., Malaval, C., Gille, A., Kero, J., and Offermanns, S. (2011). Nicotinic acid inhibits progression of atherosclerosis in mice through its receptor GPR109A expressed by immune cells. *J Clin Invest* **121**(3), 1163-73.
- Macfarlane, G. J., Hunt, I. M., and Silman, A. J. (1998). Predictors of chronic shoulder pain: a population based prospective study. *J Rheumatol* **25**(8), 1612-5.
- Macfarlane, G. T., Gibson, G. R., Beatty, E., and Cummings, J. H. (1992). Estimation of Short-Chain Fatty-Acid Production from Protein by Human Intestinal Bacteria Based on Branched-Chain Fatty-Acid Measurements. *FEMS Microbiol Ecol* **101**(2), 81-88.

- Macfarlane, S., and Macfarlane, G. T. (2003). Regulation of short-chain fatty acid production. *Proc Nutr Soc* **62**(1), 67-72.
- Macia, L., Tan, J., Vieira, A. T., Leach, K., Stanley, D., Luong, S., Maruya, M., McKenzie, C. I., Hijikata, A., Wong, C., *et al.* (2015). Metabolite-sensing receptors GPR43 and GPR109A facilitate dietary fibre-induced gut homeostasis through regulation of the inflammasome. *Nat Commun* **6**.
- MacLennan, C. A., van Oosterhout, J. J. G., White, S. A., Drayson, M. T., Zijlstra, E. E., and Molyneux, M. E. (2007). Finger-prick blood samples can be used interchangeably with venous samples for CD4 cell counting indicating their potential for use in CD4 rapid tests. *Aids* **21**(12), 1643-1645.
- Magnusdottir, S., Ravcheev, D., de Crecy-Lagard, V., and Thiele, I. (2015). Systematic genome assessment of B-vitamin biosynthesis suggests co-operation among gut microbes. *Front Genet* **6**, 148.
- Maheshwari, A., and Thuluvath, P. J. (2011). Endocrine diseases and the liver. *Clin Liver Dis* **15**(1), 55-67.
- Marchesi, J. R., Dutilh, B. E., Hall, N., Peters, W. H., Roelofs, R., Boleij, A., and Tjalsma, H. (2011). Towards the human colorectal cancer microbiome. *PLoS One* **6**(5), e20447.
- Marchesini, G., Brizi, M., Morselli-Labate, A. M., Bianchi, G., Bugianesi, E., McCullough, A. J., Forlani, G., and Melchionda, N. (1999). Association of nonalcoholic fatty liver disease with insulin resistance. *Am J Med* **107**(5), 450-5.

- Marchesini, G., Bugianesi, E., Forlani, G., Cerrelli, F., Lenzi, M., Manini, R., Natale, S., Vanni, E., Villanova, N., Melchionda, N., *et al.* (2003). Nonalcoholic fatty liver, steatohepatitis, and the metabolic syndrome. *Hepatology* **37**(4), 917-23.
- Margulis, L. (1981). *Symbiosis in cell evolution*. WH freeman.
- Mariadason, J. M., Corner, G. A., and Augenlicht, L. H. (2000). Genetic reprogramming in pathways of colonic cell maturation induced by short chain fatty acids: comparison with trichostatin A, sulindac, and curcumin and implications for chemoprevention of colon cancer. *Cancer Res* **60**(16), 4561-72.
- Marleau, S., Harb, D., Bujold, K., Avallone, R., Iken, K., Wang, Y., Demers, A., Sirois, M. G., Febbraio, M., Silverstein, R. L., *et al.* (2005). EP 80317, a ligand of the CD36 scavenger receptor, protects apolipoprotein E-deficient mice from developing atherosclerotic lesions. *FASEB J* **19**(13), 1869-71.
- Marques, C., Oliveira, C. S., Alves, S., Chaves, S. R., Coutinho, O. P., Corte-Real, M., and Preto, A. (2013). Acetate-induced apoptosis in colorectal carcinoma cells involves lysosomal membrane permeabilization and cathepsin D release. *Cell Death Dis* **4**, e507.
- Marques, T. M., Wall, R., Ross, R. P., Fitzgerald, G. F., Ryan, C. A., and Stanton, C. (2010). Programming infant gut microbiota: influence of dietary and environmental factors. *Curr Opin Biotechnol* **21**(2), 149-56.
- Maslowski, K. M., Vieira, A. T., Ng, A., Kranich, J., Sierro, F., Yu, D., Schilter, H. C., Rolph, M. S., Mackay, F., Artis, D., *et al.* (2009). Regulation of inflammatory responses by gut microbiota and chemoattractant receptor GPR43. *Nature* **461**(7268), 1282-6.

- Matchett, W. H. (1972). Inhibition of tryptophan synthetase by indoleacrylic acid. *J Bacteriol* **110**(1), 146-54.
- Matsuda, K., Toyoda, H., Nishio, H., Nishida, T., Dohgo, M., Bingo, M., Matsuda, Y., Yoshida, S., Harada, S., Tanaka, H., *et al.* (1998). Control of the bacterial wilt of tomato plants by a derivative of 3-indolepropionic acid based on selective actions on *Ralstonia solanacearum*. *J Agric Food Chem* **46**(10), 4416-4419.
- Matsuishi, T., Stumpf, D. A., Seliem, M., Eguren, L. A., and Chrislip, K. (1991). Propionate mitochondrial toxicity in liver and skeletal muscle: acyl CoA levels. *Biochem Med Metab Biol* **45**(2), 244-53.
- Mayer, E. A., Tillisch, K., and Gupta, A. (2015). Gut/brain axis and the microbiota. *J Clin Invest* **125**(3), 926-38.
- McCullough, A. J. (2006). Pathophysiology of nonalcoholic steatohepatitis. *J Clin Gastroenterol* **40 Suppl 1**, S17-29.
- McGarry, J. D., and Foster, D. W. (1980). Regulation of hepatic fatty acid oxidation and ketone body production. *Annu Rev Biochem* **49**(1), 395-420.
- McNeil, N. I. (1984). The contribution of the large intestine to energy supplies in man. *Am J Clin Nutr* **39**(2), 338-42.
- McNeil, N. I., Cummings, J. H., and James, W. P. (1978). Short chain fatty acid absorption by the human large intestine. *Gut* **19**(9), 819-22.
- Memon, R. A., Tecott, L. H., Nonogaki, K., Beigneux, A., Moser, A. H., Grunfeld, C., and Feingold, K. R. (2000). Up-regulation of peroxisome proliferator-activated receptors (PPAR-alpha) and PPAR-gamma messenger ribonucleic acid expression in the liver in murine obesity: troglitazone induces expression of PPAR-gamma-

- responsive adipose tissue-specific genes in the liver of obese diabetic mice. *Endocrinology* **141**(11), 4021-31.
- Mereschkowsky, C. (1905). *Über natur und ursprung der chromatophoren im pflanzenreiche*. Biol Centralbl 15: 593–604
- Miller, S. J., Zaloga, G. P., Hoggatt, A. M., Labarrere, C., and Faulk, W. P. (2005). Short-chain fatty acids modulate gene expression for vascular endothelial cell adhesion molecules. *Nutrition* **21**(6), 740-8.
- Miri-Dashe, T., Osawe, S., Tokdung, M., Daniel, N., Choji, R. P., Mamman, I., Deme, K., Damulak, D., and Abimiku, A. (2014). Comprehensive reference ranges for hematology and clinical chemistry laboratory parameters derived from normal Nigerian adults. *PLoS One* **9**(5), e93919.
- Mirvish, S. S., Davis, M. E., Lisowyj, M. P., and Gaikwad, N. W. (2008). Effect of feeding nitrite, ascorbate, hemin, and omeprazole on excretion of fecal total apparent N-nitroso compounds in mice. *Chem Res Toxicol* **21**(12), 2344-51.
- Mitrou, P., Petsiou, E., Papakonstantinou, E., Maratou, E., Lambadiari, V., Dimitriadis, P., Spanoudi, F., Raptis, S. A., and Dimitriadis, G. (2015). The role of acetic acid on glucose uptake and blood flow rates in the skeletal muscle in humans with impaired glucose tolerance. *Eur J Clin Nutr* **69**(6), 734-9.
- Mizejewski, G. J., Lindau-Shepard, B., and Pass, K. A. (2013). Newborn screening for autism: in search of candidate biomarkers. *Biomark Med* **7**(2), 247-60.
- Mortensen, P. B., and Clausen, M. R. (1996). Short-chain fatty acids in the human colon: relation to gastrointestinal health and disease. *Scand J Gastroenterol Suppl* **216**(S216), 132-48.

- Mozaffari, S., Rahimi, R., and Abdollahi, M. (2010). Implications of melatonin therapy in irritable bowel syndrome: a systematic review. *Curr Pharm Des* **16**(33), 3646-55.
- Mulak, A., and Bonaz, B. (2015). Brain-gut-microbiota axis in Parkinson's disease. *World J Gastroenterol* **21**(37), 10609-20.
- Muller, N., Myint, A. M., and Schwarz, M. J. (2011). Kynurenine pathway in schizophrenia: pathophysiological and therapeutic aspects. *Curr Pharm Des* **17**(2), 130-6.
- Murillo, G., and Mehta, R. G. (2001). Cruciferous vegetables and cancer prevention. *Nutr Cancer* **41**(1-2), 17-28.
- Murphy, E. F., Cotter, P. D., Healy, S., Marques, T. M., O'Sullivan, O., Fouhy, F., Clarke, S. F., O'Toole, P. W., Quigley, E. M., Stanton, C., *et al.* (2010). Composition and energy harvesting capacity of the gut microbiota: relationship to diet, obesity and time in mouse models. *Gut* **59**(12), 1635-42.
- Murrell, J., Farlow, M., Ghetti, B., and Benson, M. D. (1991). A mutation in the amyloid precursor protein associated with hereditary Alzheimer's disease. *Science* **254**(5028), 97-9.
- Nakahata, Y., Kaluzova, M., Grimaldi, B., Sahar, S., Hirayama, J., Chen, D., Guarente, L. P., and Sassone-Corsi, P. (2008). The NAD⁺-dependent deacetylase SIRT1 modulates CLOCK-mediated chromatin remodeling and circadian control. *Cell* **134**(2), 329-40.
- Nastasi, C., Candela, M., Bonfeld, C. M., Geisler, C., Hansen, M., Krejsgaard, T., Biagi, E., Andersen, M. H., Brigidi, P., Odum, N., *et al.* (2015). The effect of short-chain fatty acids on human monocyte-derived dendritic cells. *Sci Rep* **5**, 16148.

- Neish, A. S. (2009). Microbes in gastrointestinal health and disease. *Gastroenterology* **136**(1), 65-80.
- Neu, J., and Rushing, J. (2011). Cesarean versus vaginal delivery: long-term infant outcomes and the hygiene hypothesis. *Clin Perinatol* **38**(2), 321-31.
- Neut, C., Guillemot, F., Gower-Rousseau, C., Biron, N., Cortot, A., and Colombel, J. F. (1995). [Treatment of diversion colitis with short-chain fatty acids. Bacteriological study]. *Gastroenterol Clin Biol* **19**(11), 871-5.
- Nichols, G. A., Hillier, T. A., and Brown, J. B. (2008). Normal fasting plasma glucose and risk of type 2 diabetes diagnosis. *Am J Med* **121**(6), 519-24.
- Nicholson, J. K. (2006). Global systems biology, personalized medicine and molecular epidemiology. *Mol Syst Biol* **2**(1), 52.
- Nilsson, N. E., Kotarsky, K., Owman, C., and Olde, B. (2003). Identification of a free fatty acid receptor, FFA(2)R, expressed on leukocytes and activated by short-chain fatty acids. *Biochem Biophys Res Commun* **303**(4), 1047-1052.
- Nohr, M. K., Egerod, K. L., Christiansen, S. H., Gille, A., Offermanns, S., Schwartz, T. W., and Moller, M. (2015). Expression of the short chain fatty acid receptor GPR41/FFAR3 in autonomic and somatic sensory ganglia. *Neuroscience* **290**, 126-37.
- Nøhr, M. K., Pedersen, M. H., Gille, A., Egerod, K. L., Engelstoft, M. S., Husted, A. S., Sichlau, R. M., Grunddal, K. V., Seier Poulsen, S., and Han, S. (2013). GPR41/FFAR3 and GPR43/FFAR2 as cosensors for short-chain fatty acids in enteroendocrine cells vs FFAR3 in enteric neurons and FFAR2 in enteric leukocytes. *Endocrinology* **154**(10), 3552-3564.

- Nordstrom, A., O'Maille, G., Qin, C., and Siuzdak, G. (2006). Nonlinear data alignment for UPLC-MS and HPLC-MS based metabolomics: quantitative analysis of endogenous and exogenous metabolites in human serum. *Anal Chem* **78**(10), 3289-95.
- O Watzlawik, J., Wootla, B., and Rodriguez, M. (2016). Tryptophan catabolites and their impact on multiple sclerosis progression. *Curr Pharm Des* **22**(8), 1049-1059.
- Ochoa-Reparaz, J., and Kasper, L. H. (2014). Gut microbiome and the risk factors in central nervous system autoimmunity. *FEBS Lett* **588**(22), 4214-4222.
- Ochoa-Zarzosa, A., Villarreal-Fernandez, E., Cano-Camacho, H., and Lopez-Meza, J. E. (2009). Sodium butyrate inhibits *Staphylococcus aureus* internalization in bovine mammary epithelial cells and induces the expression of antimicrobial peptide genes. *Microb Pathog* **47**(1), 1-7.
- Ohigashi, S., Sudo, K., Kobayashi, D., Takahashi, O., Takahashi, T., Asahara, T., Nomoto, K., and Onodera, H. (2013). Changes of the intestinal microbiota, short chain fatty acids, and fecal pH in patients with colorectal cancer. *Dig Dis Sci* **58**(6), 1717-26.
- Ohira, H., Fujioka, Y., Katagiri, C., Mamoto, R., Aoyama-Ishikawa, M., Amako, K., Izumi, Y., Nishiumi, S., Yoshida, M., Usami, M., *et al.* (2013). Butyrate attenuates inflammation and lipolysis generated by the interaction of adipocytes and macrophages. *J Atheroscler Thromb* **20**(5), 425-42.
- Ohkawara, S., Furuya, H., Nagashima, K., Asanuma, N., and Hino, T. (2005). Oral administration of *butyrivibrio fibrisolvens*, a butyrate-producing bacterium, decreases the formation of aberrant crypt foci in the colon and rectum of mice. *J Nutr* **135**(12), 2878-83.

- Oliveira, C. S., Pereira, H., Alves, S., Castro, L., Baltazar, F., Chaves, S. R., Preto, A., and Corte-Real, M. (2015). Cathepsin D protects colorectal cancer cells from acetate-induced apoptosis through autophagy-independent degradation of damaged mitochondria. *Cell Death Dis* **6**, e1788.
- Orozco, M. N., Solomons, N. W., Arriaga, C., Hernández, L., Campos, R., Soto, M. J., and Schümann, K. (2011). Studies on variation in fecal reactive oxidative species generation in free-living populations in Guatemala. *Pure Appl Chem* **84**(2), 325-333.
- Ortega, J. F., de Conti, A., Tryndyak, V., Furtado, K. S., Heidor, R., Horst, M. A., Fernandes, L. H. G., Tavares, P. E. L. M., Pogribna, M., Shpyleva, S., *et al.* (2016). Suppressing activity of tributyrin on hepatocarcinogenesis is associated with inhibiting the p53-CRM1 interaction and changing the cellular compartmentalization of p53 protein. *Oncotarget* **7**(17), 24339-24347.
- Owen, R. W., Spiegelhalder, B., and Bartsch, H. (2000). Generation of reactive oxygen species by the faecal matrix. *Gut* **46**(2), 225-32.
- Pacheco, R. G., Esposito, C. C., Muller, L. C., Castelo-Branco, M. T., Quintella, L. P., Chagas, V. L., de Souza, H. S., and Schanaider, A. (2012). Use of butyrate or glutamine in enema solution reduces inflammation and fibrosis in experimental diversion colitis. *World J Gastroenterol* **18**(32), 4278-87.
- Pallos, J., Bodai, L., Lukacsovich, T., Purcell, J. M., Steffan, J. S., Thompson, L. M., and Marsh, J. L. (2008). Inhibition of specific HDACs and sirtuins suppresses pathogenesis in a *Drosophila* model of Huntington's disease. *Hum Mol Genet* **17**(23), 3767-3775.

- Pandey, R., Swamy, K. V., and Khetmalas, M. B. (2013). Indole: A novel signaling molecule and its applications. *Indian J Biotechnol* **12**(3), 297-310.
- Panel, N. I. o. H. C. D. (2001). National institutes of health consensus development conference statement: phenylketonuria: screening and management, October 16–18, 2000. *Pediatrics* **108**(4), 972-982.
- Park, J. S., Lee, E. J., Lee, J. C., Kim, W. K., and Kim, H. S. (2007). Anti-inflammatory effects of short chain fatty acids in IFN-gamma-stimulated RAW 264.7 murine macrophage cells: involvement of NF-kappaB and ERK signaling pathways. *Int Immunopharmacol* **7**(1), 70-7.
- Parks, D. J., Blanchard, S. G., Bledsoe, R. K., Chandra, G., Consler, T. G., Kliewer, S. A., Stimmel, J. B., Willson, T. M., Zavacki, A. M., Moore, D. D., *et al.* (1999). Bile acids: natural ligands for an orphan nuclear receptor. *Science* **284**(5418), 1365-8.
- Parnell, J. A., and Reimer, R. A. (2010). Effect of prebiotic fibre supplementation on hepatic gene expression and serum lipids: a dose-response study in JCR:LA-cp rats. *Br J Nutr* **103**(11), 1577-84.
- Peisl, B. Y. L., Schymanski, E. L., and Wilmes, P. (2017). Dark matter in host-microbiome metabolomics: Tackling the unknowns—A review. *Anal Chim Acta* doi: 10.1016/j.aca.2017.12.034.
- Penetar, D. M., McNeil, J. F., Ryan, E. T., and Lukas, S. E. (2008). Comparison among plasma, serum, and whole blood ethanol concentrations: Impact of storage conditions and collection tubes. *J Anal Toxicol* **32**(7), 505-510.

- Peng, L., Hertz, L., Huang, R., Sonnewald, U., Petersen, S., Westergaard, N., Larsson, O., and Schousboe, A. (1994). Utilization of glutamine and of TCA cycle constituents as precursors for transmitter glutamate and GABA. *Dev Neurosci* **15**(3-5), 367-377.
- Perez, R., Stevenson, F., Johnson, J., Morgan, M., Erickson, K., Hubbard, N. E., Morand, L., Rudich, S., Katznelson, S., and German, J. B. (1998). Sodium butyrate upregulates Kupffer cell PGE(2) production and modulates immune function. *J Surg Res* **78**(1), 1-6.
- Pfeiffer, R. F. (2003). Gastrointestinal dysfunction in Parkinson's disease. *Lancet Neurol* **2**(2), 107-116.
- Pietz, J., Kreis, R., Rupp, A., Mayatepek, E., Rating, D., Boesch, C., and Bremer, H. J. (1999). Large neutral amino acids block phenylalanine transport into brain tissue in patients with phenylketonuria. *J Clin Invest* **103**(8), 1169-1178.
- Pinheiro, C., Longatto-Filho, A., Scapulatempo, C., Ferreira, L., Martins, S., Pellerin, L., Rodrigues, M., Alves, V. A., Schmitt, F., and Baltazar, F. (2008). Increased expression of monocarboxylate transporters 1, 2, and 4 in colorectal carcinomas. *Virchows Arch* **452**(2), 139-46.
- Pluskal, T., Castillo, S., Villar-Briones, A., and Oresic, M. (2010). MZmine 2: modular framework for processing, visualizing, and analyzing mass spectrometry-based molecular profile data. *BMC Bioinformatics* **11**(1), 395.
- Pluznick, J. (2014). A novel SCFA receptor, the microbiota, and blood pressure regulation. *Gut Microbes* **5**(2), 202-7.
- Pluznick, J. L. (2013). Renal and cardiovascular sensory receptors and blood pressure regulation. *Am J Physiol Renal Physiol* **305**(4), F439-44.

- Poorkaj, P., Bird, T. D., Wijsman, E., Nemens, E., Garruto, R. M., Anderson, L., Andreadis, A., Wiederholt, W. C., Raskind, M., and Schellenberg, G. D. (1998). Tau is a candidate gene for chromosome 17 frontotemporal dementia. *Ann Neurol* **43**(6), 815-825.
- Portillo-Sanchez, P., Bril, F., Maximos, M., Lomonaco, R., Biernacki, D., Orsak, B., Subbarayan, S., Webb, A., Hecht, J., and Cusi, K. (2015). High Prevalence of Nonalcoholic Fatty Liver Disease in Patients With Type 2 Diabetes Mellitus and Normal Plasma Aminotransferase Levels. *J Clin Endocrinol Metab* **100**(6), 2231-8.
- Pottathil, M., and Lazazzera, B. A. (2003). The extracellular Phr peptide-Rap phosphatase signaling circuit of *Bacillus subtilis*. *Front Biosci* **8**, d32-45.
- Prasad, K. N., and Sinha, P. K. (1976). Effect of sodium butyrate on mammalian cells in culture: a review. *In Vitro* **12**(2), 125-32.
- Pratt, D. S., and Kaplan, M. M. (2000). Evaluation of abnormal liver-enzyme results in asymptomatic patients. *N Engl J Med* **342**(17), 1266-71.
- Probert, C. S., Jones, P. R., and Ratcliffe, N. M. (2004). A novel method for rapidly diagnosing the causes of diarrhoea. *Gut* **53**(1), 58-61.
- Puddu, A., Sanguineti, R., Montecucco, F., and Viviani, G. L. (2014). Evidence for the gut microbiota short-chain fatty acids as key pathophysiological molecules improving diabetes. *Mediators Inflamm* **2014**, 162021.
- Pugh, R. N., Murray-Lyon, I. M., Dawson, J. L., Pietroni, M. C., and Williams, R. (1973). Transection of the oesophagus for bleeding oesophageal varices. *Br J Surg* **60**(8), 646-9.

- Qian, G., Tang, L., Wang, F., Guo, X., Massey, M. E., Williams, J. H., Phillips, T. D., and Wang, J. S. (2013). Physiologically based toxicokinetics of serum aflatoxin B1-lysine adduct in F344 rats. *Toxicology* **303**, 147-51.
- Qin, J., Li, R., Raes, J., Arumugam, M., Burgdorf, K. S., Manichanh, C., Nielsen, T., Pons, N., Levenez, F., and Yamada, T. (2010a). A human gut microbial gene catalogue established by metagenomic sequencing. *Nature* **464**(7285), 59-65.
- Qin, J., Li, R., Raes, J., Arumugam, M., Burgdorf, K. S., Manichanh, C., Nielsen, T., Pons, N., Levenez, F., Yamada, T., *et al.* (2010b). A human gut microbial gene catalogue established by metagenomic sequencing. *Nature* **464**(7285), 59-65.
- Rajendran, V., and Binder, H. J. Short chain fatty acid stimulation of electroneutral Na-Cl absorption: role of apical SCFA-HCO₃⁻ and SCFA-Cl Exchanges 1994, pp. 104-104. Kluwer Academic Publication.
- Rambaran, R. N., and Serpell, L. C. (2008). Amyloid fibrils: abnormal protein assembly. *Prion* **2**(3), 112-7.
- Reaven, G. M. (2005). Insulin resistance, the insulin resistance syndrome, and cardiovascular disease. *Panminerva medica* **47**(4), 201-10.
- Reddy, B. S., Watanabe, K., Weisburger, J. H., and Wynder, E. L. (1977). Promoting effect of bile acids in colon carcinogenesis in germ-free and conventional F344 rats. *Cancer Res* **37**(9), 3238-42.
- Reddy, J. K., and Rao, M. S. (2006). Lipid metabolism and liver inflammation. II. Fatty liver disease and fatty acid oxidation. *Am J Physiol Gastrointest Liver Physiol* **290**(5), G852-8.

- Redfern, C. H., Degtyarev, M. Y., Kwa, A. T., Salomonis, N., Cotte, N., Nanevich, T., Fidelman, N., Desai, K., Vranizan, K., Lee, E. K., *et al.* (2000). Conditional expression of a Gi-coupled receptor causes ventricular conduction delay and a lethal cardiomyopathy. *Proc Natl Acad Sci U S A* **97**(9), 4826-31.
- Remely, M., Aumueller, E., Merold, C., Dworzak, S., Hippe, B., Zanner, J., Pointner, A., Brath, H., and Haslberger, A. G. (2014). Effects of short chain fatty acid producing bacteria on epigenetic regulation of FFAR3 in type 2 diabetes and obesity. *Gene* **537**(1), 85-92.
- Ricos, C., Alvarez, V., Cava, F., Garcia-Lario, J. V., Hernandez, A., Jimenez, C. V., Minchinela, J., Perich, C., and Simon, M. (1999). Current databases on biological variation: pros, cons and progress. *Scand J Clin Lab Inv* **59**(7), 491-500.
- Ridlon, J. M., Kang, D. J., and Hylemon, P. B. (2006). Bile salt biotransformations by human intestinal bacteria. *J Lipid Res* **47**(2), 241-59.
- Roberfroid, M. (2004). *Inulin-type fructans: functional food ingredients*. CRC Press.
- Roberfroid, M. B. (2007). Inulin-type fructans: functional food ingredients. *J Nutr* **137**(11 Suppl), 2493S-2502S.
- Robishaw, J. D., Smigel, M. D., and Gilman, A. G. (1986). Molecular basis for two forms of the G protein that stimulates adenylate cyclase. *J Biol Chem* **261**(21), 9587-9590.
- Roediger, W. E. (1980). Role of anaerobic bacteria in the metabolic welfare of the colonic mucosa in man. *Gut* **21**(9), 793-8.
- Roediger, W. E. W., and Moore, A. (1981). Effect of Short-Chain Fatty-Acid on Sodium-Absorption in Isolated Human-Colon Perfused through the Vascular Bed. *Dig Dis Sci* **26**(2), 100-106.

- Ross, J. W., and Lawson, N. S. (1995). Analytic goals, concentration relationships, and the state of the art for clinical laboratory precision. *Arch Pathol Lab Med* **119**(6), 495-513.
- Roy, C. C., Kien, C. L., Bouthillier, L., and Levy, E. (2006). Short-chain fatty acids: ready for prime time? *Nutr Clin Pract* **21**(4), 351-66.
- Rumberger, J. M., Arch, J. R., and Green, A. (2014). Butyrate and other short-chain fatty acids increase the rate of lipolysis in 3T3-L1 adipocytes. *PeerJ* **2**, e611.
- Ruppin, H., Bar-Meir, S., Soergel, K. H., Wood, C. M., and Schmitt, M. G., Jr. (1980). Absorption of short-chain fatty acids by the colon. *Gastroenterology* **78**(6), 1500-7.
- Russell, R. I. (1986). Small Intestinal Investigative Tests and Techniques. *Curr Opin Gastroenterol* **2**(2), 243-249.
- Saathoff, E., Schneider, P., Kleinfeldt, V., Geis, S., Haule, D., Maboko, L., Samky, E., de Souza, M., Robb, M., and Hoelscher, M. (2008). Laboratory reference values for healthy adults from southern Tanzania. *Trop Med Int Health* **13**(5), 612-25.
- Sachdev, A. H., and Pimentel, M. (2013). Gastrointestinal bacterial overgrowth: pathogenesis and clinical significance. *Ther Adv Chronic Dis* **4**(5), 223-31.
- Saemann, M. D., Bohmig, G. A., Osterreicher, C. H., Burtscher, H., Parolini, O., Diakos, C., Stockl, J., Horl, W. H., and Zlabinger, G. J. (2000). Anti-inflammatory effects of sodium butyrate on human monocytes: potent inhibition of IL-12 and up-regulation of IL-10 production. *FASEB Journal* **14**(15), 2380-2382.

- Sakakibara, S., Yamauchi, T., Oshima, Y., Tsukamoto, Y., and Kadowaki, T. (2006). Acetic acid activates hepatic AMPK and reduces hyperglycemia in diabetic KK-A(y) mice. *Biochem Biophys Res Commun* **344**(2), 597-604.
- Sampson, T. R., and Mazmanian, S. K. (2015). Control of brain development, function, and behavior by the microbiome. *Cell Host Microbe* **17**(5), 565-76.
- Samuel, B. S., Shaito, A., Motoike, T., Rey, F. E., Backhed, F., Manchester, J. K., Hammer, R. E., Williams, S. C., Crowley, J., Yanagisawa, M., *et al.* (2008). Effects of the gut microbiota on host adiposity are modulated by the short-chain fatty-acid binding G protein-coupled receptor, Gpr41. *Proc Natl Acad Sci U S A* **105**(43), 16767-72.
- Santos-Rosa, H., Schneider, R., Bannister, A. J., Sherriff, J., Bernstein, B. E., Emre, N. C. T., Schreiber, S. L., Mellor, J., and Kouzarides, T. (2002). Active genes are trimethylated at K4 of histone H3. *Nature* **419**(6905), 407-411.
- Sartor, R. B. (2008). Microbial influences in inflammatory bowel diseases. *Gastroenterology* **134**(2), 577-94.
- Schmid-Schonbein, G. W., and Delano, F. (2009). Methods for detecting autodigestion. In (Google Patents).
- Schmidt, C. W. (2004). Metabolomics: what's happening downstream of DNA. *Environ Health Perspect* **112**(7), A410-5.
- Schotta, G., Ebert, A., and Reuter, G. (2003). SU(VAR)3-9 is a conserved key function in heterochromatic gene silencing. *Genetica* **117**(2), 149-158.

- Schwartz, A., Taras, D., Schafer, K., Beijer, S., Bos, N. A., Donus, C., and Hardt, P. D. (2010). Microbiota and SCFA in lean and overweight healthy subjects. *Obesity (Silver Spring)* **18**(1), 190-5.
- Sealy, L., and Chalkley, R. (1978). The effect of sodium butyrate on histone modification. *Cell* **14**(1), 115-21.
- Senga, T., Iwamoto, S., Yoshida, T., Yokota, T., Adachi, K., Azuma, E., Hamaguchi, M., and Iwamoto, T. (2003). LSSIG is a novel murine leukocyte-specific GPCR that is induced by the activation of STAT3. *Blood* **101**(3), 1185-1187.
- Setji, T. L., Holland, N. D., Sanders, L. L., Pereira, K. C., Diehl, A. M., and Brown, A. J. (2006). Nonalcoholic steatohepatitis and nonalcoholic Fatty liver disease in young women with polycystic ovary syndrome. *J Clin Endocrinol Metab* **91**(5), 1741-7.
- Shapira, M. (2016). Gut Microbiotas and Host Evolution: Scaling Up Symbiosis. *Trends Ecol Evol* **31**(7), 539-549.
- Shin, H. J., Anzai, N., Enomoto, A., He, X., Kim, D. K., Endou, H., and Kanai, Y. (2007). Novel liver-specific organic anion transporter OAT7 that operates the exchange of sulfate conjugates for short chain fatty acid butyrate. *Hepatology* **45**(4), 1046-1055.
- Silverman, J. F., Pories, W. J., and Caro, J. F. (1989). Liver pathology in diabetes mellitus and morbid obesity. Clinical, pathological, and biochemical considerations. *Pathol Annu* **24 Pt 1**, 275-302.
- Siperstein, M. D., and Guest, M. J. (1960). Studies on the site of the feedback control of cholesterol synthesis. *J Clin Invest* **39**(4), 642-52.
- Siris, E. S., Chines, A. A., Altman, R. D., Brown, J. P., Johnston, C. C., Jr., Lang, R., McClung, M. R., Mallette, L. E., Miller, P. D., Ryan, W. G., *et al.* (1998).

- Risedronate in the treatment of Paget's disease of bone: an open label, multicenter study. *J Bone Miner Res* **13**(6), 1032-8.
- Skendzel, L. P., Barnett, R. N., and Platt, R. (1985). Medically useful criteria for analytic performance of laboratory tests. *Am J Clin Pathol* **83**(2), 200-5.
- Smet, I. D., Boever, P. D., and Verstraete, W. (2007). Cholesterol lowering in pigs through enhanced bacterial bile salt hydrolase activity. *Br J Nutr* **79**(02), 185.
- Smith, C. A., O'Maille, G., Want, E. J., Qin, C., Trauger, S. A., Brandon, T. R., Custodio, D. E., Abagyan, R., and Siuzdak, G. (2005). METLIN: a metabolite mass spectral database. *Ther Drug Monit* **27**(6), 747-51.
- Smith, H. W., Finkelstein, N., Aliminosa, L., Crawford, B., and Graber, M. (1945). The Renal Clearances of Substituted Hippuric Acid Derivatives and Other Aromatic Acids in Dog and Man. *J Clin Invest* **24**(3), 388-404.
- Smith, W. C. (1989). Method for separating the cellular components of blood samples. In (Google Patents).
- Soga, T., Kamohara, M., Takasaki, J., Matsumoto, S., Saito, T., Ohishi, T., Hiyama, H., Matsuo, A., Matsushime, H., and Furuichi, K. (2003). Molecular identification of nicotinic acid receptor. *Biochem Biophys Res Commun* **303**(1), 364-9.
- Soliman, M. L., and Rosenberger, T. A. (2011). Acetate supplementation increases brain histone acetylation and inhibits histone deacetylase activity and expression. *Mol Cell Biochem* **352**(1-2), 173-80.
- Solis, G., de Los Reyes-Gavilan, C. G., Fernandez, N., Margolles, A., and Gueimonde, M. (2010). Establishment and development of lactic acid bacteria and bifidobacteria microbiota in breast-milk and the infant gut. *Anaerobe* **16**(3), 307-10.

- Soscia, S. J., Kirby, J. E., Washicosky, K. J., Tucker, S. M., Ingelsson, M., Hyman, B., Burton, M. A., Goldstein, L. E., Duong, S., Tanzi, R. E., *et al.* (2010). The Alzheimer's disease-associated amyloid beta-protein is an antimicrobial peptide. *PLoS One* **5**(3), e9505.
- Spaepen, S., Vanderleyden, J., and Remans, R. (2007). Indole-3-acetic acid in microbial and microorganism-plant signaling. *FEMS Microbiol Rev* **31**(4), 425-48.
- Stefanis, L. (2012). alpha-Synuclein in Parkinson's disease. *Cold Spring Harb Perspect Med* **2**(2), a009399.
- Steffan, J. S., Bodai, L., Pallos, J., Poelman, M., McCampbell, A., Apostol, B. L., Kazantsev, A., Schmidt, E., Zhu, Y. Z., Greenwald, M., *et al.* (2001). Histone deacetylase inhibitors arrest polyglutamine-dependent neurodegeneration in *Drosophila*. *Nature* **413**(6857), 739-43.
- Storey, J. D. (2003). The positive false discovery rate: A Bayesian interpretation and the q-value. *Ann Stat* **31**(6), 2013-2035.
- Storey, J. D., and Tibshirani, R. (2003). Statistical significance for genomewide studies. *Proc Natl Acad Sci U S A* **100**(16), 9440-5.
- Strahl, B. D., and Allis, C. D. (2000). The language of covalent histone modifications. *Nature* **403**(6765), 41-5.
- Streeter, C. C., Gerbarg, P. L., Saper, R. B., Ciraulo, D. A., and Brown, R. P. (2012). Effects of yoga on the autonomic nervous system, gamma-aminobutyric-acid, and allostasis in epilepsy, depression, and post-traumatic stress disorder. *Med Hypotheses* **78**(5), 571-9.

- Subramanian, A., Tamayo, P., Mootha, V. K., Mukherjee, S., Ebert, B. L., Gillette, M. A., Paulovich, A., Pomeroy, S. L., Golub, T. R., Lander, E. S., *et al.* (2005). Gene set enrichment analysis: a knowledge-based approach for interpreting genome-wide expression profiles. *Proc Natl Acad Sci U S A* **102**(43), 15545-50.
- Sun, R., Lin, S.-F., Gradoville, L., Yuan, Y., Zhu, F., and Miller, G. (1998). A viral gene that activates lytic cycle expression of Kaposi's sarcoma-associated herpesvirus. *Proc Natl Acad Sci U S A* **95**(18), 10866-10871.
- Sun, S., Li, W., Zhang, H., Zha, L., Xue, Y., Wu, X., and Zou, F. (2012). Requirement for store-operated calcium entry in sodium butyrate-induced apoptosis in human colon cancer cells. *Biosci Rep* **32**(1), 83-90.
- Surya, R., Helies-Toussaint, C., Martin, O. C., Gauthier, T., Gueraud, F., Tache, S., Naud, N., Jouanin, I., Chantelauze, C., Durand, D., *et al.* (2016). Red meat and colorectal cancer: Nrf2-dependent antioxidant response contributes to the resistance of preneoplastic colon cells to fecal water of hemoglobin- and beef-fed rats. *Carcinogenesis* **37**(6), 635-645.
- Suzuki, Y., Suda, T., Furuhashi, K., Suzuki, M., Fujie, M., Hahimoto, D., Nakamura, Y., Inui, N., Nakamura, H., and Chida, K. (2010). Increased serum kynurenine/tryptophan ratio correlates with disease progression in lung cancer. *Lung Cancer* **67**(3), 361-5.
- Swann, J. R., Want, E. J., Geier, F. M., Spagou, K., Wilson, I. D., Sidaway, J. E., Nicholson, J. K., and Holmes, E. (2011). Systemic gut microbial modulation of bile acid metabolism in host tissue compartments. *Proc Natl Acad Sci U S A* **108** **Suppl 1**(Suppl 1), 4523-30.

- Tada, S., Okuno, T., Yasui, T., Nakatsuji, Y., Sugimoto, T., Kikutani, H., and Sakoda, S. (2011). Deleterious effects of lymphocytes at the early stage of neurodegeneration in an animal model of amyotrophic lateral sclerosis. *J Neuroinflamm* **8**(1), 19-19.
- Taggart, A. K., Kero, J., Gan, X., Cai, T.-Q., Cheng, K., Ippolito, M., Ren, N., Kaplan, R., Wu, K., and Wu, T.-J. (2005). (D)- β -hydroxybutyrate inhibits adipocyte lipolysis via the nicotinic acid receptor PUMA-G. *J Biol Chem* **280**(29), 26649-26652.
- Tang, J., Yan, H., and Zhuang, S. (2013). Histone deacetylases as targets for treatment of multiple diseases. *Clin Sci (Lond)* **124**(11), 651-62.
- Tang, Y., Chen, Y., Jiang, H., Robbins, G. T., and Nie, D. (2011). G-protein-coupled receptor for short-chain fatty acids suppresses colon cancer. *Int J Cancer* **128**(4), 847-56.
- Tao, R., de Zoeten, E. F., Ozkaynak, E., Chen, C., Wang, L., Porrett, P. M., Li, B., Turka, L. A., Olson, E. N., Greene, M. I., *et al.* (2007). Deacetylase inhibition promotes the generation and function of regulatory T cells. *Nat Med* **13**(11), 1299-307.
- Taylor, D. P., Burt, R. W., Williams, M. S., Haug, P. J., and Cannon-Albright, L. A. (2010). Population-based family history-specific risks for colorectal cancer: a constellation approach. *Gastroenterology* **138**(3), 877-885.
- Taylor, S. J., Chae, H. Z., Rhee, S. G., & Exton, J. H. (1991). Activation of the β 1 isozyme of phospholipase C by α subunits of the Gq class of G proteins. *Nature*, 350(6318), 516..
- Tazoe, H., Otomo, Y., Karaki, S., Kato, I., Fukami, Y., Terasaki, M., and Kuwahara, A. (2009). Expression of short-chain fatty acid receptor GPR41 in the human colon. *Biomed Res* **30**(3), 149-56.

- Thangaraju, M., Carswell, K. N., Prasad, P. D., and Ganapathy, V. (2009). Colon cancer cells maintain low levels of pyruvate to avoid cell death caused by inhibition of HDAC1/HDAC3. *Biochem J* **417**(1), 379-89.
- Theoharides, T. C., Alysandratos, K. D., Angelidou, A., Delivanis, D. A., Sismanopoulos, N., Zhang, B., Asadi, S., Vasiadi, M., Weng, Z., Miniati, A., *et al.* (2012). Mast cells and inflammation. *Biochim Biophys Acta* **1822**(1), 21-33.
- Thibault, R., Blachier, F., Darcy-Vrillon, B., de Coppet, P., Bourreille, A., and Segain, J. P. (2010). Butyrate utilization by the colonic mucosa in inflammatory bowel diseases: a transport deficiency. *Inflamm Bowel Dis* **16**(4), 684-95.
- Thirabunyanon, M., and Hongwittayakorn, P. (2013). Potential probiotic lactic acid bacteria of human origin induce antiproliferation of colon cancer cells via synergic actions in adhesion to cancer cells and short-chain fatty acid bioproduction. *Appl Biochem Biotechnol* **169**(2), 511-25.
- Tlaskalova-Hogenova, H., Stepankova, R., Hudcovic, T., Tuckova, L., Cukrowska, B., Lodinova-Zadnikova, R., Kozakova, H., Rossmann, P., Bartova, J., Sokol, D., *et al.* (2004). Commensal bacteria (normal microflora), mucosal immunity and chronic inflammatory and autoimmune diseases. *Immunol Lett* **93**(2-3), 97-108.
- Tlaskalová-Hogenová, H., Štěpánková, R., Kozáková, H., Hudcovic, T., Vannucci, L., Tučková, L., Rossmann, P., Hrnčíř, T., Kverka, M., and Zákostelská, Z. (2011). The role of gut microbiota (commensal bacteria) and the mucosal barrier in the pathogenesis of inflammatory and autoimmune diseases and cancer: contribution of germ-free and gnotobiotic animal models of human diseases. *Cell Mol Immunol* **8**(2), 110.

- Tolman, K. G., and Dalpiaz, A. S. (2007). Treatment of non-alcoholic fatty liver disease. *Ther Clin Risk Manag* **3**(6), 1153-63.
- Tomoeda, K., Awata, H., Matsuura, T., Matsuda, I., Ploechl, E., Milovac, T., Boneh, A., Scott, C. R., Danks, D. M., and Endo, F. (2000). Mutations in the 4-hydroxyphenylpyruvic acid dioxygenase gene are responsible for tyrosinemia type III and hawkinsinuria. *Mol Genet Metab* **71**(3), 506-10.
- Topping, D. L., and Clifton, P. M. (2001). Short-chain fatty acids and human colonic function: roles of resistant starch and nonstarch polysaccharides. *Physiol Rev* **81**(3), 1031-64.
- Torii, T., Kanemitsu, K., Wada, T., Itoh, S., Kinugawa, K., and Hagiwara, A. (2010). Measurement of short-chain fatty acids in human faeces using high-performance liquid chromatography: specimen stability. *Ann Clin Biochem* **47**(Pt 5), 447-52.
- Trayhurn, P. (2005). Endocrine and signalling role of adipose tissue: new perspectives on fat. *Acta Psychiatr Scand* **184**(4), 285-93.
- Triba, M. N., Le Moyec, L., Amathieu, R., Goossens, C., Bouchemal, N., Nahon, P., Rutledge, D. N., and Savarin, P. (2015). PLS/OPLS models in metabolomics: the impact of permutation of dataset rows on the K-fold cross-validation quality parameters. *Mol Biosyst* **11**(1), 13-9.
- Trutschel, D., Schmidt, S., Grosse, I., and Neumann, S. (2015). Experiment design beyond gut feeling: statistical tests and power to detect differential metabolites in mass spectrometry data. *Metabolomics* **11**(4), 851-860.
- Tsang, R. S. (2002). The relationship of *Campylobacter jejuni* infection and the development of Guillain-Barre syndrome. *Curr Opin Infect Dis* **15**(3), 221-8.

- Tunaru, S., Kero, J., Schaub, A., Wufka, C., Blaukat, A., Pfeffer, K., and Offermanns, S. (2003). PUMA-G and HM74 are receptors for nicotinic acid and mediate its anti-lipolytic effect. *Nat Med* **9**(3), 352-5.
- Tuomola, M., Vahva, M., and Kallio, H. (1996). High-performance liquid chromatography determination of skatole and indole levels in pig serum, subcutaneous fat, and submaxillary salivary glands. *J Agric Food Chem* **44**(5), 1265-1270.
- Turnbaugh, P. J., Hamady, M., Yatsunencko, T., Cantarel, B. L., Duncan, A., Ley, R. E., Sogin, M. L., Jones, W. J., Roe, B. A., Affourtit, J. P., *et al.* (2009). A core gut microbiome in obese and lean twins. *Nature* **457**(7228), 480-4.
- Tyanova, S., Temu, T., Sinitcyn, P., Carlson, A., Hein, M. Y., Geiger, T., Mann, M., and Cox, J. (2016). The Perseus computational platform for comprehensive analysis of (prote)omics data. *Nat Methods* **13**(9), 731-40.
- Usami, M., Kishimoto, K., Ohata, A., Miyoshi, M., Aoyama, M., Fueda, Y., and Kotani, J. (2008). Butyrate and trichostatin A attenuate nuclear factor κ B activation and tumor necrosis factor α secretion and increase prostaglandin E₂ secretion in human peripheral blood mononuclear cells. *Nutr Res* **28**(5), 321-328.
- Van Immerseel, F., De Buck, J., Boyen, F., Bohez, L., Pasmans, F., Volf, J., Sevcik, M., Rychlik, I., Haesebrouck, F., and Ducatelle, R. (2004). Medium-chain fatty acids decrease colonization and invasion through hilA suppression shortly after infection of chickens with *Salmonella enterica* serovar Enteritidis. *Appl Environ Microbiol* **70**(6), 3582-7.

- Vanholder, R., De Smet, R., and Lesaffer, G. (1999). p-cresol: a toxin revealing many neglected but relevant aspects of uraemic toxicity. *Nephrol Dial Transplant* **14**(12), 2813-5.
- Vernon, G., Baranova, A., and Younossi, Z. (2011). Systematic review: the epidemiology and natural history of non-alcoholic fatty liver disease and non-alcoholic steatohepatitis in adults. *Aliment Pharmacol Ther* **34**(3), 274-285.
- Vinolo, M. A., Rodrigues, H. G., Hatanaka, E., Sato, F. T., Sampaio, S. C., and Curi, R. (2011). Suppressive effect of short-chain fatty acids on production of proinflammatory mediators by neutrophils. *J Nutr Biochem* **22**(9), 849-55.
- Vítek, L., Jirsa, M., Brodanová, M., Kaláb, M., Mareček, Z., Danzig, V., Novotný, L., and Kotal, P. (2002). Gilbert syndrome and ischemic heart disease: a protective effect of elevated bilirubin levels. *Atherosclerosis* **160**(2), 449-456.
- Vogt, J. A., and Wolever, T. M. S. (2003). Fecal acetate is inversely related to acetate absorption from the human rectum and distal colon. *J Nutr* **133**(10), 3145-3148.
- Vujkovic-Cvijin, I., Dunham, R. M., Iwai, S., Maher, M. C., Albright, R. G., Broadhurst, M. J., Hernandez, R. D., Lederman, M. M., Huang, Y., Somsouk, M., *et al.* (2013). Dysbiosis of the gut microbiota is associated with HIV disease progression and tryptophan catabolism. *Sci Transl Med* **5**(193), 193ra91.
- Wakatsuki, A., Okatani, Y., Lzumiya, C., and Lkenoue, N. (1999). Melatonin protects against ischemia and reperfusion-induced oxidative lipid and DNA damage in fetal rat brain. *J Pineal Res* **26**(3), 147-152.

- Waldecker, M., Kautenburger, T., Daumann, H., Busch, C., and Schrenk, D. (2008). Inhibition of histone-deacetylase activity by short-chain fatty acids and some polyphenol metabolites formed in the colon. *J Nutr Biochem* **19**(9), 587-93.
- Wallace, J. L. (2012). NSAID gastropathy and enteropathy: distinct pathogenesis likely necessitates distinct prevention strategies. *Br J Pharmacol* **165**(1), 67-74.
- Wallin, I. E. (1927). *Symbiogenesis and the Origin of Species*. Рипол Классик.
- Wang, M., Li, M., Chapkin, R. S., Ivanov, I., and Donovan, S. M. (2013). Fecal microbiome and metabolites differ between breast and formula-fed human infants. *FASEB J* **27**(1 Supplement), 850.4.
- Wang, M., Li, M., Wu, S., Lebrilla, C. B., Chapkin, R. S., Ivanov, I., and Donovan, S. M. (2015a). Fecal microbiota composition of breast-fed infants is correlated with human milk oligosaccharides consumed. *J Pediatr Gastroenterol Nutr* **60**(6), 825-33.
- Wang, X., He, H., Lu, Y., Ren, W., Teng, K. Y., Chiang, C. L., Yang, Z., Yu, B., Hsu, S., Jacob, S. T., *et al.* (2015b). Indole-3-carbinol inhibits tumorigenicity of hepatocellular carcinoma cells via suppression of microRNA-21 and upregulation of phosphatase and tensin homolog. *Biochim Biophys Acta* **1853**(1), 244-53.
- Wattenberg, L. W., and Loub, W. D. (1978). Inhibition of polycyclic aromatic hydrocarbon-induced neoplasia by naturally occurring indoles. *Cancer Res* **38**(5), 1410-3.
- Weaver, G. A., Tangel, C. T., Krause, J. A., Parfitt, M. M., Jenkins, P. L., Rader, J. M., Lewis, B. A., Miller, T. L., and Wolin, M. J. (1997). Acarbose enhances human colonic butyrate production. *J Nutr* **127**(5), 717-23.

- Weisberg, S. P., McCann, D., Desai, M., Rosenbaum, M., Leibel, R. L., and Ferrante, A. W. (2003). Obesity is associated with macrophage accumulation in adipose tissue. *J Clin Invest* **112**(12), 1796-1808.
- Weiss, A., Träger, U., Wild, E. J., Grueninger, S., Farmer, R., Landles, C., Scahill, R. I., Lahiri, N., Haider, S., and Macdonald, D. (2012). Mutant huntingtin fragmentation in immune cells tracks Huntington's disease progression. *J Clin Invest* **122**(10), 3731-3736.
- Weng, J. R., Tsai, C. H., Kulp, S. K., and Chen, C. S. (2008). Indole-3-carbinol as a chemopreventive and anti-cancer agent. *Cancer Lett* **262**(2), 153-63.
- Westgard, J. O., Seehafer, J. J., and Barry, P. L. (1994). European Specifications for Imprecision and Inaccuracy Compared with Operating Specifications That Assure the Quality Required by Us Clia Proficiency-Testing Criteria. *Clin Chem* **40**(7), 1228-1232.
- Whitehead, L., Dobler, M. R., Radetich, B., Zhu, Y., Atadja, P. W., Claiborne, T., Grob, J. E., McRiner, A., Pancost, M. R., Patnaik, A., *et al.* (2011). Human HDAC isoform selectivity achieved via exploitation of the acetate release channel with structurally unique small molecule inhibitors. *Bioorg Med Chem* **19**(15), 4626-34.
- Wikoff, W. R., Anfora, A. T., Liu, J., Schultz, P. G., Lesley, S. A., Peters, E. C., and Siuzdak, G. (2009). Metabolomics analysis reveals large effects of gut microflora on mammalian blood metabolites. *Proc Natl Acad Sci U S A* **106**(10), 3698-703.
- Willett, W. C., Stampfer, M. J., Colditz, G. A., Rosner, B. A., and Speizer, F. E. (1990). Relation of meat, fat, and fiber intake to the risk of colon cancer in a prospective study among women. *N Engl J Med* **323**(24), 1664-72.

- Williamson, J. R. (1967). Effects of fatty acids, glucagon and anti-insulin serum on the control of gluconeogenesis and ketogenesis in rat liver. *Adv Enzyme Regul* **5**, 229-55.
- Willing, B. P., Dicksved, J., Halfvarson, J., Andersson, A. F., Lucio, M., Zheng, Z., Jarnerot, G., Tysk, C., Jansson, J. K., and Engstrand, L. (2010). A Pyrosequencing Study in Twins Shows That Gastrointestinal Microbial Profiles Vary With Inflammatory Bowel Disease Phenotypes. *Gastroenterology* **139**(6), 1844-U105.
- Wilson, F. A., and Dietschy, J. M. (1972). Approach to the malabsorption syndromes associated with disordered bile acid metabolism. *Arch Intern Med* **130**(4), 584-94.
- Wise, D. R., and Thompson, C. B. (2010). Glutamine addiction: a new therapeutic target in cancer. *Trends Biochem Sci* **35**(8), 427-33.
- Wishart, D. S., Tzur, D., Knox, C., Eisner, R., Guo, A. C., Young, N., Cheng, D., Jewell, K., Arndt, D., and Sawhney, S. (2007a). HMDB: the human metabolome database. *Nucleic Acids Res* **35**(suppl_1), D521-D526.
- Wishart, D. S., Tzur, D., Knox, C., Eisner, R., Guo, A. C., Young, N., Cheng, D., Jewell, K., Arndt, D., Sawhney, S., *et al.* (2007b). HMDB: the Human Metabolome Database. *Nucleic Acids Res* **35** (Database issue), D521-6.
- Wisker, E., Maltz, A., and Feldheim, W. (1988). Metabolizable Energy of Diets Low or High in Dietary Fiber from Cereals When Eaten by Humans. *J Nutr* **118**(8), 945-952.
- Wolever, T. M., Josse, R. G., Leiter, L. A., and Chiasson, J. L. (1997). Time of day and glucose tolerance status affect serum short-chain fatty acid concentrations in humans. *Metabolism* **46**(7), 805-11.

- Wolever, T. M. S., and Chiasson, J. L. (2000). Acarbose raises serum butyrate in human subjects with impaired glucose tolerance. *Br J Nutr* **84**(1), 57-61.
- Wolkoff, A., Chowdhury, J. R., and Arias, I. (1983). Hereditary jaundice and disorders of bilirubin metabolism. *Metabolic basis of inherited disease/[edited by] John B. Stanbury...[et al.]*.
- Wong, J. M., de Souza, R., Kendall, C. W., Emam, A., and Jenkins, D. J. (2006). Colonic health: fermentation and short chain fatty acids. *J Clin Gastroenterol* **40**(3), 235-43.
- Xiong, Y. M., Miyamoto, N., Shibata, K., Valasek, M. A., Motoike, T., Kedzierski, R. M., and Yanagisawa, M. (2004). Short-chain fatty acids stimulate leptin production in adipocytes through the G protein-coupled receptor GPR41. *Proc Natl Acad Sci U S A* **101**(4), 1045-1050.
- Yagi, K. (1984). Assay for blood plasma or serum. *Methods in enzymology* **105**, 328-331.
- Yamashita, H., Fujisawa, K., Ito, E., Idei, S., Kawaguchi, N., Kimoto, M., Hiemori, M., and Tsuji, H. (2007). Improvement of obesity and glucose tolerance by acetate in Type 2 diabetic Otsuka Long-Evans Tokushima Fatty (OLETF) rats. *Biosci Biotechnol Biochem* **71**(5), 1236-43.
- Yamazaki, H., Tsuboya, T., Tsuji, K., Dohke, M., and Maguchi, H. (2015). Independent Association Between Improvement of Nonalcoholic Fatty Liver Disease and Reduced Incidence of Type 2 Diabetes. *Diabetes Care* **38**(9), 1673-1679.
- Yano, J. M., Yu, K., Donaldson, G. P., Shastri, G. G., Ann, P., Ma, L., Nagler, C. R., Ismagilov, R. F., Mazmanian, S. K., and Hsiao, E. Y. (2015). Indigenous bacteria from the gut microbiota regulate host serotonin biosynthesis. *Cell* **161**(2), 264-76.

- Yatsuneneko, T., Rey, F. E., Manary, M. J., Trehan, I., Dominguez-Bello, M. G., Contreras, M., Magris, M., Hidalgo, G., Baldassano, R. N., Anokhin, A. P., *et al.* (2012). Human gut microbiome viewed across age and geography. *Nature* **486**(7402), 222-7.
- Yonezawa, T., Haga, S., Kobayashi, Y., Katoh, K., and Obara, Y. (2009). Short-chain fatty acid signaling pathways in bovine mammary epithelial cells. *Regul Pept* **153**(1-3), 30-6.
- Younossi, Z. M., Koenig, A. B., Abdelatif, D., Fazel, Y., Henry, L., and Wymer, M. (2015). Global Epidemiology of Non-Alcoholic Fatty Liver Disease—Meta-Analytic Assessment of Prevalence, Incidence and Outcomes. *Hepatology*.
- Yu, S., Matsusue, K., Kashireddy, P., Cao, W.-Q., Yeldandi, V., Yeldandi, A. V., Rao, M. S., Gonzalez, F. J., and Reddy, J. K. (2003). Adipocyte-specific gene expression and adipogenic steatosis in the mouse liver due to peroxisome proliferator-activated receptor γ 1 (PPAR γ 1) overexpression. *J Biol Chem* **278**(1), 498-505.
- Yuan, M., Breitkopf, S. B., Yang, X., and Asara, J. M. (2012). A positive/negative ion-switching, targeted mass spectrometry-based metabolomics platform for bodily fluids, cells, and fresh and fixed tissue. *Nat Protoc* **7**(5), 872.
- Zaibi, M. S., Stocker, C. J., O'Dowd, J., Davies, A., Bellahcene, M., Cawthorne, M. A., Brown, A. J., Smith, D. M., and Arch, J. R. (2010). Roles of GPR41 and GPR43 in leptin secretory responses of murine adipocytes to short chain fatty acids. *FEBS Lett* **584**(11), 2381-6.
- Zeuzem, S. (2000). Gut-liver axis. *Int J Colorectal Dis* **15**(2), 59-82.

- Zhang, J., Yi, M., Zha, L., Chen, S., Li, Z., Li, C., Gong, M., Deng, H., Chu, X., Chen, J., *et al.* (2016). Sodium Butyrate Induces Endoplasmic Reticulum Stress and Autophagy in Colorectal Cells: Implications for Apoptosis. *PLoS One* **11**(1), e0147218.
- Zhang, Y., Li, D., Lv, J., Li, Q., Kong, C., and Luo, Y. (2017). Effect of cinnamon essential oil on bacterial diversity and shelf-life in vacuum-packaged common carp (*Cyprinus carpio*) during refrigerated storage. *Int J Food Microbiol* **249**, 1-8.
- Zimmerman, M. A., Singh, N., Martin, P. M., Thangaraju, M., Ganapathy, V., Waller, J. L., Shi, H. D., Robertson, K. D., Munn, D. H., and Liu, K. B. (2012). Butyrate suppresses colonic inflammation through HDAC1-dependent Fas upregulation and Fas-mediated apoptosis of T cells. *Am J Physiol Gastrointest Liver Physiol* **302**(12), G1405-G1415.
- Zuo, L., Lu, M., Zhou, Q., Wei, W., and Wang, Y. (2013). Butyrate suppresses proliferation and migration of RKO colon cancer cells through regulating endocan expression by MAPK signaling pathway. *Food Chem Toxicol* **62**, 892-900.

CHAPTER 3. AFLATOXIN B₁ DISRUPTS GUT-MICROBIAL METABOLISMS OF
SHORT CHAIN FATTY ACIDS, LONG CHAIN FATTY ACIDS AND BILE ACIDS
IN MALE F344 RATS

3.1 Introduction

Aflatoxins (AFs) are a class of food-borne mycotoxins mainly produced by *Aspergillus Flavus* and *A. Parasiticus* (Kumar *et al.*, 2016). These toxigenic fungi commonly contaminate soil, and colonize on the surface of cereals, especially for maize, and groundnuts, once humidity (> 17.5%) and temperature (> 24 °C) meet their growth needs (Trenk and Hartman, 1970). Such environmental conditions have made the tropical area more susceptible for the food contamination and human exposure to AFs, especially in the low- and middle-income developing nations (Qian *et al.*, 2013b). Aflatoxin B₁ (AFB₁) is widely recognized as the most harmful AF, due to its potent toxicity, genotoxicity, and carcinogenicity as well as acute aflatoxicosis in animals and human populations (Kew, 2013; Qian *et al.*, 2013c; Wang and Groopman, 1999). Accordingly, the detection and assessment of AFB₁ contamination in human food and animal feed has been a global concern for food safety and public health (Henry *et al.*, 1999; Torres *et al.*, 2014). On the other hand, remarkable efforts have been made to develop novel prevention/intervention strategies against AFB₁-induced adverse health effects, including liver cancer risks and growth/developmental disorders in high-risk and vulnerable populations (Mitchell *et al.*, 2014; Xue *et al.*, 2016).

Human gastrointestinal tract harbors a complex microbiota that contains more than 100 trillion microbes with over 400 species and carries 150 times more genes than the human genome (Qin *et al.*, 2010). The gut-microbiota constantly provides host with hundreds of micronutrients and functional metabolites, which actively participate into the host enterohepatic cross-talk, as well as the physiological regulations of many organs and systems (Ursell *et al.*, 2014). In recent years, next-generation sequencing (NGS) technologies have uncovered all kinds of intricate connections among gut-microbiota, dietary composition and host health (Chakraborty *et al.*, 2010; Holmes *et al.*, 2012). In this three-way relationship, oral exposure to xenobiotics or dietary composition could lead to the alteration of gut-microbiota, and the changes of gut-microbiota may further influence host health in a significant way (Brown and Hazen, 2015). Emerging evidences have demonstrated the causative links between gut-microbial microbiome/metabolome and a series of health problems in host, e.g. obesity, metabolic syndrome, non-alcoholic fatty liver disease (NAFLD), colon cancer, inflammatory bowel disease (IBD), and cardiovascular disease (Flint *et al.*, 2012; Holmes *et al.*, 2012; Lee and Hase, 2014; Louis *et al.*, 2014; Ursell *et al.*, 2014). Therapeutic manipulation of gut-microbiota has also exhibited the potential to mitigate a number of metabolic diseases such as obesity, type-2 diabetes mellitus (T2DM), IBD and NAFLD, most probably by modifying gut-microbiota dependent metabolites, which are either derived from food by gut-microbiota, or the endogenous metabolites of gut-microbes (Kootte *et al.*, 2012; Schulberg and De Cruz, 2016).

We have previously performed 16S rRNA analysis and found the compositional change of fecal microbiome in F344 rats following repeated oral exposure to AFB₁ (Wang

et al., 2016). Through 16S rRNA sequencing technique, notable enrichment of *Clostridiales spp.* and depletion of *Lactobacillales spp.* were found in the rat feces. In the work presented here, the potential impact of such compositional changes on host health at metabolic level was further explored by examining a group of fecal organic acids that are highly associated with gut-microbiota. The studied metabolites include acetic acid, lactic acid, propionic acid, butyric acid, valeric acid, hexanoic acid, cholic acid, deoxycholic acid, pentadecanoic acid (15:0), 3-phenyllactic acid, pyruvic acid, and linoleic acid (cis-9,cis-12-18:2). The metabolism of these organic acids heavily depends on the metabolic pathways and community structure of gut-microbiota, and also play important roles in host physiology and global metabolic pathways.

3.2 Materials and methods

3.2.1 Chemicals and reagents

Pyridine, 2-nitrophenylhydrazine, N-(3-dimethylaminopropyl)-N'-ethylcarbodiimide hydrochloride (EDC), 2-ethylbutyric acid, acetic acid, propionic acid, butyric acid, valeric acid, hexanoic acid, cholic acid, pentadecanoic acid, 3-phenyllactic acid, pyruvic acid, linoleic acid, deoxycholic acid, bisphenol A, hippuric acid, heptadecanoic acid, AFB₁ and dimethyl sulfoxide (DMSO) were all purchased from Sigma-Aldrich Inc. (St. Louis, MO, USA). AFB₁ stock solution (25 mg/ml) was prepared in DMSO and diluted to appropriate treatment concentrations upon using. All other reagents and analytical solvents, methanol, acetonitrile and water were purchased at the highest grade commercially available from Honeywell (Morris Plains, NJ, USA).

3.2.2 *Animal treatment*

Male Fischer 344 rats (100–120 g) were purchased from Harlan Laboratory (Indianapolis, IN, USA). The animal housing environment was under controlled light/dark cycle (12 hr/12 hr) with a temperature of 22 ± 2 °C and relative humidity of 50 %–70%. Purified AIN 76A diet and tap water were maintained every day. Upon arrival, animals were allowed for one week of environmental acclimation. One hundred male F344 rats were divided into four groups and were gavaged with 0, 5, 25, and 75 μg AFB₁/kg body weight (B. W.) per day, respectively. DMSO was used as vehicle solvent. The details of animal protocol were reported in earlier publications, together with body indexes, histopathological assessment and AFB₁-Lys pharmacokinetic data (Mohammadagheri *et al.*, 2016; Qian *et al.*, 2014; Qian *et al.*, 2016; Qian *et al.*, 2013c). Briefly, animals were daily administered with AFB₁ by gavage for four weeks. From the second week to the fourth week, rat feces were daily collected, and weekly pooled for each group. All fecal samples were stored in -80 °C freezer. Animal husbandry and care, AFB₁ dosing protocol, and sample collection were approved and in strict accordance with the requirements and regulations of the Institutional Animal Care and Use Committee at the University of Georgia.

3.2.3 *Sample quenching and extraction*

Sample extraction procedure was similar to what previously published with modifications (de Jonge *et al.*, 2012; Hernández Bort *et al.*, 2014). Cold methanol (-80 °C) based quenching and extraction were applied to the fecal samples for sample pre-treatment. The purpose of using cold methanol was to avoid the loss of volatile compounds, and also

because methanol is a solvent chemically appropriate for the reaction of 2-NPH derivatization (Peters *et al.*, 2004; Torii *et al.*, 2010; Winder *et al.*, 2008). To perform sample extraction, 200 mg rat feces was transferred to the Mobio PowerLyzer tube with pre-loaded glass beads (0.1 mm i.d.). One milliliter of cold methanol was immediately added into the tube, and fecal pellet was gently crushed using a glass pestle. After grinding, 0.5 mL cold methanol was slowly added to wash the pestle. Then the tube was capped tightly and fastened on a rotary vortex to undergo 20 min vortex at maximum level using a Vortex-Genie 2 Mixer (Scientific Industries). During vortex, sample tube was put back on ice for 2 min in every 5 min, and finally underwent centrifugation at 12,000 rpm for 10 min to spin down cellular debris. A volume of 100 μ L supernatant was transferred to an Eppendorf tube, and 50 μ L internal standard (2-ethylbutyric acid) stock solution was spiked into the supernatant to achieve a concentration of 1 μ g/ μ L, which was used to compensate technical variabilities.

3.2.3 2-Nitrophenylhydrazine (2-NPH) derivatization

To perform derivatization, 150 μ L sample extract (with internal standard added) was mixed with 45 μ L derivatization solution which was freshly prepared by mixing 15 μ L EDC solution (0.05 g/mL H₂O), 15 μ L 2-NPH solution (12.5 mg/mL methanol) and 15 μ L 3% pyridine in methanol (v/v). After mild vortex, the tubes were transferred to water bath at 60 °C for 60 min. The tubes then were allowed to stay in room temperature for 5 min and went through brief centrifugation in order to collect the liquid left on the tube wall. All sample vials were kept in 4 °C sample cooling tray and the analysis was finished within 24 hours.

3.2.4 HPLC analysis

An Agilent 1200 HPLC system, consisted of a degasser, a quarterly pump, an autosampler, a diode-array detector, and a fluorescence detector, was used to perform HPLC-profiling analysis. The chromatographic separation was conducted in a Nucleosil C18 reversed-phase column (250 mm × 4 mm i.d.; ES industries, NJ, USA) with particle size of 5 μm and pore diameter of 120 Å. The injection volume was 100 μL and flow rate was kept at 1 mL/min. Column oven temperature was set as 40 °C. Mobile phase A was pH 4.5 acidified water adjusted by hydrochloric acid. Mobile phase B was acetonitrile. The gradient eluting condition was: 90% A to 80% A in 0–12 min; 80% A to 70% A in 12–20 min; 70% A to 60% A in 20–30 min; 60% A to 45% A in 30–41 min; 45% A to 10% A in 41–43 min; then keeping at 10% A in 43–58 min; finally, from 10% A to 90% A in 58–61 min for re-balance. The detection channel is 400 nm by DAD, with reference wavelength at 510 ± 60 nm. The representative chromatogram is shown in **Figure 3-1**. Lower limit of detection (LLOD), regression standard curves, as well as the other necessary quantitative parameters used for HPLC-profiling analysis are listed in **Table 3-1**. SCFAs were recovered using the recovery rates averaged from the feces spiked with SCFA standards of ~50%, ~100%, and ~200% of their levels in control group (**Table 3-3**). The concentrations of other interested analytes were determined using the recovery rates of structurally close standards which have similar or close structure to the analytes. Specifically, the recovery rate of hippuric acid was used to recover phenyl acids (PAs); heptadecanoic acid was used to recover long chain fatty acids (LCFAs), and bisphenol A was used to recover bile acids. Further, 2-ethylbutyric acid was used to eliminate the technical variabilities, since it has similar structure with SCFAs. Bisphenol A was used as standard to calculate recoveries for

bile acid and derivatives because it is considered to have close structure with estradiol, which was previously used as internal standard for quantitative analysis of bile acid (Junichi et al., 1978; Rubin, 2011). Plus, in current method, no other commercially available compound was found to be chromatographically separable with bile constituents for the calibration of recovery.

3.2.5 Method validation and optimization

Methanol blanks were spiked with SCFA standards to generate test solutions with concentrations of ~50%, ~100%, and ~200% of the actual SCFA amounts measured in the sample extracts. The test solutions were derivatized using 2-NPH and EDC and were immediately used for HPLC-profiling analysis. The analytical precision of the method was validated based on: (1) inter-day coefficient of variation (CV) of the peak intensities of SCFAs at three spike levels in three consecutive days, with one bunch performed per day; (2) inter-assay CV of the peak intensities of SCFAs at three spike levels in seven consecutive assays; (3) intra-assay CV of the peak intensities of SCFAs at three spike levels, with four repeats conducted at each level. Analytical accuracy was examined using recoveries with CV, and the formula to calculate recovery rate is: $\text{recovery \%} = (\text{analyte amount measured in the extract of standard-spiked feces} - \text{analyte amount measured in the extract of non-spiked feces}) \times 100 / (\text{amount of spiked analyte})$ (Han *et al.*, 2013b).

3.2.6 16S rRNA analysis

Briefly, total fecal genomic DNA which contains 16S rRNA was extracted using QIAamp DNA stool mini kits (QIAGEN, Valencia, California). A 2-step Quadruple-index

PCR method was used to prepare the 16S rRNA gene libraries according to Klindworth et al. (2013). Sequencing of these 16S rRNA fragment libraries was performed in the Georgia Genomic Facility (University of Georgia, Athens, Georgia) using the Illumina MiSeq with v2 500 cycle chemistry, resulting in paired-end 250 base reads to obtain approximately 30 000 reads per sample.

The 16S rRNA fragment amplified in this study is from site 358 to 784 under *Escherichia coli* system of nomenclature (Klindworth et al., 2013). The raw paired-end, demultiplexed sequence read was merged using FLASH 1.2.9 in Geneious 8.1 software (Biomatters Inc, San Francisco, California). All internal tags, base spacers, and locus-specific primers of merged sequences were trimmed and sequences outranged 400–450 base-pairs were discarded. Outputs from Geneious 8.1 were quality filtered using QIIME pipeline (Quantitative Insights Into Microbial Ecology) (Caporaso et al., 2010). Representative sequences for each OTU were compared with the Greengene 16S rRNA gene database 13-8 release (DeSantis et al., 2006) using uclust algorithm with the similarity threshold of 90%. The top 3 database hits that matched the above representative sequences for each OTU were selected.

3.2.7 Statistics and software

Data normality examination, homogeneity test, one-way ANOVA, and Welch's T-test, were all performed using SPSS 22. Levene statistic was used to test homogeneity of variances and Welch-Brown-Forsythe statistic was used to test the equality of means. Tukey's test was used for post-hoc analysis in ANOVA. When data failed to follow normality of distribution, Kruskal-Wallis H test was applied to replace one-way ANOVA.

Mixed-effects model regression was performed using STATA 14.1. Pearson's correlation analysis, and construction of heat map and hierarchical tree were performed using R. Mann-Whitney U test was used to compare the differences of fecal organic acids (except for SCFAs) when dose effect was the only factor being analyzed, with p value < 0.05 considered to be statistically significant.

3.3 Results

3.3.1 *Validation and optimization of HPLC-profiling method*

Our initial effort was to optimize conditions for fecal sample extraction and metabolites enrichment. However, centrifugal evaporation resulted in significant loss of SCFAs (20%–50%) in the sample extracts, as found by HPLC analysis (data not shown). For this reason, sample enrichment was avoided during sample preparation. Nonetheless, interested analytes are still detected from fecal samples. In terms of pre-column derivatization and HPLC-profiling analysis, the validation work included intra-assay precision, inter-assay precision, inter-day precision, and accuracy. Shown in **Table 3-3**, most values of measured metabolites showed CV less than 8%. The sensitivity and LLOD were determined for all analyzed metabolites, as shown in the **Table 3-1**. Internal standards were used to confirm the precision and accuracy, and recovery rate was ranged from 33% to 74% for the all SCFA standards spiked into fecal samples of the control and AFB₁-dosed rats, with CV less than 5%. Using this validated method, the peak identity and concentrations of interested metabolites were further determined from the chromatogram of fecal extracts, as shown in **Figure 3-1**. Four categories of metabolites were measured in the study: SCFAs, including acetic acid, butyric acid, hexanoic acid, lactic acid, propionic

acid, and valeric acid; LCFAs, including linoleic acid (cis-9, cis-12-18:2) and pentadecanoic acid (15:0), bile acids, including cholic acid, deoxycholic acid, and other metabolites, such as 3-phenyllactic acid and pyruvic acid (**Table 3-1**).

3.3.2 *Aflatoxin B₁ exposure affects SCFA production of gut-microbiota*

Rats were exposed to AFB₁ at doses of 0, 5, 25, and 75 µg/kg b.w., which are noted as control, low-dose, middle-dose and high-dose groups in the study. As shown in **Figure 3-2** and **Table 3-4**, significant change of fecal SCFA levels was found in AFB₁-exposed groups. The measured levels of SCFAs in the untreated control group were comparable over the time course from 2- to 4-week, but notable reduction of acetic acid, propionic acid, butyric acid, hexanoic acid, and lactic acid were detected in the rat feces of AFB₁-exposed groups. In the low-dose group, fecal SCFA levels seemed to be affected by the time of exposure. The fecal levels of acetic acid, propionic acid, butyric acid, lactic acid, valeric acid and hexanoic acid were 46.6%, 39.9%, 68.4%, 79.9%, 95.3% and 63% of the control after two weeks of exposure, but the percentages went to 70.7%, 77.6%, 35.1%, 34.4%, 75.6%, and 86.7% of the control after four weeks of exposure, indicating the time-effect of AFB₁-exposure on SCFA levels in the low-dose group. The fecal levels of SCFAs in the middle-and high-dose groups were generally not affected by the exposure time, except for propionic acid in middle-dose group at 2-week, and lactic acid and hexanoic acid in high-dose group at 4-week, which showed about 50% changes of fecal levels compared with control. As shown in **Table 3-4**, the fecal levels of six SCFAs in the middle-dose group, were 17.7%, 31.1%, 26.1%, 20.1%, 90.7%, and 19.9% of the control in 2-week, and were 21.6%, 15.3%, 24.6%, 17.2%, 88.9%, and 27.3% of the control in 4-week. Similarly, In

the high-dose group the six SCFAs were 22%, 22.2%, 21.9%, 12.1%, 44.2%, and 20.5% of the control in 2-week, and were 25%, 34.4%, 17.2%, 6.8%, 42.2%, and 52% of the control in 4-week. Remarkable changes were found for fecal propionic acid level in middle-dose group, which was reduced from 31.1% of control to 15.3% of control from 2-week to 4-week; valeric acid in high-dose group, which was reduced from 12.1% of control to 6.8% of control; and lactic acid in high-dose group, which was elevated from 20.5% of control to 52% of control from 2-week to 4-week.

To examine the AFB₁ dose-, time-, and time × dose interaction effects on fecal SCFA levels, mixed-effects regression model was applied to analyze the linear correlation between the AFB₁-dose/time and SCFA levels. As shown in **Table 3-2**, significant dose effect and dose × time interaction effect were found. Further, Pearson's correlation analysis was performed to examine the possible link between the changes of SCFA levels and the community structure of gut-microbiota. The correlation results were shown in the hierarchical tree and heat map in **Figure 3-3**. Briefly, strains belonging to *Firmicutes Clostridiales* order were highly clustered and showed inverse correlation with the fecal levels of SCFAs following AFB₁-exposure, while *Lactobacillales Streptococcus* and *Clostridiales Roseburia*, two SCFA-producing strains, were depleted in the feces. All 6 SCFAs are correlated in the same cluster of Pearson's r distance.

3.3.3 Aflatoxin B₁ exposure affects metabolism of other gut-microbiota dependent organic acids

We next examined the impacts of AFB₁ treatment on a set of key organic acids after 4 weeks of AFB₁ exposure, including cholic acid, deoxycholic acid, 3-phenyllactic acid,

pyruvic acid, pentadecanoic acid (15:0), and linoleic acid (cis-9, cis-12-18:2). Oral AFB₁ exposure significantly elevated fecal LCFAs (linoleic acid and pentadecanoic acid). Specifically, the level of linoleic acid was 95.51 ± 24.18 ng/mg in the control group, and increased to $1,274.82 \pm 363.02$ ng/mg in the low-dose group and $1,079.18 \pm 760.29$ ng/mg in the middle-dose group; the level of pentadecanoic acid in the control group was 20.26 ± 21.99 ng/mg, and increased to 64.76 ± 36.57 ng/mg in the low-dose group and 74.60 ± 53.35 ng/mg in the middle-dose group; the most significantly altered organic acid was linoleic acid, with over 10-fold increase found in low- and middle-dose groups (**Figure 3-4**).

Oral AFB₁ exposure also significantly elevated fecal levels of cholic acid, pyruvic acid, and 3-phenyllactic acid. The level of cholic acid in the control group was 56.15 ± 27.15 ng/mg, and increased to 128.46 ± 15.35 ng/mg in the low-dose group and 122.60 ± 7.32 ng/mg in the middle-dose group; the level of pyruvic acid in the control group was 38.46 ± 26.92 ng/mg, and increased to 75.57 ± 22.18 ng/mg in the low-dose group and 175.23 ± 74.98 ng/mg in the middle-dose group, and the level of 3-phenyllactic acid in the control group was 28.82 ± 9.04 ng/mg, and increased to 83.89 ± 18.10 ng/mg in the low-dose group and 107.84 ± 74.9 ng/mg in the middle-dose group, respectively.

On the other hand, the level of deoxycholic acid was significantly reduced, to about the half level (5.13 ± 5.09 ng/mg) in the low-dose group from 10.18 ± 8.69 ng/mg in the control group, and completely dropped to undetectable level in the middle-dose group.

3.4 Discussion

Results of this study clearly demonstrated that up to 2-week oral AFB₁ exposure disrupted metabolism of gut microbiota-dependent organic acids, as evidenced by significant reduction in fecal level of SCFAs and deoxycholic acid, and significant increases in LCFAs and other organic acids such as pyruvic acid, 3-phenyllactic acid, and cholic acid. All these microbial metabolites play key roles in the metabolism of gut-microbiota and the maintenance of host nutrition and health.

The detection of trace amounts of SCFAs in complex media, e.g. bio-fluids and fecal extracts, has been reported by several studies using HPLC-profiling combined with pre-column derivatization with 2-NPH (Han *et al.*, 2013a; Miwa *et al.*, 1985; Peters *et al.*, 2004), but the application of this method has not yet reported in AFB₁-exposed rat models. The chemical derivatization is usually performed in mild aqueous or alcohol environment, in which carbonyl compounds (carboxylic acid, aldehyde and ketone) bonded to 2-NPH and form hydrazides. The reaction is activated by water-soluble EDC which serves as carbodiimide crosslinker. Before in-lab analysis, method validation was conducted to confirm whether the analytical procedure is suitable and reliable for a specific analytical task (VanHook, 2016). The accuracy and reliability of analytical method were further carefully validated (**Table 3-3**). The measured values and inter-class ratio of SCFAs in our study are comparable with several other publications (Cummings *et al.*, 1987; Torii *et al.*, 2010; Zhao *et al.*, 2006).

In this study we found significant inhibitory effects of AFB₁-exposure on synthesis of SCFAs, which has not previously reported. The decrease in SCFAs was consistent with the depletion of SCFA-producing strains such as *Lactobacillales Streptococcus* and

Clostridiales Roseburia (Duncan *et al.*, 2002; Kleessen *et al.*, 1997). SCFAs are a group of beneficial aliphatic acids that are mainly produced by the anaerobic bacterial fermentation of resistant starches and insoluble fibers in the gastrointestinal tract of human and other mammals (Brockman, 2005). They are structurally constructed by 1–6 carbon atom(s), including formic acid (C1), acetic acid (C2), propionic acid (C3), butyric acid (C4), valeric acid (C5), hexanoic acid (C6), and a variety of branched-chain isomers of these acids. A variety of nutritional and physiological associations of SCFAs with liver diseases, general immunity, IBD, cardiovascular disease, and diabetes were found in many epidemiological studies and in various *in vivo* and *in vitro* models (Corrêa-Oliveira *et al.*, 2016; Galisteo *et al.*, 2008; Morrison and Preston, 2016; Wong *et al.*, 2006; Zhao *et al.*, 2006). Acetic acid, butyric acid and propionic acid can be produced by gut-microbiota via fermentation of insoluble fibers (Corrêa-Oliveira *et al.*, 2016; Morrison and Preston, 2016; Torii *et al.*, 2010). SCFAs were mainly produced from the fermentation process of certain strains such as *Lactobacillales Streptococcus*. The aflatoxin-caused reduction in these microbial strains (Wang *et al.*, 2015) could eventually affect the fermentation process and cause reduction of SCFAs. Mixed-effects model analysis showed that—three major SCFAs, i.e. acetic acid, butyric acid and propionic acid were the most significantly affected by AFB₁-dose and dose × time interaction, but not time of treatment (**Table 3-2**). It was demonstrated in our earlier 16S rRNA analysis, that the adaption of gut-microbiota community structure was featured by the elevation of relative abundances of *Clostridiales spp.*, but decrease of *Lactobacillales Streptococcus* and *Clostridiales Roseburia* (Wang *et al.*, 2016). Given that dose-response was also found for specific gut-microbial strains, Pearson’s correlation analysis between fecal SCFA levels and gut-microbial strains was

performed to show their correlation. We found that strains from *Firmicutes Clostridiales*, an order associated with diarrhea in human and other mammals (Suchodolski *et al.*, 2015), were highly clustered, and exhibited inverse correlation with SCFAs. By contrast, the relative abundances of *Lactobacillales Streptococcus* and *Clostridiales Roseburia* were positively correlated with fecal SCFAs. Both of these microbes are SCFA-producing strains (Duncan *et al.*, 2002; Kleessen *et al.*, 1997). The depletion of SCFAs in feces reflected the suppression of microbial fermentation on resistant starches and insoluble fibers. This may further result in a wide range of adverse consequences, because the receptors of SCFAs such as GPR43, GPR41, OLF78, GPR109A, are extensively distributed in different organs and systems, and are involved in a myriad of regulatory axis and pathways, such as mobility of gut epithelium, liver lipogenesis, global immunity, cell cycle, oncogenesis, apoptosis and proliferation (Brown *et al.*, 2003; Natarajan and Pluznick, 2014; Smith *et al.*, 2013). Moreover, dietary supply of SCFAs has recently been found to be able to protect against type-I diabetes in mice model (Wen and Wong, 2017).

In addition to SCFAs, there are a great number of organic acids present in gut and feces that play important physiological roles. They are either food-derived nutrients or the metabolic products generated in gut-microbiota and host metabolisms. Interested organic acids in our study included fecal linoleic acid (cis-9, cis-12-18:2), pentadecanoic acid (15:0), pyruvic acid, 3-phenyllactic acid, cholic acid, and deoxycholic acid, which were remarkably altered in the feces following AFB₁ exposure (Figure 4). Linoleic acid is an omega-6 polyunsaturated fatty acid known as an essential dietary nutrient that cannot be *de novo* synthesized by human body. The unsaturated fatty acids are known to carry with various health-promoting functions, such as antioxidant defense, suppression of blood

levels of triglycerides and cholesterol, maintenance of glucose tolerance, and mitigation of hyperinsulinemia (Whelan and Fritsche, 2013). Most of these beneficial functions has been identified in conjugated linoleic acids, mainly as *cis*-9, *trans*-11 C18:2, *trans*-9, *trans*-11 C18:2 and *trans*-10, *cis*-12 C18:2 (Worley and Powers, 2016; Yatsunenکو *et al.*, 2012). Pentadecanoic acid is known to carry a variety of regulatory functions in cell signaling, glucose utilization, and the maintenance of the integrity and stability of gut epithelium (Santaren *et al.*, 2014). The abnormal accumulation of linoleic acid and pentadecanoic acid in rat feces suggested a suppressed intestinal absorption of LCFAs, which is disadvantageous for host health. The deficient bioavailability may be caused by several conditions. First, the decrease of SCFAs may affect the epithelial delivery of nutrients to hepatic portal vein, since SCFAs are well known nutrients that are able to enhance colonic blood flow and epithelial motility by providing energy and activating G-protein receptors (Scheppach, 1994). Second, certain gut-microbial strains are capable of transferring LCFAs into their conjugated forms which are easier to be absorbed (Druart *et al.*, 2014). For example, *Lactobacillus*, *Propionibacterium* and *Bifidobacterium* species can produce conjugated linoleic acid from dietary linoleic acid by using microbial lipoxygenases and cyclooxygenases—a process known to facilitate the absorption of LCFAs (Yatsunenکو *et al.*, 2012). Our previous 16S rRNA analysis demonstrated that these strains were suppressed by AFB₁, which could affect the uptake and reduce bioavailability of LCFAs (Wang *et al.*, 2016).

Bile acids are endogenous steroid acids synthesized from cholesterol by liver cells of most vertebrates. Different species have distinct molecular forms of bile acids generated, but some major types of bile acids are shared by different species, e.g. cholic acid and

chenodeoxycholic acid in human and rat (Whittaker and Chipley, 1986). In human, bile acids are stored in the gallbladder, and are released into duodenum with bile juice under the dietary stimulation. Upon arriving small intestine, bile acids participate in the digestion and absorption of fats and fat-soluble vitamins and can be further metabolized into a variety of secondary metabolites by gut-microbiota. In the current work, cholic acid and deoxycholic acid were selected as representative primary and secondary bile acids to probe the microbial metabolism of bile acids, since they are found in both human and rat feces at comparatively high levels. We found a remarkable elevation of cholic acid level with a significant reduction of deoxycholic acid level in AFB₁ exposed rat feces. The significant elevation of cholic acid is generally considered to be harmful to host health. Abnormal increase of cholic acid is associated with liver pathogenesis such as cirrhosis and steatosis (Mouzaki *et al.*, 2016), and is also known as a risk factor for intestinal inflammation (Camilleri, 2011). Besides, extra cholic acid in gut may partially contribute to the incidence of colon cancer by stimulating the growth of a small-size benign adenoma to larger size (Rowland, 2012). In correspondence with the increase of cholic acid, we found severe liver damages and pathogenesis in the AFB₁-treated rats (Qian *et al.*, 2016; Qian *et al.*, 2013c). The abnormal reduction of deoxycholic acid can be attributed to the relative abundances of the deoxycholic acid-producing microbes, such as *Lachospiraceae*, *Clostridiaceae*, and *Ruminococcaceae*, were all decreased by AFB₁ exposure (Wang *et al.*, 2016). In both human studies and rodent models these strains can metabolize primary bile acids into secondary bile acids (Labbé *et al.*, 2014). There are also interactions among primary bile acids, secondary bile acids, and SCFAs in regulating host health, and the elevation of intestinal primary bile acids with decreased secondary bile acid was associated with the

incidences of dysbiosis and IBD in humans (Lefebvre *et al.*, 2009). The increase of fecal cholic acid in combination with the decrease of SCFAs were previously observed in the patients with colon cancer (Weir *et al.*, 2013).

Pyruvic acid is a well-known energetic α -keto acid that is involved in a number of important metabolic pathways of both gut-microbiota and host. It serves as energy supply to cells through Krebs cycle, and can be transferred to SCFAs by *Lactobacilli* strains through glycolytic pathway (Pessione, 2012). Pyruvic acid can be transferred to carbohydrates via gluconeogenesis, or participate in the biosynthesis of fatty acids after binding with acetyl-CoA (Kim *et al.*, 2016). Since pyruvic acid takes such a central role in the catabolism of carbohydrates, its unusual accumulation in rat feces reflected a suppressed energy utilization and disruption of glycolysis of gut-microbiota. This may also result in the decrease of microbial synthesis of SCFAs (VanHook, 2016). It seems that the reduction of SCFAs is not only caused by alteration of community structure of gut-microbiota, but also related with the specific metabolic pathway. Lastly, 3-phenyllactic acid, a central intermediate product in the upstream of phenylalanine catabolism (Stark *et al.*, 1979), was accumulated in the rat feces following exposure to AFB₁. The abnormal accumulation of 3-phenyllactic acid suggested the disruption of gut-microbial phenylalanine pathway (Camilleri, 2011). The phenylalanine pathway is known to generate L-3,4-dihydroxyphenylalanine (L-DOPA) and tyrosine. L-DOPA is the precursor to a number of important neurotransmitters such as dopamine, norepinephrine, and epinephrine. In addition, L-DOPA itself also mediates neurotrophic factor release by the brain and central neuro system (CNS) (Lopez *et al.*, 2008). For these reasons, the down-regulation

of phenylalanine pathway may interfere with host CNS function and cause related health problems.

Dietary AFB₁ exposure and AFB₁-induced adverse health effects remain a major public health problem in many tropical developing nations. The range of dosage used in this study (5–75 µg/kg B. W.) was relevant to human exposure, based on 300 g corn consumption per day (Gwirtz and Garcia-Casal, 2014) and oral exposure levels ranged from 100 to 1000 µg/kg corn for high-risk human populations in Kenya, Ghana, and Guangxi area of China (Azziz-Baumgartner *et al.*, 2005; Groopman *et al.*, 1992; Tang *et al.*, 2009). The dose was multiplied by an adjusting factor of 6.2 in order to transfer human exposure to that in rats (Nair and Jacob, 2016).

Regarding the mechanisms behind the metabolite alterations found in this study, there are several mechanisms involved: (1) AFB₁, as a natural antimicrobial agent, can selectively inhibit certain bacterial strains and influence on the growth of other strains, as shown in the compositional changes of gut-microbiota revealed by 16s rRNA analysis; (2) AFB₁, as a potent hepatic toxin, can damage liver—the major metabolic organ and in turn induce the metabolic changes for the supply of nutrients and metabolites to host cells and tissues, including gut cells, which may play an important role in the metabolism of gut-microbiota. However, the more specific mechanism related to how AFB₁ induces changes of gut-microbiota community structure and the dependent metabolites still need to be clarified in future study.

Taken together, as summarized in **Figure 3-5** based on our previous studies (Qian *et al.*, 2014; Qian *et al.*, 2013a; Qian *et al.*, 2013c; Wang *et al.*, 2016), oral exposure to AFB₁ in rat results in significant toxic effects, biochemical alterations, and induction of

preneoplastic GST-P positive liver foci. With same study design, here we show that AFB₁ can induces the adverse change of community structure of gut-microbiota and significant disruption of multiple metabolic pathways, such as production of SCFAs, secretion and metabolism of bile acids, absorption of LCFAs, catabolism of phenylalanine, and metabolism of pyruvic acid. These pathways take central and key positions in the global metabolism of gut-microbiota and maintenance of host health, for examples, energy-delivery pathways related with pyruvic acid, including gluconeogenesis, fatty acid synthesis, Krebs cycle and production of lactic acid. Therefore, our data suggest that gut-microbiota may partially be involved in the pathological mechanism and progressions of AFB₁-exposure induced adverse health outcomes in F344 rat model, and presumably also in humans.

TABLES

Table 3-1. Analytical parameters of HPLC-profiling analysis used for the measurement of interested fecal metabolites

Component	Category	RT*	Detection Channel	Regression (X, AUC; Y, ng/ μ L)	R ²	Linear Range ng/ μ L	LLO D ng/ μ L
Acetic acid	SCFA	14.9	400 nm	$y = 0.0063x - 0.3726$	0.9993	0.016–64.8	0.008
Propionic acid	SCFA	19.6	400 nm	$y = 0.021x - 0.9273$	0.999	0.07–143	0.03
Butyric acid	SCFA	25.1	400 nm	$y = 0.0256x - 0.4994$	0.9991	0.078–79.5	0.04
Valeric acid	SCFA	31.5	400 nm	$y = 0.0208x - 0.4974$	0.999	0.054–56.1	0.03
Hexanoic acid	SCFA	37.6	400 nm	$y = 0.0309x - 0.356$	0.9994	0.074–75.6	0.04
Lactic acid	SCFA	13.8	400 nm	$y = 0.0244x - 0.2351$	0.9991	0.11–14.33	0.05
Pyruvic acid	Alpha-keto acid	41.3	400 nm	$y = 0.0166x + 0.7136$	0.9997	6.2–500	0.19
2-Ethylbutyric acid	IS for SCFA	34.2	400 nm	$y = 0.1662x - 0.4527$	0.9991	0.56–1138	0.28
Niacin	PA	22.1	210 nm	$y = 0.0313x - 6.1768$	0.9954	1–430	0.25
3-Phenyllactic acid	PA	31.2	400 nm	$y = 0.1003x - 0.7134$	0.9994	4.7–300	0.58
Hippuric acid	IS for PA	26.3	400 nm	$y = 0.6161x + 2.8275$	0.9996	4.45–570	2.25
Cholic acid	SA	45.1	400 nm	$y = 0.1219x - 6.6046$	0.9930	3.9–250	0.49

Deoxycholic acid	SA	47.1	400 nm	$y = 0.0371x - 4.8658$	0.993 0	2.5–330	0.64
Cholesterol	Sterol	47.4	400 nm	$y = 0.0686x - 2.4795$	0.990 0	1.95–125	0.98
Bisphenol A	IS for SA	35.0	210 nm	$y = 0.0148x - 6.9647$	0.992	0.33–685	0.17
Linoleic acid	LCFA	50.9	400 nm	$y = 0.3705x - 31.314$	0.994 8	3.9–1000	3.9
Pentadecanoic acid	LCFA	51.2	400 nm	$y = 0.0636x - 0.3641$	0.999 0	1.95–500	0.5
Heptadecanoic acid	IS for LCFA	54.5	400 nm	$y = 0.1436x - 4.5852$	0.995 2	2.15–275	1.07

The minimum data point in the linear regression range ($R^2 > 0.999$) was noted as LOQ. Abbreviations: IS, internal standard for quality control; R^2 , regression coefficient; LLOD, lower limit of detection; LCFA, long chain fatty acid; PA, phenyl acid; RT, retention time (min) in chromatogram; SA, steroid acid; SCFA, short chain fatty acid. The analyte level which generated a signal-to-noise (S/N) ratio of 3 was noted as the LLOD for that analyte. Niacin and cholesterol were not detected in most sample extracts.

Table 3-2. Mixed-effects model analysis between AFB₁-treatment (dose, time and interaction) and fecal levels of SCFAs

SCFAs	Fixed Effect			Random Effect							
	Dose	S. E.	<i>p</i>	Time	S. E.	<i>p</i>	I	S. E.	<i>p</i>	Estimate	S. E.
Acetic acid	-0.1103	0.025	< 0.001	0.1613	0.133	0.227	10.361	2.149	< 0.001	31.288	6.021
Propionic acid	-0.0617	0.015	< 0.001	0.054	0.082	0.509	6.718	1.301	< 0.001	11.798	2.270
Butyric acid	-0.1442	0.015	< 0.001	-0.0202	0.086	0.921	13.226	1.663	< 0.001	18.316	3.525
Valeric acid	-0.0028	0.001	< 0.001	-0.0007	0.004	0.863	7.900	0.977	< 0.001	0.026	0.005
Hexanoic acid	-0.0179	0.004	< 0.001	-0.0074	0.022	0.740	2.113	0.365	< 0.001	0.881	0.170
Lactic acid	-0.0207	0.003	< 0.001	0.0228	0.018	0.210	1.280	0.298	< 0.001	0.586	0.112

*Estimate of interaction effect resulted by both dose and treatment time on fecal SCFA levels.

**I, Interaction effect.

Table 3-3. Results of precision and accuracy tests of 2-NPH derivatization combined HPLC-profiling analysis

	SCFAs	Low Level			Middle Level			High Level		
		Mean	S.D.	%C.V.	Mean	S.D.	%C.V.	Mean	S.D.	%C.V.
Intra-assay precision	Acetic acid	2752	6.38	0.23	4815	48.03	1.00	18181	159.34	0.88
	Propionic acid	203	0.33	0.16	1876	24.47	1.30	12212	115.10	0.94
	Butyric acid	244	2.74	1.12	1629	36.30	2.23	9249	146.74	1.59
	Valeric acid	254	1.59	0.63	1529	49.83	3.26	8391	134.81	1.61
	2-Ethylbutyric acid	52	0.21	0.41	535	21.38	3.99	1626	61.50	3.78
	Hexanoic acid	612	8.91	1.46	9527	339.38	3.56	15588	193.44	1.24
	Lactic acid	587	21.62	3.68	6358	93.24	1.47	9889	177.22	1.79
Inter-assay precision	Acetic acid	2642	168.04	6.36	4668	192.73	4.13	17106	1446.57	8.46
	Propionic acid	213	14.00	6.58	1885	34.42	1.83	11457	1277.65	11.15
	Butyric acid	263	16.68	6.33	1656	28.29	1.71	8667	1001.05	11.55
	Valeric acid	260	9.24	3.56	1564	27.76	1.77	7943	930.39	11.71
	2-Ethylbutyric acid	58	3.89	6.74	845	54.19	6.42	1789	368.02	20.57
	Hexanoic acid	637	15.30	2.40	10363	368.01	3.55	15064	602.41	4.00
	Lactic acid	587	10.44	1.78	6244	64.01	1.03	25436	869.88	3.42
Inter-day precision	SCFAs	Day 1	Day 2	Day 3	Day 4	Mean	S.D.	Upper Range	Lower Range	%C.V.
	Acetic acid	7790	6647	6996	6888	7080	428.73	7509	6651	6.06
	Propionic acid	5105	4226	4545	4460	4584	322.70	4907	4261	7.04
	Butyric acid	4124	3364	3667	3599	3688	275.47	3964	3413	7.47

Valeric acid	3533	304 5	313 5	3057	319 3	199. 64	3392	2993	6.25	
2-Ethylbutyric acid	4841	402 5	426 7	4017	428 7	334. 94	4622	3952	7.81	
Hexanoic acid	2779	246 4	266 1	2526	265 7	198. 97	2856	2459	7.49	
Lactic acid	6736	586 3	613 7	5834	614 2	362. 44	6505	5780	0.06	
		Low Level			Middle Level			High Level		
Compound	Mea n%	S.D.	C.V	Mea n%	S.D.	C.V	Mea n%	S.D.	C.V	
Acetic acid	64.6 5	1.97	3.05	66.7 6	3.52	5.28	66.9 6	1.95	2.91	
Propionic acid	47.3 1	2.15	4.55	53.3 0	1.63	3.05	47.8 2	1.30	2.71	
Butyric acid	49.6 8	1.84	3.71	56.6 2	2.08	3.67	51.8 4	1.86	3.59	
Valeric acid	51.4 0	1.42	2.77	52.5 7	2.70	5.14	46.8 0	1.60	3.42	
2-Ethylbutyric acid	77.7 5	1.67	2.15	78.6 8	1.30	1.66	70.2 7	3.51	5.00	
Hexanoic acid	50.0 3	1.81	3.63	55.3 4	3.45	6.23	50.9 3	2.22	4.37	
Lactic acid	77.2 5	3.32	4.49	48.8 7	1.96	3.86	68.2 6	1.45	2.17	
Hippuric acid	13.9 0	1.06	7.65	9.74	0.30	3.03	25.6 3	1.34	5.23	
Heptadecanoic acid	47.3 3	4.32	9.13	45.0 0	2.63	5.85	23.7 6	1.86	7.83	
Bisphenol A	75.1 3	0.01	1.63	107. 07	1.99	1.86	109. 48	3.60	3.29	

Accur
acy*

*Accuracy was calculated from recovery rate (%) of spiked standards at three concentrations. The low level, middle level and high level of the amounts of spiked compounds were ~50%, ~100%, and ~200% of their levels measured in the control group. The 100% levels of the spike standards were: acetic acid, 20 μ mole/g; butyric acid, 10 μ mole/g; propionic acid, 15 μ mole/g; valeric acid, 0.5 μ mole/g; hexanoic acid, 4 μ mole/g; hippuric acid, 0.25 μ mole/g; heptadecanoic acid, 0.25 μ mole/g; bisphenol A, 0.15 μ mole/g; 2-ethylbutyric acid (for pyruvic acid), 0.45 μ mole/g; hippuric acid, 0.2 μ mole/g. The feces used for test was 200 mg, so the spiked amounts at 100% level were: 4 μ mole, 2 μ mole, 3 μ mole, 0.1 μ mole, 0.8 μ mole, 0.05 μ mole, 0.05 μ mole, 0.03 μ mole, 0.09 μ mole and 0.04 μ mole, accordingly. The mole unit is used here for the convenience of unit conversion between different metabolites in same category, and also because the biological effects are usually mole based.

Table 3-4. Fecal SCFA levels ($\mu\text{mole/g}$ feces) of rats treated with 0, 5, 25, and 75 $\mu\text{g AFB}_1/\text{kg B. W.}$

SCFA	AFB ₁ Dose ($\mu\text{g}/\text{kg B. W.}$)	Treatment Time		
		2-wk	3-wk	4-wk
Acetic acid	0	19.33 \pm 3.38	20.11 \pm 1.60	21.48 \pm 0.83
	5	9.00 \pm 0.88**	5.15 \pm 1.81**	15.19 \pm 5.08*
	25	3.43 \pm 0.76**	4.00 \pm 0.80**	4.65 \pm 0.70**
	75	4.25 \pm 1.17**	8.03 \pm 1.90**	5.36 \pm 1.32**
Propionic acid	0	11.46 \pm 2.31	15.85 \pm 0.99	11.41 \pm 1.57
	5	4.57 \pm 0.31**	4.06 \pm 0.84**	8.85 \pm 1.50*
	25	3.56 \pm 1.23**	2.56 \pm 1.02**	1.75 \pm 0.14**
	75	2.54 \pm 0.75**	4.88 \pm 2.65**	3.92 \pm 1.75**
Butyric acid	0	15.42 \pm 1.91	19.37 \pm 3.04	19.72 \pm 2.87
	5	10.54 \pm 3.63*	11.64 \pm 1.95*	6.92 \pm 1.34**
	25	4.03 \pm 0.77**	8.11 \pm 5.42**	4.86 \pm 1.81**
	75	3.38 \pm 0.89**	3.02 \pm 0.92**	3.4 \pm 0.49**
Valeric acid	0	0.43 \pm 0.14	0.44 \pm 0.17	0.45 \pm 0.11
	5	0.41 \pm 0.15	0.50 \pm 0.28	0.34 \pm 0.01
	25	0.39 \pm 0.24	0.32 \pm 0.09	0.4 \pm 0.22
	75	0.19 \pm 0.05	0.26 \pm 0.09	0.19 \pm 0.04
Hexanoic acid	0	3.51 \pm 0.58	2.58 \pm 1.20	2.56 \pm 1.40
	5	2.21 \pm 1.00*	0.79 \pm 0.06**	2.22 \pm 0.67*
	25	0.7 \pm 0.12**	0.94 \pm 0.39**	0.70 \pm 0.27**
	75	0.72 \pm 0.09**	0.74 \pm 0.15**	1.33 \pm 0.24**
Lactic acid	0	1.74 \pm 0.33	1.73 \pm 0.53	3.23 \pm 1.42
	5	1.39 \pm 0.46	1.36 \pm 0.82*	1.11 \pm 0.50**
	25	0.35 \pm 0.16**	0.43 \pm 0.22**	0.57 \pm 0.24**
	75	0.21 \pm 0.05**	0.13 \pm 0.02**	0.22 \pm 0.07**

Data are represented as means \pm standard deviation (S.D.), $n = 5$. The significant difference between the means of treatment groups and control was determined using one-way ANOVA with Tukey's post hoc test. * indicates $p < 0.05$ and ** indicates $p < 0.01$ between the treatment group and control, in order to show dose-response of AFB₁ exposure.

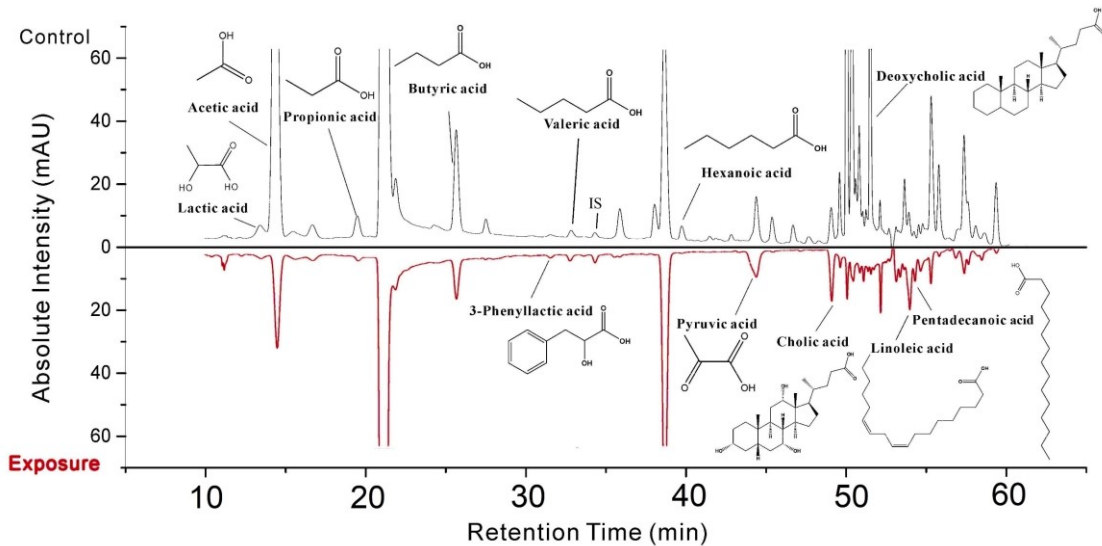


Figure 3-1. HPLC-profiling chromatograms of fecal extracts from control (upper) and exposure group (lower) after 2-NPH derivatization. 2-ethyl butyric acid was used as internal standard (IS). The detection channel of DAD is 400 nm with a reference channel as 510 ± 60 nm. Down-regulated organic acids are labeled on the upper panel, whereas up-regulated organic acids are labeled on the lower panel. Specific retention time and relevant information are available in **Table 3-1**.

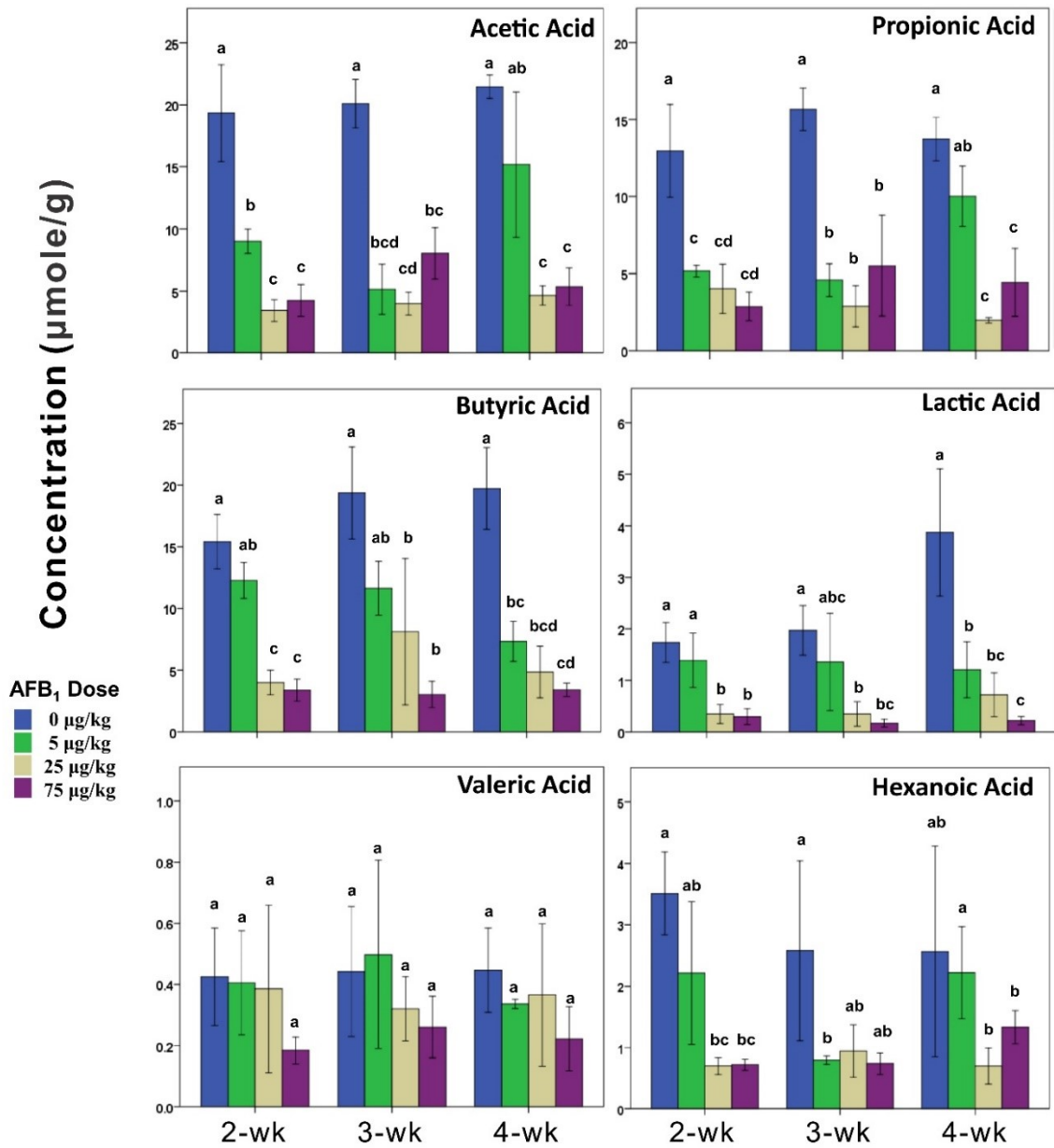


Figure 3-2. Fecal SCFA levels of rats treated with 0, 5, 25, and 75 µg AFB₁/kg body weight (B. W.). X-axis indicates duration of treatment. Significance of one-way ANOVA or Kruskal-Wallis H Test is indicated by string labels: same string indicating $p > 0.05$; string with partly overlapped character(s) indicating $p < 0.05$; totally different string indicating $p < 0.01$. Error bar indicates standard deviation ($n = 5$). Specific data is available in Table 3-4.

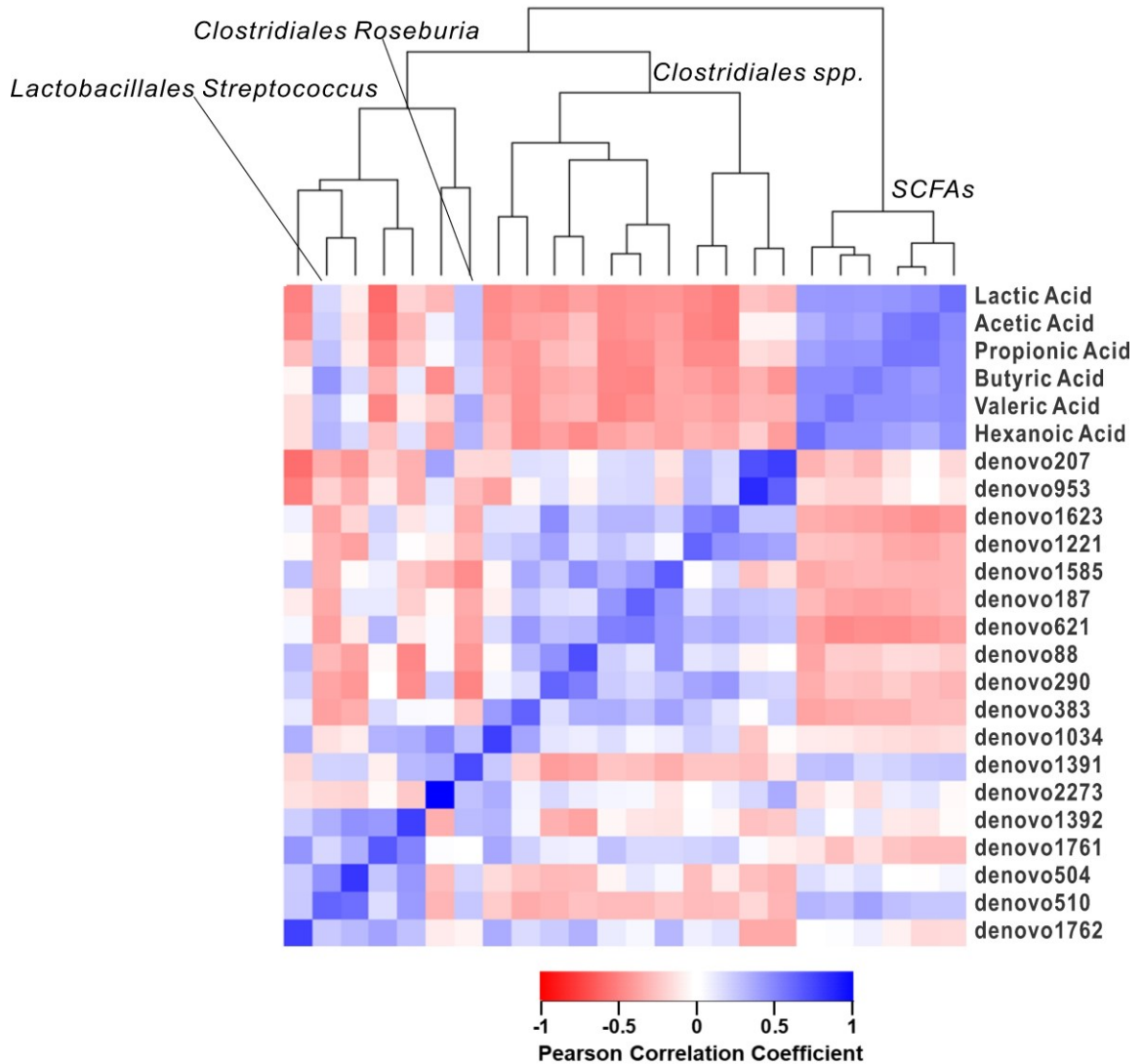


Figure 3-3. Hierarchical cluster tree and heat map to show cross correlations for short chain fatty acids and top 18 significantly altered gut microbial strains discovered by previous 16s rRNA data. Data were transferred to fold change of exposure group versus control. Hierarchical clusters are constructed based on Pearson's r distance. Red-blue color bar indicates Pearson's correlation coefficient between two correlated components. Short chain fatty acids are negatively correlated with the *Clostridial Ruminococcaceae* strains that are frequently seen in the stools from patients with Crohn's disease and obesity. The suppressed strains belong to *Lactobacillales* and *Clostridial Roseburia*. Phylogenetic taxa information can be accessed in reference (Wang et al., 2016).

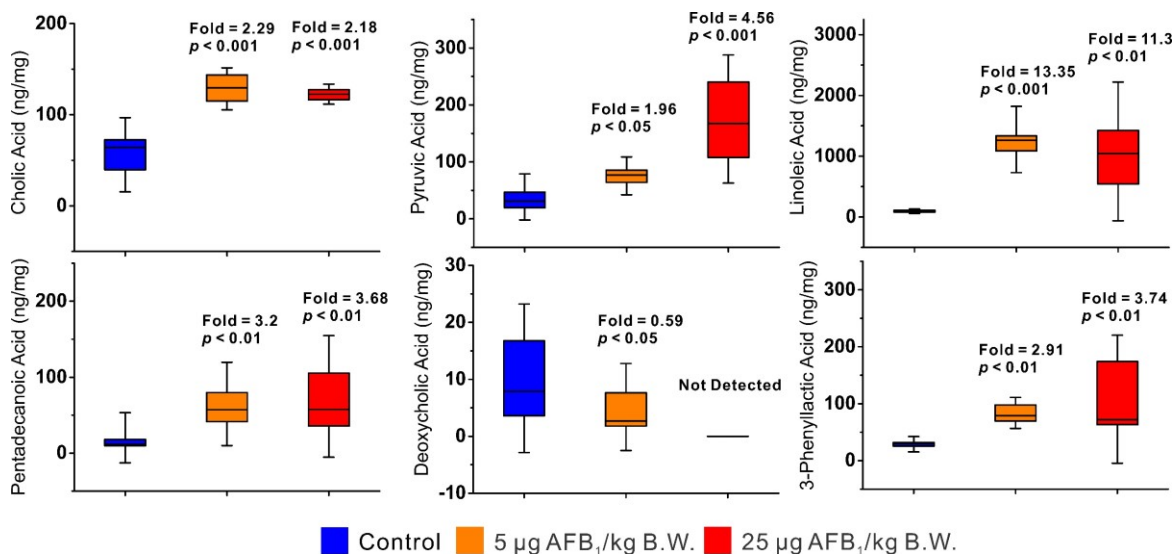


Figure 3-4. Fecal concentrations of cholic acid, deoxycholic acid, linoleic acid, pentadecanoic acid, pyruvic acid and 3-phenyllactic acid measured from the experimental groups treated with 0, 5 and 25 µg AFB₁/kg B. W. via HPLC-profiling analysis. Non-parametric Mann-Whitney U test was applied for all comparisons (n = 10). Box with middle vertical line represents 25%, 50% and 75% percentile of data. Vertical lines of box plots indicate S. D., multiplied with 1.5-fold coefficient in order to stretch out from box.

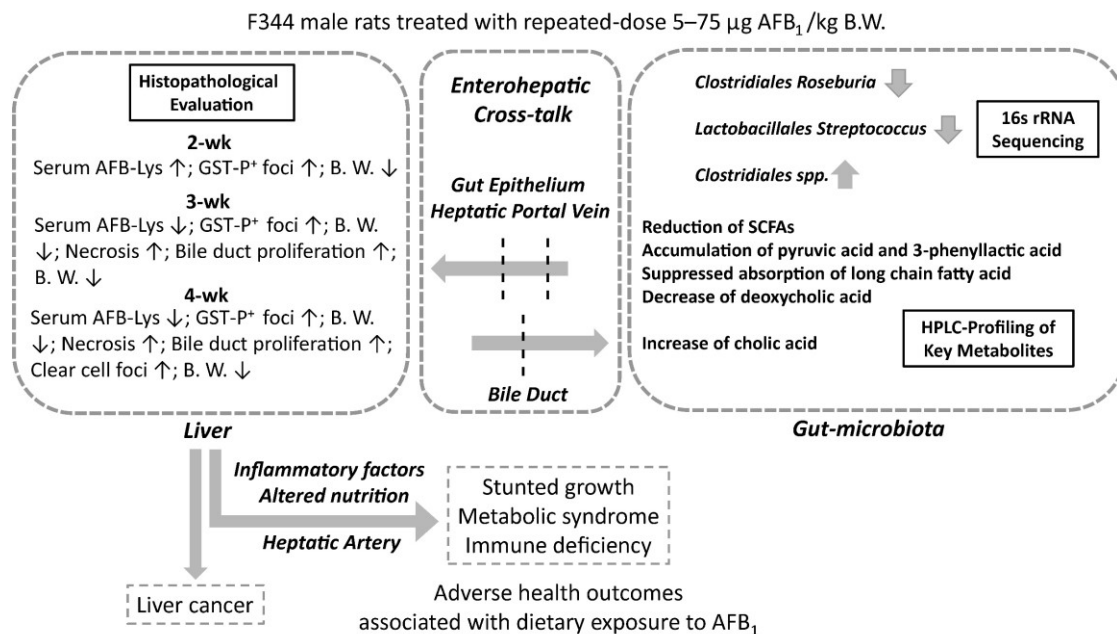


Figure 3-5. Summary of the adverse health outcomes associated with dietary exposure to AFB_1 in F344 rat model. Grey arrow indicates the changing trend of microbial taxa induced by AFB_1 -treatment. The establishment of rat model for AFB_1 oral exposure, as well as the 16s rRNA analysis have been published already (Qian et al., 2014; Qian et al., 2013a; Qian et al., 2013c; Wang et al., 2016). Briefly, male F344 rats were gavaged with AFB_1 at doses of 0, 5, 10, 25, 50 and 75 $\mu\text{g}/\text{kg B. W.}$ per day. The major pathological changes are summarized on the left panel. After three weeks of exposure to 75 $\mu\text{g AFB}_1/\text{kg B. W.}$, bile duct proliferation, liver GST-P⁺ foci co-occurred, followed by proliferation foci formation after four weeks and dramatic alanine transaminase, aspartate transaminase and creatine kinase elevations after five weeks of treatment.

Reference

- Arai, T., Ito, T., and Koyama, Y. (1967). Antimicrobial activity of aflatoxins. *J Bacteriol* 93(1), 59-64.
- Atroshi, F., Rizzo, A., Westermarck, T., and Ali-Vehmas, T. (1998). Effects of tamoxifen, melatonin, coenzyme q10, and l-carnitine supplementation on bacterial growth in the presence of mycotoxins. *Pharmacol Res* 38(4), 289-295.
- Azziz-Baumgartner, E., Lindblade, K., Gieseke, K., Rogers, H. S., Kieszak, S., Njapau, H., Schleicher, R., McCoy, L. F., Misore, A., DeCock, K., *et al.* (2005). Case-control study of an acute aflatoxicosis outbreak, Kenya, 2004. *Environ Health Perspect* 113, 1779-1783.
- Brockman, R. (2005). Glucose and short-chain fatty acid metabolism. Quantitative aspects of ruminant digestion and metabolism (J. Dijkstra, J. M. Forbes, J. France, Eds.), pp. 291-310. CAB International, Wallingford, UK.
- Brown, A. J., Goldsworthy, S. M., Barnes, A. A., Eilert, M. M., Tcheang, L., Daniels, D., Muir, A. I., Wigglesworth, M. J., Kinghorn, I., and Fraser, N. J. (2003). The Orphan G protein-coupled receptors GPR41 and GPR43 are activated by propionate and other short chain carboxylic acids. *J Biol Chem* 278, 11312-11319.
- Brown, J. M., and Hazen, S. L. (2015). The gut microbial endocrine organ: bacterially-derived signals driving cardiometabolic diseases. *Annu Rev Med* 66, 343.
- Camilleri, M. (2011). Managing symptoms of irritable bowel syndrome in patients with inflammatory bowel disease. *Gut* 60, 425-428.

- Caporaso, J. G., Kuczynski, J., Stombaugh, J., Bittinger, K., Bushman, F. D., Costello, E. K., Fierer, N., Pena, A. G., Goodrich, J. K., and Gordon, J. I. (2010). QIIME allows analysis of high-throughput community sequencing data. *Nat Methods* **7**(5), 335.
- Chakraborty, S., Zawieja, S., Wang, W., Zawieja, D. C., and Muthuchamy, M. (2010). Lymphatic system: a vital link between metabolic syndrome and inflammation. *Ann N Y Acad Sci* **1207**, 94-102.
- Corrêa-Oliveira, R., Fachi, J. L., Vieira, A., Sato, F. T., and Vinolo, M. A. R. (2016). Regulation of immune cell function by short-chain fatty acids. *Clin Transl Immunology* **5**, 73-80.
- Cummings, J., Pomare, E., Branch, W., Naylor, C., and Macfarlane, G. (1987). Short chain fatty acids in human large intestine, portal, hepatic and venous blood. *Gut* **28**, 1221-1227.
- DeSantis, T., Hugenholtz, P., Keller, K., Brodie, E., Larsen, N., Piceno, Y., Phan, R., and Andersen, G. L. (2006). NAST: a multiple sequence alignment server for comparative analysis of 16S rRNA genes. *Nucleic Acids Res* **34**, W394-W399.
- de Jonge, L. P., Douma, R. D., Heijnen, J. J., and van Gulik, W. M. (2012). Optimization of cold methanol quenching for quantitative metabolomics of *Penicillium chrysogenum*. *Metabolomics* **8**, 727-735.
- Druart, C., Neyrinck, A. M., Vlaeminck, B., Fievez, V., Cani, P. D., and Delzenne, N. M. (2014). Role of the Lower and Upper Intestine in the Production and Absorption of Gut Microbiota-Derived PUFA Metabolites. *PLoS One* **9**, e87560.

- Duncan, S. H., Hold, G. L., Barcenilla, A., Stewart, C. S., and Flint, H. J. (2002). *Roseburia intestinalis* sp. nov., a novel saccharolytic, butyrate-producing bacterium from human faeces. *Int J Syst Evol Microbiol* **52**, 1615-1620.
- Flint, H. J., Scott, K. P., Louis, P., and Duncan, S. H. (2012). The role of the gut microbiota in nutrition and health. *Nat. Rev. Gastroenterol. Hepatol.* **9**, 577-589.
- Galisteo, M., Duarte, J., and Zarzuelo, A. (2008). Effects of dietary fibers on disturbances clustered in the metabolic syndrome. *J Nutr Biochem* **19**, 71-84.
- Groopman, J. D., Jiaqi, Z., Donahue, P. R., Pikul, A., Lisheng, Z., Jun-shi, C., and Wogan, G. N. (1992). Molecular dosimetry of urinary aflatoxin-DNA adducts in people living in Guangxi Autonomous Region, People's Republic of China. *Cancer Res* **52**, 45-52.
- Gwartz, J. A., and Garcia-Casal, M. N. (2014). Processing maize flour and corn meal food products. *Ann N Y Acad Sci* **1312**, 66-75.
- Haskard, C. A., El-Nezami, H. S., Kankaanpaa, P. E., Salminen, S., and Ahokas, J. T. (2001). Surface binding of aflatoxin B1 by lactic acid bacteria. *Appl Environ Microbiol* **67**(7), 3086-3091.
- Han, J., Gagnon, S., Eckle, T., and Borchers, C. H. (2013a). Metabolomic Analysis of Key Central Carbon Metabolism Carboxylic Acids as Their 3-Nitrophenylhydrazones by UPLC/ESI-MS. *Electrophoresis* **34**, 2891-2900.
- Han, J., Gagnon, S., Eckle, T., and Borchers, C. H. (2013b). Metabolomic analysis of key central carbon metabolism carboxylic acids as their 3-nitrophenylhydrazones by UPLC/ESI-MS. *Electrophoresis* **34**, 2891-2900.
- Henry, S. H., Bosch, F. X., Troxell, T. C., and Bolger, P. M. (1999). Reducing liver cancer-global control of aflatoxin. *Science* **286**, 2453-2454.

- Hernández Bort, J. A., Shanmukam, V., Pabst, M., Windwarder, M., Neumann, L., Alchalabi, A., Krebichl, G., Koellensperger, G., Hann, S., Sonntag, D., *et al.* (2014). Reduced quenching and extraction time for mammalian cells using filtration and syringe extraction. *J Biotechnol* **182-183**, 97-103.
- Holmes, E., Li, Jia V., Marchesi, Julian R., and Nicholson, Jeremy K. (2012). Gut Microbiota Composition and Activity in Relation to Host Metabolic Phenotype and Disease Risk. *Cell Metab.* **16**, 559-564.
- Junichi, G., Masatoshi, H., Hiroaki, K., and Toshio, N. (1978). A new method for simultaneous determination of bile acids in human bile without hydrolysis. *Clin Chim Acta* **87**(1), 141-147.
- Kew, M. C. (2013). Aflatoxins as a cause of hepatocellular carcinoma. *J Gastrointestin Liver Dis.* **22**, 305-310.
- Kim, M., Qie, Y., Park, J., and Kim, C. H. (2016). Gut microbial metabolites fuel host antibody responses. *Cell Host Microbe* **20**, 202-214.
- Kleessen, B., Stoof, G., Proll, J., Schmiedl, D., Noack, J., and Blaut, M. (1997). Feeding resistant starch affects fecal and cecal microflora and short-chain fatty acids in rats. *J Anim Sci* **75**, 2453-2462.
- Klindworth, A., Pruesse, E., Schweer, T., Peplies, J., Quast, C., Horn, M., and Glöckner, F. O. (2013). Evaluation of general 16S ribosomal RNA gene PCR primers for classical and next-generation sequencing-based diversity studies. *Nucleic Acids Res* **41**(1), e1-e1.
- Kootte, R. S., Vrieze, A., Holleman, F., Dallinga-Thie, G. M., Zoetendal, E. G., de Vos, W. M., Groen, A. K., Hoekstra, J. B., Stoes, E. S., and Nieuwdorp, M. (2012). The

- therapeutic potential of manipulating gut microbiota in obesity and type 2 diabetes mellitus. *Diabetes Obes Metab* **14**, 112-20.
- Kumar, P., Mahato, D. K., Kamle, M., Mohanta, T. K., and Kang, S. G. (2016). Aflatoxins: A global concern for food safety, human health and their management. *Front Microbiol* **7**, 2170.
- Labbé, A., Ganopolsky, J. G., Martoni, C. J., Prakash, S., and Jones, M. L. (2014). Bacterial bile metabolising gene abundance in Crohn's, ulcerative colitis and type 2 diabetes metagenomes. *PLoS One* **9**, e115175.
- Lee, W.-J., and Hase, K. (2014). Gut microbiota-generated metabolites in animal health and disease. *Nat Chem Biol* **10**(6), 416-424.
- Lefebvre, P., Cariou, B., Lien, F., Kuipers, F., and Staels, B. (2009). Role of bile acids and bile acid receptors in metabolic regulation. *Physiol Rev* **89**, 147-91.
- Lopez, V. M., Decatur, C. L., Stamer, W. D., Lynch, R. M., and McKay, B. S. (2008). L-DOPA Is an Endogenous Ligand for OA1. *PLoS Biol* **6**, e236.
- Louis, P., Hold, G. L., and Flint, H. J. (2014). The gut microbiota, bacterial metabolites and colorectal cancer. *Nat Rev Microbiol* **12**, 661-672.
- Mitchell, N. J., Xue, K. S., Lin, S., Marroquin-Cardona, A., Brown, K. A., Elmore, S. E., Tang, L., Romoser, A., Gelderblom, W. C., and Wang, J. S. (2014). Calcium montmorillonite clay reduces AFB1 and FB1 biomarkers in rats exposed to single and co-exposures of aflatoxin and fumonisin. *J Appl Toxicol* **34**, 795-804.
- Miwa, H., Hiyama, C., and Yamamoto, M. (1985). High-performance liquid chromatography of short-and long-chain fatty acids as 2-nitrophenylhydrazides. *J Chromatogr A* **321**, 165-174.

- Mohammadagheri, N., Najafi, R., and Najafi, G. (2016). Effects of dietary supplementation of organic acids and phytase on performance and intestinal histomorphology of broilers. *Vet Res Forum* **7**, 189-195.
- Morrison, D. J., and Preston, T. (2016). Formation of short chain fatty acids by the gut microbiota and their impact on human metabolism. *Gut Microbes* **7**, 189-200.
- Mouzaki, M., Wang, A. Y., Bandsma, R., Comelli, E. M., Arendt, B. M., Zhang, L., Fung, S., Fischer, S. E., McGilvray, I. G., and Allard, J. P. (2016). Bile Acids and Dysbiosis in Non-Alcoholic Fatty Liver Disease. *PLoS One* **11**, e0151829.
- Nair, A. B., and Jacob, S. (2016). A simple practice guide for dose conversion between animals and human. *J Basic Clin Pharm* **7**, 27-31.
- Natarajan, N., and Pluznick, J. L. (2014). From microbe to man: the role of microbial short chain fatty acid metabolites in host cell biology. *Am J Physiol Cell Physiol* **307**(11), C979-C985.
- Pessione, E. (2012). Lactic acid bacteria contribution to gut microbiota complexity: lights and shadows. *Front Cell Infect Microbiol* **2**, 86-100.
- Peters, R., Hellenbrand, J., Mengerink, Y., and Van der Wal, S. (2004). On-line determination of carboxylic acids, aldehydes and ketones by high-performance liquid chromatography-diode array detection-atmospheric pressure chemical ionisation mass spectrometry after derivatization with 2-nitrophenylhydrazine. *J Chromatogr A* **1031**, 35-50.
- Qian, G., Tang, L., Guo, X., Wang, F., Massey, M. E., Su, J., Guo, T. L., Williams, J. H., Phillips, T. D., and Wang, J. S. (2014). Aflatoxin B1 modulates the expression of

- phenotypic markers and cytokines by splenic lymphocytes of male F344 rats. *J Appl Toxicol* **34**, 241-249.
- Qian, G., Tang, L., Lin, S., Xue, K. S., Mitchell, N. J., Su, J., Gelderblom, W. C., Riley, R. T., Phillips, T. D., and Wang, J.-S. (2016). Sequential dietary exposure to Aflatoxin B₁ and Fumonisin B₁ in F344 rats increases liver preneoplastic changes indicative of a synergistic interaction. *Food Chem Toxicol* **95**, 188-195.
- Qian, G., Tang, L., Wang, F., Guo, X., Massey, M. E., Williams, J. H., Phillips, T. D., and Wang, J.-S. (2013a). Physiologically based toxicokinetics of serum Aflatoxin B₁-lysine adduct in F344 rats. *Toxicology* **303**, 147-151.
- Qian, G., Tang, L., Wang, F., Guo, X., Massey, M. E., Williams, J. H., Phillips, T. D., and Wang, J.-S. (2013b). Physiologically based toxicokinetics of serum Aflatoxin B₁-lysine adduct in F344 rats. *Toxicology* **303**, 147-151.
- Qian, G., Wang, F., Tang, L., Massey, M. E., Mitchell, N. J., Su, J., Williams, J. H., Phillips, T. D., and Wang, J.-S. (2013c). Integrative toxicopathological evaluation of Aflatoxin B₁ exposure in F344 rats. *Toxicol Pathol* **41**, 1093-1105.
- Qin, J., Li, R., Raes, J., Arumugam, M., Burgdorf, K. S., Manichanh, C., Nielsen, T., Pons, N., Levenez, F., and Yamada, T. (2010). A human gut microbial gene catalogue established by metagenomic sequencing. *Nature* **464**(7285), 59-65.
- Rowland, I. (2012). Metabolism of Fats Bile Acids and Steroids. Role of the gut flora in toxicity and cancer. pp. 265. Elsevier, Amsterdam, Netherlands.
- Rubin, B. S. (2011). Bisphenol A: an endocrine disruptor with widespread exposure and multiple effects. *J Steroid Biochem Mol Biol* **127**(1-2), 27-34.

- Santaren, I. D., Watkins, S. M., Liese, A. D., Wagenknecht, L. E., Rewers, M. J., Haffner, S. M., Lorenzo, C., and Hanley, A. J. (2014). Serum pentadecanoic acid (15: 0), a short-term marker of dairy food intake, is inversely associated with incident type 2 diabetes and its underlying disorders. *Am J Clin Nutr* **100**, 1532-1540.
- Scheppach, W. (1994). Effects of short chain fatty acids on gut morphology and function. *Gut* **35**, S35-S38.
- Schulberg, J., and De Cruz, P. (2016). Characterisation and therapeutic manipulation of the gut microbiome in inflammatory bowel disease. *Intern Med J* **46**, 266-273.
- Smith, P. M., Howitt, M. R., Panikov, N., Michaud, M., Gallini, C. A., Bohlooly-y, M., Glickman, J. N., and Garrett, W. S. (2013). The microbial metabolites, short-chain fatty acids, regulate colonic Treg cell homeostasis. *Science* **341**, 569-573.
- Stark, A., Essigmann, J., Demain, A., Skopek, T., and Wogan, G. (1979). Aflatoxin B1 mutagenesis, DNA binding, and adduct formation in *Salmonella typhimurium*. *Proc Natl Acad Sci* **76**, 1343-1347.
- Suchodolski, J. S., Foster, M. L., Sohail, M. U., Leutenegger, C., Queen, E. V., Steiner, J. M., and Marks, S. L. (2015). The fecal microbiome in cats with diarrhea. *PLoS One* **10**, e0127378.
- Tang, L., Xu, L., Afriyie-Gyawu, E., Liu, W., Wang, P., Tang, Y., Wang, Z., Huebner, H., Ankrah, N.-A., and Ofori-Adjei, D. (2009). Aflatoxin–albumin adducts and correlation with decreased serum levels of vitamins A and E in an adult Ghanaian population. *Food Addit Contam* **26**, 108-118.

- Torii, T., Kanemitsu, K., Wada, T., Itoh, S., Kinugawa, K., and Hagiwara, A. (2010). Measurement of short-chain fatty acids in human faeces using high-performance liquid chromatography: specimen stability. *Ann Clin Biochem* **47**(5), 447-452.
- Torres, O., Matute, J., Gelineau-Van Waes, J., Maddox, J., Gregory, S., Ashley-Koch, A., Showker, J., Voss, K., and Riley, R. (2014). Human health implications from co-exposure to aflatoxins and fumonisins in maize-based foods in Latin America: Guatemala as a case study. *World Mycotoxin J* **8**, 143-159.
- Trenk, H. L., and Hartman, P. A. (1970). Effects of moisture content and temperature on aflatoxin production in corn. *Appl Microbiol* **19**, 781-784.
- Ursell, L. K., Haiser, H. J., Van Treuren, W., Garg, N., Reddivari, L., Vanamala, J., Dorrestein, P. C., Turnbaugh, P. J., and Knight, R. (2014). the intestinal metabolome—an intersection between microbiota and host. *Gastroenterology* **146**, 1470-1476.
- VanHook, A. M. (2016). Another reason to eat more fiber. *Sci Signal* **9**(441), ec184-ec184.
- Wang, J.-S., and Groopman, J. D. (1999). DNA damage by mycotoxins. *Mutat Res* **424**, 167-181.
- Wang, J., Tang, L., Glenn, T. C., and Wang, J.-S. (2016). Aflatoxin B1 induced compositional changes in gut microbial communities of male F344 rats. *Toxicol Sci* **150**:54-63.
- Weir, T. L., Manter, D. K., Sheflin, A. M., Barnett, B. A., Heuberger, A. L., and Ryan, E. P. (2013). Stool microbiome and metabolome differences between colorectal cancer patients and healthy adults. *PLoS One* **8**, e70803.
- Wen, L., and Wong, F. S. (2017). Dietary short-chain fatty acids protect against type 1 diabetes. *Nat Immunol* **18**, 484-486.

- Whelan, J., and Fritsche, K. (2013). Linoleic Acid. *Adv Nutr* **4**(3), 311-312.
- Whittaker, B. L., and Chipley, J. R. (1986). Interaction of aflatoxin B1 with bacterial DNA: possible relationship to bacteriophage induction in lysogenic *Bacillus megaterium*. *J Environ Pathol Toxicol Oncol* **6**, 295-304.
- Winder, C. L., Dunn, W. B., Schuler, S., Broadhurst, D., Jarvis, R., Stephens, G. M., and Goodacre, R. (2008). Global metabolic profiling of *Escherichia coli* cultures: an evaluation of methods for quenching and extraction of intracellular metabolites. *Anal Chem* **80**, 2939-2948.
- Wong, J. M., De Souza, R., Kendall, C. W., Emam, A., and Jenkins, D. J. (2006). Colonic health: fermentation and short chain fatty acids. *J Clin Gastroenterol* **40**, 235-243.
- Worley, B., and Powers, R. (2016). PCA as a practical indicator of OPLS-DA model reliability. *Curr Metabolomics* **4**(2), 97-103.
- Xue, K. S., Cai, W., Tang, L., and Wang, J.-S. (2016). Aflatoxin B 1-lysine adduct in dried blood spot samples of animals and humans. *Food Chem Toxicol* **98**, 210-219.
- Yatsunenکو, T., Rey, F. E., Manary, M. J., Trehan, I., Dominguez-Bello, M. G., Contreras, M., Magris, M., Hidalgo, G., Baldassano, R. N., and Anokhin, A. P. (2012). Human gut microbiome viewed across age and geography. *Nature* **486**, 222-227.
- Zhao, G., Nyman, M., and Åke Jönsson, J. (2006). Rapid determination of short-chain fatty acids in colonic contents and faeces of humans and rats by acidified water-extraction and direct-injection gas chromatography. *Biomed Chromatogr* **20**, 674-682.

CHAPTER 4. ASSESSMENT OF THE ADVERSE IMPACTS OF AFLATOXIN B₁ ON GUT-MICROBIOTA DEPENDENT METABOLISM IN F344 RATS

4.1 Introduction

The adverse impacts of aflatoxin B₁ (AFB₁) on gut-microbiota dependent metabolism in F344 rats were assessed via ultra-high performance liquid chromatograph (UHPLC)-profiling and UHPLC-mass spectrometer (MS) metabolomic analyses. UHPLC-profiling analysis found 1100 raw peaks from the feces samples collected at week 4, of which 335 peaks showed peak shape qualified for quantitation. A total of 24, 40 and 71 peaks were significantly decreased (> 2 -fold, $p < 0.05$) among the exposure groups treated with 5, 25, and 75 $\mu\text{g AFB}_1/\text{kg}$ body weight (B. W.), respectively. Supervised orthogonal partial least squares projection to latent structures-discriminant analysis revealed 11 differential peaks that may be used to predict AFB₁-induced adverse changes of the metabolites. UHPLC-MS based metabolomic analysis discovered 494 features that were significantly altered by AFB₁, and 234 of them were imputatively identified using Human Metabolome Data Base (HMDB). Metabolite set enrichment analysis showed that the highly disrupted metabolic pathways were: protein biosynthesis, pantothenate and CoA biosynthesis, betaine metabolism, cysteine metabolism, and methionine metabolism. Eight features were rated as indicative metabolites for AFB₁ exposure: 3-decanol, xanthylic acid, norspermidine, nervonyl carnitine, pantothenol, threitol, 2-hexanoyl carnitine, and 1-nitrohexane. These data suggest that AFB₁ could significantly reduce the variety of

nutrients in gut and disrupt a number of gut-microbiota dependent metabolic pathways, which may contribute to the AFB₁-associated stunted growth, liver diseases and the immune toxic effects that have been observed in animal models and human populations.

AFB₁ is a potent toxic and carcinogenic mycotoxin produced by *Aspergillus flavus* and *A. parasiticus* (Wang and Groopman, 1999). The two fungi can colonize on the surface of post-harvested cereals, groundnuts, and corns in humid and hot environment, which results in a high chance of human dietary exposure to AFB₁ (Eaton and Groopman, 2013). Acute exposure to AFB₁ causes aflatoxicosis and death in human and other animals; whereas chronic AFB₁ exposure induces hepatocellular carcinoma (HCC) and immune toxic effects (Mace et al., 1997; Jiang et al., 2008; Qian et al., 2014). There were also evidences showing that dietary exposure to AFB₁ is associated with and malnutrition-related stunted growth (Khlanguiset et al., 2011; Lombard, 2014; Knipstein et al., 2015). For these reasons, regulation of AFB₁ contamination in food and assessment of dietary AFB₁ exposure in human populations have received continuous and widely attention.

Metabolomic analysis is able to profile hundreds to thousands of metabolites present in biological samples (Dettmer et al., 2007; Zivkovic and German, 2009; Ramirez et al., 2013; Calvani et al., 2014). The frequently employed instruments for metabolomic analysis are liquid chromatography-mass spectrometry (LC-MS) and gas chromatography-mass spectrometry (GC-MS) (Wang et al., 2010). The fragmentation spectrum, retention time, parent-product ion transition, and m/z of the detected features can be used for the imputative identification and characterization of chemical entities through open-access or commercial databases (Patti et al., 2012; Ramautar et al., 2013). However, the detective scope of MS-based metabolomics is sometimes affected by different setting factors, e.g.

ionization strategy, mode of analyzer, mobile phases, voltages of capillary tube (Beckonert et al., 2007). One compromising strategy is to perform chromatography based metabolic profiling prior to metabolomics analysis. The metabolic profiling analysis is independent of ion fragmentation, but more relies on the resolution of chromatogram, and the signals recorded by conservative detectors like flame ionization detector (FID), electron capture detector (ECD), ultraviolet-diode (UV-DAD) and fluorescent detector (FLD) (Georgakoudi et al., 2002; Andersen and Frisvad, 2004; Menter, 2006). Ultra-high performance liquid chromatography (UHPLC) has largely enhanced the resolution of chromatographic profiling analysis (Guillarme and Veuthey, 2015). In addition to “clearer” chromatograms, the combination of UHPLC with MS could further provide preliminary elucidation of the alterations of metabolic pathways.

We have previously conducted a series of studies to investigate the adverse health outcomes and pathogenesis induced by AFB₁ in F344 rat model (Qian et al., 2013a; Qian et al., 2013b; Qian et al., 2014; Qian et al., 2016). We also found that AFB₁ induced depletion of beneficial gut-microbial strains and increase of harmful gut-microbes (Wang et al., 2016). Moreover, a set of key fecal metabolites were remarkably affected by AFB₁, such as short chain fatty acids (SCFAs), pyruvic acid, cholic acid, deoxycholic acid and long chain fatty acids (Zhou et al., 2018). The cell components and dependent metabolites of gut-microbiota count for around 25–50% of solid material of human stool (Rose et al., 2015). Accordingly, fecal analysis of metagenome and metabolites is considered to be a standard non-invasive approach to investigate gut-microbiota (Barbosa, 2013; Thomas et al., 2015). Since these metabolites play important roles in maintaining host immune function, energy metabolism, and liver function, the disturbance of metabolic homeostasis

of these metabolites may lead to various adverse health outcomes (Prasad Maharjan and Ferenci, 2003; Ursell et al., 2014; Sinha et al., 2016). In this regard, the AFB₁-induced changes of gut-microbiota dependent metabolism need to be further investigated and analyzed in a high throughput way. In this work, UHPLC-based metabolic profiling and UHPLC-MS-based metabolomic analysis were used to examine gut-microbiota dependent metabolism. Multivariate analyses such as principal component analysis (PCA), supervised partial least squares projection to latent structures-discriminant analysis (PLS-DA), orthogonal (O)PLS-DA, and random forest were performed to screen and rate the chromatographic peaks that can reflect the impairment of gut-microbiota dependent metabolism. Metabolite set enrichment analysis (MSEA) was further used to characterize the adverse impact of AFB₁ on gut-microbiota dependent metabolic pathways.

4.2. Methods and material

4.2.1 *Reagents and chemicals*

Dimethyl sulfoxide (DMSO) and aflatoxin B₁ (AFB₁) standard were purchased from Sigma-Aldrich (St. Louis, MO, USA). AFB₁ stock solution (25 mg/mL) was prepared in DMSO and diluted to appropriate treatment concentrations upon use. All eluting solvents (methanol and water) were LC-MS grade reagents purchased from J. T. Baker (Phillipsburg, NJ, USA). Formic acid of LC-MS grade was ordered from Fluka (Buchs, Switzerland).

4.2.2 *Animal study*

The dosing protocol has been systematically validated and reported in previous publications (Qian et al., 2013a; Qian et al., 2013b; Qian et al., 2014; Qian et al., 2016). The doses applied are relevant to the exposure level in tropical area (Zhou et al., 2018). Briefly, 100 male F344 rats (100–120 g) were purchased from Harlan Laboratory (Indianapolis, IN, USA). After 1 week of environmental acclimation, the rats were divided into 4 experimental groups, with 5 cages assigned for each group. The animal housing conditions were: light/dark cycle of 12 hr/12 hr, temperature of 22 ± 2 °C, relative humidity of 50–70%. Purified AIN 76A diet and tap water were maintained every day. The 4 experimental groups were daily gavaged with 0, 5, 25, and 75 mg AFB₁/kg body weight (B. W.), respectively, in a consecutive duration of 5 weeks. Rat feces were daily collected from week 2 to the week 4 and were pooled by each cage at each week. All samples were stored in –80 °C freezer. Animal husbandry, care, AFB₁-exposure, and sample collection strictly followed the requirements and regulations of Institutional Animal Care and Use Committee at the University of Georgia.

4.2.3 *Sample quenching and extraction*

Cold methanol was used to quench fecal sample and extract metabolites (de Jonge et al., 2012; Hernandez Bort et al., 2014). The specific operations were published in previous works (Zhou et al., 2018). In brief, fecal pellet (200 mg) was transferred to the Mobio PowerLyzer Glass Bead tubes (Mobio, Carlsbad, CA). The tubes were pre-loaded with glass beads (diameter, 0.1 mm) to facilitate the breakup of feces and lysis of cells. One milliliter cold methanol (–80 °C) was immediately added. The fecal pellet was ground using a glass pestle. Following this, 0.5 mL methanol was slowly added to wash the pestle.

The tube was then capped and fastened on a rotary vortex to undergo vortex for 20 mins. After vortex, the tube was placed on ice for 5 minutes, and was further centrifugated at 12,000 rpm for 15 mins to spin down cellular debris. The supernatant was used for analysis.

4.2.4 UHPLC-profiling analysis

Chromatographic profiling of fecal metabolome was performed using Thermo Scientific Dionex UltiMate 3000 UHPLC system. The system consists of rapid separation (RS) tertiary pump module, advanced sample tray, ultraviolet-diode detector (UV-DAD), fluorescent detector (FLD), and is equipped with a C18 reversed-phase column (length, 150 mm; i.d., 2.1 mm; particle size, 2.2 μm ; pore diameter, 120 \AA ; Thermo Fisher, Norcross, GA, USA). The detector unit is capable of scanning 8 detective channels simultaneously. Phase A was water containing 0.1% formic acid (v/v), and phase B was methanol with 0.1% formic acid (v/v). The injection volume was 30 μL . The gradient elution program started with a flow rate of 0.3 mL/min. The gradient eluting ratio was 95% to 85% A, from 0 min to 10 min; 85% to 30% A, from 10 min to 45 min; 30% to 10% A, from 45 min to 60 min; 10% to 5% A, from 60 min to 68 min, then keep to 97 min; 5% A to 0% A, from 97 min to 100 min with flow rate 0.5 mL/min, then keep to 120 min; 0% A to 95% A, from 120 min to 123 min, with flow rate back to 0.3 mL/min. Oven temperature was set as 45 $^{\circ}\text{C}$. The excitation wavelengths of FLD detective channels were set as 230 nm, 280 nm and 330 nm, with zero-order model automatically locating the maximum absorption wavelength. The wavelengths of DAD detective channels were set as 210 nm, 250 nm, 280 nm and 340 nm. The representative chromatograms are shown in **Figure 4-1**, with the possible target analyte categories listed in **Table 4-1**.

4.2.5 UHPLC-MS metabolomic analysis

UHPLC-MS metabolomic analysis was performed in an Acquity ultra-high performance liquid chromatography (UHPLC) system combined to Xevo Triple Quadrupole (TQD) mass spectrometer with electrospray ionization (ESI). The system was equipped with the same C18 reversed-phase column used for UHPLC-profiling analysis. A volume of 9 μ L extract was injected for each sample. The parameters for the MS settings are: capillary voltage, 2.8 kV; detective range of m/z, 50 to 1500; source temperature, 350 °C; desolvation temperature, 50 °C; desolvation gas, 800 L/h; cone gas, 50 L/h. Data acquisition was performed in ESI (+) mode, with precursor scanning mode, and centroid file format. Ultra-high purity nitrogen was used as desolvation gas and cone gas. Sample extracts were randomly picked from the control group and the middle-dose group for metabolomics analysis (n = 6). Mobile phase A was 0.1% formic acid in water and B was 0.1% formic acid in acetonitrile. A constant flow rate of 0.4 mL/min was used and the gradient elution was applied with the following proportions (v/v) of solvent A: 0 to 1.5 min, at 98% A; 1.5 to 7.0 min, from 98% to 75% A; 7.0 to 10.0 min, from 75% to 40% A; 10.0 to 15.0 min, from 40% to 5% A; 15.0 to 20.0 min, at 5% A; 20.0 to 26.0 min, from 5% to 98% A; followed by 4.0 min of re-equilibration.

4.2.6 Data processing and statistics

UHPLC-profiling data were pre-processed with Thermo Fisher Chromeleon 7.0. The data pre-processing includes peak detection, filtering, alignment, labeling of peaks and formation of library. When multiple peaks were generated from different detective channels for one metabolite, only the channel with highest signal was used for quantitative analysis. To standardize the peak intensities collected by different detectors and channels, data were transformed to fold-change by dividing with the mean intensities of the peaks measured in control samples. The statistical difference of the metabolite levels between control and exposure groups was tested using Welch's t-test. Principal component analysis (PCA), supervised partial least squares projection to latent structures-discriminant analysis (PLS-DA), orthogonal (O)PLS-DA, random forest, Pearson's correlation, and hierarchical clustering analyses were all performed in R (Team, 2000). Statistical supervision on PLS and OPLS include the R² and Q² quality metrics, and permutation diagnostics (Wold et al., 2001). Auto-scaling was applied to remove the dependence of the rank of the metabolites on the average concentration and the magnitude of the fold changes (van den Berg et al., 2006). The raw files collected by UHPLC-LC-MS were processed using Progenesis QI (Waters, MA, USA), including the mass detection, deconvolution of total ion chromatogram (TIC), grouping of isotope features, alignment of ion peaks, and formation of extracted ion chromatogram (XIC). Processed metabolomic data were next normalized through median division and auto-scaled, and finally analyzed using random forest model and OPLS-DA in order to find most differential metabolites. The prediction power, sensitivity, and specificity were determined by receiver operating characteristic (ROC) analyses. The metabolite set enrichment analysis (MSEA) was performed using MetaboAnalyst (Xia and Wishart, 2016).

4.3 Results

4.3.1 *Aflatoxin B₁ induced global shift of gut-microbiota dependent metabolism*

For convenience, in the following part of this article the AFB₁ doses of 5, 25, and 75 µg /kg B. W. were noted as low-, middle-, and high-dose. UHPLC-profiling analysis detected 1100 raw peaks from fecal samples at week 4 (n = 60, 3 samplings × 5 cages × 4 groups). The representative chromatograms were shown in **Figure 4-1**. A conservative peak filtering was applied to refine the raw chromatograms, with the filtering criteria of tailing factor of 0.5–2 and signal-to-noise (S/N) ratio > 5. Eventually Chromeleon module cropped 335 peaks between 19 min and 109 min from the aligned chromatograms. A total of 111 detected peaks were marked as common peaks since they were present in over 80% samples, and Pearson's correlation coefficients were used to rate the pairwise correlations of the peaks (**Figure 4-2**). Among the total 6105 pairwise correlations, 1521 pairs are significantly correlated with $p < 0.01$, and 779 pairs were correlated with $p < 0.05$, such that 37.3% of the detected peaks were correlated with AFB₁ treatment. Volcano plot analysis showed the shift of fecal metabolome (**Figure 4-3**). The screening criteria for significant fold change was set as > 2-fold ($q < 0.05$). The peak counts in different exposure groups exhibited dose dependent changes. Compared with control samples, there were 24, 40 and 71 peaks significantly reduced in the low-, middle-, and high-dose groups, respectively. The number of up-regulated peaks slightly decreased, with 18, 11 and 10 in the three exposure groups, respectively. Of note, in the high-dose group 27.2% of the common peaks exhibited significant fold-changes, with the majority of these peaks reduced by AFB₁ (**Figure 4-3**).

About 37.3% of the detected metabolites exhibited associated dose-responses to AFB₁ exposure, suggesting the necessity to perform multivariate analysis (MVA). Prior to MVA, a stepwise refinement of variables was applied to the dataset in order to enhance the reliability and statistical power of MVA models. In the first step, 26 peaks with significant alteration were retained from the 111 common peaks. The retaining criteria was that the peak showed significant fold-change (> 2-fold, $q < 0.01$) in at least two exposure groups, as compared with the control group. Principal component analysis (PCA) was used to assess whether these peaks could fairly represent the metabolic change induced by AFB₁, and 55.5% of sample variance was explained by the top 5 PCs (**SI Figure 4-1**). The 26 peaks were next processed with supervised projections to latent structures discriminant analysis (PLS-DA) and orthogonal (O) PLS to extract the differential peaks in response to AFB₁-exposure. All test parameters are shown in **Figure 4-4**. Permutation diagnostics indicated that the PLS and OPLS models could well fit the analysis. For the PLS model, t1/t2 together correlated/summarized 32% of the X variance, and the top 3 PCs achieved an explanatory R²_Y value of 0.552 and predictive Q²_Y value of 0.438 (**Figure 4-4 A and B**). With the concern of the undesirable Q²_Y of PLS modeling, we turned to binominal OPLS model to predict “Yes/No” of the adverse changes of gut-microbiota dependent metabolism (**Figure 4-4 C and D**). Permutation diagnostics showed a qualified R²_Y value of 0.808, and a Q²_Y value of 0.645 with $p < 0.05$. PC1 captured 26% of variance of X matrix. Therefore, OPLS-DA model may generate more reliable statistical results here.

Variable importance in projection (VIP) statistics were calculated using OPLS-DA model. By grouping all samples from exposure groups into one group, we applied OPLS-DA model and ranked the relative importance of the 26 differential peaks in differing

samples with different treatments according to their VIP scores. There were 11 peaks showing VIP score >1: M2, M215, M281, M264, M311, M11, M6, M324, M31, M254 and M224. These differential peaks were taken as indicative peaks for the adverse alterations of gut-microbiota dependent metabolism induced by AFB1 (**Table 4-2**). The mean decrease in accuracy (MDA) calculated from random forest model was provided as secondary quantitative reference to rate the relative importance of peaks in separating samples with different treatments.

4.3.2 *Aflaxoin B₁ disrupts gut-microbiota dependent metabolic pathways*

UHPLC-MS based metabolomic analysis discovered 494 significant responding features from 1744 detected features. The chemical entities of the 178 features were imputatively identified through Human Metabolome Data Base (HMDB). The relative intensities of the top 50 differential metabolites ranked by t-test are shown in **Figure 4-5 A**, including 23 down-regulated metabolites and 27 up-regulated ones. The 178 identified metabolites were submitted to MetaboAnalyst module for pathway analysis (Xia and Wishart, 2002). Representative components of major fecal metabolite categories modified by the AFB1 are listed in **Table 4-3**. The disrupted metabolic pathways were summarized by using MetaboAnalyst online modules, based on KEGG database (**Figure 4-5 B** and **Table 4-4**). The top 5 significantly disrupted metabolic pathways were protein biosynthesis, methionine metabolism, pantothenate and CoA biosynthesis, glycine, serine and threonine metabolism, and pyruvate metabolism. **Figure 4-6 A** listed the top 15 indicative metabolites ranked by their percentages of selected frequency (%) calculated by random forest model (**Table 4-5**). The top 5 differential metabolites, including 3-decanol, D-

threitol, phenylacetic acid, pantothenol and 2-hexanoyl carnitine, together achieved an AUC of 0.962 in ROC diagnostics (**Figure 4-6 B**). In order to obtain a conservative selection of metabolites as indicators for AFB₁ treatment in rats, we input the top 30 differential metabolites ranked by Welch t-test into OPLS-DA model and compared the results with that obtained from random forest model (**Table 4-5**). The predictive component t1 explained 38% variance of sample with a qualified R²_Y of 0.977 and Q²_Y of 0.887. Xanthylic acid, 3-decanol, norspermidine, neuronul carnitine, pantothenol, D-threitol, 2-hexenoyl carnitine, and 1-nitrohexane were marked as indicative metabolites by both OPLS-DA and random forest models. The alterations of the 8 metabolites were shown in **Figure 4-7**.

4.4 Discussion

In this study, the global shift of fecal metabolites was detected using 7 representative detective channels of UHPLC (**Table 4-1**). The fecal metabolites, as proxy of gut-microbiota dependent metabolism, exhibited highly dose-dependent correlations and compositional shift in response to AFB₁ exposure (**Figure 4-2 and Figure 4-3**). Multivariate analysis (MVA) models were used to identify the indicative peaks of the impairment of gut-microbiota dependent metabolism, and OPLS-DA was found to be the most effective model (**Figure 4-4, SI Figure 4-1 and Table 4-2**). UHPLC-LC-MS based metabolomic analysis was employed to characterize the changes of gut-microbiota dependent metabolic pathways (**Table 4-3 and Figure 4-5**). The most affected pathways include: protein biosynthesis; methionine metabolism; pantothenate and CoA biosynthesis; glycine, serine and threonine metabolism; pyruvate metabolism; betaine metabolism;

cysteine metabolism; arginine and proline metabolism; urea cycle; oxidation of branched chain fatty acids (**Table 4-4** and **Figure 4-5**). The indicative metabolites of the disrupted metabolic pathways were identified using random forest model (**Figure 4-6 A**). The predicting power was examined using ROC, and the first 5 differential features showed AUC of 0.962 (**Figure 4-6 B**). Xanthylic acid, 3-decanol, norspermidine, nervonyl carnitine, pantothenol, D-threitol, 2-hexenoyl carnitine, and 1-nitrohexane were marked as top differential metabolites by both OPLS-DA and random forest model (**Table 4-5** and **Figure 4-7**).

Gut-microbiota actively interact with host physiology and play an irreplaceable role in the maintenance of host nutritional status and a number of physiological regulations (Kaiko and Stappenbeck, 2014). In this work, we found that AFB₁ induced remarkable dose-responses for the metabolites contained in the feces (**Figure 4-2** and **Figure 4-3**). The hierarchical clusters in **Figure 4-2** stand for the metabolic pathways that are potentially involved in the related metabolic events of gut-microbiota. There are key nutrients and metabolites that may take pivotal roles in metabolism. AFB₁ reduced diversity of nutrients in a dose-dependent manner which may result in adverse impact on host nutritional provision (Martens et al., 2009). In the field of metabolomics, PCA, PLS-DA and OPLS-DA have been widely used to extract principle components, or to identify distinct metabolic pattern (Luo et al., 1999). The ranking of important metabolites heavily depends on the specific algorithm and index to use, e.g. variable importance in projection (VIP) scores (Galindo-Prieto et al., 2014). Our stepwise analysis retained a panel of 11 predictive indicators for AFB₁ induced impairment of gut-microbial metabolism (**Table 4-2**). This impairment includes disorder of community structure (Wang et al., 2016) and

derangements of major gut-microbiota dependent metabolites such as short chain fatty acids, long chain fatty acids and secondary bile acid (Zhou et al., 2018). Further structural elucidation for these indicative metabolites will be one important aspect of our future work.

Extensive alterations of gut-microbiota related metabolites, including amino acids, aliphatic acids, vitamins and polyamines were induced by AFB1 (**Figure 4-5** and **Table 4-3**). Of note, the levels of a variety of amino acids were changed significantly, such as the decreases of L-Arginine and L-Threonine, and increases of L-Lysine, L-Carnitine, Cysteinyl-histidine and L-Cysteine. These changes may have remarkable impact on host health, because host body growth and various physiological regulatory functions heavily depend on a sufficient provision and metabolism of these amino acids (Zeng et al., 2016). In addition, we noticed the disruption of L-tryptophan pathway in AFB1 exposure group, including the down-regulated S-farnesyl-L-cysteine and taurine, and elevated cyclic 3-hydroxyl melatonin, methyl dopa and L-beta-aspartyl-L-glutamic acid. The metabolism of L-tryptophan by gut-microbiota is known for its production of serotonin, melatonin and many other neurotransmitters. Accordingly, the disorganization of L-tryptophan metabolism may affect the performance of host neuro system in a significant way (Fujigaki et al., 2017). Although it has not been fully established whether gut-microbiota can produce neuropeptide-like compounds, the microbes do routinely produce small molecule neurotransmitters from host diet. For example, serotonin can be synthesized by several strains that belong to *Candida*, *Streptococcus*, *Escherichia* and *Enterococcus* (Alkasir et al., 2017); dopamine and noradrenaline can be generated by *Escherichia*, *Bacillus* and *Saccharomyces* (Lyte, 2011); and some strains belonging to *Lactobacillus* and

Bifidobacterium are able to produce gamma-aminobutyric acid (GABA) and acetylcholine (Messaoudi et al., 2011).

Metabolomic analysis revealed the reduction of fecal short chain fatty acids (SCFAs) in AFB₁ exposure group, such as lactic acid, valeric acid, acetic acid, and phenylacetic acid (**Table 4-3**). These changes were in agreement with our data collected using HPLC-profiling analysis (Zhou et al., 2018), and were consistent with the results of earlier 16S rRNA analysis that lactic acid bacteria were depleted by AFB₁ (Wang et al., 2016). The decrease of intestinal supply of SCFAs may contribute to the incidences of a myriad of adverse health outcomes, in that the receptors of SCFAs (GPR43, GPR41, OLFER78, GPR109A) are broadly distributed in different organs and systems, and participate into the regulations of a number of important physiological functions, as well as cellular events, e.g. mobility of gut epithelium, liver detoxification, liver lipogenesis, cell cycle, proliferation and apoptosis (Brown et al., 2003; Smith et al., 2013; Natarajan and Pluznick, 2014).

We found that the concentrations of several vitamins were elevated in the rat feces after AFB₁ exposure (**Table 4-3**), such as biotin, ubiquinone-1 and -4. Unlike SCFAs that are primarily synthesized by gut-microbiota, most of vitamins are consumed from food (Kamei et al., 1986; Sugahara et al., 2015). The abnormal elevations of these vitamins in feces were highly indicative of the impairment of gut absorption of vitamins. These vitamins perform necessary bio-chemical functions in global metabolism. For example, biotin is a driving coenzyme that is widely involved in the metabolisms of fatty acids, amino acids, and saccharides (LeBlanc et al., 2013). Ubiquinone-1 and -4 are important intermediates in the synthesis of Coenzyme Q (CoQ), and the primary role of CoQ is to

create a proton gradient across the inner mitochondrial membrane and drive ATP formation (Green, 1959). In addition, organic amines, including ornithine, spermine, norspermidine and putrescine, were all decreased (**Table 4-3**). Such changes may possibly be resulted by the domination of Bacteroides after AFB₁ treatment (Wang et al., 2016)—Bacteroides have comparatively higher expression of spermine oxidase (SMO) (Goodwin et al., 2011a; Goodwin et al., 2011b). The catalyzing process of these amines by SMO could produce a high level of reactive oxygen species (ROS) and causes DNA damage to intestinal epithelium once ROS is largely accumulated (Agostinelli et al., 2007).

It is suggested that random forest is the most robust model for the classification, regression and ranking of important variables when dealing with the dataset with small sample size and large amount of variables (Cutler et al., 2007; Gunduz and Fokoue, 2015). Indeed, we input the 178 metabolites into several statistical models, such as PCA, OPLS-DA, supportive vector machine (SVM), and random forest model, and the results from random forest model showed highest AUC in ROC diagnostics. As shown in **Figure 4-6**, the differential metabolites between control and exposure groups were rated by random forest model according to their statistical power to predict AFB₁ treatment. The top 5 differential metabolites were able to predict AFB₁ exposure with an AUC of 0.962 (**Figure 4-6 B**). The indicative metabolites identified by both OPLS-DA and random forest model include 3-decanol, xanthylic acid, norspermidine, nervonyl carnitine, pantothenol, D-threitol, 2-hexenoyl carnitine, and 1-nitrohexane (**Table 4-5** and **Figure 4-7**). They could be combined with the indicative peaks generated by UHPLC-profiling analysis to predict the impairment of gut-microbiota dependent metabolic pathways, as well as the corresponding changes of community structure of gut-microbiome following AFB₁

exposure in rats. Metagenomics data will be collected in our future work, which will be able to provide further evidences in terms of the molecular biological events induced by AFB₁—such metabolic changes of gut-microbiota may be very complex and are involved with several factors, e.g. community structure alteration, toxin-induced enzyme changes, as well as the health status of host.

To summarize, our data have demonstrated that oral exposure to AFB₁ could disrupt a number of gut-microbiota dependent metabolic pathways, including energy utilization, vitamin absorption, and essential metabolisms of fatty acids, amino acids and carbohydrates in rats. The results further completed previous findings gained via 16S rRNA and HPLC-profiling analyses. The adverse changes of the metabolic pathways may contribute the AFB₁-induced hepatic pathogenesis, immune toxicity, and stunted growth that were revealed by previous studies in the same rat model. Moreover, we have shown that the combination of UHPLC-profiling and UHPLC-MS based metabolomics could be used to identify the indicative peaks and metabolites and assess and predict the adverse alterations of gut-microbiota dependent metabolisms induced by AFB₁.

TABLES

Table 4-1. Detective channels and major analytes in UHPLC-profiling analysis.

Detector	Channel	Target analytes	Reference
----------	---------	-----------------	-----------

FLD	230 nm	phenylalanine, tyrosine, tryptophan and derivatives	(Determann et al., 1998; Thomas et al., 2002; Andersen and Frisvad, 2004)
FLD	280 & 330 nm	NADH, tyrosine, tryptophan, serotonin, melatonin, aromatic amines, collagen and elastin	(Georgakoudi et al., 2002; Menter, 2006)
DAD	210 nm	metabolites with (-COOH) or (-OH)	(Caruso et al., 1994)
DAD	250 nm	steroids, prostaglandin, glucuronide, furans, indoles	(Salari et al., 1987)
DAD	280 nm	steroid, folic acid, riboflavin, furans, tryptophan	(Dorfman, 1953)
DAD	340 nm	kynurenine, xanthurenic acid, flavonoids	(Soto et al., 2011)

Table 4-2. Indicative peaks discovered in UHPLC-profiling analysis.

Metabolite	Retention Time	Detective Channel	VIP Score*	MDA**
M2	18.09	FLD Ex 280 nm	1.65	0.014
M6	21.32	DAD UV 250 nm	1.19	0.009

M11	23.37	DAD UV 250 nm	1.24	0.022
M31	33.20	FLD Ex 280 nm	1.12	0.014
M215	61.54	DAD UV 250 nm	1.59	0.018
M224	67.92	DAD UV 280 nm	1.01	0.007
M254	67.69	FLD Ex 330 nm	1.05	0.014
M264	68.10	DAD UV 250 nm	1.46	0.014
M281	73.94	DAD UV 210 nm	1.56	0.006
M324	65.82	FLD Ex 230 nm	1.16	0.005
M311	95.82	DAD UV 250 nm	1.42	0.010

*VIP score is calculated from control and using the binary OPLS-DA model for all four groups.

**MDA (mean decrease accuracy) is calculated from all four groups using random forest model (500 trees).

Table 4-3. Representative metabolites detected by UHPLC-MS based metabolomics

Imputative Identities	Trend	Fold-change ^a	<i>p</i> -value ^a	<i>m/z</i>	RT ^b
-----------------------	-------	--------------------------	------------------------------	------------	-----------------

Ornithine	Down	>30	<0.001	87.1181	28.02
Spermine	Down	4.41	0.092	83.1720	29.07
Norspermidine	Down	8.50	0.022	87.0925	28.44
Putrescine	Down	>30	<0.001	65.5738	15.68
N1-Acetylspermine	Up	9.41	0.136	97.1730	7.28
L-Arginine	Down	16.77	0.058	59.0451	29.42
L-Threonine	Down	8.75	0.054	119.1435	3.42
L-Lysine	Up	29.67	0.063	102.1420	1.06
L-Carnitine	Up	>30	<0.001	116.1352	8.58
Cysteinyl-histidine	Up	>30	<0.001	141.0374	8.9
L-Cysteine	Up	>30	<0.001	56.1072	12.88
Ubiquinone-1	Up	>30	<0.001	99.1400	4.5
Biotin	Up	3.18	0.120	97.1293	8.02
Ubiquinone-4	Up	>30	<0.001	167.1993	6.09
Vitamin A2	Down	3.54	0.019	103.0739	5.73
Pantothenol	Up	>30	<0.001	84.1438	1.08
Homocystine	Down	>30	<0.001	105.1169	5.72
Betaine aldehyde	Down	14.75	0.048	103.0980	3.3
Betaine	Up	>30	<0.001	72.1071	6.69
Proline betaine	Down	>30	<0.001	98.1242	3.71
S-Farnesyl-L-cysteine	Down	>30	<0.001	124.1636	0.74
Taurine	Down	>30	<0.001	64.6602	9
3-Hydroxyl melatonin	Up	12.95	0.120	135.0381	14.11
L-Aspartyl-L-glutamic acid	Up	4.06	0.113	103.1263	23.82
N-Acetyl-L-aspartic acid	Up	>30	0.093	74.1146	1.6
Lactic acid	Down	3.43	0.060	66.0315	12.8
Valeric acid	Down	>30	<0.001	135.1012	12.29
Acetic acid	Down	>30	<0.001	121.0491	26.74
Phenylacetic acid	Down	1.62	0.019	61.1152	10.54
D-Phenyllactic acid	Up	>30	<0.001	121.0914	25.9
2-Keto-glutaramic acid	Up	>30	<0.001	64.1130	16.44

a. Fold-change and *p*-value were automatically calculated with one-way ANOVA by Progenesis QI. The quantitation was based on total ion intensity (area under curve) of extracted ion chromatogram (XIC) for the specific ion.

b. RT, aligned retention time of feature shown in total ion chromatograms (TICs) of UHPLC-LC-MS metabolomics.

Table 4-4. Gut-microbiota dependent metabolic pathways disrupted by AFB₁.

Pathway	Hits/Total ^a	<i>p</i> -value	FDR ^b
---------	-------------------------	-----------------	------------------

Protein biosynthesis	4/19	0.0001	0.0014
Methionine metabolism	4/24	0.0010	0.0054
Pantothenate and CoA biosynthesis	3/10	0.0001	0.0014
Glycine, serine and threonine metabolism	3/26	0.0014	0.0065
Pyruvate metabolism	3/20	0.0047	0.0115
Betaine metabolism	2/10	0.0003	0.0029
Cysteine metabolism	2/8	0.0009	0.0054
Arginine and proline metabolism	2/26	0.0039	0.0115
Urea cycle	2/20	0.0039	0.0115
Oxidation of branched chain fatty acids	2/14	0.0154	0.0265

a. The detected metabolites divided by the total number of metabolites in that pathway documented in MetaboAnalyst.

b. FDR, false discovery rate to conceptualize the rate of type I errors in null hypothesis testing when conducting multiple comparisons.

Table 4-5. Differential metabolites found by Random Forest and OPLS-DA models.

Random Forest model		OPLS-DA model	
Metabolite	Freq.	Metabolite	VIP

3-Decanol	0.94	2,4,6-Tribromophenol	1.51
D-Threitol	0.94	3-Decanol	1.27
Phenylacetic acid	0.92	Xanthylic acid	1.18
Pantothenol	0.86	Galactaric acid	1.13
2-Hexenoyl carnitine	0.52	Norspermidine	1.08
6-Thioinosine-5'-monophosphate	0.48	Nervonyl carnitine	1.06
1,2,3,4-Tetrahydro-beta-carboline	0.44	Pantothenol	1.05
3,6,10-Trimethyltetradecane	0.42	D-Threitol	1.04
3-Aminopropoxy guanidine	0.38	1,1'-Thiobisethanethiol	1.04
Nervonyl carnitine	0.36	2-Hexenoylcarnitine	1.04
Iso-Valeraldehyde	0.36	1-Nitrohexane	1.02
L-Lysine	0.34	3,4,5-Trimethoxy phenylacetate	0.97
5-Methoxytryptophol	0.30	Vitamin A2	0.95
Norspermidine	0.30	2,5-Dimethyl-2,4-hexadiene	0.95
Steroid derivative	0.30	6-Phenyl undecane	0.94

Abbreviations: Freq. (selected frequency), the percentage being selected by all individual trees in the ensemble in making decision (500 trees), indicating the relative importance of metabolite in clustering samples with different treatments; VIP (variance importance in projection), a measure of a metabolite's importance in clustering samples with different treatments, calculated a weighted sum of the squared correlations between the PLS-DA components and the original variable.

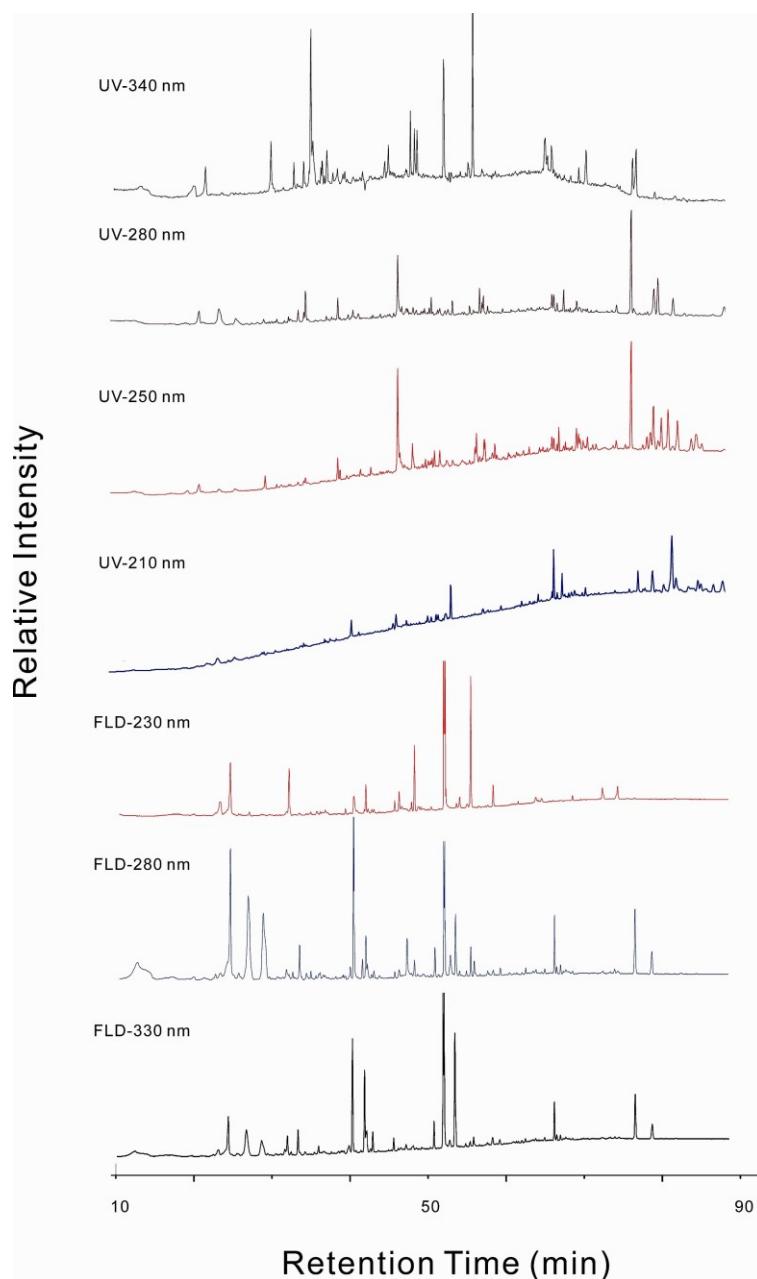


Figure 4-1. Representative chromatograms documented by UHPLC-profiling analysis of control sample. Signals were simultaneously collected from seven detective channels. The peaks were automatically labeled, picked and aligned by Chromeleon for further statistical analysis. UV bands 210 nm (UV-C), 254 nm (UV-C), 280 nm (UV-B) and 340 nm (UV-A) were set as monitor channels of DAD. FLD was employed with channels of excitation wavelength at 230 nm, 280 nm and 330 nm.

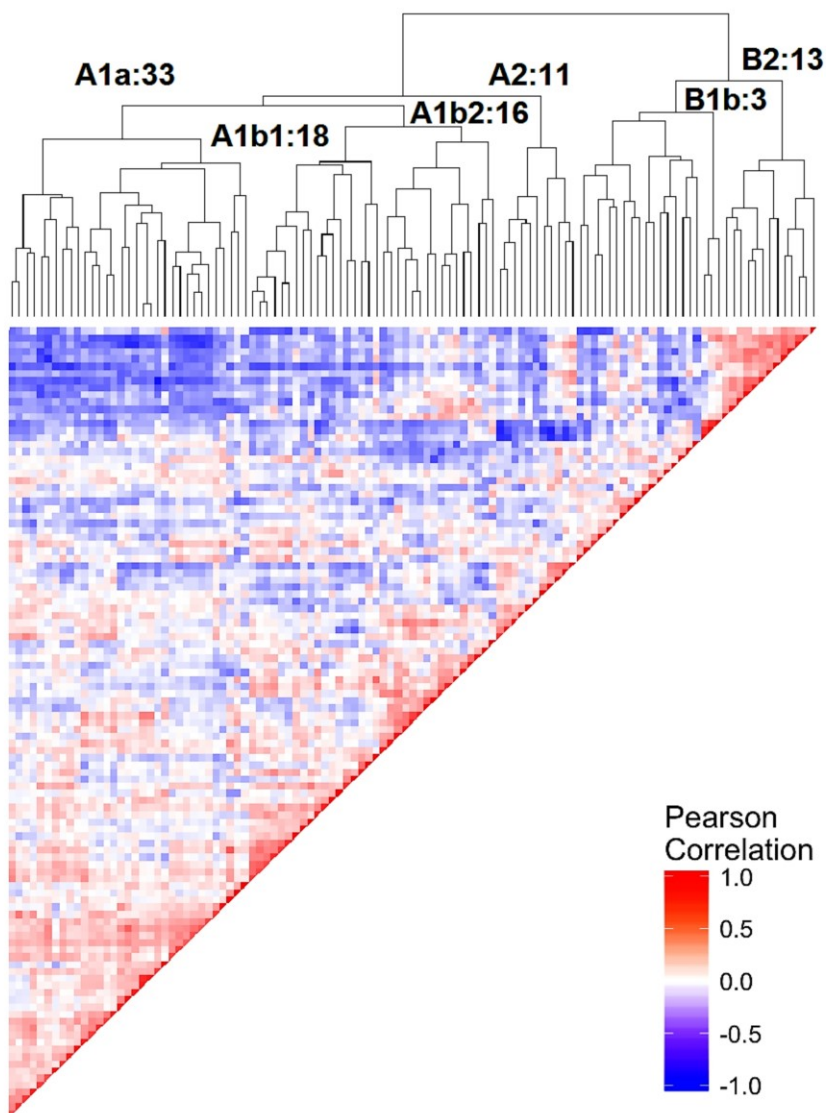
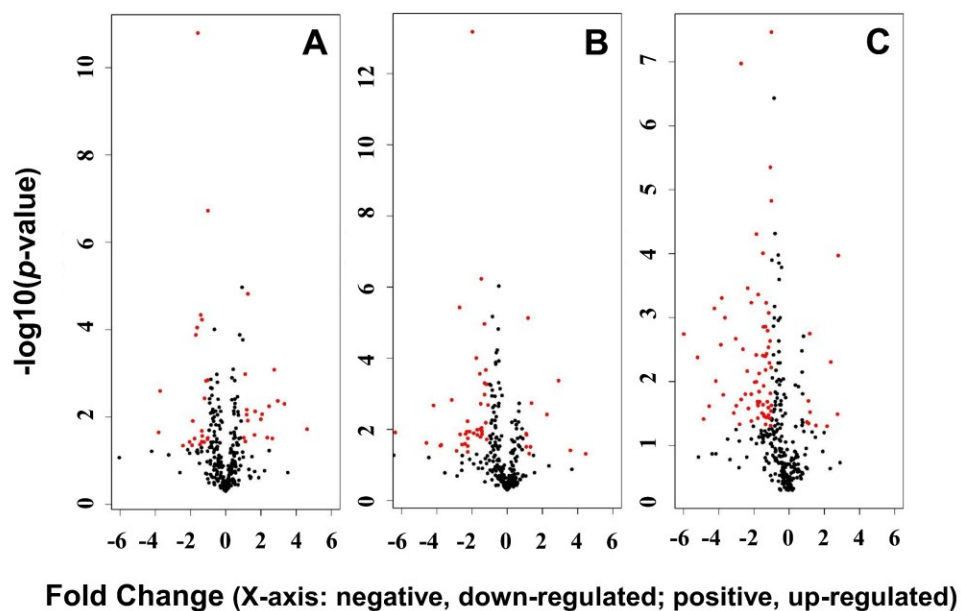


Figure 4-2. Heat map to show the correlations of 111 common metabolites upon AFB₁-treatment. The hierarchical reorganization was based on the Pearson's correlation coefficient. Data from seven detective channels were transformed to fold-change before correlation analysis and demonstrated normal distribution. Positive correlation is indicated by red color; negative correlation is indicated by blue color. The results indicated the necessity to perform multiple variable analysis (MVA) with dimension reduction technique, as well as the extensive metabolic pathway correlation.



<u>Low-Dose/Control</u>				<u>Middle-Dose/Control</u>				<u>High-Dose/Control</u>			
Up	Down	Lost	Gain	Up	Down	Lost	Gain	Up	Down	Lost	Gain
18	24	1	5	11	40	0	5	10	71	4	6

Figure 4-3. Volcano plots of all 335 differential metabolites detected by UHPLC-profiling analysis. The plots illustrate the global changes of gut-microbiota dependent metabolome in response to AFB₁ exposure of 3 different doses. Each dot represents a ratio of metabolite calculated by comparing the chromatographic intensity of the metabolite in the treatment group with that in the control group. The data for all metabolites are plotted as log₂ fold-change (X axis) versus the -log₁₀ of p-value (Y axis). The cut-off threshold for the screening of significant responding metabolites was set as fold-change > 2 and adjusted p < 0.05 by Welch's t-test, marked as red spots.

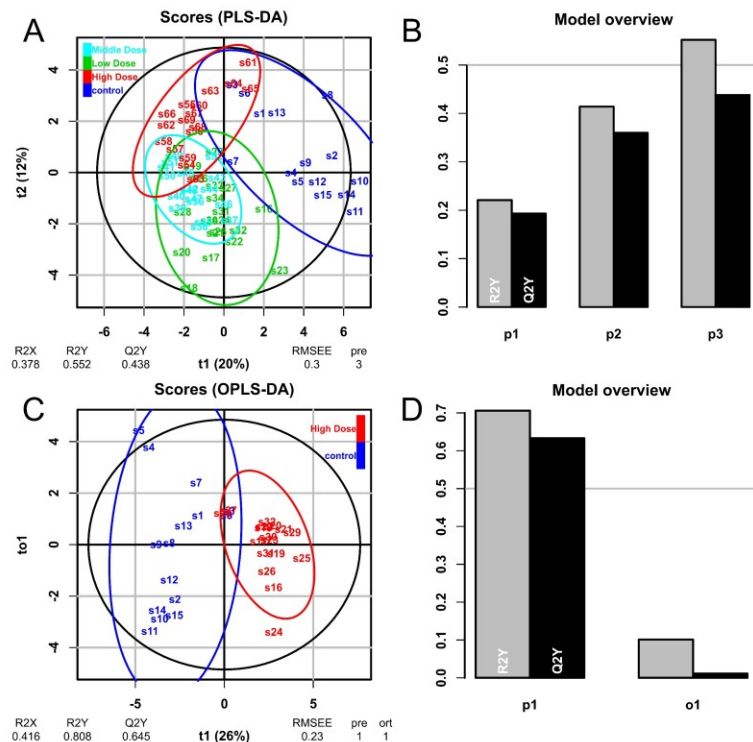
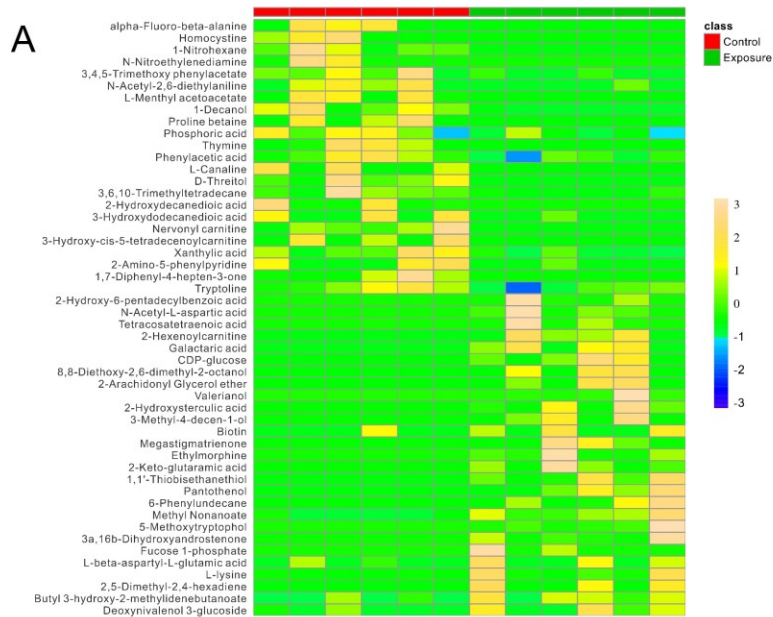
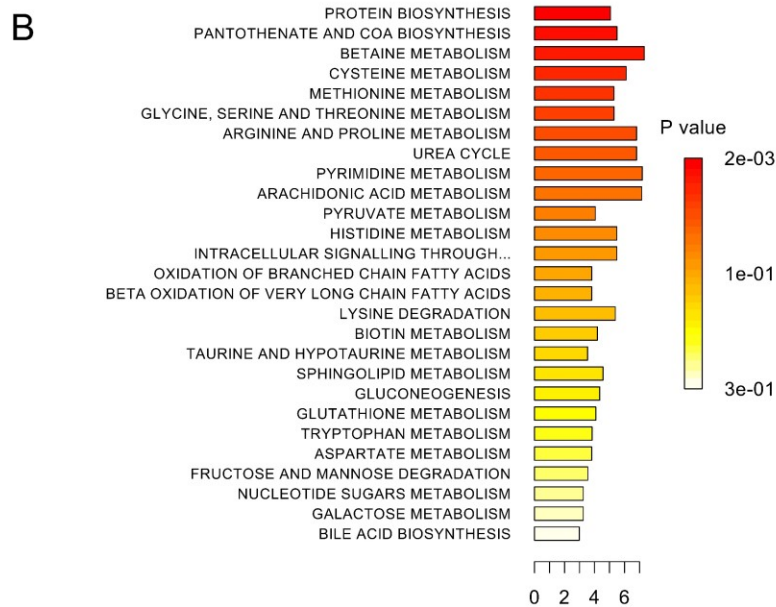


Figure 4-4. Examination of multiple variable analysis (MVA) models to extract differential metabolites from data pool. Supervised partial least squares (PLS) and Orthogonal (O) PLS: (A) score plots of PLS-DA, (B) model overview on the parameters of first three principal components of PLS, (C) score plots of OPLS-DA, (D) model overview on the parameters of first principal component of OPLS. Each dot represents a biological sample point. All data were auto-scaled and show normal distribution. Coordinates in axis are marked for illustration purpose only and selected arbitrary, and therefore do not have clear biological meanings. Percentage associated with each PC is the proportion of an eigenvalue for the respective PC in the sum of eigenvalues for all PCs. The components t_1 and t_2 are reflected on the horizontal and vertical axis respectively. The R2Y value is equivalent to the y-block cumulative variance captured, while the Q2Y is based on the 10 times cross-validated results and indicates predictive performance of the modeling.



Heat Map



Metabolite Set Enrichment Analysis

Figure 4-5. Overview of the does-responses of metabolites with significant dose-response to AFB₁-exposure and the biochemical pathways that are associated with these metabolites. (A) Heap map to show the dose-responses of top 50 significantly altered metabolites ranked by t-test. The map was constructed based on Euclidean distance with an algorithm of average distance, and data standardization via feature auto-scaling. (B) The biochemical pathways ranked by Metabolite Set Enrichment Analysis (MSEA). Specific statistical parameters are available in **Table 4-4**. Data were normalized by median and standardized by pareto-scaling.

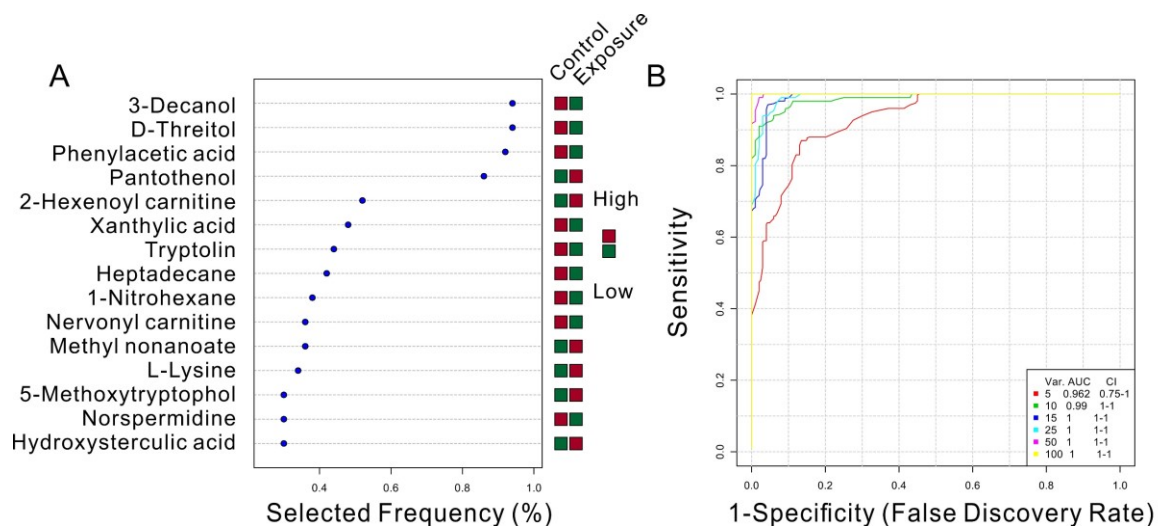


Figure 4-6. Evaluation of predictive power of indicative metabolites using receiver operating characteristic (ROC) curve based exploratory analysis (random forest model built-in). (A) Top 15 differential metabolites ranked according to the importance in discriminating samples with different treatments via random forest model (500 trees). (B) Validation of the differential metabolites extracted by random Forest model using ROC curves. ROC analysis was performed with built-in multivariate random forests algorithm. Monte-Carlo cross validation (MCCV) with balanced subsampling was used to generate ROC curves. ROC curves are based on all optional models averaged from all CVs. The 95% confidence interval was presented. In multivariate exploratory ROC analysis overview, feature importance was evaluated using two thirds (2/3) of the samples. The top 2, 3, 5, 10 ...100 (max) important features are then used to build classification models which is validated on the 1/3 the samples that were left out. ROC curves were used to compare the models with the combination of different number of features.

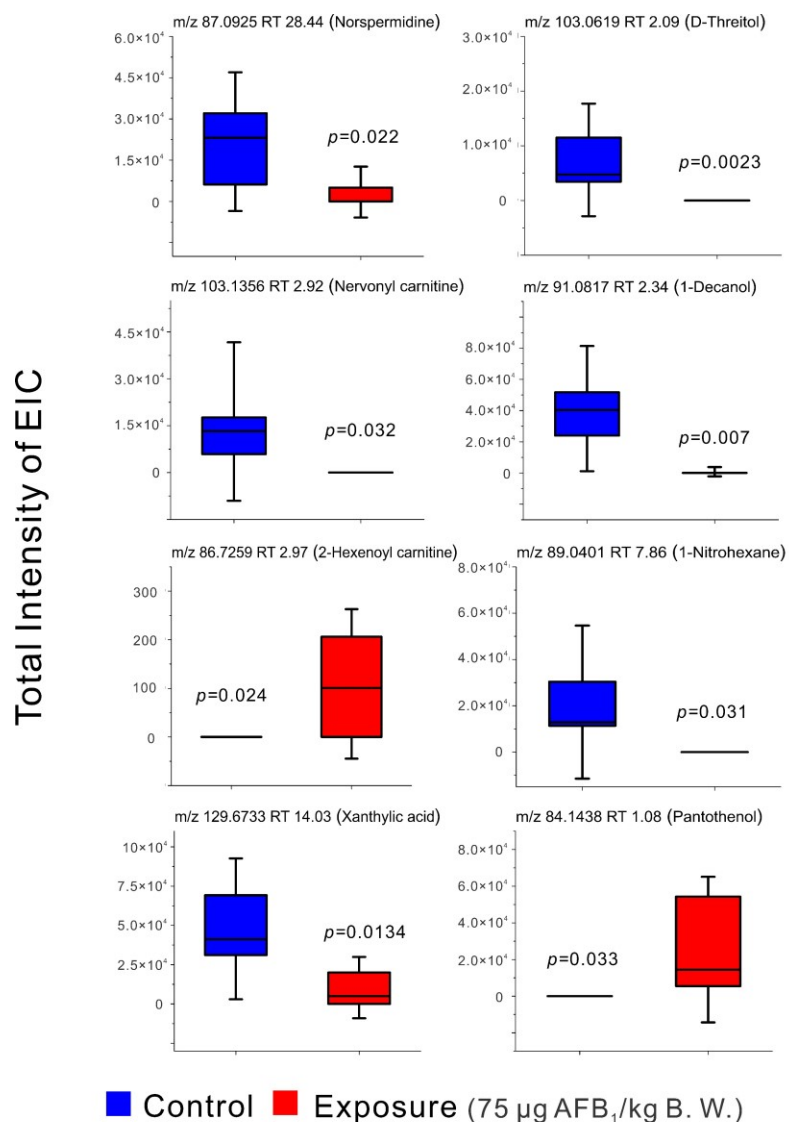
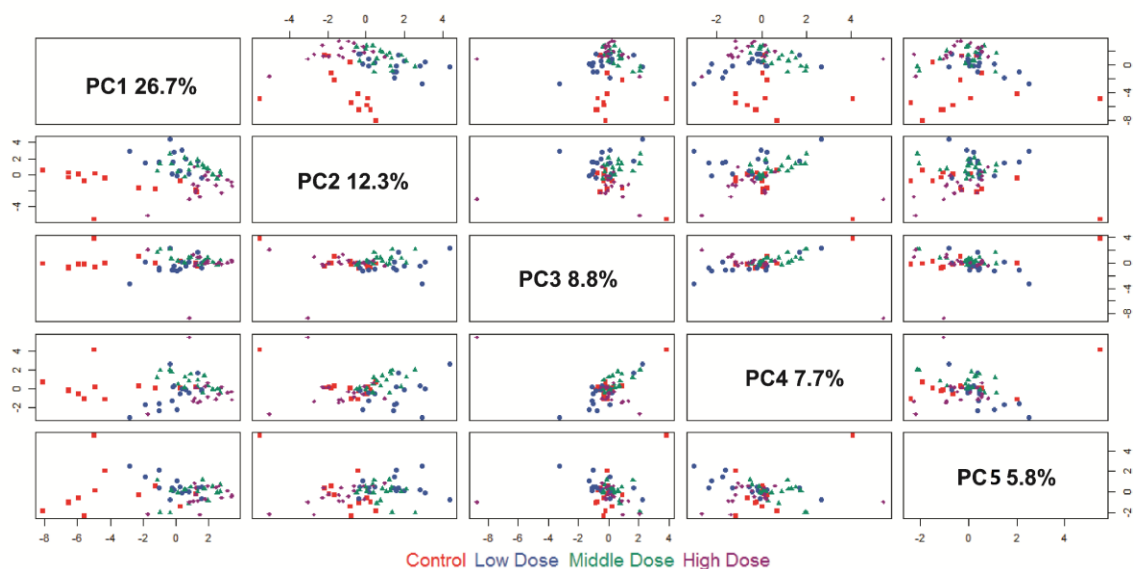


Figure 4-7. Box plots to show the alterations of indicative metabolites induced by AFB₁. The ion peak intensities were integrated from Extracted Ion Chromatograms (EICs) which were generated from the Total Ion Chromatograms (TICs) of metabolomics analysis in ESI (+) mode. The rat feces were from the experimental groups treated with 0 and 75 μg AFB₁/kg body weight (B. W.). Quantitative ions and retention times were noted on each box plots with imputative identifications acquired from HMDB. Non-parametric Mann-Whitney U test was applied for all comparisons ($n = 6$). Box plots represent 25%, 50% and 75% percentile of data. Vertical lines of box plots indicate standard deviation (SD), multiplied with an adjusting coefficient of 1.5 in order to stretch out from box.



SI Figure 4-1. Score plot matrix of relationships between first five principal components of PCA. Control, low-dose, middle-dose and high-dose correspond to 0, 5, 25, and 75 $\mu\text{g AFB}_1/\text{kg B. W.}$ doses, respectively. Overlapped area is found between groups of exposure. Clear separation was shown between exposure groups and controls. Coordinates in axis are for illustration purpose only and selected arbitrary and therefore do not have clear biological meanings. Percentage associated with each PC is the proportion of an eigenvalue for the respective PC in the sum of eigenvalues for all PCs. With PC1 to PC5, a regression function of AFB_1 exposure level was obtained with R squared of 0.458 between predicted AFB_1 dose and actual AFB_1 doses.

Reference

- Agostinelli, E., Tempera, G., Molinari, A., Salvi, M., Battaglia, V., Toninello, A., and Arancia, G. (2007). The physiological role of biogenic amines redox reactions in mitochondria. New perspectives in cancer therapy. *Amino Acids* **33**(2), 175-187.
- Alkasir, R., Li, J., Li, X., Jin, M., and Zhu, B. (2017). Human gut microbiota: the links with dementia development. *Protein Cell* **8**(2), 90-102.
- Andersen, B., and Frisvad, J. C. (2004). Natural occurrence of fungi and fungal metabolites in moldy tomatoes. *J Agric Food Chem* **52**(25), 7507-13.
- Barbosa, M. R. Chemical composition and formation of human feces-Problems and solutions of large mergers demographics in developing countries 2013.
- Beckonert, O., Keun, H. C., Ebbels, T. M., Bundy, J., Holmes, E., Lindon, J. C., and Nicholson, J. K. (2007). Metabolic profiling, metabolomic and metabonomic procedures for NMR spectroscopy of urine, plasma, serum and tissue extracts. *Nat Protoc* **2**(11), 2692-703.
- Brown, A. J., Goldsworthy, S. M., Barnes, A. A., Eilert, M. M., Tcheang, L., Daniels, D., Muir, A. I., Wigglesworth, M. J., Kinghorn, I., and Fraser, N. J. (2003). The Orphan G protein-coupled receptors GPR41 and GPR43 are activated by propionate and other short chain carboxylic acids. *J Biol Chem* **278**(13), 11312-11319.
- Calvani, R., Brasili, E., Praticò, G., Capuani, G., Tomassini, A., Marini, F., Sciubba, F., Finamore, A., Roselli, M., Marzetti, E., *et al.* (2014). Fecal and urinary NMR-based metabolomics unveil an aging signature in mice. *Exp Gerontol* **49**, 5-11.

- Caruso, U., Fowler, B., Minniti, G., and Romano, C. (1994). Determination of tryptophan and ten of its metabolites in a single analysis by high-performance liquid chromatography with multiple detection. *J Chromatogr A* **661**(1-2), 101-104.
- Cutler, D. R., Edwards, T. C., Jr., Beard, K. H., Cutler, A., Hess, K. T., Gibson, J., and Lawler, J. J. (2007). Random forests for classification in ecology. *Ecology* **88**(11), 2783-92.
- de Jonge, L. P., Douma, R. D., Heijnen, J. J., and van Gulik, W. M. (2012). Optimization of cold methanol quenching for quantitative metabolomics of *Penicillium chrysogenum*. *Metabolomics* **8**(4), 727-735.
- Determann, S., Lobbes, J. M., Reuter, R., and Rullkotter, J. (1998). Ultraviolet fluorescence excitation and emission spectroscopy of marine algae and bacteria. *Marine Chem* **62**(1-2), 137-156.
- Dettmer, K., Aronov, P. A., and Hammock, B. D. (2007). MASS SPECTROMETRY-BASED METABOLOMICS. *Mass Spectrom Rev* **26**(1), 51-78.
- Dorfman, L. (1953). Ultraviolet Absorption of Steroids. *Chem Rev* **53**(1), 47-144.
- Eaton, D. L., and Groopman, J. D. (2013). *The toxicology of aflatoxins: human health, veterinary, and agricultural significance*. Elsevier.
- Fujigaki, H., Yamamoto, Y., and Saito, K. (2017). L-Tryptophan-kynurenine pathway enzymes are therapeutic target for neuropsychiatric diseases: Focus on cell type differences. *Neuropharmacology* **112**, 264-274.
- Galindo-Prieto, B., Eriksson, L., and Trygg, J. (2014). Variable influence on projection (VIP) for orthogonal projections to latent structures (OPLS). *J Chemom* **28**(8), 623-632.

- Georgakoudi, I., Jacobson, B. C., Muller, M. G., Sheets, E. E., Badizadegan, K., Carr-Locke, D. L., Crum, C. P., Boone, C. W., Dasari, R. R., Van Dam, J., *et al.* (2002). NAD(P)H and collagen as in vivo quantitative fluorescent biomarkers of epithelial precancerous changes. *Cancer Res* **62**(3), 682-7.
- Goodwin, A. C., Destefano Shields, C. E., Wu, S., Huso, D. L., Wu, X., Murray-Stewart, T. R., Hacker-Prietz, A., Rabizadeh, S., Woster, P. M., Sears, C. L., *et al.* (2011a). Polyamine catabolism contributes to enterotoxigenic *Bacteroides fragilis*-induced colon tumorigenesis. *Proc Natl Acad Sci U S A* **108**(37), 15354-9.
- Goodwin, A. C., Murray-Stewart, T. R., and Casero, R. A., Jr. (2011b). A simple assay for mammalian spermine oxidase: a polyamine catabolic enzyme implicated in drug response and disease. *Methods Mol Biol* **720**, 173-81.
- Green, D. E. (1959). Electron transport and oxidative phosphorylation. *Advances in Enzymology and Related Areas of Molecular Biology, Volume 21*, 73-129.
- Guillarme, D., and Veuthey, J.-L. (2015). *UHPLC in life sciences*. Royal Society of Chemistry.
- Gunduz, N., and Fokoue, E. (2015). Robust classification of high dimension low sample size data. *arXiv preprint arXiv:1501.00592*.
- Hernandez Bort, J. A., Shanmukam, V., Pabst, M., Windwarder, M., Neumann, L., Alchalabi, A., Krebiehl, G., Koellensperger, G., Hann, S., Sonntag, D., *et al.* (2014). Reduced quenching and extraction time for mammalian cells using filtration and syringe extraction. *J Biotechnol* **182-183** (Supplement C), 97-103.

- Jiang, Y., Jolly, P. E., Preko, P., Wang, J. S., Ellis, W. O., Phillips, T. D., and Williams, J. H. (2008). Aflatoxin-related immune dysfunction in health and in human immunodeficiency virus disease. *Clin Dev Immunol* **2008**, 790309.
- Kaiko, G. E., and Stappenbeck, T. S. (2014). Host-microbe interactions shaping the gastrointestinal environment. *Trends Immunol* **35**(11), 538-48.
- Kamei, M., Fujita, T., Kanbe, T., Sasaki, K., Oshiba, K., Otani, S., Matsui-Yuasa, I., and Morisawa, S. (1986). The distribution and content of ubiquinone in foods. *Int J Vitam Nutr Res* **56**(1), 57-63.
- Khlangwiset, P., Shephard, G. S., and Wu, F. (2011). Aflatoxins and growth impairment: a review. *Crit Rev Toxicol* **41**(9), 740-55.
- Knipstein, B., Huang, J., Barr, E., Sossenheimer, P., Dietzen, D., Egner, P. A., Groopman, J. D., and Rudnick, D. A. (2015). Dietary aflatoxin-induced stunting in a novel rat model: evidence for toxin-induced liver injury and hepatic growth hormone resistance. *Pediatr Res* **78**(2), 120-7.
- LeBlanc, J. G., Milani, C., de Giori, G. S., Sesma, F., Van Sinderen, D., and Ventura, M. (2013). Bacteria as vitamin suppliers to their host: a gut microbiota perspective. *Curr Opin Biotechnol* **24**(2), 160-168.
- Lombard, M. J. (2014). Mycotoxin exposure and infant and young child growth in Africa: what do we know? *Ann Nutr Metab* **64**(Suppl. 2), 42-52.
- Luo, R. F., Misra, M., and Himmelblau, D. M. (1999). Sensor fault detection via multiscale analysis and dynamic PCA. *Ind Eng Chem Res* **38**(4), 1489-1495.

- Lyte, M. (2011). Probiotics function mechanistically as delivery vehicles for neuroactive compounds: Microbial endocrinology in the design and use of probiotics. *Bioessays* **33**(8), 574-581.
- Mace, K., Aguilar, F., Wang, J. S., Vautravers, P., Gomez-Lechon, M., Gonzalez, F. J., Groopman, J., Harris, C. C., and Pfeifer, A. M. (1997). Aflatoxin B₁-induced DNA adduct formation and p53 mutations in CYP450-expressing human liver cell lines. *Carcinogenesis* **18**(7), 1291-7.
- Martens, E. C., Koropatkin, N. M., Smith, T. J., and Gordon, J. I. (2009). Complex glycan catabolism by the human gut microbiota: the Bacteroidetes Sus-like paradigm. *J Biol Chem* **284**(37), 24673-7.
- Menter, J. M. (2006). Temperature dependence of collagen fluorescence. *Photochem Photobiol Sci* **5**(4), 403-10.
- Messaoudi, M., Violle, N., Bisson, J. F., Desor, D., Javelot, H., and Rougeot, C. (2011). Beneficial psychological effects of a probiotic formulation (*Lactobacillus helveticus* R0052 and *Bifidobacterium longum* R0175) in healthy human volunteers. *Gut Microbes* **2**(4), 256-61.
- Natarajan, N., and Pluznick, J. L. (2014). From microbe to man: the role of microbial short chain fatty acid metabolites in host cell biology. *Am J Physiol Renal Physiol* **307**(11), C979-C985.
- Patti, G. J., Yanes, O., and Siuzdak, G. (2012). Metabolomics: the apogee of the omic triology. *Nat Rev Mol Cell Biol* **13**(4), 263.

- Prasad Maharjan, R., and Ferenci, T. (2003). Global metabolite analysis: the influence of extraction methodology on metabolome profiles of *Escherichia coli*. *Anal Biochem* **313**(1), 145-154.
- Qian, G., Tang, L., Guo, X., Wang, F., Massey, M. E., Su, J., Guo, T. L., Williams, J. H., Phillips, T. D., and Wang, J. S. (2014). Aflatoxin B₁ modulates the expression of phenotypic markers and cytokines by splenic lymphocytes of male F344 rats. *J Appl Toxicol* **34**(3), 241-9.
- Qian, G., Tang, L., Lin, S., Xue, K. S., Mitchell, N. J., Su, J., Gelderblom, W. C., Riley, R. T., Phillips, T. D., and Wang, J.-S. (2016). Sequential dietary exposure to aflatoxin B₁ and fumonisin B₁ in F344 rats increases liver preneoplastic changes indicative of a synergistic interaction. *Food Chem Toxicol* **95**, 188-195.
- Qian, G., Wang, F., Tang, L., Massey, M. E., Mitchell, N. J., Su, J., Williams, J. H., Phillips, T. D., and Wang, J.-S. (2013a). Integrative Toxicopathological Evaluation of Aflatoxin B₁ Exposure in F344 Rats. *Toxicol Pathol* **41**(8), 1093-1105.
- Qian, G. Q., Tang, L. L., Wang, F., Guo, X., Massey, M. E., Williams, J. H., Phillips, T. D., and Wang, J. S. (2013b). Physiologically based toxicokinetics of serum aflatoxin B-1-lysine adduct in F344 rats. *Toxicology* **303**(1), 147-151.
- Ramautar, R., Berger, R., van der Greef, J., and Hankemeier, T. (2013). Human metabolomics: strategies to understand biology. *Curr Opin Chem Biol* **17**(5), 841-6.
- Ramirez, T., Daneshian, M., Kamp, H., Bois, F. Y., Clench, M. R., Coen, M., Donley, B., Fischer, S. M., Ekman, D. R., and Fabian, E. (2013). Metabolomics in toxicology and preclinical research. *Altex* **30**(2), 209.

- Rose, C., Parker, A., Jefferson, B., and Cartmell, E. (2015). The Characterization of Feces and Urine: A Review of the Literature to Inform Advanced Treatment Technology. *Crit Rev Environ Sci Technol* **45**(17), 1827-1879.
- Salari, H., Yeung, M., Douglas, S., and Morozowich, W. (1987). Detection of prostaglandins by high-performance liquid chromatography after conversion to p-(9-anthroyloxy)phenacyl esters. *Anal Biochem* **165**(1), 220-9.
- Sinha, R., Ahn, J., Sampson, J. N., Shi, J., Yu, G., Xiong, X., Hayes, R. B., and Goedert, J. J. (2016). Fecal Microbiota, Fecal Metabolome, and Colorectal Cancer Interrelations. *PLoS ONE* **11**(3), e0152126.
- Smith, P. M., Howitt, M. R., Panikov, N., Michaud, M., Gallini, C. A., Bohlooly-y, M., Glickman, J. N., and Garrett, W. S. (2013). The microbial metabolites, short-chain fatty acids, regulate colonic Treg cell homeostasis. *Science* **341**(6145), 569-573.
- Soto, M. E., Ares, A. M., Bernal, J., Nozal, M. J., and Bernal, J. L. (2011). Simultaneous determination of tryptophan, kynurenine, kynurenic and xanthurenic acids in honey by liquid chromatography with diode array, fluorescence and tandem mass spectrometry detection. *J Chromatogr A* **1218**(42), 7592-600.
- Sugahara, H., Odamaki, T., Fukuda, S., Kato, T., Xiao, J. Z., Abe, F., Kikuchi, J., and Ohno, H. (2015). Probiotic *Bifidobacterium longum* alters gut luminal metabolism through modification of the gut microbial community. *Sci Rep* **5**, 13548.
- Team, R. C. (2000). R language definition. *Vienna, Austria: R foundation for statistical computing*.

- Thomas, A. H., Lorente, C., Capparelli, A. L., Pokhrel, M. R., Braun, A. M., and Oliveros, E. (2002). Fluorescence of pterin, 6-formylpterin, 6-carboxypterin and folic acid in aqueous solution: pH effects. *Photochem Photobiol Sci* **1**(6), 421-6.
- Thomas, V., Clark, J., and Dore, J. (2015). Fecal microbiota analysis: an overview of sample collection methods and sequencing strategies. *Future Microbiol* **10**(9), 1485-504.
- Ursell, L. K., Haiser, H. J., Van Treuren, W., Garg, N., Reddivari, L., Vanamala, J., Dorrestein, P. C., Turnbaugh, P. J., and Knight, R. (2014). The intestinal metabolome: an intersection between microbiota and host. *Gastroenterology* **146**(6), 1470-1476.
- van den Berg, R. A., Hoefsloot, H. C., Westerhuis, J. A., Smilde, A. K., and van der Werf, M. J. (2006). Centering, scaling, and transformations: improving the biological information content of metabolomics data. *BMC Genomics* **7**, 142.
- Wang, J., Tang, L., Glenn, T. C., and Wang, J. S. (2016). Aflatoxin B1 Induced Compositional Changes in Gut Microbial Communities of Male F344 Rats. *Toxicol Sci* **150**(1), 54-63.
- Wang, J. H., Byun, J., and Pennathur, S. (2010). Analytical approaches to metabolomics and applications to systems biology. *Semin Nephrol* **30**(5), 500-11.
- Wang, J. S., and Groopman, J. D. (1999). DNA damage by mycotoxins. *Mutat Res* **424**(1-2), 167-81.
- Wold, S., Sjostrom, M., and Eriksson, L. (2001). PLS-regression: a basic tool of chemometrics. *Chemometrics and Intelligent Laboratory Systems* **58**(2), 109-130.

- Xia, J., and Wishart, D. S. (2002). Using MetaboAnalyst 3.0 for Comprehensive Metabolomics Data Analysis. *Curr Protoc Bioinformatics* 55(1), 14-10.
- Xia, J., and Wishart, D. S. (2016). Using metaboanalyst 3.0 for comprehensive metabolomics data analysis. *Curr Protoc Bioinformatics* 14 (10). 1-14.10. 91.
- Zeng, S., Long, W., Tian, L., Xie, S., Chen, Y., Yang, H., Liang, G., and Liu, Y. (2016). Effects of dietary aflatoxin B1 on growth performance, body composition, haematological parameters and histopathology of juvenile Pacific white shrimp (*Litopenaeus vannamei*). *Aquacult Nutr* 22(5), 1152-1159.
- Zhou, J., Tang, L., Wang, J., and Wang, J.-S. (2018). Aflatoxin B1 Disrupts Gut-microbial Metabolisms of Short Chain Fatty Acids, Long Chain Fatty Acids and Bile Acids in Male F344 Rats. *Toxicol Sci*
- Zivkovic, A. M., and German, J. B. (2009). Metabolomics for assessment of nutritional status. *Curr Opin Clin Nutr Metab Care* 12(5), 501.

CHAPTER 5. AFLATOXIN B₁ DISRUPTS GUT-MICROBIOTA DEPENDENT
METABOLIC PATHWAYS OF CALORIFIC CARBOHYDRATES, AMINO ACIDS,
ORGANIC ACIDS AND LIPIDS MALE F344 RATS

5.1 Introduction

Our preliminary studies have demonstrated the adverse effects of aflatoxin B₁ (AFB₁) on gut-microbiota community structure and dependent metabolites in F344 rats. Here, the adverse impact was explored using both gas chromatography-electron ionization-quadrupole mass spectrometer (GC-EI-Q-MS) and high-resolution liquid chromatography hybrid linear ion trap-orbitrap mass spectrometer (HRLC-LTQ-Orbitrap MS). Male F344 rats were daily gavaged with 0, 5, 25 and 75 µg AFB₁ kg⁻¹ body weight. The feces collected in week 4 were used for analysis. A total of 1490 features were aligned from the raw data collected by GC-MS using XCMS. Sixty out of top 100 differential features were imputatively identified based on NIST database. For the raw data collected by HRLC-LTQ-Orbitrap MS, 3925 MS1 features were aligned using MZmine, whereas 2498 MS2 features (234 groups) were aligned using XCMS. The MS1 m/z and MS2 fragmentation patterns matched 86 metabolites documented in Human Metabolome Database (HMDB), MassBank and METLIN databases. The key metabolites altered by AFB₁ belong to carbohydrates, amino acids, bile constituents, phospholipids, glycerolipids, and fatty acids. The top 5 impacted metabolic pathways revealed by (a) GC-MS and (b) nanoHRLC-MS/MS include—(a): valine-leucine metabolism; bile acid and steroid synthesis; GTPs

Synthesis; N-acetyl-D-glucosamine synthesis; carbohydrate conversion; (b): retinol metabolism; glycerolipid metabolism; pentose and glucuronate interconversion; glycerophospholipid metabolism; arginine and proline metabolism. The results are highly consistent with previous findings, suggesting that the impairment of gut-microbiota by AFB₁ is an important contributor to the AFB₁-induced stunted growth and the disruptions of liver-gut axis, immune function and energy homeostasis in rats.

AFB₁ is a Group 1 carcinogen that can induce hepatocellular carcinoma (HCC) in human (Wang and Groopman, 1999). It has a TD50 of 0.0032 mg kg⁻¹ day⁻¹ in rats (Gold *et al.*, 2005). The mycotoxin is generated by *Aspergillus Flavus* and *A. Parasiticus*—two fungus that can easily grow on the cereals and groundnuts at a routine temperature (24 °C–35 °C), and the fungal colonization could be easily boosted by moderate humidity (Wang and Groopman, 1999). In recent years, the global climate change and extreme weather conditions have driven the contamination of AFB₁ to become an emerging risk for food safety in the world wide, and, in turn, more effort has been put on the investigation of adverse effects of AFB₁ (Battilani *et al.*, 2016; Mary *et al.*, 2017; Sriwattanapong *et al.*, 2017).

“Next-generation sequencing” techniques have uncovered an extremely complex gut-microbiota in gastrointestinal tracts of human and other mammals (Peisl *et al.*, 2017; Qin *et al.*, 2010). The microbial flora contains over 1000 bacterial species and 100-fold more genes than host genome (Huang *et al.*, 2017). Substantial data have uncovered the intricate interaction between the gut-microbiota and host health—an interplay that influences a variety of aspects of host health, e.g. fat storage, energy metabolism, immune function, central neuron system (CNS) function, and cardiovascular circulation (Chi *et al.*,

2017; Gao *et al.*, 2017; Yoo *et al.*, 2015). Could AFB₁ affect gut-microbiota in human and animals and further lead to adverse health outcomes? Our previous 16S rRNA sequencing and metabolic profiling analyses of feces have shown that oral exposure to AFB₁ may induce community structure change of gut-microbiota and affect gut-microbiota dependent nutritional provision (Wang *et al.*, 2016; Zhou *et al.*, 2018). A set of key metabolites tightly associated with the liver-gut axis and immune system were found to be altered by AFB₁ in male F344 rats (Qian *et al.*, 2014; Qian *et al.*, 2016; Qian *et al.*, 2013; Qian *et al.*, 2012). At this point, more specific evidences are needed in order to elucidate the changes of specific metabolic pathways.

Metabolomics is considered to be a proper approach to investigate gut-microbiota dependent metabolic pathways since it is able to capture the changes of hundreds to thousands of metabolites and nutrients present in complex metabolome (Peisl *et al.*, 2017). However, as an integrative analytical approach, the detective scope of metabolomics depends on a number of factors including sample pre-treatment, instrumental design and settings, the modes of detector and data collection, statistical analysis, bioinformatic interpretation of data, as well as the consistency with reference data (Beger *et al.*, 2016; Dunn *et al.*, 2017; Peisl *et al.*, 2017). As such, multiple platforms may be together employed to explore gut-microbiota and its physiological significances.

Currently, both gas chromatography–mass spectrometry (GC-MS) and liquid chromatography–mass spectrometry (LC-MS) are widely used to perform metabolomics analysis, since they have different detective scopes (Barbosa, 2013; Chi *et al.*, 2017; Smirnov *et al.*, 2016). With similar instrumental parameters and columns, GC-EI-Q MS usually generates reproducible fragmentation patterns for the targeted analytes, making it

an integral and comparable tool to elucidate the metabolic pathway changes for most sample types (Grün *et al.*, 2008; Trimigno *et al.*, 2017). The constant ionization energy and standardized instrumental settings have generated highly reproducible standard fragment-rich mass spectra in the fields of metabolomics, environmental chemistry, pharmacology, and gut-microbiota studies etc. (Garcia and Barbas, 2011; Shadoff *et al.*, 1977). To extend the detective scope of metabolites, here we also applied “high resolution LC linear ion trap-Orbitrap Hybrid MS” (nanoHRLC-LTQ-Orbitrap MS) to perform rapid untargeted LC/MS/MS metabolomics analysis. The core unit of the system is the C-trap united linear ion trap and Orbitrap analyzer, which ensures an integration of collision-induced dissociation (CID) and orbitrap that can largely fasten MS/MS analysis (Kalli *et al.*, 2013). The gut-microbiota dependent biochemical pathways that were disrupted by AFB₁ were summarized using open-access cheminformatics databases, metabolite set enrichment analysis (MSEA), pathway analysis and network analysis (Shannon *et al.*, 2003; Shen *et al.*, 2016). By applying these statistical models and bioinformatics methods we aim to reveal the gut-microbiota dependent metabolic pathways disrupted by AFB₁ and retained a small number of key metabolites for further structural elucidation.

5.2 Method and materials

5.2.1 Chemicals and reagents

Pyridine, dimethyl sulfoxide (DMSO), Aflatoxin B₁ (purity \geq 98%), 2-deoxy-d-ribose, D-mannose, D-ribitol, D-fructose, D-ribose, D-galactose, D-glucose, D-galactitol, N-acetyl-D-glucosamine, *myo*-inositol, D-lactose, D-trehalose, L-lysine, L-proline, L-alanine, L-tyrosine, methoxyamine, and *N,O*-bis(trimethylsilyl)trifluoroacetamide

(BSTFA) with 1% trimethylchlorosilane (TMCS) were all purchased from Sigma-Aldrich Inc. (St. Louis, MO, USA). Methanol, acetonitrile, formic acid, water and chloroform of GC-MS grade were purchased from J. T. Baker (Phillipsburg, NJ, USA). AFB₁ stock solution (25 mg mL⁻¹) was prepared in DMSO and was freshly diluted upon dosing.

5.2.2 *Animal study*

One hundred male F344 rats (100–120 g) were purchased from Harlan Laboratory (Indianapolis, IN, USA). Upon arrival, animals were allowed for one week of environmental acclimation, and were divided into 4 groups, with 5 cages per group. The 4 experimental groups were then gavaged with 0, 5, 25, and 75 mg AFB₁ kg⁻¹ body weight (B. W.) day⁻¹, respectively. Animals were daily dosed from Monday to Friday per week in a consecutive duration of 5 weeks. The animal housing environment was under controlled light/dark cycle (12 hr) with a temperature of 22 ± 2 °C and relative humidity of 50 to 70%. Purified AIN 76A diet and tap water were maintained every day. The detailed protocol was validated and reported in our previous publications, including body indexes, histopathological assessment, and AFB₁-Lys pharmacokinetic data (Qian *et al.*, 2014; Qian *et al.*, 2016; Qian *et al.*, 2013). From week 2 to week 4, rat feces were daily collected for each cage and pooled by each week. All samples were stored in –80 °C freezer until using. Animal husbandry and care, dosing and sample collection were in strict accordance with the requirements and regulations of the Institutional Animal Care and Use Committee at the University of Georgia.

5.2.3 *Sample extraction and derivatization prior to GC-MS analysis*

Cold methanol was used to perform sample quenching and extraction of global metabolites (de Jonge *et al.*, 2012). Briefly, a pellet of 50 mg frozen rat feces was taken to a tube which contained pre-loaded glass beads (PowerLyzer, i.d. 0.1 mm, Mo Bio, Carlsbad, CA). Four hundred milliliter of $-80\text{ }^{\circ}\text{C}$ cold methanol was immediately added. Then the fecal pellet was sufficiently grinded using a fine glass pestle. An aliquot of $800\text{ }\mu\text{L}$ chloroform was mixed with the sample and the tube was vortexed for 15 min. After vortex, an aliquot of $400\text{ }\mu\text{L}$ water was added into the tube to achieve phase separation. The tubes were then well sealed before frozen centrifugation at 12,000 rpm for 10 min and then placed into the refrigerator at $4\text{ }^{\circ}\text{C}$ for 5 min stabilization. Following this step, $100\text{ }\mu\text{L}$ upper phase and $100\text{ }\mu\text{L}$ lower phase were taken from the sample extract and re-combined in a new tube. The mixture was dried using a centrifugal evaporation. After dryness, $300\text{ }\mu\text{L}$ methanol was added to bring down the liquid left on the wall and further evaporation was continued until sample extract is fully dried. For each group, 6 sub-samplings were randomly conducted for each of the 5 pooled samples, totally generating 120 measurements of GC-MS. After thorough dryness, a volume of $80\text{ }\mu\text{L}$ methoxyamine (15 mg mL^{-1} pyridine) was added into the glass tube. An aliquot of $2\text{ }\mu\text{L}$ 5 mg mL^{-1} epigallocatechin gallate (EGCG) in pyridine was spiked as internal standard in order to eliminate instrumental and operational bias, since EGCG is present in the end part of chromatogram and leaves no disturbance on the other components (**Figure 5-1**). The glass tubes then underwent vortex for 10 min of homogenization, followed by a frozen centrifugation at 4000 rpm for another 10 min to collect the liquid left on the tube wall. The solution was finally transferred to standard glass sample vial and were placed into an air bath shaker, keeping at $35\text{ }^{\circ}\text{C}$ for 90 min to process derivatization. After that, an aliquot of $80\text{ }\mu\text{L}$

BSTFA with 1% TMCS was carefully spiked into the vial to process the second step of derivatization at 70 °C for 12 hours. For nanoLC-MS/MS analysis, the sample supernatants from control group and middle dose group (25 mg AFB₁ kg⁻¹ B. W. day⁻¹) were directly taken out for analysis without derivatization (n = 6).

5.2.4 GC-MS condition

GC-EI-Q MS metabolomics was performed in an Agilent 5973-6890 system equipped with a J&W DB-5MS column. Ultra-high purity grade helium was used as carrier gas. The front inlet was set as splitless mode with gas-saver and a heating temperature of 275 °C. The ion source temperature was set at 230 °C and quadrupole temperature was set at 150 °C. The injection volume was 2 µL. The flow rate was 0.6 mL min⁻¹. The oven initial temperature was 50 °C. After a holding time of 2 mins, the oven temperature ramped to 320 °C at a rate of 3.5 °C min⁻¹, followed with a holding time for 10.5 min at 320 °C. To protect MS detector, a solvent delay time of 10.5 min was applied. Full-scan mode was performed with m/z ranged from 50 to 800. The representative total ion chromatogram (TIC) is shown in **Figure 5-1**. The labeled peaks were confirmed by spiking standard chemicals.

5.2.5 nanoLC-CID-MS/MS condition

Untargeted LC-MS metabolomics was performed in a Thermo Orbitrap Elite™ Hybrid Ion Trap-Orbitrap Mass Spectrometer equipped with a nanoC18 column (length, 130 mm; i.d., 100 µm; particle size, 5 µm; pore size, 150 Å; max flow rate, 500 nL/min; packing material, Bruker Micron Magic 18). It has a maximum resolution power of over

120,000 at m/z 400 for a 768 ms transient. A further advancement comes from the coupled nanoLC system, which may significantly avoid the nebulization at high temperature and therefore keeps more analytes stable for detection. Mobile phase A is 0.1% formic acid/water solution; mobile phase B is 0.1% formic acid/acetonitrile. A volume of 10 μ L of each sample was injected for analysis. A constant flow rate of 500 nL/min was applied to perform a gradient profiling with the following proportional change of solvent A (v/v): 0 to 1.5 min at 98% A, 1.5 to 15.0 min from 98% to 75% A, 15.0 to 20.0 min from 75% to 40% A, 20.0 to 25.0 min from 40% to 5% A, 25.0 to 28.0 min kept at 5% A, 28.0 to 30.0 min from 5% to 98% A, and the washing elution ended with a 4 min of re-equilibration. The LTQ-Orbitrap Elite MS was set in positive full scan mode within range of 50 to 1500 m/z . Settings of the electrospray ionization were: heater temperature of 300 °C, sheath gas of 35 arbitrary unit, auxiliary gas of 10 arbitrary unit, the capillary temperature of 350 °C and source voltage was +3.0 kV. Collision-induced dissociation (CID) scan with a Fourier transform resolving power of 120,000 (transient = 192 ms; scan repetition rate = 4 Hz) at 400 m/z over 50–1500 m/z was used to induce MS/MS fragmentation (Najdekr *et al.*, 2016). The following settings were applied: activation value q_c of 0.25, the activation time of 10 ms and normalized collision energy of 35%. The applied collision energy for CID mode is suggested by Thermo Fisher and is considered to be proper for informative fragmentation of the majority of small molecule compounds. The cloud plot generated by XCMS and the data normalization conducted by MetaboAnalyst were presented in **Figure 5-8 A and B**.

5.2.6 Data processing and statistics

Raw GC-MS files were submitted to XCMS for peak picking, isotope grouping, and alignment. The total intensities of extracted ion chromatography (EIC) was automatically integrated for each feature ion, and were then normalized using cyclic locally weighted scatterplot smoothing (LOESS) technique before further analysis (Savage, 1972). A two-tailed Welch's t-test was used to test the significance of fold change and the *p* value was adjusted for multiple comparisons before further data-mining (Storey *et al.*, 2004). After peak deconvolution via Agilent AMDIS modules, the fragmentation pattern of the peaks containing the interested features were searched through National Institute of Standards and Technology (NIST) Standard Reference Database to characterize the entities of these chemicals. The imputatively identified metabolites were searched through Human Metabolome Database (HMDB) to acquire functional and pathway information. Non-parametric Mann-Whitney U test was used to examine the significance of fold change for the metabolites that were determined by standard calibration ($n = 10$). Principal component analysis (PCA), supervised partial orthogonal least squares projection to latent structures (OPLS-DA) and Random Forest were applied to the dataset in order to extract PCs and key metabolites. Metabolite set enrichment analysis and pathway enrichment analysis were conducted to reveal the biochemical pathways disrupted by AFB₁ according to Xia *et al.* (Shen *et al.*, 2016). KEGG-based compound-gene network analysis was performed in CytoScape 3.0 in order to reveal the global compound-gene correlation and the biochemical pathways disrupted by AFB₁ (Saito *et al.*, 2012).

nanoLC-CID-MS/MS data were initially processed using MZmine 2.29 (Pluskal *et al.*, 2010). The steps of processing include baseline-correction, MS1 detection,

chromatogram building, deconvolution, isotope grouping, and peak alignment through linear mode random sample consensus (RANSAC). Specifically, baseline-correction was performed with m/z bin of 1, based on amu of base peak. Asymmetric baseline corrector was used as correcting method with a smoothing factor of 1 and asymmetry factor of 0.001. The method used for MS1 detection was wavelet transform. The wavelet transform was set with noise level of 15000, scale level of 10 and wavelet window size of 20%. The centroid was set with a noise level of 500. Chromatogram deconvolution was based on the wavelet algorithm. The used parameter includes S/N threshold of 20, wavelet scale between 0.25 and 5, and a peak duration range from 0 to 10. The isotope grouping was based on m/z tolerance of 0.006 or 20 ppm and the tolerance of retention time was 0.5 min. RANSAC aligner was set with a m/z tolerance of 0.005 amu or 20 ppm, retention time tolerance of 1.5 min and 0.5 min after correction. The iteration of RANSAC was 100 with a minimum number of points 30%. The processed dataset was normalized by sum, auto-scaled and showed well-shaped normal distribution by examining density plot (van den Berg *et al.*, 2006). A one-tailed Welch's t-test with adjusted- p value (q) was used to examine the significance of change (Hochberg and Benjamini, 1990; Storey *et al.*, 2004). XCMS was used to form fragmentation patterns so that the results of MS1 searching can further rely on fragmentation-based identity characterization once it is available in HMDB, MassBank or METLINE. Similar with GC-MS data processing, the enriched pathway analysis, principal component analysis (PCA), supervised partial orthogonal least squares projection to latent structures (OPLS-DA) and Random Forests models were performed using MetaboAnalyst (Shen *et al.*, 2016).

5.3 Results

5.3.1 GC-MS metabolomic analysis

The chemical derivatization protocol suggested by manufacturer (Sigma-Aldrich, MO, USA) was briefly optimized. **SI Table 5-1** shows the peak number generated when different reaction temperature and solvent were tested according to the suggested derivatization protocol. Shown in **SI Table 5-2**, we examined the extracting efficacy of several frequently used solvent mixtures, including methanol/methyl tert-butyl ether/water (2:2:1), BUME (butanol/methanol at 3:1) and several adjusted Folch system solvents (Eggers and Schwudke, 2016; Howlett *et al.*, 2017; Lofgren *et al.*, 2016). Of them, a mixture of methanol, chloroform and water with ratio of 1:2:1 generated highest scanning peak number of 1094 ± 69 .

For convenience, in the following part of this article the four experimental groups treated with 0, 5, 25, and 75 mg AFB₁ kg⁻¹ B. W. day⁻¹ are noted as control, low-dose, middle-dose and high-dose groups, respectively. The peak detection, deconvolution, alignment and integration of GC-MS data were processed through XCMS online modules. After data pre-treatment, 1490 feature ions were aligned from the 120 measurements of the fecal samples. Seen from the volcano plots of total feature ions (**Figure 5-2**), the counts of significantly upregulated features (> 1.5 -fold, $q < 0.05$) were 278, 405 and 10 in the low-dose, middle-dose and high-dose groups, respectively. The down-regulated features demonstrated straightly decreasing trend, with count number of 638, 902 and 1106 showing in the three AFB₁-treated groups (**Figure 5-2 D**). The top 100 differential feature ions were imputatively identified by searching their fragmentation pattern through NIST database and a set of 60 metabolites were identified. Compared with the control group, there were

43 down-regulated and 17 elevated metabolites in the middle-dose group. Of note, there were 127 feature ions showing increasing trend from low-dose to middle-dose treatment (**Figure 5-2 B and C**). Most of these components were later attributed to carbohydrates and amino acids. **Figure 5-3** shows the heatmap of the normalized intensities of these metabolites in the control and middle-dose groups. The major categories of these metabolites include carbohydrates, organic acids, steroids and amino acids (**SI Table 5-3**). In addition to the fragmentation pattern based imputative identification through NIST database, we also determined fecal concentrations of 16 structurally similar carbohydrates and amino acids using standard calibration method. The quantitative parameters such as regression curves, lower limit of detection and recoveries were all included in **Table 5-1**. A set of 16 structurally similar carbohydrate and amino acid standards were spiked to determine their concentrations in feces. Significant changes were confirmed for 11 of them (**Figure 5-4**). The fecal concentrations of these 11 metabolites are listed in **Table 5-2** and **Figure 5-4**.

To extract the key metabolites altered by AFB₁. The 60 imputatively identified metabolites were further analyzed using principal component analysis (PCA). **SI Figure 5-2 A** shows the matrix of the clusters separated by the first 5 principal components (PCs). PC1 to PC5 together explained 91.4% variance of values, and the regression constructed with them showed a fair R² of 0.697 between the actual values and the predicted values of exposure level (**SI Figure 5-2 B**). The binary supervised model of OPLS-DA (**Figure 5-5**) was next applied to extract the key metabolites according to the method published by Etienne *et al* (Giacomoni *et al.*, 2015). The ‘double-check’ of supervision includes the R2 and Q2 quality metrics and 10 times permutation diagnostics. Permutation diagnostics

generated a R2Y of 0.858 and a Q2Y of 0.845. The first PC predicts 31% of data variance. Differential metabolites were obtained by inputting extracted ion intensities of the identified metabolites obtained in middle-dose group into OPLS-DA model. By doing so, a list of metabolites with VIP score over 1 was obtained (**SI Table 5-3**). Random Forest model was also applied to find the key metabolites by further ranking the components according to mean decrease accuracy (MDA) score (**Figure 5-6** and **SI Table 5-3**).

5.3.2 nanoLC-MS/MS metabolomic analysis

A total of 3923 MS1 features were found by MZmine with the settings mentioned in material and method part. There were 140 MS1 features showing q -value < 0.05 . Their chemical entities were imputatively characterized by searching through HMDB. In addition, data were processed with XCMS online module and generated 234 feature groups, containing 2498 MS2 features. The fragmentation patterns were searched through “fragment similarity search” module offered by METLIN and the results were used together with MS1 to characterize the identification of metabolites. By performing the above two approaches, 86 metabolites were imputatively identified (**SI Table 5-5**). The total intensities of MS1 integrated from extracted ion chromatography (EIC) were used for quantitative analysis for these metabolites, the data were normalized by sum, pareto-scaled, and then used for quantitative analysis according to material and method part of this article. **Figure 5-9** shows the heatmap of these metabolites. There were 36 metabolites showing elevated intensities and 48 metabolites showing decreased intensities following treatment.

Figure 5-10 A shows the OPLS-DA scores plot. In the OPLS-DA model, the explained sum of squares for T (x) and orthogonal T (y) were found to be 71.2% and 11.2%, respectively. Three parameters R2X, R2Y and Q2Y were used to supervise the validity of the OPLS-DA model through 10-fold cross validation (**Figure 5-10 B**). R2X and R2Y represent the fraction of the variance of the x and y variable explained by the model, while Q2Y suggests the predictive performance of the model. The model reported R2X value of 0.712, R2Y value of 0.96 and Q2 value of 0.939. Therefore, we the 86 metabolites could well represent the change of fecal metabolome caused by AFB₁. To extract distinct metabolites from dataset, OPLS-DA model and Random Forests model were both used. **Table 5-4** shows the ranking of the signature metabolites which were extracted using both OPLS-DA and Random Forest models. The annotations, retention time, and m/z of these signature metabolites were listed in **SI Table 5-5**. **Figure 5-11** shows the relative intensities (auto-scaled and normalized intensities) of the differential lipids between control and exposure groups.

5.4 Discussion

We profiled the changes of fecal metabolome induced by AFB₁ and observed extensive dose-dependent shift of the metabolome (**Figure 5-2**). Data showed that AFB₁ disrupted fecal long chain fatty acids, cholesterol, amino acids and carbohydrates in a remarkable way. Analytical parameters for a set of key carbohydrates and amino acids were fixated using standard calibration (**Table 5-1**) and the concentrations of these compounds in different dose groups were shown in **Table 5-2**. We found accumulation of calorific carbohydrates and reduction of beneficial pentoses. The signature metabolites that were

stimulated by AFB₁ were extracted using a combination of different statistical models, presented in **Figure 5-5**, **Figure 5-6** and **Table 5-3**. Finally, to assess the impact of AFB₁ on the metabolic pathways we employed both pathway impact analysis (**Figure 5-7**) and gene-compound network analysis (**SI Figure 5-1**).

Shown in **SI Table 5-1**, Pyridine outperformed DMSO and DMF with the least number of background peaks. DMSO resulted in unacceptable noise peak number. The disturbing peak number reached approximate 500 counts though apparently highest peak counts was gained. With respect to the reaction temperature used for the derivatization with methoxyamine hydrochloride, the scanned peaks under the selected three reaction temperatures, i.e. 35 °C, 55 °C and 70 °C, were found to generate comparable results. A temperature of 35 °C was finally selected for derivatizing reaction. In terms of the second step of derivatization with BSTFA (1% TMCS), we tested the suggested time and found that a reaction time of 12 hour is sufficient to achieve the maximum peak number. The efficiency of extraction of metabolites for different extracting solvents were evaluated and compared (**SI Table 5-2**). The adjusted Folch-system was finally selected to perform the sample extraction since it detected highest peak number with least background peaks, probably benefited by the combination of aqueous and organic phases. As briefly mentioned in the introduction part, the instrumental settings for GC-MS based metabolomics are basically comparable with similar instrumental settings conducted in different labs. It generates stable fragmentation of analyzed metabolites though the detective scope for GC-MS mainly targets the small molecules of less polarity (Beger *et al.*, 2016). Variation of data quality, however, could be caused by the sample extraction and derivatization procedures. The most significant checkpoints to pinpoint the

variabilities are the solvents used for sample extraction and derivatization, as well as the temperature and time to process derivatization. These factors need to be examined before instrumental analysis since the efficacy of extraction is dependent on the specific biochemical properties of sample (Beger *et al.*, 2016; Calvani *et al.*, 2014; Dettmer *et al.*, 2007; Dunn *et al.*, 2017; Garcia and Barbas, 2011). After validation, we applied the derivatization to analyze the extract of rat feces.

Upon AFB₁ treatment, the metabolome demonstrated dose-response at global level (**Figure 5-2**). The counts of the significantly elevated features (> 1.5-fold, $q < 0.05$) were 278, 405 and 10 in the low-dose, middle-dose and high-dose groups, and the down-regulated features were of 638, 902 and 1106 in the 3 exposure groups. In the high-dose group the components were all reduced (**Figure 5-2 C**), with many feature ions completely fell out of detective range. To include these data into statistical analysis and model fitting may result in statistical errors, thus this dataset was excluded from further analysis. Next, we located the total ion chromatogram (TIC) peaks that contain the top 100 significantly altered feature ions (ranked by Welch t-test) after deconvolution of chromatogram using AMDIS. The identities of these peaks were imputatively annotated according to the fragmentation pattern documented in NIST database. Seen from **SI Table 5-3**, GC-EI-Q MS revealed the changes of metabolites that belong to a wide range of categories, including carbohydrates, amino acids, fatty acids, steroids and derivatives. Since the chemical entities of these metabolites were imputative, further discussion of biological significance was based on categorical level.

We found that in the middle-dose group the utilization of carbohydrate was generally suppressed, since a number of calorific carbohydrates were accumulated in the

feces. The remarkable decrease of the count of metabolites in the high-dose group might be caused by the deficient gut-microbiota dependent catabolism of carbohydrates and amino acids as carbon source or “raw materials” to produce secondary metabolites (**Table 5-2** middle-dose group). Severe disruption of metabolisms was also observed in the metabolites of other categories, such as long chain fatty acids, short chain fatty acids and bile constituents. To explain these changes, related literatures were searched and collected, and possible mechanisms were given to explain the changes induced by AFB₁. Only middle-dose group was used to compare with control, since volcano plots already showed the global changing trend of metabolome were consistent with the increase of AFB₁ dose, and both low-dose and high-dose groups contain too little useful information.

The accumulated carbohydrates and related derivatives include: glucose (2.72 fold, standard calibration), rhamnose (3 fold), fructose (3.69 fold, standard calibration), turanose (2.038 fold), galactose (2 fold, standard calibration), galactitol (1.538 fold), glycerol (1.355 fold), ribose (1.26 fold), 3-beta-D-galactosyl-sn-glycerol (1.36 fold), arabinose (1.39 fold), and trehalose (12.23 fold, standard calibration) (**Table 5-2** middle-dose group data and **SI Table 5-3**). The results suggest a suppressed utilization and metabolism of calorific carbohydrates of gut-microbiota. In agreement with such change, a group of secondary or degradative metabolites of these carbohydrates showed decrease changes, including, threose (0.598), arabitol (0.845), N-acetyl glucosamine (0.894 fold), mannose (0.85 fold, standard calibration). Mannose can be produced from fructose or glucose by microbial mannose isomerases and further used as basic components of bacterial cell wall (Cleasby *et al.*, 1996; Elbaz and Ben-Yehuda, 2010). Straightforward decrease was seen in 2-deoxy-D-ribose. The concentration of this deoxy pentose was reduced to 37% of control in low-

dose group, and 40% of control in middle-dose group. The monosaccharide is a preferred carbon source for diarrhea-associated pathogens with deoxyribose kinase (Martinez-Jehanne *et al.*, 2009), so that the decrease might be induced by the domination of diarrhea-associated pathogens which largely consumed 2-deoxy-D-ribose as carbon source. Of note, three primary carbohydrates: glucose, fructose and trehalose, which are utilized by most gut-microbial strains as carbon source, were all elevated in feces. Such pronounced accumulation suggested suppressed intensities of the majority of gut-microbial strains upon AFB₁ exposure.

SCFAs and related derivatives were mostly reduced in the middle-dose group, such as acetic acid (0.745 fold), lactic acid (0.445 fold), formic acid (0.648 fold), butanoic acid (0.736 fold), 3-hydroxybutyric acid (0.44 fold), 6-hydroxyhexanoic acid (0.656 fold), 2-hydroxybutanedioic acid (0.792 fold), ethanedioic acid (0.888 fold), 2,5-dihydroxyphenylacetic acid (0.628 fold), vinylformic acid (0.605 fold). This suggests that the synthetic pathways of SCFA and secondary metabolites were blocked or suppressed by AFB₁. Short or medium chain aliphatic acids, especially SCFAs, are able to maintain the nutritional and immunomodulatory functions of host physiology (Sun and O'Riordan, 2013). The entry of small molecule aliphatic acids into bacterial cytoplasm is through free diffusion across the bacterial membrane in nonionized form. Once inside the bacterial cytoplasm, the nonionized acids undergo dissociate and result in accumulation of protons, which evokes inhibitory effect on numerous pathogens such as *Clostridium Difficile*, *Streptococcus Mutans*, *S. Gordonii*, *S. Sanguis*, *Candida albicans* (Huang *et al.*, 2011; May *et al.*, 1994), but not the probiotic strains that belong to *Lactobacillus sp*, *Bifidobacterium sp*, and *Saccharomyces boulardii* etc (Amaya-Farfan, 1999). Plus, many reports also

revealed the positive association between the intestinal amount of organic acids and villus heights in duodenum and jejunum, as well as inhibited intestinal infectious processes (Mohammadagheri *et al.*, 2016). There is a mechanistic link between catabolism of calorific hexoses and microbial synthesis of short chain fatty acids (Louis *et al.*, 2014). Thus, the reduction of SCFAs and derivatives were likely resulted from deficient catabolism of calorific carbohydrates caused by AFB₁ treatment. By contrast, food-sourced long chain fatty acids were found to be accumulated in the feces (**Figure 5-1**), including arachidonic acid (7.27 fold), 9,12-octadecadienoic acid (1.436 fold), octadecanoic acid (1.103 fold), oleic acid (1.297 fold) and erucic acid (1.517 fold). This indicates that the absorption of food-sourced long chain fatty acids was affected by AFB₁. In accordance with the absorption of these long chain fatty acids, a number of possible secondary metabolic products or metabolic intermediates of them also demonstrated decreasing trend in feces, including 2,6,10,14-tetramethyl pentadecanoic acid (0.677 fold), dihydroxy octadecatrienoic acid (0.772 fold), and 9,10-12,13-diepoxy-octadecanoate (0.753 fold). The absorption of long chain fatty acids and production of SCFAs were previously found to be driven and mediated by the gut-microbiota shown in rat and zebra fish models (Groopman *et al.*, 1992; Rabot *et al.*, 2010; Semova *et al.*, 2012). Data from these works also showed that *Firmicutes* strains may increase the number of lipid droplets in enterocytes by facilitating the absorption, whereas *Bacteroidetes* or *Proteobacteria* strain could not. Therefore, the alteration of SCFA and fatty acid levels observed in the middle-dose exposure group might be caused by the community structure change induced by AFB₁, which were shown in our previous 16s rRNA sequencing data (Tang *et al.*, 2015).

The levels of cholesterol metabolites in feces were universally reduced, such as cholesterol (0.547 fold), cholesterol ester (0.786 fold), chenodeoxycholic acid (0.795 fold), (22R)-20 α ,22-dihydroxycholesterol (0.447 fold), (22R)-22-hydroxycholesterol (0.797 fold), 5-cholestene (0.711 fold), and cholest-5-ene-3 β ,7 α -diol (0.935 fold). Since these metabolites are produced in liver as derivatives of cholesterol, their consistent decreases indicate disruption of cholesterol metabolism in liver (Chrostek *et al.*, 2014). This is in line with our previous observations on the hepatic pathogenesis and development of liver cancer in same study design (Qian *et al.*, 2013).

In the middle-dose group L-lysine, L-proline and L-tyrosine were all elevated over 2-fold in feces. Food-sourced proteins are hydrolyzed into peptides and amino acids by both host- and bacteria secreted proteases and peptidases (Gaudet *et al.*, 2015). Therefore, the reduced level of these amino acids in the low-dose group might be resulted by the suppressed microbial exo-enzymes (i.e. extracellular enzymes) such as proteases and peptidases. However, with the increase of dose, both the diversity and intensity of gut-microbiota were reduced (Tang *et al.*, 2015). In accordance with this change, the endo-enzymes (i.e. cytoplasmic enzymes)-based modification and metabolism were suppressed and finally resulted in the accumulation of metabolites in feces. Such enzyme-based explanation could also apply to mannose and N-acetyl-D-glucosamine. The two carbohydrates demonstrated divergent trends of change, possibly because of the dose-dependent sequence of inhibition on exo-enzymes and endo-enzymes.

According to above discussion, the metabolomics data suggest that AFB₁ disrupted gut-microbiota dependent metabolisms of SCFA, long chain fatty acids, cholesterol, amino acids and carbohydrates. These changes may further induce a wide range of adverse health

outcomes in the experimental rats. PCA was next used to examine whether these metabolites could stand for the global metabolic changes induced by AFB₁. As a major type of unsupervised discriminant multivariate analysis (MVA), the assumption of PCA is that all observed variables are correlated with underlying variables which are corresponding to the clustering of subjects. The analysis provides basic information on the dependent structures of data and predictive model for the exposure. Importantly, PCA is considered to be a practical indicator of PLS-DA or OPLS-DA model reliabilities (Worley and Powers, 2016). Seen from **SI Figure 5-2**, PC1 to PC5 explained 91.4% data variance. The principal component regression (PCR) analysis constructed with them showed linear regression coefficient of 0.697 between the actual values and the predicted values of exposure level (**SI Figure 5-2 B**). This indicates that sample pre-treatment process successfully retained the differential composition between control and exposure groups, and the GC-MS metabolomics protocol properly profiled these components.

The binary supervised model of OPLS-DA was next applied to extract the key metabolites altered by AFB₁ according to the method published by Etienne et al (Thévenot et al., 2015). Seen from **Figure 5-5**, the “double-check” of supervision includes the R² and Q² quality metrics and 10 times permutation diagnostics. Both higher R²Y of 0.858 and Q²Y of 0.845 were shown with $p < 0.05$ for the permutation diagnostics, which justified the fitness of the model. The first predictive component predicts 31% of data variance. Differential metabolites were obtained by inputting extracted ion intensities of the identified metabolites obtained in middle-dose group into OPLS-DA model. There were 10 metabolites with VIP score over 1 revealed by OPLS-DA (**Table 5-3**). We found that the mean decrease accuracy (MDA) based ranking of metabolites provided by Random

Forests model is consistent with the VIP score-based ranking (**Table 5-3** and **Figure 5-6**). The 10 metabolites with high VIP score were all included in the MDA based ranking list, including D-lactic acid, 3-hydroxybutyric acid, erucic acid, cholesterol, 20 α , 22R-dihydroxycholesterol, N-acetyl-L-alanine, α , α -trehalose, L-arabinose, galactitol and turanose. The metabolite panel was considered to be the signature metabolites in response to AFB₁ treatment. These metabolites also stand for the several major metabolite categories affected by AFB₁, such as carbohydrates, amino acids, long chain fatty acids, SCFAs, and cholesterol derivatives.

We applied metabolite set enrichment analysis to summarize the metabolic changes occurred at pathway level. The results from control and middle-dose groups were used for MSEA and pathway enrichment analysis, which uses the records documented in KEGG database (Shen *et al.*, 2016). The disrupted biochemical pathways are listed on **Figure 5-7 A**, with the topological presentation shown in **Figure 5-7 B**. The most significantly altered metabolic pathways were found to be galactose metabolism, protein biosynthesis, propanoate metabolism, and several metabolic pathways of amino acids (valine, leucine, isoleucine, alanine etc.). In addition, glycolysis, glycogenesis, pyruvate pathway, and homeostasis of global energy supply are also among the most severely affected pathways. In general, the biochemical pathways correlated by KEGG-based enrichment analysis are consistent with the literature-based data interpretation. We also constructed KEGG-based network to reveal the global compound-gene correlation (**SI Figure 5-1**). The reports from several bioinformatics methods were generally consistent.

The AFB₁-induced liver pathogenesis has been analyzed and characterized by our previous works (Qian *et al.*, 2013). Here nanoLC-MS/MS metabolomics found a set of

signature fats and lipids that are associated with gut-liver axis. To be specific, we identified 18 signature metabolites by applying statistical modeling analysis (**Figure 5-10, Table 5-4, and Figure 5-11**). Though their specific structures cannot be confirmed at this point, the chemical entities estimated by HMDB, Massbank and METLIN indicate that they belong to lipids, including fatty acyls, glycerolipid and glycerophospholipid. Of them, we found elevated levels of diglyceride (DG), monoacylglyceride (MG), 19,20-dihydroxy-4Z,7Z,10Z,13Z,16Z-docosapentaenoic acid (19,20-DiHDEPA), phosphatidylethanolamine, PC(DiMe(9,3)/DiMe(9,3)), S-(2-Methylbutanoyl)-dihydrolipoamide, and palmitoyl glucuronide. Usually these lipids are carried by bile from liver to gut, and their elevation may be resulted by AFB₁-induced hepatic steatosis (Amaya-Farfan, 1999; Jeannot *et al.*, 2012). Propionic acid is able to inhibit lipogenesis and cholesterologenesis in liver (Demigne *et al.*, 1995; Hara *et al.*, 1999). The reduced supply of propionic acid from gut to liver may also contribute to the elevated lipids, and such reduction was reported by our previous work. The hepatic steatosis was further indicated by the increase of other three signature metabolites: 5beta-pregnane-3alpha,21-diol-11,20-dione, 11beta,20-dihydroxy-3-oxopregn-4-en-21-oic acid (DHOPA) and 3-oxo-4,6-choladienoic acid. The first two metabolites are transformed from corticosterone in liver and then carried to gut by bile. Hypercortisolism is associated with steatosis, obesity and metabolic syndrome (Tarantino and Finelli, 2013). The increase of 3-oxo-4,6-choladienoic acid is consistent with the elevation of fecal bile acid that was formerly reported. The rat diet did not contain extra lipids. The elevated lipids in gut were more likely transported from liver. In fact, after fourth weeks of treatment, histological examination found liver steatosis and cirrhosis induced by the treatment of AFB₁ (Qian *et al.*, 2016; Qian *et al.*, 2013). Similar with lipids,

the elevation of vitamin A and derivatives (retinol and 4-oxo-retinoic acid) may also be resulted from the damaged liver tissue, since vitamin A is fat-soluble and is stored in the liver. Liver regulates a variety of biochemical reactions in detoxification of drugs and metabolism of nutrients or metabolites. It takes a central role in plasma protein synthesis, hormone synthesis, as well as maintenance of glucose and lipid homeostasis. There are numerous studies reporting that oral exposure to AFB₁ could affect lipid metabolism in liver, including tri-, di-, monoglycerides, glycerolipid, cholesterol and phospholipids etc. Lu et al. have reported disruption of hepatic gluconeogenesis and lipid metabolism following acute AFB₁ exposure in rat (Lu *et al.*, 2013).

L-carnitine can facilitate the catabolism of medium- to long-chain fatty acids by transporting acyl- group into mitochondria where the carbon chain undergoes β -oxidation (Miller *et al.*, 2002). Endogenous synthesis of L-carnitine is an important metabolic function of the liver, and part of synthesized L-carnitine is released into gut through bile (Groopman *et al.*, 1992). There are several reports demonstrating that liver diseases, such as primary biliary cirrhosis and other liver diseases (Fortin, 2011; Tang *et al.*, 2015). We found a 37.8-fold down-regulation of L-carnitine in the feces from the exposure group. This remarkable reduction of L-carnitine could be caused by liver cirrhosis, for which specific histological examination was reported previously (Qian *et al.*, 2013).

The other signature metabolites (**Table 5-4**) include L-urobilin, creatine, propyl decanoate, 7-hexadecenoic acid methyl ester and 5,8-tetradecadienoic acid. Creatine is produced in liver and kidney. The synthesis relies on methionine, glycine, and arginine, and two enzymes, i.e. l-arginine:glycine amidinotransferase (AGAT) and guanidinoacetate methyltransferase (GAMT) (da Silva *et al.*, 2009). Creatine was almost not detected in the

exposure group. It was reported before that decline in hepatic functional capacity results in reduced creatine production (MacAulay *et al.*, 2006), thus the observed reduction of fecal creatine might be caused by the liver damages. L-urobilin, propyl decanoate, 7-hexadecenoic acid methyl ester and 5,8-tetradecadienoic acid were found to be reduced by over 40 folds. L-urobilin and propyl decanoate are microbial derivatives of liver-secreted bilirubin and food-contained decanoic acid, respectively. 7-hexadecenoic acid methyl ester belong to mono-unsaturated fatty acids, which can be synthesized by microbes through both anaerobic and aerobic pathways (Russell and Nichols, 1999). Conversion from arachidonic acid to 5,8-tetradecadienoic acid could occur through the peroxisomal oxidative enzymes from gut-microbiota (Spector *et al.*, 1997). The reduction of the acid suggested dysfunction of related enzymes. During steatosis, extra lipids were produced in liver, and were further brought to gut through bile excretion. Once entering gut, these lipids could change the composition of gut-microbial strains. It has been widely known that diet with high concentration of lipids and fats could enrich certain gut-microbial strains that are associated with obesity, metabolic syndrome, as well as several types of cardiovascular diseases in human and animal models (Chang *et al.*, 2011; Guo *et al.*, 2017; Lecomte *et al.*, 2015; Murphy *et al.*, 2015). Hybrid LTQ-Orbitrap LC-MS seems to be a proper platform for further lipidomic analysis of bile constituents in the future.

5.5 Conclusion

Gut-microbiota are able to impart specific function in the metabolism of nutrients in host. The regulation is realized via the small molecules produced by gut microbiota, including the food-derived micronutrients, microbial signaling molecules and a small

portion of host secreted molecules from bile and gut epithelium (Scheppach *et al.*, 1994). The major categories include aliphatic acids, lipids, hydrocarbons, phenyl acids, bile compositions, vitamins, steroids, amino acids, organic amines and a rich pool of microbe-derived secondary metabolites of these components. These metabolites offer a wide range of functions, and some of them can be easily detected since they have considerable high concentrations shown in feces. The gut-microbial metabolome thus plays a dominant role in regulating the development and performance of host systems, organs, and tissues. By contrast, the disruption of gut-microbiota is associated with many gastrointestinal diseases, hepatic diseases, cancer, obesity, autism and a variety of allergic or inflammatory symptoms (Smith *et al.*, 2017). Our findings in the current study generally agree with these knowledges.

In this work, we captured the alteration of fecal metabolites from AFB₁-treated F344 male rats using GC-MS and nanoLC-MS/MS based metabolomics. To mine useful information from the metabolomics data, multiple statistical models and bioinformatics tools were applied. The data were acquired using validated methods with sufficient sample size, three dose levels and pretreatment of sample. The biological explanation and interpretation were consistent with previous pathological findings and the results of 16S rRNA analysis. Taken together, oral exposure to AFB₁ in F344 male rats may disrupt gut-microbial utilization of carbohydrates and amino acids, absorption of food-sourced long chain fatty acids, bile synthesis and secretion, and also largely reduce production of SCFAs (Zhou *et al.*, 2018). The adverse health outcomes predicted from metabolomics data may be further examined in future, and the structures of key metabolites could be structurally elucidated.

TABLES

Table 5-1. Analytical parameters of GC-MS analysis used for the measurement of amino acids and carbohydrates.

Compound	RT	Q Ion	Regression Equation ^a	R ²	Recovery ^b	Linear Range ^c	LLOD ^d
2-Deoxy-D-ribose	32.55	73	$y = 1e-06x + 6.4$	0.996	0.222	1.25–400	0.625
D-Mannose	35.93	73	$y = 2e-07x - 0.66$	0.999	0.203	1.25–400	0.625
D-Ribitol	37.35	73	$y = 1e-07x - 1.2$	0.998	0.239	1.25–400	0.625
D-Fructose	41.68	73	$y = 1e-06x - 2.03$	0.996	0.232	1.25–400	0.625
D-Ribose	42.14	73	$y = 9e-07x - 14.5$	0.996	0.257	1.25–400	0.625
D-Galactose	42.20	73	$y = 3e-07x - 2.42$	0.999	0.298	1.25–400	0.625
D-Glucose	42.42	73	$y = 1e-06x - 16.57$	0.991	0.562	1.25–400	0.625
D-Galactitol	43.50	73	$y = 4e-06x - 9.89$	0.993	0.305	1.25–400	0.625
GlcNAc	47.34	73	$y = 1e-06x + 12.36$	0.999	0.249	1.25–400	0.625
<i>myo</i> -inositol	47.46	73	$y = 4e-07x - 10.31$	0.995	0.193	1.25–400	0.625
D-Lactose	61.39	73	$y = 1e-06x - 4.96$	0.995	0.249	1.25–400	0.625
D-Trehalose	62.62	73	$y = 1e-06x - 11.92$	0.991	0.217	1.25–400	0.625
L-Proline	22.4	307	$y = 1e-05x + 22.75$	0.944	0.243	9–575	4.5
L-Lysine	43.01	174	$y = 6e-06x + 16.84$	0.993	0.133	15.6–500	7.8
L-Tyrosine	43.52	218	$y = 9e-07x + 32.87$	0.998	0.358	25–400	12.5
L-Alanine	15.3	116	$y = 2e-06x + 101.4$	0.992	0.267	75–1200	37.5

Abbreviation: RT, retention time; Q Ion, most abundant fragment ion used for quantitation; R², linear regression coefficient; LLOD, lower limit of detection; GlcNAc, N-Acetyl-D-glucosamine.

a. Y, ng μL^{-1} of analyte; X, peak area. The ion peak intensities used for quantitation were integrated from Extracted Ion Chromatograms (XICs).

b. Recovery rate was calculated from blank extract containing ~50%, ~100% and ~200% concentrations of an analyte measured in mixed sample extract (n = 10, control group).

Recovery% = (amount of analyte measured in the spiked extract – analyte amount measured in the extract) \times 100/(spiked analyte amount in the extract). Blank extract was generated from the samples that were thoroughly washed. Blank extract was generated from samples which were thoroughly washed.

c. The range in which regression curve maintains $R^2 > 0.99$. Unit of linear range is $\mu\text{g mL}^{-1}$.

d. The analyte level which generated a signal-to-noise (S/N) ratio of 3 was noted as the LLOD for that analyte. The unit of LLOD is $\mu\text{g mL}^{-1}$.

Table 5-2. Fecal concentrations of key carbohydrates and amino acids determined by standard calibration (Figure 5-5).

Metabolite	Dose*	Concentration in feces (ng mg ⁻¹)					
		Mean	STD	Median	Ratio	Trend	<i>p</i> **
2-Deoxy-D-ribose	0	1375.07	183.15	1275.78			
	5	508.59	77.26	494.47	0.37	Down	<0.0001
	25	545.92	152.91	502.45	0.40	Down	<0.0001
D-Mannose	0	340.69	111.86	357.69			
	5	122.38	37.59	135.84	0.36	Down	0.001
	25	288.69	77.18	294.29	0.85	Down	0.112
D-Fructose	0	12022.08	2510.93	12087.09			
	5	15262.07	3238.84	15724.89	1.27	Up	0.049
	25	44408.66	16726.81	46244.21	3.69	Up	<0.0001
D-Galactose	0	2175.87	582.41	2180.88			
	5	1886.38	449.48	1981.40	0.87	Down	0.257
	25	4346.70	3070.31	3118.29	2.00	Up	0.226
D-Glucose	0	9746.52	1550.97	9879.19			
	5	10767.25	3039.79	10215.85	1.10	Up	0.597
	25	26544.67	5334.65	28526.41	2.72	Up	<0.0001
N-Acetyl-D-glucosamine	0	768.87	120.28	749.39			
	5	495.31	56.19	478.17	0.64	Down	<0.0001
	25	835.15	198.60	845.66	1.09	Up	0.288
D-Trehalose	0	496.06	197.91	519.84			
	5	2008.69	1219.08	1530.23	4.05	Up	<0.0001
	25	6068.40	1780.92	5441.29	12.23	Up	<0.0001
L-Lysine	0	3037.01	881.80	2711.68			
	5	1174.31	361.46	1229.62	0.39	Down	<0.0001
	25	7602.95	2660.96	6759.64	2.50	Up	<0.0001
L-Proline	0	18758.05	2919.63	19441.99			
	5	20710.88	11028.55	17906.75	1.10	Up	<0.0001
	25	48716.21	12224.2	51352.98	2.60	Up	<0.0001
L-Alanine	0	14354.25	3238.78	14853.32			
	5	3346.25	435.66	3138.63	0.23	Down	<0.0001
	25	12905.08	5026.46	12094.36	0.90	Down	0.364

	0	1378.64	247.42	1374.36			
L-Tyrosine	5	1155.53	216.34	1045.81	0.84	Down	0.034
	25	2726.71	595.30	2525.14	1.98	Up	<0.0001

* mg AFB₁ kg⁻¹ B. W. day⁻¹.

** Kruskal-Wallis H test, n = 10.

Table 5-3. Key metabolites (GC-MS) extracted by Random Forests and OPLS-DA models.

Random Forests model		OPLS-DA model	
Component	MDA	Component	VIP
(22R)-20alpha,22-Dihydroxycholesterol	0.055	D-Lactic acid	1.383
D-Lactic acid	0.040	alpha, alpha-Trehalose	1.344
N-Acetyl-L-alanine	0.035	N-Acetyl-L-alanine	1.331
Turanose	0.033	(22R)-20alpha,22-Dihydroxycholesterol	1.317
Acetic acid	0.025	Turanose	1.312
Cholesterol	0.023	Erucic acid	1.280
(R)-3-Hydroxybutyric acid	0.016	Galactitol	1.257
5,6-Dihydroxyindole-2-carboxylate	0.014	Cholesterol	1.250
9,12-Octadecadienoic acid	0.013	(R)-3-Hydroxybutyric acid	1.241
Vinylformic acid	0.013	L-Arabinose	1.193
L-Arabinose	0.013	Tetramethylpentadecanoic acid	1.186
Tetramethylpentadecanoic acid	0.012	Vinylformic acid	1.178
Erucic acid	0.011	Sphinganine	1.177
Galactitol	0.010	3-beta-D-Galactosyl-sn-glycerol	1.161
6-Hydroxyhexanoic acid	0.009	Formic acid	1.156

Abbreviations: MDA, Mean Decrease Accuracy, calculated by Random Forests model (500 trees), indicating the relative importance of metabolite in clustering samples with different treatments. VIP (variance importance in projection), a measure of a metabolite's importance in clustering samples with different treatments, calculated a weighted sum of the squared correlations between the OPLS-DA components and the original variable.

Table 5-4. Key metabolites (nanoHRLC-MS/MS) extracted by Random Forests and OPLS-DA models.

Random forests model Component	AI	OPLS-DA model Component	VIP
L-Urobilin	5.08	3-Hydroxy-cis-5-tetradecenoylcarnitine	1.41
Dodecanedioylcarnitine	2.66	7-Hexadecenoic acid, methyl ester	1.41
12-phenoxydodecoxybenzene	2.63	L-Histidinol	1.39
Lyso PE(16:0/0:0)	2.37	Piperochromenoic acid	1.34
Heptadecenoic acid	1.62	Dihydromaleimide beta-D-glucoside	1.34
Taurolithocholic acid 3-sulfate	1.83	Palmitoyl glucuronide	1.33
PE(22:2(13Z,16Z)/P-18:0)	1.54	L-Urobilin	1.32
Stearic acid	1.61	Squamoxinone	1.30
Trihexosylceramide	1.29	N-Nitrosothiazolidine-4-carboxylic acid	1.28
3-4-Hydroxy-3-methoxyphenyl-1,2-propanediol	1.23	3-4-Hydroxy-3-methoxyphenyl-1,2-propanediol	1.27
Palmitoyl glucuronide	1.23	4-Hydroxyenterodiol	1.27
Z-22-Hentriacontene-2,4-dione	1.17	Glycerol trihexanoate	1.26
Mahanimbinol	1.13	3,17-Androstenediol glucuronide	1.26
2-Hydroxyhexadecanoylcarnitine	1.01	Retinal	1.25
2-Isopentyl-7-azaindole	1.08	3,7-Dihydroxy-12-oxocholanoic acid	1.24

Abbreviations: AI, averaged importance, or mean importance measure, calculated by Random Forests model (500 trees), indicating a (weighted) mean of the individual trees improvement in the splitting criterion produced by each variable (Strobl *et al.*, 2007). VIP (variance importance in projection), a measure of a metabolite's importance in clustering samples with different treatments, calculated a weighted sum of the squared correlations between the PLS-DA components and the original variable.

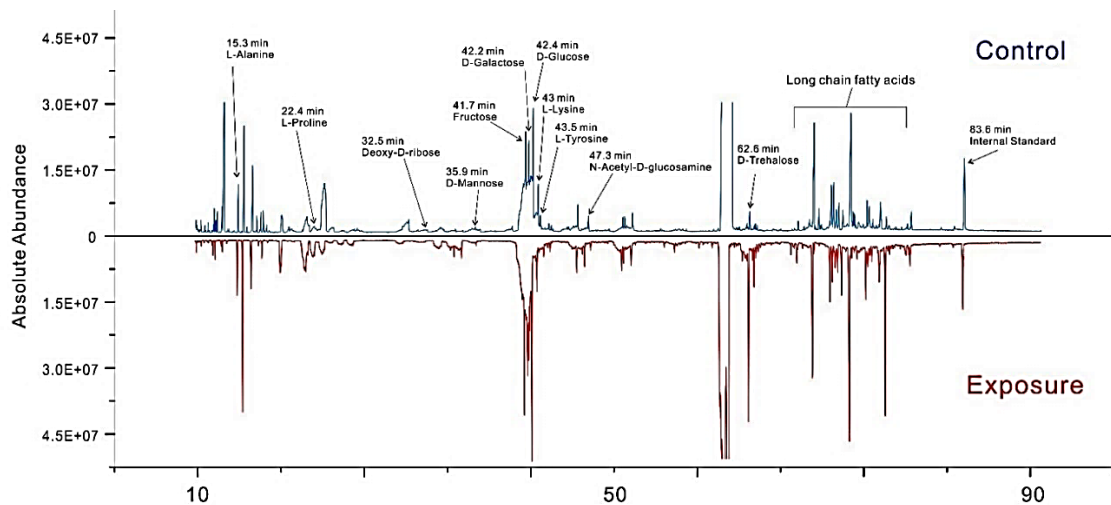


Figure 5-1. Typical GC-MS total ion chromatogram (TIC) of fecal metabolites. The labeled interested amino acids and carbohydrates were located in the chromatogram by standard spikes.

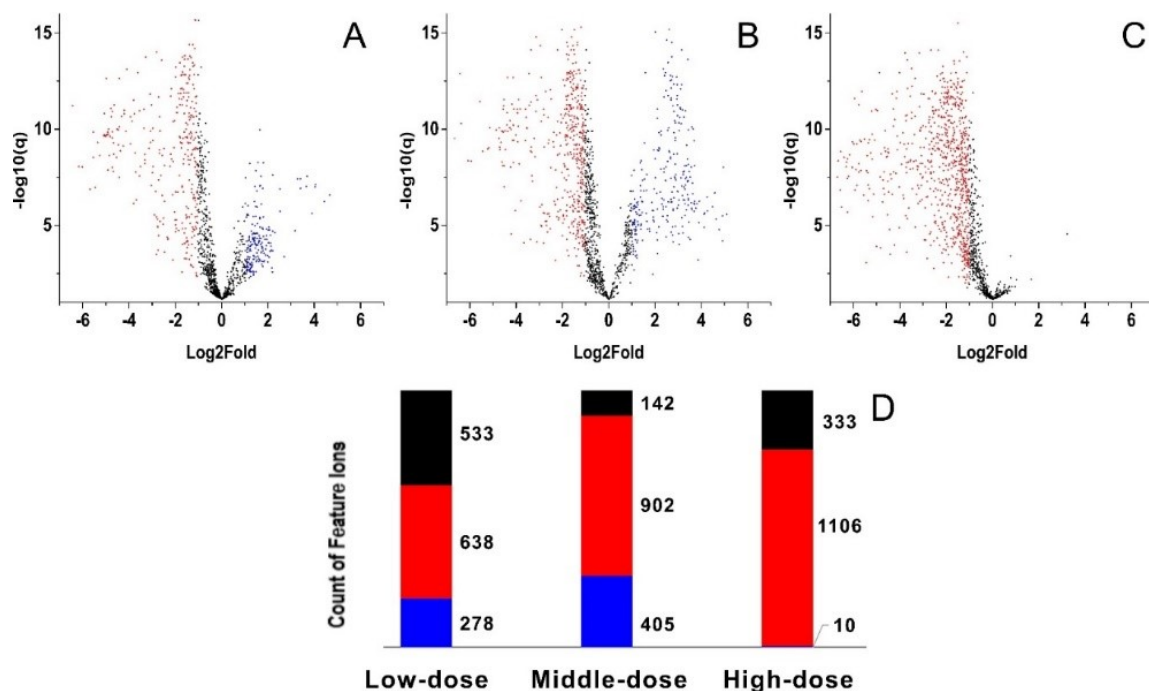


Figure 5-2. Volcano plots of 1490 feature ions detected by GC-MS. The plots illustrate the compositional changes of fecal metabolome in rats treated with (A) 5, (B) 25 and (C) 75 $\mu\text{g AFB}_1 \text{ kg}^{-1} \text{ B. W. day}^{-1}$. Each dot represents a ratio of metabolite calculated by comparing the extracted ion chromatography (EIC) intensity of the metabolite in the treatment group with that in the control group. The data for all metabolites are plotted as log2 fold-change (X axis) versus the $-\log_{10}$ of q -value (Y axis). The cut-off threshold for the screening of significant responding metabolites was set as fold-change > 2 and $q < 0.05$ by Welch's t-test, marked as red spots.

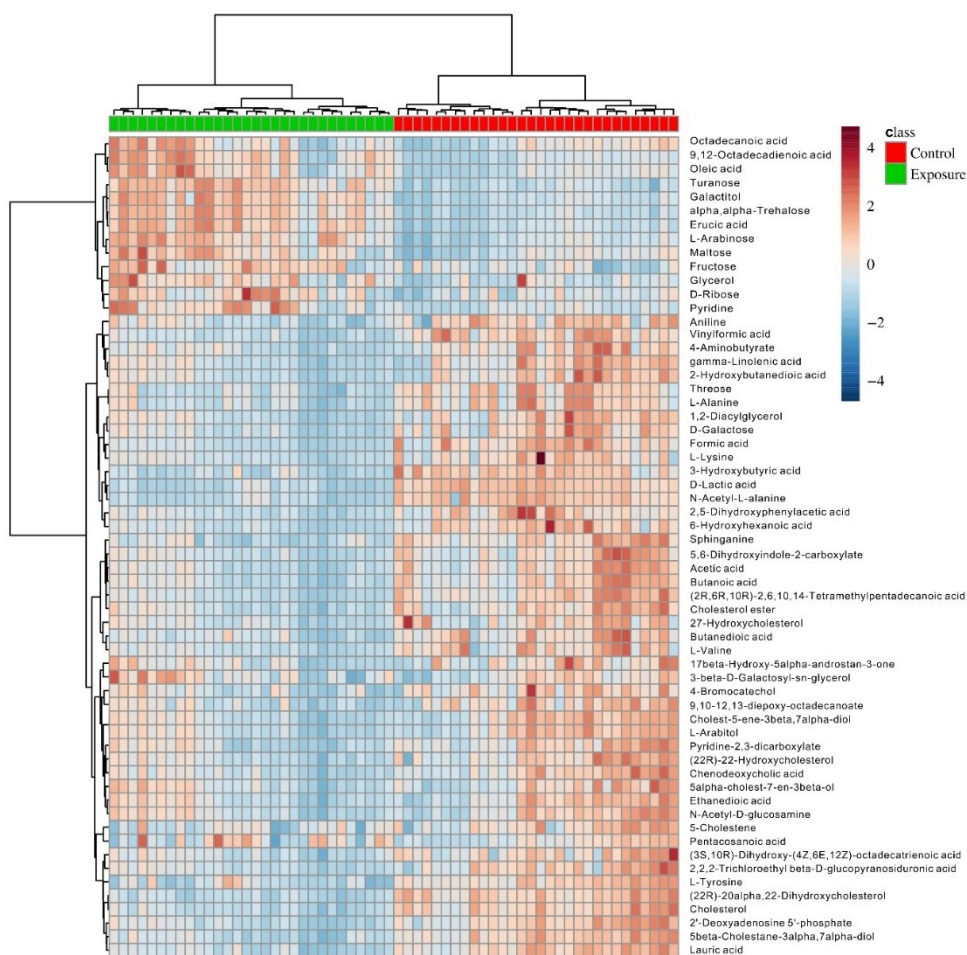


Figure 5-3. Heatmap overview of the alterations of metabolites profiled by GC-MS between control and middle-dose groups. Heat map shows the level changes of metabolites. The hierarchical reorganization was based on the Pearson's correlation coefficient with average distance. Data were normalized using locally weighted scatterplot smoothing (LOESS) algorithm. The exposure group was treated with 25 $\mu\text{g AFB}_1 \text{ kg}^{-1} \text{ B. W.}$

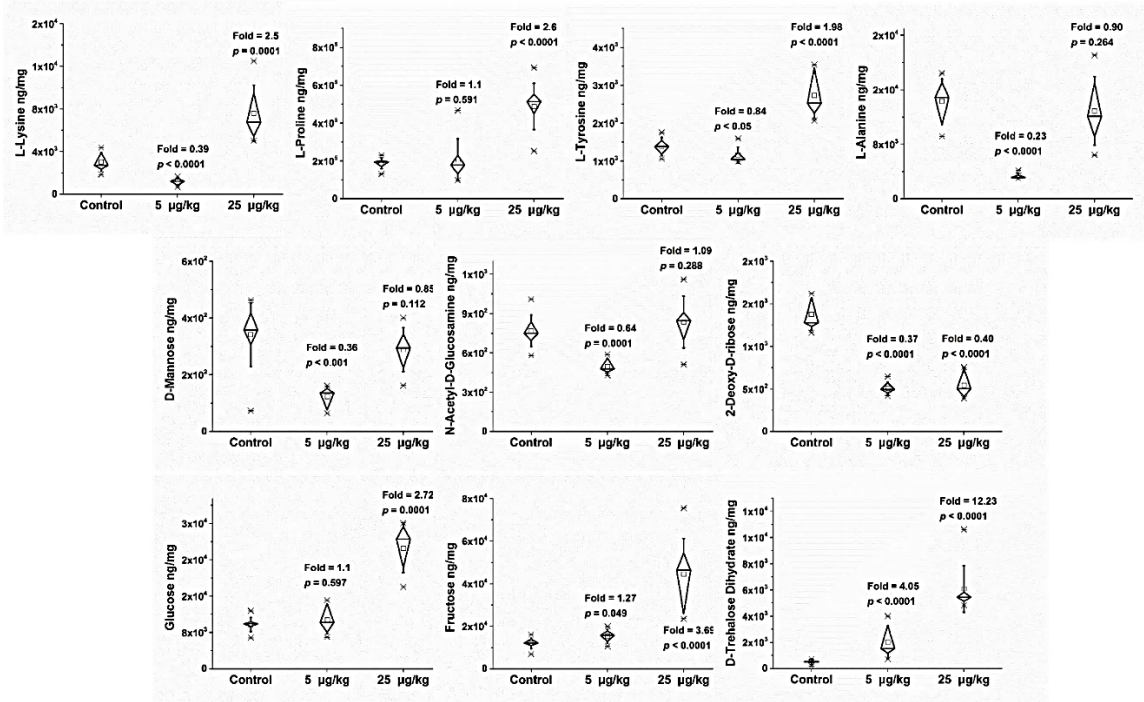


Figure 5-4. Differential metabolites measured by standard calibration. The ion peak intensities were integrated from Extracted Ion Chromatograms (XICs). Non-parametric Mann-Whitney U test was applied for all comparisons (n = 10). Violin plots represent 25%, 50% and 75% percentile of data. Whisker of box plots indicate standard deviation (S. D., n = 10).

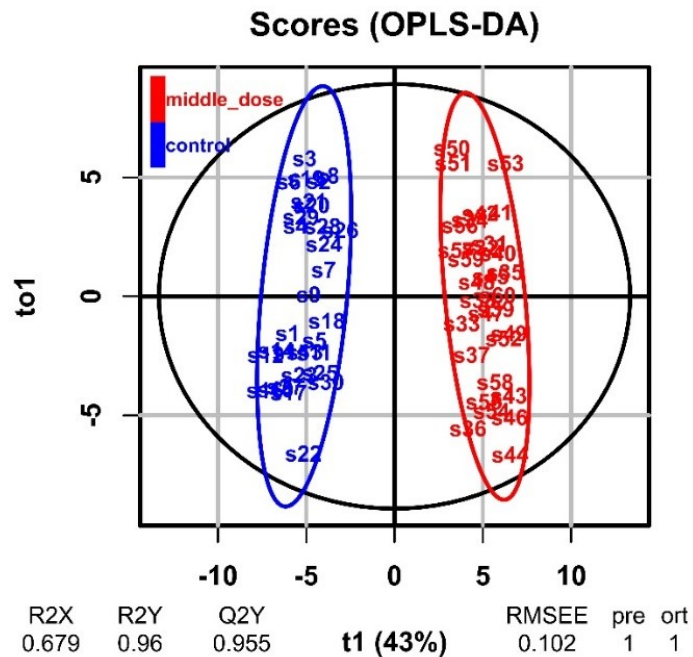


Figure 5-5. Score plot and model supervision of OPLS-DA model for GC-MS metabolomics data. Each dot represents a biological sample point. All data were auto-scaled and show normal distribution. The components t1 and t2 are reflected on the horizontal and vertical axis respectively. The R2Y value is equivalent to the y-block cumulative variance captured, while the Q2Y is based on the 10 times cross-validated results and indicates predictive performance of the modeling. The color-coded circle represents 95% confidential interference.

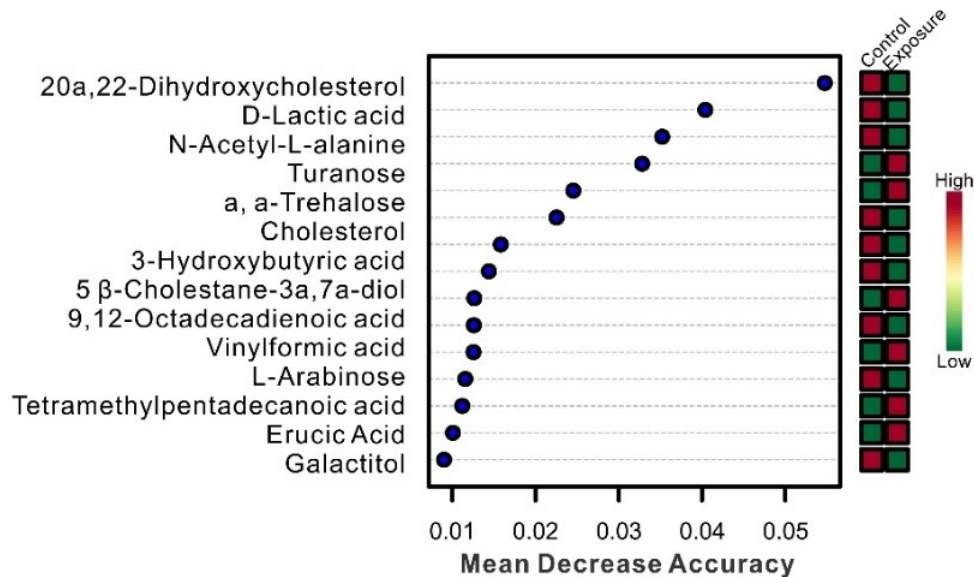


Figure 5-6. Key metabolites (GC-MS) ranked by Random Forests model to evaluate the contribution of metabolites to the discrimination between control and AFB₁-treated groups. Mean decrease accuracy (MDA) was calculated by Random Forests model (500 trees), indicating the relative importance of metabolite in clustering samples with different treatments. The more the accuracy of the random forest decreases due to the exclusion of that single variable, the more important that variable is. The variable with a larger mean decrease in accuracy is more important for classification of the data.

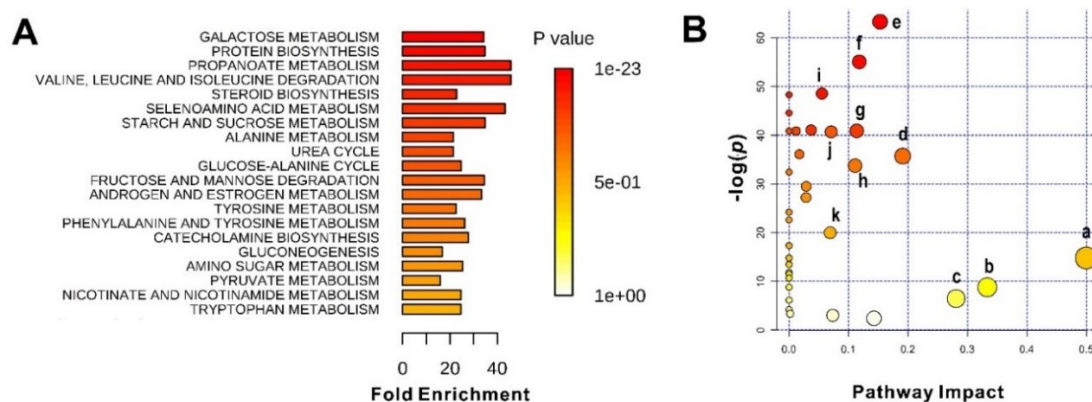


Figure 5-7. Metabolite set enrichment analysis (MSEA) and pathway enrichment analysis for the detected metabolites (KEGG rat database). (A) MSEA of metabolic pathways with $q < 0.05$ for the significance of alteration. The color code indicates q values, and the enrichment fold (X-axis) indicates extent of response for the metabolic pathway. (B) Pathway enrichment analysis to show the biochemical pathways affected by AFB₁ (global test with topology analysis based on relative-betweenness centrality). Specific results of pathway analysis are available on SI Table 4. (a) Phenylalanine, tyrosine and tryptophan biosynthesis; (b) Valine, leucine and isoleucine biosynthesis; (c) Glycerolipid metabolism; (d) Tyrosine metabolism; (e) Pyruvate metabolism; (f) Steroid biosynthesis; (g) Alanine, aspartate and glutamate metabolism; (h) Glyoxylate and dicarboxylate metabolism; (i) Primary bile acid synthesis; (j) TCA cycle; (k) Amino sugar and nucleotide sugar metabolism.

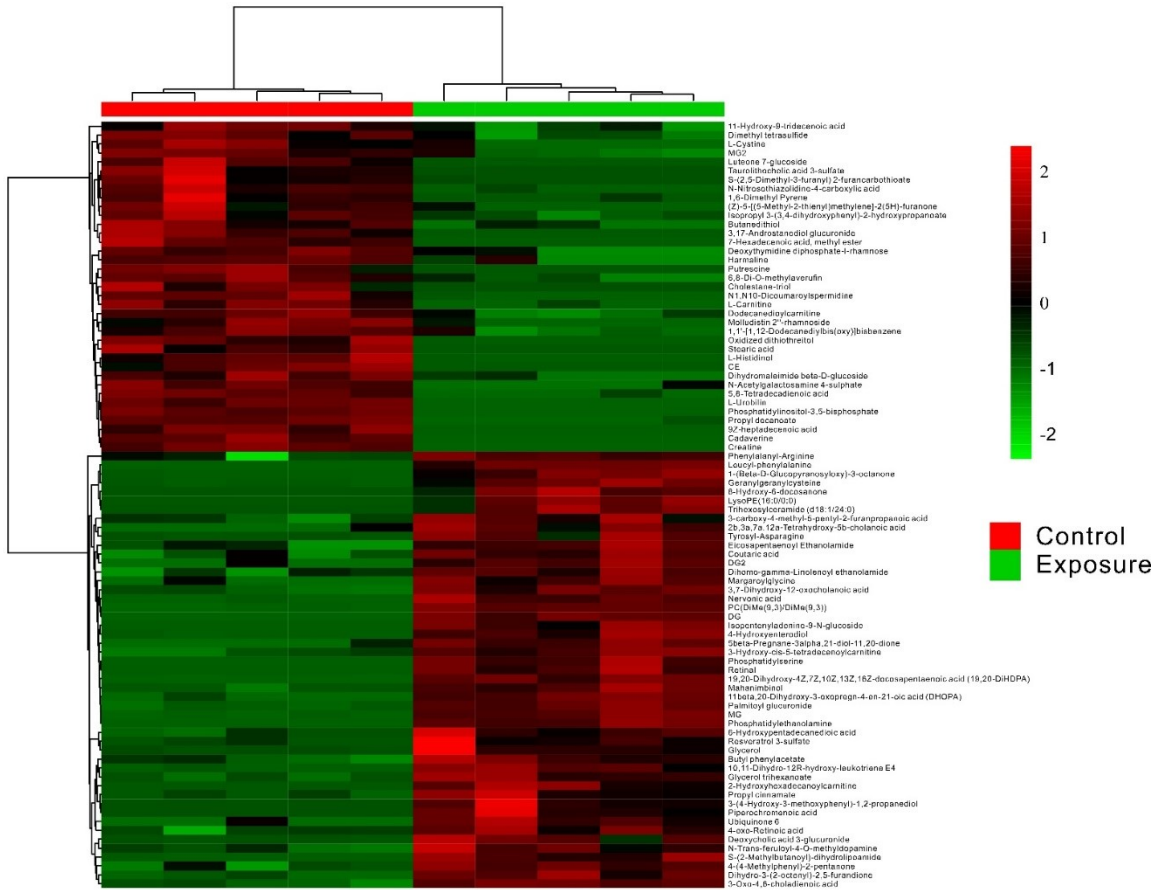


Figure 5-9. Heat map based on the Pearson distance measure and the average cluster algorithm. Heat map here provides intuitive visualization of the metabolic remodeling in disease groups compared to the control group. Red color indicates a high level of metabolites and green color indicates a low level of metabolites, while black color means an equal level in groups.

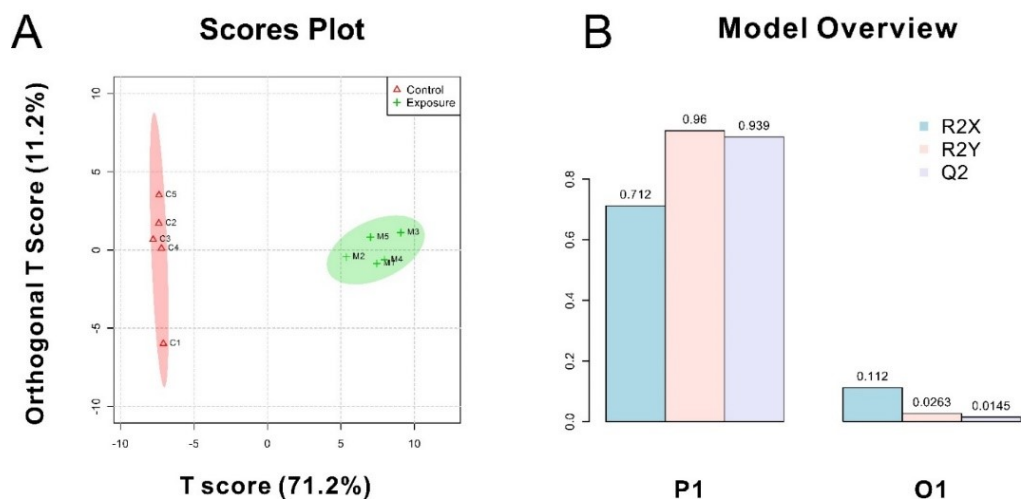


Figure 5-10. Score plot and model supervision of OPLS-DA model for nanoLC-MS/MS metabolomics data. Each dot represents a biological sample point. All data were auto-scaled and show normal distribution. The components t and orthogonal t are reflected on the horizontal and vertical axis respectively. The R^2Y value is equivalent to the y -block cumulative variance captured, while the Q^2Y is based on the 10 times cross-validated results and indicates predictive performance of the modeling. The color-coded circle represents 95% confidential interference.

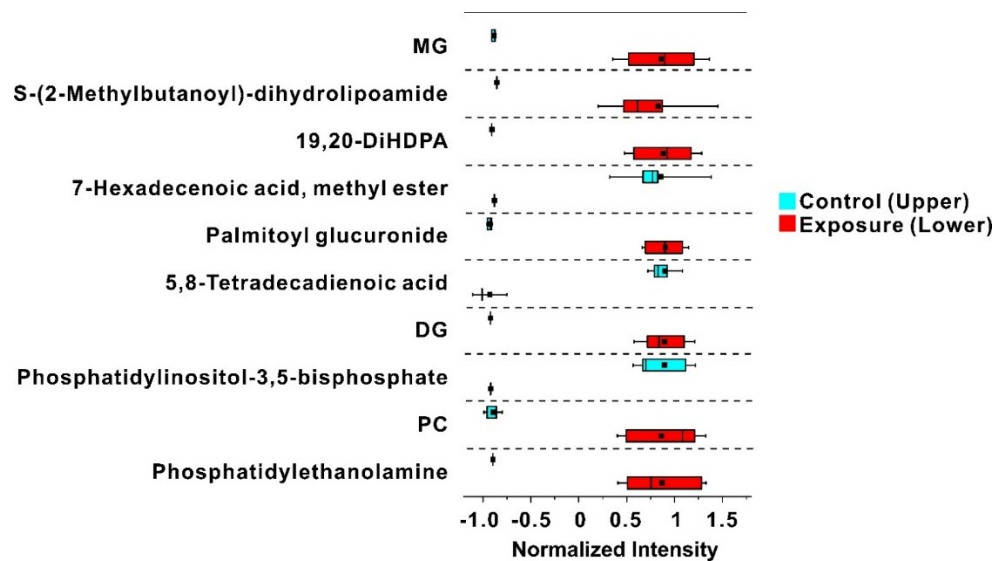


Figure 5-11. Comparison of intensities of signature lipid components between control group (upper) and exposure group (lower). The intensities of ion peaks were normalized by sum and pareto-scaled ($n = 5$). The horizontal lines of box plots indicate the 25th percentile, mean and 75th percentile. Abbreviations: DG, diglyceride (14:0/18:0/0:0) or (14:0/18:0/0:0) or (18:0/14:0/0:0) or (16:0/16:0/0:0) or (16:0/0:0/16:0); 19,20-DiHDPA, (4Z,7Z,10Z,13Z,16Z)-19,20-dihydroxydocosa-4,7,10,13,16-pentaenoic acid; MG, monoradyglycerol (0:0/20:5(5Z,8Z,11Z,14Z,17Z)/0:0) or (0:0/20:5(5Z,8Z,11Z,14Z,17Z)/0:0) or (20:5(5Z,8Z,11Z,14Z,17Z)/0:0/0:0); PC, phosphatidyl choline (DiMe(9,3)/DiMe(9,3)). Specific data are available on SI Table 5-5.

SI Table 5-1. Comparison of the counts of peak detected by GC-MS by using different solvents for chemical derivatization.

Derivatization	Temperature	Derivatization solvent					
		Pyridine		DMSO		DMF	
		Peak count	Blank	Peak count	Blank	Peak count	Blank
Step 1	35 °C	342 ± 7	13	505 ± 15	388	345 ± 33	23
	55 °C	347 ± 3	8	643 ± 6	311	336 ± 8	28
	70 °C	343 ± 6	10	624 ± 6	479	348 ± 5	24
Step 2	70 °C	363 ± 3	11	563 ± 66	492	366 ± 8	27

Peak count: number of peaks detected by AMDIS in total ion chromatographic (TIC), mean ± SD, n = 3. Step 2 was not examined since 70 °C is widely applied for sufficient derivatization.

SI Table 5-2. Comparison of the counts of peaks detected by GC-MS analysis by using different solvents for sample extraction.

Extraction solvent	Peak count
Methanol/Chloroform 2:1	798 ± 6
Methanol/Chloroform 1:1	850 ± 4
Methanol/Chloroform 1:2	939 ± 44
Methanol	476 ± 44
Methanol/Water 1:1	730 ± 13
BUME	550 ± 2
Methanol/MTBE/Water 2:2:1	608 ± 4
Methanol/Chloroform/Water 1:2:1	1094 ± 69

Peak count: number of peaks detected by AMDIS in deconvoluted total ion chromatographic (TIC), mean ± SD, n = 3. BUME, Butanol/Methanol 3:1. MTBE, Methyl-Tertiary-Butyl-Ether.

SI Table 5-3. Fold-change and statistical parameters for the 60 differential metabolites detected by GC-MS.

Imputative Identity	Middle-dose vs Control	mz@RT	MDA	VIP score	q	Trend
(22R)-20alpha,22-Dihydroxycholesterol	0.447	M370T69	0.054 8	1.31 7	1.310E -18	DOW N
D-Lactic acid	0.445	M73T14	0.040 4	1.38 3	4.182E -26	DOW N
N-Acetyl-L-alanine	0.480	M117T14	0.035 2	1.33 1	7.191E -20	DOW N
Acetic acid	0.745	M149T17	0.024 5	1.06 8	1.718E -08	DOW N
Cholesterol	0.547	M371T69	0.022 5	1.25 0	2.123E -15	DOW N
3-Hydroxybutyric acid	0.444	M147T23	0.015 8	1.24 1	7.346E -16	DOW N
5,6-Dihydroxyindole-2-carboxylate	0.651	M220T17	0.014 4	1.12 4	2.327E -09	DOW N
Vinylformic acid	0.605	M73T37	0.012 6	1.17 8	2.293E -13	DOW N
D-Galactose	0.677	M299T43	0.011 6	1.18 6	6.113E -12	DOW N
6-Hydroxyhexanoic acid	0.656	M118T14	0.009 0	1.06 8	5.312E -11	DOW N
Lauric acid	0.870	M95T71	0.008 8	0.74 1	1.778E -04	DOW N
Formic acid	0.648	M145T17	0.008 6	1.15 6	1.400E -12	DOW N
L-Tyrosine	0.741	M75T44	0.007 7	1.01 9	1.161E -08	DOW N
2,5-Dihydroxyphenylacetic acid	0.628	M74T14	0.006 2	1.03 4	1.934E -10	DOW N
L-Alanine	0.521	M116T16	0.005 5	1.08 9	2.784E -10	DOW N
Threose	0.598	M147T16	0.004 9	1.03 7	3.511E -09	DOW N
Butanedioic acid	0.676	M145T19	0.004 8	1.04 0	2.372E -08	DOW N
L-Lysine	0.618	M247T23	0.004 4	1.06 0	1.457E -09	DOW N

2'-Deoxyadenosine 5'-phosphate	0.745	M216T70	0.004 4	1.01 1	4.483E -08	DOW N
L-Valine	0.521	M144T19	0.004 1	1.15 2	2.907E -11	DOW N
Butanoic acid	0.736	M75T17_1	0.003 9	1.09 6	3.729E -09	DOW N
Sphinganine	0.682	M207T13	0.003 8	1.17 7	3.846E -11	DOW N
(2R,6R,10R)-2,6,10,14-Tetramethylpentadecanoic acid	0.761	M217T48	0.003 5	1.03 2	1.317E -08	DOW N
(3S,10R)-Dihydroxy-(4Z,6E,12Z)-octadecatrienoic acid	0.772	M145T69	0.003 3	0.90 0	8.890E -07	DOW N
2,2,2-Trichloroethyl beta-D-glucopyranosiduronic acid	0.714	M217T69	0.002 7	0.95 2	4.632E -08	DOW N
Chenodeoxycholic acid	0.795	M258T72	0.001 7	0.91 5	4.818E -07	DOW N
27-Hydroxycholesterol	0.720	M368T70	0.001 4	1.00 4	3.516E -07	DOW N
(22R)-22-Hydroxycholesterol	0.797	M388T72	0.001 1	0.90 8	2.113E -06	DOW N
L-Arabitol	0.845	M205T68	0.001 1	0.81 4	6.285E -06	DOW N
Cholesterol ester	0.786	M257T71	0.001 0	1.01 9	1.013E -07	DOW N
Aniline	0.761	M95T69	0.001 0	0.84 0	3.016E -06	DOW N
9,10-12,13-Diepoxy-octadecanoate	0.753	M119T71_2	0.001 0	0.85 4	1.592E -06	DOW N
1,2-Diacylglycerol	0.803	M191T48	0.001 0	0.91 6	1.885E -07	DOW N
4-Bromocatechol	0.788	M207T71	0.000 8	0.78 5	1.517E -05	DOW N
4-Aminobutyrate	0.741	M130T18	0.000 8	0.95 5	3.994E -07	DOW N
Pyridine-2,3-dicarboxylate	0.838	M208T13	0.000 7	0.89 5	2.652E -06	DOW N
5 α -Cholest-7-en-3 β -ol	0.935	M460T71	0.000 7	0.27 1	2.177E -01	DOW N
2-Hydroxybutanedioic acid	0.792	M117T54	0.000 6	0.89 8	1.022E -06	DOW N
Cholest-5-ene-3beta,7alpha-diol	0.845	M205T68	0.000 4	0.81 4	6.285E -06	DOW N

N-Acetyl-D-glucosamine	0.894	M320T70	0.000 4	0.63 1	1.164E -03	DOW N
17beta-Hydroxy-5alpha-androstan-3-one	0.837	M217T39	0.000 2	0.50 0	3.045E -03	DOW N
5-Cholestene	0.711	M385T70	0.000 1	0.95 8	2.955E -07	DOW N
Ethanedioic acid	0.888	M148T12	0.000 1	0.66 6	6.353E -04	DOW N
gamma-Linolenic acid	0.817	M129T54	0.000 1	0.89 3	1.929E -06	DOW N
5beta-Cholestane-3alpha,7alpha-diol	0.790	M189T69	0.000 1	0.96 6	3.113E -08	DOW N
Turanose	2.038	M361T63	0.032 8	1.31 2	6.914E -16	UP
9,12-Octadecadienoic acid	1.436	M75T51	0.012 6	0.97 5	1.841E -08	DOW N
L-Arabinose	1.390	M218T63	0.012 6	1.19 3	1.224E -11	UP
Erucic acid	1.517	M319T63	0.011 2	1.28 0	3.698E -14	UP
Galactitol	1.538	M363T63	0.010 1	1.25 7	2.781E -13	UP
Oleic Acid	1.297	M337T51	0.004 0	0.86 6	2.251E -06	DOW N
Maltose	1.226	M219T63	0.002 7	0.93 5	2.170E -06	DOW N
alpha, alpha-Trehalose	1.776	M362T63	0.001 7	1.34 4	3.955E -17	UP
Glycerol	1.355	M133T22	0.001 5	0.71 6	1.337E -04	DOW N
Fructose	1.746	M355T69	0.001 0	0.93 9	5.894E -06	DOW N
Pyridine	1.436	M171T12	0.001 0	0.86 5	5.767E -06	DOW N
Octadecanoic acid	1.103	M77T51	0.000 9	0.47 6	1.625E -02	DOW N
3-beta-D-Galactosyl-sn-glycerol	1.357	M148T63	0.000 7	1.16 1	7.822E -11	UP
D-Ribose	1.260	M205T63	0.000 5	0.76 2	1.106E -04	DOW N
Pentacosanoic acid	1.003	M440T67	0.000 0	0.02 0	9.606E -01	DOW N

SI Table 5-4. Results of GC-MS pathway analysis (MSEA, only significant components included) performed using MetaboAnalyst.

Metabolic pathway	Significant Hits/Total compounds	<i>q</i>	FDR	impact
Pyruvate metabolism	3/22	1.13E-26	1.13E-26	0.15318
Steroid biosynthesis	2/35	4.10E-23	2.11E-23	0.11826
Primary bile acid biosynthesis	4/46	2.71E-20	9.15E-21	0.05530
Pentose phosphate pathway	1/19	3.34E-20	9.15E-21	0.00000
Nicotinate and nicotinamide metabolism	1/13	1.36E-18	3.06E-19	0.00000
Galactose metabolism	3/26	4.39E-17	6.84E-18	0.03729
Alanine, aspartate and glutamate metabolism	3/24	4.98E-17	6.84E-18	0.11392
Arginine and proline metabolism	1/44	4.98E-17	6.84E-18	0.01198
beta-Alanine metabolism	1/19	4.98E-17	6.84E-18	0.00000
Citrate cycle (TCA cycle)	2/20	5.45E-17	7.33E-18	0.07086
Steroid hormone biosynthesis	2/70	5.18E-15	6.60E-16	0.01746
Tyrosine metabolism	3/42	7.44E-15	9.04E-16	0.19116
Glyoxylate and dicarboxylate metabolism	2/16	5.08E-14	5.95E-15	0.11111
Aminoacyl-tRNA biosynthesis	4/67	1.82E-13	2.07E-14	0.00000
Butanoate metabolism	4/20	3.23E-12	3.59E-13	0.02899
Glycolysis or Gluconeogenesis	1/26	3.03E-11	3.31E-12	0.02862
Ubiquinone and other terpenoid-quinone biosynthesis	2/3	5.85E-10	6.34E-11	0.00000
Biosynthesis of unsaturated fatty acids	4/42	2.69E-09	2.91E-10	0.00000
Amino sugar and nucleotide sugar metabolism	2/37	3.59E-08	3.89E-09	0.06921
Selenoamino acid metabolism	1/15	4.71E-07	5.16E-08	0.00000
Phenylalanine, tyrosine and tryptophan biosynthesis	1/4	5.60E-06	5.94E-07	0.50000
Phenylalanine metabolism	1/9	5.60E-06	5.94E-07	0.00000
Synthesis and degradation of ketone bodies	1/5	1.83E-05	2.14E-06	0.00000
Propanoate metabolism	1/20	8.89E-05	1.08E-05	0.00000

Fatty acid biosynthesis	3/43	0.0001138	1.45E-05	0.00000
Methane metabolism	1/9	0.0002316	3.12E-05	0.00000
Valine, leucine and isoleucine biosynthesis	1/11	0.001373	0.0001841	0.33333
Valine, leucine and isoleucine degradation	1/38	0.001373	0.0001841	0.00000
Pantothenate and CoA biosynthesis	1/15	0.001373	0.0001841	0.00000
Glycerolipid metabolism	1/18	0.0092925	0.0018069	0.28098
Biotin metabolism	1/5	0.010753	0.0024281	0.00000
Pentose and glucuronate interconversions	2/14	0.061189	0.016731	0.00000
Purine metabolism	1/68	0.10644	0.037631	0.00193
Starch and sucrose metabolism	3/23	0.10644	0.050231	0.07345
Sphingolipid metabolism	1/21	0.10644	0.090684	0.14286

SI Table 5-5. Summary of nanoLC-MS/MS metabolomics data.

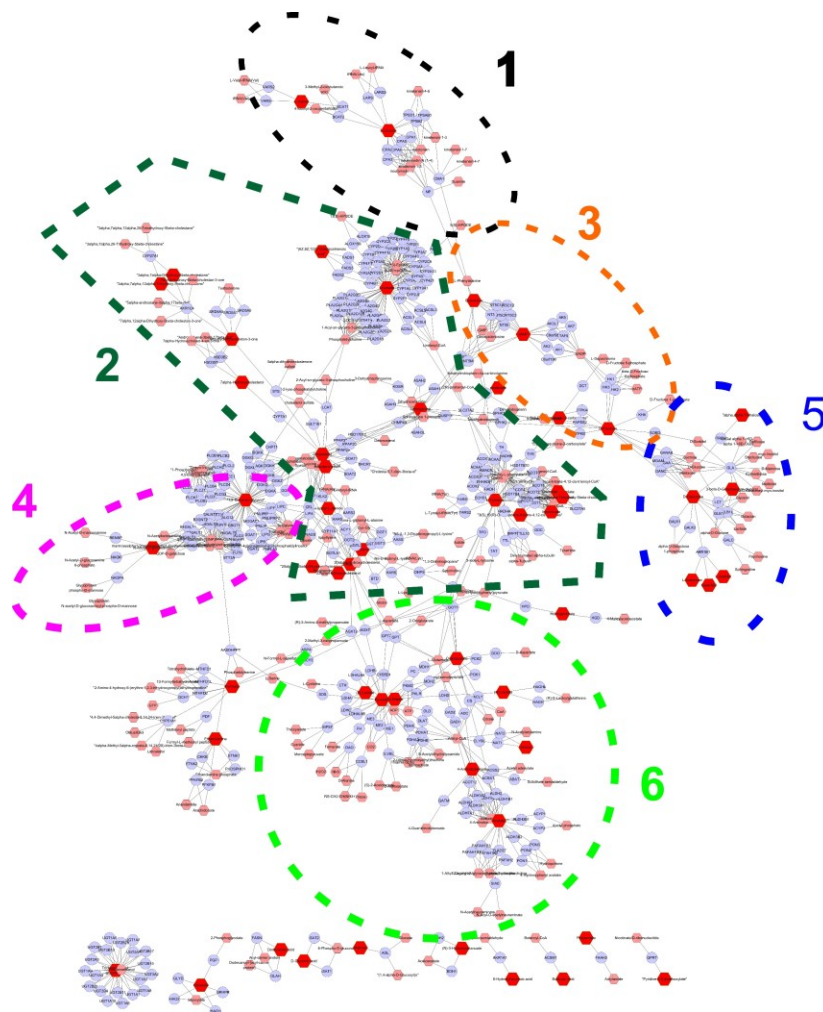
m/z	RT		MS1 30 ppm threshold	MS/MS 100 ppm threshold for both	adjusted p
337.2527	0.160266	Up	Ubiquinone 6		0.01388001
457.2561	0.456282	Up		10,11-Dihydro-12R-hydroxy-leukotriene E4	0.00126909
503.2981	0.563484	Up	2b,3a,7a,12a-Tetrahydroxy-5b-cholanoic acid		0.0182688
405.2249	0.696388	Up	Isopentenyladenine-9-N-glucoside		0.00812974
340.2596	0.755621	Up		8-Hydroxy-6-docosanone	0.04166214
186.0608	0.85413	Down	L-Histidinol		0.01430053
172.0444	0.868412	Down	N-Acetylgalactosamine 4-sulphate		0.01430053
198.0973	0.881952	Up		Vanillyl glycol	0.04461579
103.1227	0.982037	Down	Cadaverine		0.00037804
89.107	1.01826	Down	Putrescine		0.01012924
86.09615	1.030368	Down	Piperidine		0.0000781
143.0013	1.059968	Down	L-Cystine		0.03050316
607.1389	1.091573	Down	Molludistin 2"-rhamnoside		0.02187826
441.0913	1.099806	Down	6,8-Di-O-methylaverufin		0.00301581
173.0118	1.119552	Down	Oxidized dithiothreitol		0.01209673
110.9751	1.129156	Down	1,3-Dichloropropene		0.03076705
177.0068	1.13494	Up	Resveratrol 3-sulfate		0.02712832
561.1336	1.144165	Down	Dihydromaleimide beta-D-glucoside		0.01128034
120.034	1.15255	Up	S-(2-Methylbutanoyl)-dihydrolipoamide		0.00923176

111.529 4	1.16426 9	Up	Tetrahydrohippuric acid		0.00562575
555.124 6	1.17206 3	Down	Luteone 7- glucoside		0.00401423
143.018 8	1.22717 3	Down	4-Hydroxymethylpyrazole		0.01430053
295.085 8	7.81396 6	Up		Tyrosyl- Asparagine	0.01339197
318.202 2	11.3708 9	Up		4- Hydroxyenterodi ol	0.00952649
259.082 4	11.7767 9	Down	Harmaline		0.02685834
437.235 6	11.9566 2	Down	N1,N10-Dicoumaroylspermidine		0.00018382
568.345 9	12.8308 2	Up		Deoxycholic acid 3-glucuronide	0.01588081
453.343 5	13.2360 8	Up		LysoPE(16:0/0:0)	0.04461579
349.200 9	14.6381 9	Up		Dihomo-gamma- Linolenoyl ethanolamide	0.01372483
306.181 3	14.6638 8	Up		1-(beta-D- Glucopyranosylo xy)-3-octanone	0.01750777
588.41	14.7932 1	Up	Trihexosylceramid e		0.03877391
320.196 8	15.7086 9	Up	Leucyl-phenylalanine		0.00401423
311.182 8	15.9938	Up	6-Hydroxypentadecanedioic acid		0.00612773
349.237 3	16.1297 4	Up		Coutaric acid	0.01430053
361.173 3	16.1884 1	Down	L-Carnitine		0.00214256
363.253 1	16.5869 2	Up	19,20-DiHDPA		0.00113767
345.242 4	16.6401 4	Up		Eicosapentaenoyl Ethanolamide	0.0222471

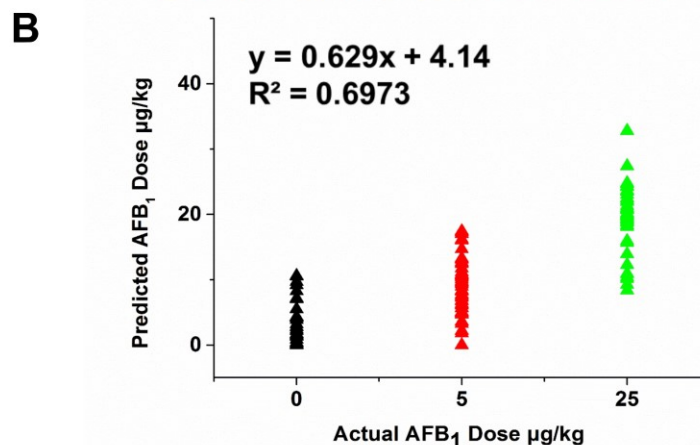
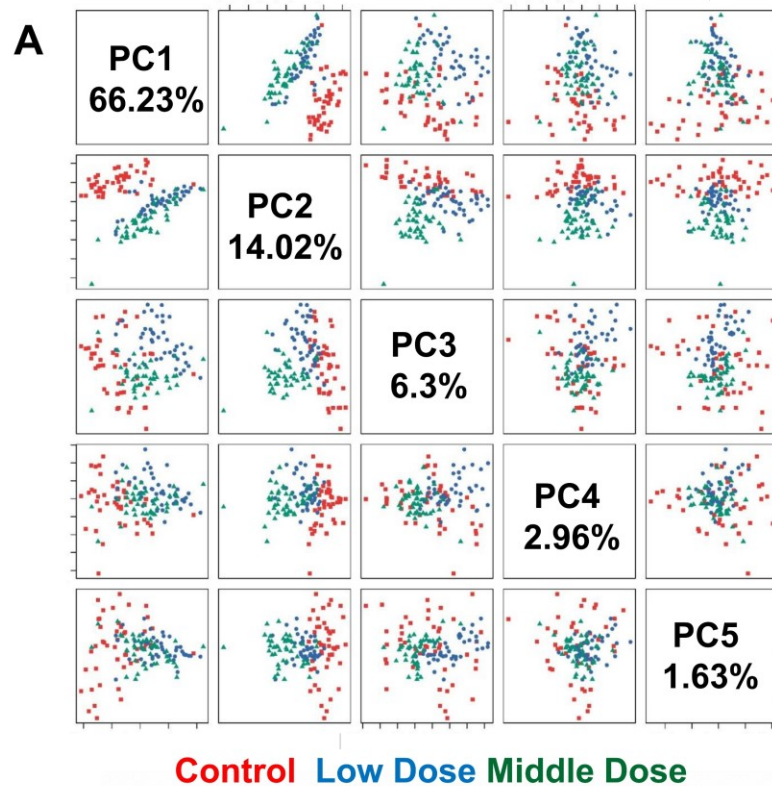
349.237 3	16.6613 3	Up		5beta-Pregnane-3alpha,21-diol-11,20-dione	0.00401423
367.247 9	16.7510 4	Up		Nervonic acid	0.0000781
452.221 5	16.7856 1	Up	Geranylgeranylecysteine		0.01333004
321.180 9	16.8769 3	Up		Phenylalanyl-Arginine	0.03634054
343.162 8	16.9131 3	Up		N-trans-Feruloyl-4-O-methyldopamine	0.01372483
435.274 3	17.0325 1	Up		11beta,20-Dihydroxy-3-oxopregn-4-en-21-oic acid (DHOPA)	0.00301581
305.092	17.1159 5	Down	11-Hydroxy-9-tridecenoic acid		0.03298289
345.130 8	17.1885 2	Down	phosphatidylinositol bisphosphate		0.00034479
595.349 7	17.2133 5	Down	L-Urobilin		0.00036523
355.263 1	17.2546 3	Down	12-phenoxydodecoxybenzene		0.01262934
315.195 5	17.2941	Up	4-oxo-Retinoic acid		0.01430053
468.249 6	17.2943	Down		3,17-Androstanediol glucuronide	0.00482093
373.273 7	17.3974 4	Down		Dodecanedioylcar nitine	0.00663949
433.258 6	17.4650 1	Up	phosphatidylserine		0.0021413
459.214 7	17.5969 8	Up		Cerivastatin	0.00920544
436.269 5	17.8709 7	Down	7-Hexadecenoic acid, methyl ester		0.00401423
425.229 9	17.9593 9	Up	Glycerol trihexanoate		0.00124504
399.252 9	18.0686 5	Up	MG(0:0/20:5(5Z,8Z,11Z,14Z,17Z)/0:0)		0.00335238

457.256 5	18.0686 5	Up	Palmitoyl glucuronide		0.0000781
417.263 5	18.0686 5	Up	Ethinodiol Diacetate		0.00233927
401.268 9	18.2147 5	Up	Piperochromenoic acid		0.03666113
333.242 5	18.3053	Up		Mahanimbinol	0.00726697
361.237 3	18.4091 5	Up	phosphatidylethanolamine		0.0021413
291.112 9	18.6983 2	Down		Etiocholanolone	0.0003923
232.133 2	18.9214 4	Up		Melatonin	0.0182688
537.267 1	19.1824 2	Up		Sodium taurocholate	0.01430053
327.231 9	19.1917 5	Up	2-Hydroxydesogestrel		0.01430053
385.237 3	19.642	Up		3-Hydroxy-cis-5-tetradecenoylcarnitine	0.01262934
284.294 8	19.9294 7	Down		Stearic acid	0.02375207
327.268 2	20.1106 9	Up		Margaroylglycine	0.00923176
317.247 4	20.1929 3	Up	Retinal		0.00370377
286.274 1	20.6951 9	Down	Heptadecenoic acid		0.00401423
225.185	20.7251 9	Down		3-Nitrotyrosine	0.0000855
783.579	20.7706	Down		PE(22:2(13Z,16Z)/P-18:0)	0.01430053
307.242 1	20.8410 3	Up	Diacylglycerol		0.00032169
353.247 7	20.8578 4	Up	4-(4-Methylphenyl)-2-pentanone		0.00754925
371.258 1	20.8578 4	Up		Docosahexaenoyl Ethanolamide	0.01430053
406.295 3	20.8578 4	Up		3,7-Dihydroxy-12-oxocholanoic acid	0.00482093

411.2508	20.87602	Up	Butyl phenylacetate		0.00147953
462.3945	21.48756	Down	(Z)-22-Hentriacontene-2,4-dione		0.03938217
563.2658	24.61766	Down		Taurolithocholic acid 3-sulfate	0.03634054
415.3574	26.73656	Up		2-Hydroxyhexadecanoylcarnitine	0.01430053
381.2977	28.41849	Down	Glycerol 1-octadecanoate		0.01118184
200.9731	29.056	Down	N-Nitrosothiazolidine-4-carboxylic acid		0.00711225
97.0007	29.13326	Down	S-(2,5-Dimethyl-3-furanyl) 2-furancarbothioate		0.03413086
128.0192	29.14718	Down	(Z)-5-[(5-Methyl-2-thienyl)methylene]-2(5H)-furanone		0.03666113
151.0352	29.19106	Down	1,6-Dimethoxy pyrene		0.03413086
317.0204	29.24864	Down	4-[(2,4-Dihydroxyphenyl)azo]benzenesulfonic acid		0.01372483
198.94	29.34011	Down	Butanedithiol		0.03081329



SI Figure 5-1. Global compound-gene network analysis of the metabolites detected in rat feces collected from the middle-dose group. The intense red hexagons represent metabolites with significant alteration. The light red hexagons (compounds) and purple balls (genes) stand for the components in the pathways. Compounds and genes are represented as nodes and the relationships among them are represented as edges; the edges represent both reactions and enzymes based on KEGG. The most activated pathways include: (1) Valine-leucine metabolism; (2) Bile acid and steroid synthesis; (3) GTPs synthesis; (4) N-acetyl-D-glucosamine synthesis; (5) Carbohydrate conversion; (6) Lactate-pyruvate glycolysis (anaerobic glycolysis).



SI Figure 5-2. Principal component analysis (PCA) for the 60 imputatively identified metabolites that were significantly altered by AFB₁. (A) Score plot matrix of the combination of first 5 PCs to show sample clustering upon AFB₁ treatment. Coordinates in axis are for illustration purpose only and selected arbitrary, and do not have clear biological meanings. Percentage associated with each PC is the proportion of an eigenvalue for the respective PC in the sum of eigenvalues for all PCs. (B) The Principal Component Regression (PCR) function between predicted AFB₁ dose and actual AFB₁ dose has a R² (linear regression coefficient) of 0.697.

Reference

- Amaya-Farfan, J. (1999). Aflatoxin B₁-induced hepatic steatosis: role of carbonyl compounds and active diols on steatogenesis. *Lancet* **353**(9154), 747-748.
- Barbosa, M. R. (2013). Chemical composition and formation of human feces-Problems and solutions of large mergers demographics in developing countries. In 10th International Symposium on Recent Advances in Environmental Health Research.
- Battilani, P., Toscano, P., Van der Fels-Klerx, H. J., Moretti, A., Camardo Leggieri, M., Brera, C., Rortais, A., Goumperis, T., and Robinson, T. (2016). Aflatoxin B1 contamination in maize in Europe increases due to climate change. *Sci Rep* **6**, 24328.
- Beger, R. D., Dunn, W., Schmidt, M. A., Gross, S. S., Kirwan, J. A., Cascante, M., Brennan, L., Wishart, D. S., Oresic, M., and Hankemeier, T. (2016). Metabolomics enables precision medicine:“a white paper, community perspective”. *Metabolomics* **12**(9), 149.
- Calvani, R., Brasili, E., Pratico, G., Capuani, G., Tomassini, A., Marini, F., Sciubba, F., Finamore, A., Roselli, M., Marzetti, E., *et al.* (2014). Fecal and urinary NMR-based metabolomics unveil an aging signature in mice. *Exp Gerontol* **49**, 5-11.
- Chang, H.-P., Wang, M.-L., Chan, M.-H., Chiu, Y.-S., and Chen, Y.-H. (2011). Antiobesity activities of indole-3-carbinol in high-fat-diet–induced obese mice. *Nutrition* **27**(4), 463-470.
- Chi, L., Mahbub, R., Gao, B., Bian, X., Tu, P., Ru, H., and Lu, K. (2017). Nicotine Alters the Gut Microbiome and Metabolites of Gut–Brain Interactions in a Sex-Specific Manner. *Chem Res Toxicol* **30**(12), 2110-2119.

- Chrostek, L., Supronowicz, L., Panasiuk, A., Cylwik, B., Gruszevska, E., and Flisiak, R. (2014). The effect of the severity of liver cirrhosis on the level of lipids and lipoproteins. *Clin Exp Med* **14**(4), 417-21.
- Cleasby, A., Wonacott, A., Skarzynski, T., Hubbard, R. E., Davies, G. J., Proudfoot, A. E., Bernard, A. R., Payton, M. A., and Wells, T. N. (1996). The x-ray crystal structure of phosphomannose isomerase from *Candida albicans* at 1.7 angstrom resolution. *Nat Struct Biol* **3**(5), 470-9.
- da Silva, R. P., Nissim, I., Brosnan, M. E., and Brosnan, J. T. (2009). Creatine synthesis: hepatic metabolism of guanidinoacetate and creatine in the rat in vitro and in vivo. *Endocrinol Metabol* **296**(2), E256-61.
- de Jonge, L. P., Douma, R. D., Heijnen, J. J., and van Gulik, W. M. (2012). Optimization of cold methanol quenching for quantitative metabolomics of *Penicillium chrysogenum*. *Metabolomics* **8**(4), 727-735.
- Demigne, C., Morand, C., Levrat, M. A., Besson, C., Moundras, C., and Remesy, C. (1995). Effect of propionate on fatty acid and cholesterol synthesis and on acetate metabolism in isolated rat hepatocytes. *Brit J Nutr* **74**(2), 209-19.
- Dettmer, K., Aronov, P. A., and Hammock, B. D. (2007). Mass spectrometry-based metabolomics. *Mass Spectrom Rev* **26**(1), 51-78.
- Dunn, W. B., Broadhurst, D. I., Edison, A., Guillou, C., Viant, M. R., Bearden, D. W., and Beger, R. D. (2017). Quality assurance and quality control processes: summary of a metabolomics community questionnaire. *Metabolomics* **13**(5), 50.
- Eggers, L. F., & Schwudke, D. (2016). Lipid Extraction: Basics of the Methyl-tert-Butyl Ether Extraction. In *Encyclopedia of Lipidomics* (pp. 1-3). Springer Netherlands.

- Elbaz, M., and Ben-Yehuda, S. (2010). The metabolic enzyme ManA reveals a link between cell wall integrity and chromosome morphology. *PLoS Genet* **6**(9), e1001119.
- Fortin, G. (2011). Chapter fifteen - l-Carnitine and Intestinal Inflammation. In *Vitamins & Hormones* (G. Litwack, Ed.), Vol. 86, pp. 353-366. Academic Press.
- Gao, B., Chi, L., Mahbub, R., Bian, X., Tu, P., Ru, H., and Lu, K. (2017). Multi-omics reveals that lead exposure disturbs gut microbiome development, key metabolites, and metabolic pathways. *Chem Research Toxicol* **30**(4), 996-1005.
- Garcia, A., and Barbas, C. (2011). Gas chromatography-mass spectrometry (GC-MS)-based metabolomics. *Methods Mol Biol* **708**, 191-204.
- Gaudet, R. G., Sintsova, A., Buckwalter, C. M., Leung, N., Cochrane, A., Li, J., Cox, A. D., Moffat, J., and Gray-Owen, S. D. (2015). INNATE IMMUNITY. Cytosolic detection of the bacterial metabolite HBP activates TIFA-dependent innate immunity. *Science* **348**(6240), 1251-5.
- Giacomini, F., Le Corguille, G., Monsoor, M., Landi, M., Pericard, P., Petera, M., Duperier, C., Tremblay-Franco, M., Martin, J. F., Jacob, D., *et al.* (2015). Workflow4Metabolomics: a collaborative research infrastructure for computational metabolomics. *Bioinformatics* **31**(9), 1493-5.
- Gold, L., Slone, T., Manley, N., Garfinkel, G., and Ames, B. (2005). Summary table by chemical of carcinogenicity results in CPDB on 1485 chemicals. *University of California, Berkeley*. Available: <http://potency.berkeley.edu/pdfs/ChemicalTable.pdf> [accessed 6/30/2005 2005].

- Groopman, J. D., Zhu, J. Q., Donahue, P. R., Pikul, A., Zhang, L. S., Chen, J. S., and Wogan, G. N. (1992). Molecular dosimetry of urinary aflatoxin-DNA adducts in people living in Guangxi Autonomous Region, People's Republic of China. *Cancer Res* **52**(1), 45-52.
- Grün, C. H., van Dorsten, F. A., Jacobs, D. M., Le Belleguic, M., van Velzen, E. J., Bingham, M. O., Janssen, H.-G., and van Duynhoven, J. P. (2008). GC-MS methods for metabolic profiling of microbial fermentation products of dietary polyphenols in human and in vitro intervention studies. *J Chromatogr B* **871**(2), 212-219.
- Guo, X., Li, J., Tang, R., Zhang, G., Zeng, H., Wood, R. J., and Liu, Z. (2017). High Fat Diet Alters Gut Microbiota and the Expression of Paneth Cell-Antimicrobial Peptides Preceding Changes of Circulating Inflammatory Cytokines. *Mediators Inflamm* **2017**, 9474896.
- Hara, H., Haga, S., Aoyama, Y., and Kiriyama, S. (1999). Short-chain fatty acids suppress cholesterol synthesis in rat liver and intestine. *J Nutr* **129**(5), 942-8.
- Hochberg, Y., and Benjamini, Y. (1990). More powerful procedures for multiple significance testing. *Stat Med* **9**(7), 811-8.
- Howlett, R. M., Davey, M. P., and Kelly, D. J. (2017). Metabolomic Analysis of *Campylobacter jejuni* by Direct-Injection Electrospray Ionization Mass Spectrometry. *Methods Mol Biol* **1512**, 189-197.
- Huang, C. B., Alimova, Y., Myers, T. M., and Ebersole, J. L. (2011). Short- and medium-chain fatty acids exhibit antimicrobial activity for oral microorganisms. *Arch Oral Biol* **56**(7), 650-4.

- Huang, G., Xu, J., Lefever, D. E., Glenn, T. C., Nagy, T., and Guo, T. L. (2017). Genistein prevention of hyperglycemia and improvement of glucose tolerance in adult non-obese diabetic mice are associated with alterations of gut microbiome and immune homeostasis. *Toxicol Appl Pharmacol* **332**, 138-148.
- Jeannot, E., Boorman, G. A., Kosyk, O., Bradford, B. U., Shymoniak, S., Tumurbaatar, B., Weinman, S. A., Melnyk, S. B., Tryndyak, V., Pogribny, I. P., *et al.* (2012). Increased incidence of aflatoxin B1-induced liver tumors in hepatitis virus C transgenic mice. *Int J Cancer* **130**(6), 1347-56.
- Kalli, A., Smith, G. T., Sweredoski, M. J., and Hess, S. (2013). Evaluation and optimization of mass spectrometric settings during data-dependent acquisition mode: focus on LTQ-Orbitrap mass analyzers. *J Proteome Res* **12**(7), 3071-86.
- Lecomte, V., Kaakoush, N. O., Maloney, C. A., Raipuria, M., Huinao, K. D., Mitchell, H. M., and Morris, M. J. (2015). Changes in gut microbiota in rats fed a high fat diet correlate with obesity-associated metabolic parameters. *PLoS One* **10**(5), e0126931.
- Lofgren, L., Forsberg, G. B., and Stahlman, M. (2016). The BUMÉ method: a new rapid and simple chloroform-free method for total lipid extraction of animal tissue. *Sci Rep* **6**, 27688.
- Louis, P., Hold, G. L., and Flint, H. J. (2014). The gut microbiota, bacterial metabolites and colorectal cancer. *Nat Rev Microbiol* **12**(10), 661-72.
- Lu, X., Hu, B., Shao, L., Tian, Y., Jin, T., Jin, Y., Ji, S., and Fan, X. (2013). Integrated analysis of transcriptomics and metabonomics profiles in aflatoxin B1-induced hepatotoxicity in rat. *Food Chem Toxicol* **55**, 444-55.

- MacAulay, J., Thompson, K., Kiberd, B. A., Barnes, D. C., and Peltekian, K. M. (2006). Serum creatinine in patients with advanced liver disease is of limited value for identification of moderate renal dysfunction: Are the equations for estimating renal function better? *Can J Gastroenterol* **20**(8), 521-526.
- Martinez-Jehanne, V., du Merle, L., Bernier-Febreau, C., Usein, C., Gassama-Sow, A., Wane, A. A., Gouali, M., Damian, M., Aidara-Kane, A., Germani, Y., *et al.* (2009). Role of deoxyribose catabolism in colonization of the murine intestine by pathogenic *Escherichia coli* strains. *Infect Immun* **77**(4), 1442-50.
- Mary, V. S., Arias, S. L., Otaiza, S. N., Velez, P. A., Rubinstein, H. R., and Theumer, M. G. (2017). The aflatoxin B1-fumonisin B1 toxicity in BRL-3A hepatocytes is associated to induction of cytochrome P450 activity and arachidonic acid metabolism. *Environ Toxicol* **32**(6), 1711-1724.
- May, T., Mackie, R. I., Fahey, G. C., Jr., Cremin, J. C., and Garleb, K. A. (1994). Effect of fiber source on short-chain fatty acid production and on the growth and toxin production by *Clostridium difficile*. *Scand J Gastroenterol* **29**(10), 916-22.
- Mller, D. M., Seim, H., Kiess, W., Lster, H., and Richter, T. (2002). Effects of oral L-carnitine supplementation on in vivo long-chain fatty acid oxidation in healthy adults. *Metabolism* **51**(11), 1389-1391.
- Mohammadagheri, N., Najafi, R., and Najafi, G. (2016). Effects of dietary supplementation of organic acids and phytase on performance and intestinal histomorphology of broilers. *Vet Res Forum* **7**(3), 189-195.

- Murphy, E. A., Velazquez, K. T., and Herbert, K. M. (2015). Influence of high-fat diet on gut microbiota: a driving force for chronic disease risk. *Curr Opin Clin Nutr Metab Care* **18**(5), 515-20.
- Najdekr, L., Friedecky, D., Tautenhahn, R., Pluskal, T., Wang, J., Huang, Y., and Adam, T. (2016). Influence of Mass Resolving Power in Orbital Ion-Trap Mass Spectrometry-Based Metabolomics. *Anal Chem* **88**(23), 11429-11435.
- Peisl, B. Y. L., Schymanski, E. L., and Wilmes, P. (2017). Dark matter in host-microbiome metabolomics: Tackling the unknowns—A review. *Anal Chim Acta* doi: 10.1016/j.aca.2017.12.034.
- Pluskal, T., Castillo, S., Villar-Briones, A., and Oresic, M. (2010). MZmine 2: modular framework for processing, visualizing, and analyzing mass spectrometry-based molecular profile data. *BMC Bioinformatics* **11**(1), 395.
- Qian, G., Tang, L., Guo, X., Wang, F., Massey, M. E., Su, J., Guo, T. L., Williams, J. H., Phillips, T. D., and Wang, J. S. (2014). Aflatoxin B1 modulates the expression of phenotypic markers and cytokines by splenic lymphocytes of male F344 rats. *J Appl Toxicol* **34**(3), 241-9.
- Qian, G., Tang, L., Lin, S., Xue, K. S., Mitchell, N. J., Su, J., Gelderblom, W. C., Riley, R. T., Phillips, T. D., and Wang, J. S. (2016). Sequential dietary exposure to aflatoxin B1 and fumonisin B1 in F344 rats increases liver preneoplastic changes indicative of a synergistic interaction. *Food Chem Toxicol* **95**, 188-95.
- Qian, G., Tang, L., Wang, F., Guo, X., Massey, M. E., Williams, J. H., Phillips, T. D., and Wang, J. S. (2013). Physiologically based toxicokinetics of serum aflatoxin B1-lysine adduct in F344 rats. *Toxicology* **303**(1), 147-51.

- Qian, G., Xue, K., Tang, L., Wang, F., Song, X., Chyu, M. C., Pence, B. C., Shen, C. L., and Wang, J. S. (2012). Mitigation of oxidative damage by green tea polyphenols and Tai Chi exercise in postmenopausal women with osteopenia. *PLoS One* **7**(10), e48090.
- Qin, J., Li, R., Raes, J., Arumugam, M., Burgdorf, K. S., Manichanh, C., Nielsen, T., Pons, N., Levenez, F., Yamada, T., *et al.* (2010). A human gut microbial gene catalogue established by metagenomic sequencing. *Nature* **464**(7285), 59-65.
- Rabot, S., Membrez, M., Bruneau, A., Gerard, P., Harach, T., Moser, M., Raymond, F., Mansourian, R., and Chou, C. J. (2010). Germ-free C57BL/6J mice are resistant to high-fat-diet-induced insulin resistance and have altered cholesterol metabolism. *FASEB J* **24**(12), 4948-59.
- Russell, N. J., and Nichols, D. S. (1999). Polyunsaturated fatty acids in marine bacteria—a dogma rewritten. *Microbiology* **145**(4), 767-779.
- Saito, R., Smoot, M. E., Ono, K., Ruscheinski, J., Wang, P. L., Lotia, S., Pico, A. R., Bader, G. D., and Ideker, T. (2012). A travel guide to Cytoscape plugins. *Nat Methods* **9**(11), 1069-76.
- Savage, D. C. (1972). Associations and physiological interactions of indigenous microorganisms and gastrointestinal epithelia. *Am J Clin Nutr* **25**(12), 1372-9.
- Scheppach, W., Loges, C., Bartram, P., Christl, S. U., Richter, F., Dusel, G., Stehle, P., Fuerst, P., and Kasper, H. (1994). Effect of free glutamine and alanyl-glutamine dipeptide on mucosal proliferation of the human ileum and colon. *Gastroenterology* **107**(2), 429-34.

- Semova, I., Carten, J. D., Stombaugh, J., Mackey, L. C., Knight, R., Farber, S. A., and Rawls, J. F. (2012). Microbiota regulate intestinal absorption and metabolism of fatty acids in the zebrafish. *Cell Host Microbe* **12**(3), 277-88.
- Shadoff, L., Hummel, R., Lamparski, L., and Davidson, J. (1977). A search for 2, 3, 7, 8-tetrachlorodibenzo-p-Dioxin (TCDD) in an environment exposed annually to 2, 4, 5-trichloro-phenoxyacetic acid ester (2, 4, 5-T) herbicides. *Bull Environ Contam Toxicol* **18**(4), 478-485.
- Shannon, P., Markiel, A., Ozier, O., Baliga, N. S., Wang, J. T., Ramage, D., Amin, N., Schwikowski, B., and Ideker, T. (2003). Cytoscape: a software environment for integrated models of biomolecular interaction networks. *Genome Res* **13**(11), 2498-504.
- Shen, X. T., Gong, X. Y., Cai, Y. P., Guo, Y., Tu, J., Li, H., Zhang, T., Wang, J. L., Xue, F. Z., and Zhu, Z. J. (2016). Normalization and integration of large-scale metabolomics data using support vector regression. *Metabolomics* **12**(5), 89.
- Smirnov, K. S., Maier, T. V., Walker, A., Heinzmann, S. S., Forcisi, S., Martinez, I., Walter, J., and Schmitt-Kopplin, P. (2016). Challenges of metabolomics in human gut microbiota research. *Int J Med Microbiol* **306**(5), 266-279.
- Smith, P., Willemsen, D., Popkes, M., Metge, F., Gandiwa, E., Reichard, M., and Valenzano, D. R. (2017). Regulation of life span by the gut microbiota in the short-lived African turquoise killifish. *Elife* **6**, e27014.
- Spector, A. A., Williard, D. E., Kaduce, T. L., and Gordon, J. A. (1997). Conversion of arachidonic acid to tetradecadienoic acid by peroxisomal oxidation. *Prostaglandins Leukot Essent Fatty Acids* **57**(1), 101-5.

- Sriwattanapong, K., Slocum, S. L., Chawanthayatham, S., Fedeles, B. I., Egner, P. A., Groopman, J. D., Satayavivad, J., Croy, R. G., and Essigmann, J. M. (2017). Editor's Highlight: Pregnancy Alters Aflatoxin B1 Metabolism and Increases DNA Damage in Mouse Liver. *Toxicol Sci* **160**(1), 173-179.
- Storey, J. D., Taylor, J. E., and Siegmund, D. (2004). Strong control, conservative point estimation and simultaneous conservative consistency of false discovery rates: a unified approach. *J Roy Stat Soc B* **66**(1), 187-205.
- Strobl, C., Boulesteix, A. L., Zeileis, A., and Hothorn, T. (2007). Bias in random forest variable importance measures: illustrations, sources and a solution. *BMC Bioinformatics* **8**, 25.
- Sun, Y., and O'Riordan, M. X. (2013). Regulation of bacterial pathogenesis by intestinal short-chain Fatty acids. *Adv Appl Microbiol* **85**, 93-118.
- Tang, Y. M., Wang, J. P., Bao, W. M., Yang, J. H., Ma, L. K., Yang, J., Chen, H., Xu, Y., Yang, L. H., Li, W., *et al.* (2015). Urine and serum metabolomic profiling reveals that bile acids and carnitine may be potential biomarkers of primary biliary cirrhosis. *Int J Mol Med* **36**(2), 377-85.
- Tarantino, G., and Finelli, C. (2013). Pathogenesis of hepatic steatosis: the link between hypercortisolism and non-alcoholic fatty liver disease. *World J Gastroenterol* **19**(40), 6735-43.
- Trimigno, A., Khakimov, B., Mejia, J. L. C., Mikkelsen, M. S., Kristensen, M., Jespersen, B. M., and Engelsens, S. B. (2017). Identification of weak and gender specific effects in a short 3 weeks intervention study using barley and oat mixed linkage β -

- glucan dietary supplements: a human fecal metabolome study by GC-MS. *Metabolomics* **13**(10), 108.
- van den Berg, R. A., Hoefsloot, H. C., Westerhuis, J. A., Smilde, A. K., and van der Werf, M. J. (2006). Centering, scaling, and transformations: improving the biological information content of metabolomics data. *BMC Genomics* **7**, 142.
- Wang, J., Tang, L., Glenn, T. C., and Wang, J. S. (2016). Aflatoxin B1 Induced Compositional Changes in Gut Microbial Communities of Male F344 Rats. *Toxicol Sci* **150**(1), 54-63.
- Wang, J. S., and Groopman, J. D. (1999). DNA damage by mycotoxins. *Mutat Res* **424**(1-2), 167-81.
- Worley, B., and Powers, R. (2016). PCA as a practical indicator of OPLS-DA model reliability. *Curr Metabolomics* **4**(2), 97-103.
- Yoo, N. Y., Jeon, S., Nam, Y., Park, Y. J., Won, S. B., and Kwon, Y. H. (2015). Dietary Supplementation of Genistein Alleviates Liver Inflammation and Fibrosis Mediated by a Methionine-Choline-Deficient Diet in db/db Mice. *J Agric Food Chem* **63**(17), 4305-11.
- Zhou, J., Tang, L., Wang, J., and Wang, J. S. (2018). Aflatoxin B1 Disrupts Gut-microbial Metabolisms of Short Chain Fatty Acids, Long Chain Fatty Acids and Bile Acids in Male F344 Rats. *Toxicol Sci* doi: 10.1093/toxsci/kfy102, kfy102.

CHAPTER 6. GREEN TEA POLYPHENOLS MODIFY GUT-MICROBIOTA
DEPENDENT METABOLISMS OF ENERGY, BILE CONSTITUENTS AND
MICRONUTRIENTS IN FEMALE SPRAGUE-DAWLEY RATS

6.1 Introduction

Our recent metagenomics analysis has uncovered remarkable modifying effects of green tea polyphenols (GTPs) on gut-microbiota community structure and energy conversion related gene orthologs in rats. How these genomic changes could further influence host health is still unclear. In this work, the alterations of gut-microbiota dependent metabolites were studied in the GTPs-treated rats. Six groups of female SD rats (n = 12/group) were administered drinking water containing 0%, 0.5%, and 1.5% GTPs (wt/vol). Their gut contents were collected at 3- and 6-month and were analyzed via high performance liquid chromatography (HPLC) and gas chromatography (GC)-mass spectrometry (MS). GC-MS based metabolomics analysis captured 2668 feature, and 57 metabolites were imputatively from top 200 differential features identified via NIST fragmentation database. A group of key metabolites were quantitated using standard calibration methods. Compared with control, the elevated components in the GTPs-treated groups include niacin (8.61-fold), 3-phenyllactic acid (2.20-fold), galactose (3.13-fold), mannose (2.05-fold), pentadecanoic acid (2.15-fold), lactic acid (2.70-fold), and proline (2.15-fold); the reduced components include cholesterol (0.29-fold), cholic acid (0.62-fold), deoxycholic acid (0.41-fold), trehalose (0.14-fold), glucose (0.46-fold), fructose (0.12-

fold), and alanine (0.61-fold). These results were in line with the genomic alterations of gut-microbiome previously discovered by metagenomics analysis. The alterations of these metabolites suggested the reduction of calorific carbohydrates, elevation of vitamin production, decreases of bile constituents, and modified metabolic pattern of amino acids in the GTPs-treated animals. Changes in gut-microbiota associated metabolism may be a major contributor to the anti-obesity function of GTPs.

Green tea is a popular beverage consumed by people all over the world (Graham, 1992) and has been recognized as health-promoting drink that offers a wide range of health benefits, although their major constituents were identified in less than three decades as GTPs (Cabrera *et al.*, 2006; Jankun *et al.*, 1997). A number of *in vivo*, *in vitro* and epidemiological studies have demonstrated that GTPs constituents, (–)-epigallocatechin-3-gallate (EGCG), (–)-epicatechin-3-gallate (ECG), (–)-epigallocatechin (EGC), and (–)-epicatechin (EC), carry various positive functions in regulating human health, including anti-oxidative stress, cancer prevention, immune enhancement, amelioration of liver diseases, prevention of osteoporosis, and improvement of arterial function (Bose *et al.*, 2008; Chen *et al.*, 1997; Chung *et al.*, 1999; Kim *et al.*, 2000; Kovacs *et al.*, 2004; Lee *et al.*, 2002; Nagao *et al.*, 2005; Rasooly *et al.*, 2013; Yang *et al.*, 1998a; Yang *et al.*, 1998b; Yang *et al.*, 2000). Importantly, GTPs has been found to be significantly associated with the prevention and mitigation of obesity and related ailments. Studies have shown that such beneficial function may be achieved by modulating liver functions, including elevation of hepatic glycolysis, suppression of liver lipogenesis, as well as the reduction of triglyceride and cholesterol (Chan *et al.*, 1999; Kim *et al.*, 2013; Muramatsu *et al.*, 1986; Suzuki *et al.*, 1998; Yang and Koo, 1997). Several studies have explored the uses of GTPs as the

complementary and alternative medicinal agents against human chronic diseases (Borges *et al.*, 2016; Li *et al.*, 2016; Peng *et al.*, 2014; Wang *et al.*, 2008).

Human gastrointestinal (GI) tract harbors a complex and dynamic microbial community (Dominguez-Bello *et al.*, 2010; Penders *et al.*, 2006). Next generation sequencing (NGS) techniques have identified more than 1000 microbial species from gut microbiota with over 200 trillion cells, which own a gene repertoire of about 150 times larger than human gene complement (Qin *et al.*, 2010a). The metabolic functions maintained by the gene products of gut-microbiota provide host with thousands of functional metabolites and nutrients, including vitamins, phenols, secondary bile acids, lipids, short chain fatty acids (SCFAs), and neurotransmitters (Clifford, 2004; Qin *et al.*, 2010b; Rowland *et al.*, 2018). These molecules actively modulate the physiological functions of GI tract and liver through enterohepatic circulation (Jia *et al.*, 2018), and participate in the regulation of other organs via peripheral circulation (Ursell *et al.*, 2014). Studies have recently uncovered a complicated “three-way” connection among gut-microbiota, host health, and the environmental inputs—dietary preference, medical treatments, and lifestyle-related factors, e.g. cigarette smoking, alcohol consumption, and physical activities (Chakraborty *et al.*, 2010; Holmes *et al.*, 2012). With regards to the influential factors involved with gut-microbiota, food consumption is recognized as the most crucial determinant which modulates the human gut-microbiota starting from infancy (Brown and Hazen, 2015; Conlon and Bird, 2014; Holmes *et al.*, 2012; Jansson *et al.*, 2009; Penders *et al.*, 2006). Certain dietary pattern, or consumption of functional food components, were found to remarkably modify the community structure of gut-microbiota, leading to the change of nutritional status, and eventually resulting in positive or adverse

health outcomes in host (Oriach *et al.*, 2016). This “three-way” relationship is essentially driven by the diversity, proportion, and the amount of the metabolites produced by gut-microbiota (Conlon and Bird, 2014; Marchesi *et al.*, 2016). Therefore, to examine and characterize gut-microbiota dependent metabolism have been considered a novel dimension for the study of human health and disease conditions.

Previous 16S rRNA sequencing analysis demonstrated that microbes of *Bacteroidetes* and *Oscillospira* families were significantly enriched whereas *Peptostreptococcaceae* family were almost depleted in the gut of the rats treated with GTPs (Wang *et al.*, 2018). The adjusted gut-microbiota community structure was supposed to influence the nutritional provision in gut in a more comprehensive way than gene orthologs. However, more specific and solid evidences are required to estimate the potential health impacts of the genome changes gut-microbiota on host. In the work presented here, gas chromatography–mass spectrometry (GC-MS) based metabolomics and high-performance liquid chromatography (HPLC)-metabolic profiling approaches were used to analyze the gut content of the rats administered with GTPs. In addition to the high-throughput metabolomics data, a set of key organic acids, carbohydrates, and amino acids were determined using standard calibration methods. The purpose of this study is to investigate how genomic changes in gut microbiome could further influence host health via modification of gut-microbiota dependent metabolisms.

6.2 Methods

6.2.1 Chemicals and reagents

Methoxyamine, N,O-bis(trimethylsilyl)trifluoroacetamide (BSTFA) with 1% trimethylchlorosilane (TMCS), N-(3-Dimethylaminopropyl)-N'-ethylcarbodiimide hydrochloride (EDC), 2-nitrophenylhydrazine, and high-purity standards (>99%), including D-mannose, D-fructose, D-galactose, D-glucose, N-acetyl-D-glucosamine, myo-inositol, D-lactose, D-trehalose, L-proline, L-alanine, acetic acid, propionic acid, butyric acid, valeric acid, hexanoic acid, cholic acid, pentadecanoic acid, 3-phenyl lactic acid, pyruvic acid, linoleic acid, deoxycholic acid, internal standards (i.e. 2-ethylbutyric acid, hippuric acid, and heptadecanoic acid) were all purchased from Sigma-Aldrich Inc (St. Louis, MO, USA). GC-MS grade hexane and chloroform were ordered from J. T. Baker (Phillipsburg, NJ, USA). HPLC grade solvents, including pyridine, dimethyl sulfoxide (DMSO), methanol, acetonitrile, and water, were purchased from Honeywell (Morris Plains, NJ, USA). Decaffeinated high-purity green tea polyphenols (GTPs) powder, consisting of 65.37% of EGCG, 19.08% of ECG, 9.87% of EC, 4.14% of EGC, and 1.54% of catechin was purchased from Zhejiang Yixin Pharmaceutical Co., Ltd. (Zhejiang, China).

6.2.2 Animal experiment

This study was conducted following the same protocol used in a recently published study which tested the chronic toxicity and no observed adverse effect level (NOAEL) of GTPs extracts (decaffeinated) in middle-aged ovariectomized SD rats (Shen *et al.*, 2017; Wang *et al.*, 2018). Briefly, 72 female Sprague-Dawley (SD) rats (6-month old, Harlan Laboratories, Indianapolis, IN, USA) were randomized and divided into 6 groups (n =

12/group), and housed in individual stainless-steel cages with a room temperature of 21 ± 2 °C and a light-dark cycle of 12 hr. The rats were administered with drinking water containing 0, 0.5%, and 1.5% GTPs (g/dL, 2 groups per treatment level) up to 6-month. The applied doses have been shown to be under NOAEL (Shen *et al.*, 2017). All rats were fed with the pelleted AIN-93M diet (Dyets, Bethlehem, PA, USA). Gut contents were collected at 3-month and 6-month, with 1 group of rats at each treatment level sacrificed at each sampling time. After sacrifice, gut content samples were rapidly taken out and transferred to 50 mL centrifuge tubes, and then immediately stored in a -80 °C freezer until analysis. The 6-month duration of treatment for the evaluation of chronic effects of a substance in rats is roughly equivalent to 12 years in human (Guideline, 2006). All procedures were approved by the Institutional Animal Care and Use Committee.

6.2.3 Gas chromatography–mass spectrometry (GC-MS) metabolomic analysis

To quench the sample used for GC-MS analysis, a 50 mg frozen sample pellet was transferred to a PowerLyzer tube, and 400 μ L cold methanol (-80 °C) was immediately added into the tube. The sample pellet was then smashed using a glass pestle. After that, an aliquot of 800 μ L chloroform was added to form a mixture. The tube was capped and vortexed for 15 min. Next, an aliquot of 400 μ L water was added to induce phase separation. The tube was later centrifuged at 4 °C and 12,000 rpm for 10 min. Following centrifugation, 100 μ L upper phase and 100 μ L lower phase were drawn out and re-combined into an analytical glass tube (length, 75 mm; inner diameter 10 mm; Fisher Scientific, Pittsburgh, PA, USA). The sample was evaporated to dryness in a centrifugal evaporator. A volume of 300 μ L methanol was used to wash the tube wall and a secondary round of evaporation

was conducted. After thorough evaporation of sample extract in a centrifugal evaporator, 80 μ L methoxyamine (15 mg/mL in pyridine) was added into the glass tube to perform pre-column derivatization. The glass tube was vortexed for 10 min in order to homogenize the mixture, and then underwent centrifugation at 4000 rpm, 4 $^{\circ}$ C for 10 min to collect the mixture solution left on the wall. The solution was then transferred to an analytical vial to for air bath at 35 $^{\circ}$ C for 90 min. After then, an aliquot of 80 μ L BSTFA with 1% TMCS was added and the vial was allowed to stay at 70 $^{\circ}$ C for 12 hr under mild shaking condition. Three extra sampling operations were performed randomly for each group to increase statistical power, generating a sample size of 15 for each group.

GC-MS metabolomics analysis was performed using an Agilent 5973-6890 system equipped with a J&W DB-5ms column (length, 30 m; inner diameter, 0.25 mm; film thickness, 0.25 μ m; temperature range, -60 – 350 $^{\circ}$ C). Ultra-high purity grade nitrogen was used as carrier gas with a constant flow rate of 0.6 mL/min. Front inlet was set as splitless and gas-saving mode with a heating temperature of 275 $^{\circ}$ C. To analyze sample, the purge time was set to 60 s, with a purge flow rate of 20 mL/min and an equilibration time of 1 min. The column temperature was initially started at 50 $^{\circ}$ C for 2 min, and then ramped to 320 $^{\circ}$ C at 3.5 $^{\circ}$ C/min, held for 10.5 min. Ion source temperature was set as 230 $^{\circ}$ C. Quadrupole temperature was set as 150 $^{\circ}$ C. Data was acquired in full-scan positive mode with a mass range of 50 to 800 amu. To protect ion detector, a solvent delay time of 10.5 min was applied in the ramping process for instrumental protection. Injection volume was 2 μ L. Typical total ion chromatograms (TIC) of GTPs-treated group and control group are shown in **Figure 6-1**. The labeled peaks were confirmed with standard spikes. All analytical parameters used for quantitation are listed on **Table 6-1**. The quantitation was

based on extracted ion chromatogram (XIC or EIC) using the most abundant ions showing in the fragmentation spectra.

6.2.4 HPLC-metabolic profiling of key metabolites

The sample extraction procedure was modified from previous publications (de Jonge *et al.*, 2012; Hernandez Bort *et al.*, 2014). Cold methanol ($-80\text{ }^{\circ}\text{C}$) was used to quench and extract samples in order to avoid the loss of volatile composition (Peters *et al.*, 2004; Torii *et al.*, 2010; Winder *et al.*, 2008). Briefly, 200 mg frozen sample pellet was transferred to a Mobio PowerLyzer tube (Qiagen, Venlo, Netherlands). The tube was preloaded with glass beads of 0.1 mm inner diameter in order to sufficiently break the cells and particles under vortex condition. One milliliter of cold methanol ($-80\text{ }^{\circ}\text{C}$) was added into the tube. Then the sample pellet was gently smashed using a glass pestle. Half milliliter of cold methanol was slowly added to wash the pestle. The tube was next capped tightly and fastened on Genie 2 mixer (VWR, Suwanee, GA, USA) to undergo 20 min vortex. Finally, the tube was centrifuged at 12,000 rpm for 10 min to spin down cellular debris.

The derivatization protocol followed our previous publication (Zhou *et al.*, 2018). Briefly, 100 μL supernatant was transferred to a microcentrifuge tube, and 50 μL internal standard (IS, 2-ethylbutyric acid) stock solution was spiked into the tube to achieve a concentration of 1 $\mu\text{g}/\mu\text{L}$. To perform 2-nitrophenylhydrazine (2-NPH) derivatization, 150 μL sample extract (with internal standard added) was mixed with 45 μL derivatization solution which was freshly prepared by mixing 15 μL EDC solution (0.05 g/mL H_2O), 15 μL 2-NPH solution (12.5 mg/mL methanol) and 15 μL 3% pyridine in methanol (v/v). After mild vortex, the tubes were transferred to process water bath at $60\text{ }^{\circ}\text{C}$ for 60 min.

The tubes then were allowed to stay in room temperature for 5 min and went through brief centrifugation in order to collect the liquid left on the tube wall. All sample vials were kept in 4 °C sample cooling tray and the analysis was finished within 24 hours. Ten samples were randomly picked from each group for quantitation and analysis. The instrumental settings and chromatographic conditions were the same described in previous work (Zhou *et al.*, 2018). A typical chromatogram from GTPs-treated group and control group are shown and compared in **Figure 6-2**. The labeled peaks were confirmed using standard spikes. All analytical parameters used for quantitative analysis were listed in **Table 6-2**.

6.2.5 Data processing and statistics

GC-MS raw files were submitted to XCMS on-line modules for peak detection, retention time correction, isotope grouping, peak alignment, and integration of extracted ion chromatography (Tautenhahn *et al.*, 2012). The processed data were then normalized using cyclic locally weighted scatterplot smoothing (LOWESS) technique (Savage, 1972). A two-tailed Welch's t-test was used to examine the statistical significance of fold change of metabolomic data. The chemical entities of the interested analytes were imputatively annotated by searching their fragmentation spectra through National Institute of Standards and Technology (NIST) Standard Reference Database coupled to Agilent Automatic Mass Deconvolution and Identification Software (AMDIS). Principal component analysis (PCA) was applied to evaluate the statistical importance of metabolite in clustering samples with different treatments using R. Heatmap and hierarchical tree were constructed based on Pearson's correlation coefficients. Two-way ANOVA was performed in SPSS 13.0 to examine the statistical significance of dose (A), time (B), and interaction (A × B) effects

of GTPs on the metabolites detected in the metabolomic analysis. Treatment time was set as within-subjects independent variable and dose was set as between-subjects independent variable. The specific metabolic pathways responding to GTPs treatment were estimated and summarized according to Human Metabolome Database (HMDB) and Kyoto Encyclopedia of Genes and Genomes (KEGG) database. Metabolite set enrichment analysis (MSEA) was conducted to summarize the alterations of metabolic pathways via MetaboAnalyst (Xia and Wishart, 2016). Non-parametric Mann-Whitney U test was performed in SPSS 13.0 to examine the significance of fold-change for the key metabolites profiled by GC-MS and HPLC using standard calibration-based quantitation. Unless otherwise stated, all data visualizations were performed in R (Team, 2013).

6.3 Results

6.3.1 *Green tea polyphenols induced dose- and time-dependent changes of gut-microbiota dependent metabolites*

For convenience, the three experimental groups were noted as control, 0.5% GTPs-treated, and 1.5% GTPs-treated, respectively. GC-MS based metabolomics analysis was performed to gain an overview on the global shift of the gut microbial metabolites. Totally 2667 feature ions were detected from 90 samples. The top 200 significantly altered feature ions ranked by Welch's t-test were noted as differential feature ions. The total ion chromatogram (TIC) peaks that contain these differential feature ions were located in the deconvoluted chromatograms using the retention time and m/z of that feature ion. The quantitative analysis was based on the total peak intensities of extracted ion chromatograms (EIC) of feature ions. The fragmentation spectra of top 200 differential peaks were

searched through NIST database and a total of 57 metabolites were imputatively identified (**Table 6-3**). Principal component analysis (PCA) model was used to examine whether the differential metabolites could reflect the global change of the gut microbial metabolites induced by GTPs-treatment. The metabolomics data of the samples collected at 3-month and 6-month were input into the PCA model to examine whether the studied 57 features could represent the overall change of samples induced by GTPs. The scores plot was shown in **Figure 6-3**. At 3-month PC1 and PC2 explained 60.1% and 10.2% of data variation; at 6-month the PC1 and PC2 explained 81% and 9.3% of data variation, respectively. Principal component regression (PCR) analysis with these 5 PCs generated a regression coefficient (R^2) of 0.86 between the expected dose and actual dose of GTPs (data not shown). Thus, not much information is lost by considering these 57 metabolites as representative components of all existing metabolites at 6-month. The dose- and time-effects of GTPs-treatment on these metabolites were visualized using heatmap and hierarchical clustering tree (**Figure 6-4 A**). The clustering tree was built based on the distance metrics of Pearson correlation coefficient. As shown in the heatmap, Cluster A (28 components) were decreased in the GTPs-treated groups, and Cluster B (29 components) were elevated in the GTPs-treated groups. Further, the components in Cluster B exhibited time-dependent changes. The highest concentrations of Cluster B1 (15 components) were observed after 3-month treatment, whereas the highest concentrations of Cluster B2 (14 components) were observed after 6-month treatment.

Following observations on the changes of metabolic patterns, two-way ANOVA was applied to examine the time- and dose-dependency of the metabolites during GTPs-treatment. The results of two-way ANOVA are listed in **Table 6-3**. Venn plot illustrates

the counts of metabolites that are significantly affected by the two main factors and interaction effect (**Figure 6-4 B**). There were 53 metabolites significantly affected by the dose effect, 14 metabolites significantly affected by the time effect, and 39 metabolites affected by the interaction effect between dose and time of GTPs-treatment. Eight metabolites were found to be significantly affected by time, dose and the interaction effects of GTPs-treatment, all observed at high dose level (**Figure 6-5**). The imputative identities and max fold changes (MFC) of the eight metabolites are pentanoic acid (MFC, 2.02; $p = 0.033$), unknown steroid (MFC, 0.89; $p = 0.0064$), aspartic acid (MFC, 1.91; $p < 0.0001$), butanedionic acid (MFC, 1.44; $p = 0.00046$), pyrimidine (MFC, 1.67; $p < 0.0001$), D-xylose (MFC, 2.65; $p < 0.0001$), ursodeoxycholic acid (MFC, 1.7; $p < 0.0001$), and cyclohexanecarboxylic acid (MFC, 0.79; $p < 0.0001$), respectively.

The potential impact of the changes of 57 differential metabolites on host health was assessed using metabolite set enrichment analysis (MSEA) (**Figure 6-6**). The metabolic pathways showing remarkable response to GTPs were summarized by MSEA, based on KEGG records. There were 32 pathways showing significant responses (**Table 6-4**). There were 6 metabolic pathways containing more than 3 significantly altered metabolites: (1) urea cycle, (2) galactose metabolism, (3) glycine, serine and threonine metabolism, (4) ammonia recycling, (5) bile acid biosynthesis, (6) valine, leucine and isoleucine degradation. These 6 major pathways extended to connect with other metabolic pathways and form 5 major “node clusters”. Shown in **Figure 6-6 B**, the “major pathways centered node clusters” are—Cluster 1: alanine metabolism, glucose-alanine cycle, urea cycle, arginine and proline metabolism, ammonia recycling, glutamate metabolism, malate-aspartate shuttle; Cluster 2: glycine, serine and threonine metabolism, methionine

metabolism; Cluster 3: fatty acid metabolism, fatty acid elongation in mitochondria; Cluster 4: galactose metabolism, nucleotide sugars metabolism, starch and sucrose metabolism; Cluster 5: glycolysis, gluconeogenesis.

Following pathway analysis, global metabolite-gene network analysis was performed and revealed the genes that were potentially affected by the metabolic changes caused by GTPs-treatment (**Figure 6-7**). The results of global metabolite-gene network analysis were consistent with the results of MSEA and present us the connections between metabolic pathways bridged by both compounds and genes. The most remarkably activated and connected metabolic pathways are: Bile acid biosynthesis, C21-steroid hormone biosynthesis and metabolism, *de novo* fatty acid biosynthesis, Fructose/Mannose metabolism, Galactose metabolism, Glycine/serine/alanine/threonine metabolism, Glycerophospholipid metabolism, Glycolysis, Gluconeogenesis, and Glycosphingolipid metabolism.

6.3.2 Determination of key metabolites in gut content

Untargeted GC-MS based metabolomics analysis provided us an overview on the metabolic pathways modified by GTPs. It was shown that the most significantly modified metabolites belong to long chain fatty acid, phenyl acid, bile constituents, carbohydrate, vitamin, and amino acid. To confirm such changes, the concentrations of a set of representative metabolites were determined using standard calibration methods via HPLC and GC-MS analyses. The high-purity standards used for quantitative analysis are shown in Materials and Methods part. The regression curves and analytical parameters are listed in **Table 6-1** and **6-2**. The specific results of the quantitation of these metabolites are shown

in **Figure 6-8**. The metabolites showing statistically significant and MFCs at 3-month include niacin (8.61; $p < 0.0001$; 1.5% GTPs-treated group), 3-phenyllactic acid (2.20; $p = 0.009$; 1.5% GTPs-treated group), D-galactose (3.13; $p < 0.0001$; 0.5% GTPs-treated group), pentadecanoic acid (2.15; $p = 0.022$; 1.5% GTPs-treated group), lactic acid (2.70; $p = 0.003$; 1.5% GTPs-treated group), and L-proline (2.15; $p < 0.0001$; 1.5% GTPs-treated group); the components with reduced MFCs were cholesterol (0.29; $p = 0.007$; 0.5% GTPs-treated group), cholic acid (0.62; $p = 0.001$; 1.5% GTPs-treated group), deoxycholic acid (0.41; $p = 0.034$; 1.5% GTPs-treated group), D-trehalose (0.14; $p < 0.0001$; 0.5% GTPs-treated group), D-glucose (0.46; $p < 0.0001$; 1.5% GTPs-treated group); D-fructose (0.12; $p < 0.0001$; 1.5% GTPs-treated group). The metabolites showing significant and MFCs at 6-month included D-mannose (2.05; $p < 0.0001$; 1.5% GTPs-treated group) and L-alanine (0.61; $p < 0.0001$; 1.5% GTPs-treated group), respectively.

6.4 Discussion

In the current study, untargeted metabolomics analysis followed by quantitation of key metabolites with GC-MS and HPLC were conducted to investigate GTPs-induced alterations of gut-microbiota dependent metabolic pathways. A total of 57 differential metabolites represented the overall changes of GTPs induced metabolome of gut-microbiota (**Figure 6-3**). The dataset of metabolites at 6-month could explain ~90% data variation, indicating that it can well stand for the global metabolic changes induced by GTPs (**Figure 6-3 B**). Fragmentation-based characterization of sample metabolomes demonstrated that GTPs treatment induced remarkable changes of metabolites in a wide range of categories, which exhibited significant time- and dose-dependent patterns (**Figure**

6-4 and **Table 6-3**). Bioinformatic analysis found that such changes cover the biochemical reactions that relate to metabolisms of carbohydrates, amino acids, lipids, organic acids, and bile constituents etc. (**Figure 6-6**, **Figure 6-7** and **Table 6-4**). Cluster analysis also demonstrated a “node cluster” formed by several pathways that were related with TCA cycle, including alanine metabolism, glucose-alanine cycle, urea cycle, arginine-proline metabolism, ammonia recycling, glutamate metabolism, and malate-aspartate shuttle (**Figure 6-6 B**). Standard calibration-based quantitation confirmed that significant alterations occurred on carbohydrates, amino acids, bile constituents, and lactic acid, but not for the other short chain fatty acids (SCFA) (**Figure 6-8**).

The gut of mammals is colonized by actively metabolizing microorganisms that play a crucial role in digesting food and providing functional metabolites and nutrients (Marchesi *et al.*, 2016). Upon exposure to xenobiotics, such as drugs, natural products, toxins and toxicants, gut flora has exhibited responsive adjustment of community structure and metabolic pathways, which further exert dynamic influence on host health (Koppel *et al.*, 2017). The changes of the metabolic pathways are usually explored via all kinds of metabolomic analyses (Smirnov *et al.*, 2016; Tang *et al.*, 2016; Xia and Wishart, 2016; You *et al.*, 2014). Among the diverse strategies that are used to refine and reduce metabolomic data pool for further analysis, the combination of t-test with PCA has been widely practiced to acquire the representative metabolite set for further pathway analysis (Lu *et al.*, 2014; Lu *et al.*, 2012; Xia *et al.*, 2009). As shown in **Figure 6-3**, the dataset collected at 6-month was much more representative than that extracted from dataset at 3-month, of which the PC1 and PC2 only explained 70% variation caused by GTPs. The metabolomic data (**Table 6-3**) at 6-month demonstrated that GTPs extensively reduced

concentrations of calorific carbohydrates (such as glucose, galactose, fructose), fatty acids (such as pentadecanoic acid and octadecanoic acid) but elevated a number of amino acids and derivatives (such as threonine, aspartic acid, leucine). The bile constituents were found to be generally reduced, suggesting that GTPs could also downregulate the synthesis and secretion of bile components. These metabolites were affected by time-, dose-, and interaction (time \times dose) effects of GTPs treatment. Untargeted metabolomic analysis (**Figure 6-4** and **Table 6-3**) found that the metabolites usually with high concentrations in gut, such as D-glucose, D-fructose, glycerol, myo-inositol, acetic acid, L-aspartic acid, L-alanine etc., were only affected by dose, whereas no metabolite was found to be affected singly by time. This indicates that the time effect of GTPs treatment is comparably weaker than dose effect in modulating the gut-microbiota dependent metabolic pathways of major nutrients and metabolites. This is consistent with previous finding that the gut-microbiota biodiversity was mainly dependent on GTPs dose (Wang *et al.*, 2018). The eight most sensitive responsive metabolites (**Figure 6-5**) were organic acid (pentanoic acid, butanedionic acid), bile metabolites (an unknown steroid, ursodeoxycholic acid), amino acid (aspartic acid), phenolic acid (cyclohexanecarboxylic acid), nucleic acid metabolite (pyrimidine) and carbohydrate (D-xylose). The changes of these metabolites indicated the alterations of biochemical reactions for the metabolisms of carbohydrates, steroids, amino acids, aliphatic acids and phenol acids, which has been reported for exposure to a wide range of xenobiotic categories (Barbosa, 2013; Kim *et al.*, 2013; Koppel *et al.*, 2017).

As shown in **Figure 6-6 A** and **Table 6-4**, the top five metabolic pathways demonstrating significant responses to GTPs include urea cycle, aspartate metabolism, malate-aspartate shuttle, arginine and proline metabolism, and beta-alanine metabolism, all

of which were related with mitochondrial TCA/Urea cycle. Next to these five pathways were the metabolisms of carbohydrates and conjugated sugars that support mitochondrial respiration and ATP-synthesis. The cluster analysis (**Figure 6-6 B**) also indicated that mitochondrial centered “energy conversion” pathways were affected. Moreover, KEGG-based compound-gene network analysis (**Figure 6-7**) found consistent results with the above pathway analysis. While the gene ortholog data were not available, network analysis was performed to show the “gene bridged” connections between the metabolic pathways. As shown in the **Figure 6-7**, the metabolic pathways connected to TCA/Urea cycle include: bile acid biosynthesis, C21-steroid hormone biosynthesis and metabolism, *de novo* fatty acid biosynthesis, fructose/mannose metabolism, galactose metabolism, glycine/serine/alanine/threonine metabolism, glycerophospholipid metabolism, glycolysis, gluconeogenesis, and glycosphingolipid metabolism, etc. The pathway analysis and network analysis together suggested that TCA/urea cycle of gut-microbiota may be boosted by GTPs and then drives the metabolisms of carbohydrates, fatty acids and lipids. This is consistent with the results of metagenomic analysis, in which a set of microbial gene orthologs related to mitochondrial respiration were significantly elevated by GTPs, such as alpha-glucosidase (ENOG4105CGS), NADH oxidase (ENOG4105CCY), and AAA-ATPase (ENOG4105F42) (Wang *et al.*). These analyses further suggest that GTPs modulated the energy conversion and branch pathways (Laparra and Sanz, 2010; Velagapudi *et al.*, 2010).

Standard-calibration based quantitation (**Figure 6-8**) demonstrated that the major dietary calorific carbohydrates, such as D-glucose, D-fructose and D-trehalose, were reduced in all GTPs-treated groups. This may be partially caused by the enrichment of

Bacteroidetes and *Oscillospira* by GTPs in the gut of rats (Wang *et al.*)—the two families were linked with the lean phenotype in mammals (Konikoff and Gophna, 2016; Tims *et al.*, 2013; Turnbaugh *et al.*, 2009; Verdum *et al.*, 2013), and were shown to be highly efficient in metabolizing carbohydrates (Lin *et al.*, 2013; Turnbaugh *et al.*, 2009). GTPs may elevate the efficiency of gut-microbiota dependent energy conversion at global level and consequently reduced calorific carbohydrates in gut by enriching these microbes. By contrast, D-mannose and D-galactose were both increased by GTPs in the gut content, and the elevation of D-galactose was more remarkable than D-mannose. Galactose has been reported to offer beneficial modifications regarding multiple physiological functions, such as liver metabolism, fertilization, blood maintenance, and pulmonary function via forming functional complex carbohydrates (Dabelsteen *et al.*, 1988; Hussain *et al.*, 2012; Roseman and Baenziger, 2003; Xia *et al.*, 2005). Galactose and mannose can be synthesized in the bacterial catabolic process of calorific carbohydrates (Macfarlane *et al.*, 2005).

Interestingly, there was no significant changes of SCFAs observed in the gut content from GTPs-treated rats, except for lactic acid, which is different with a recent report that tea polyphenols elevated the production of SCFA in Caco cell-bacteria co-culture system (Sun *et al.*, 2018). In our study, remarkable elevation was only observed for lactic acid at 3-month (2.7 fold; $p = 0.003$; 0.5% GTPs-treated group). In addition, acetic acid demonstrated remarkable decrease at 6-month in 1.5% GTPs-treated groups (0.6-fold of control, $p = 0.013$). It seems that GTPs may not target bacterial anaerobic metabolism of indigestible fibers—the major source of gut SCFAs. Consistently, 16S rRNA sequencing analysis also showed non-significant change for *Lactobacillales*, such as *Lactobacillus*,

Leuconostoc, *Pediococcus*, *Lactococcus*, and *Streptococcus*. Therefore, we conclude that the gut-microbiota dependent formation of SCFAs is not a major target pathway of GTPs.

L-alanine (reduced by ~40%) and L-proline (increased by ~2 fold) were both markedly altered in our study, which may suggest that the metabolisms of amino acids may not respond in the same trend. These results reflected complex adjustment of community structure of gut-microbiota following GTPs treatment, since different microbial strains have diverse preferences on the metabolic pathways of amino acids (Dai *et al.*, 2011). Gut-microbiota is known to play important roles in the digestion and absorption of amino acids, as well as the catabolism and fermentation of amino acids in gut (Wang *et al.*, 2009). In the intestine of healthy adults, the most abundant amino acid fermenting bacteria belong to *Clostridium*, *Proteobacteria*, *Peptostreptococci*, and *Streptococcus*.

Gut niacin was elevated in the GTPs-treated groups, with remarkable increase seen in 0.5% GTPs-treated group at 6-month (8.61-fold of change, $p < 0.0001$), 1.5% GTPs-treated groups at both 3-month (4.24-fold of control, $p = 0.001$) and 6-month (3.66-fold of change, $p = 0.027$). B group vitamins are well known to take the central regulating role in mitochondrial energy metabolism, including the oxidative decarboxylation of the branched-chain keto acid, CoA formation and fatty acid oxidation (Depeint *et al.*, 2006). Niacin (vitamin B3) is especially needed for the mitochondrial synthesis of NADH, which supplies protons for the oxidative phosphorylation. A PubSEED-based investigation showed that niacin can be synthesized by 162 of the 256 gut microbes of common human gut bacteria (Magnusdottir *et al.*, 2015). Therefore, GTPs may enrich gut vitamin-producing strains and then contribute to the TCA/Urea cycle and energy conversion.

Cholesterol and cholic acid, two major constituents of bile, were significantly reduced in the GTPs-treated groups (**Figure 6-8**). The reduction of cholic acid may be caused by the decrease of cholesterol since cholic acid is synthesized from the latter. Consistently, gut deoxycholic acid, a derivative of cholic acid, was markedly reduced in the 1.5% GTPs-treated group at 6-month. In line with the above HPLC-profiling results, metabolomics data also indicated an overall suppression of bile constituents, such as deoxycholic acid, cholan-24-oic acid, ursodeoxycholic acid, cholesterol, and coprostan-3-ol—all reduced in 1.5% GTPs-treated groups at both 3-month and 6-month (**Table 6-3**). It is well known that bile constituents are endogenously synthesized from cholesterol by liver cells of most vertebrates. Though different species have distinct molecular forms of bile constituents, but cholic acid and chenodeoxycholic acid are both generated in human and rats. The alteration of bile constituents in gut, especially bile acid and deoxycholic acid, play a crucial role in modulating gut-microbiota (Tremaroli and Backhed, 2012). Besides, the elevation of cholic acid in gut is associated with liver pathogenesis and is also known as a risk factor for intestinal inflammation (Camilleri *et al.*, 2011; Mouzaki *et al.*, 2016), and extra cholic acid may partially contribute to the incidence of colon cancer by stimulating the growth of benign adenoma (Rowland, 2012). The modulation of the secretion and metabolism of bile constituents have been long noticed as a major aspect of the health benefits offered by GTPs (Stalmach *et al.*, 2010; Yang and Koo, 1999). In addition to bile constituents, significant accumulation of pentadecanoic acid was observed in the GTPs-treated groups at 3-month (MFC, 2.15; $p = 0.022$), which indicated the suppression of fat absorption following GTPs administration. It was suggested that the decrease in body fat after administration of GTPs is partly due to the inhibition of lipid

absorption, which is linked with mechanism of bile constituents in liver (Koo and Noh, 2007; Wang *et al.*, 2006).

Taken together, the results from untargeted and targeted metabolomics analysis demonstrated the decrease of calorific carbohydrates, reduction of bile synthesis, reduced absorption of fatty acids, altered metabolisms of amino acids, elevation of beneficial hexoses and vitamins in the gut of the GTPs-treated rats. The pathway changes were remarkable after 6-month treatment, especially for mitochondria TCA/Urea cycle related pathways. However, the production of SCFAs was not significantly affected by GTPs. The gut-microbiota dependent metabolic changes, accompanied with the alteration of gut-microbiome, may partially contribute to the health benefits observed with green tea consumption. It seems the overall beneficial effects of GTPs on host health rely on the consequences of integrated mechanisms. Our data showed that the gut-microbiota dependent metabolism could be a very important and indispensable contributor to the health-promoting bioactivity of GTPs, especially for the mitigation of obesity and reduction of extra calories.

TABLES

Table 6-1. Analytical parameters of GC-MS analysis used for the measurement of key metabolites.

Compound	RT	Q-ion	Regression Function ^a	R ²	Recovery Rate ^b	Linear Range ^c	LLOD ^d
2-Deoxy-D-ribose	32.55	73	$y = 1E-06x + 6.4$	0.996	0.222	1.25~400	0.625
D-Mannose	35.93	73	$y = 2E-07x - 0.66$	0.999	0.203	1.25~400	0.625
D-Ribitol	37.35	73	$y = 1E-07x - 1.2$	0.998	0.239	1.25~400	0.625
D-Fructose	41.68	73	$y = 1E-06x - 2.03$	0.996	0.232	1.25~400	0.625
D-Ribose	42.14	73	$y = 9E-07x - 14.5$	0.996	0.257	1.25~400	0.625
D-Galactose	42.20	73	$y = 3E-07x - 2.42$	0.999	0.298	1.25~400	0.625
D-Glucose	42.42	73	$y = 1E-06x - 16.57$	0.991	0.562	1.25~400	0.625
D-Galactitol	43.50	73	$y = 4E-06x - 9.89$	0.993	0.305	1.25~400	0.625
GlcNAc	47.34	73	$y = 1E-06x + 12.36$	0.999	0.249	1.25~400	0.625
<i>myo</i> -inositol	47.46	73	$y = 4E-07x - 10.31$	0.995	0.193	1.25~400	0.625
D-Lactose	61.39	73	$y = 1E-06x - 4.96$	0.995	0.249	1.25~400	0.625
D-Trehalose	62.62	73	$y = 1E-06x - 11.92$	0.991	0.217	1.25~400	0.625
L-Proline	22.4	307	$y = 1E-05x + 22.75$	0.944	0.243	9~575	4.5
L-Alanine	15.3	116	$y = 2E-06x + 101.4$	0.992	0.267	75~1200	37.5

Abbreviation: RT, retention time; Q ion, fragment ion used for quantitation; R², linear regression coefficient; LLOD, lower limit of detection; GlcNAc, N-Acetyl-D-glucosamine.

a. Y, ng/μL of analyte; X, peak area integrated from extracted ion chromatogram (EIC) of Q ion.

b. Recovery rate was calculated from blank extract containing ~50%, ~100% and ~200% peak area of an analyte measured in mixed control sample extract (n = 10, from control group). Recovery % = (amount of analyte measured in the spiked sample – analyte amount measured in the control) × 100/(spiked analyte amount in the extract). Three replicates were used to generate final recovery rate.

- c. The range in which regression curve maintains $R^2 > 0.99$. Unit of linear range is $\mu\text{g/mL}$.
- d. The analyte level which generated a signal-to-noise (S/N) ratio of 3 was noted as the LLOD for that analyte. The unit of LLOD is $\mu\text{g/mL}$.

Table 6-2. Analytical parameters of HPLC-profiling used for the measurements of key metabolites.

Compound	RT	Detective Channel	Regression	R ²	Recovery Rate ^a	Linear Range	LLOD ^b
Acetic acid	14.9	400 nm	$y = 0.0063x - 0.373$	0.999 3	0.66	0.016–64.8	0.008
Propionic acid	19.6	400 nm	$y = 0.021x - 0.927$	0.999	0.49	0.07–143	0.03
Butyric acid	25.1	400 nm	$y = 0.0256x - 0.499$	0.999 1	0.53	0.078–79.5	0.04
Valeric acid	31.5	400 nm	$y = 0.0208x - 0.497$	0.999	0.50	0.054–56.1	0.03
Hexanoic acid	37.6	400 nm	$y = 0.0309x - 0.356$	0.999 4	0.52	0.074–75.6	0.04
Lactic acid	13.8	400 nm	$y = 0.0244x - 0.235$	0.999 1	0.65	0.11–14.33	0.05
Pyruvic acid	41.3	400 nm	$y = 0.0166x + 0.714$	0.999 7	IS 1	6.2–500	0.19
2-Ethylbutyric acid	34.2	400 nm	$y = 0.1662x - 0.453$	0.999 1	0.76	0.56–1138	0.28
Niacin	22.1	210 nm	$y = 0.0313x - 6.177$	0.995 4	IS 2	1–430	0.25
3-Phenyllactic acid	31.2	400 nm	$y = 0.1003x - 0.713$	0.999 4	IS 2	4.7–300	0.58
Hippuric acid	26.3	400 nm	$y = 0.6161x + 2.828$	0.999 6	0.16	4.45–570	2.25
Cholic acid	45.1	400 nm	$y = 0.1219x - 6.605$	0.993 0	IS 3	3.9–250	0.49
Deoxycholic acid	47.1	400 nm	$y = 0.0371x - 4.866$	0.993 0	IS 3	2.5–330	0.64

Cholesterol	47.4	400 nm	$y = 0.0686x - 2.48$	0.990 0	IS 3	1.95–125	0.98
Bisphenol A	35.0	210 nm	$y = 0.0148x - 6.965$	0.992	0.97	0.33–685	0.17
Linoleic acid	50.9	400 nm	$y = 0.3705x - 31.314$	0.994 8	IS 4	3.9–1000	3.9
Pentadecanoic acid	51.2	400 nm	$y = 0.0636x - 0.3641$	0.999 0	IS 4	1.95–500	0.5
Heptadecanoic acid	54.5	400 nm	$y = 0.1436x - 4.5852$	0.995 2	0.39	2.15–275	1.07

The minimum data point in the linear regression range ($R^2 > 0.999$) was noted as LOQ. Abbreviations: IS, internal standard for quality control; R^2 , regression coefficient; LLOD, lower limit of detection; LCFA, long chain fatty acid; PA, phenyl acid; RT, retention time (min) in chromatogram; SA, steroid acid; SCFA, short chain fatty acid. The analyte level which generated a signal-to-noise (S/N) ratio of 3 was noted as the LLOD for that analyte. More specifics of methodology are available in previous publication.

Table 6-3. Two-way ANOVA examination on the statistical significance of the dose, time, and interaction effects of GTPs-treatment on the metabolites measured by GC-MS.

m/z	RT	Annotation	Category	E/C 1	E/C 2	VIP ^c	p-value		
							Dose	Time	Interaction
<i>Metabolites significantly affected by dose-time interaction of GTPs-treatment</i>									
129	43.9	Pentadecanoic acid	LCFA	0.69 2	0.78 9	0.01 4	<0.00 1	>0.05	<0.001
59.1	51.6	Octadecanoic acid	LCFA	0.70 8	0.78 0	0.07 6	<0.00 1	>0.05	<0.001
211	38.6	Phosphoric acid	IA	0.58 4	0.64 6	1.47 0	<0.00 1	>0.05	<0.001
221	18.1	Cyclohexanecarboxylic acid	OA	0.59 8	0.63 5	1.21 9	<0.00 1	<0.05	<0.01
73.1	40.3	Benzoic acid	OA	1.52 1	2.08 5	1.51 8	<0.00 1	>0.05	<0.001
61.1	13.6	Propanoic acid	SCFA	0.63 9	0.69 5	0.64 2	>0.05	>0.05	<0.001
119	11.2	Pentanoic acid	SCFA	0.74 8	1.00 8	1.11 5	<0.00 1	<0.05	<0.001
101	14.1	Hexanoic acid	SCFA	0.64 4	0.68 4	1.15 0	<0.00 1	>0.05	<0.001
77.1	23.3	Butanedionic acid	SCFA	0.69 4	1.02 5	0.05 8	<0.00 1	<0.05	<0.05
190	21.2	Butanoic Acid	SCFA	0.72 4	1.00 3	0.08 6	<0.00 1	>0.05	<0.05
147	24	Pyrimidine	OC	0.72 0	1.01 5	0.32 2	<0.00 1	<0.01	<0.05
297	55.8	3-Pyridinecarboxylic acid	OC	0.61 4	0.82 6	0.44 6	<0.00 1	>0.05	<0.05
400	68.8	Unknown steroid	CD	0.61 7	0.59 2	1.45 1	<0.00 1	<0.05	<0.01
259	70.6	Deoxycholic acid	CD	0.57 1	0.64 5	1.32 6	<0.00 1	>0.05	<0.05
430	72.3	Cholan-24-oic acid	CD	0.97 6	0.91 0	0.30 0	<0.00 1	>0.05	<0.001
355	67.7	Prosta-5,13-dien-1-oic acid	CD	0.56 3	0.69 2	1.00 5	<0.00 1	>0.05	<0.05
414	72.6	Ursodeoxycholic acid	CD	0.61 0	0.73 6	0.07 6	<0.00 1	<0.05	<0.001
355	70	Cholesterol	CD	0.62 5	0.73 7	0.86 7	<0.01	>0.05	<0.001
330	68.4	Coprostan-3-ol	CD	0.66 9	0.78 7	0.38 0	<0.01	>0.05	<0.001
55.2	71.7	Stigmastanol	CD	0.57 6	0.46 8	1.72 7	<0.00 1	>0.05	<0.05

311	72. 6	beta-Sitosterol	CD	0.64 9	0.75 7	0.40 7	<0.00 1	>0.05	<0.001
385	70. 2	Cholestan-3-yl acetate	CD	0.49 3	0.48 5	1.45 9	<0.00 1	>0.05	<0.001
100	30. 7	Aspartic acid	AA	0.59 8	1.33 6	0.31 7	<0.00 1	<0.00 1	<0.001
73. 1	25. 9	Threonine	AA	0.66 2	1.85 5	1.32 1	<0.00 1	>0.05	<0.001
100	43. 5	Tyrosine	AA	0.62 9	1.12 2	0.43 7	<0.00 1	>0.05	<0.05
159	21. 5	Leucine	AA	0.64 3	1.14 0	0.00 2	>0.05	>0.05	<0.001
75. 1	19. 3	Valine	AA	0.50 4	0.86 4	0.45 1	>0.05	>0.05	<0.05
174	22. 7	Glycine	AA	0.38 8	0.88 1	0.99 9	<0.00 1	>0.05	<0.001
75. 1	22. 4	Isoleucine	AA	0.58 9	1.09 3	0.05 3	<0.00 1	>0.05	<0.05
91. 1	34	Glutamine	AA	0.62 6	1.08 6	0.26 8	<0.00 1	>0.05	<0.05
89. 1	11. 6	Propylene glycol	C	0.69 7	0.87 1	0.54 9	<0.00 1	>0.05	<0.001
85. 2	71. 7	1,4-Cyclohexadiene	C	0.63 0	0.52 9	1.33 9	<0.01	>0.05	<0.001
355	50. 8	Methyl α -D- galactoside	C	0.62 1	0.73 8	0.78 3	<0.01	>0.05	<0.001
161	42. 4	Glucose	C	0.75 3	1.01 7	0.11 8	<0.00 1	>0.05	<0.01
307	35. 9	Xylose	C	1.11 4	1.83 0	1.03 2	<0.00 1	<0.05	<0.001
249	48. 6	Fucose	C	0.67 2	0.79 9	0.36 2	<0.00 1	>0.05	<0.001
160	42. 9	Galactose	C	0.85 8	1.16 7	0.24 6	<0.00 1	>0.05	<0.001
204	57. 9	Turanose	C	0.70 2	0.68 3	1.13 2	<0.00 1	>0.05	<0.001
158	10. 8	Diethylamine	C	0.68 7	0.78 1	0.54 8	<0.05	>0.05	<0.001
<i>Metabolites significantly affected by dose and time effects of GTPs-treatment</i>									
121	11. 5	Pyridine	OC	0.48 9	0.52 9	1.70 8	<0.00 1	<0.01	>0.05
204	37. 6	Xylopyranose	C	0.41 0	0.45 9	2.20 7	<0.00 1	<0.01	>0.05
73. 1	49. 6	1-Monolinoleoyl glycerol	C	2.13 6	2.49 6	2.98 4	<0.00 1	<0.05	>0.05

291	45	Pantothenic acid	VB	0.59 2	0.70 6	0.90 8	>0.05	<0.05	>0.05
84.	31.	Serine	AA	0.50	0.72	1.22	<0.00	<0.05	>0.05
1	2			8	1	4	1		
205	69.	Corticosterone	CD	0.51	0.49	2.08	<0.00	<0.05	>0.05
	9			8	3	4	1		
<i>Metabolites significantly affected by dose effect of GTPs-treatment</i>									
155	21.	Glycerol	C	0.66	0.85	0.49			
	7			8	4	8	<0.01	>0.05	>0.05
315	55.	Myo-inositol derivative	C	0.60	0.66	1.26			
	4			0	2	6	<0.01	>0.05	>0.05
217	41.	Fructose	C	0.45	0.48	2.05	<0.00		
	7			7	1	9	1	>0.05	>0.05
73.	35.	Ribose	C	0.72	0.47	2.67	<0.00		
1	2			6	7	2	1	>0.05	>0.05
73.	61.	Dulcitol	C	0.82	0.43	2.97	<0.00		
1	7			1	6	2	1	>0.05	>0.05
339	67	Phosphatidylcholine	Choline	0.72	0.97	0.15	<0.00		
				5	6	0	1	>0.05	>0.05
174	46.	Hexadecanoic acid	LCFA	0.65	0.93	0.08	<0.00		
	7			8	9	9	1	>0.05	>0.05
77.	43.	2- Hydroxyphenylpentan oic acid	PA	1.01	1.45	1.42	<0.00		
1	3			6	7	0	1	>0.05	>0.05
220	16.	Acetic acid	SCFA	0.52	0.55	1.67	<0.00		
	5			3	7	2	1	>0.05	>0.05
75.	15.	Alanine	AA	0.46	0.57	1.39	<0.00		
1	1			5	4	8	1	>0.05	>0.05
249	15.	Hydroxylamine	Oam	0.46	0.72	0.83	<0.00		
	4			0	3	8	1	>0.05	>0.05

Abbreviation: LCFA, long chain fatty acid; IA, inorganic acid, OA, organic acid; SCFA, short chain fatty acid; OC, organoheterocyclic compound; CD, cholesterol and derivative; AA, amino acid; C, carbohydrate, OAm, organic amine; VB, vitamin B; PA, phenolic acid. RT, retention time of feature ion aligned from all TICs (total ion chromatograms). Annotation, most plausible chemical entity acquired from NIST database based on the fragmentation spectrum. E/C1, extracted ion chromatogram peak intensity of a metabolite detected in 0.5% GTPs-treated group versus control after 6-month treatment. E/C2, extracted ion chromatogram peak intensity of a metabolite detected in 1.5% GTPs-treated group versus control, after 6-month treatment. VIP, Variable Importance in Projection (VIP) calculated using OPLS-DA, to evaluate the importance of a metabolite in clustering samples with different treatments.

Table 6-4. Significantly modified metabolic pathways revealed by MSEA^a.

Pathway	Hits/Total	adjusted- <i>p</i>	FDR
Urea cycle* (Cluster 1)	3/20	4.00E-10	1.83E-10
Aspartate metabolism	1/12	5.36E-10	1.83E-10
Malate-aspartate shuttle (Cluster 1)	1/8	5.36E-10	1.83E-10
Arginine and proline metabolism (Cluster 1)	2/26	9.42E-08	2.54E-08
Beta-alanine metabolism	2/13	3.62E-07	8.00E-08
Galactose metabolism* (Cluster 4)	5/25	3.00E-06	4.40E-07
Starch and sucrose metabolism (Cluster 4)	1/14	3.02E-06	4.40E-07
Fructose and mannose degradation	1/18	3.02E-06	4.40E-07
Nucleotide sugars metabolism (Cluster 4)	1/9	8.10E-06	1.11E-06
Steroidogenesis	2/32	2.37E-05	3.02E-06
Glycine, serine and threonine metabolism* (Cluster 2)	3/26	6.60E-05	7.87E-06
Ammonia recycling* (Cluster 1)	4/18	1.41E-04	1.54E-05
Bile acid biosynthesis*	4/49	1.43E-04	1.54E-05
Glucose-alanine cycle (Cluster 1)	2/12	3.80E-04	3.93E-05
Tyrosine metabolism	1/38	1.22E-03	1.07E-04
Phenylalanine and tyrosine metabolism	1/13	1.22E-03	1.07E-04
Catecholamine biosynthesis	1/5	1.22E-03	1.07E-04
Selenoamino acid metabolism	1/15	5.82E-03	5.14E-04
Alanine metabolism (Cluster 1)	1/6	5.82E-03	5.14E-04
Beta oxidation of very long chain fatty acids	1/14	6.45E-03	5.89E-04
Insulin signaling	2/19	9.00E-03	8.18E-04
Butyrate metabolism	1/9	1.24E-02	1.13E-03
Valine, leucine and isoleucine degradation*	3/36	1.25E-02	1.14E-03
Fatty acid metabolism (Cluster 3)	1/29	2.13E-02	1.89E-03
Fatty acid elongation in mitochondria (Cluster 3)	1/26	2.13E-02	1.89E-03
Steroid biosynthesis	1/31	2.67E-02	2.46E-03
Propanoate metabolism	2/18	2.67E-02	2.46E-03
Glycolysis (Cluster 5)	1/21	2.84E-02	2.75E-03
Gluconeogenesis (Cluster 5)	2/27	2.84E-02	2.75E-03
Pyrimidine metabolism	1/36	4.65E-02	4.69E-03
Purine metabolism	1/45	4.65E-02	4.69E-03
Glutamate metabolism (Cluster 1)	1/18	4.65E-02	4.69E-03
Methionine metabolism (Cluster 2) <i>non-significant</i>	2/24	1	0.7

* Pathway contains more than 3 detected components. There are four clusters revealed in network analysis. Cluster 1: Alanine metabolism, Glucose-alanine cycle, Urea cycle, Arginine and proline metabolism, Ammonia recycling, Glutamate metabolism, Malate-aspartate shuttle. Cluster 2: Glycine, serine and threonine metabolism, Methionine metabolism. Cluster 3: Fatty acid metabolism, Fatty acid elongation in mitochondria. Cluster 4: Galactose metabolism, Nucleotide sugars metabolism, Starch and sucrose metabolism. Cluster 5: Glycolysis, Gluconeogenesis.

- a. MSEA, metabolite set enrichment analysis performed using MetaboAnalyst online modules.
- b. The count of the detected metabolites divided by the total number of metabolites in that pathway according to KEGG.
- c. FDR, false discovery rate to conceptualize the rate of type I errors in null hypothesis testing when conducting multiple comparisons.

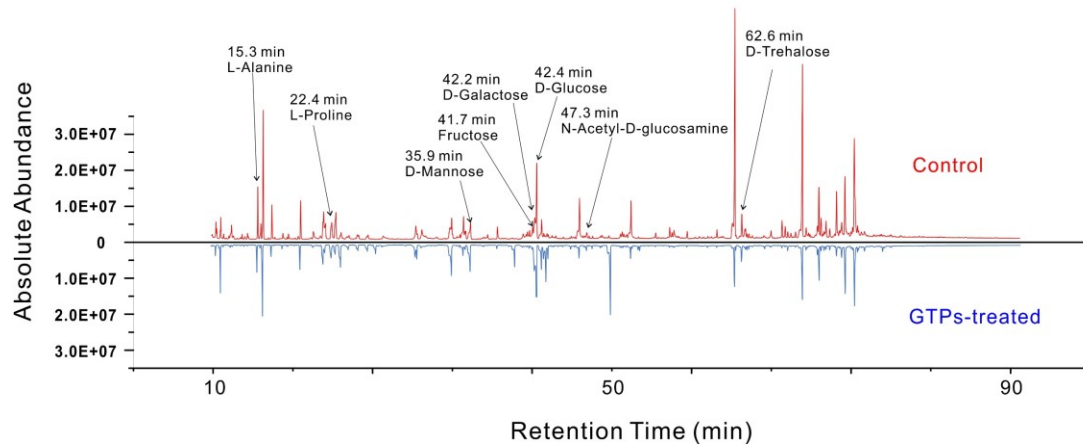


Figure 6-1. GC-MS total ion chromatogram (TIC) of gut content metabolites. Several interested amino acids and carbohydrates were located in the chromatogram by spiking standards. A solvent delay time of 10.5 min was applied. The determined concentrations of these nutrients were calculated based on extracted ion chromatogram (XIC) using standard calibration method. Specific results are listed in **Figure 6-8**.

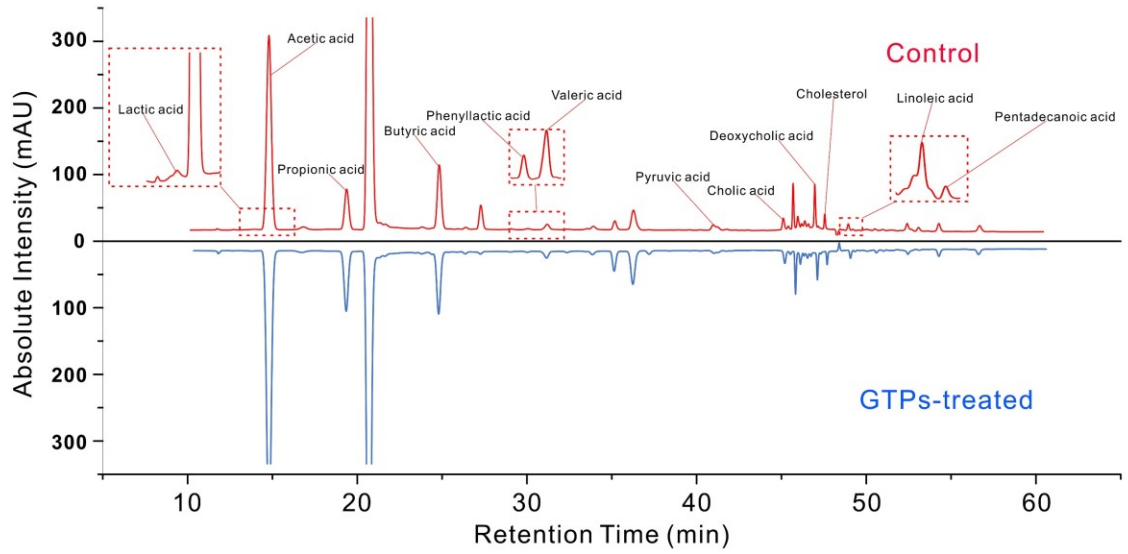


Figure 6-2. HPLC-profiling chromatograms of gut content metabolites from control (upper) and GTPs-treated group (lower). The detection channel of DAD is 400 nm with a reference channel as 510 ± 60 nm. Specific results are available in **Figure 6-8**.

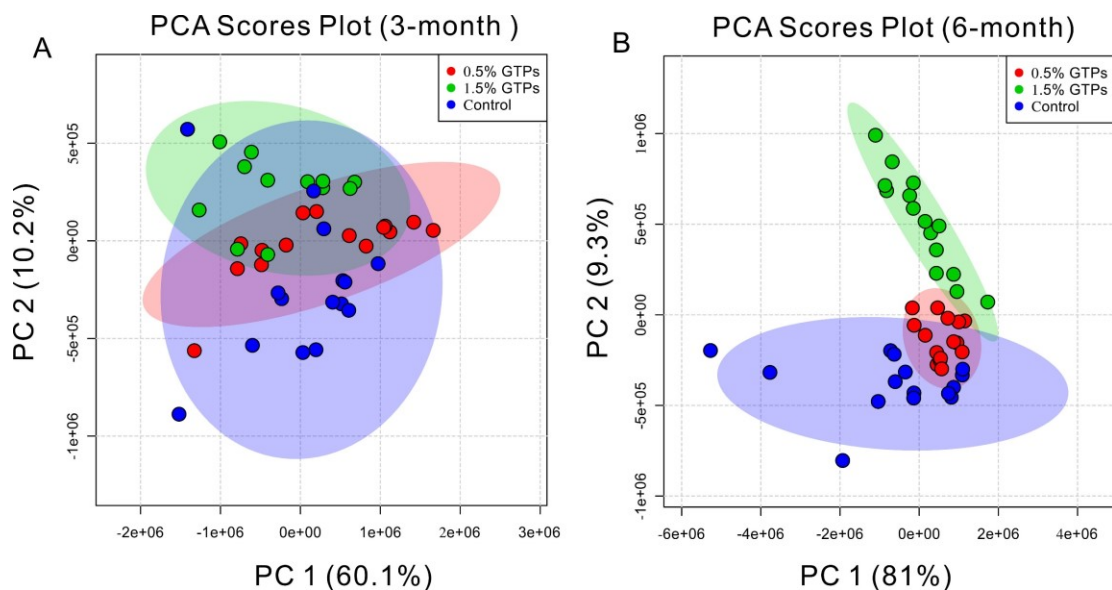


Figure 6-3. Score plot of principal component analysis (PCA) of the 57 metabolites significantly modified by GTPs. (A) Dataset collected at 3-month; (B) Dataset collected at 6-month. The color-coded circle represents 95% confidential interference, with 0.5% and 1.5% correspond to the treatments of drinking water containing 0.5% and 1.5% GTPs, respectively. Coordinates in axis are for illustration purpose only and selected arbitrary and therefore do not have clear biological meanings. Percentage associated with each PC is the proportion of an eigenvalue for the respective PC in the sum of eigenvalues for all PCs. With the top 5 PCs extracted from dataset of 6-month, the regression function between predicted GTPs dose and actual doses of GTPs has a R^2 (linear regression coefficient) of 0.86.

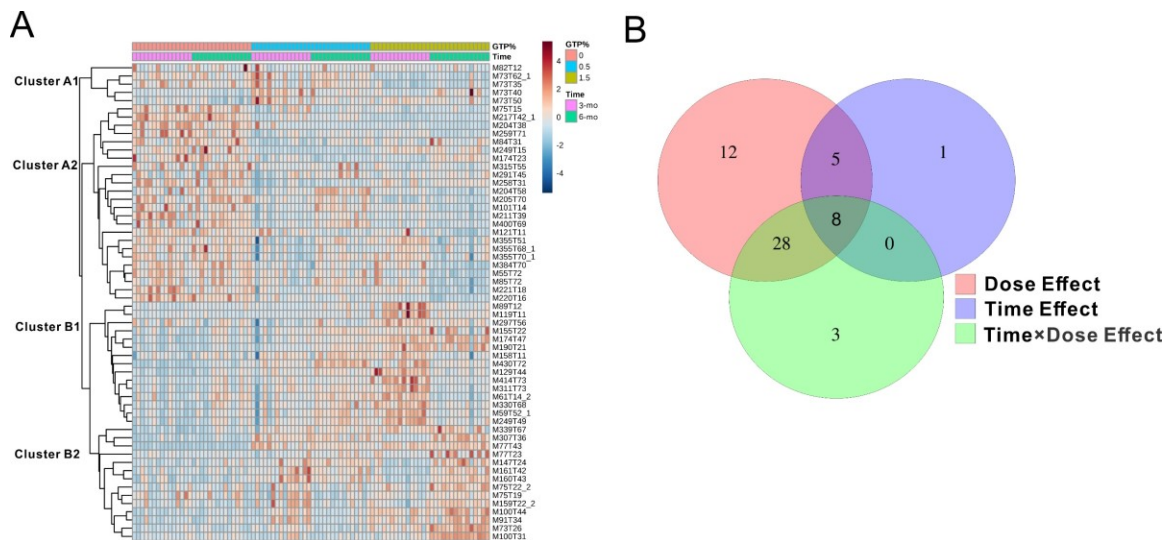


Figure 6-4. Overview of the alterations of metabolites profiled by GC-MS during the course of GTPs-treatment. (A) Heat map shows the level changes of metabolites. The hierarchical reorganization was based on the Pearson’s correlation coefficient with average distance. Data were normalized using locally weighted scatterplot smoothing (LOESS) algorithm. (B) Venn plot demonstrates the time, dose, and interaction effects of GTPs on significantly altered metabolites revealed by two-way ANOVA (see **Table 6-3**).

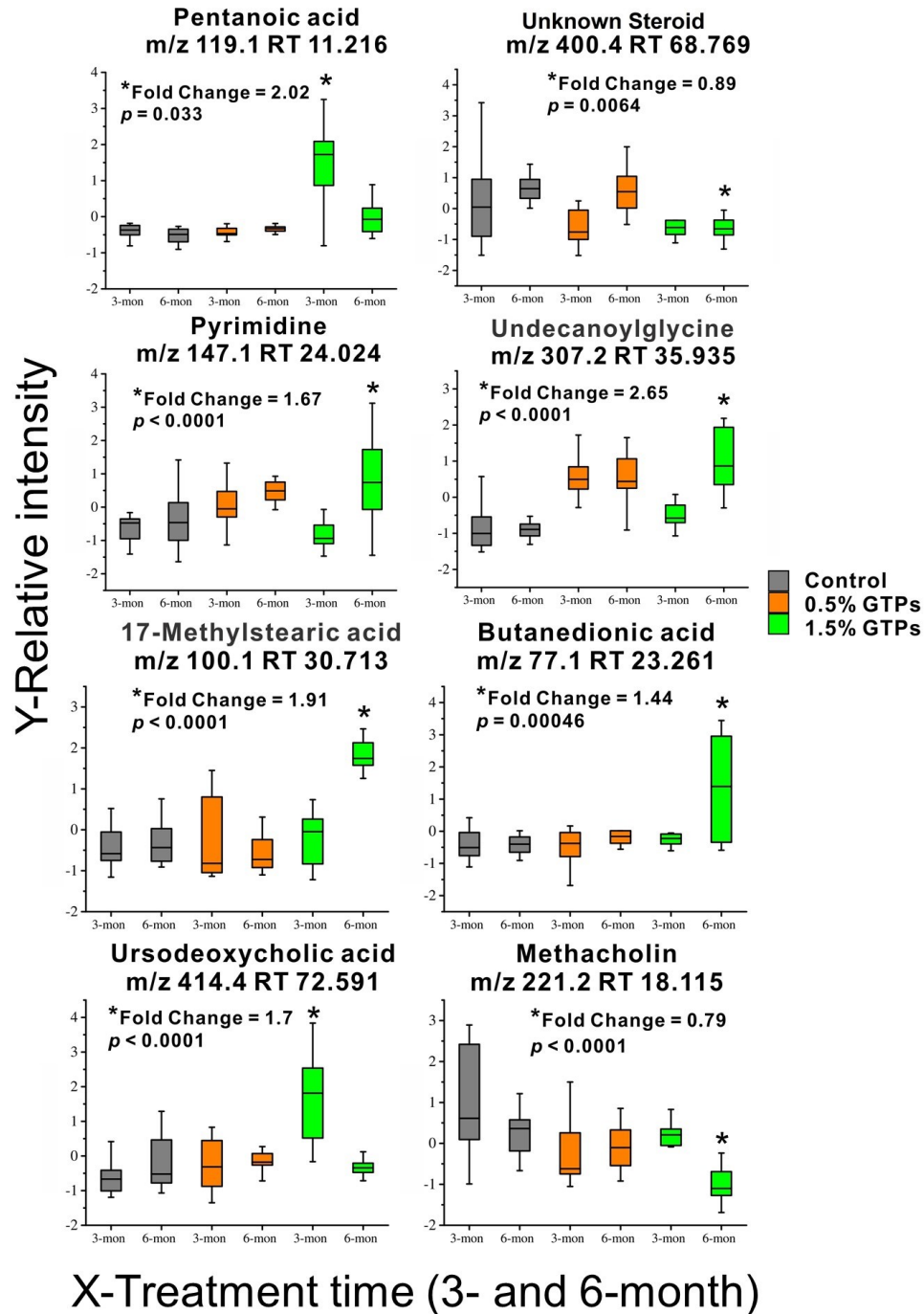


Figure 6-5. Box plots to show the alterations of eight signature metabolites that were affected by the dose, time and interaction effects of GTPs-treatment. The ion peak intensities were integrated from Extracted Ion Chromatograms (XICs). Non-parametric Mann-Whitney U test was applied for all comparisons (n = 10). Box plots represent 25%, 50% and 75% percentile of data. Whisker of box plots indicate standard deviation (S. D.).

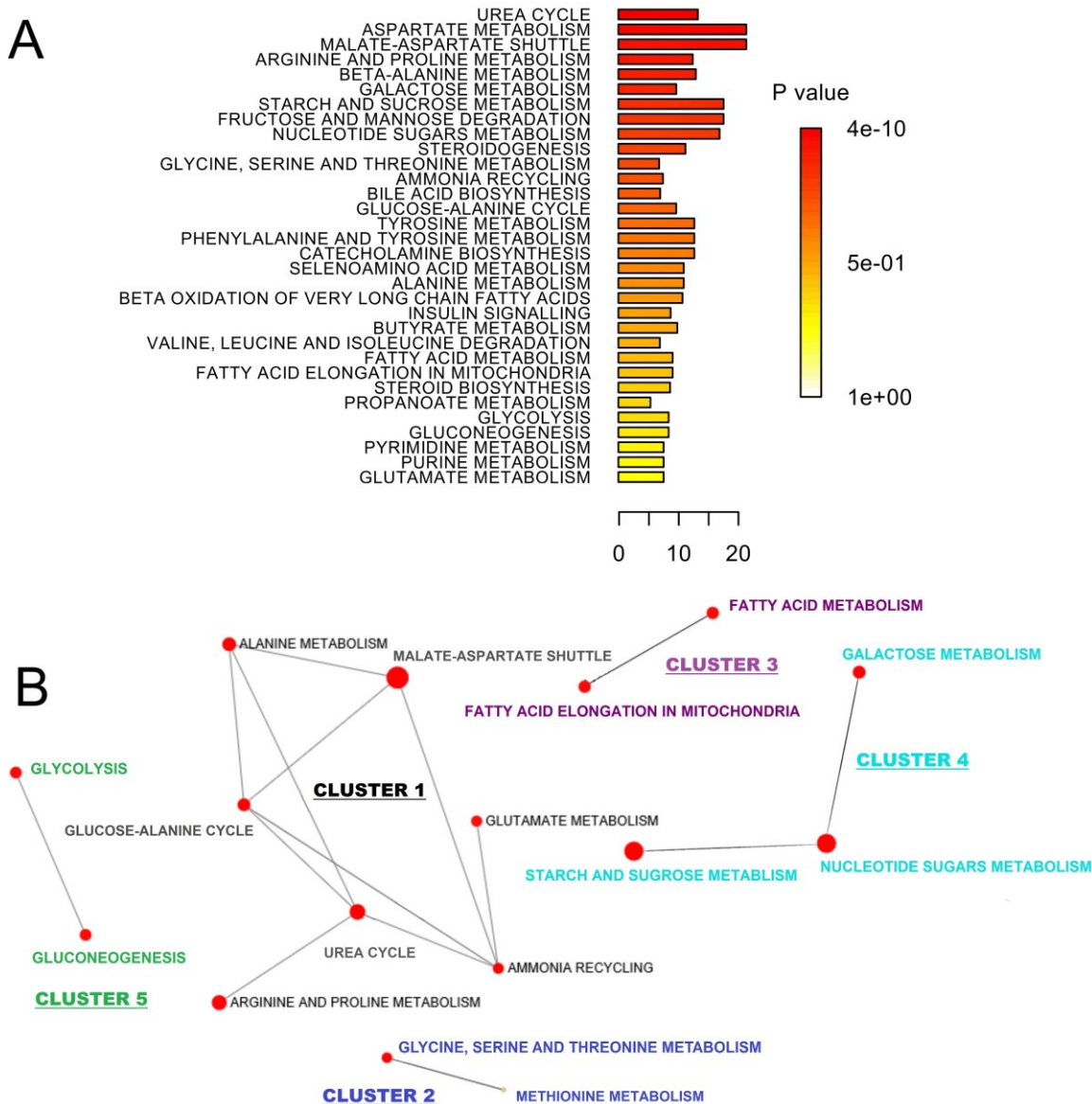


Figure 6-6. Metabolite set enrichment analysis (MSEA) of detected metabolites and network view of GTPs-modified metabolic pathways. (A) MSEA of metabolic pathways with adjusted- $p < 0.05$ for the significance of alteration. Specific statistics are listed in Table 3. The color code indicates adjusted- p values, and the enrichment fold (X-axis) indicates extent of response for the metabolic pathway. (B) Network view of metabolic pathways that share same metabolites. The node size reflects the total number of components in a pathway; the node color reflects the p value of the pathway, with a darker color corresponding to lower adjusted- p values. There are four clusters of nodes. Cluster 1: Alanine metabolism, Glucose-alanine cycle, Urea cycle, Arginine and proline metabolism, Ammonia recycling, Glutamate metabolism, Malate-aspartate shuttle. Cluster 2: Glycine, serine and threonine metabolism, Methionine metabolism. Cluster 3: Fatty acid metabolism, Fatty acid elongation in mitochondria. Cluster 4: Galactose metabolism, Nucleotide sugars metabolism, Starch and sucrose metabolism. Cluster 5: Glycolysis and Gluconeogenesis.

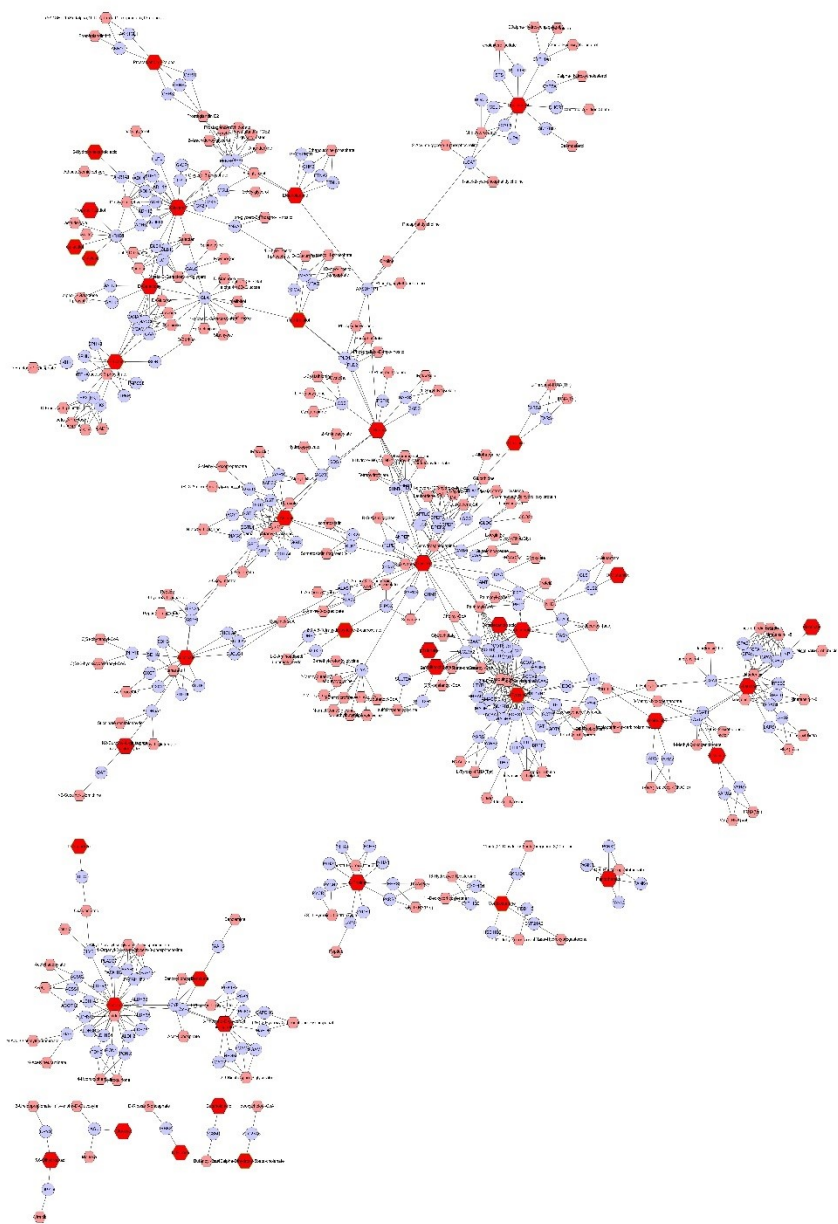


Figure 6-7. Global compound-gene network analysis of metabolites detected in feces of rats administered with 1.5% GTPs in drinking water. The intense red hexagons represent metabolites with significant alteration. The light red hexagons (compounds) and purple balls (genes) stand for the components in the pathways. Compounds and genes are represented as nodes and the relationships among them are represented as edges; the edges represent both reactions and enzymes based on KEGG. The most activated pathways include: bile acid biosynthesis, C21-steroid hormone biosynthesis and metabolism, butanoate metabolism, de novo fatty acid biosynthesis, biopterin metabolism, arachidonic acid metabolism, fructose and mannose metabolism, galactose metabolism, glycerophospholipid metabolism, glycine/serine/alanine/threonine metabolism, glycolysis and gluconeogenesis, glycosphingolipid metabolism.

Compound	GTPs w/V%	3-month				6-month			
		Mean	Median	E/C ^a	<i>p</i> ^b	Mean	Median	E/C ^a	<i>p</i> ^b
Lactic acid	0	16.41	14.5			24.25	22.8		
	0.5	19.82	15.25	1.21	0.63	15.03	14.48	0.62	0.131
	1.5	44.3	43.63	2.7	0.003	45.73	44.23	1.89	0.076
Acetic acid	0	3287.2	3088.57			2502.85	2508.87		
	0.5	1966.9	1716.25	0.6	0.013	2113.19	2216.34	0.84	0.326
	1.5	2627.5	1780.58	0.8	0.151	1903.48	1168.18	0.76	0.257
Propionic acid	0	1775.3	1628.19			1230.62	1181.8		
	0.5	2089.5	1024.3	1.18	0.096	1321.77	1222.65	1.07	0.705
	1.5	1888.8	1176.38	1.06	0.88	1149.34	843	0.93	0.29
Butyric acid	0	1995.9	1998.74			1818.61	1959.59		
	0.5	1370.1	1419.64	0.69	0.082	1422.83	1364.26	0.78	0.082
	1.5	1509.6	1244.69	0.76	0.049	1435.41	1168.18	0.79	0.462
Valeric acid	0	132.02	123.54			116.57	118.07		
	0.5	187.91	105.31	1.42	0.406	117.03	109.63	1	0.744
	1.5	172.8	125.02	1.31	0.762	140.23	110.17	1.2	1
Niacin	0	187.63	151.9			220.71	216.52		
	0.5	291.95	170.56	1.56	0.29	936.72	940.84	4.24	0.001
	1.5	1615.3	1043.6	8.61	<0.0001	806.86	667.92	3.66	0.027
3-Phenylactic acid	0	111.02	96.46			127.41	103.1		
	0.5	150.37	101.83	1.35	0.514	237.1	218.34	1.86	0.034
	1.5	244.42	192.9	2.2	0.009	116.67	66.38	0.92	0.009
Pyruvic acid	0	85.37	81.19			74.19	69.1		
	0.5	90.49	74.51	1.06	0.94	73.55	69.4	0.99	0.94
	1.5	112.01	97.23	1.31	0.364	85.47	69.24	1.15	0.821
Cholic acid	0	162.23	161.76			201.38	203.82		
	0.5	115.74	109.27	0.71	0.002	137.65	138.16	0.68	<0.0001
	1.5	119.31	126.38	0.74	0.013	124.77	142.89	0.62	0.001
Deoxycholic acid	0	42.95	31.14			54.77	60.86		
	0.5	60.14	59.06	1.4	0.07	39.23	35.26	0.72	0.11
	1.5	42.9	39	1	0.568	22.62	17.57	0.41	0.034
Cholesterol	0	15	15.54			15.6	14.93		
	0.5	4.32	4.69	0.29	0.007	8.93	5.89	0.57	0.076
	1.5	7.28	6.17	0.49	0.044	10.92	10.11	0.7	0.047
Pentadecanoic acid	0	22.98	16.6			23.98	19.84		
	0.5	29	23.2	1.26	0.462	28.16	10.4	1.17	0.762
	1.5	49.3	43.25	2.15	0.022	45.03	25.42	1.88	0.131
D-Mannose	0	384.59	382.7			367.62	370.26		
	0.5	384.39	379.06	1	0.954	454.02	449.27	1.24	0.05
	1.5	392.03	358	1.02	0.817	752.49	737.72	2.05	<0.0001
D-Fructose	0	495.21	313.27			426.22	307.77		
	0.5	216.71	98.64	0.44	0.033	137.19	151.36	0.32	<0.0001
	1.5	57.75	58.76	0.12	<0.0001	128.26	134.2	0.3	<0.0001
D-Galactose	0	489.17	426.3			544.55	450.03		
	0.5	1529.6	1673.22	3.13	<0.0001	958.9	899.18	1.76	<0.0001
	1.5	728.35	639.51	1.49	0.057	1289.53	1320.4	2.37	<0.0001
D-Glucose	0	6125.6	6059.32			5642.64	5405.55		
	0.5	5005.1	3612.37	0.82	0.386	4348.45	3987.06	0.77	0.273
	1.5	2830.5	2615.2	0.46	<0.0001	4900.41	5336.35	0.87	0.525
N-Acetyl-D-glucosamine	0	766.18	743.84			897.5	840.28		
	0.5	853.96	813.38	1.11	0.05	894	861.97	1	0.386
	1.5	943.2	837.68	1.23	0.043	871.87	854.09	0.97	0.644
Trehalose	0	655.48	708.11			689.97	650.2		
	0.5	91.36	81.28	0.14	<0.0001	745.47	754.17	1.08	0.326
	1.5	452.87	433.83	0.69	0.176	555.86	603.48	0.81	0.0453
L-Alanine	0	7415.5	7001.85			6866.68	5837.11		
	0.5	4554.3	4335.23	0.61	<0.001	4204.78	4109.42	0.61	<0.0001
	1.5	4498.5	4546.29	0.61	<0.0001	4485.27	4572.21	0.65	<0.0001
L-Proline	0	3594.6	3235.71			3994.07	3324.32		
	0.5	6207.3	7080.07	1.73	0.013	4840.99	4434.79	1.21	0.133
	1.5	7330.7	6890.07	2.04	<0.0001	8581.52	8235.31	2.15	<0.0001

Figure 6-8. Key metabolites determined using HPLC-profiling and GC-MS analyses. Blue color bar indicates the relative level of the compound determined in the three experimental groups. Half-transparent bar stands for the results at 3-month and fully filled bar stands for the results at 6-month. Abbreviations: a. E/C, the mean concentration (ng/mg gut content) determined in exposure group versus that in control group. b. *p*-value is calculated from Kruskal-Wallis H test, n = 10.

Reference

- Barbosa, M. R. (2013). Chemical composition and formation of human feces-Problems and solutions of large mergers demographics in developing countries. In 10th International Symposium on Recent Advances in Environmental Health Research.
- Borges, C. M., Papadimitriou, A., Duarte, D. A., De Faria, J. M. L., and De Faria, J. B. L. (2016). The use of green tea polyphenols for treating residual albuminuria in diabetic nephropathy: A double-blind randomised clinical trial. *Sci Rep* 6, 28282.
- Bose, M., Lambert, J. D., Ju, J., Reuhl, K. R., Shapses, S. A., and Yang, C. S. (2008). The major green tea polyphenol,(-)-epigallocatechin-3-gallate, inhibits obesity, metabolic syndrome, and fatty liver disease in high-fat-fed mice. *J Nutr* 138(9), 1677-1683.
- Brown, J. M., and Hazen, S. L. (2015). The gut microbial endocrine organ: bacterially derived signals driving cardiometabolic diseases. *Annu Rev Med* 66, 343-59.
- Cabrera, C., Artacho, R., and Giménez, R. (2006). Beneficial effects of green tea—a review. *J Am Coll Nutr* 25(2), 79-99.
- Camilleri, M., Carlson, P., McKinzie, S., Zucchelli, M., D'Amato, M., Busciglio, I., Burton, D., and Zinsmeister, A. R. (2011). Genetic susceptibility to inflammation and colonic transit in lower functional gastrointestinal disorders: preliminary analysis. *Neurogastroenterol Motil* 23(10), 935-e398.
- Chakraborty, S., Zawieja, S., Wang, W., Zawieja, D. C., and Muthuchamy, M. (2010). Lymphatic system: a vital link between metabolic syndrome and inflammation. *Ann Ny Acad Sci* 1207(s1), E94-E102.

- Chan, P. T., Fong, W. P., Cheung, Y. L., Huang, Y., Ho, W. K., and Chen, Z. Y. (1999). Jasmine green tea epicatechins are hypolipidemic in hamsters (*Mesocricetus auratus*) fed a high fat diet. *J Nutr* 129(6), 1094-101.
- Chen, L., Lee, M. J., Li, H., and Yang, C. S. (1997). Absorption, distribution, elimination of tea polyphenols in rats. *Drug Metab Dispos* 25(9), 1045-50.
- Chung, J. Y., Huang, C., Meng, X., Dong, Z., and Yang, C. S. (1999). Inhibition of activator protein 1 activity and cell growth by purified green tea and black tea polyphenols in H-ras-transformed cells: structure-activity relationship and mechanisms involved. *Cancer Res* 59(18), 4610-7.
- Clifford, M. N. (2004). Diet-derived phenols in plasma and tissues and their implications for health. *Planta Medica* 70(12), 1103-14.
- Conlon, M. A., and Bird, A. R. (2014). The impact of diet and lifestyle on gut microbiota and human health. *Nutrients* 7(1), 17-44.
- Dabelsteen, E., Graem, N., Clausen, H., and Hakomori, S. (1988). Structural variations of blood group A antigens in human normal colon and carcinomas. *Cancer Res* 48(1), 181-7.
- Dai, Z. L., Wu, G., and Zhu, W. Y. (2011). Amino acid metabolism in intestinal bacteria: links between gut ecology and host health. *Front Biosci (Landmark Ed)* 16, 1768-86.
- de Jonge, L. P., Douma, R. D., Heijnen, J. J., and van Gulik, W. M. (2012). Optimization of cold methanol quenching for quantitative metabolomics of *Penicillium chrysogenum*. *Metabolomics* 8(4), 727-735.

- Depeint, F., Bruce, W. R., Shangari, N., Mehta, R., and O'Brien, P. J. (2006). Mitochondrial function and toxicity: role of the B vitamin family on mitochondrial energy metabolism. *Chem Biol Interact* 163(1-2), 94-112.
- Dominguez-Bello, M. G., Costello, E. K., Contreras, M., Magris, M., Hidalgo, G., Fierer, N., and Knight, R. (2010). Delivery mode shapes the acquisition and structure of the initial microbiota across multiple body habitats in newborns. *Proc Natl Acad Sci U S A* 107(26), 11971-5.
- Graham, H. N. (1992). Green tea composition, consumption, and polyphenol chemistry. *Prev Med* 21(3), 334-50.
- Guideline, I.-H. T. (2006). S4A: duration of chronic toxicity testing in animals (rodent and non-rodent toxicity testing).
- Hernandez Bort, J. A., Shanmukam, V., Pabst, M., Windwarder, M., Neumann, L., Alchalabi, A., Krebiehl, G., Koellensperger, G., Hann, S., Sonntag, D., et al. (2014). Reduced quenching and extraction time for mammalian cells using filtration and syringe extraction. *J Biotechnol* 182-183(Supplement C), 97-103.
- Holmes, E., Li, J. V., Marchesi, J. R., and Nicholson, J. K. (2012). Gut microbiota composition and activity in relation to host metabolic phenotype and disease risk. *Cell Metab* 16(5), 559-64.
- Hussain, M. R. M., Hassan, M., Shaik, N. A., and Iqbal, Z. (2012). The role of Galactose in human health and disease. *Cent Eur J Med* 7(4), 409-419.
- Jankun, J., Selman, S. H., Swiercz, R., and Skrzypczak Jankun, E. (1997). Why drinking green tea could prevent cancer. *Nature* 387(6633), 561-561.

- Jansson, J., Willing, B., Lucio, M., Fekete, A., Dicksved, J., Halfvarson, J., Tysk, C., and Schmitt-Kopplin, P. (2009). Metabolomics reveals metabolic biomarkers of Crohn's disease. *PLoS One* 4(7), e6386.
- Jia, W., Xie, G., and Jia, W. (2018). Bile acid-microbiota crosstalk in gastrointestinal inflammation and carcinogenesis. *Nat Rev Gastroenterol Hepatol* 15(2), 111-128.
- Kim, J. J., Tan, Y., Xiao, L., Sun, Y. L., and Qu, X. (2013). Green tea polyphenol epigallocatechin-3-gallate enhance glycogen synthesis and inhibit lipogenesis in hepatocytes. *BioMed Res Int* 2013, 920128.
- Kim, S., Lee, M. J., Hong, J., Li, C., Smith, T. J., Yang, G. Y., Seril, D. N., and Yang, C. S. (2000). Plasma and tissue levels of tea catechins in rats and mice during chronic consumption of green tea polyphenols. *Nutr Cancer* 37(1), 41-8.
- Konikoff, T., and Gophna, U. (2016). Oscillospira: a Central, Enigmatic Component of the Human Gut Microbiota. *Trends Microbiol* 24(7), 523-524.
- Koo, S. I., and Noh, S. K. (2007). Green tea as inhibitor of the intestinal absorption of lipids: potential mechanism for its lipid-lowering effect. *J Nutr Biochem* 18(3), 179-183.
- Koppel, N., Maini Rekdal, V., and Balskus, E. P. (2017). Chemical transformation of xenobiotics by the human gut microbiota. *Science* 356(6344), eaag2770.
- Kovacs, E. M., Lejeune, M. P., Nijs, I., and Westerterp-Plantenga, M. S. (2004). Effects of green tea on weight maintenance after body-weight loss. *Br J Nutr* 91(3), 431-7.
- Laparra, J. M., and Sanz, Y. (2010). Interactions of gut microbiota with functional food components and nutraceuticals. *Pharmacol Res* 61(3), 219-25.

- Lee, M. J., Maliakal, P., Chen, L., Meng, X., Bondoc, F. Y., Prabhu, S., Lambert, G., Mohr, S., and Yang, C. S. (2002). Pharmacokinetics of tea catechins after ingestion of green tea and (-)-epigallocatechin-3-gallate by humans: formation of different metabolites and individual variability. *Cancer Epidemiol Biomarkers Prev* 11(10 Pt 1), 1025-32.
- Li, Y., Wang, C., Huai, Q., Guo, F., Liu, L., Feng, R., and Sun, C. (2016). Effects of tea or tea extract on metabolic profiles in patients with type 2 diabetes mellitus: a meta-analysis of ten randomized controlled trials. *Diabetes Metab Res Rev* 32(1), 2-10.
- Lin, A., Bik, E. M., Costello, E. K., Dethlefsen, L., Haque, R., Relman, D. A., and Singh, U. (2013). Distinct distal gut microbiome diversity and composition in healthy children from Bangladesh and the United States. *PLoS One* 8(1), e53838.
- Lu, K., Abo, R. P., Schlieper, K. A., Graffam, M. E., Levine, S., Wishnok, J. S., Swenberg, J. A., Tannenbaum, S. R., and Fox, J. G. (2014). Arsenic exposure perturbs the gut microbiome and its metabolic profile in mice: an integrated metagenomics and metabolomics analysis. *Environ Health Perspect* 122(3), 284-91.
- Lu, K., Knutson, C. G., Wishnok, J. S., Fox, J. G., and Tannenbaum, S. R. (2012). Serum metabolomics in a *Helicobacter hepaticus* mouse model of inflammatory bowel disease reveal important changes in the microbiome, serum peptides, and intermediary metabolism. *J Proteome Res* 11(10), 4916-26.
- Macfarlane, S., Woodmansey, E. J., and Macfarlane, G. T. (2005). Colonization of mucin by human intestinal bacteria and establishment of biofilm communities in a two-stage continuous culture system. *Appl Environ Microbiol* 71(11), 7483-92.

- Magnusdottir, S., Ravcheev, D., de Crecy-Lagard, V., and Thiele, I. (2015). Systematic genome assessment of B-vitamin biosynthesis suggests co-operation among gut microbes. *Front Genet* 6, 148.
- Marchesi, J. R., Adams, D. H., Fava, F., Hermes, G. D., Hirschfield, G. M., Hold, G., Quraishi, M. N., Kinross, J., Smidt, H., Tuohy, K. M., et al. (2016). The gut microbiota and host health: a new clinical frontier. *Gut* 65(2), 330-9.
- Mouzaki, M., Wang, A. Y., Bandsma, R., Comelli, E. M., Arendt, B. M., Zhang, L., Fung, S., Fischer, S. E., McGilvray, I. G., and Allard, J. P. (2016). Bile Acids and Dysbiosis in Non-Alcoholic Fatty Liver Disease. *PLoS One* 11(5), e0151829.
- Muramatsu, K., Fukuyo, M., and Hara, Y. (1986). Effect of green tea catechins on plasma cholesterol level in cholesterol-fed rats. *J Nutr Sci Vitaminol* 32(6), 613-22.
- Nagao, T., Komine, Y., Soga, S., Meguro, S., Hase, T., Tanaka, Y., and Tokimitsu, I. (2005). Ingestion of a tea rich in catechins leads to a reduction in body fat and malondialdehyde-modified LDL in men. *Am J Clin Nutr* 81(1), 122-9.
- Oriach, C. S., Robertson, R. C., Stanton, C., Cryan, J. F., and Dinan, T. G. (2016). Food for thought: The role of nutrition in the microbiota-gut-brain axis. *Clin Nutr Exp* 6(Supplement C), 25-38.
- Penders, J., Thijs, C., Vink, C., Stelma, F. F., Snijders, B., Kummeling, I., van den Brandt, P. A., and Stobberingh, E. E. (2006). Factors influencing the composition of the intestinal microbiota in early infancy. *Pediatrics* 118(2), 511-21.
- Peng, X., Zhou, R., Wang, B., Yu, X., Yang, X., Liu, K., and Mi, M. (2014). Effect of green tea consumption on blood pressure: a meta-analysis of 13 randomized controlled trials. *Sci Rep* 4, 6251.

- Peters, R., Hellenbrand, J., Mengerink, Y., and Van der Wal, S. (2004). On-line determination of carboxylic acids, aldehydes and ketones by high-performance liquid chromatography-diode array detection-atmospheric pressure chemical ionisation mass spectrometry after derivatization with 2-nitrophenylhydrazine. *J Chromatogr A* 1031(1-2), 35-50.
- Qin, J., Li, R., Raes, J., Arumugam, M., Burgdorf, K. S., Manichanh, C., Nielsen, T., Pons, N., Levenez, F., and Yamada, T. (2010a). A human gut microbial gene catalogue established by metagenomic sequencing. *Nature* 464(7285), 59-65.
- Qin, J., Li, R., Raes, J., Arumugam, M., Burgdorf, K. S., Manichanh, C., Nielsen, T., Pons, N., Levenez, F., Yamada, T., et al. (2010b). A human gut microbial gene catalogue established by metagenomic sequencing. *Nature* 464(7285), 59-65.
- Rasooly, R., Hernlem, B., He, X., and Friedman, M. (2013). Non-linear relationships between aflatoxin B(1) levels and the biological response of monkey kidney vero cells. *Toxins (Basel)* 5(8), 1447-61.
- Roseman, D. S., and Baenziger, J. U. (2003). The Man/GalNAc-4-SO 4-receptor: relating specificity to function. *Methods Enzymol* 363, 121-133.
- Rowland, I. (Ed.). (2012). Role of the gut flora in toxicity and cancer. Elsevier.
- Rowland, I., Gibson, G., Heinken, A., Scott, K., Swann, J., Thiele, I., and Tuohy, K. (2018). Gut microbiota functions: metabolism of nutrients and other food components. *Eur J Nutr* 57(1), 1-24.
- Savage, D. C. (1972). Associations and physiological interactions of indigenous microorganisms and gastrointestinal epithelia. *Am J Clinical Nutr* 25(12), 1372-9.

- Shen, C. L., Brackee, G., Song, X., Tomison, M. D., Finckbone, V., Mitchell, K. T., Tang, L., Chyu, M. C., Dunn, D. M., and Wang, J. S. (2017). Safety Evaluation of Green Tea Polyphenols Consumption in Middle-aged Ovariectomized Rat Model. *J Food Sci* 82(9), 2192-2205.
- Smirnov, K. S., Maier, T. V., Walker, A., Heinzmann, S. S., Forcisi, S., Martinez, I., Walter, J., and Schmitt-Kopplin, P. (2016). Challenges of metabolomics in human gut microbiota research. *Int J Med Microbiol* 306(5), 266-279.
- Stalmach, A., Mullen, W., Steiling, H., Williamson, G., Lean, M. E., and Crozier, A. (2010). Absorption, metabolism, and excretion of green tea flavan-3-ols in humans with an ileostomy. *Mol Nutr Food Res* 54(3), 323-34.
- Sun, H., Chen, Y., Cheng, M., Zhang, X., Zheng, X., and Zhang, Z. (2018). The modulatory effect of polyphenols from green tea, oolong tea and black tea on human intestinal microbiota in vitro. *J Food Sci Technol* 55(1), 399-407.
- Suzuki, H., Ishigaki, A., and Hara, Y. (1998). Long-term effect of a trace amount of tea catechins with perilla oil on the plasma lipids in mice. *Int J Vitam Nutr Res* 68(4), 272-4.
- Tang, D. Q., Zou, L., Yin, X. X., and Ong, C. N. (2016). HILIC-MS for metabolomics: An attractive and complementary approach to RPLC-MS. *Mass Spectrom Rev* 35(5), 574-600.
- Tautenhahn, R., Patti, G. J., Rinehart, D., and Siuzdak, G. (2012). XCMS Online: A Web-Based Platform to Process Untargeted Metabolomic Data. *Anal Chem* 84(11), 5035-5039.
- Team, R. C. (2013). R: A language and environment for statistical computing.

- Tims, S., Derom, C., Jonkers, D. M., Vlietinck, R., Saris, W. H., Kleerebezem, M., de Vos, W. M., and Zoetendal, E. G. (2013). Microbiota conservation and BMI signatures in adult monozygotic twins. *ISME J* 7(4), 707-17.
- Torii, T., Kanemitsu, K., Wada, T., Itoh, S., Kinugawa, K., and Hagiwara, A. (2010). Measurement of short-chain fatty acids in human faeces using high-performance liquid chromatography: specimen stability. *Annal Clin Biochem* 47(5), 447-452.
- Tremaroli, V., and Backhed, F. (2012). Functional interactions between the gut microbiota and host metabolism. *Nature* 489(7415), 242-249.
- Turnbaugh, P. J., Hamady, M., Yatsunencko, T., Cantarel, B. L., Duncan, A., Ley, R. E., Sogin, M. L., Jones, W. J., Roe, B. A., Affourtit, J. P., et al. (2009). A core gut microbiome in obese and lean twins. *Nature* 457(7228), 480-4.
- Ursell, L. K., Haiser, H. J., Van Treuren, W., Garg, N., Reddivari, L., Vanamala, J., Dorrestein, P. C., Turnbaugh, P. J., and Knight, R. (2014). The intestinal metabolome: an intersection between microbiota and host. *Gastroenterology* 146(6), 1470-6.
- Velagapudi, V. R., Hezaveh, R., Reigstad, C. S., Gopalacharyulu, P., Yetukuri, L., Islam, S., Felin, J., Perkins, R., Boren, J., Oresic, M., et al. (2010). The gut microbiota modulates host energy and lipid metabolism in mice. *J Lipid Res* 51(5), 1101-12.
- Verdam, F. J., Fuentes, S., de Jonge, C., Zoetendal, E. G., Erbil, R., Greve, J. W., Buurman, W. A., de Vos, W. M., and Rensen, S. S. (2013). Human intestinal microbiota composition is associated with local and systemic inflammation in obesity. *Obesity* (Silver Spring, Md.) 21(12), E607-15.

- Wang, J., Tang, L., Zhou, H., Zhou, J., Glenn, T. C., Shen, C. L., and Wang, J. S. (2018). Long-term treatment with green tea polyphenols modifies the gut microbiome of female sprague-dawley rats. *J Nutr Biochem* 56, 55-64.
- Wang, J. S., Luo, H., Wang, P., Tang, L., Yu, J., Huang, T., Cox, S., and Gao, W. (2008). Validation of green tea polyphenol biomarkers in a phase II human intervention trial. *Food Chem Toxicol* 46(1), 232-40.
- Wang, S., Noh, S. K., and Koo, S. I. (2006). Green tea catechins inhibit pancreatic phospholipase A2 and intestinal absorption of lipids in ovariectomized rats. *J Nutr Biochem* 17(7), 492-498.
- Wang, W. W., Qiao, S. Y., and Li, D. F. (2009). Amino acids and gut function. *Amino Acids* 37(1), 105-10.
- Winder, C. L., Dunn, W. B., Schuler, S., Broadhurst, D., Jarvis, R., Stephens, G. M., and Goodacre, R. (2008). Global metabolic profiling of Escherichia coli cultures: an evaluation of methods for quenching and extraction of intracellular metabolites. *Anal Chem* 80(8), 2939-48.
- Xia, B., Royall, J. A., Damera, G., Sachdev, G. P., and Cummings, R. D. (2005). Altered O-glycosylation and sulfation of airway mucins associated with cystic fibrosis. *Glycobiology* 15(8), 747-75.
- Xia, J., Psychogios, N., Young, N., and Wishart, D. S. (2009). MetaboAnalyst: a web server for metabolomic data analysis and interpretation. *Nucleic Acids Res* 37(Web Server issue), W652-60.
- Xia, J., and Wishart, D. S. (2016). Using MetaboAnalyst 3.0 for comprehensive metabolomics data analysis. *Curr Protoc Bioinformatics* 14(10) 1-91.

- Yang, C. S., Chen, L., Lee, M. J., Balentine, D., Kuo, M. C., and Schantz, S. P. (1998a). Blood and urine levels of tea catechins after ingestion of different amounts of green tea by human volunteers. *Cancer Epidemiol Biomarkers Prev* 7(4), 351-4.
- Yang, G. Y., Liao, J., Kim, K., Yurkow, E. J., and Yang, C. S. (1998b). Inhibition of growth and induction of apoptosis in human cancer cell lines by tea polyphenols. *Carcinogenesis* 19(4), 611-6.
- Yang, G. Y., Liao, J., Li, C. C., Chung, J., Yurkow, E. J., Ho, C. T., and Yang, C. S. (2000). Effect of black and green tea polyphenols on c-jun phosphorylation and H₂O₂ production in transformed and non-transformed human bronchial cell lines: possible mechanisms of cell growth inhibition and apoptosis induction. *Carcinogenesis* 21(11), 2035-2039.
- Yang, T. T., and Koo, M. W. (1997). Hypocholesterolemic effects of Chinese tea. *Pharmacol Res* 35(6), 505-12.
- Yang, T. T., and Koo, M. W. (1999). Chinese green tea lowers cholesterol level through an increase in fecal lipid excretion. *Life Sci* 66(5), 411-423.
- You, L., Zhang, B., and Tang, Y. J. (2014). Application of stable isotope-assisted metabolomics for cell metabolism studies. *Metabolites* 4(2), 142-65.
- Zhou, J., Tang, L., Wang, J., and Wang, J. S. (2018). Aflatoxin B1 Disrupts Gut-microbial Metabolisms of Short Chain Fatty Acids, Long Chain Fatty Acids and Bile Acids in Male F344 Rats. *Toxicol Sci* doi: 10.1093/toxsci/kfy102, kfy102-kfy102.

CHAPTER 7. GREEN TEA POLYPHENOLS BOOST GUT-MICROBIOTA
DEPENDENT MITOCHONDRIAL TCA/UREA CYCLE AND ENERGY
CONVERSION OF IN SPRAGUE DAWLEY RATS

7.1 Introduction

Here we report the modifying effects of green tea polyphenols (GTPs) on gut-microbiota dependent TCA/urea cycle and related metabolic pathways in Sprague Dawley rats. GTPs were administered through drinking water under no-observed-adverse-effect-level (NOAEL) doses 0, 0.5% and 1.5% g/dL. Gut-content samples were collected at both 3- and 6-month and were analyzed using hydrophilic interaction liquid chromatography (HILIC)-heated electrospray ionization (HESI)-tandem mass spectrometry (MS). Through untargeted metabolomic analysis, a total of 2177 features were aligned from 60 samples, with 91 features showing significant dose and/or time dependent responses to the treatment. Targeted metabolic profiling analysis was conducted with established reference MS/MS library. The two approaches together revealed fold-changes of 39 metabolites that relate to TCA/urea cycle and related metabolic pathways. At 6-month, in the 1.5% GTPs-treated group, significant fold-changes were found for argininosuccinic acid (0.9-fold), dihydrouracil (1.14-fold), fumaric acid (1.19-fold), malic acid (2.17-fold), citrulline (1.86-fold) and succinic acid (0.4-fold). Metabolic mapping analysis with 1891 gene orthologs and 72 related metabolites revealed remarkable alterations and correlations of TCA/urea cycle, carbohydrate metabolism, nucleotide metabolism, energy metabolism, bile acid metabolism, and the metabolisms of different amino acids. These results agreed with the

findings of metagenomic analysis of gut-content and were in line with the clinical chemistry results of blood. Of note, in the gut-content of GTPs-treated rats we observed enrichment of *Clostridiales ruminococcaceae*, *C. Lachnospiraceae*, *Bacteroidetes bacteroidaceae*, and decreases of “adverse health outcome”-associated OTUs. Taken together, our study suggested that GTPs could boost gut-microbiota dependent energy conversion in gut by altering the community structure and mitochondrial TCA/urea cycle of the gut-microbiota. Such modifying effects could be an important mechanistic part of the health-promoting function of green tea discovered in human populations and animal models.

Green tea has been considered a recreational and health-promoting beverage since ancient times (Weisburger, 1997). The major functional compositions of green tea leaves (*Camellia sinensis*) include flavonoids, amino acids and polysaccharides (Balentine *et al.*, 1997). As primary flavonoids contained in tea leaves, green tea polyphenols (GTPs) constitute up to 30% dry weight of tea leaves (Balentine *et al.*, 1997; Graham, 1992). In both *in vitro* and *in vivo* assays, GTPs have demonstrated the similar beneficial effects associated with drinking green tea, including antioxidant activity, cancer protection, alleviation of high blood pressure, enhancement of bone quality, the reductions of body fat, cholesterol level and blood sugar etc. (Chen *et al.*, 2017b; Luo *et al.*, 2006; Qian *et al.*, 2012; Shen *et al.*, 2015a; Shen *et al.*, 2008; Tang *et al.*, 2008). Accordingly, GTPs have addressed remarkable attention from both industry and academia, with significant efforts made to explore its novel clinical uses as well as the behind mechanisms (Taylor, 1998).

Our previous studies have demonstrated that GTPs could effectively modify gut-microbiota community structure and the dependent metabolites in Sprague Dawley (SD)

rats. In GTPs exposure group, we observed significant enrichment of *C. Ruminococcaceae*, *C. Lachnospiraceae* and *B. Bacteroidaceae*, as well as the elevation of the gene orthologs (GOs) that are related with mitochondrial TCA cycle and ATP synthesis (Wang *et al.*, 2018). Through normal phase-based metabolomics, we found that not only the calorific carbohydrates (glucose, fructose and trehalose) were largely reduced, but also the metabolisms of bile acids, fatty acids, and amino acids were all positively modulated in the gut. The alterations of these metabolites could be explained by the shift of gut-microbiota community structure. It has been reported that the major part of cellular metabolites generated by gut-microbiota are hydrophilic, and may reflect and represent the metabolic changes of the microbiota (Marcobal *et al.*, 2013). However, in our studies the water-soluble compositions of the microbiota dependent metabolites have not been specifically investigated because of the undesirable separation of hydrophilic metabolites in the reverse phase chromatography-based analysis.

In recent years, hydrophilic interaction liquid chromatography (HILIC) silica column has been widely employed to analyze hydrophilic metabolites (Tang *et al.*, 2016). In practice, HILIC column is frequently coupled with liquid chromatography (LC)-triple quadrupole (TsQ)-mass spectrometry (MS) that is featured by the function of selected reaction monitoring (SRM) analysis. The parent ion selected in the first quadrupole (MS1 or Q1) is dissociated to fragment ions in the collision cell, and only a specific fragment ion (daughter ion) is selected in the second quadrupole for quantitative purpose (MS2, or Q3) (Bajad *et al.*, 2006; Lu *et al.*, 2008). This two-stage transition of ion pair is corresponding to specific chemical structure and therefore can be used for the quantitative analysis of the interested compounds. Though the detective limit of TsQ-MS is sometimes not satisfying,

heated electrospray ionization (HESI) can be introduced in the TsQ-MS to enhance the sensitivity for the ion detection (Rodriguez-Aller *et al.*, 2013). In the current study we applied HILIC-based untargeted/targeted metabolomic analyses to observe the shift of hydrophilic metabolites contained in the gut-content following GTPs administration. Bioinformatics analysis was then used to integrate previous data and explore the mechanistic scheme. The current work aims to provide a comprehensive picture to describe the changes of gut-microbiota induced by GTPs.

7.2 Materials and methods

7.2.1 Chemicals and reagents

LC-MS grade acetonitrile, formic acid and water were purchased from Honeywell (Morris Plains, NJ, USA). High-purity green tea polyphenols (GTPs, decaffeinated) powder was ordered from Zhejiang Yixin Pharmaceutical Co., Ltd. (Zhejiang, China). The mixture contains 65.37% of EGCG, 19.08% of ECG, 9.87% of EC, 4.14% of EGC, and 1.54% of catechin.

7.2.2 Animal study

The protocol of animal study was described in previous studies. In brief, 72 female Sprague-Dawley (SD) rats (6-month old, Harlan Laboratories, Indianapolis, IN, USA) were randomized and divided into 6 groups (n = 12). The rats were housed in individual stainless-steel cages with a room temperature of 21 ± 2 °C and a light-dark cycle of 12 hours. After environmental acclimation, the rats were administered with drinking water containing 0, 0.5%, and 1.5% GTPs (g/dL, 2 groups/treatment) for 6-month. All rats were fed with the pelleted AIN-93M diet (Dyets, Bethlehem, PA, USA). Gut-content samples

were collected at 3-month and 6-month. Each time half of rats in dosing group were sacrificed for sample collection. After sacrifice, gut-content was immediately taken out and transferred to 50 mL Eppendoff tubes and were stored in a $-80\text{ }^{\circ}\text{C}$ freezer until use. All procedures were approved by the local Institutional Animal Care and Use Committee. For each sampling time and dosing group, a total of 10 samples were randomly chosen for untargeted metabolic analysis. Six samples were randomly chosen from samples at 6-month for SRM analysis.

7.2.3 Sample pre-treatment

Sample extraction procedure was consistent with several earlier publications. Briefly, cold methanol ($-80\text{ }^{\circ}\text{C}$) was used to quench gut-content and consequent extraction of metabolome. Around 200 mg frozen gut-content was weighed and placed into a Mobio PowerLyzer tube containing glass beads of 0.1 mm inner diameter (Qiagen, Venlo, Netherlands). One milliliter cold methanol was added in the tube and the pellet was ground using a glass pestle. The tube was then capped tightly and fastened on Genie 2 mixer (VWR, Suwanee, GA, USA) for 20 min vortex. The tube was centrifugated at 12,000 rpm for 10 min in order to spin down the cellular debris. Only supernatant was used for further analysis.

7.2.4 Metabolomic analysis

To perform metabolomic analysis, Agilent 1100 High-performance liquid chromatography (HPLC) system was coupled with Finnigan Triple Quadrupole (TsQ) Ultra mass spectrometer (Thermo Electron Corporation, San Jose, CA, USA). The HPLC system was equipped with Atlantis HILIC Silica (SiO_2) column (Waters, 150 mm \times 2 mm,

3 μm i.d., pH range 1–6). A 0.1 mm internal diameter fused silica capillary was used to introduce sample into the electrospray chamber after chromatographic separation. Heated electrospray ionization spray voltage was 3200 V in positive mode. Ultra-high purity nitrogen was used as sheath gas (30 psi) and auxiliary gas (10 psi). Argon was used as the collision gas (1.5 mTorr). Capillary temperature was 325 $^{\circ}\text{C}$. Flow rate was 150 $\mu\text{L}/\text{min}$. Mobile phase A was water containing 0.1% formic acid; mobile phase B was acetonitrile containing 0.1% formic acid. The gradient was: t = 0 min, 100% B; t = 30 min, 0% B; t = 42 min, 0% B; t = 44 min, 100% B; t = 50 min, 100% B. Data were collected in centroid files. Both untargeted and targeted metabolomic analyses were applied. Untargeted metabolomic analysis was performed in full-scan positive (+) mode with the following settings: sample volume was 15 μL ; scan range was 150–1500 amu; scan time was 1 s; scan width was 1 m/z; unit resolution of Q1 peak width was 0.7 amu. Scan time for Q1 was based on the following calculation: **(1)** (1500–150 amu)/0.7 amu = 1938 measures; **(2)** 1938 measures \times 0.5 ms (dwell time) \approx 1 s. Dwell time of 0.5 ms is the commonly recommended minimum dwell time for Thermo Ultra mass spectrometry. Selected reaction monitor (SRM) mode was used for targeted metabolomic analysis. Injection volume was 15 μL . Collision voltage was selected from 15 eV, 25 eV, and 35 eV, depending on the closest collision voltage recorded in the reference library. The scanned parent-product transition was also based on the reference MS/MS library (Bajad *et al.*, 2006; Lu *et al.*, 2008). Gas pressure was 1.5 mtorr. Transition scan time was 0.05 s. Scan width was 1 m/z.

7.2.5 Data processing and statistics

Raw MS files were submitted to on-line XCMS modules for peak detection, retention time correction, isotope grouping, and peak alignment. Quantitative analysis was based on the total ion intensities integrated by extracted ion chromatography (XIC). The processed data were normalized using cyclic locally weighted scatterplot smoothing (LOWESS) technique. Two-tailed Welch's t-test was used to examine the statistical significance of fold change. Analysis of variance simultaneous component analysis (ASCA) was used to screen the metabolites that showed remarkable responses to time/dose/interaction effects of GTPs treatment (leverage threshold, 0.9; alpha threshold, 0.05). ASCA and pathway impact analysis were both processed through MetaboAnalyst (Xia *et al.*, 2015). Microbial correlation analysis was based on Pearson's correlation. Gene diversity data of family-level OTUs were retrieved from Integrated Microbial Genomes & Microbiomes (IMG/M) (Chen *et al.*, 2017a).

7.3 Results

7.3.1 Normal phase chromatography-based metabolomic analysis

A total of 2177 features were aligned from the 60 samples measured by MS. There were 35 features demonstrating significant dose-dependency (**Fig. 7-1 A**) and 54 features showing significant time-dependency (**Fig. 7-1 B**). Of note, two features were significantly affected by the interaction effect of treatment (**Fig. 7-1 C, D and E**). The majority of the hydrophilic metabolites were the dietary components and complex lipids that are undistinguishable without high-purity standards (**SI Table 7-1**). A set of 15 metabolites were found to fall into the TCA/urea/pyrimidine pathways (**Table 7-1**). SRM analysis identified 24 metabolites that relate to TCA/urea cycle and the metabolisms of pyrimidine,

purine and diverse amino acids (**Table 7-2**). The detected TCA/urea cycle associated metabolites include malic acid (2.17-fold, $p < 0.01$), fumaric acid (1.19-fold, not significant), citrulline (1.86-fold, $p < 0.01$), argininosuccinic acid (0.9-fold, $p < 0.01$), dihydrouracil (1.14-fold, $p < 0.01$), aspartic acid (1.34-fold, $p < 0.05$), succinic acid (0.4-fold, $p < 0.05$), argmatine (0.35-fold, $p < 0.05$). These results are summarized in **Figure 7-7**. Meantime, there were also several metabolites showing remarkable changes in purine and pyrimidine pathway. Pyrimidine pathway: dihydroorotic acid (0.83-fold, $p = 0.062$), cytosine (6.01-fold, $p = 0.0039$), allantoin (2.68-fold, $p = 0.0244$), ureidosuccinate (2.57-fold, $p = 0.0024$). Purine pathway: inosinic acid (0.93-fold, $p = 0.019$), adenosine 3',5'-cyclic phosphate (0.96-fold, $p = 0.0168$), 3-hydroxy-4-aminopyridine sulfate (0.97-fold, $p = 0.0433$). The fold changes of these metabolites at 6-month were used for pathway impact analysis through MetaboAnalyst 3.0. The results were listed in **Table 7-3**. The most significantly impacted metabolic pathways include “TCA cycle (0.106)”, “cysteine and methionine metabolism (0.257)”, “glycine, serine and threonine metabolism (0.535)”, “purine metabolism (0.119)”, and “valine, leucine and isoleucine biosynthesis (0.667)”.

7.3.2 Correlation analysis of family-level taxa

The relative contributions of the significantly altered OTUs to the interested metabolic pathways were estimated by the relative abundances of OTUs and their gene diversities in the metabolic pathways being examined. The results were presented in **Figure 7-2**. Compared with other enriched OTUs, (p) *Ruminococcaceae* and (u) *Bacteroidaceae* demonstrated highest contribution to the examined metabolic pathways. Correlation analysis was performed to explore the connections between the family-level OTUs. The

results are presented in the circular plots shown in **Figure 7-3**. The specific operational taxonomic group labels are listed in **SI Table 7-2**. There were two clusters formed in the decreased OTUs: a-b-f-g-n and c-d-e (**Fig. 7-3 B**). Among the increased OTUs, p-q-r-w demonstrated most extensive correlation with the other enriched OTUs; (p) *Ruminococcaceae* and (t) *Dehalobacteriaceae* exhibited clustered correlation which is exclusive to the other OTUs (**Fig. 7-3 C**). By examining the correlation between the elevated OTUs with decreased OTUs shown in **Figure 7-3 D**, we found that (d) *Peptostreptococcaceae*, (f) *Prevotellaceae*, and (g) *Bifidobacteriaceae* showed inverse correlation with the most enriched OTUs. Specifically, (d) *Peptostreptococcaceae* was inversely correlated with (v) *Porphyromonadaceae*, (u) *Bacteroidaceae*, and (s) *Lachnospiraceae*; (f) *Prevotellaceae* was inversely correlated with (w) *Alphaproteobacteria|o_RF32*, (r) *Peptococcaceae*, and (q) *Desulfovibrionaceae*; (g) *Bifidobacteriaceae* was inversely correlated with (u) *Bacteroidaceae*, (r) *Peptococcaceae*, and (q) *Desulfovibrionaceae*.

Specifically, correlation analysis revealed three clusters of the enriched OTUs and the decreased OTUs : (1) (s) *Lachnospiraceae* (u) *Bacteroidaceae* and (v) *Porphyromonadaceae* were inversely correlated with (d) *Peptostreptococcaceae* (associated with colon cancer); (2) (r) *Desulfovibrionaceae* and (q) *Peptococcaceae* were inversely correlated with (f) *Prevotellaceae* (opportunistic pathogen); (3) (u) *Bacteroidaceae*, (r) *Desulfovibrionaceae* and (q) *Peptococcaceae* were inversely correlated with (g) *Bifidobacteriaceae* (contain opportunistic pathogen).

7.3.3 Integration of metabolomics, metagenomics and clinical chemistry data

To analyze the alteration of global metabolic pathways, metabolomics and metagenomics data collected at 6-month were input into KEGG online mapper. The metabolomic data included the results from previous GC-MS metabolomic analysis, HPLC-profiling data, and the compounds listed in **Table 7-1** and **Table 7-2**, together covering 72 metabolites. The metagenomics data include 1891 GOs. **Figure 7-4** illustrates the mapping analysis of the metabolic pathways using the metabolomics and metagenomics data. The metabolic pathways filled by the metabolites and GOs were highly coincided in TCA/urea cycle and the “energy conversion” related metabolisms of purine, pyrimidine, lipids, fats, carbohydrates, and amino acids. This is consistent with the significant changes of the 6 mitochondrial biogenesis related GOs discovered by previous metagenomic analysis (**Fig. 7-5** and **SI Table 7-5**) and is also consistent with the clinical chemistry analysis of rat serum (**Fig. 7-6** and **SI Table 7-6**). At 6-month, in the 1.5% GTPs-treated group the fold change of the six “energy conversion” related GOs were: AAA-ATPase (1.63-fold; $p < 0.001$), NADH-flavin oxidoreductase (1.78-fold; $p < 0.0001$), fumarate reductase (2.74-fold; $p < 0.001$), alpha glucosidase (1.81-fold; $p < 0.0001$), 4Fe-4S ferredoxin, iron-sulfur binding domain protein (5.86-fold; $p < 0.001$), molybdopterin oxidoreductase (5.58-fold; $p < 0.001$). Clinical chemistry analysis showed that at 6-month, in 1.5% GTPs-treated group total cholesterol, triglycerides, glucose were 108.7 ± 2.5 mg/dL, 37.14 ± 1.62 mg/dL, and 153.4 ± 3.2 mg/dL, respectively. The values were reduced to 125.5 ± 3.8 mg/dL ($p < 0.05$), 49.25 ± 2.48 mg/dL ($p < 0.05$), and 160.8 ± 3.7 mg/dL ($p > 0.05$), respectively. We observed significant elevation of blood urea nitrogen (BUN) following GTPs treatment. At 6-month, BUN in control group was 16.08 ± 0.81 mg/dL,

and the value was increased to 18.50 ± 0.64 mg/dL by 1.5% GTPs-treatment ($p < 0.05$). Finally, the general alterations of TCA/urea cycle are summarized in **Figure 7-7**.

7.4 Discussion

In this study, the results of HILIC-LC-MS based metabolomic analysis further fulfilled our exploration on how GTPs could modify gut-microbiota and the dependent metabolites in rat model. We found that GTPs caused significant time- and dose-dependent alterations of the hydrophilic metabolites and nutrients in the gut of GTPs-treated rats (**Table 7-1**, **Table 7-2**, **Fig. 7-1 A and B**). The altered metabolic pathways include TCA cycle, bile acid metabolism and the metabolisms of purine, pyrimidine, and various amino acids (**Table 7-3**). In addition, calorific lipids and fats were accumulated in the gut of GTPs-treated rats (**SI Table 7-1**). Meantime, GTPs enriched OTUs that have high gene diversities in TCA/urea cycle and the “energy conversion” related pathways, such as glycolysis, gluconeogenesis, and fatty acid degradation (**Fig. 7-2**). The taxonomic groups associated with healthy physiological phenotypes were enriched by GTPs, whereas the taxonomic groups containing opportunistic pathogens and related with adverse health outcome were reduced by GTPs (**Fig. 7-3** and **SI Table 7-2**). To gain an overview on the global metabolic changes caused by GTPs, data published in several earlier works were integrated (**Fig. 7-4** and **Table 7-2**) and were input into KEGG metabolic mapping analysis (**Fig. 7-5**). The gene ortholog and mapping analyses showed that TCA/urea cycle may play a central role in reducing the serum glucose, triglyceride and total cholesterol, which was supported by clinical chemistry analysis (**Fig. 7-6**). These results also indicated that GTPs may reduce the absorption of calorific food components by boosting the TCA/urea cycle,

glycolysis, ATP synthesis and the metabolisms of amino acids of gut-microbiota (**Fig. 7-7**).

The untargeted metabolomics also revealed that the majority of these fatty acids and lipids were accumulated in the gut content (**SI Table 7-1**). Though specific structures of these components could not be elucidated without spikes of high-purity standards, the results are consistent with previous metabolomic analysis using gas chromatography–mass spectrometry (GC-MS). Our data suggested that green tea polyphenols could suppress the absorption of calorific fats and lipids in both human and rodent models. In terms of the mechanism, several studies have been done to investigate the mechanism behind the anti-obesity function of green tea extract (Dulloo *et al.*, 1999; Murase *et al.*, 2005; Xu *et al.*, 2015). The mechanism was considered to be the catechin-induced precipitation of fats and lipids in the micelles of gut content (Ikeda *et al.*, 1992). But to our best knowledge, no such study has been conducted with a specific focus on the role of gut-microbiota in the anti-obesity function of GTPs except for our earlier microbiome analysis conducted in the same rat model (Wang *et al.*, 2018). Of note, we observed significant time-/dose- dependent shift of the gut-content metabolome caused by GTPs. Of note, two features m/z 416.144 (3.351 min) and m/z 359.11 (3.367 min) were found to be significantly affected by the interaction effect of time and dose of GTPs treatment (**Fig. 7-1 C, D and E**). The identities of metabolites were tentatively characterized with HMDB, showing to be trihydroxy-3',7'-dimethoxyflavanone (m/z , 416.144; retention time, 3.351) and myricanol 5-(6-galloylglucoside) (m/z , 359.110; retention time, 3.367). They might be generated from the gut-microbiota dependent metabolism of GTPs in gut and may be used to predict the dietary exposure to GTPs.

These genes belong to the mitochondrial respiratory chain complex which functions to maintain oxidative phosphorylation, also termed as the respiratory chain. This is not surprising since GTPs are well known free radical scavenger (Rehman *et al.*, 2014). Oxidative phosphorylation is an important cellular process that uses carbohydrates to create adenosine triphosphate (ATP), also termed as mitochondrial biogenesis (Frye *et al.*, 2016). The evidences from these two aspects together reflected the stimulation of gut-microbiota dependent TCA cycle and ATP synthesis. The intermediate metabolites of TCA/urea cycle showed remarkable alterations following GTPs treatment (**Table 7-1**, **Table 7-2** and **Fig. 7-7**). Consistently, previous metagenomic analysis found that the gene orthologs (GOs) related with mitochondrial TCA cycle and ATP synthesis were significantly increased, including AAA-ATPase, NADH-flavin oxidoreductase, fumarate reductase, alpha glucosidase, 4Fe-4S ferredoxin iron-sulfur binding domain protein, and molybdopterin oxidoreductase (**Fig. 7-5**). In addition, we also noticed the elevation of metabolisms of purine and pyrimidine, which are tightly linked with mitochondrial energy conversion (Loffler *et al.*, 2005; Song *et al.*, 2013; Vogels and Van der Drift, 1976). Pyrimidine can be synthesized from glutamine and uridine monophosphate (UMP), which were generated from ribose-5-P (pentose phosphate pathway, PPP) and aspartic acid (TCA cycle), respectively. Purine can be synthesized by glutamine and AMP, which were generated from glycine (glycolysis) and ribose-5-P (PPP), respectively. The purine nucleotide pathway is a metabolic process in which fumaric acid is generated from aspartic acid in order to provide the fumaric acid consumed in TCA cycle (Song *et al.*, 2013). The catabolism of pyrimidine could provide acetyl-CoA and succinyl-CoA to TCA cycle (Vogels and Van der Drift, 1976). There it seems the boosted TCA/urea cycle further

elevated pyrimidine and purine metabolisms by consuming the intermediates generated by these two pathways. More specific molecular evidences in terms of how GTPs affect mitochondrial TCA/urea cycle is not known in this study. To our knowledge, the specific mechanisms are complex and have a myriad of factors involved, such as SIRT-1, PGC-1 α , Bak/Bax and MPTP etc. (Sandoval-Acuna *et al.*, 2014). Considering that gut-microbiota is a highly complex mixture of different microbial strains, more detailed mechanism could be very difficult to elucidate.

Two sulfate-reducing OTUs, (q) *Desulfovibrionaceae*, (t) *Dehalobacteriaceae* and (r) *Peptococcaceae* exhibited positive correlations with (p) *Ruminococcaceae* (**Fig. 7-2 A** and **C**). Evidences have shown a negative correlation between high fat diets with *Ruminococcus* and *Oscillospira* (family *Rumminococcaceae*), and *Dehalobacterium* (family *Dehalobacteriaceae*), *Butyribrio* and *R. gnavus* (family *Lachnospiraceae*), of which all belong to *Clostridiales* order, phylum *Firmicutes* (O'Connor *et al.*, 2014). The elevation of the above strains may be resulted by the precipitation of fats and lipids in gut following physical binding of catechins. It is well known that (p) *Ruminococcaceae* and (s) *Lachnospiraceae* are associated with healthy gut status and lean phenotype (Wong *et al.*, 2006). On the other hand, the sulfur metabolism of gut-microbiota has been linked with the anti-oxidative capacity and detoxification of xenobiotics (Carbonero *et al.*, 2012). Of note, two decreased OTUs (d) *Peptostreptococcaceae* (over-represented in the guts of colorectal cancer patients) and (f) *Prevotellaceae* (opportunistic pathogen) were negatively correlated with the strains discussed above (**Fig. 7-2 D**). (g) *Bifidobacteriaceae* was also inversely correlated yet its role is controversial in different publications (Million *et al.*, 2013), for which reason it will not be discussed here. As shown in **Figure 7-2 B**, two clusters exist

among the decreased OTUs: cluster 1, (n) *Alcaligenaceae* (opportunistic pathogen), (b) *Rikenellaceae* (high fat diet), (f) *Prevotellaceae*, (opportunistic pathogen), and (g) *Bifidobacteriaceae*; cluster 2, (d) *Peptostreptococcaceae* (colorectal cancer related), (e) *Verrucomicrobiaceae*. More specific reasons for such clustering keep unknown in the current study and need to be investigated in future work.

As mentioned in the results part above, certain correlations among the altered OTUs were discovered, from which we gained interesting findings (**Fig. 7-3**). The reduction of opportunistic pathogens may be a result of the competition of carbon source with the beneficial strains, since (s) *Lachnospiraceae*, (u) *Bacteroidaceae* and (v) *Porphyromonadaceae* were all highly active in energy conversion (**SI Table 7-2 and 3**). The other two links may relate to sulfur-reducing reactions because both (r) *Desulfovibrionaceae* and (q) *Peptococcaceae* are active sulfur-reducing OTUs. In the family of (r) *Desulfovibrionaceae*, members of the genera *Desulfovibrio*, *Desulfobaculum*, and *Desulfocurvus* are able to utilize sulfate as electron acceptor which is reduced to sulfide, most species can also use sulfite and thiosulfate. Similarly, many genera in (q) *Peptococcaceae*, such as *Desulfitibacter*, *Desulfitispora* and *Desulfurispora* could use sulfide and sulfite as electron acceptors (Kuever, 2014). In addition, (p) *Ruminococcaceae*, (u) *Bacteroidaceae* and (s) *Lachnospiraceae* highly contributed to the global energy metabolism, including TCA cycle, ATP synthesis, amino acid synthesis, glycolysis/gluconeogenesis and fatty acids metabolism. The members of these families have been reported as beneficial bacteria in gut that are associated with a wide range of positive health outcomes (Montel *et al.*, 2014; Thushara *et al.*, 2016; Walter *et al.*, 2013). By contrast, although (w) *RF32. unclassified* and (v) *Porphyromonadaceae* were

significantly elevated in the 1.5% GTPs group at 6-month, they have bare contribution to “energy conversion” pathways. Significant reductions of cholic acid, deoxycholic acid and cholesterol were found in previous HPLC-profiling analysis. In terms of the metabolizer of bile acids, *Clostridiales Lachnospiraceae*, *C. Ruminococcaceae* and *C. Blautia* have been found to carry with highly active 7 α -dehydroxylating activities (Chen *et al.*, 2011; Kakiyama *et al.*, 2013b; Liu *et al.*, 2004).

Our previous analysis showed that GTPs enriched *C. Lachnospiraceae* and *C. Ruminococcaceae* and significantly reduced cholic acid level in the gut of rats (Wang *et al.*, 2018). Studies have uncovered that the derivatization and metabolism of bile acids by gut-microbiota is a crucial factor in deciding the physiological health statuses of host gastrointestinal (GI) tract and liver (Louis *et al.*, 2014; Ma *et al.*, 2018; O'Connor *et al.*, 2014; Wolf *et al.*, 2014). Also, one recent mice study has proven that, regardless of specific phylogenetic composition, a reduced fecal bile acid level, induced by an elevated level of bile salt hydrolase (BSH) of gut-microbiota, can modulate host lipid metabolism, cholesterol metabolism and eventually lead to weight loss by regulating related key genes in liver and intestine (Joyce *et al.*, 2014). BSH has been found in many probiotic genera like *Lactobacillus*, *Bifidobacterium*, *Enterococcus*, *Clostridium* and *Bacteroides* spp., and is rarely seen in pathogen or opportunistic pathogens (Begley *et al.*, 2006). Thus, the dynamics of gut-microbiota community structure could affect the metabolism of bile acid and in turn exert significant influence on liver and gut. Indeed, studies have clearly demonstrated the association between the pathogenesis/carcinogenesis of liver-gut axis and the gut-microbiota dependent bile acid metabolism, such as nonalcoholic steatohepatitis (Wolf *et al.*, 2014), liver cancer (Ma *et al.*, 2018), colorectal cancer (Louis *et al.*, 2014),

cirrhosis (Kakiyama *et al.*, 2013a), and inflammation bowel disease (Duboc *et al.*, 2013) etc. From a view of systematic biology, the metabolic status of gut-microbiota also participates into the global immune system by affecting gut autoimmune lymph tissue (GALT) (Li *et al.*, 2018). Taken the above information into consideration, the modulation of bile acid by *C. Lachnospiraceae* and *C. Ruminococcaceae* may lead to a healthy intestinal environment and enhance the epithelial absorption of nutrients. The *Lachnospiraceae* and *Ruminococcaceae* are two of the most abundant families in the mammalian gut environment and have been positively associated with gut health. The two families share a common role as active plant degraders (Biddle *et al.*, 2013). This might be the reason that they were largely enriched following oral administration of GTPs.

As already presented in the results part, significant alterations were found for the metabolites between TCA and urea cycles (**Fig. 7-7**). The two pathways are associated with purine metabolism, pyrimidine metabolism, glycolysis, gluconeogenesis, as well as the metabolisms of diverse amino acids. It is well-known that gut-microbiota plays a pivotal role in regulating host energy balance—not only the host environment contributes to the composition of gut microbiota, but the microbiota in turn influence the digestive efficiency and energy homeostasis of host (Cani and Delzenne, 2009a). Dysfunctional energy homeostasis of gut-microbiota can result in obesity and is related with diabetes (Baothman *et al.*, 2016; Meijnikman *et al.*, 2017). In addition to energy homeostasis, TCA cycle of gut-microbiota has been reportedly linked with host redox homeostasis, oxidative stress, and the latter is also connected with lipid metabolism (Cani and Delzenne, 2009b; Holmes *et al.*, 2012). GTPs boosted TCA/urea cycle which further connected with TCA/urea cycle, carbohydrate metabolism, nucleotide metabolism, energy metabolism, and the

metabolisms of amino acids (**Fig. 7-4**). The metabolic changes of gut-microbiota are consistent with clinical chemistry data (**Fig. 7-6**), which demonstrated reductions of serum glucose, triglycerides, total cholesterol, and the increase of blood urea nitrogen. Gut-microbiota dependent urea metabolism has been noticed for its correlation with host urea balance (Davila *et al.*, 2013; Shen *et al.*, 2015b), but to our best knowledge it has not been mechanistically linked with GTPs. Considering the results of metabolomic analysis, metagenomic analysis and clinical chemistry, we believe that gut-microbiota may be an important factor involved with the elevation of serum urea following green tea administration in rats.

To summarize, data from metabolomics, metagenomics and clinical chemistry together demonstrated that GTPs could boost TCA/urea cycle of gut-microbiota and meantime enrich *Ruminococcaceae*, *Bacteroidaceae* and *Lachnospiraceae*. Besides, the strains featured for sulfide-reducing activities were also enriched, including (q) *Desulfovibrionaceae*, and (r) *Peptococcaceae*. The adjustment of gut-microbiome co-occurred with the GTPs-induced positive modifications of the metabolisms of bile constituents, carbohydrates, fats, lipids and amino acids. Our results represent a comprehensive picture of the changes of gut-microbiota induced by GTPs, suggesting that gut-microbiota dependent mitochondrial TCA/urea cycle is a key factor for the health-promoting function of GTPs. However, more detailed information and mechanisms for the underlying changes of mitochondrial metabolism remain obscure and need to be explored in future in order to improve clinical medical practice of GTPs.

TABLES

Table 7-1. Signature metabolites significantly affected by time/dose effects of GTPs treatment.

AS CA	m/z	RT	Imputative ID	E/ C	<i>p</i> - valu e	Lever age	SPE	Metabolic pathway
Tim e	358.1 00	4.47 2	Dihydroorotic acid	0. 83	6.29 E- 02	2.83E -03	9.43E- 17	Pyrimidine metabolism
Tim e	253.0 04	11.2 92	2- Hydroxyethanes ulfonate	0. 85	1.04 E- 01	5.20E -03	1.17E- 16	Taurine metabolite
Tim e	459.0 18	11.1 69	Diadenosine pentaphosphate	0. 90	1.10 E- 02	4.40E -03	1.63E- 16	Glycerophosp holipid metabolism
Tim e	332.1 56	10.7 28	Argininosuccinic acid	0. 90	6.71 E- 03	3.35E -03	1.30E- 16	Urea cycle
Tim e	393.0 18	12.8 83	Inosinic acid	0. 93	1.90 E- 02	4.26E -03	1.30E- 17	Purine synthesis
Tim e	405.9 76	12.5 33	Adenosine 3',5'- cyclic phosphate	0. 96	1.68 E- 02	2.68E -03	3.25E- 17	Purine metabolism
Tim e	212.9 94	11.2 53	3-Hydroxy-4- aminopyridine sulfate	0. 97	4.33 E- 02	3.82E -03	8.46E- 17	Pyridine amines metabolism
Tim e	252.9 60	16.5 63	Dihydrouracil	1. 14	1.62 E- 03	2.08E -03	1.45E- 16	Urea cycle
Tim e	322.0 87	16.0 68	1H-Indole-2,3- dione	1. 27	1.01 E- 03	1.91E -03	1.63E- 18	Indole derivative
Dos e	162.0 29	14.8 24	Indole	1. 41	3.48 E- 05	1.48E -03	8.04E +11	Tryptophan metabolism
Dos e	175.0 13	13.7 57	Glyceric acid 1,3-biphosphate	1. 50	2.89 E- 04	1.40E -03	2.88E +13	Glycolysis
Dos e	592.4 43	3.34 2	Aspidospermidin e	1. 56	1.05 E- 05	1.49E -03	1.73E +12	Tryptophan metabolism
Dos e	290.9 55	3.28 6	Inositol 1,3,4,5,6-	1. 75	6.52 E- 07	2.27E -03	6.73E +13	Cell replication

			pentakisphosphate					
Dose	404.0	3.39	N-(1-Deoxy-1-fructosyl) phenylalanine	1.99	2.94E-06	2.19E-03	1.87E+14	Phenylalanine metabolism

Abbreviation: RT, Retention Time; E/C, Ratio of peak intensity (Extracted Ion Chromatogram) in 1.5% GTPs-treated group versus control group at 6-month; *p*-values were calculated from Welch T-test, two-tailed. Leverage and SPE score was calculated using analysis of variance-simultaneous component analysis (ASCA) according to Neuda et al. (Nueda *et al.*, 2007). Leverage was used to evaluate the importance of the metabolite to the model, and SPE was a test of the fitness of the model for the particular metabolite. Variables with low SPE and higher leverage usually have more significant contribution to the model and were the compounds showing remarkable response to the treatment. Full list is available in the **SI Table 7-1**.

Table 7-2. TCA/Urea cycle targeted metabolomic analysis performed with SRM.

Transition*	CE	RT	Metabolite	E/C	p-value	Primary pathway
<i>Elevated Metabolites</i>						
112→95	15	12.52	Cytosine	6.01	0.0039	Pyrimidine metabolism
136→90	15	17.65	Homocysteine	4.53	0.0013	Amino acid
113→70	35	18.25	Uracil	2.77	0.0064	Pyrimidine metabolism
159→99	15	15.92	Allantoin	2.68	0.0244	Uric acid metabolite
175→132	15	19.5	Ureidosuccinate	2.57	0.0024	Pyrimidine metabolism
133→115	15	19.54	Malic acid	2.17	0.0077	Urea cycle
150→133	15	18.2	Methionine	1.99	0.0172	Amino acid
174→131	15	15.24	Citrulline	1.86	0.0098	Urea cycle
106→60	15	18.84	Serine	1.73	0.0684	Amino acid
132→86	15	15.16	(Iso)leucine	1.65	0.0648	Amino acid
173→93	15	18.13	Shikimic acid	1.62	0.0216	Tryptophan pathway
116→70	15	16.77	Proline	1.62	0.0393	Amino acid
124→80	15	11.33	Taurine	1.56	0.0262	Tryptophan pathway
120→44	35	17.44	Homoserine	1.54	0.1060	Amino acid
118→55	15	18.75	Valine	1.24	0.2855	Amino acid
115→71	15	18.8	Fumaric acid	1.19	0.0036	Urea/TCA cycle
142→95	15	18.65	Histidinol	1.12	0.3586	Amino acid
<i>Decreased Metabolites</i>						
104→60	15	18.62	Choline	0.98	0.4676	Vitamin-like nutrient
147→84	15	19.47	Lysine	0.76	0.2769	Amino acid
122→78	15	16.58	Nicotinic acid	0.76	0.1782	Vitamin
76→30	15	18.9	Glycine	0.74	0.3136	Amino acid
345→122	25	14.85	ThPP	0.70	0.1086	Vitamin
117→73	15	16.31	Succinic acid	0.40	0.0332	TCA cycle
131→72	15	18.72	Agmatine	0.35	0.0181	Arginine metabolism

*Transition, the specific pair of m/z values associated to the precursor and fragment ions selected is referred to as a "transition" and can be written as parent m/z → fragment m/z. Abbreviation: CE, Collision Energy (eV); RT, Retention Time; E/C, ratio of peak intensities (Extracted Ion Chromatogram) of a metabolite measured in exposure group versus control; ThPP, Thiamine pyrophosphate. *p*-values were calculated from Welch T-test, two-tailed.

Table 7-3. Pathway impact analysis based on the metabolites showing remarkable change in targeted and untargeted metabolomic analysis.

Pathway	Hit/Total	<i>p</i> value	Impact
Arginine and proline metabolism	4/44	0.004	0.070
Alanine, aspartate and glutamate metabolism	4/24	0.022	0.025
Citrate cycle (TCA cycle)	3/20	0.007	0.106
Cysteine and methionine metabolism	3/28	0.009	0.257
Valine, leucine and isoleucine degradation	3/38	0.044	0.036
Glycine, serine and threonine metabolism	3/32	0.119	0.535
Purine metabolism	2/68	0.003	0.119
Butanoate metabolism	2/20	0.004	<0.001
Valine, leucine and isoleucine biosynthesis	2/11	0.107	0.667
Pantothenate and CoA biosynthesis	2/15	0.149	<0.001
Pyrimidine metabolism	2/41	0.330	0.065
Primary bile acid biosynthesis	2/46	0.339	0.060
Methane metabolism	2/9	0.516	0.400
Cyanoamino acid metabolism	2/6	0.516	<0.001

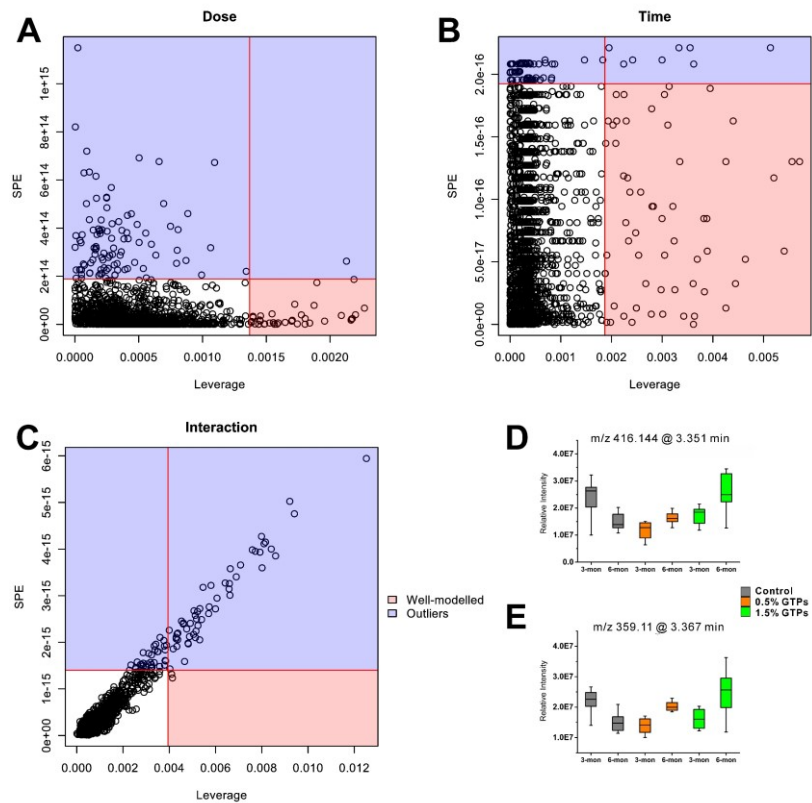


Figure 7-1. Leverage/SPE scatter plots to screen the important metabolites that demonstrated significant responses to (A) time-, (B) dose-, and (C) interaction effects of GTPs administration. The leverage and squared prediction error (SPE) scores were calculated via ASCA model using MetaboAnalyst. X-axis indicates modeling leverage; Y-axis indicates SPE. Two feature ions (D and E) showed remarkable response to the interaction effect of treatment time and dose.

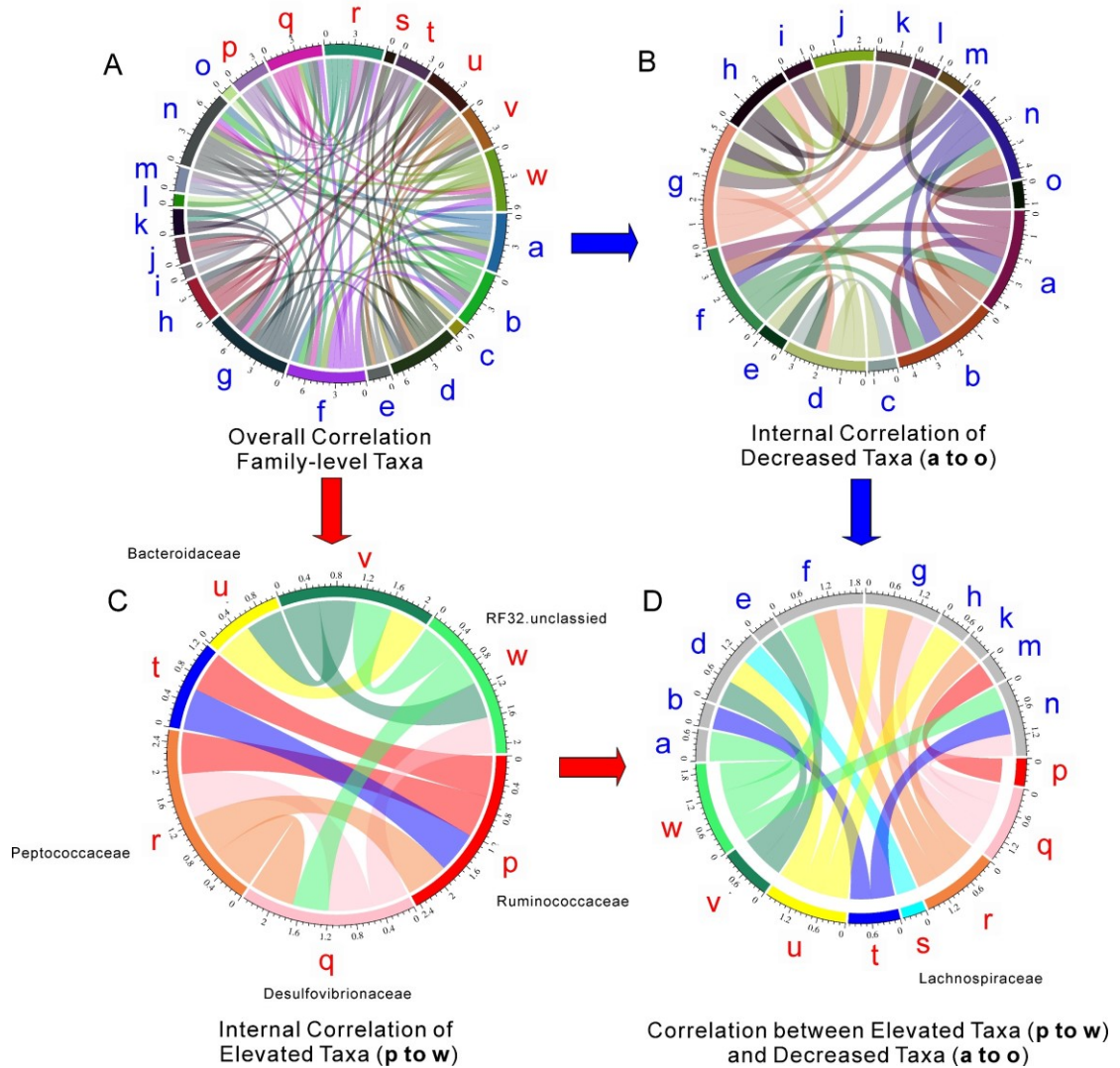


Figure 7-2. Correlation analysis of elevated and decreased operational taxonomic units (OTUs) of gut-microbiota. (A) Overall correlation of 23 family-level OTUs. (B) Correlation between decreased OTUs. (C) Correlation between elevated OTUs. (D) Correlation between elevated OTUs and decreased OTUs. Cutoff value for Pearson correlation coefficient is 0.5. Specific values are available in the **SI Table 7-2**.

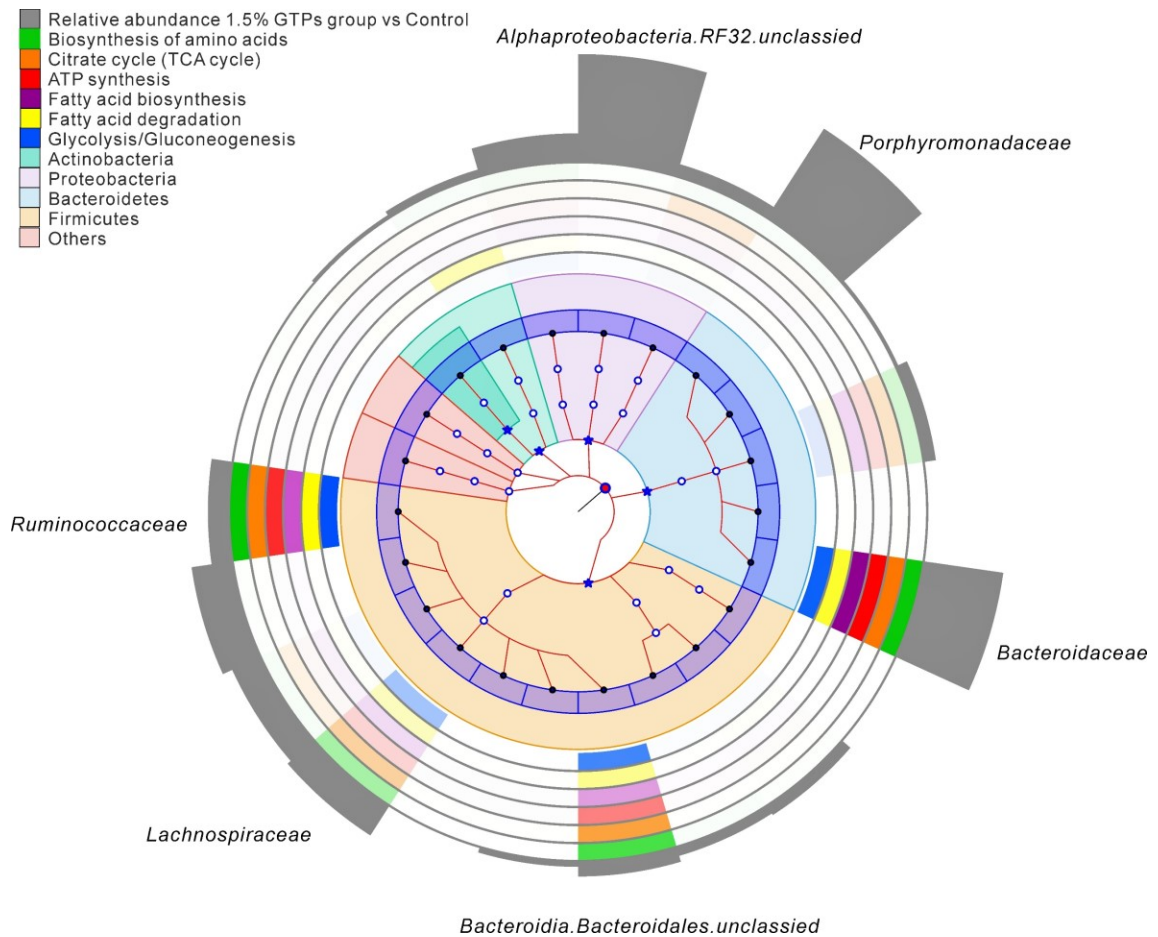


Figure 7-3. Relative contribution to gut-microbiota dependent metabolism by specific OTUs. Inside phylogenetic tree was constructed with the 23 family-level OTUs which showed significant alteration following GTPs administration. The color clades which cover the phylogenetic tree indicate four major phyla of gut-microbiota—*Firmicutes*, *Bacteroidetes*, *Actinobacteria*, and *Proteobacteria*. The rainbow color-coded circular bars indicate the relative contribution of gut-microbiota family group to the interested metabolic pathways. The outside grey histogram indicates the ratio of family relative abundance measured in 1.5% GTPs treated group versus control at 6-month. Specific values are available in the **SI Table 7-3**.

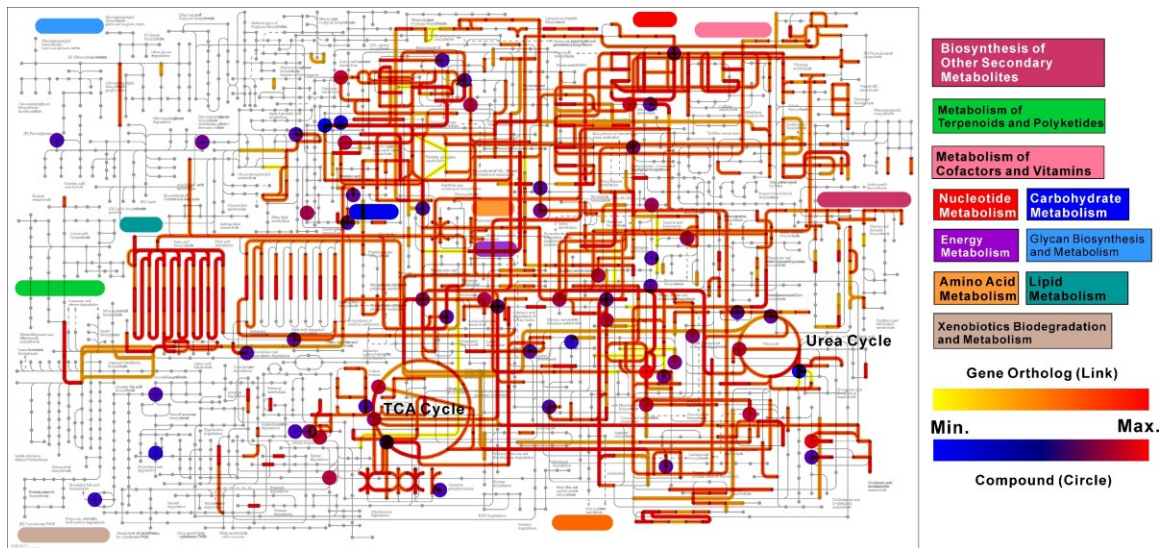


Figure 7-4. Metabolic mapping of metabolomic and metagenomic data on KEGG map of gut-microbiota biosynthesis pathways. Fold changes of a total of 72 metabolites and 1891 GO at 6-month were input into iPath online module.

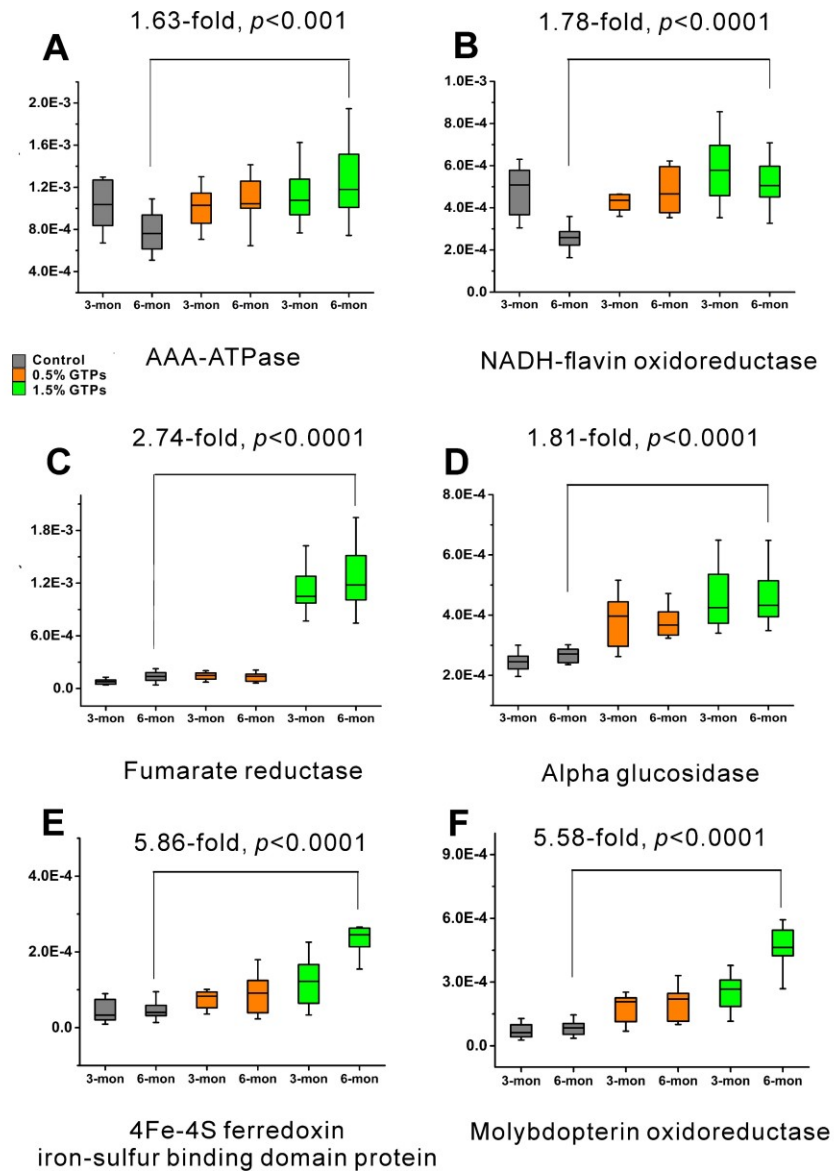


Figure 7-5. Relative abundances of TCA/Urea cycle related Gene Orthologs (GOs) revealed by metagenomic analysis that showed significant alteration in previous analysis. (A) AAA-ATPase (ENOG4105F42); (B) NADH-flavin oxidoreductase (ENOG4105CCY); (C) Fumarate reductase (ENOG4105DAB); (D) Alpha glucosidase (ENOG4105CGS); (E) 4Fe-4S ferredoxin, iron-sulfur binding domain protein (ENOG4105D3S); (F) Molybdopterin oxidoreductase (ENOG4108J2R). Specific data are available in **SI Table 7-5**. Data were retrieved from previous metagenomic analysis (Wang *et al.*, 2018).

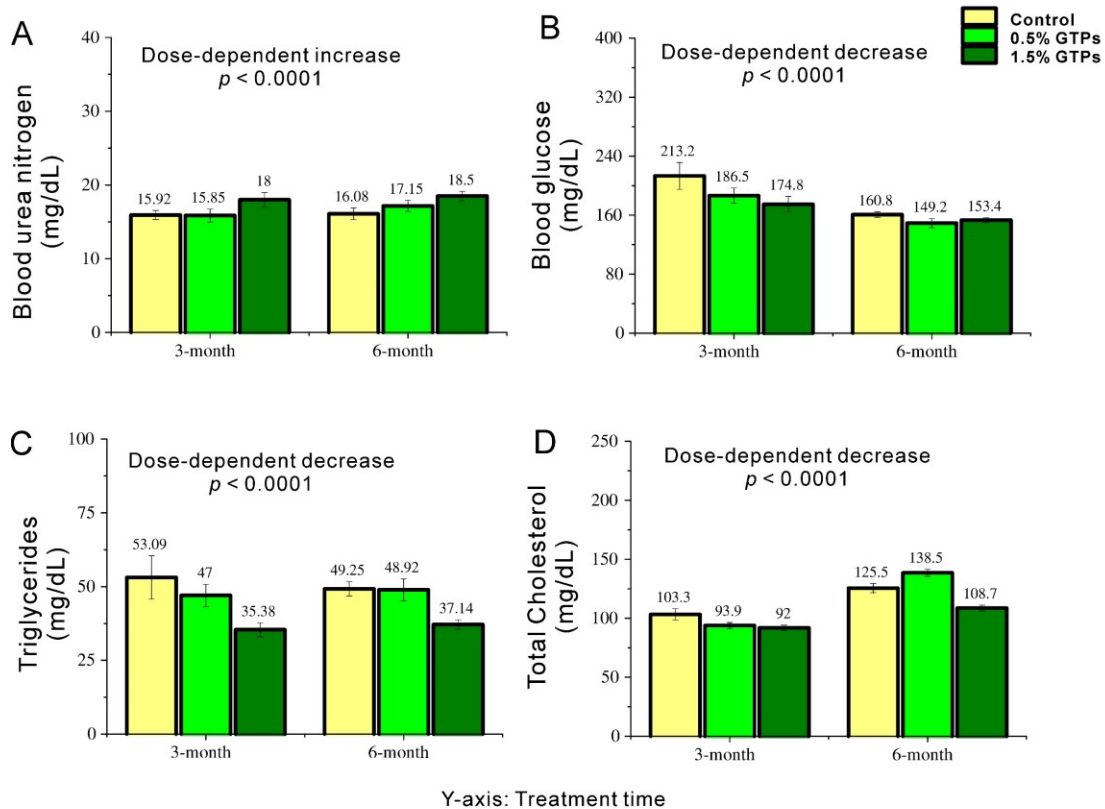


Figure 7-6. Serum chemistry analysis of the rats treated with GTPs. (A) Blood Triglycerides; (B) Blood Glucose; (C) Blood Total Cholesterol; (D) Blood Urea Nitrogen. Specific data are available in SI Table 6. Data were retrieved from previous clinical chemistry analysis (Shen *et al.*, 2017).

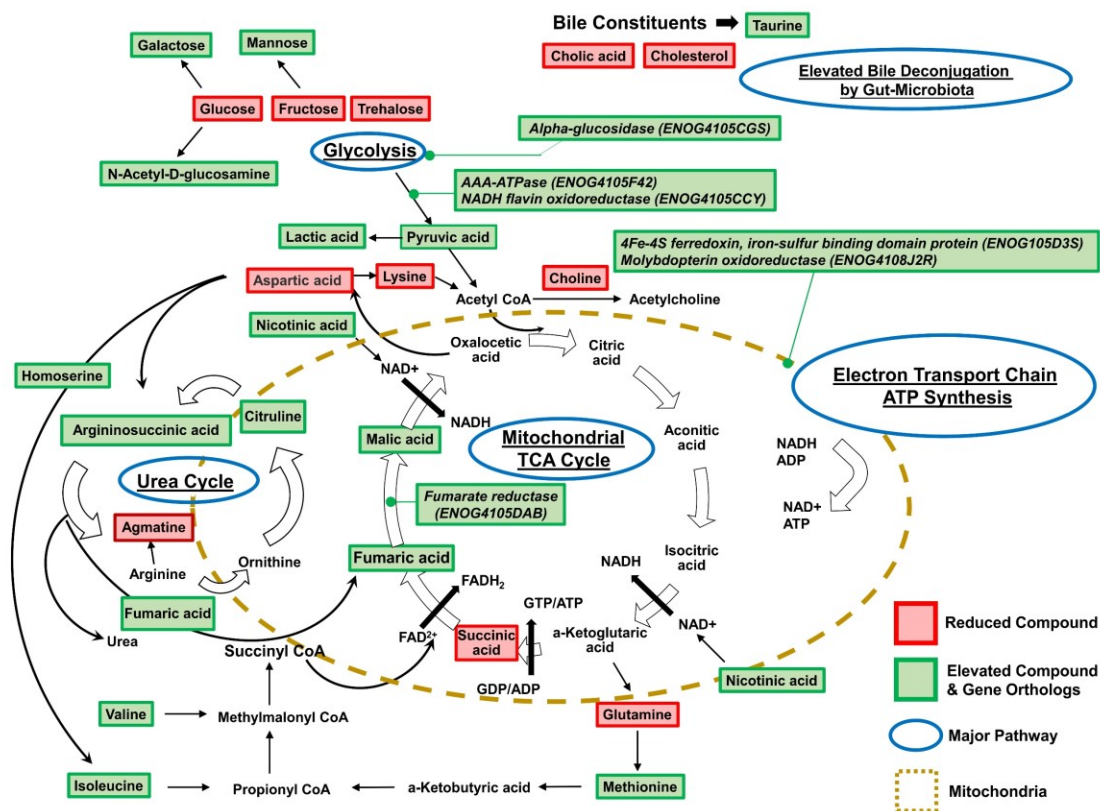


Figure 7-7. Summary of impact of GTPs on the mitochondrial TCA/urea cycle and associated metabolic pathways of gut-microbiota.

SI Table 7-1. Summary of untargeted metabolomic analysis.

Depend ency	m/z	RT	Imputative Identity	Fold	ANOVA <i>p</i>
Time	1008.663	14.209	(23S,24S)-17,23-Epoxy-24,29-dihydroxy-27-norlanost-8-ene-3,15-dione	0.94	1.0169E-02
Time	1042.657	14.294	1-Stearoylglycerophosphoglycerol	0.87	8.9828E-02
Dose	1042.846	14.192	TG(20:4(5Z,8Z,11Z,14Z)/20:0/20:4(5Z,8Z,11Z,14Z))	1.69	2.7023E-05
Time	1076.777	14.295	Theasapogenol A	1.10	4.2667E-03
Time	1110.664	14.234	LysoPC(20:5(5Z,8Z,11Z,14Z,17Z))	0.91	4.3259E-02
Time	1178.656	14.256	(3b,6a,12b,17a,20S)-Dammar-24-ene-3,6,12,17,20-pentol 20-[glucosyl-(1->2)-[rhamnosyl-(1->6)]-glucoside] 6-xyloside	0.98	7.4035E-03
Dose	160.010	14.689	3-keto-2-Methylbutyrate	1.78	7.5206E-06
Time	160.989	13.270	2-(Dimethylamino)acetonitrile	1.04	1.1629E-02
Time	165.005	2.527	Sanguisorbic acid dilactone	0.89	1.5222E-03
Dose	167.941	17.240	3-Chloro-4-(dichloromethylene)-2,5-pyrrolidinedione	1.70	1.1862E-04
Time	170.053	14.984	1,3-Diacetoxy-4,6,12-tetradecatriene-8,10-diyne	0.80	5.5229E-03
Time	171.116	15.017	Cardanolmonoene	1.16	5.1708E-05
Time	170.985	16.331	Acetylthiophene	0.96	2.1943E-03
Time	176.967	11.624	(E)-S-1-Propenyl thiosulfate	0.72	4.6205E-01
Time	177.952	10.787	4,5-Dihydro-2-methylthiazole	0.70	4.3655E-01
Time	188.043	15.033	3-Hydroxymugineic acid	0.92	1.8986E-04
Time	188.025	16.259	5,6-dihydroxy-2-(4-hydroxy-3-methoxyphenyl)-7-methoxy-4H-chromen-4-one	1.18	3.6763E-04
Time	199.922	10.776	DG(15:0/16:1(9Z)/0:0)	0.70	4.9968E-01
Time	202.047	14.931	Hydroxybenzoic acid	1.04	1.3375E-04
Dose	213.939	15.861	DG(16:1(9Z)/18:0/0:0)	1.43	1.0876E-04
Time	216.034	14.909	Phenol sulphate	0.78	2.4755E-02
Time	238.961	15.891	Quindoxin	1.37	1.6535E-04
Time	253.004	11.292	2-Hydroxyethanesulfonate	0.85	1.0378E-01
Dose	302.126	3.319	2-Ethylidihydro-3(2H)-thiophenone	1.39	1.6040E-04
Time	304.134	10.780	Benzo[a]pyrene-7,8-diol	0.83	7.1968E-02
Time	307.947	13.458	TG(20:3(5Z,8Z,11Z)/o-18:0/20:3(5Z,8Z,11Z))	1.28	2.7411E-04
Time	308.841	14.219	PS(22:6(4Z,7Z,10Z,13Z,16Z,19Z)/20:3(8Z,11Z,14Z))	1.03	2.8312E-02
Time	320.807	14.874	DG(14:1(9Z)/22:0/0:0)	0.94	1.7019E-03
Time	351.038	15.878	5-(4-Chloro-3-hydroxy-1-butynyl)-2,2'-bithiophene	1.53	5.5431E-04
Dose	388.062	3.394	ent-Epicatechin-(4alpha->8)-ent-epicatechin 3-gallate	1.89	1.0446E-05
Time	393.018	12.883	Inosinic acid	0.93	1.8999E-02
Interact ion	416.144	3.351	unknown	1.28	2.3013E-04

Time	437.047	13.337	Lentinic acid	1.08	8.9200E-04
Time	461.151	13.256	Pelargonidin 3-O-[b-D-Glucopyranosyl-(1->2)-[4-hydroxycinnamoyl-(->6)]-b-D-glucopyranoside](E-) 5-O-b-D-glucopyranoside	1.11	2.3147E-05
Time	477.161	13.805	Dulxanthone E	1.03	2.3339E-05
Time	478.156	13.807	a-L-Arabinofuranosyl-(1->3)-b-D-xylopyranosyl-(1->4)-D-xylose	1.13	2.9436E-05
Dose	498.951	13.076	Ganglioside GD3 (d18:0/18:1(11Z))	1.43	1.3063E-05
Time	498.651	14.437	Cardiolipin	0.95	4.6810E-01
Dose	512.227	12.977	Histidiny-Serine	1.56	6.6540E-05
Dose	542.330	3.255	LysoPC(20:5(5Z,8Z,11Z,14Z,17Z))	1.52	2.8734E-04
Time	546.241	13.236	Dihydrozeatin-9-N-glucoside-O-glucoside	1.20	9.2032E-05
Dose	556.350	3.256	3-Methylthiohexyl hexanoate	1.59	5.5700E-04
Dose	557.434	3.248	TG(22:4(7Z,10Z,13Z,16Z)/22:6(4Z,7Z,10Z,13Z,16Z,19Z)/22:4(7Z,10Z,13Z,16Z))	1.60	9.2456E-07
Time	561.923	13.376	TG(22:6(4Z,7Z,10Z,13Z,16Z,19Z)/20:4(8Z,11Z,14Z,17Z)/22:6(4Z,7Z,10Z,13Z,16Z,19Z))	1.01	2.2105E-03
Dose	563.149	3.168	Lupiwighteone hydrate 7-glucoside	1.61	7.4740E-04
Time	567.645	14.553	Cyanidin 3-[6-(4-glucosylferuloyl)sophoroside] 5-glucoside	1.08	1.7846E-03
Dose	570.388	3.247	Glabric acid	1.69	6.5743E-08
Dose	571.384	3.266	LysoPC(P-18:0)	1.45	7.7586E-07
Dose	584.393	3.236	Cyclopassifloic acid B	1.70	5.4172E-10
Dose	585.367	3.243	LysoPC(20:4(5Z,8Z,11Z,14Z))	1.54	2.7974E-06
Time	588.847	13.495	28-Glucosyl-30-methyl-3b,23-dihydroxy-12-oleanene-28,30-diate 3-[glucosyl-(1->3)-xylosyl-(1->2)-glucoside]	0.82	1.1724E-01
Time	593.155	12.333	8,8'-Methylenebiscatechin	1.03	3.2210E-03
Time	594.162	12.311	Epicatechin-(2beta->7,4beta->6)-catechin	1.12	2.2456E-03
Time	597.166	12.380	7,8-Dihydrovomifoliol 9-[apiosyl-(1->6)-glucoside]	1.03	2.3188E-02
Time	598.158	12.364	Dihydro-4-hydroxy-5-S-glutathionyl-benzo[a]pyrene	1.13	1.5225E-03
Time	612.140	12.361	3,5-Digalloylepicatechin	0.83	7.7992E-02
Time	618.145	12.356	Kaempferol 7-(6"-galloylglucoside) (3b,16a)-Dihydroxy-12-oleanen-28-oic acid 3-[glucosyl-(1->2)-arabinoside] 28-[rhamnosyl-(1->4)-glucosyl-(1->4)-glucosyl] ester	1.15	8.6142E-03
Dose	619.320	3.350	4"-Methyl-6"-(3,4-dihydroxy-E-cinnamoyl) isoorientin	1.44	1.0303E-05
Time	625.156	12.295	Epifisetinidol-(4beta->8)-catechin	0.96	5.2612E-02
Time	626.150	12.310	Epifisetinidol-(4beta->8)-catechin	1.00	2.5905E-03

Time	639.080	12.301	3,5-Digalloylepicatechin	1.08	2.6089E-03
Time	648.271	12.242	Histidiny-Histidine	0.92	1.3411E-02
Dose	695.167	3.313	7-Hydroxy-6-methyl-8-ribityl lumazine	1.60	4.3456E-07
Dose	719.963	13.818	Ganglioside GM2 (d18:1/16:0)	1.43	6.6945E-10
Dose	761.556	14.004	PC(14:0/14:0)	1.56	4.3179E-08
Time	798.446	14.300	PE(18:3(6Z,9Z,12Z)/20:5(5Z,8Z,11Z, 14Z,17Z))	1.10	6.4203E-04
Time	804.665	14.332	PE(22:0/22:5(4Z,7Z,10Z,13Z,16Z))	1.02	2.4615E-02
Dose	806.566	13.842	PG(16:0/16:0)	1.72	1.8574E-07
Dose	809.566	13.887	CE(MonoMe(13,5))	1.71	4.9579E-08
Dose	810.564	13.723	PC(14:0/22:6(4Z,7Z,10Z,13Z,16Z,19 Z))	1.70	6.1595E-07
Dose	811.565	13.741	PE(15:0/20:3(5Z,8Z,11Z))	1.61	2.3538E-07
Dose	833.563	13.680	PC(20:5(5Z,8Z,11Z,14Z,17Z)/14:1(9 Z))	1.64	1.8502E-09
Dose	885.453	12.181	(2b,3b)-Dihydroxy-30-nor-12,20(29)- oleanadiene-28-glucopyranosyloxy- 23-oic acid 3-glucuronide	1.52	6.4116E-05
Dose	906.821	14.307	TG(15:0/24:1(15Z)/15:0)	1.91	1.3524E-07
Time	974.661	14.219	Cholesterol sulfate	0.91	1.0154E-01
Dose	974.828	14.333	TG(20:3(5Z,8Z,11Z)/18:1(11Z)/20:3(5Z,8Z,11Z))	1.73	4.4468E-06
Time	358.100	4.472	Dihydroorotic acid	0.83	6.2918E-02
Time	459.018	11.169	Diadenosine pentaphosphate	0.90	1.1016E-02
Time	332.156	10.728	Argininosuccinic acid	0.90	6.7146E-03
Time	405.976	12.533	Adenosine 2',3'-cyclic phosphate	0.96	1.6762E-02
Time	212.994	11.253	3-Hydroxy-4-aminopyridine sulfate	0.97	4.3328E-02
Time	252.960	16.563	Ureidosuccinic acid	1.14	1.6187E-03
Interact ion	359.110	3.367	unknown	1.14	1.0624E-03
Time	322.087	16.068	1H-Indole-2,3-dione	1.27	1.0145E-03
Dose	162.029	14.824	Indole	1.41	3.4829E-05
Dose	160.981	14.884	Fumaric acid	1.48	2.6364E-05
Dose	175.013	13.757	Glyceric acid 1,3-biphosphate	1.50	2.8916E-04
Dose	696.234	3.303	Glycylalanylprolylmethionylphenylal anylvalinamide	1.52	9.9884E-06
Dose	592.443	3.342	Aspidospermidine	1.56	1.0538E-05
Dose	290.955	3.286	Inositol 1,3,4,5,6-pentakisphosphate	1.75	6.5157E-07
Dose	404.048	3.397	N-(1-Deoxy-1- fructosyl)phenylalanine	1.99	2.9430E-06

SI Table 7-2. Relative abundance of gut-microbiome family-level taxa in 1.5% GTPs-treated groups at 6-month.

Phylogenetic assignment	1.5% GTPs-treatment	Fold change
(a) k__Bacteria p__Bacteroidetes c__Bacteroidia o__Bacteroidales f__unclassified	ND	ND
(b) k__Bacteria p__Bacteroidetes c__Bacteroidia o__Bacteroidales f__Rikenellaceae	ND	ND
(c) k__Bacteria p__Tenericutes c__Mollicutes o__RF39 f__unclassified	0.00038	0.015
(d) k__Bacteria p__Firmicutes c__Clostridia o__Clostridiales f__Peptostreptococcaceae	0.00025	0.048
(e) k__Bacteria p__Verrucomicrobia c__Verrucomicrobiae o__Verrucomicrobiales f__Verrucomicrobiaceae	0.00259	0.053
(f) k__Bacteria p__Bacteroidetes c__Bacteroidia o__Bacteroidales f__Prevotellaceae	0.00112	0.154
(g) k__Bacteria p__Actinobacteria c__Actinobacteria o__Bifidobacteriales f__Bifidobacteriaceae	0.00311	0.169
(h) k__Bacteria p__Firmicutes c__Erysipelotrichia o__Erysipelotrichales f__Erysipelotrichaceae	0.04216	0.274
(i) k__Bacteria p__Firmicutes c__Clostridia o__Clostridiales f__Christensenellaceae	0.00030	0.316
(j) k__Bacteria p__Actinobacteria c__Coriobacteriia o__Coriobacteriales f__Coriobacteriaceae	0.00560	0.390
(k) k__Bacteria p__Firmicutes c__Bacilli o__Lactobacillales f__Lactobacillaceae	0.00271	0.515
(l) k__Bacteria p__Firmicutes c__Bacilli o__Lactobacillales f__Streptococcaceae	0.00379	0.617
(m) k__Bacteria p__Bacteroidetes c__Bacteroidia o__Bacteroidales f__unclassified	0.05313	0.682
(n) k__Bacteria p__Proteobacteria c__Betaproteobacteria o__Burkholderiales f__Alcaligenaceae	0.00421	0.701

(o)	k__Bacteria p__Firmicutes c__Clostridia o__Clostridiales f__unclassified	0.20846	0.853
(p)	k__Bacteria p__Firmicutes c__Clostridia o__Clostridiales f__Ruminococcaceae*	0.32593	1.176
(q)	k__Bacteria p__Proteobacteria c__Deltaproteobacteria o__Desulfovibrionales f__Desulfovibrionaceae	0.00767	1.601
(r)	k__Bacteria p__Firmicutes c__Clostridia o__Clostridiales f__Peptococcaceae	0.00666	1.736
(s)	k__Bacteria p__Firmicutes c__Clostridia o__Clostridiales f__Lachnospiraceae*	0.06401	1.963
(t)	k__Bacteria p__Firmicutes c__Clostridia o__Clostridiales f__Dehalobacteriaceae	0.00103	2.302
(u)	k__Bacteria p__Bacteroidetes c__Bacteroidia o__Bacteroidales f__Bacteroidaceae*	0.25901	4.470
(v)	k__Bacteria p__Bacteroidetes c__Bacteroidia o__Bacteroidales f__Porphyromonadaceae	0.00525	5.871
(w)	k__Bacteria p__Proteobacteria c__Alphaproteobacteria o__Rhodospirillales f__Rhodospirillaceae	0.00150	appear

Abbreviations: ND, not detected. Taxonomic groups with asterisk (p, s, u) were previously found to be reduced by AFB₁ but enriched in 1.5% GTPs-treated group.

SI Table 7-3. Family-level OTU average gene diversities in the metabolic pathways stimulated by GTPs.

OTU	Relative intensity*	Biosynthesis of amino acids	TCA cycle	Fatty acid biosynthesis	Fatty acid degradation	Glycolysis and Gluconeogenesis	ATP synthesis
a	0.00025	117.39	20.89	22.00	5.11	37.67	22.11
b	0.00025	85.50	14.00	16.50	2.50	30.00	14.50
c	0.00038	19.16	3.93	0.46	0.66	21.13	4.26
d	0.00025	117.90	18.62	14.19	8.62	77.71	11.29
e	0.00259	80.50	12.00	7.83	1.33	20.33	19.33
f	0.00112	64.70	15.50	10.30	2.80	27.40	18.70
g	0.00311	24.45	104.67	7.79	8.48	12.67	6.98
h	0.04216	78.14	6.71	7.43	3.71	67.86	7.71
i	0.00030	113.00	26.00	17.00	19.00	10.00	7.00
j	0.00560	92.88	13.00	6.88	3.63	34.88	15.50
k	0.00271	82.01	7.15	15.02	3.37	52.38	11.02
l	0.00379	85.50	14.00	16.50	2.50	30.00	14.50
m	0.05313	60.32	13.92	11.40	3.96	23.56	12.36
n	0.00421	158.56	27.37	31.91	36.14	40.61	42.30
o	0.20846	91.82	11.18	10.27	3.68	26.05	7.55
p	0.32593	110.00	12.14	12.05	3.82	31.05	8.95
q	0.00767	118.11	23.16	16.32	4.95	44.11	22.11
r	0.00666	134.50	23.45	16.95	16.68	39.41	30.86
s	0.06401	133.43	10.61	12.17	5.65	38.78	9.52
t	0.00103	121.00	25.00	15.00	9.00	42.00	29.00
u	0.25901	118.24	21.59	22.59	5.12	37.47	22.71
v	0.00525	62.57	19.71	11.43	4.00	28.57	9.00
w	0.00150	109.25	21.75	23.75	18.50	35.25	31.00

* Relative intensity at 6-month.

SI Table 7-4. Relative contribution of family level OTUs to the gut-microbiota dependent metabolic pathways (1.5% GTPs-treated group, 6-month).

Taxa	Relative contribution to metabolic pathways					
	Biosynthesis of amino acids	Citrate cycle (TCA cycle)	ATP Synthesis	Fatty acid biosynthesis	Fatty acid degradation	Glycolysis
<i>Phylogenetic families reduced by 1.5% GTPs treatment at 6-month</i>						
a	8.32	9.50	9.56	9.56	9.80	9.46
b	6.06	6.36	6.27	7.17	4.79	7.54
c	2.05	2.70	2.78	0.30	1.91	8.02
d	8.36	8.46	4.88	6.17	16.52	19.52
e	58.23	55.65	85.24	34.72	26.07	52.11
f	20.29	31.16	35.74	19.79	23.74	30.44
g	21.23	582.80	36.95	41.45	199.10	38.98
h	918.81	505.86	552.58	535.34	1179.40	2826.82
i	9.43	13.91	3.56	8.69	42.85	2.96
j	145.12	130.23	147.61	65.87	153.34	193.07
k	61.97	34.65	50.76	69.55	68.80	140.22
l	90.38	94.88	93.42	106.87	71.44	112.34
m	893.86	1322.52	1116.39	1035.15	1586.50	1236.85
n	185.99	205.84	302.43	229.36	1146.09	168.76
o	5338.87	4167.79	2675.76	3659.07	5784.88	5366.01
<i>Phylogenetic families elevated by 1.5% GTPs treatment at 6-month</i>						
p*	10000	7075.83	4959.27	6712.47	9388.69	10000
q	252.58	317.54	288.20	213.86	286.19	334.18
r	249.71	279.13	349.21	192.83	837.22	259.21
s	2382.16	1214.46	1035.96	1331.36	2727.09	2452.77
t	34.64	45.88	50.60	26.31	69.65	42.59
u*	8542.01	10000	10000	10000	10000	9589.82
v	91.68	185.15	80.38	102.62	158.45	148.30
w	45.77	58.42	79.15	60.96	209.52	52.31

* indicates the families demonstrating highest contribution to the interested metabolic pathways at global level. The contribution was estimated by multiplying average gene diversity (i.e. gene richness in a specific metabolic pathway) of gut-microbiota family with the relative abundances at 6-month ($\times 10^{-4}$, percentage of maxima value among all taxa).

SI Table 7-5. Energy Conversion related gene orthologs (GO) significantly modified by GTPs.

Gene Orthologs	Time	Control		0.5% GTPs-treated		1.5% GTPs-treated	
		Mean	SD	Mean	SD	Mean	SD
AAA-ATPase	3-month	1.029E-03	2.115E-04	1.004E-03	1.899E-04	1.114E-03	2.158E-04
	6-month	7.746E-04	1.864E-04	1.070E-03	2.042E-04	1.266E-03	3.299E-04
Fumarate reductase	3-month	7.690E-05	2.746E-05	1.684E-04	1.053E-04	1.996E-04	6.818E-05
	6-month	1.346E-04	5.292E-05	1.319E-04	4.531E-05	3.695E-04	1.233E-04
NADH-flavin oxidoreductase	3-month	2.457E-04	2.824E-05	3.780E-04	7.808E-05	4.563E-04	9.702E-05
	6-month	2.610E-04	3.398E-05	3.624E-04	6.515E-05	4.658E-04	1.083E-04
Alpha glucosidase	3-month	4.822E-04	1.156E-04	4.567E-04	9.942E-05	5.893E-04	1.600E-04
	6-month	2.832E-04	1.137E-04	4.773E-04	9.765E-05	5.115E-04	1.108E-04
4Fe-4S ferredoxin, iron-sulfur binding domain protein	3-month	5.079E-05	4.461E-05	9.176E-05	7.306E-05	1.169E-04	5.871E-05
	6-month	4.535E-05	2.190E-05	9.144E-05	4.916E-05	2.658E-04	1.087E-04
Molybdopterin oxidoreductase	3-month	8.032E-05	5.742E-05	1.950E-04	1.008E-04	2.470E-04	7.733E-05
	6-month	9.189E-05	5.223E-05	1.982E-04	7.913E-05	5.127E-04	1.847E-04

SI Table 7-6. Clinical chemistry data from reference serum analysis.

Parameter	Time	OVX-control	OVX+0.5%GTPs	OVX+1.5%GTPs
CHOL-total	3-month	103.3 ^{ax} ±4.9	93.9 ^{abx} ±2.5	92.0 ^{bx} ±2.2
	6-month	125.5 ^{by} Δ*±3.8	138.5 ^{ax} Δ*±3.0	108.7 ^{cz} Δ±2.5
TRIG	3-month	53.09 ^{ax} Δ±7.37	47.00 ^{abx} ±3.84	35.38 ^{bx} ±2.35
	6-month	49.25 ^{ax} ±2.48	48.92 ^{ax} ±3.70	37.14 ^{bx} ±1.62
GLU	3-month	213.2 ^{ax} Δ*±18.1	186.5 ^{abx} Δ±10.3	174.8 ^{bx} ±10.6
	6-month	160.8 ^{ax} ±3.7	149.2 ^{ax} ±6.3	153.4 ^{ax} ±3.2
BUN	3-month	15.92 ^{bx} ±0.62	15.85 ^{bx} ±0.88	18.00 ^{ax} Δ*±0.97
	6-month	16.08 ^{bxy} ±0.81	17.15 ^{abxy} Δ±0.76	18.50 ^{axy} Δ*±0.64

Data are presented as mean ± SEM (mg/dL). BUN, blood urea nitrogen; CHOL, cholesterol; GLU, glucose; TRIG, triglycerides. All four parameters did not show significant difference between sham control and ovariectomy (OVX) control.

Within a given column (dose), values that share the same superscript letter (a, b, c, or d) are not statistically different from each other among the OVX groups (OVX-control, OVX+0.5% GTPs, OVX+1.5% GTPs) without adjustment for multiple comparisons.

Within a given row (time), values that share the same superscript letter (x, y, or z) are not statistically different from each other among the OVX groups (OVX-control, OVX+0.5% GTPs, OVX+1.5% GTPs) after adjustment for multiple comparisons.

Δ Indicates a difference from the 0-month data of the control treatment at $p < 0.05$.

* indicates a difference after adjustment

Reference

- Bajad, S. U., Lu, W., Kimball, E. H., Yuan, J., Peterson, C., and Rabinowitz, J. D. (2006). Separation and quantitation of water soluble cellular metabolites by hydrophilic interaction chromatography-tandem mass spectrometry. *J Chromatogr A* **1125**(1), 76-88.
- Balentine, D. A., Wiseman, S. A., and Bouwens, L. C. (1997). The chemistry of tea flavonoids. *Crit Rev Food Sci Nutr* **37**(8), 693-704.
- Baothman, O. A., Zamzami, M. A., Taher, I., Abubaker, J., and Abu-Farha, M. (2016). The role of Gut Microbiota in the development of obesity and Diabetes. *Lipids Health Dis* **15**(1), 108.
- Begley, M., Hill, C., and Gahan, C. G. (2006). Bile salt hydrolase activity in probiotics. *Appl Environ Microbiol* **72**(3), 1729-38.
- Biddle, A., Stewart, L., Blanchard, J., and Leschine, S. (2013). Untangling the genetic basis of fibrolytic specialization by Lachnospiraceae and Ruminococcaceae in diverse gut communities. *Diversity* **5**(3), 627-640.
- Cani, P. D., and Delzenne, N. M. (2009a). The role of the gut microbiota in energy metabolism and metabolic disease. *Curr Pharm Des* **15**(13), 1546-58.
- Cani, P. D., and Delzenne, N. M. (2009b). The role of the gut microbiota in energy metabolism and metabolic disease. *Curr Pharm Des* **15**(13), 1546-1558.
- Carbonero, F., Benefiel, A. C., Alizadeh-Ghamsari, A. H., and Gaskins, H. R. (2012). Microbial pathways in colonic sulfur metabolism and links with health and disease. *Front Physiol* **3**, 448.

- Chen, I. A., Markowitz, V. M., Chu, K., Palaniappan, K., Szeto, E., Pillay, M., Ratner, A., Huang, J., Andersen, E., Huntemann, M., *et al.* (2017a). IMG/M: integrated genome and metagenome comparative data analysis system. *Nucleic Acids Res* **45**(D1), D507-D516.
- Chen, L., Mo, H., Zhao, L., Gao, W., Wang, S., Cromie, M. M., Lu, C., Wang, J. S., and Shen, C. L. (2017b). Therapeutic properties of green tea against environmental insults. *J Nutr Biochem* **40**, 1-13.
- Chen, Y., Yang, F., Lu, H., Wang, B., Chen, Y., Lei, D., Wang, Y., Zhu, B., and Li, L. (2011). Characterization of fecal microbial communities in patients with liver cirrhosis. *Hepatology* **54**(2), 562-72.
- Davila, A.-M., Blachier, F., Gotteland, M., Andriamihaja, M., Benetti, P.-H., Sanz, Y., and Tomé, D. (2013). Re-print of “Intestinal luminal nitrogen metabolism: Role of the gut microbiota and consequences for the host”. *Pharmacol Res* **69**(1), 114-126.
- Duboc, H., Rajca, S., Rainteau, D., Benarous, D., Maubert, M. A., Quervain, E., Thomas, G., Barbu, V., Humbert, L., Despras, G., *et al.* (2013). Connecting dysbiosis, bile-acid dysmetabolism and gut inflammation in inflammatory bowel diseases. *Gut* **62**(4), 531-9.
- Dulloo, A. G., Duret, C., Rohrer, D., Girardier, L., Mensi, N., Fathi, M., Chantre, P., and Vandermander, J. (1999). Efficacy of a green tea extract rich in catechin polyphenols and caffeine in increasing 24-h energy expenditure and fat oxidation in humans. *Am J Clin Nutr* **70**(6), 1040-1045.
- Frye, R. E., Rose, S., Chacko, J., Wynne, R., Bennuri, S. C., Slattery, J. C., Tippett, M., Delhey, L., Melnyk, S., Kahler, S. G., *et al.* (2016). Modulation of mitochondrial

- function by the microbiome metabolite propionic acid in autism and control cell lines. *Transl Psychiatry* **6**(10), e927.
- Graham, H. N. (1992). Green tea composition, consumption, and polyphenol chemistry. *Prev Med* **21**(3), 334-50.
- Holmes, E., Li, J. V., Marchesi, J. R., and Nicholson, J. K. (2012). Gut microbiota composition and activity in relation to host metabolic phenotype and disease risk. *Cell Metab* **16**(5), 559-64.
- Ikeda, I., Imasato, Y., Sasaki, E., Nakayama, M., Nagao, H., Takeo, T., Yayabe, F., and Sugano, M. (1992). Tea catechins decrease micellar solubility and intestinal absorption of cholesterol in rats. *Biochim Biophys Acta* **1127**(2), 141-6.
- Joyce, S. A., MacSharry, J., Casey, P. G., Kinsella, M., Murphy, E. F., Shanahan, F., Hill, C., and Gahan, C. G. (2014). Regulation of host weight gain and lipid metabolism by bacterial bile acid modification in the gut. *Proc Natl Acad Sci U S A* **111**(20), 7421-6.
- Kakiyama, G., Pandak, W. M., Gillevet, P. M., Hylemon, P. B., Heuman, D. M., Daita, K., Takei, H., Muto, A., Nittono, H., and Ridlon, J. M. (2013a). Modulation of the fecal bile acid profile by gut microbiota in cirrhosis. *J Hepatol* **58**(5), 949-955.
- Kakiyama, G., Pandak, W. M., Gillevet, P. M., Hylemon, P. B., Heuman, D. M., Daita, K., Takei, H., Muto, A., Nittono, H., Ridlon, J. M., *et al.* (2013b). Modulation of the fecal bile acid profile by gut microbiota in cirrhosis. *J Hepatol* **58**(5), 949-55.
- Kuever, J. (2014). The Family Desulfovibrionaceae. In *The Prokaryotes: Deltaproteobacteria and Epsilonproteobacteria* (E. Rosenberg, E. F. DeLong, S.

- Lory, E. Stackebrandt, and F. Thompson, Eds.) doi: 10.1007/978-3-642-39044-9_272, pp. 107-133. Springer Berlin Heidelberg, Berlin, Heidelberg.
- Li, B., Selmi, C., Tang, R., Gershwin, M. E., and Ma, X. (2018). The microbiome and autoimmunity: a paradigm from the gut-liver axis. *Cell Mol Immunol* doi: 10.1038/cmi.2018.7.
- Liu, Q., Duan, Z. P., Ha, D. K., Bengmark, S., Kurtovic, J., and Riordan, S. M. (2004). Synbiotic modulation of gut flora: effect on minimal hepatic encephalopathy in patients with cirrhosis. *Hepatology* **39**(5), 1441-9.
- Loffler, M., Fairbanks, L. D., Zameitat, E., Marinaki, A. M., and Simmonds, H. A. (2005). Pyrimidine pathways in health and disease. *Trends Mol Med* **11**(9), 430-437.
- Louis, P., Hold, G. L., and Flint, H. J. (2014). The gut microbiota, bacterial metabolites and colorectal cancer. *Nat Rev Microbiol* **12**(10), 661-72.
- Lu, W., Bennett, B. D., and Rabinowitz, J. D. (2008). Analytical strategies for LC-MS-based targeted metabolomics. *J Chromatogr B* **871**(2), 236-42.
- Luo, H., Tang, L., Tang, M., Billam, M., Huang, T., Yu, J., Wei, Z., Liang, Y., Wang, K., Zhang, Z. Q., *et al.* (2006). Phase IIa chemoprevention trial of green tea polyphenols in high-risk individuals of liver cancer: modulation of urinary excretion of green tea polyphenols and 8-hydroxydeoxyguanosine. *Carcinogenesis* **27**(2), 262-8.
- Ma, C., Han, M., Heinrich, B., Fu, Q., Zhang, Q., Sandhu, M., Agdashian, D., Terabe, M., Berzofsky, J. A., Fako, V., *et al.* (2018). Gut microbiome-mediated bile acid metabolism regulates liver cancer via NKT cells. *Science* **360**(6391).

- Marcobal, A., Kashyap, P. C., Nelson, T. A., Aronov, P. A., Donia, M. S., Spormann, A., Fischbach, M. A., and Sonnenburg, J. L. (2013). A metabolomic view of how the human gut microbiota impacts the host metabolome using humanized and gnotobiotic mice. *ISME J* **7**(10), 1933-1943.
- Mejnikman, A. S., Gerdes, V. E., Nieuwdorp, M., and Herrema, H. (2017). Evaluating Causality of Gut Microbiota in Obesity and Diabetes in Humans. *Endocr Rev* **39**(2): 133-153.
- Million, M., Lagier, J. C., Yahav, D., and Paul, M. (2013). Gut bacterial microbiota and obesity. *Clin Microbiol Infect* **19**(4), 305-13.
- Montel, M. C., Buchin, S., Mallet, A., Delbes-Paus, C., Vuitton, D. A., Desmasures, N., and Berthier, F. (2014). Traditional cheeses: rich and diverse microbiota with associated benefits. *Int J Food Microbiol* **177**, 136-54.
- Murase, T., Haramizu, S., Shimotoyodome, A., Nagasawa, A., and Tokimitsu, I. (2005). Green tea extract improves endurance capacity and increases muscle lipid oxidation in mice. *Am J Physiol Regul Integr Comp Physiol* **288**(3), R708-15.
- Nueda, M. J., Conesa, A., Westerhuis, J. A., Hoefsloot, H. C., Smilde, A. K., Talon, M., and Ferrer, A. (2007). Discovering gene expression patterns in time course microarray experiments by ANOVA-SCA. *Bioinformatics* **23**(14), 1792-800.
- O'Connor, A., Quizon, P. M., Albright, J. E., Lin, F. T., and Bennett, B. J. (2014). Responsiveness of cardiometabolic-related microbiota to diet is influenced by host genetics. *Mamm Genome* **25**(11-12), 583-99.
- Qian, G., Xue, K., Tang, L., Wang, F., Song, X., Chyu, M. C., Pence, B. C., Shen, C. L., and Wang, J. S. (2012). Mitigation of oxidative damage by green tea polyphenols

- and Tai Chi exercise in postmenopausal women with osteopenia. *PLoS One* **7**(10), e48090.
- Rehman, H., Krishnasamy, Y., Haque, K., Thurman, R. G., Lemasters, J. J., Schnellmann, R. G., and Zhong, Z. (2014). Green tea polyphenols stimulate mitochondrial biogenesis and improve renal function after chronic cyclosporin a treatment in rats. *PLoS One* **8**(6), e65029.
- Rodriguez-Aller, M., Gurny, R., Veuthey, J. L., and Guillarme, D. (2013). Coupling ultra high-pressure liquid chromatography with mass spectrometry: constraints and possible applications. *J Chromatogr A* **1292**, 2-18.
- Sandoval-Acuna, C., Ferreira, J., and Speisky, H. (2014). Polyphenols and mitochondria: An update on their increasingly emerging ROS-scavenging independent actions. *Arch Biochem Biophys* **559**, 75-90.
- Shen, C. L., Brackee, G., Song, X., Tomison, M. D., Finckbone, V., Mitchell, K. T., Tang, L., Chyu, M. C., Dunn, D. M., and Wang, J. S. (2017). Safety Evaluation of Green Tea Polyphenols Consumption in Middle-aged Ovariectomized Rat Model. *J Food Sci* **82**(9), 2192-2205.
- Shen, C. L., Han, J., Wang, S., Chung, E., Chyu, M. C., and Cao, J. J. (2015a). Green tea supplementation benefits body composition and improves bone properties in obese female rats fed with high-fat diet and caloric restricted diet. *Nutr Res* **35**(12), 1095-105.
- Shen, C. L., Yeh, J. K., Liu, X. Q., Dunn, D. M., Stoecker, B. J., Wang, P. W., Tang, Y. T., and Wang, J. S. (2008). Effect of green tea polyphenols on chronic

- inflammation-induced bone loss in female rats. *FASEB J* **22**(1 Supplement), 314.3-314.3.
- Shen, T. C., Albenberg, L., Bittinger, K., Chehoud, C., Chen, Y. Y., Judge, C. A., Chau, L., Ni, J., Sheng, M., Lin, A., *et al.* (2015b). Engineering the gut microbiota to treat hyperammonemia. *J Clin Invest* **125**(7), 2841-50.
- Song, C. W., Kim, D. I., Choi, S., Jang, J. W., and Lee, S. Y. (2013). Metabolic engineering of *Escherichia coli* for the production of fumaric acid. *Biotechnol Bioeng* **110**(7), 2025-34.
- Tang, D. Q., Zou, L., Yin, X. X., and Ong, C. N. (2016). HILIC-MS for metabolomics: An attractive and complementary approach to RPLC-MS. *Mass Spectrom Rev* **35**(5), 574-600.
- Tang, L., Tang, M., Xu, L., Luo, H., Huang, T., Yu, J., Zhang, L., Gao, W., Cox, S. B., and Wang, J. S. (2008). Modulation of aflatoxin biomarkers in human blood and urine by green tea polyphenols intervention. *Carcinogenesis* **29**(2), 411-7.
- Taylor, N. (1998). *Green tea*. Kensington Books.
- Thushara, R. M., Gangadaran, S., Solati, Z., and Moghadasian, M. H. (2016). Cardiovascular benefits of probiotics: a review of experimental and clinical studies. *Food Funct* **7**(2), 632-42.
- Vogels, G. D., and Van der Drift, C. (1976). Degradation of purines and pyrimidines by microorganisms. *Bacteriol Rev* **40**(2), 403-68.
- Walter, J., Martinez, I., and Rose, D. J. (2013). Holobiont nutrition: considering the role of the gastrointestinal microbiota in the health benefits of whole grains. *Gut Microbes* **4**(4), 340-6.

- Wang, J., Tang, L., Zhou, H., Zhou, J., Glenn, T. C., Shen, C. L., and Wang, J. S. (2018). Long-term treatment with green tea polyphenols modifies the gut microbiome of female sprague-dawley rats. *J Nutr Biochem* **56**, 55-64.
- Weisburger, J. H. (1997). Tea and health: a historical perspective. *Cancer Lett* **114**(1-2), 315-7.
- Wolf, M. J., Adili, A., Piotrowitz, K., Abdullah, Z., Boege, Y., Stemmer, K., Ringelhan, M., Simonavicius, N., Egger, M., Wohlleber, D., *et al.* (2014). Metabolic activation of intrahepatic CD8⁺ T cells and NKT cells causes nonalcoholic steatohepatitis and liver cancer via cross-talk with hepatocytes. *Cancer Cell* **26**(4), 549-64.
- Wong, J. M., de Souza, R., Kendall, C. W., Emam, A., and Jenkins, D. J. (2006). Colonic health: fermentation and short chain fatty acids. *J Clin Gastroenterol* **40**(3), 235-43.
- Xia, J., Sinelnikov, I. V., Han, B., and Wishart, D. S. (2015). MetaboAnalyst 3.0—making metabolomics more meaningful. *Nucleic Acids Res* **43**(W1), W251-W257.
- Xu, Y., Zhang, M., Wu, T., Dai, S., Xu, J., and Zhou, Z. (2015). The anti-obesity effect of green tea polysaccharides, polyphenols and caffeine in rats fed with a high-fat diet. *Food Funct* **6**(1), 297-304.

CHAPTER 8. SUMMARY

The current dissertation sufficiently investigated the impacts of green tea polyphenols (GTPs) and aflatoxin B₁ (AFB₁) on gut-microbiota in rodent models. The studies were conducted in two different rat strains with unrelated doses, different rat models and different exposure times, thus the data can hardly be integrated for any meaningful analysis. However, the major findings can still be inspiring. Opposite modifying effects exerted by GTPs and AFB₁ were found in 6 aspects, with each aspect covering a number of metabolic pathways: (1) bile constituents, (2) calorific lipids and fats, (3) amino acids and derivatives, (4) calorific carbohydrates, (5) beneficial monosaccharide and (6) short chain fatty acids.

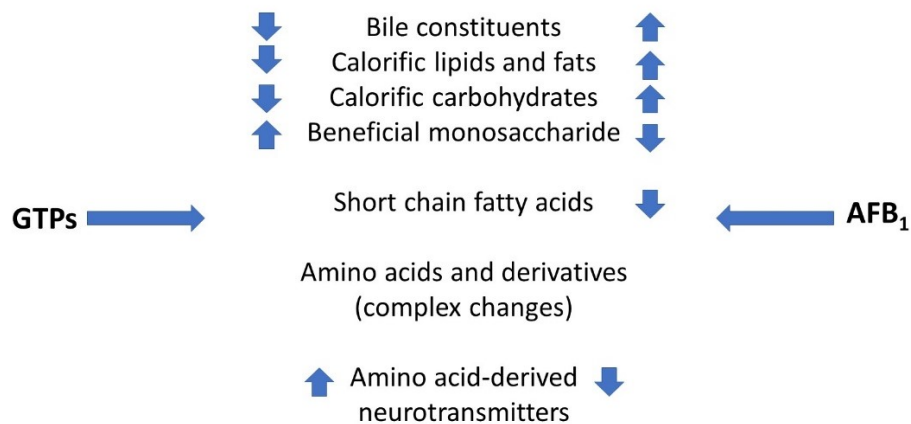


Figure 8-1. Comparing the major changes of gut-microbiota dependent metabolites following exposures to GTPs and AFB₁.

The possible mechanisms were explored by integrating metabolomics data with available reference data, such as 16s rRNA survey, metagenomics data, histopathological data and clinical chemistry data. And the mechanisms seem to be largely different. The treatment of AFB₁ induced decrease of a number of beneficial gut-microbiota strains, such as lactic acid bacteria. Marked enrichment of *Clostridiales spp.* and depletion of *Lactobacillales spp.* were discovered following AFB₁ treatment. Importantly, *Lactobacillales streptococcus* and *Clostridiales roseburia*, two SCFA-producing strains, were depleted in the feces. Due to the changes of community structure, global metabolism of gut-microbiota was disrupted in the AFB₁-treated rats. The efficiency of energy conversion, bile constituent metabolism and long chain fatty acid metabolism were all suppressed, which was indicated by the accumulation of bile acid, pyruvic acid and linoleic acid in the rat feces. Besides, the metabolism of phenylalanine was perturbed, suggesting the impairment of gut-microbiota dependent metabolisms of amino acids.

The modifying effects of GTPs administration on gut-microbiota are totally different. The driving force of the generally boosted gut-microbiota dependent metabolisms seem to be the mitochondrial TCA/Urea cycle. This might be initiated by the binding between GTPs and known GTPs receptors. The altered metabolism may also be involved with the enrichment of *Clostridiales ruminococcaceae*, *C. Lachnospiraceae*, *Bacteroidetes bacteroidaceae*, and decreases of various “adverse outcome pathway”-associated OTUs. The changes of community structure may result in adaptations of abundances of functional genes in different pathways. Eventually, calorific carbohydrates, lipids and fats were consumed. However, the levels of short chain fatty acids were not significantly modified.

We consider that the primary limit of current studies is the short of a combinational exposure to AFB₁ and GTPs under same experimental settings, which may explore whether or not GTPs are able to reverse the AFB₁-induced impairment of gut-microbiota in rats. The secondary limit is that we don't know whether gut-microbiota may naturally recover from the AFB₁-induced impairment and how long it needs to recover completely. Besides, there are many details that need to be investigated. Could the supplement of any probiotics reverse the adverse impacts of AFB₁ but strengthen GTPs benefits on gut-microbiota? What would the physiological outcomes be? How would the changes of gut-microbiota dependent metabolisms affect rodent physiology when the community structure of gut-microbiota is conditionally controlled? These issues may be investigated in the future.